

## ABSTRACT

Title of Document: MICELLE AND AGGREGATE FORMATION  
IN AMPHIPHILIC BLOCK COPOLYMER  
SOLUTIONS

Bryna Christine Clover, Doctor of Philosophy, 2010

Directed By: Sandra C. Greer, Professor Emerita,  
Department of Chemistry and Biochemistry

The amphiphilic nature of many block copolymers causes self-aggregation and micelle formation in solvents that are miscible with only one of the block polymers (selective solvents). Micelle and aggregate formation of amphiphilic block copolymers in selective solvents is a function of temperature and concentration. Such self-aggregation has been examined here in a variety of block copolymer systems.

In dilute solutions of Pluronic P85 (PEO<sub>26</sub>PPO<sub>40</sub>PEO<sub>26</sub>) (where PEO is poly(ethylene oxide) and PPO is poly(propylene oxide)) in D<sub>2</sub>O, transitions between clustered unimers, spherical micelles, cylindrical micelles, and finally lamellar micelles were observed with increasing temperature. The effect of pressure on this system was examined through small angle neutron scattering (SANS) techniques. At temperatures above 95 °C, a new phase of “demixed lamellae” was observed. Pressure effects on the transition temperatures between the phases of this system were investigated.

The self-aggregation of Reverse Pluronic 17R4 (PPO<sub>14</sub>PEO<sub>24</sub>PPO<sub>14</sub>) in D<sub>2</sub>O has also been examined. The phase diagram of this system was determined through visual cloud-point techniques. Three distinct regions have been observed in solutions of this system, as a function of temperature and concentration: a cloudy, one-phase region; a clear, one-phase system; and a region of phase separation. Copolymer structures were examined in the clear and cloudy one-phase regions through SANS and dynamic light scattering (DLS) techniques. A network, or clustering, of unimers was observed in the cloudy phase. Aggregates in the clear, one-phase region could not be identified definitively as micelles.

Finally, micellization of PEO<sub>132</sub>-PB<sub>89</sub> (where PB is polybutadiene) has been studied in solutions of deuterated methanol and deuterated cyclohexane. Spherical micelles were observed in solutions of deuterated methanol. These micelles change little in size or shape over a 50 °C temperature span. The difference in aggregates in protonated and deuterated solvents was also examined. In deuterated cyclohexane, the copolymer formed flexible, cylindrical micelles below 40 °C. These micelles became spherical in shape at higher temperatures.

MICELLE AND AGGREGATE FORMATION IN  
AMPHIPHILIC BLOCK COPOLYMER SOLUTIONS

By

Bryna Christine Clover

Dissertation submitted to the Faculty of the Graduate School of the  
University of Maryland, College Park, in partial fulfillment  
of the requirements for the degree of  
Doctor of Philosophy  
2010

Advisory Committee:  
Professor Emerita Sandra C. Greer, Chair  
Professor Philip DeShong  
Associate Professor Srinivasa Raghavan  
Professor Robert Walker  
Distinguished University Professor John Weeks

© Copyright by  
Bryna C. Clover  
2010

## Dedication

To my family, without whom I could never have gotten where I am today.

## Acknowledgements

First and foremost, I would like to thank Professor Sandra Greer, for all of her guidance, insight, and advice. Thank you for sticking with me, even as your life took you on a new path and all the way to California. I appreciate your faith in my abilities to complete this dissertation in this unusual situation, especially when my own faith faltered.

To Dr. Don Jacobs, thank you for so many helpful discussions, both related to our dear 17R4 and the life of an educator in general. Also, thank you for the experience of working with you and your students at Wooster.

I thank Dr. Boualem Hammouda, at the National Institute of Standards and Technology, for his guidance and advice with all things SANS-related.

Dr. Srinivasa Raghavan, I thank you for the use of your dynamic light scattering and rheometry instruments, as well as for your guidance and beneficial dialogue. Mr. Hee Young Lee and Dr. Mikhail Anisimov, thank you for sharing your knowledge and expertise.

To Dr. Robert Walker, thank you for taking in a “lost” graduate student and for allowing me the opportunity to be a pseudo-member of your group. The concern and interest that both you and Dr. Philip DeShong kept in my advancement was very much appreciated during Dr. Greer’s absence.

Thank you to Mr. Christopher Ploetz and Dr. Alexander Norman for your continued support and assistance, even after you had embarked on your next journey.

Finally, to my family and friends, thank you for all your encouragement, faith, and motivation throughout this experience.

# Table of Contents

Dedication	ii
Acknowledgements	iii
Table of Contents	v
List of Tables	vii
List of Figures	ix
Chapter 1: Introduction	1
1.1 Polymers, Block Copolymers and Pluronics	1
1.2 Micelles	3
1.3 Micelle Formation	5
1.4 Driving Forces of Micellization	7
1.5 Isotope Effects on Hydrogen Bonding	9
1.6 Summary of Experiments	13
Chapter 2: Experimental Techniques	15
2.1 Rheology	15
2.1.1 Theory	15
2.2.2 Instrument	17
2.2 Dynamic Light Scattering	17
2.2.1 Theory	17
2.1.2 Data Collection	19
2.1.3 Data Analysis	20
2.2 Small Angle Neutron Scattering	21
2.2.1 Theory	21
2.2.2 Data Collection	24
2.2.3 SANS Analysis	24
<i>General Analysis</i>	25
<i>Linear Analyses</i>	31
<i>Empirical Non-linear Models</i>	33
Chapter 3: Polymer Systems and Characterization	42
3.1 Pluronic P85: PEO <sub>26</sub> PPO <sub>40</sub> PEO <sub>26</sub>	42
3.2 Reverse Pluronic 17R4: PPO <sub>14</sub> PEO <sub>24</sub> PPO <sub>14</sub>	42
3.3 Polybutadiene-Poly(ethylene oxide): PBd <sub>89</sub> PEO <sub>132</sub>	45
Chapter 4: Aqueous Pluronic System under Pressure	48
4.1 Introduction	48



4.2	Experimental details	50
4.2.1	Materials	50
4.2.2	Solution preparation	50
4.2.3	SANS experimental	51
4.2.4	SANS analysis	52
4.3	Results and discussion	52
4.4	Summary and conclusions	59
Chapter 5: Reverse Pluronic Triblock in Aqueous Solvent		60
5.1	Introductory background	60
5.2	17R4 in D <sub>2</sub> O – glossary	71
5.3	17R4 in D <sub>2</sub> O – phase diagram	72
5.3.1	Introduction	72
5.3.2	Experimental	73
	<i>Solution preparation</i>	73
	<i>Experimental setup of visual observations</i>	74
	<i>Stability of cloudy phase</i>	74
	<i>Effects of filtration on solution in Region I</i>	76
	<i>Region I to Region II equilibration time</i>	77
	<i>Phase separation equilibration time</i>	79
	<i>Determination of Region I to Region II transition temperatures</i>	81
	<i>Determination of phase separation transition temperatures</i>	81
5.3.3	Results and discussion	82
	<i>Region I to Region II transition</i>	82
	<i>Phase separation transition</i>	83
5.3.4	Conclusions	84
5.4	Characterization of copolymer structures	87
5.4.1	Experimental	89
	<i>Solutions</i>	89
	<i>Rheometry</i>	89
	<i>Dynamic light scattering</i>	90
	<i>Small angle neutron scattering – procedure</i>	91
	<i>Small angle neutron scattering – data analysis</i>	91
5.4.2	Results and discussion, Region I	96
	<i>Rheometry of <math>\omega=0.23</math> 17R4/D<sub>2</sub>O sample</i>	96
	<i>SANS of <math>\omega=0.23</math> 17R4/D<sub>2</sub>O solution</i>	97
	<i>SANS of <math>\omega=9.5 \times 10^{-3}</math> and <math>\omega=0.11</math> solutions</i>	106
	<i>Comparison of clusters in different concentration solutions</i>	111
	<i>Summary of Region I</i>	112
5.4.3	Results and discussion, Region II	113
	<i>Rheometry of <math>\omega=0.23</math> 17R4/D<sub>2</sub>O sample</i>	113
	<i>Dynamic light scattering of <math>\omega=0.23</math> 17R4/D<sub>2</sub>O sample</i>	114
	<i>Small angle neutron scattering of <math>\omega=0.23</math> 17R4/D<sub>2</sub>O sample</i>	115
	<i>Reversibility of aggregation</i>	124
	<i>Summary of Region II</i>	124
5.5	Summary	125

Chapter 6: Diblock Poly(ethylene oxide)-Polybutadiene in Organic Solvents	132
6.1 Introduction	132
6.2 Experimental	140
6.2.1 Solution preparation	140
6.2.2 Dynamic light scattering	141
6.2.3 Solvent properties	142
<i>Refractive indices</i>	142
<i>Viscosities</i>	143
6.2.4 Small angle neutron scattering	144
<i>Procedure</i>	144
<i>Analysis methods</i>	144
6.3.1 Copolymer in deuterated methanol	149
<i>Dynamic light scattering</i>	149
<i>Small angle neutron scattering</i>	150
<i>Summary of CD<sub>3</sub>OD results</i>	155
6.3.2 Copolymer in deuterated cyclohexane	159
<i>Dynamic light scattering</i>	159
<i>Small angle neutron scattering</i>	162
<i>Summary of C<sub>6</sub>D<sub>12</sub> results</i>	173
6.4 Conclusions	176
 Chapter 7: Summary and Conclusions	 178
 Appendices	 183
 References	 269

## List of Tables

5.1	Phase separation equilibrium time of 17R4/D <sub>2</sub> O	80
5.2	Porod exponents of cluster in 17R4/D <sub>2</sub> O, Region I	99
5.3	Radii of gyration of Region I unimers of $\omega=0.23$ 17R4/D <sub>2</sub> O	104
5.4	Unimer Porod exponents of $\omega=0.23$ solution in Region I	105
5.5	Absolute and background scattering intensities of unimers in $\omega=0.23$ 17R4/D <sub>2</sub> O solution	106
5.6	Correlation length fit parameters of $\omega=0.11$ 17R4/D <sub>2</sub> O scattering in Region I	108
5.7	Two-region Guinier-Porod model results for $\omega=9.5 \times 10^{-3}$ 17R4/D <sub>2</sub> O solution in Region I	110
5.8	Dynamic light scattering results of $\omega=0.23$ 17R4/D <sub>2</sub> O in Region II	115
5.9	Radius of gyration of copolymer aggregate in Region II of $\omega=0.23$ 17R4/D <sub>2</sub> O solution	119
5.10	Region II SANS analysis with three-region Guinier-Porod model	122
5.11	Porod exponents of copolymer aggregate in $\omega=0.23$ solution of 17R4/D <sub>2</sub> O in Region II	123
6.1	Hydrodynamic radii of PEO <sub>132</sub> -PB <sub>89</sub> in CD <sub>3</sub> OD	149
6.2	Intermediate Q-scaling exponents of PEO <sub>132</sub> -PB <sub>89</sub> in CD <sub>3</sub> OD	152
6.3	Radii of gyration and spherical radii of PEO <sub>132</sub> -PB <sub>89</sub> in CD <sub>3</sub> OD	153
6.4	Spherical radii and polydispersities of PEO <sub>132</sub> -PB <sub>89</sub> in CD <sub>3</sub> OD determined from Schulz sphere model	154
6.5	Polydisperse core-shell model fit results for PEO <sub>132</sub> -PB <sub>89</sub> in CD <sub>3</sub> OD	155
6.6	Comparison of all spherical micelle dimensions of PEO <sub>132</sub> -PB <sub>89</sub> in CD <sub>3</sub> OD, determined through multiple techniques	158
6.7	Hydrodynamic radii of PEO <sub>132</sub> -PB <sub>89</sub> in C <sub>6</sub> D <sub>12</sub>	159
6.8	Intermediate Q-scaling exponents of PEO <sub>132</sub> -PB <sub>89</sub> in CD <sub>3</sub> OD at low temperatures	164
6.9	Fitting parameters of flexible cylinder model for PEO <sub>132</sub> -PB <sub>89</sub> in CD <sub>3</sub> OD	167
6.10	Intermediate Q-scaling exponents of PEO <sub>132</sub> -PB <sub>89</sub> in CD <sub>3</sub> OD at high temperatures	168
6.11	Dimensions of spherical micelles of PEO <sub>132</sub> -PB <sub>89</sub> in CD <sub>3</sub> OD as determined through linear Guinier and Schulz sphere models	171
6.12	Polydisperse core-shell model fit results for PEO <sub>132</sub> -PB <sub>89</sub> in CD <sub>3</sub> OD	172
6.13	Dimensions of flexible cylinders of PEO <sub>132</sub> -PB <sub>89</sub> in CD <sub>3</sub> OD, determined through multiple analysis techniques	174
6.14	Dimensions of spherical micelles of PEO <sub>132</sub> -PB <sub>89</sub> in CD <sub>3</sub> OD, determined through multiple analysis techniques	175
A.1	Uncertainties in DLS and PEO-PB copolymer systems, used to calculate uncertainties in $R_h$	185

A.2	Uncertainties in DLS and 17R4/D <sub>2</sub> O systems, used to calculate uncertainties in $R_h$	186
B.1	Densities and scattering length densities of polymers and solvents	188
C.1	Aggregation temperatures of 17R4 in D <sub>2</sub> O	190
C.2	Cloud-point temperatures of 17R4 in D <sub>2</sub> O	190
C.3	Phase separation temperatures of 17R4 in D <sub>2</sub> O	190
C.4	DynaLS analysis results for 17R4 in D <sub>2</sub> O	193
C.5	Correlation length model results for 17R4 in D <sub>2</sub> O at $\omega=0.23$ in Region I	196
C.6	Linear Porod plot results for 17R4 in D <sub>2</sub> O at $\omega=0.23$ in Region I	196
C.7	Linear Guinier plot results for 17R4 in D <sub>2</sub> O at $\omega=0.23$ in Region I	197
C.8	Two-region Guinier-Porod model results for 17R4 in D <sub>2</sub> O at $\omega=0.23$ in Region I	197
C.9	Correlation length model results for 17R4 in D <sub>2</sub> O at $\omega=0.11$	198
C.10	Two-region Guinier-Porod model results for 17R4 in D <sub>2</sub> O at $\omega=9.5 \times 10^{-3}$	198
C.11	Correlation length model results for 17R4 in D <sub>2</sub> O at $\omega=0.23$ in Region II	199
C.12	Linear Guinier plot results for 17R4 in D <sub>2</sub> O at $\omega=0.23$ in Region II	199
C.13	Linear Porod plot results for 17R4 in D <sub>2</sub> O at $\omega=0.23$ in Region II	200
C.14	Two-region Guinier-Porod model results for 17R4 in D <sub>2</sub> O at $\omega=0.23$ in Region II	200
C.15	Three-region Guinier-Porod model results for 17R4 in D <sub>2</sub> O at $\omega=0.23$ in Region I	201
D.1	Refractive indices of CD <sub>3</sub> OD	202
D.2	Refractive indices of C <sub>6</sub> D <sub>12</sub>	203
D.3	Viscosities of CD <sub>3</sub> OD	204
D.4	Viscosities of C <sub>6</sub> D <sub>12</sub>	204
D.5	DynaLS analysis results for PEO <sub>132</sub> -PB <sub>89</sub> in CD <sub>3</sub> OD	206
D.6	Linear Guinier plot results for PEO <sub>132</sub> -PB <sub>89</sub> in CD <sub>3</sub> OD	210
D.7	Linear Porod plot results for PEO <sub>132</sub> -PB <sub>89</sub> in CD <sub>3</sub> OD	210
D.8	Schulz sphere model results of PEO <sub>132</sub> -PB <sub>89</sub> in CD <sub>3</sub> OD	211
D.9	Polydisperse core-shell model results of PEO <sub>132</sub> -PB <sub>89</sub> in CD <sub>3</sub> OD	211
D.10	DynaLS analysis results for PEO <sub>132</sub> -PB <sub>89</sub> in C <sub>6</sub> D <sub>12</sub>	212
D.11	Linear Porod plot results of PEO <sub>132</sub> -PB <sub>89</sub> in C <sub>6</sub> D <sub>12</sub>	220
D.12	Lamellae model results of PEO <sub>132</sub> -PB <sub>89</sub> in C <sub>6</sub> D <sub>12</sub>	220
D.13	Flexible cylinder model results of PEO <sub>132</sub> -PB <sub>89</sub> in C <sub>6</sub> D <sub>12</sub>	221
D.14	Linear Guinier plot results for PEO <sub>132</sub> -PB <sub>89</sub> in C <sub>6</sub> D <sub>12</sub>	221
D.15	Schulz sphere model results for PEO <sub>132</sub> -PB <sub>89</sub> in C <sub>6</sub> D <sub>12</sub>	222
D.16	Polydisperse core-shell model results for PEO <sub>132</sub> -PB <sub>89</sub> in C <sub>6</sub> D <sub>12</sub>	222

## List of Figures

1.1	Poly(ethylene oxide) and poly(propylene oxide) structures	1
1.2	Schematics of block copolymers	2
1.3	Schematics of micelle structures	5
1.4	Micellization lines in aqueous and organic solvents	7
1.5	Enthalpically and entropically driven micellizations	9
2.1	Polymer viscosity as a function of shear rate	16
2.2	Small angle neutron scattering (SANS) geometry	21
2.3	Guinier and Porod regimes of scattering particles	26
2.4	Clustering of poly(ethylene oxide) unimers	27
2.5	Q-scaling exponents and representative particle structures	30
2.6	Sample SANS intensity from cylindrical body	37
2.7	Core-shell micelle model	39
2.8	Flexible cylinder model	41
3.1	Size exclusion chromatograph of 17R4	44
3.2	<sup>1</sup> H-NMR of 17R4	44
3.3	Proton identification in 17R4	45
3.4	<sup>1</sup> H-NMR of PEO <sub>132</sub> PB <sub>89</sub>	46
3.5	Size exclusion chromatograph of PEO <sub>132</sub> PB <sub>89</sub>	46
4.1	SANS scattering from 0.5% P85/D <sub>2</sub> O solution	54
4.2	P85/D <sub>2</sub> O at 65 °C and varying pressures	55
4.3	P85 structures in D <sub>2</sub> O	55
4.4	P85 Guinier factor variation with pressure	57
4.5	Pressure effects on P85 phase boundaries	58
5.1	Schematic of possible micelles of copolymers with hydrophobic ends	61
5.2	Aqueous 25R4 and 25R2 phase diagrams	62
5.3	Aqueous 25R8 phase diagram	65
5.4	Phase diagram of PPO <sub>19</sub> PEO <sub>113</sub> PPO <sub>19</sub> in water	66
5.5	17R4/H <sub>2</sub> O phase diagram, by Zhou and Chu	67
5.6	17R4/H <sub>2</sub> O phase diagram, by Jacobs et al.	70
5.7	Precision water bath	74
5.8	Film formation on surface of 17R4/D <sub>2</sub> O solution	75
5.9	17R4/D <sub>2</sub> O phase diagram	84
5.10	17R4/D <sub>2</sub> O phase diagram with Zhou and Chu 17R4/H <sub>2</sub> O diagram	85
5.11	Intersection of 17R4/H <sub>2</sub> O cloud-point and coexistence curves	86
5.12	17R4/D <sub>2</sub> O solution concentrations of structure investigation	88
5.13	Shear viscosity of 17R4/D <sub>2</sub> O in Region I of $\omega=0.23$ solution	97
5.14	Neutron scattering of $\omega=0.23$ 17R4/D <sub>2</sub> O solution in Region I	98
5.15	Correlation length model fit to $\omega=0.23$ 17R4/D <sub>2</sub> O at 29.8 °C	99
5.16	Clusters of 17R4 unimers in D <sub>2</sub> O	101
5.17	SANS analyses fits of $\omega=0.23$ at 29.8 °C	103
5.18	SANS scattering intensity of $\omega=0.11$ 17R4/D <sub>2</sub> O solution	107

5.19	SANS scattering intensity of $\omega=9.5 \times 10^{-3}$ 17R4/D <sub>2</sub> O solution	109
5.20	Comparison of Region I cluster scattering in three 17R4/D <sub>2</sub> O solutions	112
5.21	Shear viscosity of 17R4/D <sub>2</sub> O in Region II of $\omega=0.23$ solution	114
5.22	$\omega=0.23$ 17R4/D <sub>2</sub> O solution Region II SANS scattering	116
5.23	SANS analyses fits of $\omega=0.23$ at 34.5 °C	118
5.24	Two-region Guinier-Porod model fit to 17R4/D <sub>2</sub> O scattering	119
5.25	Region II SANS data fit by three-region Guinier-Porod model	121
5.26	17R4/D <sub>2</sub> O aggregation reversibility	124
5.27	Comparison of all aqueous 17R4 phase diagrams	126
5.28	17R4 copolymer conformations in Regions I and II	128
6.1	Self-aggregation morphologies of PEO-PB in water	134
6.2	PEO-PB morphologies in water by Won et al.	135
6.3	Dynamic light scattering results of PEO <sub>132</sub> -PB <sub>89</sub> in methanol	137
6.4	Molecular structures of PEO-PB	138
6.5	Dynamic light scattering results of PEO <sub>132</sub> -PB <sub>89</sub> in cyclohexane	139
6.6	Refractive indices of deuterated methanol and deuterated cyclohexane	143
6.7	SANS scattering from a worm-like body	147
6.8	Hydrodynamic radii of PEO <sub>132</sub> -PB <sub>89</sub> in CD <sub>3</sub> OD and CH <sub>3</sub> OH	150
6.9	SANS intensity of PEO <sub>132</sub> -PB <sub>89</sub> in CD <sub>3</sub> OD	151
6.10	Linear Porod plot of PEO <sub>132</sub> -PB <sub>89</sub> in CD <sub>3</sub> OD at 21.3 °C	151
6.11	Linear Guinier plot of PEO <sub>132</sub> -PB <sub>89</sub> in CD <sub>3</sub> OD at 21.3 °C	152
6.12	Schulz sphere model fit to SANS data of PEO <sub>132</sub> -PB <sub>89</sub> in CD <sub>3</sub> OD at 21.3 °C	154
6.13	Polydisperse core-shell model fit to SANS data of PEO <sub>132</sub> -PB <sub>89</sub> in CD <sub>3</sub> OD at 21.3 °C	155
6.14	Hydrodynamic radii of PEO <sub>132</sub> -PB <sub>89</sub> in C <sub>6</sub> D <sub>12</sub> and C <sub>6</sub> H <sub>12</sub>	160
6.15	DLS mean scattering intensity of PEO <sub>132</sub> -PB <sub>89</sub> in C <sub>6</sub> D <sub>12</sub>	161
6.16	SANS of PEO <sub>132</sub> -PB <sub>89</sub> in C <sub>6</sub> D <sub>12</sub>	163
6.17	Linear Porod plot of PEO <sub>132</sub> -PB <sub>89</sub> in C <sub>6</sub> D <sub>12</sub> at 21.3 °C	164
6.18	Lamellae form factor model fit to SANS data of PEO <sub>132</sub> -PB <sub>89</sub> in C <sub>6</sub> D <sub>12</sub> at 21.3 °C	165
6.19	Flexible cylinder model fit to SANS data of PEO <sub>132</sub> -PB <sub>89</sub> in C <sub>6</sub> D <sub>12</sub> at 21.3 °C	167
6.20	SANS scattering data of PEO <sub>132</sub> -PB <sub>89</sub> in C <sub>6</sub> D <sub>12</sub> at high temperatures	168
6.21	Linear Porod plot of PEO <sub>132</sub> -PB <sub>89</sub> in C <sub>6</sub> D <sub>12</sub> at 49.3 °C	169
6.22	Linear Guinier and Schulz sphere models fit to SANS data of PEO <sub>132</sub> -PB <sub>89</sub> in C <sub>6</sub> D <sub>12</sub> at 49.3 °C	170
6.23	Polydisperse core-shell model fit to SANS data of PEO <sub>132</sub> -PB <sub>89</sub> in C <sub>6</sub> D <sub>12</sub> at 49.3 °C	172

# Chapter 1: Introduction

## 1.1 Polymers, Block Copolymers and Pluronics

Large, macromolecules formed from smaller molecules are given the general term of “polymers.” Homopolymers are formed when all of the units creating the macromolecule are the same. For example, the homopolymer poly(ethylene oxide) (PEO) is a macromolecule of repeating ethylene oxide units. This polymer is written as  $-(\text{CH}_2\text{CH}_2\text{O})_n-$ , where  $n$  is the number of repeated molecules; the structure is presented in Figure 1.1a.

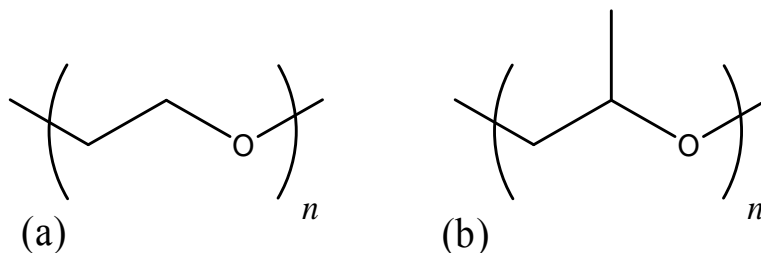


**Figure 1.1:** (a) Poly(ethylene oxide), PEO, and (b) poly(propylene oxide), PPO;  $n$  is the number of repeat units.

If a string, or “block,” of one such homopolymer is covalently bonded to a block of a different polymer, a block copolymer is produced.<sup>1</sup> Block copolymers can be formed with two or more distinct blocks. For example, diblock AB is formed when a block of repeating A units is bonded to a block of repeating B units. Triblock copolymers can be formed when three separate blocks of A, B, and C polymers are

bond together to form, or when two different blocks A and B are bonded in an ABA or BAB fashion.<sup>2</sup> These kinds of copolymers are shown graphically in Figure 1.2.

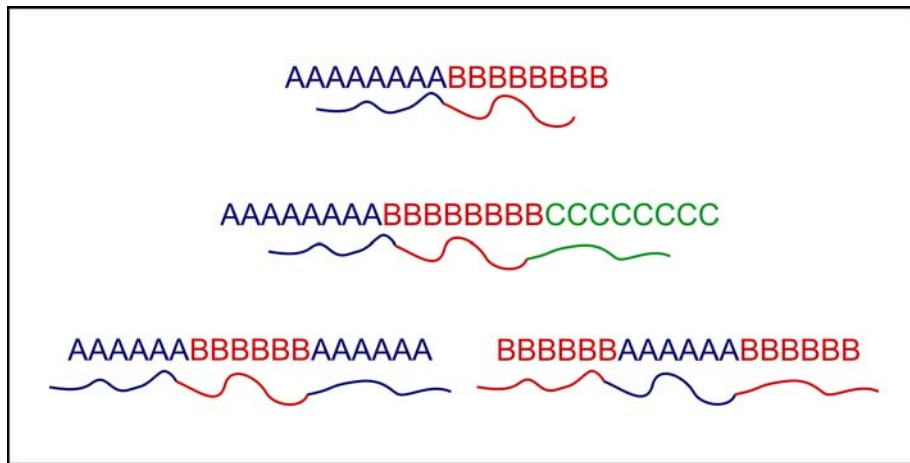


**Figure 1.2:** Schematic representations of AB diblock, ABC triblock, ABA triblock, and BAB triblock copolymers.

All block copolymers must be synthetically prepared,<sup>3</sup> which permits the synthesis of copolymers with chemically incompatible blocks.<sup>4</sup> Copolymers can be synthesized to be amphiphilic; that is the copolymer has one block that is hydrophilic while a second block is hydrophobic. This incompatibility of sections leads to interesting and important physical properties and uses.<sup>4, 5</sup>

Many of these amphiphilic copolymers are composed of the poly(oxyalkenes).<sup>6</sup> The poly(oxyalkene) discussed above, PEO, is one of the most basic hydrophilic polymers and is found in many amphiphilic copolymers. Poly(propylene oxide) (PPO) on the other hand (Figure 1.1b), has just one more carbon per repeating unit than PEO, but it is hydrophobic in nature. The simplicity of these polymers, and their different properties, make copolymers of these polymers



favorites for study. These properties also allow a large number of industrial applications.<sup>6</sup>

Copolymers of the PEO-PPO-PEO variety are known by the commercial trade name “Pluronics,” from BASF Chemical Company. More commonly, these are known as poloxamers.<sup>7</sup> Inverting this block sequence, PPO-PEO-PPO, results in the commercially known “Reverse Pluronics” or “Pluronic-R” copolymers. These copolymers have the nonproprietary name of meroxapols.<sup>7</sup> Triblock copolymers of PEO and PPO are seen in a number of applications.<sup>6</sup> Such applications range from pharmaceutical and medicinal products, such burn and wound dressings and products for controlled drug release, to cleaning products, where the copolymers act as “foam controlling agents.”<sup>6</sup> Interestingly, PEO-PPO-PEO copolymers are found to produce foam, while the Reverse Pluronics reduce foam formation in solutions.<sup>6</sup>

Commercial Pluronic triblocks have been reported to have considerable amounts of impurities.<sup>6</sup> These include both diblock PEO-PPO and pure PPO. Nearly 10% of Pluronic samples have been suggested to be PPO and other hydrophobic impurities.<sup>6</sup> It is not clear at this time what effects these impurities have on the behaviors of Pluronics in selective solvents.<sup>6</sup>

## 1.2 Micelles

Amphiphilic copolymers are usually considered to be those with one hydrophilic and one hydrophobic block, as described above. More generally, however, these molecules can be regarded as having one block that will dissolve in a solvent (not necessarily water),<sup>8</sup> while the other does not. In this regard,<sup>8</sup> one block can be considered

solvophilic and the other solvophobic. When placed in a selective solvent, *i.e.* a solvent that dissolves only one portion of the copolymer, these molecules form aggregates such as lamella, vesicles, and micelles,<sup>8</sup> the last of which is the main focus below.

Micelle formation in diblock copolymers occurs when the solvophobic blocks of multiple polymer strands cluster together forming a *core*. Surrounding this core of solvophobic blocks, the solvophilic blocks form a shielding layer, known as the *corona*,<sup>9</sup> as shown in Figure 1.3. Block copolymer molecules that remain unassociated in the solvent are then referred to here as *unimers*. Triblock copolymers of the ABA variety have also been shown to form micelles in solvents selective for the A-blocks.<sup>5,10</sup> As with diblock copolymer micelles, the solvophobic B-blocks form the core of the micelles, while the solvophilic A-blocks form the protective corona. Micelle formation of triblock copolymers in solvents selective for the B polymer, however, has been suggested to be more difficult, with multiple possibilities of morphologies for the micelles.<sup>6</sup> Such morphologies include the flowerlike micelle and bridged micelles.<sup>5,10</sup> The shapes of micelles from triblock copolymers are also shown in Figure 1.3.

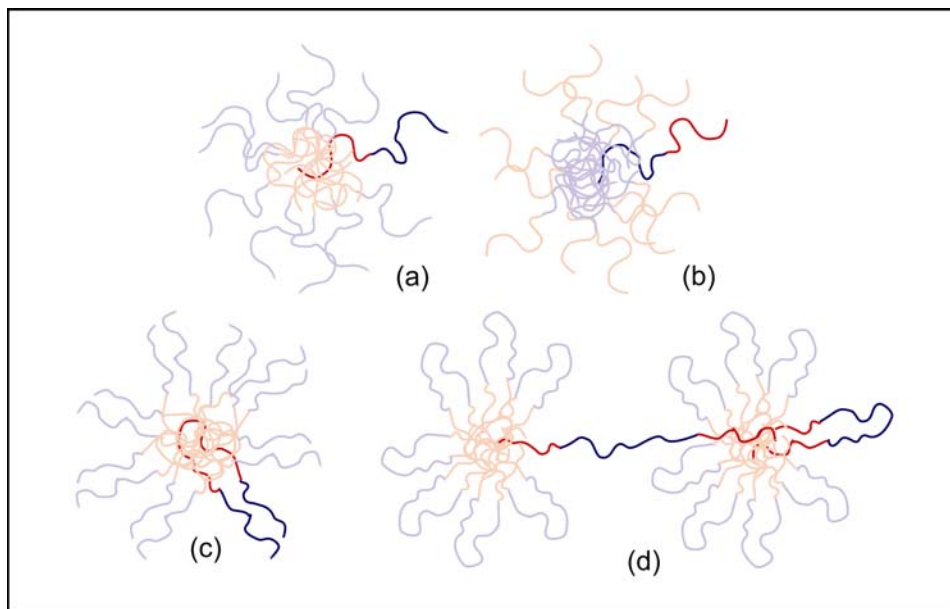


**Figure 1.3:** Schematic representations of (a) regular and (b) reverse micelles from diblock copolymers. Solvents can be selective for either the outer blocks or inner blocks of triblock copolymers. Schematic representation of a copolymer in a solvent selective for the outer blocks is shown (c). Schematic (d) presents possible conformations of a triblock in a solvent selective for the inner block. Flower micelles, are shown, as well as the bridging of a copolymer chain between micelles.

Generally, the term “micelle” is used to refer to this structure when the selective solvent is polar in nature.<sup>8</sup> This results in a micelle structure with a polar corona and a nonpolar core. Micelles can also form in nonpolar selective solvents. Micelles formed in polar solvents shall be referred to here as *regular micelles*, while those formed in nonpolar solvents shall be referred to as *reverse micelles*.

### 1.3 Micelle Formation

Micelle formation occurs only after a specific concentration of unimers has been reached. This critical micelle concentration, CMC, is defined as the point where there is a “sharp increase in the number of molecules associated into micelles” at a fixed

temperature.<sup>9</sup> After this CMC has been reached, additional unimers generally form micelles, and the free unimer concentration remains relatively constant.<sup>11</sup> It is important to note another term here: the CMT, or critical micelle temperature, which is the temperature above or below which micellization occurs at a fixed concentration.<sup>9</sup>

Micellization is not only a function of concentration and temperature, but also of solvent type, with this behavior differing between organic and aqueous systems.<sup>12</sup> At low temperature, poly(oxyalkanes), such as PEO and PPO, are soluble and somewhat compatible with water. At these temperatures, unimers generally exist in solution, except at high concentrations. With increased temperatures, poly(oxyalkanes) (other than PEO) become more hydrophobic and micelles form.<sup>12</sup> Critical micelle concentrations are thus lowered at higher temperatures in water, as depicted in Figure 1.4a. In nonpolar organic solvents, however, amphiphilic poly(oxyalkanes) generally form micelles at low temperatures and break into unimers as the temperature is increased. At higher temperatures, compatibility between carbon-containing solvents and the carbon-backbones of both copolymer blocks increases, allowing the copolymer to maintain a unimer formation in solution (Figure 1.4b).<sup>12</sup> Micellization of amphiphilic block copolymers in polar organic solvents has received little attention in the literature,<sup>5</sup> and it does not necessarily conform to either of these descriptions. Work by Alexandridis and Yang<sup>13</sup> with the polar solvent formamide suggests that polar organic solvents may cause micellization in a manner similar to that seen in aqueous solvents.

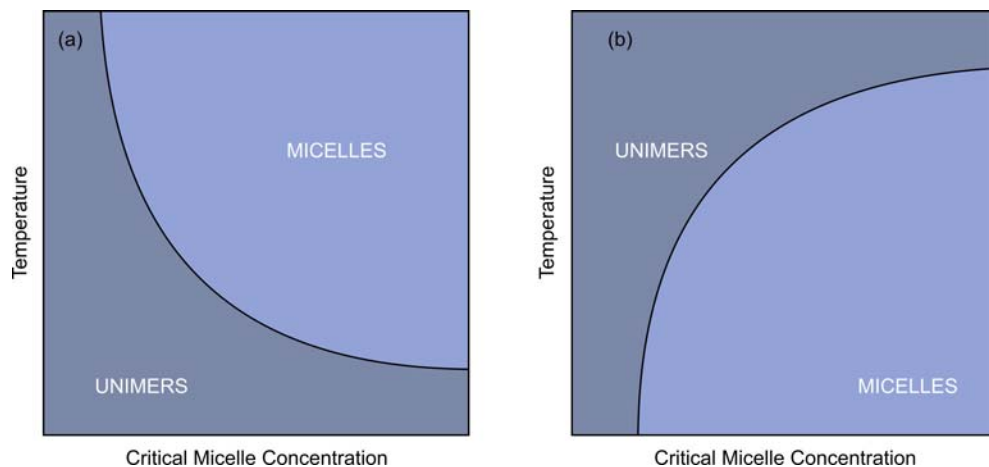


**Figure 1.4:** Micellization line displaying the CMC as a function of temperature for (a) aqueous solvents and (b) nonpolar organic solvents, adapted from Greer.<sup>14</sup>

#### 1.4 Driving Forces of Micellization

Current models of micellization have shown that the thermodynamic forces which drive micelle formation differ greatly with solvent properties.<sup>12</sup> Micelle formation will only occur if the change in Gibbs free energy upon micellization,  $\Delta G_{\text{mic}}$ , has a negative value.<sup>12</sup> That is, the free energy of the micellar system is less than the free energy of the dissociated unimers in solution. This  $\Delta G_{\text{mic}}$  is controlled by the change in enthalpy upon micellization,  $\Delta H_{\text{mic}}$ , and the change in entropy upon micellization,

$\Delta S_{\text{mic}}$  :

$$\Delta G_{\text{mic}} = \Delta H_{\text{mic}} - T\Delta S_{\text{mic}} \quad (1.1)$$

The enthalpy term of the Gibbs free energy equation is greatly controlled by the solvent quality, and this term reflects the interactions among all molecules in the system.

In organic solvent systems, this  $\Delta H_{\text{mic}}$  term is often negative, this is true for both protic and aprotic organic solvents.<sup>12</sup> The ordering of unimers in the solvent upon

micelle formation also causes a negative  $\Delta S_{\text{mic}}$  term. Such an ordering of unimers is depicted in Figure 1.5a. This implies that micellization in organic solvents is enthalpically driven. This also corresponds to the previous discussion of micellization in organic solvents, above: only at low temperatures will the enthalpic term drive micellization. At higher temperatures, the entropic term will cause the free energy to become positive, and micelles will not form.

In contrast, experimental evidence has shown that the  $\Delta H_{\text{mic}}$  in aqueous solvents is positive.<sup>12</sup> Therefore, the driving force leading to a negative  $\Delta G_{\text{mic}}$  in aqueous solvents must be the entropic term. The formation of micelles by the ordering of free polymer chains decreases the disorder of unimer molecules. However, in aqueous solutions the strong hydrogen bonding nature of the solvent greatly impacts the overall  $\Delta S_{\text{mic}}$  of the system. Water will form a highly ordered structure around the hydrophobic carbon chain of the unimer to minimize polymer-solvent interactions and increase solvent-solvent hydrogen bonds, but upon micelle formation, the number of solvent molecules involved in these ordered hydrogen-bonded structures is decreased, as shown in Figure 1.5b.<sup>12, 15, 16</sup> These ordered solvent structures are sometimes referred to as “cages.” This releases a number of solvent molecules in the system, greatly increasing the disorder and entropy of the bulk solvent.<sup>12, 15, 16</sup> This increase in entropy is greater than the loss of entropy due to the ordering of unimers into micelles. This effect causes an entropically driven micelle formation in protic solvents.<sup>12</sup> This argument for micellization in aqueous systems agrees with that discussed in the previous section. At high temperatures, micelles will be present in solution. At low temperatures, the entropy term may be smaller than the enthalpy term, causing a positive free energy, and leaving unimers in solution.

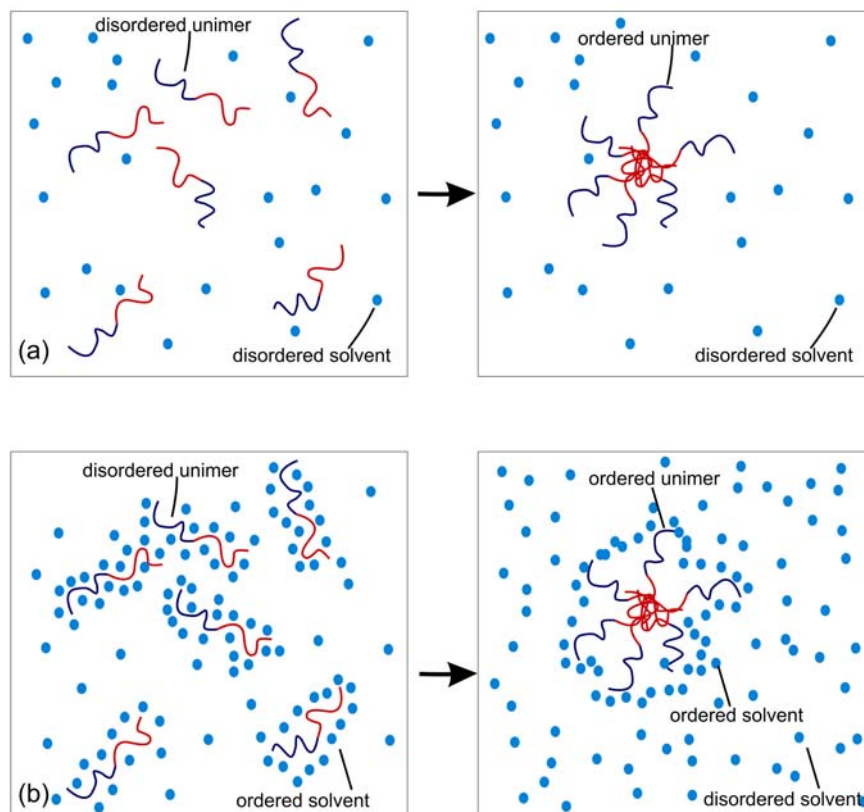


**Figure 1.5:** Representation of (a) enthalpically and (b) entropically driven micelle formation. Upon micellization, unimers in both circumstances experience a decrease in disorder. In aqueous solutions, however, water molecules gain energetically favorable disorder. (Adapted from Raghavan.)<sup>16</sup>

### 1.5 Isotope Effects on Hydrogen Bonding

H<sub>2</sub>O and D<sub>2</sub>O are often taken to be interchangeable when examining the copolymer behavior in aqueous solutions. Many physical properties of these two liquids such as density, viscosity, and even heat capacity have distinct differences.<sup>17,</sup>  
<sup>18</sup> Although often small, these differences do have pronounced effects on system behaviors. For instance, while H<sub>2</sub>O is needed to sustain life, D<sub>2</sub>O is actually lethal in large doses.<sup>17</sup> With this in mind, the differences in polymer solution behavior caused by solvent isotope exchange should not be ignored.

The hydrogen bonding strengths in H<sub>2</sub>O and D<sub>2</sub>O have been shown to differ.<sup>19</sup> Because deuterium atoms are heavier than their single-neutron counterpart, the out of phase vibrations in hydrogen bonds with donated deuterium atoms are smaller than those in hydrogen bonds with donated hydrogen atoms. With smaller vibrations, the strength of D<sub>2</sub>O hydrogen bonds is larger than that of hydrogen bonds in H<sub>2</sub>O. This larger strength of hydrogen bonds in D<sub>2</sub>O is believed to lead to a greater overall structuring within bulk D<sub>2</sub>O, as compared to bulk H<sub>2</sub>O.<sup>17, 20</sup> Many of the differences in physical properties between H<sub>2</sub>O and D<sub>2</sub>O are due to this difference in fluid structures.<sup>20</sup>

With these differences in hydrogen bond strength and solvent structure in mind, solvation of a polymer chain in D<sub>2</sub>O and H<sub>2</sub>O is considered. If a polymer is able to partake in hydrogen bonding with the solvent, this hydrogen bond will be stronger in D<sub>2</sub>O. This polymer characteristic will cause an increase in solvation in D<sub>2</sub>O compared to solvation in H<sub>2</sub>O.

Conversely, the hydrophobicity of polymers with hydrocarbon chains must also be considered with respect to these two solvents. Many studies have suggested that hydrophobic interactions are greater in D<sub>2</sub>O than H<sub>2</sub>O: that is, solutes become *more* hydrophobic in D<sub>2</sub>O.<sup>17, 20, 21</sup> This is often accredited to the greater structure in D<sub>2</sub>O, but it has been indicated that this is not necessarily the case.<sup>17, 21</sup> Some suggest that the structure of solvation cage around the hydrophobe should be considered as well as the structure of the bulk D<sub>2</sub>O.<sup>17, 21</sup> While the cause of this higher hydrophobicity in D<sub>2</sub>O remains uncertain, the self-aggregation of many hydrophobic bodies occurs at lower temperatures and concentrations in D<sub>2</sub>O than in H<sub>2</sub>O.<sup>17, 20, 21</sup>



It is difficult to predict the changes in polymer aggregation behavior that will occur upon changing the solvent from H<sub>2</sub>O to D<sub>2</sub>O since there is an increase in both hydrogen bond strength and hydrophobicity. For example, polymerization temperatures of actin were found to be lower in D<sub>2</sub>O than in H<sub>2</sub>O at low concentrations.<sup>22</sup> However, at higher concentrations of actin, this temperature was found to be higher in D<sub>2</sub>O solutions than in H<sub>2</sub>O solutions.<sup>22</sup>

A study into the solvent isotope effects on several Pluronic copolymers has recently been reported.<sup>23</sup> For each Pluronic studied, it was shown that the increased hydrophobic nature of D<sub>2</sub>O with the increased alkane chain of these copolymers caused self-aggregation at lower temperatures than in H<sub>2</sub>O. The authors also presented theoretical calculations that demonstrated that the enthalpy of micellization is significantly higher in D<sub>2</sub>O than in H<sub>2</sub>O. This calculation also showed that there are fewer hydrogen bonds between Pluronics and D<sub>2</sub>O, compared to the number between Pluronics and H<sub>2</sub>O. Micelle sizes were shown, experimentally and through calculations, to be larger in D<sub>2</sub>O than in H<sub>2</sub>O. Solutions formed from 50/50 isotopic mixtures presented results that were of average values of the pure D<sub>2</sub>O and H<sub>2</sub>O when aggregation number, heat capacity (at constant pressure) and density profiles were examined. The authors describe these results as an effect of the stronger D<sub>2</sub>O-D<sub>2</sub>O hydrogen bonds. Calculations show the free energy cost of a copolymer-D<sub>2</sub>O hydrogen bond is greater than that of a copolymer-H<sub>2</sub>O hydrogen bond. Because of this, hydrogen bonding between D<sub>2</sub>O molecules is preferred over copolymer-D<sub>2</sub>O bonding. It is believed that this will also cause lower CMT values in D<sub>2</sub>O than in H<sub>2</sub>O in aqueous poly(alkyl oxide) solutions.

There is also difficulty in predicting solution separation behavior upon solvent isotope exchange. Changes in lower critical solution temperatures (LCST) depend greatly on the chemical composition of the solute in solution. For example, poly(vinyl methyl ether) (PVME) and poly(N-isopropyl acrylamide) (PNIPAM) were both observed to have a higher LCST in D<sub>2</sub>O than in H<sub>2</sub>O.<sup>24, 25</sup> Poly(ethylene glycol) and Pluronic 10R5 (PPO<sub>22</sub>PEO<sub>8</sub>PPO<sub>22</sub>) have lower LCSTs in D<sub>2</sub>O than in H<sub>2</sub>O.<sup>25</sup> This difference can be understood by examining the structures of these polymers. PVME and PNIPAM both have electronegative atoms protruding into solution. This allows D<sub>2</sub>O molecules to hydrogen bond to the copolymer, while avoiding the carbon backbone of the copolymer. Conversely, the electronegative oxygen in the poly(alkane oxides) of PEG and 10R5 are hidden within the polymer backbone. This would make hydrogen bonding to the copolymer more difficult and necessitate that water molecules come in close proximity to the hydrophobic carbon chain within the copolymer. It is thus expected that solvent exchange of H<sub>2</sub>O for D<sub>2</sub>O will cause lower LCST values in the solutions of poly(alkyl oxides) studied here.

It is also important to address the issue of isotope exchange in the organic solvents used in the PEO-PB systems. Like D<sub>2</sub>O/H<sub>2</sub>O, CD<sub>3</sub>OD has a slightly higher boiling point and density than in its protonated counterpart.<sup>26, 27</sup> This suggests that there is possibly more intermolecular interactions in the bulk CD<sub>3</sub>OD solution, due to stronger hydrogen bonds. Because of this, it is expected that copolymer aggregation will occur at lower temperatures in the deuterated solvent, as has been seen in aqueous solutions.

It is more difficult to predict the changes that may occur upon replacement of cyclohexane with deuterated cyclohexane. These solvents do not partake in hydrogen bonding. Interestingly, the boiling point of  $C_6H_{12}$  is higher than that of  $C_6D_{12}$ , but the density of  $C_6H_{12}$  is lower than that of  $C_6D_{12}$ .<sup>28, 29</sup>

## 1.6 Summary of Experiments

Here, the formation of aggregates and micelles from diblock and triblock copolymers is examined in a variety of solvents. The phase transitions of a dilute solution of the copolymer Pluronic P85 ( $PEO_{26}PPO_{40}PEO_{26}$ ) in  $D_2O$  were examined under pressure using the small angle neutron scattering (SANS) technique.<sup>30</sup> This work was performed with Dr. B. Hammouda at the NIST Center for Neutron Research (NCNR) in Gaithersburg, MD. At low temperatures, solvated copolymer chains are present in solution. These chains also attach to one another, presumably at the PPO blocks, to form large clusters. As temperature is increased, spherical micelles, cylindrical micelles, and finally lamellar micelles form in solution. Transitions between micelle types were observed with increasing temperature. The transition temperatures between micelle types were observed to increase with increased pressure. Above 95 °C, a new “demixed lamellae” phase was observed. This phase is made of stacked lamellae with pockets of solvent. The transition to this phase signifies the approach of a solution phase separation. As pressure was increased, this phase appeared at lower temperatures.

The phase diagram of the Reverse Pluronic 17R4 ( $PPO_{14}PEO_{24}PPO_{14}$ ) in  $D_2O$  was also examined using visual observation, dynamic light scattering, and SANS

techniques. This polymer solution was observed to have three distinct regions. At low concentrations and temperatures, the polymer solution is cloudy and consists of solvated chains and large clusters. As temperature is increased, the copolymer forms aggregates, and the solution clears abruptly. These aggregates are formed from multiple chains and are ellipsoidal in shape, but are not considered micelles here. As temperature is further increased, a solution phase separation is approached, causing additional particle-solvent interactions and possibly prohibiting micellization. The phase diagram of this system is complicated. This system is deserving of further exploration as few studies into these Reverse Pluronics exist. The phase diagram research on this project was performed with Dr. S. Greer at the University of Maryland, College Park and with collaborative efforts from Dr. D. Jacobs from The College of Wooster, Wooster, OH. SANS measurements and analysis were performed with Dr. B. Hammouda of the NCNR at NIST.

Finally, PEO<sub>132</sub>-PB<sub>89</sub> (where PB is polybutadiene) was examined in two organic solvents: deuterated methanol and deuterated cyclohexane. This copolymer was previously examined by Ploetz and Greer through DLS techniques in protonated solvents. Here, SANS is used to verify the micelle confirmations predicted by Ploetz and Greer. PEO<sub>132</sub>-PB<sub>89</sub> forms spherical micelles in deuterated methanol. A solvent isotope effect is observed in this system, as Ploetz and Greer observed both spherical and cylindrical micelles in the protonated solvent. In deuterated cyclohexane, the copolymer forms worm-like cylindrical micelles at low temperatures. These micelles disassemble into spherical micelles and unimers as temperature is increased. This supports the observations of Ploetz and Greer in protonated cyclohexane.

## Chapter 2: Experimental Techniques

### 2.1 Rheology

#### 2.1.1 Theory

The viscosity of a liquid is often referred to as its “resistance to flow;” more formally, this property is a measurement of how a fluid responds to a shear stress. A shear stress,  $\sigma$ , is the ratio between a shearing force,  $F$ , and the area upon which this force is directed,  $A$ , so that

$$\sigma = \frac{F}{A}. \quad (2.1)$$

This shear stress produces a strain on the liquid, causing layers within the fluid to move with different rates. This velocity gradient is referred to as the shear rate,  $\dot{\gamma}$ .<sup>31</sup>

The viscosity of a solution,  $\eta$ , describes the relationship between the shear stress and shear rate, so that

$$\eta = \frac{\dot{\gamma}}{\sigma}. \quad (2.2)$$

Fluids exist for which  $\eta$  is constant and has no dependence on  $\dot{\gamma}$ .<sup>32</sup> In these fluids, the relationship between shear stress and shear rate is linear, obeying Newton’s Law of viscosity. These fluids are known as “Newtonian fluids,” and their viscosities as “Newtonian viscosities.” Viscosities of these liquids display no dependence on shear rate, and so they are also known as “zero-shear” viscosities.<sup>31</sup>

Polymer solutions, however, have been shown to be “non-Newtonian;” that is, the flow of the solution is described by multiple viscosities depending on shear placed upon the liquid. Viscosities of these solutions have a dependence on the shear rate applied to the fluid. Polymer solutions can display Newtonian viscosities at small shear rates.<sup>31</sup> However, at higher shear rates, viscosities become power-law dependent upon shear rates. Polymer solutions sometimes resolve to a second Newtonian viscosity region at high shear rates. (Figure 2.1) These lower Newtonian viscosities are “not due to the *original* fluid,” but rather have been attributed to turbulence in the sample and aggregation or degradation of the polymer.<sup>31</sup> The “zero-shear” viscosities of these solutions correspond to those of the first Newtonian viscosity, at low shear rates.

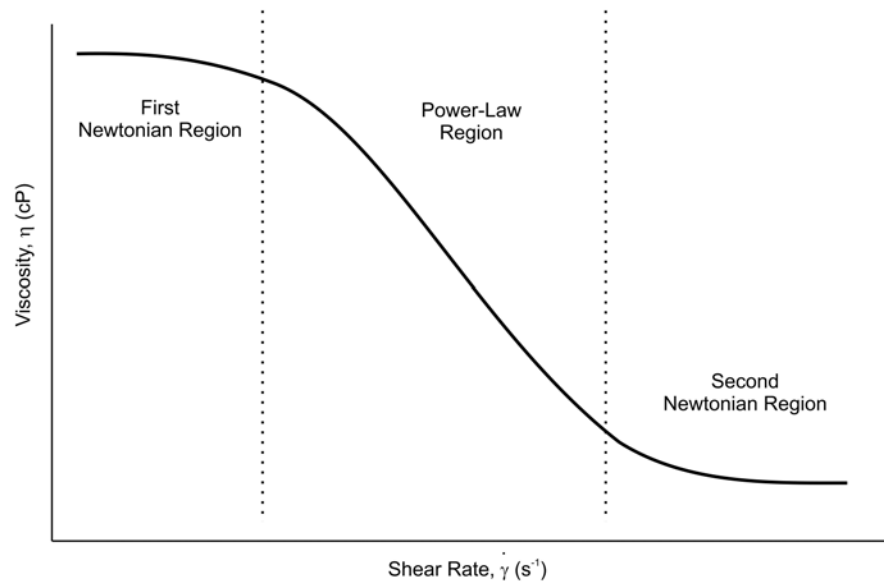


Figure 2.1: The viscosity of polymer solutions shows a dependence on the shear rate,  $\dot{\gamma}$ . At low shear rates, a Newtonian region exists, where the viscosity has no dependence on shear rate, and corresponds to the “zero-shear” viscosity.

### 2.2.2 Instrument

An AR2000 stress controlled rheometer (TA Instruments, Newark, DE) was used for steady state rheological experiments. A cone-and-plate geometry (400 mm diameter, 1° 58' 47" cone angle) was used and a gap of 47  $\mu\text{m}$  was kept between the cone and plate.

## 2.2 Dynamic Light Scattering

### 2.2.1 Theory

Dynamic light scattering (DLS) is a widely used method for determining properties of macromolecules in solution. Based on the electromagnetic interactions between the electrons of these molecules and an incident beam of monochromatic light,<sup>33</sup> DLS exploits the time-dependent Brownian motion of these molecules or assemblies of molecules to yield their hydrodynamic radii.

In DLS, an autocorrelation function of the scattered intensity over time is determined.<sup>34</sup> An autocorrelation function shows the relationship of the measured intensities at separate times in data collection.<sup>35</sup> The normalized autocorrelation function is:

$$g_{(2)}(\tau) = \frac{\langle I(t)I(t + \tau) \rangle}{\langle I(t) \rangle^2}, \quad (2.3)$$

where the brackets symbolize the average over time,  $I$  is the intensity of scattered light, and  $\tau$  is the time delay between data collections.<sup>34</sup> The intensity is measured as the number of photons arriving at the photon detector at a given time.<sup>34</sup>

If Gaussian behavior in fluctuations of intensity is assumed, then the relationship between the intensity autocorrelation function and the electric field autocorrelation function is described by the Siegret relation as follows:<sup>34</sup>

$$g_{(2)}(\tau) = 1 + b |g_{(1)}(\tau)|^2. \quad (2.4)$$

Here  $b$  is an instrumental constant approximately equal to one, and  $g_{(1)}(\tau)$  is the electric field autocorrelation function, which is equal to:

$$g_{(1)}(\tau) = \frac{\langle E(t)E^*(t+\tau) \rangle}{\langle E(t) \rangle^2}, \quad (2.5)$$

where  $E$  is the time-dependent electric field, and the  $*$  signifies the complex conjugate.<sup>34</sup> Fluctuations in this electric field are caused by the movement and scattering variations of the molecules.<sup>34, 36</sup>

It has been shown that for a solution of polydisperse, non-interacting spheres,  $g_{(1)}(\tau)$  takes the form of the exponential decay.<sup>34, 37</sup>

$$g_{(1)}(\tau) = \int P(\Gamma) \exp(-\Gamma\tau) d\Gamma. \quad (2.6)$$

Here  $\Gamma$  is the rate of exponential decay which is related to the scattering vector,  $Q$ , and the diffusion coefficient,  $D$ , of the particles by:

$$\Gamma = Q^2 D. \quad (2.7)$$

The scattering vector is related to the refractive index of a solvent,  $n$ , the scattering angle  $\theta$ , and the light wavelength as:

$$Q = \frac{4n\pi}{\lambda} \sin\left(\frac{\Theta}{2}\right). \quad (2.8)$$

The  $P(\Gamma)$  term in Equation (2.6) represents a function that describes the distribution in the decay rates due to the polydispersity. Determination of this distribution is



difficult, however, as multiple functions may fit the experimental data within the error.<sup>38</sup> Through the use of complex computer-based algorithms,<sup>38</sup> the best  $P(\Gamma)$  is determined and  $D$  can be used to determine the size of the molecules.

The diffusion coefficient of spherical particles is related to their size through the Stokes-Einstein equation,<sup>39</sup>

$$D = \frac{k_B T}{6\pi \eta R_h}, \quad (2.9)$$

where  $k_B$  is the Boltzmann constant,  $T$  is the absolute temperature,  $\eta$  is the viscosity of the solvent, and  $R_h$  is the hydrodynamic radius. The hydrodynamic radius calculated in this manner is the radius of the particle as seen by the solvent that flows around the particle.<sup>9</sup> This definition presumes a spherical particle and provides only an estimate of the particle size, as it may include a solvation layer surrounding the particle as it moves through the solvent.

### 2.1.2 Data Collection

DLS data were collected on a PhotoCor instrument, comprised of a 632.8 nm laser, photo-multiplier tube, 288-channel multi-tau correlator, and precision goniometer.<sup>40</sup> Data were taken at a scattering angle of  $90^\circ$  and the laser was allowed to warm up for at least 20 minutes prior to use. The instrument was set on self-beating mode, and a data collection time of  $2.5 \cdot 10^{-8}$  s was selected. Data were analyzed at 60, 200, and 300 seconds into one 5-minute acquisition and at 90 and 300 seconds into a second acquisition.

### 2.1.3 Data Analysis

The correlation function was fitted using DynaLS version 2.8.3 (Alango Ltd),<sup>38</sup> and Gaussian distributions of hydrodynamic radii were determined. DynaLS is an important analysis tool, as it can account for multiple scatterers in solution. Data from channels lower than number 50 were removed from analysis owing to the irregular scatter in these areas. The high channel numbers were also excluded, where the autocorrelation function had decayed to a “foot” or the baseline.<sup>41</sup>

The peak area, peak position  $R_h$  value, the mean  $R_h$  within the peak, and the standard deviation of this mean are reported by the DynaLS program. Different values between the mean and position of scattering peak indicate a skewed peak. The peak position  $R_h$  value will be reported, however the standard deviation of the  $R_h$  is usually overestimated by DynaLS.<sup>41</sup> The uncertainty in the  $R_h$  was estimated by propagation of error for one sample that showed a single scattering body. It was found that the uncertainty in the resulting  $R_h$  did not exceed 10%. Because not all samples measured are systems with a single type of scattering body, a 10% error is applied conservatively to all  $R_h$  values. See Appendix A for this sample propagation of error and the explanation of one exception to the 10% generalization.

DLS scattering was measured at least four times for each sample. Here, the reported  $R_h$  value for a sample is the average of the  $R_h$  values from the repetitions. The error reported with this average  $R_h$  corresponds to the propagation of 10% error in  $R_h$  from each repetition. That is, if the scattering from a sample was measured five times (repetitions A, B, C, D, and E), the  $R_h$  value reported here is the average from each of these repetitions, as:

$$R_h = \frac{R_{h,A} + R_{h,B} + R_{h,C} + R_{h,D} + R_{h,E}}{5}. \quad (2.10)$$

The error reported for the average  $R_h$  will be determined by:

$$u_{R_h} = \sqrt{\left(\frac{1}{5}\right)^2 \times \left[ (0.1 \times R_{h,A})^2 + (0.1 \times R_{h,B})^2 + (0.1 \times R_{h,C})^2 + (0.1 \times R_{h,D})^2 + (0.1 \times R_{h,E})^2 \right]}. \quad (2.11)$$

## 2.2 Small Angle Neutron Scattering

### 2.2.1 Theory

Small angle neutron scattering (SANS) is an important characterization method. This technique uses the scattering of neutrons from particles within a sample to determine the size and shape of nanometer-sized objects. As shown in Figure 2.2, a sample is placed in the path of an incident beam of neutrons where nuclei within the sample scatter neutrons by an angle,  $\theta$ , and these scattered neutrons are collected at a detector located a distance,  $L_{sd}$ , away from the sample.

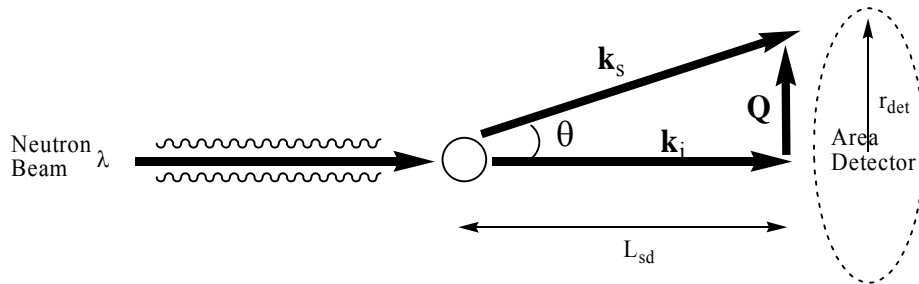


**Figure 2.2:** Geometry of neutron beam scattered through sample. The scattering vector,  $Q$ , is equal to the difference of scattering wave vector,  $k_s$ , and the incident wave vector,  $k_i$ , when neutrons are scattered at an angle,  $\theta$ . Detection of neutrons occurs at a detector of radius,  $r_{det}$ , located at a distance,  $L_{sd}$ , away from the sample. Adapted from Hiemenz and Rajagopalan.<sup>36</sup>

This detector measures the flux of neutrons scattered from the interaction with the nuclei of the sample.<sup>42, 43</sup> This flux is described by the equation

$$I(\lambda, Q) = I_o(\lambda)\Delta\Omega\eta(\lambda)T(\lambda)V_s \frac{\partial\Sigma}{\partial\Omega}(Q), \quad (2.12)$$

where  $I_o$ ,  $\Delta\Omega$ ,  $\eta$ , and  $T$  are all detector-dependent.  $I_o$  is the flux of incident radiation,  $\Delta\Omega$  is an element based on detector pixel size, and  $\eta$  is the detector efficiency. These variables depend only on the wavelength of neutron radiation for the experiment. The final three variables offer information regarding the sample:  $T$  is the transmission of neutrons by the sample,  $V_s$  is the sample volume within the neutron beam, and

$\frac{\partial\Sigma}{\partial\Omega}(Q)$  is the differential scattering cross-section.<sup>42, 43</sup>

All but the final term are constant at a constant wavelength, which is the case in most SANS experiments.  $\frac{\partial\Sigma}{\partial\Omega}(Q)$  instead depends on the scattering vector,  $Q$ .<sup>42, 43</sup>

$$Q = \frac{4\pi}{\lambda} \sin\left(\frac{\theta}{2}\right) \approx \frac{4\pi}{\lambda} \frac{r_{\text{det}}}{L_{\text{sd}}}. \quad (2.13)$$

As all terms in Equation (2.13) are held constant with constant neutron beam wavelength, our main information regarding our samples comes from the differential cross-section term. Within this term lies important information regarding the “size, shape, and interactions between, scattering centers in the sample.”<sup>43</sup> This term is expressed by

$$\frac{\partial\Sigma}{\partial\Omega}(Q) = NV^2(\Delta\rho_n)^2 P(Q)S(Q) + B \quad (2.14)$$

where  $N$  is the number of nuclei within the sample,  $V$  is the volume of one of these scattering nuclei, and  $B$  is a background signal. The remaining factors are described below.

The term  $(\Delta\rho_n)^2$  is considered the “contrast.”<sup>43</sup> This represents the difference in scattering length densities between solute and solvent. The scattering length density depends on individual nuclei of the molecule, and can differ between isotopes of the same atom. If the solvent is deuterated and the solute is hydrogenated, one can better distinguish solute from the solvent and  $\Delta\rho_n$  can be maximized, leading to higher scattering intensity.

The next factor,  $P(q)$ , is termed the form or shape factor.<sup>43</sup> This describes the change in  $\frac{\partial\Sigma}{\partial\Omega}(Q)$  due to the interactions of neutrons scattered by different nuclei within the same molecule.<sup>43</sup> This function is dependent on both the size and shape of the molecules within a sample. Mathematical equations have been developed to describe different molecular shapes, ranging from a swollen coil that can be used to describe a single polymer chain, to a core-shell model which is used as an approximation of micellar core and corona structures.<sup>42, 43</sup>

Finally, the term  $S(q)$  is the structure factor.<sup>42</sup> This term describes the transformation of  $\frac{\partial\Sigma}{\partial\Omega}(Q)$  due to interference between neutrons scattered from nuclei in different molecules of the sample. This function depends upon the ordering and proximity of molecules within the sample. It is important to note that  $\frac{\partial\Sigma}{\partial\Omega}(Q)$  is often

abbreviated as  $I(Q)$ , or, the scattering intensity as a function of  $Q$ . Such will be the case throughout this work.

### 2.2.2 Data Collection

Small angle neutron scattering (SANS) measurements were made at the National Institute of Standards and Technology Center for Neutron Research in Gaithersburg, MD, on the NG3 30-m instrument.<sup>44</sup> Samples were the same as those used in DLS measurements, and were held in demountable titanium cells with quartz crystal windows and 1 mm sample path lengths. Three sample-to-detector distances were used (1.33 m, 4.00 m, and 13.17 m) with a neutron beam wavelength of 6 Å to obtain a  $Q$  range of 0.003433 to 0.461 Å<sup>-1</sup>. The scattered intensity,  $I(Q)$ , as a function of the wave vector,  $Q$ , was generated through circular averaging of the collected scattered intensity after background scattering was removed. The ten-cell sample holder of the instrument was set at 10 °C intervals between 20-100 °C.

### 2.2.3 SANS Analysis

Analysis of SANS data begins with a general observation of scattering trends. Linear plots are then used to gain preliminary information from the data. After linear fits are performed, empirical non-linear fits are used to point analyses toward proper modeling functions that predict the shape and properties of scattering particles. Each of these is an important step and will be described further. Agreement among methods indicates reliability in analysis findings.

### *General Analysis*

The first steps in analyzing SANS data are to examine the intensity as a function of  $Q$  in general. It is important to note scattering in regions of high- and low- $Q$  values and any peaks that may be apparent in the data.

Typically, scattering from dilute polymer solutions presents two regions of  $Q$ -values that offer information about the scattering particle.<sup>45</sup> A  $Q$ -value can be related to a length scale,  $d$ , of a specific probed area.<sup>43</sup> If Equation (2.13) is recalled, and the Bragg law of diffraction,

$$\lambda = 2d \sin\left(\frac{\theta}{2}\right), \quad (2.15)$$

is inserted, then the length scale of the probed region is related to  $Q$  through<sup>43</sup>

$$Q = \frac{2\pi}{d}. \quad (2.16)$$

At values of  $Q$  corresponding to a probed region of length scale smaller than the size of the scattering particle, specific relationships, known as the Guinier approximations, can be used to determine dimensions of the scattering particles.<sup>43</sup> These Guinier approximations will be discussed later in this chapter. Figure 2.3a displays this so-called “Guinier regime” with respect to a scattering body.<sup>45</sup> Because of the inverse relationship between  $d$  and  $Q$ , the Guinier regime of large length scales often occurs at low- $Q$  values.

A second important  $Q$ -range is that which corresponds to a probed area of length scales smaller than those of the scattering particle. Here, the intensity  $Q$ -dependence offers insight into the shape of the scattering body and its local

structure.<sup>45</sup> This Q-range of length scales smaller than the size of the scattering body is often referred to as the “Porod regime,” and is graphically depicted in Figure 2.3b.

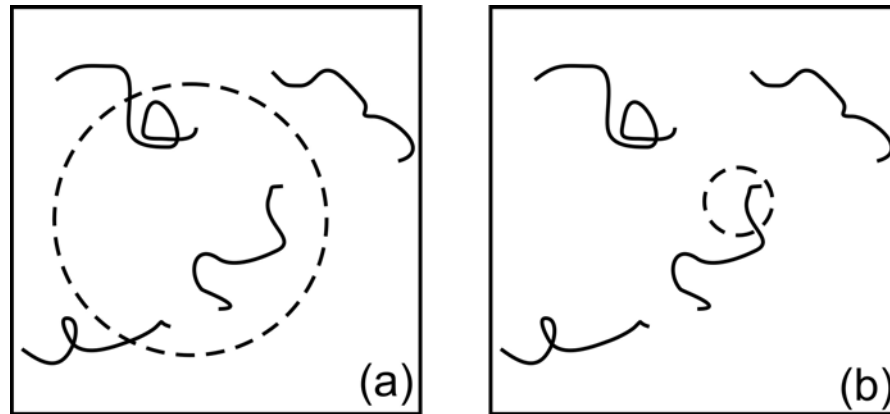


**Figure 2.3:** Depiction of Guinier (a) and Porod (b) regions compared to scattering particles. Probed regions are depicted by the dashed circle. Adapted from Hammouda.<sup>45</sup>

In samples showing scattering from multiple scattering bodies, it is possible for the Guinier and Porod regimes of different bodies to overlap. For example, in solutions of polymers it is possible for the polymer to cluster together, forming a very large scattering object, while still displaying scattering from individual unimers in solution.<sup>46</sup> This is seen in solutions of PEO alone in  $D_2O$ ,<sup>46</sup> and is shown in Figure 2.4. If this occurs, the Guinier regime of the smaller structure can overlap with the Porod region of the larger, as both would occur at small Q-values.



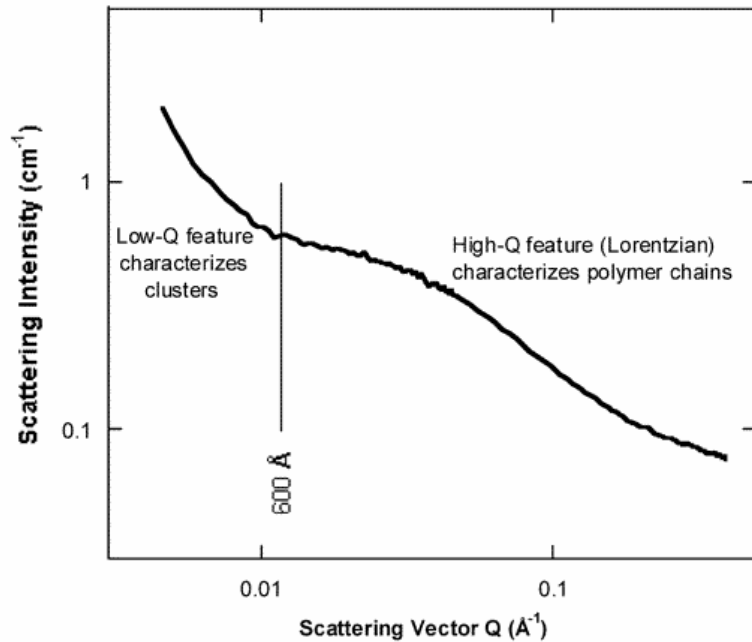


**Figure 2.4:** Clustering of PEO unimers in D<sub>2</sub>O occurs at Q values smaller than 0.0105 Å<sup>-1</sup> (corresponding to d lengths of 600 Å), while at larger Q values, scattering from polymer chains is apparent. Adapted from Hammouda et al.<sup>46</sup>

It is also important to note that larger structures, such as clusters or crystals, may scatter beyond the SANS Q-range, typically 0.001 Å<sup>-1</sup> to 0.45 Å<sup>-1</sup>, which corresponds to probing lengths of 63000 Å to 14 Å.<sup>45</sup> Often only the tail of the Porod regime scattering from these bodies is observed, while the Guinier regime occurs at smaller Q-values.

Scattering from particles with axes of different lengths (such as ellipsoids or cylinders) will also have an intermediate Q-regime. Such particles have at least two distinct radius of gyration,  $R_g$ , values: those corresponding to rotation on the smaller axis and one corresponding to the rotation of the entire object. These dimensions will be apparent in the scattering data and are often marked by a change in slope of  $I(Q)$ . Scattering from these particles does display a Guinier regime, at Q-values lower than

those corresponding to the large  $R_g$ , and a Porod regime at Q-values higher than the smallest dimension.

Between these scattering regimes an intermediate regime is apparent. Q-scaling in this intermediate regime indicates the dimensionality of the structure. This scaling of the intensity as a function of Q will be discussed later. The  $R_g$  corresponding to the large particle dimension can give insight into the length of a particle. It is possible that only the Porod and intermediate regimes of a large structure will be visible in the SANS data window. When this occurs, no inference of particle length can be made. This is shown in an example of PEO/water solution in Figure 2.4.

In addition to these Guinier and Porod scattering regions, it is also important to note any peaks in the data, usually appearing at mid-Q ranges, between the Porod and Guinier regimes. Sharp peaks are often seen in SANS data of soft materials, and these can be representative of multiple system characteristics. Often only one peak will be apparent in the scattering data, with various peaks occurring only in certain situations.<sup>45</sup> In systems with periodic scattering length densities, such as those seen in lamellar systems, Bragg peaks will arise representing the average distance between density domains.<sup>45</sup> A peak can also be observed in concentrated systems with a high degree of inter-particle interactions, where the peak represents the distance between interacting particles, due to the structure factor,  $S(Q)$ .<sup>45</sup> Finally, multiple, higher-order peaks at high-Q values can be observed from very dilute systems due to the oscillating Bessel function that describes single-particle scattering.<sup>45</sup> Each of these

peaks offers further insight into the form and structure of particles in solution, as well as any inter-particle interactions.

As mentioned earlier, the scaling of  $I(Q)$ , as  $Q^{-m}$ , can give much insight into the shape of a scattering particle. In the Guinier regime of a dilute solution of 3D particles, there is usually no  $Q$ -dependence. Scattering with a  $Q^0$  dependence is often an indication of the Guinier regime.

Scaling in the Porod regime is related to the particle-solvent interface<sup>47</sup> and offers information regarding the fractal dimensions of a particle.<sup>45</sup> Fractal particles are those that have a self-similarity at different length scales.<sup>48</sup> Porod exponents,  $m$ , indicate the fractal dimension of a body. Surface fractals have Porod exponents between 3 and 4; exponents near 3 describe the scattering from a rough body, while that of 4 represents a smooth body. Mass fractals, or those particles without a distinct surface from which to scatter, display scattering with a different power-dependence of  $Q$ . Porod exponents between 1 and 3 are often indicative of these mass fractals. A Porod exponent of 1 represents scattering off of a very dilute particle, and  $m=3$  is scattering off a very dense particle. Such mass particles include swollen polymers (where  $m=5/3$ ) and even collapsed polymers (where  $m=3$ ).<sup>45</sup> Notice that a highly collapsed mass fractal can begin to scatter as a rough surface fractal, both having Porod exponents near 3.

Representative  $Q$ -scaling exponents are shown in Figure 2.5a.<sup>45</sup> Note that some values of exponents can be representative of multiple scattering body shapes or fractals. Polydispersity and data smearing can also affect the  $I(Q)$  slope at high- $Q$ , skewing this scaling.<sup>49</sup>

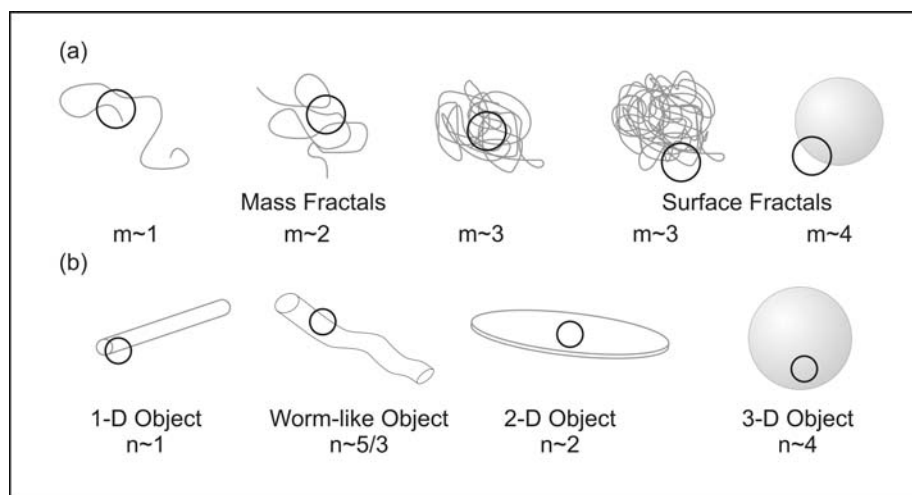


**Figure 2.5:** Examples of Q-scaling exponents: (a) Porod Q-scaling offers information on the particle-solvent interface while (b) intermediate regime scaling offers information regarding body shape. Adapted from Hammouda.<sup>45</sup>

Scaling within the intermediate regime indicates particle dimension. Here, the variable  $n$  will be used to describe scaling of  $Q$  in the intermediate regime, as  $Q^{-n}$ . Scaling of  $Q^{-2}$  is indicative of plates or lamellae (2-D objects);  $Q^{-1}$  scattering is indicative of a cylinder or rod (somewhat 1-D); and in between,  $Q^{-3/2}$  represents worm-like particles. Scattering from a smooth sphere has a dependence of  $Q^{-4}$ , but it is difficult to observe this separately from the Porod regime scaling, as both have the same value. Also, it is difficult to see a true “intermediate regime” for particles of equal lengths of axes. Thus, spherical a shape is often inferred from a Guinier regime smoothly flowing into the Porod regime. These particle dimensions are displayed in Figure 2.5b.

### *Linear Analyses*

The next stage of SANS analysis involves simple, linear plots. A valuable relationship in small angle scattering, the Guinier approximation, offers an estimation of particle size without dependence upon any model of scattering. Using a series of expansions at low QR values, and further approximations of the spherical form factor, Guinier approximated:<sup>43</sup>

$$I(Q) = I_0 \exp\left(\frac{-Q^2 R_g^2}{3}\right). \quad (2.17)$$

Here,  $R_g$  is the radius of gyration of the particle, and  $I_0$  is the scattering intensity at  $Q=0$ , or  $NV^2(\Delta\rho_n)^2$ , from Equation (2.14). The radius of gyration for a sphere is related to the spherical radius,  $R$ , through<sup>45</sup>

$$R = R_g \sqrt{\frac{3}{5}}. \quad (2.18)$$

This approximation holds only within the Guinier region of  $Q$  values, or where  $QR_g < \sqrt{3}$ .<sup>45</sup> By taking the natural log of Equation (2.17), a linear relationship can be obtained, and by plotting  $\ln[I(Q)]$  versus  $Q^2$ , the radius of gyration of the scattering particle can be estimated from the slope of the line of data.

This approximation works well for spheres, and it has been used for other geometries of particles. However, modifications to the Guinier approximation have been made to suit these other forms better by extending similar approximations to the form factors of cylinders and even sheets.<sup>50, 51</sup> These modified Guinier approximations for the cylinder lead to the formula:

$$I(Q) = Q^{-1} I_0 \exp\left(\frac{-Q^2 R_g^2}{2}\right). \quad (2.19)$$

In this case,  $R_g$  is the cross-sectional radius of gyration of the cylinder and is related to the cross sectional radius through<sup>50, 51</sup>

$$R_g = R / \sqrt{2}. \quad (2.20)$$

The value of  $R_g$  can be determined by plotting the linear relationship obtained when the natural log is taken of Equation (2.19) on axes of  $\ln(IQ)$  versus  $Q^2$ . This approximation can only be made over  $Q$ -values where  $QR_g < \sqrt{2}$ .<sup>51</sup> The Guinier approximation has also been modified for sheets, such as lamella.<sup>51</sup>

These Guinier approximations are important tools in SANS analysis because they allow the determination of the effective particle size without relying upon models. Also, with the modifications, the appropriate particle shape can be determined from the linear behavior of the scattering data. That is, scattering data from a cylinder will not appear linear when plotted on the spherical Guinier approximation axes,  $\ln(I)$  versus  $Q^2$ , but will appear linear on  $\ln(IQ)$  versus  $Q^2$  axes.<sup>49</sup>

A second common linear plot used in both the Porod and intermediate regimes, is the Porod plot, derived from Porod's Law for a spherical particle.<sup>45</sup> This plot offers a simple method to determine the  $Q$ -scaling factor of  $I(Q)$ . A simple equation:

$$I(Q) = \frac{A}{Q^m} + B, \quad (2.21)$$

where  $A$  is a multiplicative scaling factor and  $B$  is the incoherent background scattering, allows for determination of the  $Q$ -scaling factor,  $m$ .<sup>45</sup> By plotting  $\log[I(Q)-B]$  vs.  $\log[Q]$ ,  $m$  is determined from the slope of the data at high- $Q$ .

This plot can be used in both the intermediate and Porod regimes, which can lead to confusion in denoting the scaling in each region. Here, the scaling factor in the Porod regime will have the variable  $m$  and will be referred to as the Porod exponent. The letter  $n$  will be used to represent the scaling exponent in the intermediate regime.

Although these linear plots do offer useful estimates of size and shape of a scattering body, they are only used as preliminary analyses due to many drawbacks. Background scattering should be removed before plotting, and poor estimates of such scattering may skew results. Also, polydispersity and smearing effects are not taken into consideration in these analyses.<sup>45</sup> Finally, the  $Q$  ranges in which these plots are performed greatly affect the results. Although general ranges are suggested, the actual range used can be difficult to determine<sup>43</sup> and greatly sways results. For example, in performing the Porod plot, it is difficult to determine where the Porod and intermediate regimes begin and end. For these reasons, it is sometimes suggested that  $R_g$  values or Porod exponents are not best determined through these linear plots.<sup>52</sup> Others argue, however, that these plots present the truest results as they are not skewed by models or tweaked to produce a best fit.<sup>49</sup>

### *Empirical Non-linear Models*

While the simple, linear plots aid in estimating information from SANS data, non-linear models offer other approaches to estimating particle size and dimension from  $I(Q)$ .<sup>45</sup> One such model is the correlation length model.<sup>45</sup> This model can be used when  $I(Q)$  has no interaction peaks. The function has the form

$$I(Q) = \frac{C}{1 + (Q\xi)^m} + B, \quad (2.22)$$

where C represents the scattering intensity at Q=0, and B is the background scattering.  $\xi$  is the correlation length, and m is a Porod exponent. The correlation length can be related to the radius of gyration of the scattering body through<sup>49</sup>

$$\xi = \frac{R_g}{\sqrt{3}}. \quad (2.23)$$

This model can describe dimensions and shape while also taking into account background scattering and using the entire Q range of scattering data. This eliminates two of the main problems with linear fits.

A second term is often added to this fit to describe the scattering of a second large body also in solution. This fit was derived to model the behavior of PEO in D<sub>2</sub>O,<sup>46</sup> and it has the formula

$$I(Q) = \frac{A}{Q^{m_1}} + \frac{C}{1 + (Q\xi)^{m_2}} + B. \quad (2.24)$$

This equation is used with polymer solutions displaying low-Q scattering from clustering as well as scattering from solvated polymer. The Porod term  $\left(\frac{A}{Q^{m_1}}\right)$  fits the Porod region of the clustering feature in solution and gives the Porod exponent of the cluster feature. The correlation term  $\left(\frac{C}{1 + (Q\xi)^{m_2}}\right)$  describes the scattering from individual polymer chains, giving the correlation length and Porod exponent for the unimers in solution.<sup>46</sup> This form of the correlation length model will be used in this



study. The variables  $m_1$  and  $m_2$  will be used for the Porod exponents of the cluster and unimer, respectively.

A new model, the Guinier-Porod model, has recently been developed by B. Hammouda<sup>51</sup> to include both the Guinier approximation and the Porod exponent through non-linear fits. The Guinier functional form:

$$I(Q) = \frac{G}{Q^n} \exp\left(\frac{-Q^2 R_g^2}{3-n}\right) \text{ for } Q \leq Q_1, \quad (2.25)$$

and the Porod functional form:

$$I(Q) = \frac{D}{Q^m} \text{ for } Q \geq Q_1, \quad (2.26)$$

are fitted over different Q-ranges. Here,  $Q_1$  has the equation

$$Q_1 = \frac{1}{R_g} \sqrt{\frac{(m-n)(3-n)}{2}} \quad (2.27)$$

and is determined within the model. In the Guinier function,  $n$  is the Guinier dimensionality. When  $n=0$ , the Guinier approximation for a sphere is obtained. Similarly the Guinier approximation for cylinders is obtained when  $n=1$ . Note that these exponent values match the Q-scaling values for the same particle shapes in the intermediate regime. The resulting  $R_g$  values can be related to the radii of the scattering particles through Equations (2.18) and (2.20), previously discussed.  $G$  and  $D$  in Equations (2.25) and (2.26) are scaling factors.

This Guinier-Porod model can also be extended to have three fitting regions, adding a second Guinier function, obtaining the function:<sup>51</sup>

$$\begin{aligned}
I(Q) &= \frac{G_2}{Q^{n_2}} \exp\left(\frac{-Q^2 R_{g2}^2}{3 - n_2}\right) \text{ for } Q \leq Q_2, \\
I(Q) &= \frac{G_1}{Q^{n_1}} \exp\left(\frac{-Q^2 R_{g1}^2}{3 - n_1}\right) \text{ for } Q_2 \leq Q_1, \\
I(Q) &= \frac{D}{Q^m} \text{ for } Q \geq Q_1,
\end{aligned} \tag{2.28}$$

where

$$Q_2 = \frac{1}{R_g} \sqrt{\frac{(n_1 - n_2)}{\frac{2}{3 - n_2} R_{g2}^2 - \frac{2}{3 - n_1} R_{g1}^2}}. \tag{2.29}$$

In the additional Guinier function,  $R_{g2}$  is the radius of gyration for the long dimension of the particle.<sup>51</sup> For instance, if the particle is a cylinder, then the first Guinier region would return a radius while a second Guinier region would allow the estimation of a length. This  $R_g$  can be related to the cylinder length through:

$$R_g = \sqrt{\frac{L^2}{12} + \frac{R^2}{3}}. \tag{2.30}$$

An example of this scattering from a cylinder is shown in Figure 2.6.

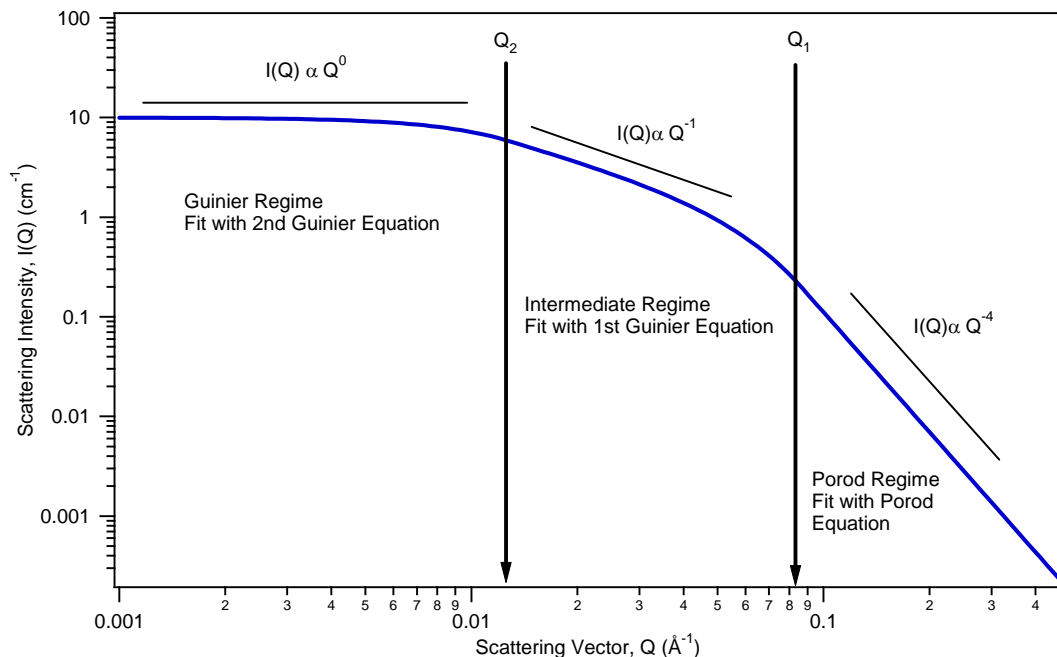


**Figure 2.6:** Sample scattering from a cylinder of  $R_{g2}$  of 100 Å and an  $R_{g1}$  of 20 Å. The three regions of the three-region Guinier-Porod fit are shown. Q-scaling exponents represent the Guinier dimensions in each region.

Other empirical models in which a shape for the scattering particle is assumed are available from NIST and are used to model scattering from specific structures.<sup>53</sup> These models use Equation (2.14), and so fits made with these models result in a great deal of information. Because these models return values for the scattering length densities, they can also determine the chemical compositions of volumes within a scattering body.

One such model is the hard sphere model. In this model, the form factor of hard spheres is described as:

$$P(Q) = \left\{ \frac{3[\sin(QR) - QR \cos(QR)]}{(QR)^3} \right\}^2, \quad (2.31)$$

where R is the radius of the scattering sphere. A Schulz polydispersity can also be included in this model. The model written by NIST averages  $P(Q)$  over the size

distribution of R and includes a volume fraction scaling factor. The model also accounts for background scattering and is normalized by an average volume,  $\langle V \rangle$ .

The polydispersity in the radius follows a Schulz distribution as:<sup>45, 53</sup>

$$f(R) = (z + 1)^{z+1} x^z \frac{\exp[-(z + 1)x]}{R_{\text{avg}} \Gamma(z + 1)}, \quad (2.32)$$

where

$$x = \frac{R}{R_{\text{avg}}},$$

$$z = \frac{1}{p^2} - 1, \quad (2.33)$$

$$p = \frac{\sigma}{R_{\text{av}}}, \text{ and}$$

$R_{\text{avg}}$  is the average radius.  $\sigma^2$  is the variance in the distribution.<sup>45, 47, 53</sup> Finally, substituting in Equation (2.14), the scattering intensity,  $I(Q)$  is described as:<sup>45, 47, 53</sup>

$$I(Q) = \left( \frac{N}{\langle V \rangle} \right) \Delta\rho^2 \int_0^\infty f(R) \left( \frac{4\pi}{3} R^3 \right)^2 \left[ \frac{3 \sin(QR) - QR \cos(QR)}{(QR)^3} \right]^2 dR. \quad (2.34)$$

A second model that presumes a particle shape, and so has a form factor within the model is the core-shell model. This model represents the core-corona structure of a micelle. A core shell particle is described as having two regions: the core of specific volume,  $v_{\text{core}}$ , and scattering length density  $\rho_{n,\text{core}}$ , and a shell of specific volume,  $v_{\text{shell}}$ , and scattering length density  $\rho_{n,\text{shell}}$  (Figure 2.7). The solvent has a scattering length density of  $\rho_{n,\text{solvent}}$ . The scattering cross section (for a dilute solution) is given by:<sup>45</sup>

$$\frac{\partial \Sigma}{\partial \Omega}(Q) = \frac{N}{V} \left[ \left( \rho_{n,\text{core}} - \rho_{n,\text{solvent}} \right) V_{\text{core}} \frac{3j(QR_{\text{core}})}{(QR_{\text{core}})} + \left( \rho_{n,\text{shell}} - \rho_{n,\text{solvent}} \right) \left( V_{\text{core+shell}} \frac{3j(QR_{\text{shell}})}{(QR_{\text{shell}})} - V_{\text{core}} \frac{3j(QR_{\text{core}})}{(QR_{\text{core}})} \right) \right]^2 \quad (2.35)$$

Here,  $V_{\text{core}}$  is the volume of the core which equals  $\left(\frac{4\pi}{3}\right)R_{\text{core}}^3$ , and  $V_{\text{core+shell}}$  is the volume of the shell which equals  $\left(\frac{4\pi}{3}\right)R_{\text{shell}}^3$ .  $V$  is the total solution volume and

$$j(QR_{\text{core}}) = \frac{\sin(QR_{\text{core}})}{(QR_{\text{core}})^2} - \frac{\cos(QR_{\text{core}})}{QR_{\text{core}}} \quad (2.36)$$

In future chapters, the thickness,  $T$ , of the shell will be used. This is equal to  $R_{\text{shell}} - R_{\text{core}}$ .

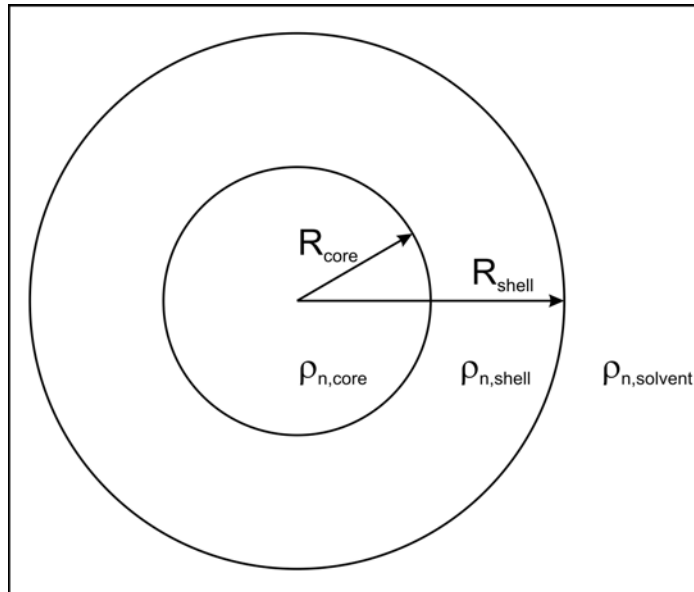


**Figure 2.7:** Representation of the core-shell model available from NIST.<sup>53</sup> The fit results in values for the core radius, shell radius, and scattering length densities of the core, shell, and surrounding solvent.

Similar core-shell models for oblate and cylindrical bodies are also available from NIST<sup>53, 54</sup> and have similar fitting parameters, just using the appropriate form

factors for those bodies. Different structure factors are used depending upon the particle shape. Particle interactions and polydispersity can also be included in these models.

In this work, polydispersity will be added to the core of these micelles, resulting in a “polydisperse core-shell model.” In this model,  $P(Q)$  is averaged over a Schulz distribution of the total radii ( $R_c+T$ ), and is normalized over the average particle volume,  $\langle V \rangle$ , in a manner similar to that discussed above for the Schulz sphere. The distribution is further discussed in the literature.<sup>53, 55</sup>

The form factor model of lyotropic lamellae with a polydisperse bilayer thickness<sup>53, 56</sup> is also used here. Again, the NIST model accounts for a scaling factor and background scattering in the calculated fit, where the fit is equal to  $scale \cdot I(Q) + B$ , and

$$I(Q) = \frac{2\pi P(Q)}{\delta Q^2}. \quad (2.37)$$

Here, the form factor,  $P(Q)$  is expressed by the equation:

$$P(Q) = \frac{2\Delta\rho^2}{Q^2} [1 - \cos(Q\delta) \exp(-Q^2\sigma^2/2)]. \quad (2.38)$$

The bilayer thickness is represented by  $\delta$ , and the polydispersity,  $p$ , in this thickness is  $\sigma/\delta$ , where  $\sigma$  is the variation in the thickness.

Finally, the model of a flexible cylinder with excluded volume will be used. This is also available from NIST.<sup>53</sup> Excluded volume is included in the model because two or more portions of the same micelle are not able to occupy the same space in the sample. The model is thoroughly described by Pedersen et al.,<sup>57</sup> with corrections provided by Chen et al.<sup>58</sup> A flexible cylinder, of total length,  $L$ , is modeled with a spherical cross-section, of radius  $R_{cs}$  (Figure 2.8).<sup>53</sup> A Schulz

distribution in the cross-sectional radius is also included. The scattering length density of the cylinder is constant over the entire assembly. The persistence length,  $l_p$ , is the length of cylinder than can be described as rigid. The Kuhn length,  $b=2l_p$ , is determined within the model. Finally, the NIST model written for Igor Pro (WaveMetrics)<sup>59</sup> also takes into account background scattering and includes a scaling factor.<sup>53</sup>

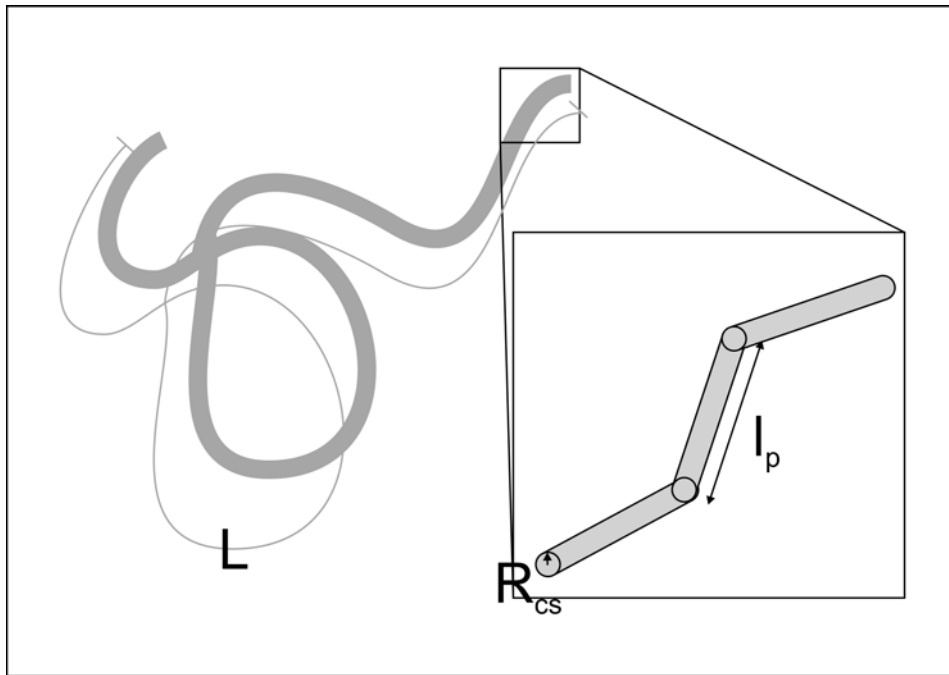


**Figure 2.8:** Representation of a flexible cylinder of contour length,  $L$ ; persistence length,  $l_p$ ; and cross-sectional radius,  $R_{cs}$ . The Kuhn length,  $b$ , is equal to  $2 \cdot l_p$ .

## Chapter 3: Polymer Systems and Characterization

### 3.1 Pluronic P85: $\text{PEO}_{26}\text{PPO}_{40}\text{PEO}_{26}$

The Pluronic P85,  $\text{PEO}_{26}\text{PPO}_{40}\text{PEO}_{26}$ , was acquired as a gift from BASF Chemical Company. The number of repeating units in each block can be calculated from information found in the copolymer name. The last number of the name, multiplied by 10, represents the weight percent of PEO in the copolymer.<sup>7</sup> For example, the name P85 indicates a copolymer with 50% PEO by weight. Using this value with the average molecular weight of the copolymer gives the repeat units of each block.

The average molecular weight of this copolymer is 4600 g/mol, as reported by BASF. Assuming that PEO accounts for 50% of the copolymer molecular weight, this copolymer has a total of approximately 52 PEO units and 40 PPO units, or  $\text{PEO}_{26}\text{-PPO}_{40}\text{-PEO}_{26}$ . This copolymer was used as received and no further characterization was performed.

### 3.2 Reverse Pluronic 17R4: $\text{PPO}_{14}\text{PEO}_{24}\text{PPO}_{14}$

Similar to Pluronics, the last number in the name of a Reverse Pluronic represents the weight percent of PEO in the copolymer.<sup>7</sup> Therefore, in 17R4, the PEO block is approximately 40% of the total copolymer molecular weight. BASF



reports that this copolymer has an average molecular weight of 2650 g/mol. With this information, the formula for 17R4 is PPO<sub>14</sub>-PEO<sub>24</sub>-PPO<sub>14</sub>.

Pluronic 17R4 was obtained as a gift from BASF Chemical Company (Batch Number: USXW93594). BASF analysis stated purity with a 0.09 wt% water content, but offered no indication of triblock, diblock, and monomer distribution within the sample. Size exclusion chromatography (SEC) data were provided by Polymer Source, Inc. These were determined in tetrahydrofuran (THF) at 35 °C.

Poly(ethylene glycol) standards were used for calibration. SEC results indicate a single peak, indicating the sample to be pure (Figure 3.1). Had other substances been present, such as PPO monomers or diblocks, multiple peaks would be observed from the SEC. The number average molecular weight was found to be 2670 g/mol, very close to that reported from BASF. The polydispersity in the sample was 1.06.

A <sup>1</sup>H-NMR in deuterated chloroform was also performed by Polymer Source, Inc. From this analysis (Figure 3.2), it was determined that the PEO:PPO block ration was 0.98, indicating there are slightly fewer PEO blocks than PPO in the copolymer. Also important, the copolymer contains approximately 5% unsaturated end groups, as opposed to the hydroxy groups expected at the termini of the molecules (Figure 3.3).<sup>60</sup>

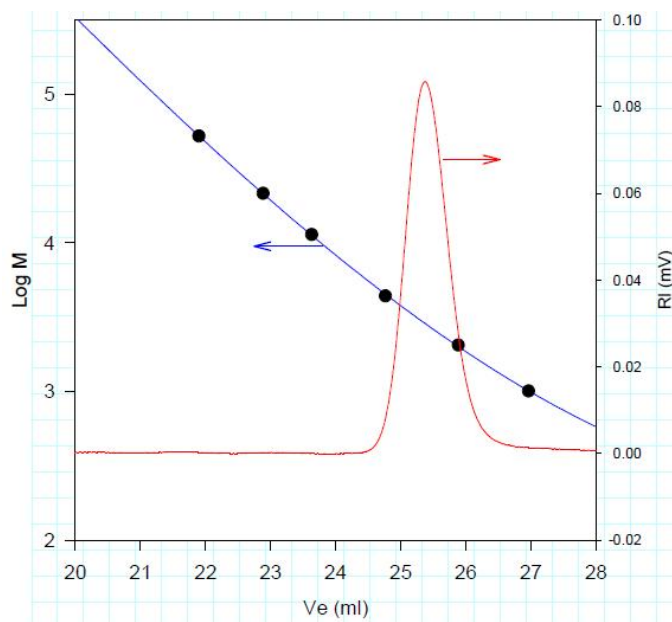


**Figure 3.1:** Size exclusion chromatography profile of 17R4. The profile determines the molecular weight and polydispersity of the copolymer. The calibration curve is shown by black data points and the SEC profile is shown in red. Performed by Polymer Source, Inc.

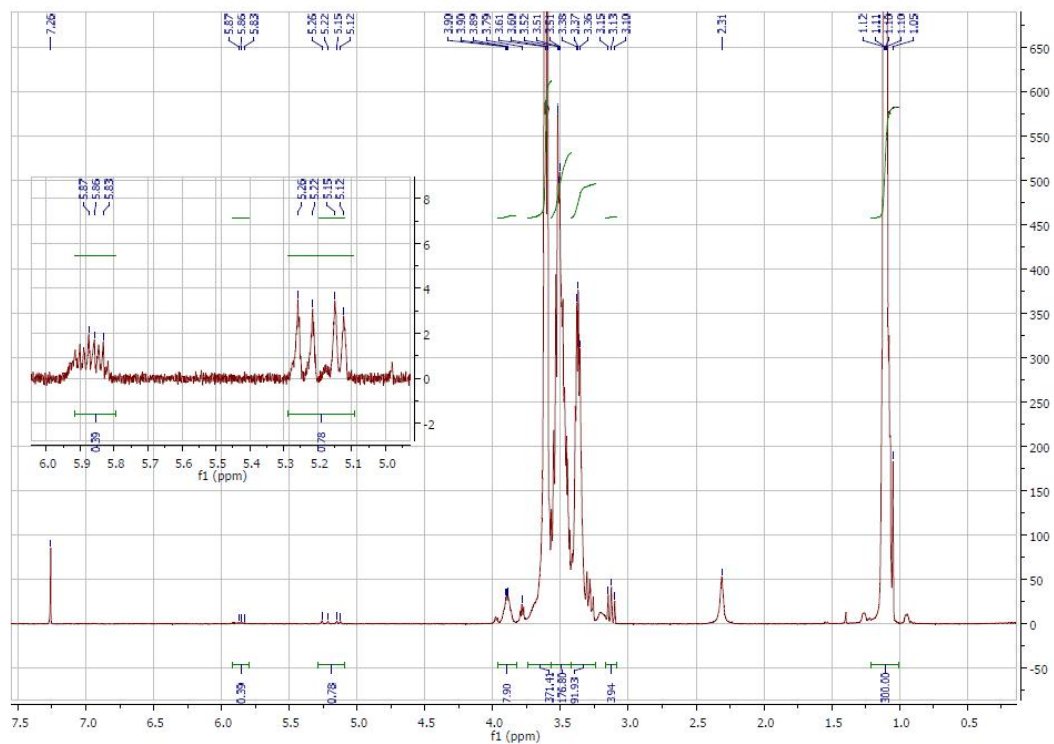
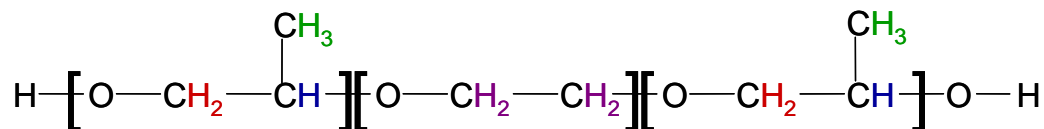


**Figure 3.2:**  $^1\text{H-NMR}$  of 17R4 in deuterated chloroform. For proton clarification see Figure 3.3.



PPO Protons:

$\text{H}_2$ : 3.50 ppm

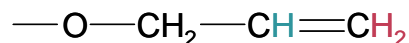
$\text{H}$ : 3.35 ppm

$\text{H}_3$ : 1.10 ppm

PEO Protons:

$\text{H}_2$ : 3.60 ppm

Unsaturated Termini:



$\text{H}_2$ : 5.1-5.3 ppm

$\text{H}$ : 5.8-5.9 ppm

**Figure 3.3:** 17R4 protons for  $^1\text{H}$ -NMR. Chemical shifts for each proton are indicated. Also, the hydroxy and unsaturated end groups are shown. Adapted from Zhang.<sup>60</sup>

### 3.3 Polybutadiene-Poly(ethylene oxide): PB<sub>89</sub>PEO<sub>132</sub>

Polybutadiene- poly(ethylene oxide) (Sample Number: P4603-BdEO) was purchased from Polymer Source, Inc. The  $^1\text{H}$ -NMR spectrum of the copolymer (Figure 3.4) provided by the manufacturer shows the ratio between PEO protons and vinylic PB protons to be roughly 3:1. This corresponds to a 1½:1 block ratio. Size exclusion chromatography (SEC) analysis, also provided by the manufacturer (Figure 3.5), determined the copolymer to have a PB block of molecular weight 4800 g/mol and a PEO block of molecular weight 5800 g/mol. This suggests that there are 89 repeating units of PB and 132 units of PEO in the copolymer. This agrees with the ~1½:1 block ratio determined by  $^1\text{H}$ -NMR. SEC results also indicated that the copolymer has a polydispersity of 1.04.

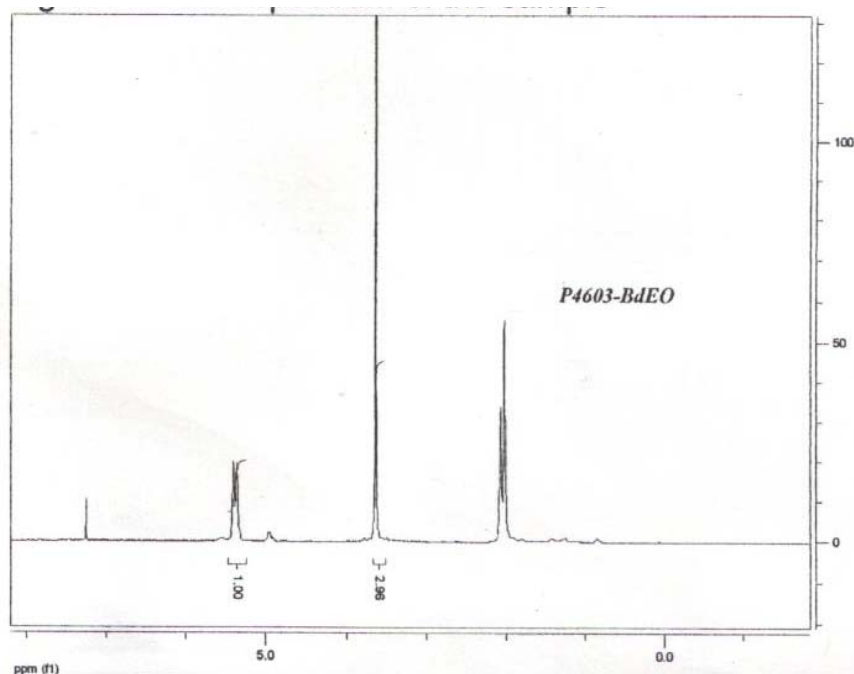


**Figure 3.4:**  $^1\text{H}$ -NMR spectrum of polybutadiene-*b*-poly(ethylene oxide), as provided by the manufacturer, Polymer Source, Inc. Ethylene oxide protons are indicated around 3.6 ppm, while vinylic butadiene protons are indicated around 5.4 ppm. The ratio between these proton signals indicate a 3:1 ratio of protons in the sample.

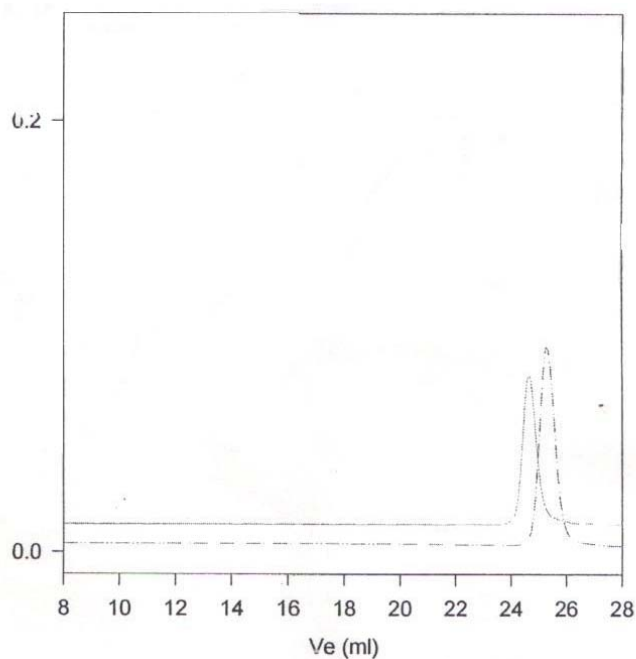


**Figure 3.5:** Size exclusion chromatography profile of the polybutadiene polymer (dashed line) and the block copolymer (solid line). Analysis of the single polymer determines the molecular weight of that block to be  $M_n=4800$ . Analysis of the diblock copolymer determines that the copolymer has a polydispersity of 1.04.

The following chapter is reproduced in part with permission from: Clover, B.; Hammouda, B. *Langmuir* **2009**. Copyright 2009 American Chemical Society. The introduction and SANS data analysis sections have been adjusted for better flow within this dissertation. Formatting has also been modified to fit that required from the Graduate School at the University of Maryland. All other sections and figures are quoted directly from the article.

## Chapter 4: Aqueous Pluronic System under Pressure

Self-aggregation in triblock copolymers is now addressed. Pluronics (those copolymers formed in the PEO-PPO-PEO fashion) have found important uses in the industrial and medicinal fields. A full understanding of their micellization behaviors in aqueous solutions is necessary for the full development of these functions.

### 4.1 Introduction

The behavior of Pluronics in aqueous solutions has been shown to depend on block architecture as well as temperature and pressure.<sup>61, 62</sup> The dependence on these thermodynamic properties is our main focus here. When these parameters are varied, Pluronics self-associate into a multitude of structures such as spherical, cylindrical, and lamellar micelles, as well as micellar crystals. Few studies, however, have examined the pressure effects on the phase behavior of Pluronics in aqueous solution, as most have examined either architecture or temperature effects.

A review of the effect of pressure on phases in lipid and surfactant solutions has been presented by Winter.<sup>63</sup> Most of the current literature examines the phase transitions between multiple lamellar or gel phases. Few studies have examined transitions between micelle-forming microstructures. A high pressure small-angle neutron scattering (SANS) study on an amphiphilic surfactant (pentaethylene glycol monoethyl ether,  $\text{CH}_3(\text{CH}_2)_7(\text{OCH}_2\text{CH}_2)_5\text{OH}$ ) showed that the radius of gyration of

spherical micelles in solution decreases between ambient pressure and 150 MPa.<sup>64</sup> It was also shown that the hydrophobic core radius increases slightly with pressure, while the hydrophilic shell becomes dehydrated and its radius decreases. In a Nuclear Magnetic Resonance (<sup>1</sup>H-NMR) study on the same surfactant, the critical micelle concentration (CMC) was examined as a function of pressure.<sup>65</sup> Up to a pressure of 150 MPa, the CMC was shown to decrease with increasing pressure, while above this pressure CMC values were shown to increase. In aqueous surfactant solutions, CMC and CMT (critical micelle temperature) values vary in opposite directions.

Recent literature searches found few pressure studies on the phase diagrams of aqueous Pluronic solutions, with a limited number on nonionic aqueous surfactants.<sup>66</sup> <sup>67</sup> Both Kostko et al.<sup>66</sup> and Mortensen et al.<sup>68</sup> examined concentrated ( $\geq 20$  wt %) aqueous Pluronic solutions. Through dynamic light studies, Kostko et al.<sup>66</sup> examined the Pluronic F108 (PEO<sub>141</sub>PPO<sub>44</sub>PEO<sub>141</sub>) and found that temperature boundaries between unimers, micelles, and clustered micelles increase with pressure. Mortensen et al.<sup>68</sup> examined Pluronic F88 (PEO<sub>96</sub> PPO<sub>39</sub> PEO<sub>96</sub>) by small-angle neutron scattering (SANS). It was observed that increasing pressure causes micelle decomposition and melting of micellar crystals. They observed that pressure enhances the solvent quality of water, thereby shifting the CMC downward.

The temperature and volume fraction dependencies of Pluronic P85 (PEO<sub>26</sub> PPO<sub>40</sub> PEO<sub>26</sub>) have been studied extensively by Mortensen<sup>68, 69</sup> and Hammouda.<sup>45</sup> SANS measurements done at ambient pressure have elucidated the volume fraction-temperature phase diagram for P85 in deuterated water (D<sub>2</sub>O). At low temperature and volume fraction, solvated unimers (dissolved copolymer chains) make up the

solution. Neutron scattering from these unimers displays clustering at low-Q values, as well as chain solvation at high-Q. Clustering at low-Q has been observed in many water-soluble systems including polypeptide chains, polyelectrolyte solutions, as well as PEO in D<sub>2</sub>O solution. At relatively low volume fraction ( $\phi < 10\%$ ), as temperature is increased, copolymers transition from unimers to spherical micelles at the CMC. These micelles then elongate into cylindrical (or rod-like) micelles, and finally lamellar micelles are formed.<sup>45, 67, 69, 70</sup> Higher order (micellar crystal) phases have also been observed at higher volume fractions.<sup>67, 69, 70</sup>

In this study, we use SANS with in-situ pressure to examine the pressure dependence of phase transitions in P85. This is important to understand the full phase diagram and develop further uses for these copolymers.

## 4.2 Experimental details

### 4.2.1 Materials

Pluronic P85 was obtained from BASF Corp., and was used as received. The average molecular weight of the copolymer is 4600 g/mol, as reported by the manufacturer. The copolymer has an average composition of PEO<sub>26</sub>PPO<sub>40</sub>PEO<sub>26</sub>.

### 4.2.2 Solution preparation

Deuterium oxide, D<sub>2</sub>O, (99.9 % D, from Cambridge Isotope Labs) was used as solvent in order to increase the scattering contrast and lower the incoherent scattering



background in SANS experiments. All scattering experiments were performed on a 0.5 % (w/w) P85/D<sub>2</sub>O solution. The sample fraction was kept low to avoid interparticle (either interchain or intermicelle) interaction effects. Such structure factor effects have been shown to appear at volume fractions as low as 4 % (at approximately 43 °C).<sup>67</sup>

#### 4.2.3 SANS experimental

The SANS technique under high pressure was used to examine the phase transitions of the aqueous P85 solution. SANS measurements were made at the National Institute of Standards and Technology Center for Neutron Research (NCNR), on the NG3-SANS instrument. Sample-to-detector distances of 2 m and 12 m were used with a 6 Å neutron wavelength.

The SANS in-situ pressure cell uses two sapphire windows separated by a 1 mm gap in which the polymer solution is contained. The entire hydrostatic pressure pump and pressure cell were filled with the sample solution. Scattering measurements were taken at every 5 °C between 25 °C and 125 °C ( $\pm 0.3$  °C), and at four different pressures: near 400 psi, 13000 psi, 26000 psi, and 39000 psi (corresponding to approximately 3 MPa, 90 MPa, 180 MPa, and 270 MPa, respectively). The lowest pressure of 2.76 MPa was chosen to allow measurements at temperatures above the boiling point of water.

#### 4.2.4 SANS analysis

The two-region Guinier-Porod model<sup>51</sup> was used to evaluate scattering P85/D<sub>2</sub>O solutions under pressure. Recall from Chapter 2, this model fits over two regions, as:

$$I(Q) = \frac{G}{Q^n} \exp\left(\frac{-Q^2 R_g^2}{3-n}\right) \text{ for } Q \leq Q_1, \quad (2.25)$$

and

$$I(Q) = \frac{D}{Q^m} \text{ for } Q \geq Q_1, \quad (2.26)$$

where

$$Q_1 = \frac{1}{R_g} \sqrt{\frac{(m-n)(3-n)}{2}}. \quad (2.27)$$

The Q-range of 0.008-0.076 Å<sup>-1</sup> was used for all fits in order to avoid clustering at low-Q in low temperature data and to avoid background scattering at high-Q. The appearance of a Bragg peak in the scattering data at high temperatures prohibited the use of this model. The emergence of this peak in the data was taken to signify the transition into a new phase. Scattering in this new phase was not fitted with a model.

### 4.3 Results and discussion

SANS data were taken from 0.5 % P85 in D<sub>2</sub>O as a function of both pressure and temperature, and both micelle formation and copolymer demixing were observed. At low temperatures, scattering from unimers in solution was observed, including high intensity scattering at low-Q, known as clustering. At high-Q, a low intensity

unimer signal was observed. The Porod exponent of the solvated unimer chains of 1 implies that unimers are stretched chains as they do not display the  $1/Q^2$  behavior typical of Gaussian coils.

As temperature is increased, unimers self-associate to form spherical micelles, displaying the typical  $1/Q^4$  behavior at high-Q and a flat low-Q signal. Upon further heating, the spherical micelles elongate into cylindrical micelles with  $1/Q$  behavior at low-Q. Scattering typical of lamellae,  $1/Q^2$  at low-Q, was seen at even higher temperatures (at 3 MPa and 90 MPa, for example). Each of these phases was previously observed at ambient pressure.<sup>45,69</sup> In a 1% solution at ambient pressure, spherical micelles form just above 30 °C, cylindrical micelles form above 60 °C, and lamellae form above 80 °C.

At temperatures above 95 °C, a Bragg peak forms at high-Q, typical of inter-lamellar spacing. This phase is referred to as demixed lamellae. The lamellar micelles phase corresponds to uniformly distributed lamellae throughout the sample, while in this new phase, lamellae are tightly stacked, thereby forming pockets of solvent. The term “demixed lamellae” is preferred to “vesicles” since vesicles connote a spherical onion-skin structure while it is not clear whether the newly observed structures are spherical. It should be noted that electron microscopy could not be performed at these high temperatures to verify the structures. The demixed lamellae phase is formed when the PEO outer blocks demix close to their cloud point temperature.<sup>71</sup> Sample scattering data of each phase are displayed in Figure 4.1.

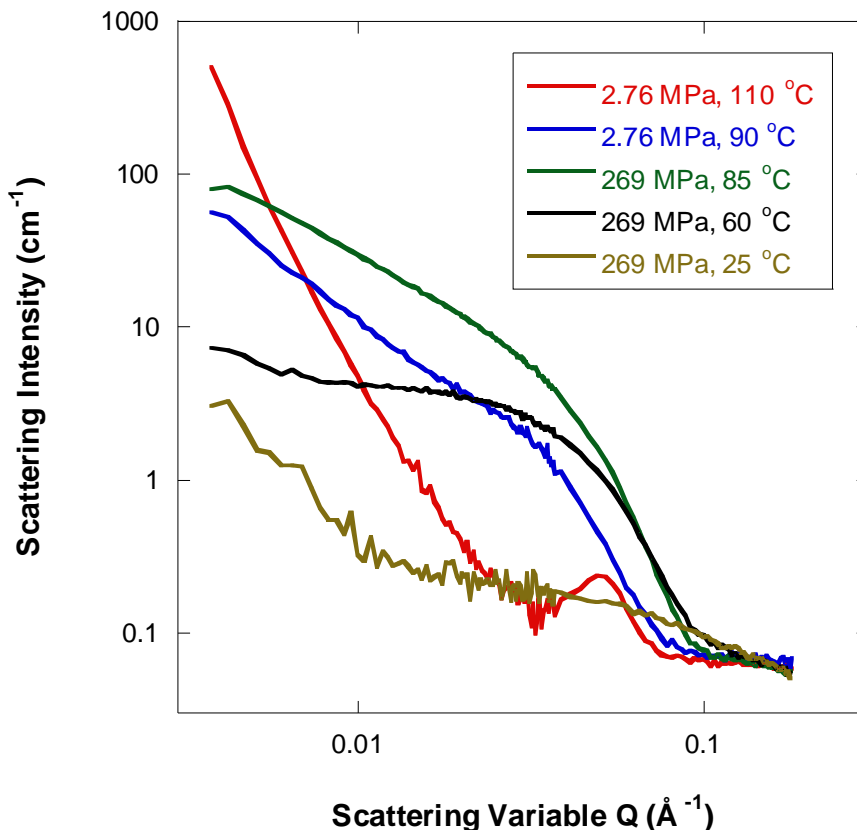


**Figure 4.1:** Scattering data from 0.5 % P85/ D<sub>2</sub>O solution at various pressure and temperature conditions. The 2.76 MPa, 110 °C data depicts a demixed lamellae structure, while the 2.76 MPa, 90 °C data represents lamellar micelles. Cylindrical micelles correspond to the 269 MPa, 85 °C data. The 269 MPa, 60 °C and 25 °C data correspond to spherical micelles and unimers in solution, respectively.

With increased pressure, the transition temperature between micellar phases increases. For example, at 65 °C, cylindrical micelles are present only at low pressures, while at high pressures, spherical micelles still exist (Figure 4.2). Note that at intermediate pressures, although the micelles are primarily spherical, both the scattering intensity and Porod exponents increase slightly. This indicates that the spheres are elongating and transitioning to cylindrical morphologies. The various observed structures (unimers, spherical micelles, cylindrical micelles, lamellar micelles, and demixed lamellae) are shown schematically in Figure 4.3.

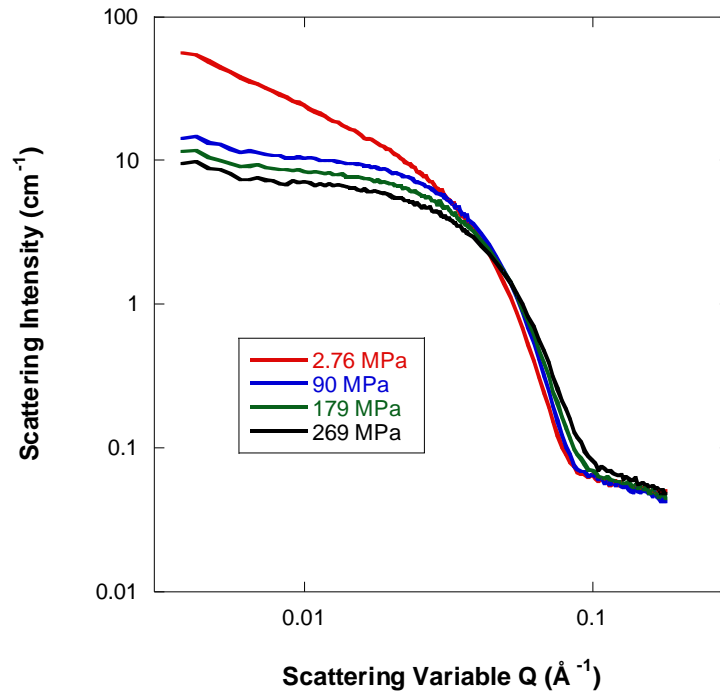


**Figure 4.2:** SANS scattering for 0.5 % P85/ D<sub>2</sub>O solution at fixed temperature of 65 °C and varying pressure. Cylindrical micelles are present at the lowest pressure, while spherical micelles remain in solution at high pressures.

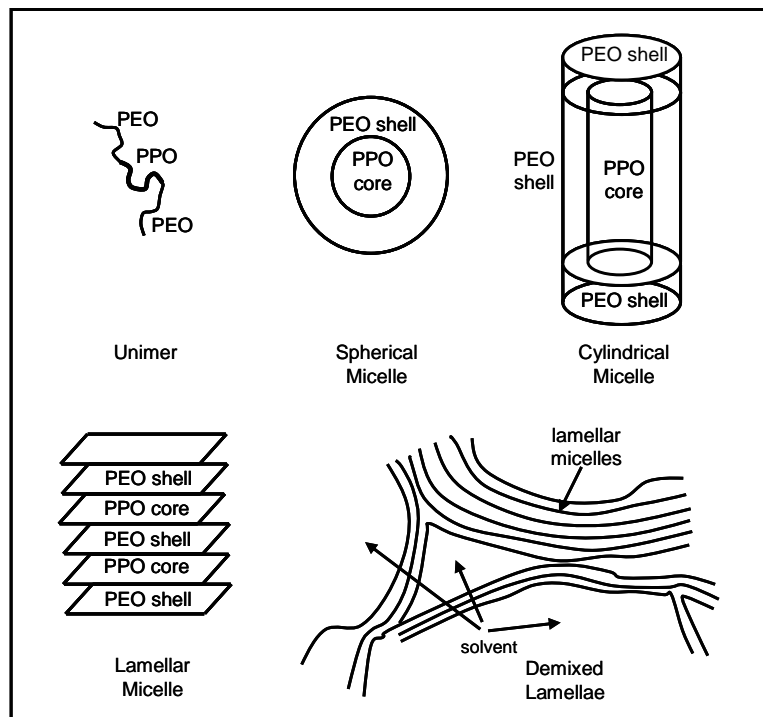


**Figure 4.3:** Schematic representation showing the observed structures.

The specific transition temperatures between the copolymer micellar phases can be determined by monitoring the low-Q Guinier factor (Equation (2.25)) at a low Q value of  $0.004 \text{ \AA}^{-1}$ . In this way, phase transitions can be monitored. For example, the Guinier factor for unimers has a lower scattering intensity than that of spherical micelles, which, in turn, is less than that of cylindrical micelles.

Plotting this Guinier factor as a function of temperature, the transitions between copolymer morphologies are clear. The sigmoid shape of the Guinier factor between copolymer morphologies characterizes the transition temperatures between phases. This temperature is the mid-point between relative intensity plateaus. By determining these transition temperatures, the phase transition lines can be drawn for the system. The sigmoid shape of the Guinier factor is seen in Figure 4.4 for the measured pressures. Note that the empirical Guinier-Porod model is not appropriate to fit the (high temperature) demixed lamellae phase since a Bragg peak shows up.

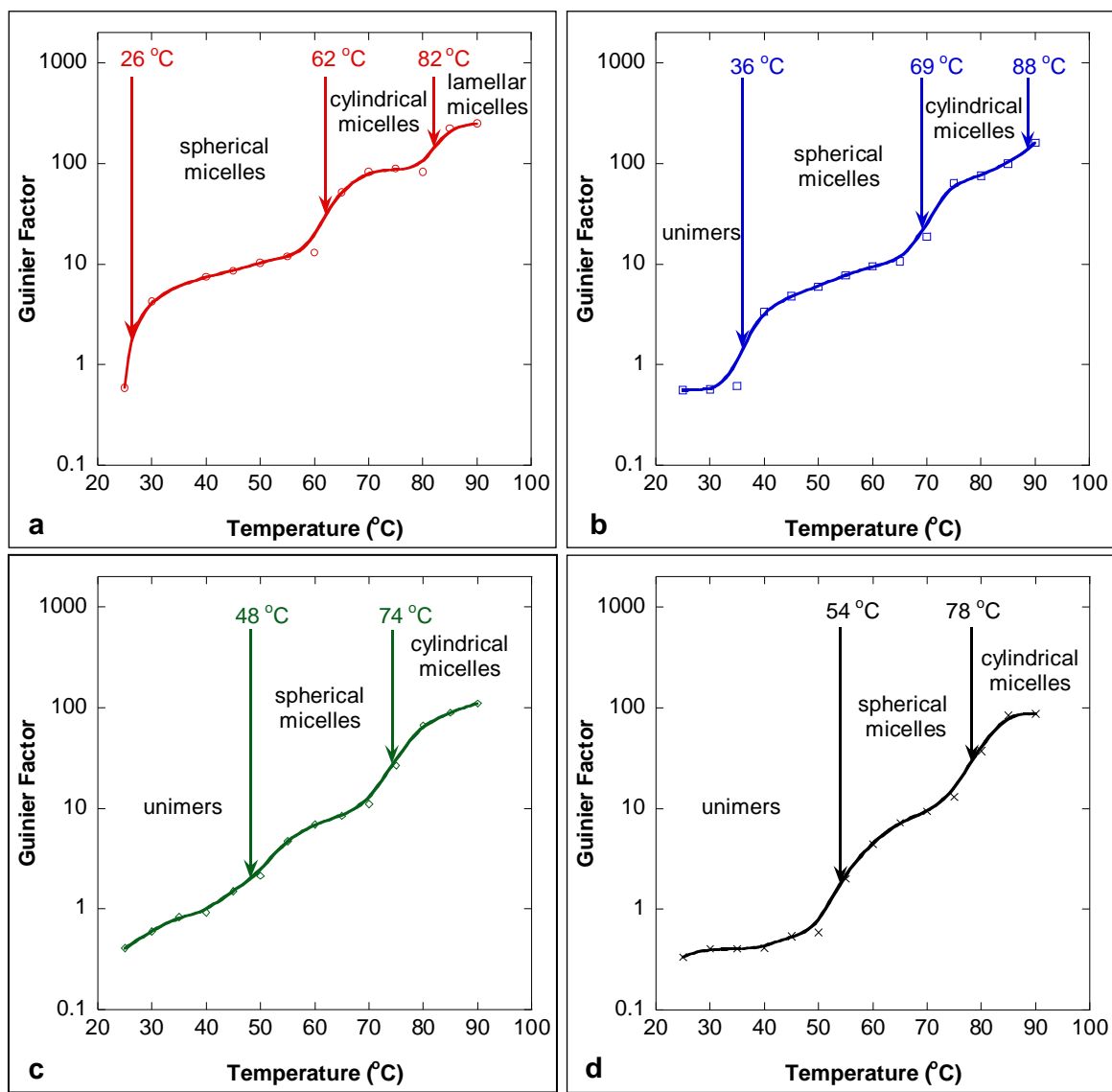


**Figure 4.4:** Variation of the Guinier factor with increasing temperature for 0.5 % P85/ D<sub>2</sub>O at the following pressures (a) 2.76 MPa, (b) 90 MPa, (c) 179 MPa, and (d) 269 MPa. Transition temperatures between unimers, spherical micelles, cylindrical micelles, and lamellar micelles are indicated.

Figure 4.5 shows the pressure effect on the phase transition lines. Transition temperatures between micelle morphologies were determined by the sigmoid method shown in Figure 4.4. The demixed micelle transition was determined, instead, by the appearance of the Bragg peak in the scattering intensity data. Increased pressure is shown to shift micellar transition phase boundaries to higher temperatures. However,

increasing pressure lowers the demixed lamella phase boundary as shown in Figure 4.5. The pressure effect on phase boundary lines is substantial. For example, the unimers-to-spherical micelles transition increases by as much as 11 °C per kBar (note that 1 kBar = 101 MPa).

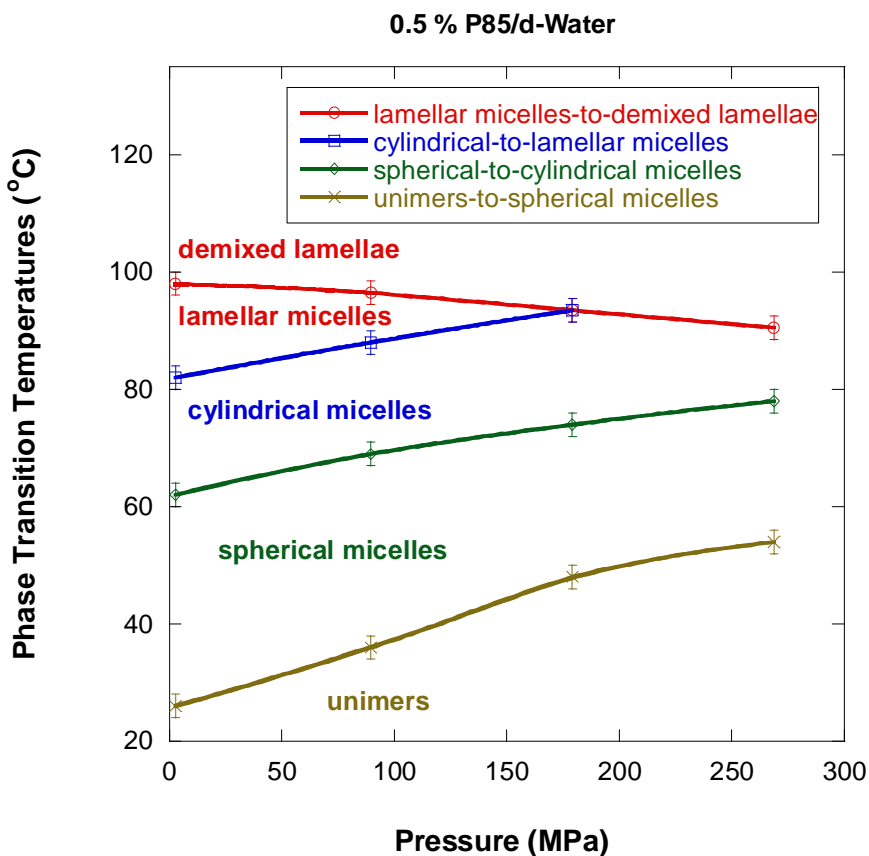


**Figure 4.5:** Effect of pressure on the phase boundary lines. Transitions between micelle morphologies were determined through the sigmoid variation of the Guinier factor, while the formation of the demixed micelle phase was determined by the appearance of the Bragg scattering peak. Statistical error bars correspond to one standard deviation.

The increase of micellar phase transition boundaries with pressure can be thought of as a *copolymer* effect in that the pressure affects aggregation. Increasing pressure is equivalent to decreasing temperature. As discussed earlier, this is seen at 65 °C in the formation of cylindrical micelles at low pressures, while spherical



micelles remain at high pressures (Figure 4.2). This leads to an increase of the transition temperature with pressure. This result is similar to the trends observed by Mortensen et al.<sup>68</sup> who focused on micellar crystals at a narrower temperature (20 °C to 50 °C) and pressure (less than 1 kBar) window.

The decrease of the demixed lamellae phase boundary with pressure can be understood as a *polymer solution* effect in that the pressure affects phase separation. This result is reminiscent of the effect of pressure on PEO/water solutions. PEO in water has been shown to phase separate upon heating, that is, it has a lower critical solution temperature (LCST). Hammouda et al.<sup>71</sup> showed that pressure reduces the LCST of PEO/water solutions. It was argued that hydrogen bonds between the PEO polymer and solvent break at increased pressures, causing the polymer to demix from solution.

#### 4.4 Summary and conclusions

The SANS characterization method has been used to investigate the various phase transitions in 0.5 % P85 in D<sub>2</sub>O. Transitions from a unimers phase to a series of micellar phases (spherical, cylindrical, and lamellar) were observed. In-situ hydrostatic pressure was found to increase the temperature of the boundary lines between these micellar transitions. Another high-temperature phase referred to as the demixed lamellae phase was observed; its boundary line was found to decrease in temperature with increasing pressure. The inter-micelle transition lines are understood as a copolymer effect, while the demixed lamellae phase is understood as a polymer solution effect.

## Chapter 5: Reverse Pluronic Triblock in Aqueous Solvent

As discussed in Chapter 1, Reverse Pluronics have a central block of hydrophilic PEO, surrounded by hydrophobic PPO. This leads to interesting and different characteristics in aqueous solutions compared to traditional Pluronics.

### 5.1 Introductory background

Early reports of triblock copolymers in solvents selective for the central block did not focus on PEO and PPO copolymers; however, the findings of that research should not be ignored here. Some of the first studies into the micellization of such block copolymers were presented by Tanaka, Kotaka, and Inagaki in 1972.<sup>72, 73</sup> In these experiments, the triblock poly(methyl methacrylate)-polystyrene-poly(methyl methacrylate) was studied in xylene, a solvent miscible only with polystyrene. Micellization was not observed to occur in this solvent. It was suggested that micellization did not occur because the center block formed a shield around the end blocks, prohibiting any further association with the end blocks of other molecules in solution. Such a formation is shown in Figure 5.1a.

In 1987, the thermodynamic favorability of these copolymers to form flower-like micelles was questioned by theoretical calculations. Hadziioannou and ten Brinke<sup>74</sup> concluded that such morphologies would not occur due to the reduction in

entropy caused by the looping of the copolymer strands to form the flower-like micelles (Figure 5.1b).

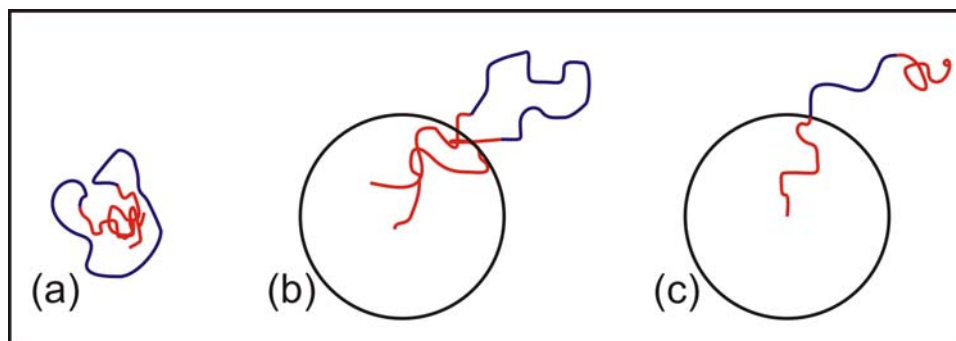


**Figure 5.1:** Schematic representations of a (a) shielded unimer strand suggested by Kotaka et al.<sup>72</sup> and (b) unimer looping necessary for micellization suggested by ten Brinke and Hadziioannou.<sup>74</sup> Hydrophobic blocks are presented in red, while the blue represents the hydrophilic central block. (c) A micelle with free end blocks, modeled by Balsara et al.,<sup>75</sup> is also depicted.

A different copolymer, poly(vinyl propylene)-polystyrene-poly(vinyl propylene) (PVP-PS-PVP), was researched by Tang et al. in the PS-selective solvent, toluene.<sup>76</sup> Again, no micellization was observed. Balsara et al.<sup>75</sup> also examined this system and found that micellization did occur at concentrations higher than those considered by Tang et al. It was also observed that the molecular weight of the central block must be comparable to that of the end blocks for micellization to occur. Balsara et al. also questioned the reliability of the entropy calculations presented by ten Brinke and Hadziioannou.<sup>75</sup> They presented theoretical calculations that suggested ten Brinke and Hadziioannou overestimated the entropic reduction caused by the looping of the copolymer chain, and that this entropic barrier could be surpassed. Balsara et al. modeled the free energies associated with two micelle formations, the flower-like micelle and a micelle in which end blocks are allowed to

be free and poorly-solvated in solution (Figure 5.1c).<sup>75</sup> The flower-like micelle was shown to be more probable thermodynamically.

From these experimental studies and theoretical calculations, it is clear that micellization of these triblocks is difficult to predict. Micellization depends greatly on the copolymer chain architecture. Such results are echoed in studies on Pluronic-R triblocks. The Reverse Pluronics labeled “25R” have been the most-studied Pluronic-R’s in the literature. In 2004, D’Errico et al.<sup>77</sup> presented the phase diagrams of 25R4 and 25R2, PPO<sub>19</sub>PEO<sub>33</sub>PPO<sub>19</sub> and PPO<sub>21</sub>PEO<sub>14</sub>PPO<sub>21</sub>, respectively. These diagrams were determined through visual inspection, using sample phase separation and birefringence. Based upon the Pluronic naming system, 25R2 consists of 20% PEO by weight, while 25R4 consists of 40% PEO.<sup>7</sup> The differences between these copolymers in weight fraction and molecular weight of the central PEO block were shown to lead to variant phase behaviors in water, as shown in the phase diagrams in Figure 5.2.

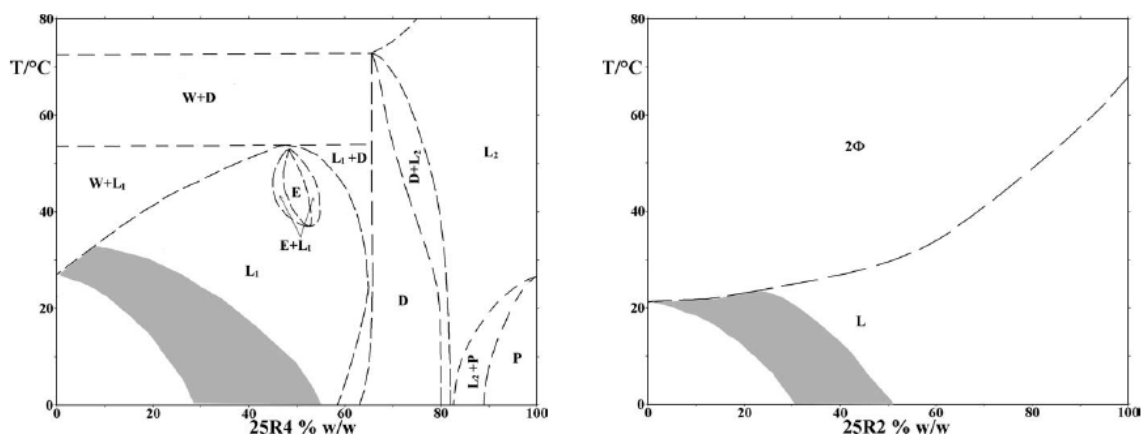


**Figure 5.2:** Phase diagrams of 25R4 and 25R2 from D’Errico et al.<sup>77</sup> The 25R4 phase contains water-rich solution ( $L_1$ ), water (W), hexagonal liquid crystal (D), lamellar liquid crystal (E), polymer-rich solution ( $L_2$ ), and paste (P) phases. 25R2 has an isotropic solution phase (L), and a two-phase ( $2\Phi$ ) region. Turbid solution areas are represented by the grey regions in each diagram.

The phase diagram of 24R4 is much more complex than that of 25R2. The appearance of birefringent concentration-temperature regions was observed in the 25R4 sample, but not in the 25R2 solutions. This birefringence was shown to be caused by a lyotropic crystalline phase (such as lamellae). Liquid phases without birefringence were observed in both copolymer solutions. Both samples also displayed a cloud-point line, above which samples separated into two-phase systems. The liquid phases of both solutions displayed a region of cloudiness. This clouding was said to indicate “anomalous micellization,”<sup>77</sup> and will be addressed later.

Through NMR self-diffusion measurements performed on 25R4, unimers (with a radius of 22 Å) were proposed to exist in a low temperature/low concentration region, which occurs below the turbid region.<sup>77</sup> Within the turbid region, diffusion coefficient values suggested copolymer chains were aggregating in solution. Finally, in concentrated solutions beyond the cloudy region, it was suggested that interconnected micelles existed. No spherical micelles were observed to form in these systems and no CMC was detected between the unimer and interconnected micelle regions.<sup>77</sup>

25R8, a reverse Pluronic with a very large central block, PPO<sub>15</sub>PEO<sub>156</sub>PPO<sub>15</sub>, was studied in D<sub>2</sub>O through SANS and DLS techniques by Mortensen et al.<sup>78</sup> Scattering data were taken over a wide range of copolymer concentrations and temperatures, allowing the depiction of the phase diagram of this copolymer (Figure 5.3). Mortensen et al. observed a phase of unimers in solution at low temperatures and concentrations. The unimers were determined to have a radius of gyration of ~37 Å. A region of solutions displaying high-intensity, low-Q SANS scattering was also

observed. Interestingly, this region also appeared turbid to the eye. It was suggested that this region contained a large network in which PPO blocks aggregated and PEO blocks remained solvated in solution, as they were in the unimer regions. These agglomerations were described as “inhomogeneous polydisperse suspension of randomly cross-linked networks.”<sup>78</sup> This and other definitions in the article imply that this is meant as one large network of cross-linked clusters.

Beyond this random network region, a correlation peak formed within the SANS data, suggesting the formation of a micellar network, where micelles with a core radius of gyration of  $\sim 40 \text{ \AA}$  were interconnected through PEO blocks in solution. Between these two regions, both the low-Q scattering and correlation peak existed simultaneously. Low-Q scattering from the random network decreased slowly to leave finally only the correlation peak of the micellar network. Crystallized micelles and lamellar regions were also observed at higher temperatures. No sharp transition into or out of the random network occurred. The authors make no observation of a distinct CMT for these copolymer solutions. It might be assumed that the CMT occurs before the onset of the correlation peak in the SANS data.

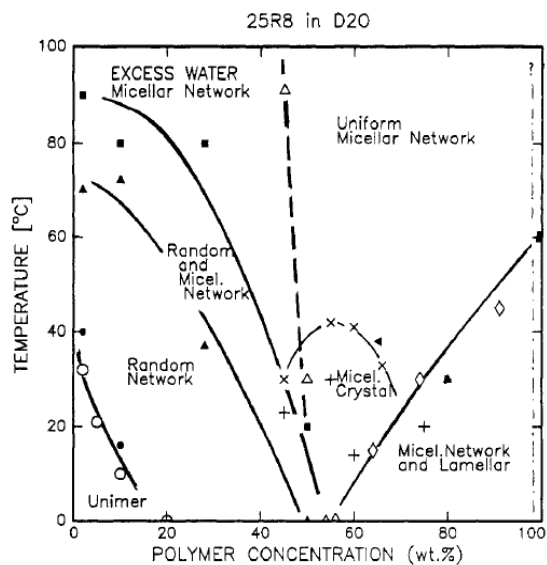


**Figure 5.3:** The phase diagram determined by Mortensen et al. for aqueous 25R8.<sup>78</sup> Neutron scattering, light scattering, and rheology measurements were used to determine boundaries, and are represented by filled symbols, open symbols, and crosses, respectively.

In an important work from 1997, Altinok et al.<sup>79</sup> examined copolymer block architecture and its affect on micelle formation, using the triblock PPO<sub>19</sub>PEO<sub>113</sub>PPO<sub>19</sub>. Unlike most studies done on Reverse Pluronic, the copolymer used was synthesized and purified prior to studies of micelle formation in aqueous solutions. The phase diagram of this copolymer in water is shown in Figure 5.4.

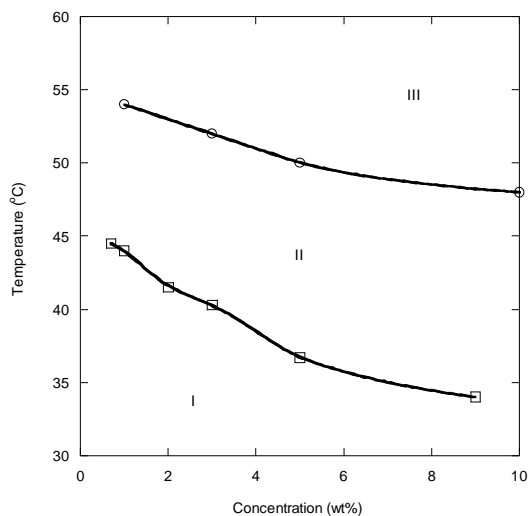


**Figure 5.4:** The phase diagram of PPO<sub>19</sub>PEO<sub>113</sub>PPO<sub>19</sub> in water, adapted from Altinok et al.<sup>79</sup> Squares represent clouding temperatures, while circles represent CMT values determined by SLS techniques. The clear unimer (I), micelle (II), and cloudy, linked micelle (III) regions are depicted.

Low concentration (1-10 wt %) solutions were observed to become cloudy as solutions were heated.<sup>79</sup> This effect was explained as micellar linking. DLS techniques were used on similar concentrations, at temperatures below solution clouding. Through this technique, the hydrodynamic radii of unimers and micelles were estimated to be 30-50 Å and 150-300 Å, respectively. The diffusion coefficients of PPO<sub>19</sub>PEO<sub>113</sub>PPO<sub>19</sub> solutions were shown to be inversely related to solution concentration. This indicated an attraction between micelles, suggesting linked micelles.

CMT values for low concentration solutions were determined through static light scattering techniques (SLS).<sup>79</sup> These CMT values occurred at much lower temperatures (~5-10 °C) than those at which clouding was initially observed. This, with DLS results, indicates that the cloudy solutions are a result of micelle linking.<sup>79</sup> This differs from results seen by Mortensen et al., in which unimers were observed to



link (and solutions became cloudy) before micellization occurred.<sup>78</sup> With these CMT values, Altinok et al. estimated a CMC value of 80 g/L at 40 °C, and this value was used to calculate thermodynamic properties of aqueous solutions of this copolymer.<sup>79</sup>  $\Delta H_{mic}^{\circ}$  and  $T\Delta S_{mic}^{\circ}$  values were shown to be similar to PEO-PPO-PEO copolymers, with  $\Delta H_{mic}^{\circ} = 193 \pm 20$  KJ/mol unimers and  $T\Delta S_{mic}^{\circ} = 208 \pm 20$  kJ/mol unimers. For such calculations, the standard states are “ideally-dilute solutions” of unimers and micelles.<sup>79</sup>

The only work found on the micellization of a reverse Pluronic outside the 25R series is the 1994 work by Zhou and Chu on Pluronic-R 17R4, PPO<sub>14</sub>PEO<sub>24</sub>PPO<sub>14</sub>.<sup>80</sup> The phase diagram of this copolymer in water is displayed in Figure 5.5.

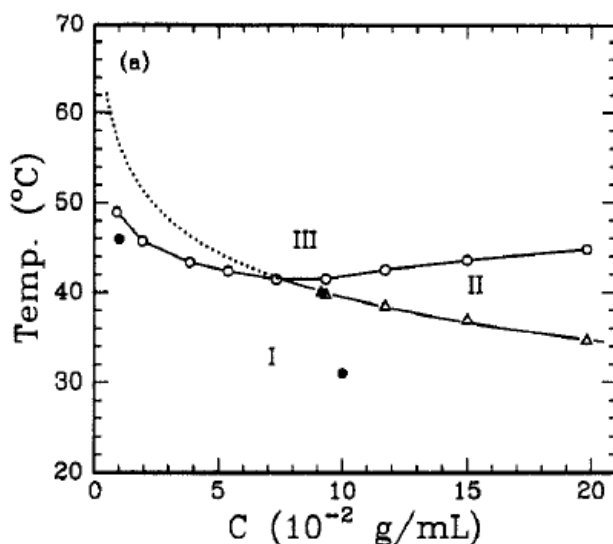


**Figure 5.5:** Phase diagram of 17R4 in H<sub>2</sub>O, as determined by Zhou and Chu using cloud point (open circles) and CMC/CMT measurements (filled/open triangles, respectively). The unimer (I), micelle (II), and two-phase (III) regions are shown. Figure reproduced from Zhou and Chu, *Macromolecules* **1994**.<sup>80</sup>

A “strong opalescent appearance” was observed in solutions near the micellization temperatures.<sup>80</sup> The authors claimed this was due to “anomalous micellization.” Originally described by Zhou and Chu when observing other Pluronic systems,<sup>80-82</sup> “anomalous micellization” is due to “composition heterogeneity of the block copolymer” and other hydrophobic impurities, such as PPO homopolymers.<sup>82</sup> It is suggested that copolymers with larger hydrophobic blocks phase separate prior to micellization of the main sample, causing light scattering and opalescence from the solution.<sup>80-82</sup> When the main copolymer micellizes, hydrophobic impurities are solubilized within the cores of these micelles and the solution clears. Zhou and Chu asserted that filtration of samples at temperatures corresponding to the greatest scattering intensity caused this anomaly to disappear. No other mention of a cloudy region was made in this work.

Critical micelle temperatures of several solutions and one critical micelle concentration at 40°C were determined. DLS techniques below and above the CMC displayed the transition from unimer solutions to solutions of coexisting unimers and micelles.<sup>80</sup> The hydrodynamic radius of the unimer was determined to be ~14 Å, while the micelle hydrodynamic radius was calculated to be 40 Å at 40.0 °C. Use of light scattering techniques at temperatures below CMT’s suggests that solutions did not display a cloudy appearance, as this would hinder such techniques. Although not discussed by the authors, the solutions displayed diffusion coefficients with an inverse dependence on temperature.<sup>80</sup> As argued by Booth et al.,<sup>79</sup> this indicates particles with attractive behaviors.

Solutions of aqueous 17R4 were also observed to phase separate at raised temperatures, showing a lower critical solution temperature (LCST).<sup>80</sup> Cloud-point measurements were used to determine the phase separation curve of the copolymer. This curve, with the CMC/CMT values is displayed in the phase diagram.

Further research has been performed by Jacobs et al. on this 17R4/H<sub>2</sub>O system.<sup>83</sup> Jacobs et al. have observed that this solution does form cloudy solutions in the “unimer region” described by Zhou and Chu. Filtering the samples resulted in no change to this cloudy appearance. Turbidity measurements were used to examine the transition between the cloudy and clear solution regions.

To determine the one-phase to two-phase transition, Jacobs et al. made refractive index measurements on both phases of the two-phase solutions.<sup>83</sup> Through these measurements, the concentration of each phase was calculated and the phase transition line was determined. Interestingly, the transition line depended on the initial copolymer concentration. This dependence would not be observed through the traditional cloud-point measurements performed on solutions of varying copolymer concentration. The cause of this concentration dependence is still under investigation. Preliminary results of Jacobs et al. are shown in Figure 5.6. The critical solution concentration, that concentration where resulting phases after separation are of equal volume, was determined to be 0.226 (v/v).

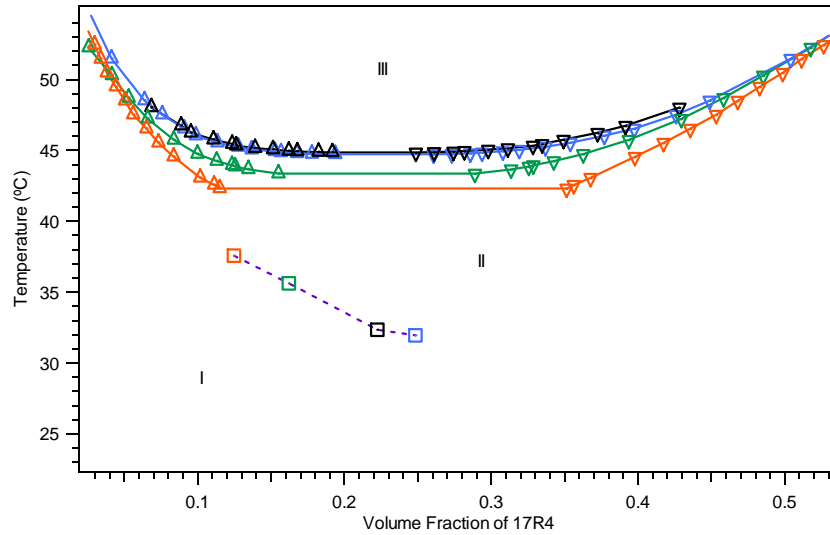


**Figure 5.6:** Concentration dependence of one-phase to two-phase transition line in 17R4/H<sub>2</sub>O solutions, as well as cloudy-to-clear temperatures determined by Jacobs et al.<sup>83</sup> as a function of temperature and volume fraction ( $\phi$ ). Turbidity measurements (squares) were used to determine the transition between cloudy (I) and clear (II) regions. Refractive index measurements on the upper (triangles) and lower (upside down triangles) phases of multiple solution concentrations over a variety of temperatures determined the one-phase to two-phase (III) transition. Solution concentrations are coded by color:  $\phi=0.125$  is in orange;  $\phi=0.163$ , green;  $\phi=0.226$ , black, and  $\phi=0.246$ , blue. Lines are drawn to help lead the eye, and do not represent lines of best fit.

After the preliminary work by Jacobs et al. and the observation of a cloudy solution region, the use of light scattering techniques by Zhou and Chu became suspect, as turbid samples cannot be used with such techniques. SANS techniques, however, can be easily performed on such turbid samples. Zhou and Chu also assumed spherical micelle formation through DLS measurements. SANS techniques are used here to give a better indication of micelle shape and to help resolve the issue of linked or single micelles that is discussed throughout Pluronic-R literature.

## 5.2 17R4 in D<sub>2</sub>O – glossary

The following terms will be used in the discussion of 17R4 copolymer behavior. They are defined here for clarity and will be discussed to a greater extent at later points in this chapter.

The phase diagram of 17R4 in D<sub>2</sub>O has three distinct regions: cloudy, one-phase; clear, one-phase; and two-phase. Here, “cloudy” means the solution is turbid and opaque to the eye; one cannot see through the sample. This phase will be referred to as “Region I.” The term “clear” represents any solution through which one can see and distinctly make out details of objects seen through the solution. To be labeled as “clear,” the sample does not have to be water-like and may display some haziness or light scattering. Solutions in this phase will be said to be in “Region II.” The term “aggregation temperature” ( $T_a$ ) is used to describe the point at which the solution changes from Region I to Region II, that is the temperature at which the solution becomes clear.

The final region consists of two phases separated within the sample. The transition into this region is detected through two sample characteristics, here called the “cloud point” and “phase separation.” The “cloud point” is referred to as the temperature at which a solution becomes very turbid and appears “speckled” or to be composed of small bubbles of different phases. The appearance of this turbidity suggests that full phase separation is soon to occur. The term “phase separation” is used to define the temperature at which two distinct phases were clearly visible in the solution. The “transition temperature” ( $T_t$ ) indicates the temperature at which the

transition into Region III occurs, and includes both the cloud point and phase separation temperatures.

It is also important to define terms to discuss the structures assumed by the copolymer within each of these phases. The term “unimer” will continue to be used to define a solvated polymer chain in solution. A “cluster” of unimers refers to the networking of unimers into multiple groups in solution. Within these clusters, solvation of the hydrophilic portions of the copolymer still occurs. The term “cluster” is used as opposed to a “network” which connotes the idea of one large spider-web of copolymers in solution. In this work, however, it is impossible to distinguish between these two formations, and so the term “cluster” will be used to represent either clusters or a network of clusters in solution.

Finally, it is necessary to distinguish a “micelle” from a generic “aggregate.” The term “micelle” means unimers have come together in an organized manner, creating a hydrophobic core and a hydrophilic shell (when in aqueous solutions). “Aggregate” is used to define a body of collected unimers that does not display signs of this organization; no distinct core/shell structure is observed.

### 5.3 17R4 in D<sub>2</sub>O – phase diagram

#### 5.3.1 Introduction

Deuterated solvents must be used for SANS measurements, and thus D<sub>2</sub>O was used as the solvent for this aqueous 17R4 system. Although the phase diagram of 17R4 had previously been examined in H<sub>2</sub>O,<sup>80, 83</sup> isotopic effects in the solvent may

cause changes in the phase boundaries of the system. H/D solvent substitution has been shown to cause stronger polymer-solvent hydrogen-bonds, as well as increased hydrophobicity.<sup>17, 19-21</sup>

17R4 in D<sub>2</sub>O was observed to form cloudy one-phase, clear one-phase, and two-phase solutions depending on temperature and copolymer concentration, as was observed by Zhou and Chu<sup>80</sup> and Jacobs et al.<sup>83</sup> for 17R4/H<sub>2</sub>O solutions. Because of the similarity, the phase diagram for 17R4/H<sub>2</sub>O was used as the preliminary diagram for 17R4/D<sub>2</sub>O. A concentration similar to the critical solution concentration of 17R4/H<sub>2</sub>O determined by Jacobs et al. was used for many of the experiments in the 17R4/D<sub>2</sub>O system. 17R4/D<sub>2</sub>O solutions were monitored visually to determine the general phase diagram of the system.

### 5.3.2 Experimental

#### *Solution preparation*

17R4, a liquid with density ( $\rho$ ) of 1.048 g/mL was used as received from BASF Corp. Deuterium oxide (D<sub>2</sub>O, 99.9%,  $\rho=1.10$  g/mL over temperature range 20-50 °C<sup>84</sup>) was obtained from Cambridge Isotopes, Inc. Solutions were prepared by massing the desired amount of polymer into a glass vial with a Teflon-lined lid, and solvent was added until the total desired weight was achieved. Measurements were performed on a Mettler H80 balance ( $\pm 0.1$  mg). All solutions samples were vigorously shaken to ensure complete mixing. Buoyancy corrections were made on sample weights prior to converting to weight fraction,  $\omega$ .

### *Experimental setup of visual observations*

Sample observations were made using a high-precision water bath (Figure 5.7). This water bath has been described elsewhere.<sup>85</sup> Water bath accuracy was at the 0.2 °C level, while the precision of the bath was at the 0.01 °C level.

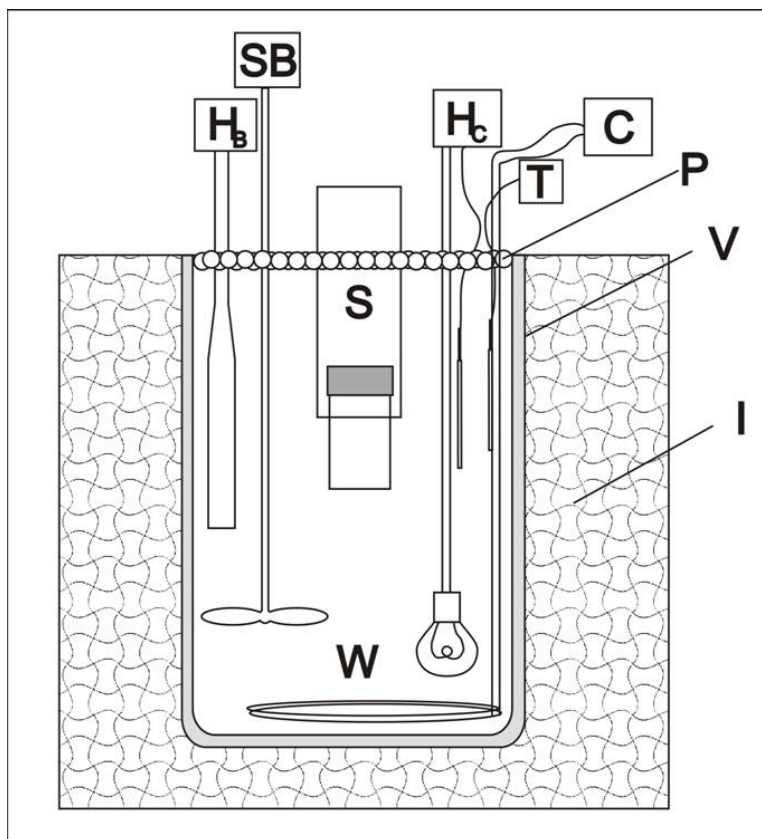


**Figure 5.7:** Precision water bath. Water bath elements include:  $H_B$ , background blade heater; SB, stirring blade; S, sample held in place with Tygon tubing;  $H_C$ , control heater (60 watt bulb) and thermometer; T, measurement thermometer. Each of these is located in the workspace, W, or a large Pyrex vessel, V, filled with water. The vessel is surrounded by insulating Styrofoam, I, and poly(propylene) balls, P, are on the water surface for further insulation. Cold water from a cooling bath, C, is used as a heat sink as water is circulated through copper coils. Figure adapted from Greer.<sup>85</sup>

### *Stability of cloudy phase*

All 17R4/D<sub>2</sub>O solutions were observed over time at room temperature. One  $\omega=0.23$  sample was observed over time at 25.52 °C ( $\pm 0.01^\circ\text{C}$ ) in the high precision



water bath. The sample was shaken vigorously and placed in the bath. Samples were allowed to sit without disruption, and general observations were made over time.

When cloudy solutions of 17R4/D<sub>2</sub>O were left undisturbed for long periods of time, a distinct white, opaque layer was observed to form at the air-solution interface and affixed to the vial wall around this interface. Solutions were observed to begin clearing from the bottom of the solution towards the air-solution interface. Samples remained hazy near the bottom of the solutions and were cloudier toward the interface and the milky layer. This is shown in Figure 5.8. This occurred both at room temperature and in the water bath, which indicates that this is not due to temperature variations on the lab bench.

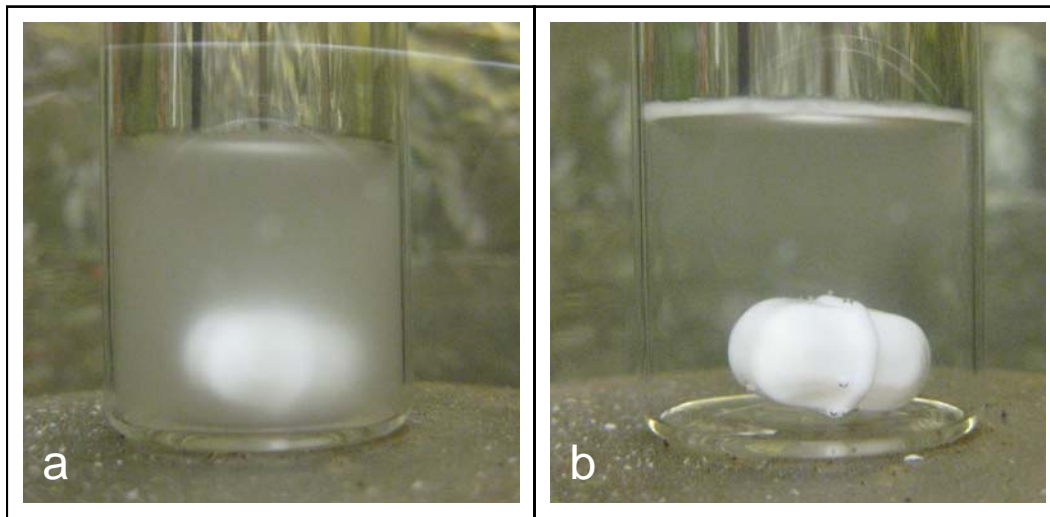


**Figure 5.8:** Formation of film at air/water interface in  $\omega=0.23$  17R4/D<sub>2</sub>O sample. Sample is shown (a) immediately after shaking and (b) after 13 days resting at  $25.52 \pm 0.01$  °C. Note formation of white film on air/water and vial/water interfaces after rest. The large white object is a magnetic stir bar.

It is speculated that this milky layer contains concentrated copolymer. As a large portion of the original cloudy copolymer moves from the solution to the interface, it is thought that the concentration of copolymer in the bulk solution thus

decreases. This would explain the clearing of the cloudiness of the bulk solution. This phenomenon was observed in all 17R4/D<sub>2</sub>O solutions prepared. However, Jacobs et al. made no observation of this film formation in 17R4/H<sub>2</sub>O solutions.

Surface adsorption of Pluronics has been studied many times,<sup>86-91</sup> but that of Reverse Pluronics is little studied.<sup>92</sup> PPO blocks have been shown to reside at the surface of the air/water interface, while soluble PEO blocks reach into the solution.<sup>92</sup> Although research has been done into Pluronic formations at the surface, a literature search offered no clues into the formation of a Pluronic film at the surface over time. In the examined literature, sample equilibration time after preparation was a day or less, or was not mentioned at all. A “foam film” produced by these copolymers in fresh aqueous solutions is researched by Sedev et al.,<sup>89, 90</sup> but it is unclear whether this is the film that is observed in 17R4 solutions here. This film formation over long equilibration times deserves further observation.

#### *Effects of filtration on solution in Region I*

As discussed above in the background information, Zhou and Chu reported that filtration of 17R4/H<sub>2</sub>O samples caused the “disappearance” of the “strong opalescent appearance” that was observed at temperatures below Region II.<sup>80</sup> In the work by Zhou and Chu, samples were filtered with a Millipore VC membrane filter of pore size 0.1 μm near the temperature of maximum light scattering. However, the type of membrane (nylon, polycarbonate, or mixed cellulose ester, for example) was not identified.

Here, a  $\omega=0.13$  17R4/D<sub>2</sub>O sample was visually monitored in a Neslab water bath to determine the temperature of maximum light scattering and cloudiness. This was found to be near 36.0 °C. It is noted that the sample was cloudy at this temperature, but was not considered to display a “strong opalescence.” Approximately 5 mL of this sample was filtered at this temperature through a Nylon filter with 0.2 mm pore size into a second vial. The sample temperature did drop slightly during the filtration process. Upon filtration, the sample remained as cloudy as the remaining unfiltered sample.

Both the filtered and unfiltered samples were allowed to sit at 25.0 °C in the Neslab bath, and they were monitored over a few weeks. After 24 days, it was noted that both samples had formed a film at the air-solution interface around the sides of the vial. Interestingly, the film in the filtered sample was clearer than that of the unfiltered sample, which was white and opaque. It was also noted that when shaken, the filtered sample did not become as cloudy as the unfiltered sample. However, it is not possible to say that the cloudy appearance “disappeared,” and the sample remained so turbid as to prohibit dynamic light scattering techniques. With these observations, and those of Jacobs et al.,<sup>83</sup> the filtration technique used by Zhou and Chu to remove the turbidity of samples in Region I could not be repeated and remains suspect.

#### *Region I to Region II equilibration time*

The equilibration time required for the Region I to Region II transition was investigated following discussions with D. T. Jacobs. Jacobs et al. saw long

equilibration times of 12+ hours (this will be considered a “slow” transition) for 17R4 in H<sub>2</sub>O, whereas preliminary observations in this lab showed transitions in 1-2 hours (“fast” transition) for 17R4 in D<sub>2</sub>O. In order to clarify the equilibration time needed for proper elucidation of the phase diagram, a 0.17 weight fraction sample was placed in the high precision water bath and brought to 34.80 °C ± 0.01 °C. This sample had been observed to clear at this temperature within one hour; i.e., this is near the “fast” transition temperature.

The water bath temperature was lowered in a stepwise fashion, and the sample was monitored for clearing. The sample was stirred at each lower temperature and allowed to sit for 12+ hours. If clearing was observed after this time, the temperature was considered to be above the “slow” transition temperature, and the temperature was again lowered. At each of these lower temperatures, the solution was observed to clear slowly from the bottom of the vial, in a manner similar to the clearing observed when copolymer gathered at the air-surface interface. In fact, such a polymer film formation was observed.

At this time in the 17R4/D<sub>2</sub>O sample, this “slow” clearing is attributed to the film formation, rather than the transition between Region I and Region II. The Region I to Region II transition temperatures presented in this work are thus those shown to occur abruptly, within 1-3 hours. By using these values, complications with longer equilibrium times and polymer film formation at the interface are avoided.

### *Phase separation equilibration time*

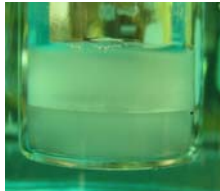
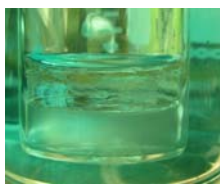


The equilibration time of the phase separation was also monitored. A  $\omega=0.22$  solution of 17R4/D<sub>2</sub>O was placed in a  $45.0 \pm 0.1$  °C Neslab temperature bath, well above the transition temperature,  $T_t$ , for this concentration, and was allowed to equilibrate over two to three days, while observations were made. The sample was placed in a beaker containing water from the bath and both were removed from the bath to make these periodic observations over time. Both were then placed back into the bath. Pictures were taken of the solution at various times in the equilibration. It is estimated that the solution temperature did not change significantly in the time the sample was removed from the bath.

Solution characteristics changed continuously over the 52 hours of observation, as shown in Table 5.1. From the observations, it is clear that the solution has a long equilibration time and may even extend beyond the 52 hours allotted here.

These long equilibration times bring a difficulty when working with 17R4/D<sub>2</sub>O solutions. It is often hard to determine when samples have equilibrated from visual observations alone. It is unclear whether these equilibration times are associated with phase separation alone or whether they are also seen in one-phase solutions. Studies in the literature often make no mention of sample equilibration times, and it is difficult to identify the necessary time scale. Because of these long equilibration times, performing experiments on equilibrated samples may be difficult due to experimental techniques and limitations. Previous studies on copolymers similar to this Reverse Pluronic have made no mention of long equilibration times

above the one-phase to two-phase transition, as this transition is often observed through cloud point techniques.

**Table 5.1:** Monitoring of equilibration time of phase separation. Changes in phase appearance over time of a  $\omega=0.22$  solution at  $45.0 \pm 0.1$  °C, well above the transition temperature,  $T_i$ . Blue appearance is due to ethylene glycol in temperature bath solution.

Approx. Equilibration Time	Visual Observations		
	Top	Bottom	
1 hour	Milky	Cloudy	
3 hours	Gel-like	Opalescent	
9 ½ hours	Clear, gel-like	Opalescent	
24 hours	Clear, gel-like near air-solution interface	Opalescent	
52 hours	Clear, gel-like	Less opalescent	

#### *Determination of Region I to Region II transition temperatures*

Samples were placed within the high precision water bath and allowed to sit for 30 minutes to come to thermal equilibrium with the bath. Following this thermal equilibration, samples were stirred vigorously for a short time and then allowed to equilibrate. Samples were given at least one to three hours for this equilibration. All samples were observed by eye. Temperatures are reported as the midpoint between the last temperature at which a solution was cloudy and the first temperature at which one could clearly see through the sample. The samples were often hazy at this point, but are considered in the clear, Region II due to their transparency. An ice/water mixture was used to bring high concentration samples to 0 °C. Temperatures signifying the cloudy-to-clear transition will be referred to here as aggregation temperatures ( $T_a$ ), based upon the observations of Zhou and Chu described earlier. The assumption that this cloudy-to-clear transition corresponds to unimer aggregation and micelle formation will be addressed in a later section of this chapter.

#### *Determination of phase separation transition temperatures*

Samples were allowed to sit undisturbed for half an hour in the precision water bath to thermally equilibrate with the bath. The solutions were then shaken vigorously and allowed to equilibrate for up to 12 hours. Phase separation, observed as meniscus formation, marked the transition into Region III. For very high and low concentration samples, this meniscus was difficult to observe and so traditional “cloud point” techniques were used. For these samples, an equilibration time of only one hour was used. As with the Region I to Region II transition, transition

temperatures are reported as the midpoint between the last temperature at which a solution was clear and one phase, and the first temperature at which a meniscus formed (or the first temperature of clouding for “cloud point” techniques). The temperatures signifying the one-phase to two-phase transition will be referred to as transition temperatures ( $T_t$ ).

### 5.3.3 Results and discussion

#### *Region I to Region II transition*

Transitions in 17R4/D<sub>2</sub> samples from an opaque, turbid solution to a clear solution were observed at a variety of concentrations, and these transitions were found to be temperature dependent. A solution was said to be within Region I if was cloudy to the point that one could not see through the sample. One can see through solutions within Region II. The temperature of this transition between Regions I and II is considered the aggregation temperature ( $T_a$ ). Very near  $T_a$ , solutions were clear so that one could see through them; however, they often remained hazy to the eye. The clearing of these solutions was observed to take longer times (2 hours). Well-above  $T_a$ , solutions became clear and water-like within 5-10 minutes.

It was observed that this transition temperature decreased with increasing concentration. At weight fractions of 0.12 and below, solutions were only slightly hazy at room temperature, and they grew cloudier as temperature was increased. No cloudy-to-clear transition was observed in these samples, however, because the one-phase to two-phase transition was reached prior to the cloudy-to-clear transition. The high concentration ( $\omega=0.48$ ) sample remained clear at all observed temperature,



indicating that the Region I to Region II transition occurs below 0 °C. Appendix C.1 includes all values for each of these temperatures and an explanation of the error bars found in Figure 5.9.

#### *Phase separation transition*

Visual observations were made as described above to determine the approximate one-phase to two-phase transition temperatures ( $T_t$ ). When observing  $T_t$  values, extreme sample turbidity or the appearance of a meniscus was used as a visual indication of the transition to the two-phase region (noted as the “cloud point” or “phase separation” points, respectively in tables and graphs of data). These temperatures are included in the phase diagram of the 17R4/D<sub>2</sub>O system, presented in Figure 5.9 below. See Appendix C.1 for all transition temperatures and an explanation of error bars found in Figure 5.9.

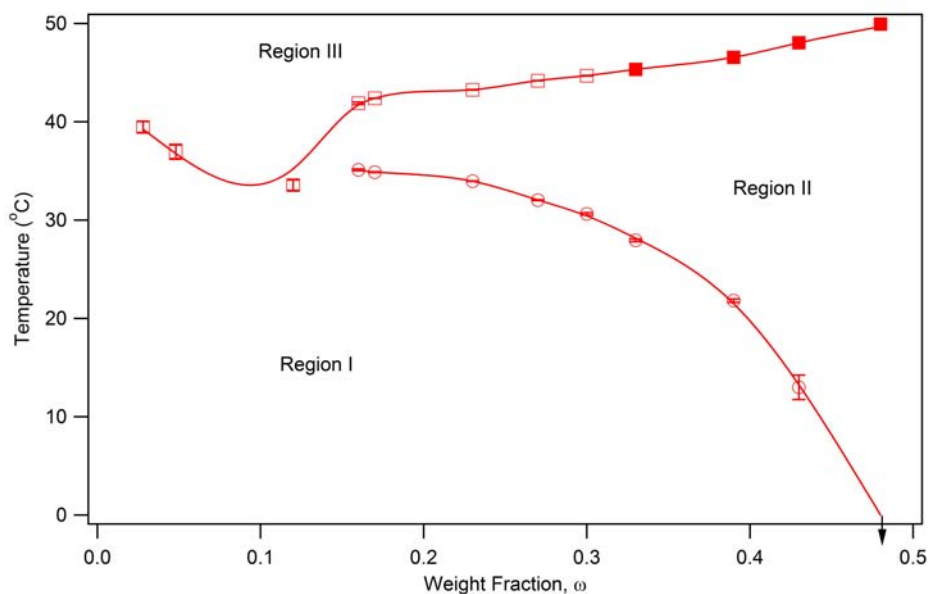


**Figure 5.9:** Phase diagram of 17R4 in D<sub>2</sub>O. The transition between the cloudy and clear regions (I and II, respectively) is shown with circles, while the transition between the one and two phase regions is shown with squares. Open squares signify observation of phase separation, while closed squares signify observation of the cloud-point. Error bars are shown, some of which are smaller than the size of the symbol used. These bars represent the absolute range of temperatures in which a transition may occur, based upon visual observations. The midpoint is indicated by the symbol. See Appendix C.1 for these data. Lines are drawn to help guide the eye. The  $\omega=0.48$  solution is clear at 0 °C, as indicated by the arrow.

### 5.3.4 Conclusions

The phase diagram of 17R4 in D<sub>2</sub>O has been determined through visual inspection, including cloud-point techniques and the observation of phase separation. The diagram is very similar to that determined by Zhou and Chu for 17R4 in H<sub>2</sub>O (Figure 5.10).<sup>80</sup> Differences in transition temperatures are not unexpected, due to the solvent isotope differences. The phase transition curves in both systems are not symmetric. It appears that the presence of Region II flattens the curve at higher concentrations. This suggests less stability of the one-phase solution after aggregate formation, because the phase separation temperature is less than it would be had the

curves been symmetric. The aggregation curves occur at very similar temperatures, suggesting there is little or no solvent isotope effect on this curve.

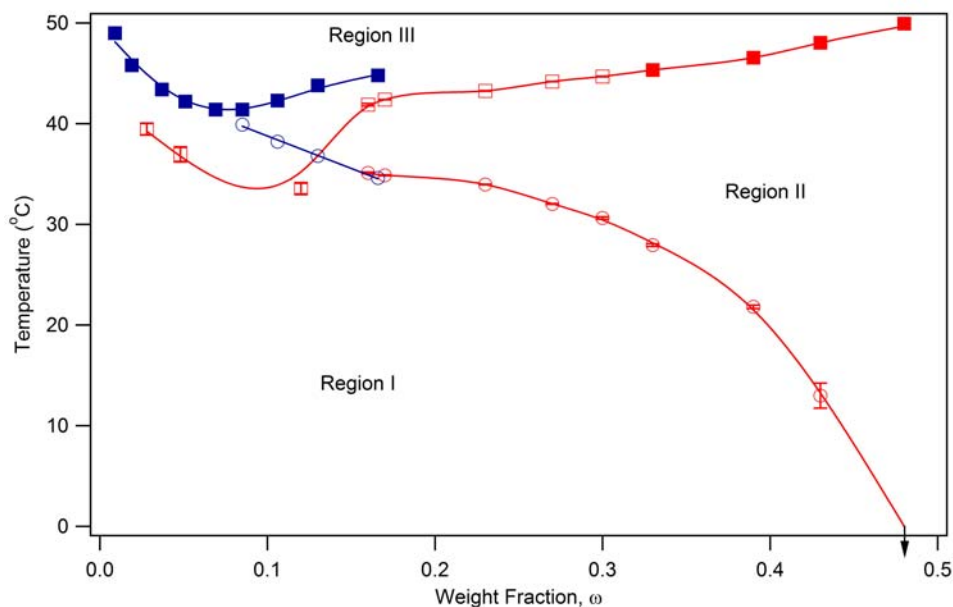


**Figure 5.10:** Phase diagrams of 17R4/D<sub>2</sub>O (red) and 17R4/H<sub>2</sub>O (blue). The H<sub>2</sub>O system was determined by Zhou and Chu.<sup>80</sup> The phase transitions are noted by squares, while the Region I to Region II transitions are shown by circles. The phase transition in H<sub>2</sub>O was determined through cloud-point techniques, while that in D<sub>2</sub>O was determined by both observations of cloud-points (filled squares) and phase separation (open squares). The arrow at  $\omega=0.48$  signifies that this concentration enters Region II below 0°C.

The phase diagrams may also be compared to that of 17R4 in H<sub>2</sub>O determined by Jacobs et al. Through refractive index techniques, Jacobs et al. have determined the coexistence curve of 17R4/H<sub>2</sub>O.<sup>83</sup> Jacobs et al. measure the concentration of coexisting phases at various temperatures above the phase transition temperature. They have observed differing coexistence curves, depending on the original solution concentration. Such an effect would not be observed through traditional cloud-point techniques employed here and by Zhou and Chu, as only the transition temperature is measured for a single concentration.

Interestingly, the phase transition curve of Zhou and Chu and those of Jacobs et al. intersect at the same temperature for a specified concentration (Figure 5.11). For example, the cloud-point of volume fraction,  $\phi$ , 0.118 solution is 42.3 °C, determined by Zhou and Chu.<sup>80</sup> This point intersects the  $\phi=0.125$  coexistence curve, close to where the top phase of the  $\phi=0.125$  solution has a concentration of 0.115 at 42.3 °C. The meaning of these intersections continues to be examined.<sup>83</sup>

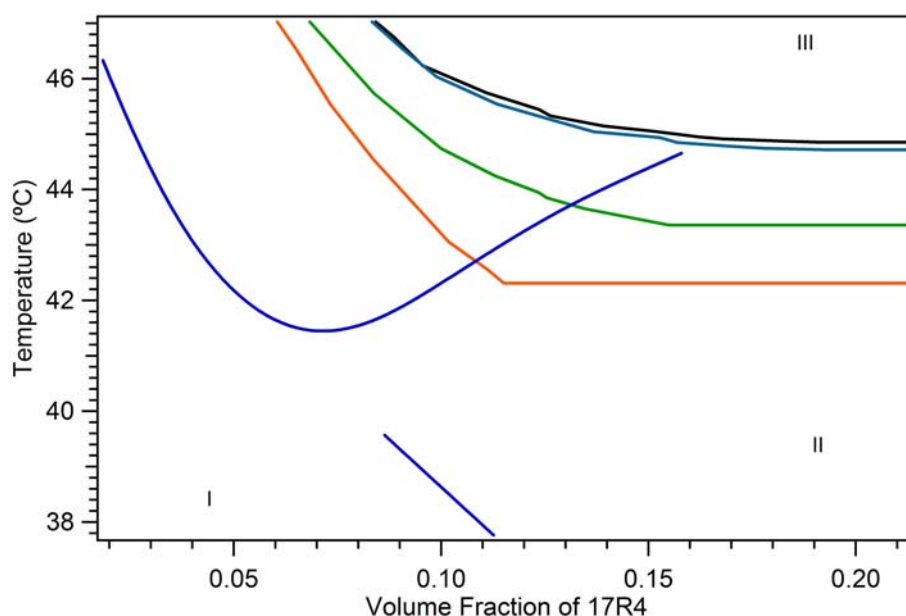


**Figure 5.11:** Coexistence curves from Jacobs et al.<sup>83</sup> with cloud-point line from Zhou and Chu.<sup>80</sup> Only the approximate curves are shown to show the intersection points. Solution concentrations are coded by color:  $\phi=0.125$  is in orange;  $\phi=0.163$ , green;  $\phi=0.226$ , black, and  $\phi=0.246$ , light blue. The cloud-point curve from Zhou and Chu is shown in dark blue. The blue line extending to low temperatures is the aggregation curve, determined by Zhou and Chu.

It is expected that the 17R4/D<sub>2</sub>O diagrams determined here through cloud-point techniques and that determined through refractive index techniques will show similar characteristics. Jacobs et al. are currently completing the coexistence curves of D<sub>2</sub>O solutions, and the phase diagrams will be compared in the near future.

If systems were at equilibrium, the same coexistence curve should be determined, no matter the technique. This suggests that one, or possibly all, of the phase diagrams have not been measured on an equilibrated system. It appears as if the transition into Region II and the subsequent aggregate formation cause a non-equilibrium state. It is hypothesized that the aggregates are unable to rearrange to obtain a proper equilibration.

The equilibration of these systems and their phase diagrams continues to be investigated.<sup>83</sup> The copolymer film formation at the air-solution interface in the 17R4/D<sub>2</sub>O system also deserves further exploration. The time lengths that should be allotted for equilibration between all regions remain unknown as well. In experiments discussed below, temperature and concentration values were chosen so as to assure the solution was within a region, and the transition areas were avoided. It is recognized, however, that this does not guarantee equilibrium.

#### 5.4 Characterization of copolymer structures

The structures assumed by the 17R4 copolymer chains in 17R4/D<sub>2</sub>O solutions were also investigated here. Due to the observations of the cloudy nature of these solutions in Region I, the results from the dynamic light scattering technique used by Zhou and Chu<sup>80</sup> were doubted. Because the small angle neutron scattering technique does not rely on the refractive index of a solution, this technique was used with both turbid and clear samples from Regions I and II. This technique also offers greater insight into the shape of the scattering body than the dynamic light scattering technique. Although dynamic light scattering could not be used to examine turbid

samples in Region I, this technique was used to compare to SANS results in Region II. Rheology techniques were also used to offer insight into solution characteristics in both regions.

The copolymer structure was investigated at three concentrations. The first,  $\omega=0.23$ , is near the critical concentration 0.226 (v/v) in 17R4/H<sub>2</sub>O solutions, as determined by Jacobs et al.<sup>83</sup> More dilute solutions, at  $\omega=0.11$  and  $\omega=9.5 \times 10^{-3}$ , were also examined. Figure 5.12 indicates these concentrations on the phase diagram. The dilute solutions will only pass through Regions I and III with increasing temperature, while the  $\omega=0.23$  solution will traverse all three regions.

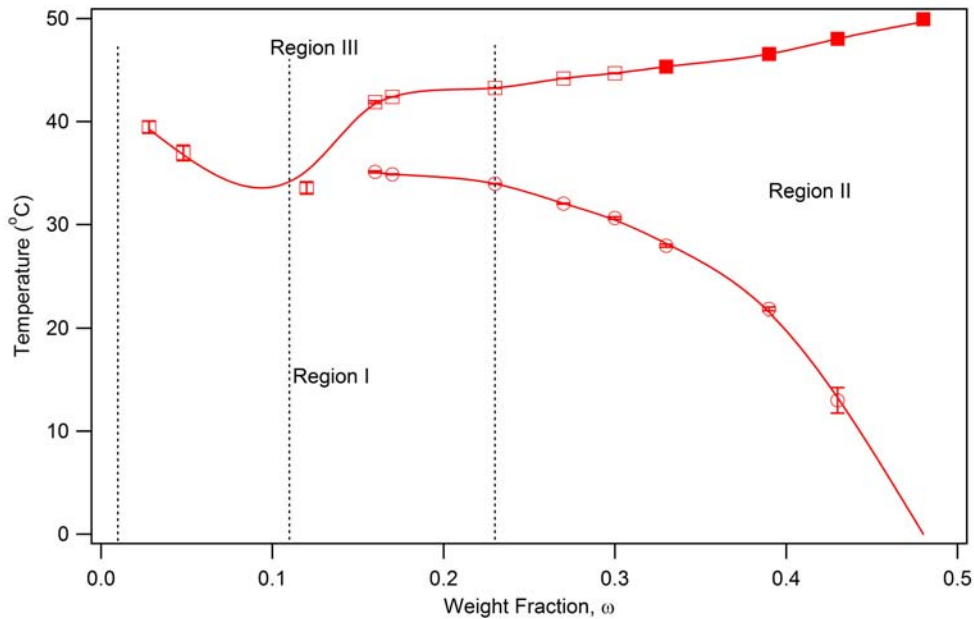


**Figure 5.12:** Phase diagram of 17R4/D<sub>2</sub>O, indicating the three concentrations ( $\omega=9.5 \times 10^{-3}$ , 0.11 and 0.23) at which copolymer structure is examined and discussed below.

### 5.4.1 Experimental

#### *Solutions*

17R4/D<sub>2</sub>O samples of  $\omega=0.23$  were prepared as previously described for the visual observations. These samples were used for rheometry, dynamic light scattering, and small angle neutron scattering experiments. A  $\omega=0.11$  17R4/D<sub>2</sub>O sample and a  $\omega=9.5 \times 10^{-3}$  17R4/D<sub>2</sub>O sample were also prepared. The  $\omega=0.11$  17R4/D<sub>2</sub>O sample was prepared as described previously, but on an electric balance, as opposed to the Mettler balance. Buoyancy corrections were still performed, as suggested in the literature.<sup>93</sup> A  $\omega=0.030$  solution was also prepared, and this solution was diluted to  $\omega=9.5 \times 10^{-3}$ . These more dilute solutions were used in SANS experiments. DLS and rheometry measurements were taken only on  $\omega=0.23$  solutions because this concentration was near the critical concentration of 17R4 in H<sub>2</sub>O. Also, Region II was not observed in the more dilute samples, and so DLS could not be performed on those samples.

#### *Rheometry*

The rheometry instrumentation was the same as described in Chapter 2. Measurements were taken at 25.0, 30.0, 35.0, and 40.0 °C ( $\pm 0.1$  °C). Sample aliquots (all of  $\omega=0.23$ ) were allowed to equilibrate on the heated plate for 1-2 minutes before rheology data were taken. To minimize evaporation, a lid was placed around the cone and sample. Rheology data were taken between 0.5-100 s<sup>-1</sup> shear rates. These shear rates included the first Newtonian region, marked by a steady viscosity value. The average of the measured viscosities in this region was taken as the zero-shear

viscosity. Error is reported as three times the standard deviation of this average value.

### *Dynamic light scattering*

Dynamic light scattering instrumentation was described earlier in Chapter 2. General DLS data collection and analysis was performed as described in Chapter 2. A  $\omega=0.23$  sample was placed within the chamber as the instrument heated to the desired temperature. After reaching and stabilizing at this temperature ( $35$  and  $39 \pm 1$  °C), the solution was shaken and replaced within the chamber. The solution was then given at least one hour to equilibrate before light scattering was measured.

Analysis techniques was done using the DynaLS program (see Chapter 2), and fitted channels were chosen to eliminate irregular scattering at low channel numbers and the “foot” of scattering at upper channel numbers. The included channel numbers are listed with the scattering results in Appendix C.3.

As shown in Equations (2.8) and (2.9), determination of the hydrodynamic radius within a sample depends on the refractive index of the solvent. The refractive index,  $n$ , of  $D_2O$  as a function of temperature was measured by Luten in 1934.<sup>94</sup> The refractive index of  $D_2O$  was not shown to vary within three significant figures in the temperature range used here. A value of  $1.32 (\pm 0.00)$  was used for the refractive index in DLS analyses. The data presented by Luten were determined at  $6563 \text{ \AA}$ ;<sup>94</sup> however, the DLS instrument used here measures scattering at  $6328 \text{ \AA}$ . The error associated with this difference of wavelength was assumed to be small compared to that of the overall DLS analysis.



### *Small angle neutron scattering – procedure*

The same SANS instrument configurations were used as previously described in Chapter 2. SANS data was taken on three 17R4/D<sub>2</sub>O concentrations:  $\omega=0.23$ ,  $\omega=0.11$  and  $\omega=9.5 \times 10^{-3}$ . Scattering data were collected at 15.5, 24.9, 29.8, 34.5, and 39.2 (all  $\pm 0.1$ ) °C on the  $\omega=0.23$  sample. The sample was allotted one hour to equilibrate at each temperature before scattering data were taken. The solution was then heated into Region III ( $44.0 \pm 0.1$  °C) for approximately seven hours. Cooling from Region III, scattering data were taken at  $25.1 \pm 0.1$  °C and finally  $6.7 \pm 0.1$  °C. Again, the sample had at least one hour to equilibrate at each cooler temperature. Scattering data were taken during this cool-down in order to determine the reversibility of aggregate formation. SANS data of the  $\omega=0.11$  sample were taken at  $11.9 \pm 1.0$ ,  $30.6 \pm 1.1$ , and  $49.3 \pm 1.3$  °C. Scattering of the  $\omega=9.5 \times 10^{-3}$  sample was measured at  $11.9 \pm 1.0$ ,  $21.3 \pm 1.0$ ,  $30.6 \pm 1.1$ ,  $39.9 \pm 1.2$ , and  $49.3 \pm 1.3$  °C.

### *Small angle neutron scattering – data analysis*

#### *-- Region I, $\omega=0.23$ sample*

Scattering in Region I of the  $\omega=0.23$  sample displayed no interaction peaks, and so simple fits could be used without taking into account a structure factor. Guinier and Porod linear fits were performed on this data. These fits were described in detail in Chapter 2. Incoherent background scattering had to be estimated and removed from the scattering intensity,  $I(Q)$ , prior to using these linear fits. Scattering at  $29.8 \pm 0.1$  °C and cooler displayed scattering intensity from clusters and unimers in

solution. In order to perform linear fits on scattering on the unimer only, scattering intensity from the clusters has to be removed, along with the background scattering.

As described in Chapter 2, the correlation length fit can fit both cluster and unimer scattering data with the equation:<sup>45</sup>

$$I(Q) = \frac{A}{Q^{m_1}} + \frac{C}{1 + (Q\xi)^{m_2}} + B. \quad (2.24)$$

Here, this fit was used prior to analysis with linear fits. The cluster,  $\frac{A}{Q^{m_1}}$ , and background, B, terms were subtracted from I(Q) and propagation of error from these terms was done before linear fittings were performed. The error in the first term was approximately 3-9% error in the cluster term, depending on temperature and Q-value, and the error in B was approximately 0.4-2.7, depending on temperature.

Linear Guinier fits were then performed on scattering data from this region, as described in Chapter 2. These fits were performed over a Q-range of 0.13-0.90 Å<sup>-1</sup>, as this fit is only accurate within  $QR_g < \sqrt{3}$ .<sup>45</sup> Fits were performed on axes ( $\ln[I(Q)]$  vs  $Q^2$ ), and yielded nearly-linear results, indicating spherical or nearly-spherical particle dimensions. Linear Porod fits were also performed on these data. The data were fitted over a Q range of 0.28-0.41 Å<sup>-1</sup>.

Following analyses with linear plots, non-linear plots without structure factors were used to analyze scattering data. In addition to the correlation length model already discussed, the two-region Guinier-Porod model was used as a second non-linear analysis tool. This model was described in Chapter 2 and uses the following equations:<sup>51</sup>

$$I(Q) = \frac{G}{Q^n} \exp\left(\frac{-Q^2 R_g^2}{3-n}\right) + B \text{ for } Q \leq Q_1, \quad (2.25)$$

and the Porod functional form

$$I(Q) = \frac{D}{Q^m} + B \text{ for } Q \geq Q_1, \quad (2.26)$$

to fit over different Q-ranges.  $Q_1$  has the equation

$$Q_1 = \frac{1}{R_g} \sqrt{\frac{(m-n)(3-n)}{2}}. \quad (2.27)$$

Recall that  $n$  is the Q-scaling exponent in the intermediate regime,  $m$  is the Porod exponent, and  $B$  is the background scattering.

This fit does not take clustering into consideration, and so cluster scattering needed to be removed from scattering data. This was again done by subtracting the cluster term, determined through the correlation length fit, from  $I(Q)$ . This did not completely remove the cluster scattering, however, and so the Guinier-Porod fit was performed using a Q-range of 0.017-0.40  $\text{\AA}^{-1}$ . The intermediate regime exponent,  $n$ , was held at zero to assume spherical unimer particles in solution.

*-- Region I, dilute solutions*

Data from the  $\omega=0.11$  solution at  $11.9 \pm 1.0$  and  $30.6 \pm 1.1$   $^{\circ}\text{C}$  displayed both cluster and unimer scatter, and so was analyzed with the correlation length model. This was fitted over the entire Q-range. At  $49.3 \pm 1.3$   $^{\circ}\text{C}$ , phase separation had begun and precluded any reliable model fitting. Only general observations of the data were made at this temperature.

Scattering data from the  $\omega=9.5 \times 10^{-3}$  solution was analyzed with the two-region Guinier-Porod model at all temperatures. From 11.9-30.6 °C, only unimer scattering was apparent, and so this model was used over the entire Q-region. At  $39.9 \pm 1.2$  °C, scattering from a second body at low-Q appeared. The two-region Guinier-Porod model was used over the Q-range of 0.0034 to 0.019 Å to analyze the large body, and over a region of 0.019 to 0.40 Å to analyze scattering at high-Q.

*-- Region II,  $\omega=0.23$  sample*

Scattering in Region II of the  $\omega=0.23$  sample displayed only very small interaction peaks, and so simple fits could again be used without taking into account a structure factor. Guinier and Porod linear fits were performed, as described in Chapter 2. Background scattering had to be removed from these scattering data before linear fits were performed. The correlation length fit was used to estimate the background scattering, as was done with Region I scattering. As no clusters were observed in this data, the coefficients used in the cluster term, A and n, were held at  $10^{-12}$  and 3, respectively. This was done to approximate a value of zero for this term and essentially remove the clustering portion for this fit.

The background term from the correlation length model was removed from I(Q) prior to performing linear fits. The error from this background term was propagated into the I(Q) error. The error in the background was small: approximately 0.14% at 34.7 °C and 0.10% at 39.5 °C. Guinier fits were performed over a Q-range of 0.0038-0.045 Å<sup>-1</sup>, and Porod fits were performed over a Q-range of 0.070-0.28 Å<sup>-1</sup>.

In addition to the correlation length plot, other non-linear fits were also performed on scattering data in Region II. The two-region Guinier-Porod model was fitted over the entire Q-range. The intermediate region exponent,  $n$ , was held at zero to represent a 3-D body shape. Slight variation of this fit from the data indicated that scattering particles were not spherical, and so the three-region Guinier-Porod fit was also used to examine scattering data in this region.

The three-region Guinier-Porod model was discussed in Chapter 2, and follows the equations:<sup>51</sup>

$$\begin{aligned}
 I(Q) &= \frac{G_2}{Q^{n_2}} \exp\left(\frac{-Q^2 R_{g2}^2}{3 - n_2}\right) \text{ for } Q \leq Q_2, \\
 I(Q) &= \frac{G_1}{Q^{n_1}} \exp\left(\frac{-Q^2 R_{g1}^2}{3 - n_1}\right) \text{ for } Q_2 \leq Q_1, \\
 I(Q) &= \frac{D}{Q^m} \text{ for } Q \geq Q_1,
 \end{aligned} \tag{2.28}$$

where

$$Q_2 = \frac{1}{R_g} \sqrt{\frac{(n_1 - n_2)}{\frac{2}{3 - n_2} R_{g2}^2 - \frac{2}{3 - n_1} R_{g1}^2}}. \tag{2.29}$$

This model can be used to fit scattering from particles with a second scattering dimension. For example, a cylinder would scatter from both the cross-sectional axis and from its length. In this fit,  $R_{g2}$  represents the radius of gyration from this long scattering dimension. The Q-scaling at length scales related to the Guinier regime is fit with  $n_2$ .

Finally, single particle form factor models for core-shell spheres and oblate particles were used for the Region II data. The entire Q-range was used with this model. These models use the difference in scattering length densities between the core, shell, and solvent, as described in Chapter 2. The scattering length density of D<sub>2</sub>O was held at  $6.3 \times 10^{-6} \text{ \AA}^{-2}$ , while the scattering length densities of the core and shell were held between  $3.4 \times 10^{-7} \text{ \AA}^{-2}$  and  $6.3 \times 10^{-6} \text{ \AA}^{-2}$ .<sup>45</sup> (See Appendix B for a discussion on scattering length density values.) These are the scattering length density values of PPO and D<sub>2</sub>O, respectively; the scattering length density of PEO is slightly larger than that of PPO. The scattering length densities of the core and shell would be some average of these values depending on the distribution of polymer blocks in the core and shell. Thus, these values could not be less than PPO or more than D<sub>2</sub>O.

Results for all analysis techniques performed on scattering data from 17R4 in D<sub>2</sub>O are presented in Appendix C.3.

#### 5.4.2 Results and discussion, Region I

##### *Rheometry of $\omega=0.23$ 17R4/D<sub>2</sub>O sample*

Zero-shear viscosities of  $\omega=0.23$  17R4/D<sub>2</sub>O sample were determined at a variety of temperatures. Within Region I, the zero-shear viscosity was determined to be  $12.5 \text{ cP} \pm 0.5 \text{ cP}$  and  $12.4 \text{ cP} \pm 0.5 \text{ cP}$ , at 25 °C and 30 °C, respectively. Note that these values are more than ten times greater than that of water. Figure 5.13 displays

the viscosities of this sample as a function of shear rate at 25 and 30 °C, and shows the average value that is taken as the zero-shear viscosity.

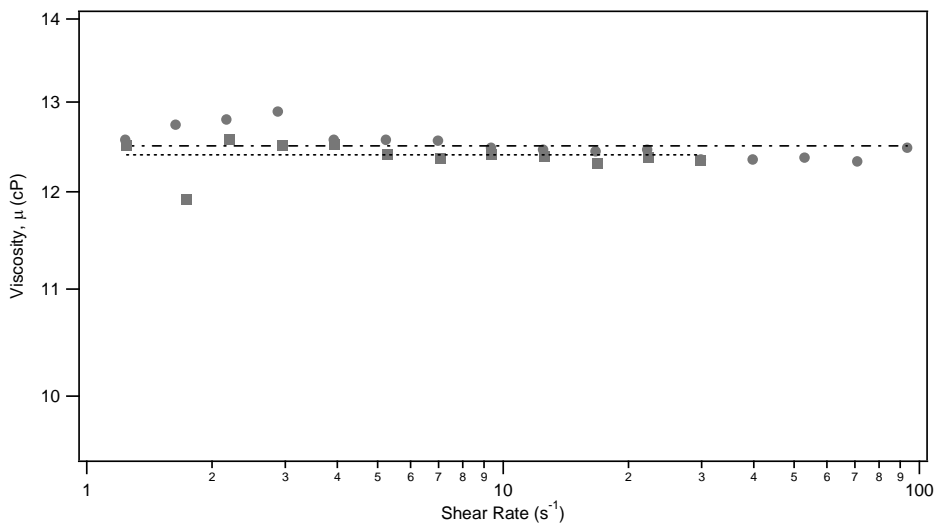


**Figure 5.13:** Determination of zero-shear viscosity for one-phase solutions in Region I of  $\omega=0.23$  solution at (●) 25 °C, (■) 30 °C. The zero-shear viscosities are shown as lines at 12.5 cP and 12.4 cP for 25 °C and 30 °C, respectively.

#### *SANS of $\omega=0.23$ 17R4/D<sub>2</sub>O solution*

At temperatures of 29.8 °C and below in the  $\omega=0.23$  copolymer solution, there is strong scattering at low-Q, but very weak scattering in the high-Q region (Figure 5.14). Such low-Q scattering can be indicative of clustering, as observed in PEO/water systems or network formation, as seen in 25R8.<sup>46, 71, 78</sup> These structures are of a large size scale, so only the Porod regime of scattering is observed. The weak scattering in the mid-to-high Q-range is suggestive of unimers in solution.

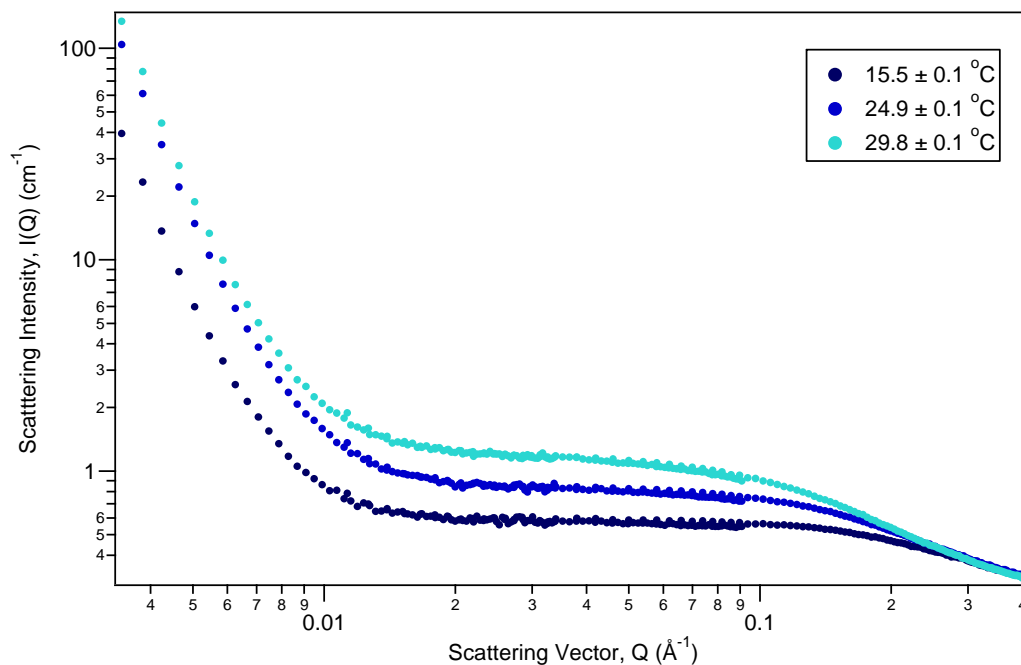


**Figure 5.14:** Neutron scattering intensity within Region I of a  $\omega=0.23$  17R4/D<sub>2</sub>O solution.

-- *Clusters*

Clusters or a network are evident by a large  $I(Q)$  scattering at low- $Q$  values.

From these data, it is not possible to distinguish the two. Here the term “cluster” will be used to mean either structure. Fits with the correlation length model indicated that these clusters have a Porod exponent of approximately 3.6, which indicates a rough surface fractal. An example of this fit to the data is shown in Figure 5.15. All Porod exponents determined in this manner are shown in Table 5.2.



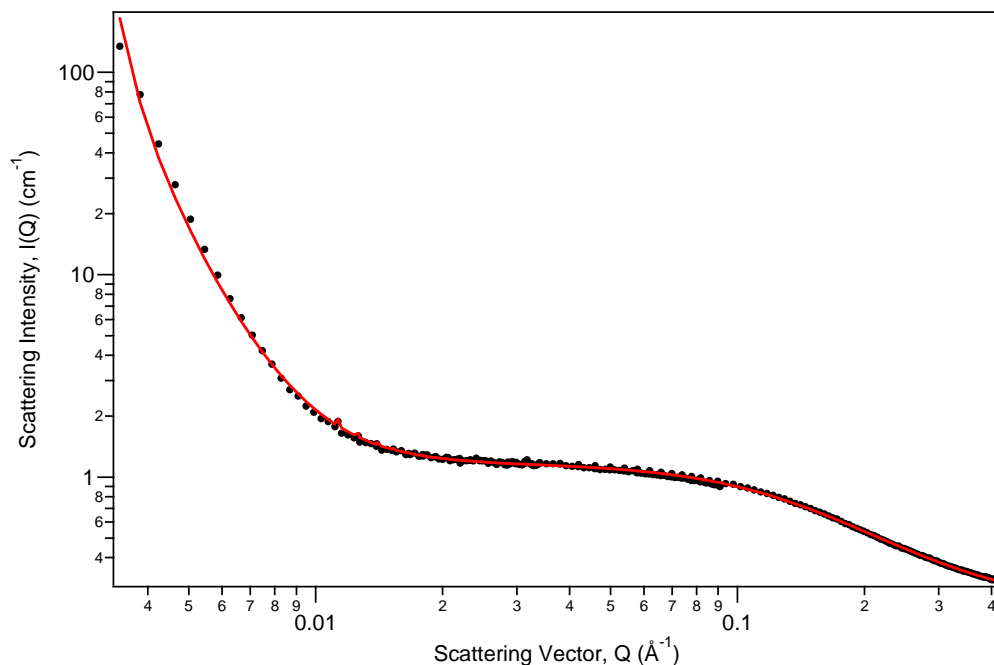


**Figure 5.15:** Correlation length model fit to scattering from  $\omega=0.23$  17R4/D<sub>2</sub>O solution at  $29.8 \pm 0.1$  °C. The fit is shown in red, while data is shown as black circles.

**Table 5.2:** Porod exponents,  $m_1$ , of cluster feature in Region I. These were determined for clusters in solutions of  $\omega=0.23$ . Uncertainties are at 99% level.

Temperature (°C)	Cluster Porod Exponent, $m_1$
15.5 ± 0.1	3.52 ± 0.03
24.9 ± 0.1	3.59 ± 0.03
29.8 ± 0.1	3.60 ± 0.02

The presence of such low-Q scattering has been seen in many similar systems, including synthetic polymers and biopolymers in D<sub>2</sub>O.<sup>45, 46, 78, 95-97</sup> The exact structure of “clusters” is currently unknown, but recent work on PEO/D<sub>2</sub>O by Hammouda,<sup>95</sup> and work on the Reverse Pluronic 25R8 by Mortensen et al.<sup>78</sup> offer insight into this structure. Recently, Hammouda has shown that PEO in D<sub>2</sub>O tends to form clusters through interactions between ethylene groups of separate chains.<sup>95</sup> Although PEO does dissolve in water, the ethylene groups “prefer” to minimize solvent and oxygen interactions, and reside near other ethylene groups. As ethylene

groups draw close to one another, they tend to “stick” to one another, causing the chains to cross-link, and a cluster network to form. The clusters seen in PEO have a Porod exponent of only 3, indicating a mass fractal. This suggests that the clusters in 17R4/D<sub>2</sub>O may be formed in a different manner, since this Porod exponent is closer to 3.6.

A similar explanation is offered by Mortensen et al. when discussing network formation in 25R8/D<sub>2</sub>O solutions.<sup>78</sup> They suggest that the hydrophobic PPO blocks group together forming “knots,” while PEO blocks extend into solution. Scattering intensity from these structures showed a Q-dependence of 4, suggesting a smooth surface fractal in solution.

Such a structure seems very plausible for the 17R4 triblock in D<sub>2</sub>O, and Figure 5.16 shows a cartoon of this possible structure. Because scattering from this structure extends beyond the SANS window, it is not possible to determine a size dimension, except to say the cluster is larger than 6000 Å, the limit of the SANS technique.<sup>45</sup>

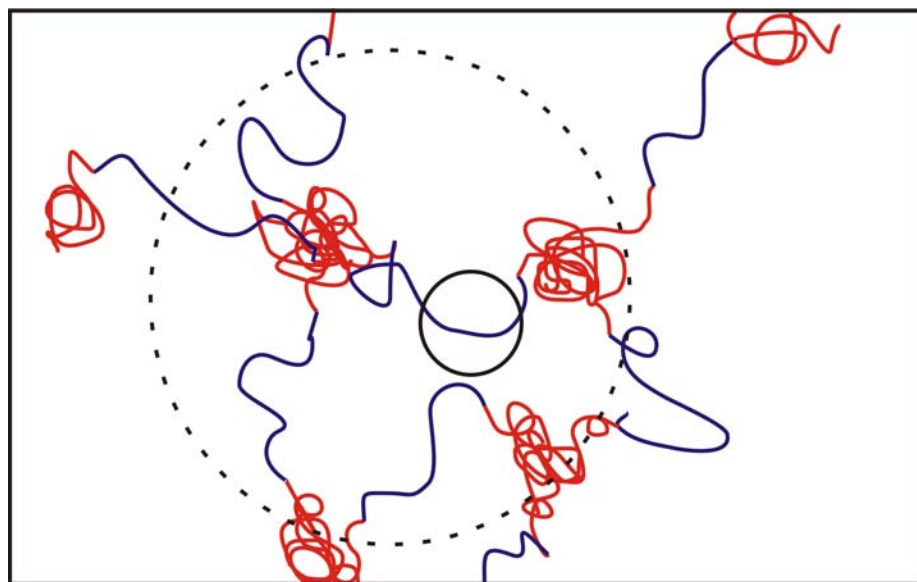


**Figure 5.16:** Cartoon of clustering of unimers in 17R4/D<sub>2</sub>O solutions. PPO is shown in red and PEO is in blue. The cluster particle is shown within the large, hashed circle; depicting scattering from low-Q dimensions. The unimer particle is shown within the small, whole circle; depicting scattering from high-Q dimensions.

It is possible that this clustering is the cause of the turbidity in 17R4/D<sub>2</sub>O samples in Region I. Although clustering is seen in PEO/D<sub>2</sub>O samples, no cloudiness has been reported in that system.<sup>46, 95-97</sup> Mortensen et al. do consider network formation as the reason for turbidity in 25R8/D<sub>2</sub>O samples.<sup>78</sup> It is possible that such cloudiness is due to larger “knots” of PPO blocks that tether the cluster together in 25R8/D<sub>2</sub>O and 17R4/D<sub>2</sub>O systems, versus the individual ethylene groups in PEO/D<sub>2</sub>O solutions.

-- *Unimers*

At high-Q values, scattering from copolymer chains is apparent. Figure 5.16 displays a cartoon view of such a high-Q window and the portion of the cluster structure that corresponds to scattering at high-Q ranges. Solvated PEO blocks

stretched between PPO “knots” will scatter in a manner similar to unimers in solution. It is not possible to distinguish scattering from unimers in this structure from free unimers in solvent. The scattering from these particles is much weaker in intensity and represents a very small particle. Scattering in this Q-range was analyzed with linear Guinier and Porod fits, the correlation length model, and the two-region Guinier-Porod model. Examples of these fits are shown in Figure 5.17.

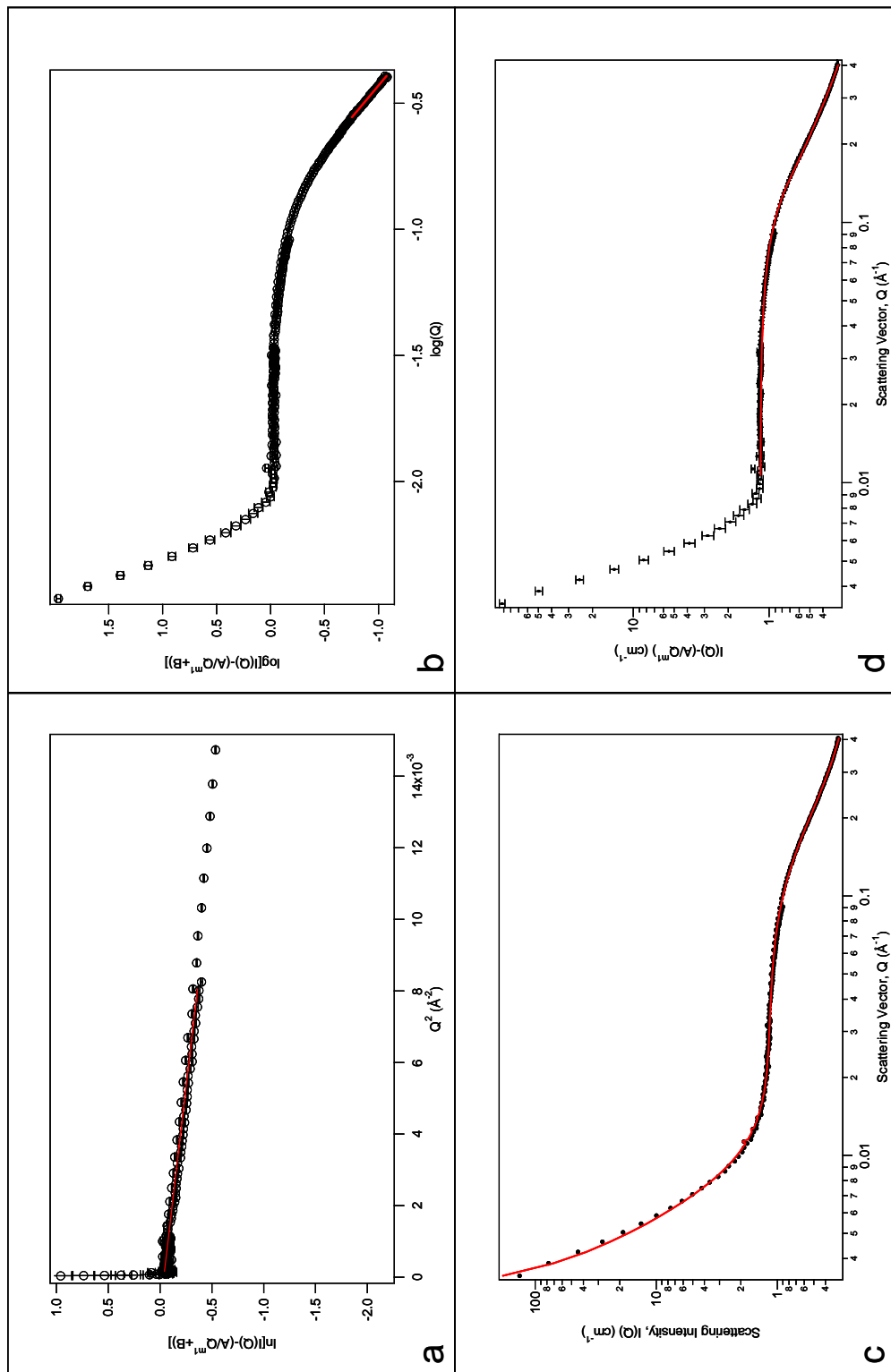


**Figure 5.17:** Examples of SANS analysis fits of  $\omega=0.23$  17R4/D<sub>2</sub>O solution at  $29.8 \pm 0.1$  °C. Fits include: (a) linear Guinier fit, (b) linear Porod fit, (c) correlation length fit, and (d) two-region Guinier-Porod model. Analyses of data from other temperatures, including goodness of fit for each model, are found in Appendix C.3.

Analyses by linear and nonlinear methods offer insight into the behavior of these copolymer chains as temperature is increased through Region I. The radii of gyration of these chains, as derived from linear Guinier fits, the Guinier-Porod model, and the correlation length model are compared in Table 5.3. All the analysis techniques give comparable dimensions. Note that because the radii are so small (especially at 15.5 °C) this scattering is at the extreme of the SANS detection limit, and it is only possible to say that these scattering bodies have a spherical radius less than or equal to 10 Å. The slight increase in radius with increasing temperature suggests greater solvation of the copolymer, presumably of the PEO block.

**Table 5.3:** Radii of gyration derived for the unimer chains in Region I of  $\omega=0.23$  17R4/D<sub>2</sub>O solution. Values are determined through (a) linear Guinier fit, (b) correlation length model, and (c) 2-region Guinier-Porod model, and are given in Å. Uncertainties are 99%.

Temperature (°C)	$R_g^a$ (Å)	$R_g^b$ (Å)	$R_g^c$ (Å)
15.5 ± 0.1	5.6 ± 0.6	6.8 ± 0.1	4.03 ± 0.03
24.9 ± 0.1	8.2 ± 0.2	8.90 ± 0.06	6.5 ± 0.2
29.8 ± 0.1	11.0 ± 0.1	11.74 ± 0.05	9.0 ± 0.6

The approximate volume of one 17R4 molecule can be determined using the molecular volumes of PPO and PEO monomers (57.77 cm<sup>3</sup>/mol and 39.04 cm<sup>3</sup>/mol, respectively).<sup>45</sup> One 17R4 chain has a volume of approximately 4.2x10<sup>3</sup> Å<sup>3</sup>, assuming no solvent interactions. If a spherical formation is assumed for the unimer, the spherical radius can be determined by using this volume. (See Appendix C.2 for calculation.) The approximate spherical radius of one 17R4 molecule was determined

to be approximately 10 Å. This suggests that the high-Q scattering intensity is from unimers in solution.

Porod exponent values for these unimers vary greatly depending on the method of analysis (Table 5.4). Low-intensity scattering and the small size of these chains add difficulty in determining reliable values. Due to the small size, and the limits of the SANS detection area, it is possible that the full Porod region of these chains is not measured, causing limitations in determining the Porod exponents. Finally, because this scattering lies at the edge of the detection limit, it is difficult to determine a reliable value of the background scattering. This also adds difficulty in determining the Porod exponents, as some background scattering is Q-dependent and may be concealed within the coherent scattering from the particle. Here, the traditional linear Porod plots are decided to offer the most plausible exponents.<sup>98</sup> This fit gave Porod exponents scaling from 2.6 – 2.0, with increasing temperature from 5 to 30 °C. This suggests copolymer strands in solution become slightly more solvated with increasing temperature. This observation agrees with the slight increase in  $R_g$  of the unimer with increasing temperature.

**Table 5.4:** Porod exponents of unimer scattering in Region I of  $\omega=0.23$  17R4/D<sub>2</sub>O solution, determined through multiple analysis techniques. Notice the differences in values depending on the fit. Errors are reported at 99% level.

Temperature (°C)	m, Linear Porod Fit	m <sub>2</sub> , Correlation Length Model	m, Guinier-Porod Model
15.5 ± 0.1	2.23 ± 0.12	3.1 ± 0.1	0.595 ± 0.009
24.9 ± 0.1	2.08 ± 0.10	2.60 ± 0.05	0.91 ± 0.09
29.8 ± 0.1	1.97 ± 0.07	2.33 ± 0.03	1.11 ± 0.03

Table 5.5 displays the absolute scattering intensity of the chain in solution, as well as the background scattering intensities. These values were determined through the correlation length model. Note that the background scattering is very close in value to the absolute scattering from the unimer chains in solution. This causes difficulty in determining reliable fits at these temperatures, and may explain the differences in Porod exponents observed through the various techniques used here.

**Table 5.5:** Absolute and background scattering intensities of  $\omega=0.23$  17R4/D<sub>2</sub>O solution in Region I. These results are from the correlation length model. Errors are shown at 99%.

Temperature (°C)	Absolute Scattering Intensity, C (cm <sup>-1</sup> )	Background Scattering Intensity, B (cm <sup>-1</sup> )
15.5 ± 0.1	0.321 ± 0.008	0.255 ± 0.003
24.9 ± 0.1	0.579 ± 0.007	0.243 ± 0.002
29.8 ± 0.1	0.943 ± 0.007	0.228 ± 0.001

To summarize, Region I of  $\omega=0.23$  solution contains unimers in solution that are most likely linked at various PPO blocks, causing a strong clustering of the unimers. The length scale of the cluster lies outside of the SANS detection limit. The unimer size is found to be 10-12 Å.

*SANS of  $\omega=9.5 \times 10^{-3}$  and  $\omega=0.11$  solutions*

Scattering data were also taken in Region I for  $\omega=9.5 \times 10^{-3}$  and  $\omega=0.11$  solutions. Neither of these solutions exhibits a clear Region II. Instead, with an increase of temperature, these solutions move directly from Region I to Region III (See Figure 5.12). SANS scattering from these solutions show that the solutions do not enter Region II. Rather, phase separation occurs at temperatures immediately



following those at which Region I scattering occurred. Phase separation was indicated as the appearance of an  $S(Q)$  peak signifying interparticle interactions as the solutions separated.

Scattering from the  $\omega=0.11$  solution is shown in Figure 5.18. The solution contains unimers and clusters at 11.9 and 30.6 °C, similar to the scattering seen in Region I of the  $\omega=0.23$  solution. Scattering data were fitted with the correlation length model. Fit results are shown in Table 5.6. At 49.3 °C, phase separation has begun in the solution and cluster scattering is still present. This suggests that the clusters also exist in one of the separated phases.

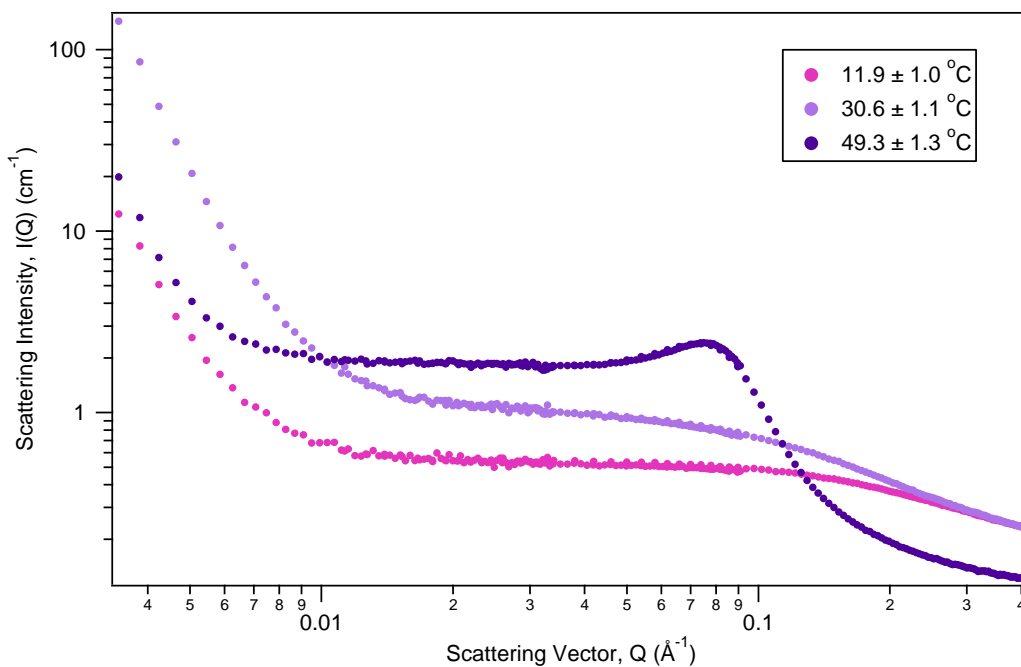


**Figure 5.18:** SANS data from  $\omega=0.11$  solution at 11.9, 30.6, and 49.3 °C, shown in pink, maroon, and red, respectively. Clusters and unimers are present at 11.9 and 30.6 °C. Phase separation is apparent at 49.3 °C, as indicated by  $S(Q)$  peak. Clusters appear to exist even into phase separation.

**Table 5.6:** Correlation length model fitting parameters for  $\omega=0.11$  sample in Region I. \*Radius of gyration determined from correlation length found through fit to model. All uncertainties are 99%.

Temperature (°C)	Cluster Porod Exponent, $m_1$	Radius of Gyration (Å)*	Unimer Porod Exponent, $m_2$
11.90 ± 1.0	3.20 ± 0.05	7.8 ± 0.1	2.42 ± 0.07
30.60 ± 1.1	3.59 ± 0.03	13.06 ± 0.07	2.11 ± 0.03

The very dilute  $\omega=9.5 \times 10^{-3}$  solution displayed slightly different scattering in Region I (Figure 5.19). At lower temperatures, no significant scattering from a cluster formation was observed, indicating that unimers exist freely in solution. At these temperatures, there is a great deal of error in low-Q scattering and so the Q-scaling in this region may be suspect. Unimer scattering was fitted with the two-region Guinier-Porod model, and results are in Table 5.7. At 40 °C, scattering from a larger aggregate in solution appears distinctly, along with the unimer scattering. It is assumed that this low-Q scattering is the beginning of clustering. Fitting of this low-Q scattering with the two-region Guinier-Porod model resulted in an intermediate Q-scaling,  $n$ , near one. This suggests this large body has a cylindrical structure. Only the  $R_g$  associated with the cross-section of this cylinder fell within the SANS window, and this  $R_g$  had a value of  $\sim 217$  Å. This information may give some insight into the general dimensions of clusters at other concentrations. As no  $R_g$  of the cluster fell within the SANS window at other concentrations, it is believed that the dimensions of the clusters grow with increased concentration. At  $49.3 \pm 1.3$  °C, a Bragg peak appeared in the data, signifying phase separation in the sample.

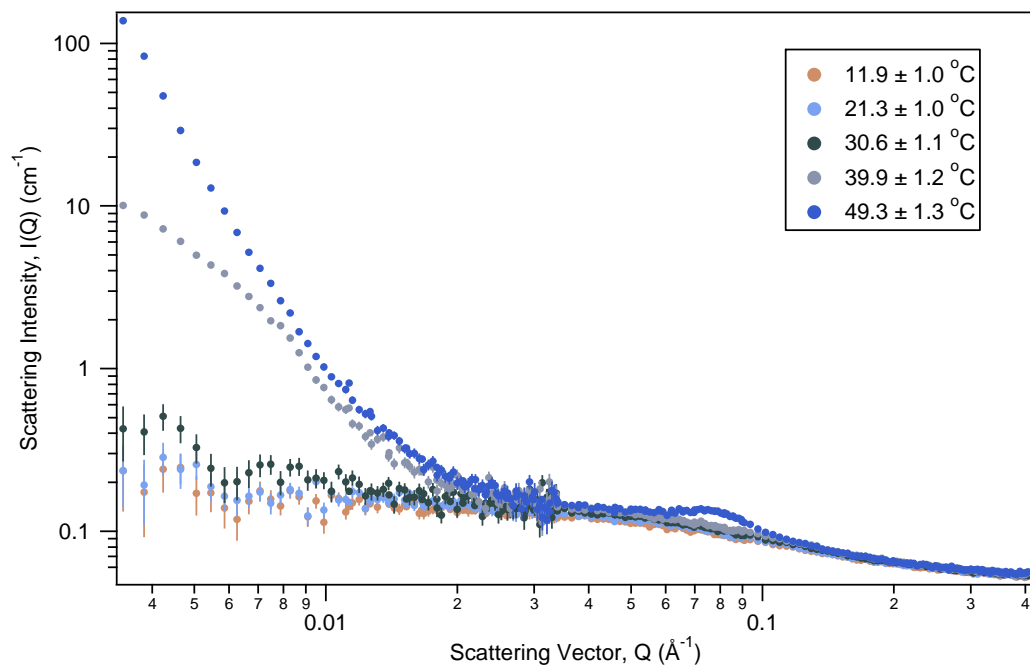


**Figure 5.19:** Region I scattering from  $\omega=9.5 \times 10^{-3}$  17R4/D<sub>2</sub>O solution. Unimer scattering is apparent at all temperatures, while clustering only becomes very apparent at 40 °C.

**Table 5.7:** Two-region Guinier-Porod model fit results to  $\omega=9.5 \times 10^{-3}$  sample. Data at 11.9-30.6 °C were modeled over the entire Q-range. The cluster and unimer scattering at 39.9 °C were modeled separately. The Porod exponent of the cluster was held at 4. Uncertainties are reported at the 99% level.

								Unimer		Cluster						
		11.9	±	1.0	21.3	±	1.0	30.6	±	1.1	39.9	±	1.2	39.9	±	1.2
Temperature	°C															
Guinier Scale, G		0.047	±	0.002	0.047	±	0.002	0.038	±	0.002	0.027	±	0.001	0.06	±	0.03
Intermediate Q-scaling*, n		0.18	±	0.04	0.19	±	0.04	0.27	±	0.04	0.39	±	0.04	0.9	±	0.3
Radius of Gyration, R <sub>g</sub>	Å	12.5	±	0.8	12.5	±	0.8	11.3	±	0.7	9.8	±	0.6	220	±	40
Porod Exponent, m		1.2	±	0.1	1.2	±	0.1	1.3	±	0.1	1.5	±	0.2	4	±	0
Background, B	cm <sup>-1</sup>	0.045	±	0.002	0.045	±	0.002	0.047	±	0.002	0.048	±	0.002	0.15	±	0.01

### *Comparison of clusters in different concentration solutions*

Clusters of copolymer chains exist in Region I of each of the different copolymer concentration solutions. When compared, clusters in each of these solutions are similar (Figure 5.20). Clusters in lower concentrations solutions exhibit less scattering intensity. However, a decreased scattering intensity is indicative of the lower solution concentration. This is especially true with the  $\omega=9.5 \times 10^{-3}$  concentration sample. This sample displays much less background and overall scattering intensities.

It is interesting that for the  $\omega=9.5 \times 10^{-3}$  solution, the most dilute solution measured, clusters are smaller than in the other solutions. In the most dilute solution, one scattering axis is small enough to lie within the SANS data window. It is believed that these clusters must become larger with greater copolymer concentration.

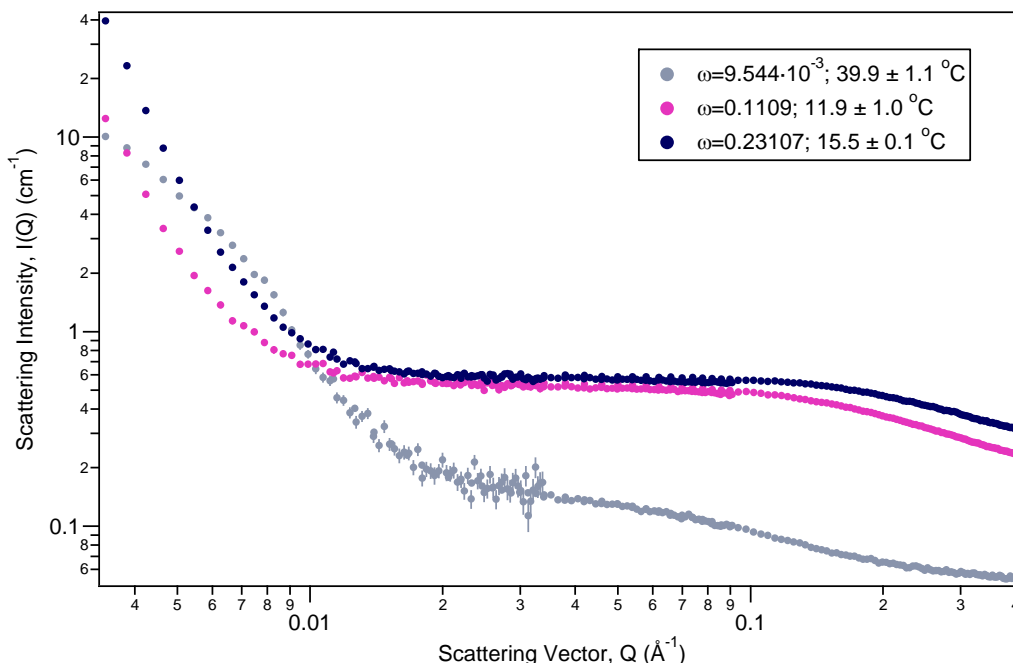


**Figure 5.20:** Comparison of Region I clusters from  $\omega=9.5 \times 10^{-3}$ ,  $\omega=0.11$ , and  $\omega=0.23$  17R4/D<sub>2</sub>O solutions. Scattering from the  $\omega=9.5 \times 10^{-3}$  solution has much less intensity due to the overall solution concentration. Also, clusters in this solution are smaller than those in the other solutions. Scattering from clusters in  $\omega=0.11$  and  $\omega=0.23$  solutions are similar.

### *Summary of Region I*

At the lowest concentrations and temperatures, 17R4 exists as unimers in solutions of D<sub>2</sub>O. These unimers were measured to have a radius of gyration of approximately 4-12 Å. Unimer dimensions were seen to vary depending on solution concentration, temperature, and the method of data analysis. It is imperative to note that the length scale of these unimers lies at the edge of the SANS detection limit, and thus to take these sizes only as approximations.

As temperature and concentration are increased, PPO becomes less soluble and clusters appear in solution. High-intensity scattering at low-Q ranges indicates cluster formation in solution. It is thought that these clusters are formed as insoluble

PPO blocks group together to avoid D<sub>2</sub>O interactions, and PEO blocks continue to be hydrated in the solvent, as they were in the unimer phase. These clusters appear to grow larger with increased concentration.

### 5.4.3 Results and discussion, Region II

#### *Rheometry of $\omega=0.23$ 17R4/D<sub>2</sub>O sample*

The zero-shear viscosity of a  $\omega=0.23$  17R4/D<sub>2</sub>O solution was determined to be  $10.3 \text{ cP} \pm 0.3 \text{ cP}$  at both 35 and 40 °C. Figure 5.21 displays the viscosity of the solution at these temperatures as a function of shear rate. The zero-shear viscosity is the average of these viscosities, and is shown as a line in the figure. Note that the zero-shear viscosity of Region II is slightly less than that of Region I:  $10.3 \pm 0.3 \text{ cP}$  and  $12.5 \pm 0.5 \text{ cP}$ , respectively. This suggests there are more interactions and connectivity among copolymers in Region I.

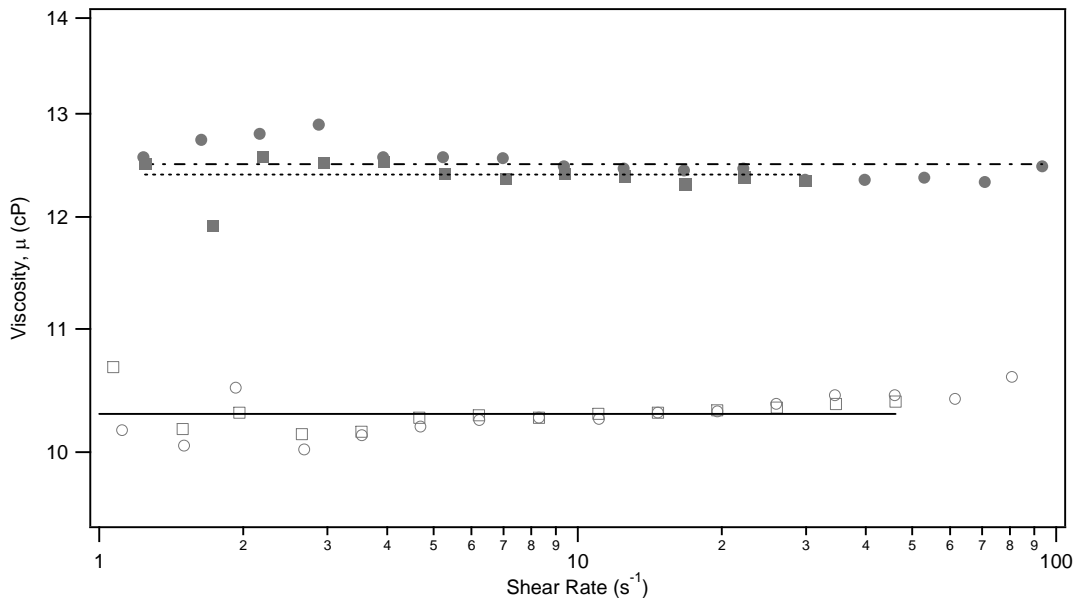


**Figure 5.21:** Determination of zero-shear viscosity for  $\omega=0.23$  17R4/D<sub>2</sub>O solution in Region II at (○) 35 and (□) 40 °C. The average zero-shear velocity for this region is 10.3 cP, shown in the figure by a black line. Region I data are shown for comparison: (●) 25 °C, (■) 30 °C. The zero-shear viscosities are shown as lines at 12.5 cP and 12.4 cP for 25 °C and 30 °C, respectively.

*Dynamic light scattering of  $\omega=0.23$  17R4/D<sub>2</sub>O sample*

Light scattering performed in Region II showed scattering from both unimers and aggregates in solution. Scattering was measured five times at each temperature. The position and mean hydrodynamic radii values from all iterations were averaged. These average  $R_h$  values are reported in Table 5.8. The error of the peak position was based off a 10% uncertainty in each  $R_h$  value, and was determined as described in Chapter 2. DLS analyses of each data collection, as obtained from the DynaLS software using optimal resolution, are reported in Appendix C.3.



**Table 5.8:** Region II DLS results for scattering corresponding to unimers and aggregates in  $\omega=0.23$  17R4/D<sub>2</sub>O solutions. a: Uncertainty in temperature is  $\pm 1$  °C. Errors are given as 99%.

Temperature	°C <sup>a</sup>	35	39
Mean Signal Intensity	Hz	8565	22387
Unimer	Peak Area	-	0.273
	Mean	Å	3.0
	Position	Å	2.8
	Error of Position	Å	0.1
Spherical Micelle	Peak Area	-	0.118
	Mean	Å	35
	Position	Å	30
	Error of Position	Å	4

*Small angle neutron scattering of  $\omega=0.23$  17R4/D<sub>2</sub>O sample*

Scattering from the  $\omega=0.23$  17R4/D<sub>2</sub>O solution at 34.7 and 39.2 °C is shown in Figure 5.22. These data display no high-intensity scattering at low-Q, an important difference in scattering from that in Region I. Scattering intensity reaches its maximum intensity in the mid-Q range, suggesting scattering from an object of moderate size. Lack of scattering peaks suggests that solutions are dilute, without much particle interaction.

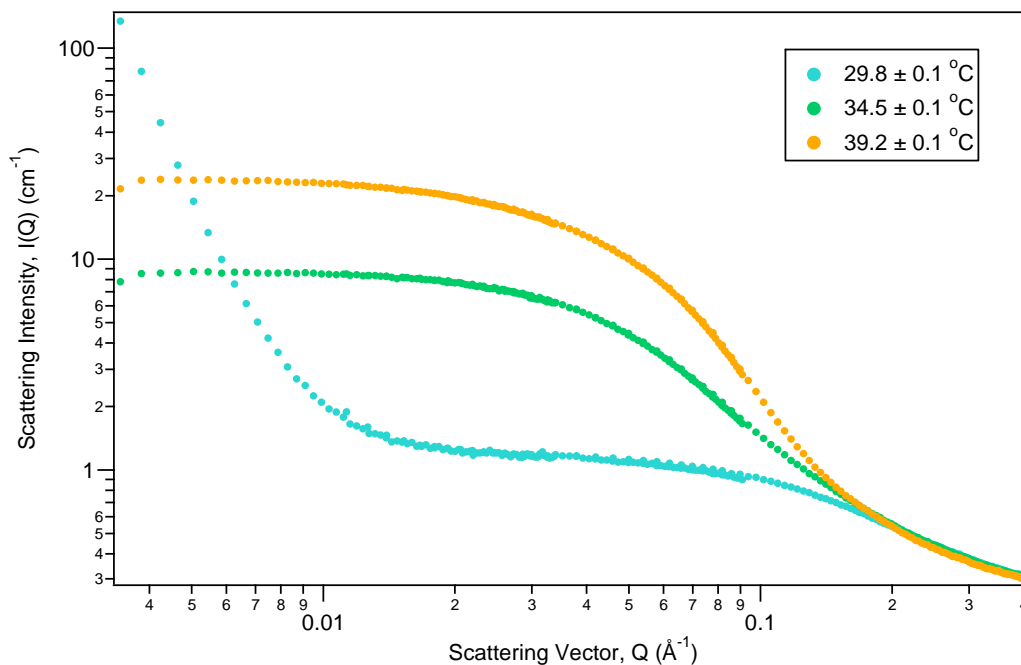


**Figure 5.22:** Neutron scattering within Region II of  $\omega=0.23$  17R4/D<sub>2</sub>O sample. Region I scattering at  $29.8 \pm 0.1$  °C is included to show the abrupt change in scattering between  $29.8$  and  $34.5$  °C.

Scattering in Region II appears to be due to spheres in solution, as there is little-to-no  $Q$ -dependence at the intermediate- and low- $Q$  range. Lack of high-intensity at low- $Q$  indicates that the clusters have been disrupted in solution and broken apart. Interestingly, the disappearance of these clusters does not seem to be gradual, as observed with 25R8.<sup>78</sup> At  $29.8$  °C, the cluster scattering is present, while at  $34.5$  °C this scattering has disappeared completely. It is possible that a decrease in clustering does occur over a short temperature range between  $29.8$ - $34.5$  °C. However, network scattering was observed in 25R8 in D<sub>2</sub>O well into the micelle region, and was taken to indicate a micellar network. It is clear that such a network is not present in Region II of this 17R4 solution.

Copolymer scattering shifts from the high-Q range in Region I to mid-Q range in Region II, indicating a larger scattering body. Scattering also grows in intensity in Region II. The near-zero Q-scaling at intermediate Q-values suggests spherical scattering particles. These characteristics suggest aggregation of unimers into larger bodies, such as micelles.

Scattering in Region II was fitted with the correlation length model, the two-region Guinier-Porod fit, and the linear Guinier and Porod plots. Example fits are shown in Figure 5.23. Radii of gyration determined through the correlation length, two-region Guinier-Porod, and linear Guinier fits show agreement (Table 5.9). The dimensions of the copolymer aggregates found through these analyses are very similar to the hydrodynamic radii found through DLS analyses (also see Table 5.9).

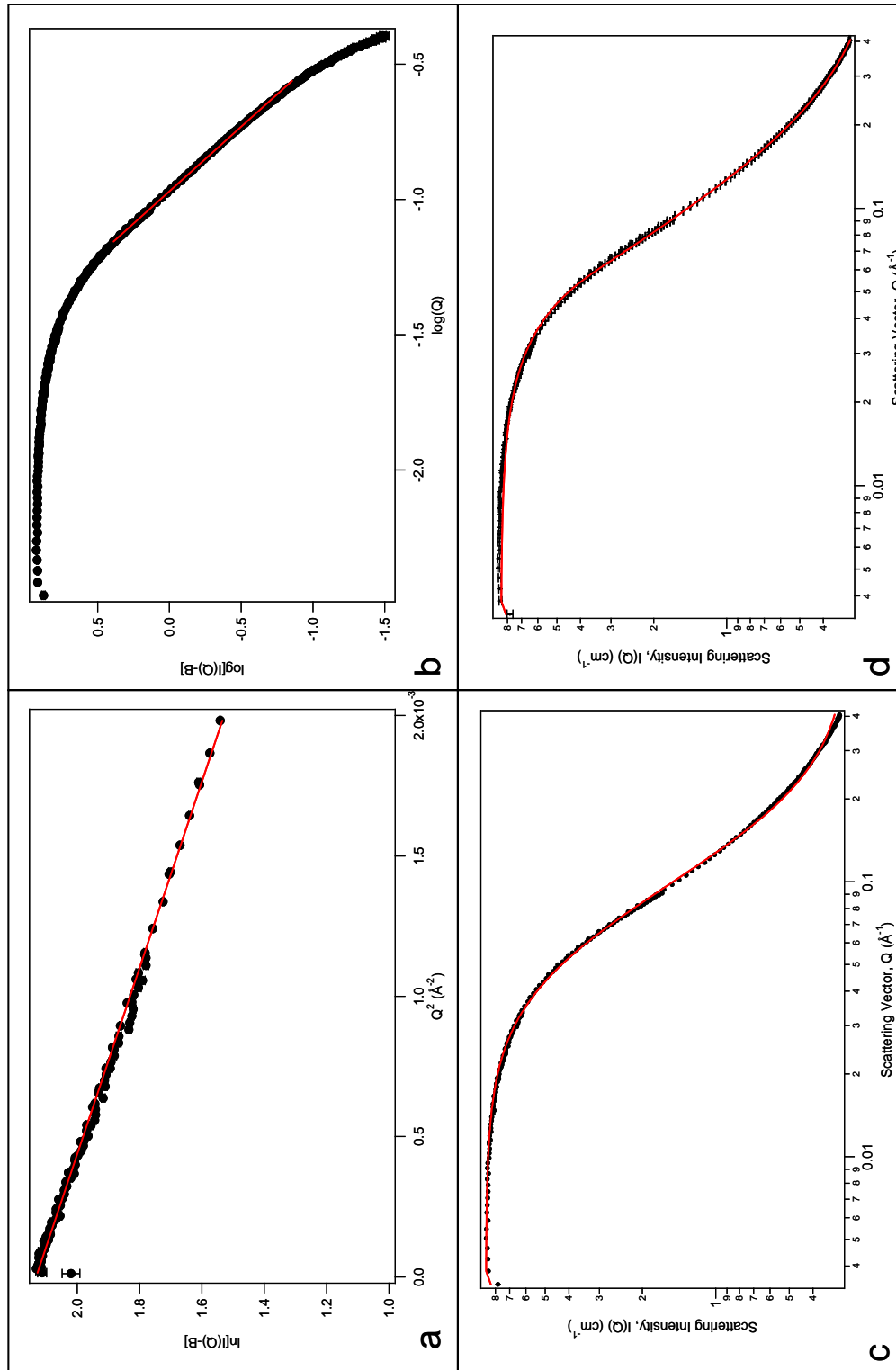


**Figure 5.23:** Example SANS analyses of  $\omega=0.23$  17R4/D<sub>2</sub>O sample with simple fits at 34.5 °C  $\pm$  0.1 °C. Fits include: (a) linear Guinier, (b) linear Porod, (c) correlation length, and (d) two-region Guinier-Porod. Analysis results at other temperatures, including reduced  $\chi^2$  values are located in Appendix C.3.

**Table 5.9:** Radii of gyration of copolymer aggregate in Region II of  $\omega=0.23$  solution. Determined through (a) linear Guinier fit, (b) correlation length model, and (c) two-region Guinier-Porod model. (d) Hydrodynamic radii, determined through DLS. 99% error is shown.

Temperature ( $^{\circ}\text{C}$ )	$R_g^a(\text{\AA})$	$R_g^b(\text{\AA})$	$R_g^c(\text{\AA})$	$R_h^d(\text{\AA})$
34.5 $\pm$ 0.1	30.0 $\pm$ 0.1	36.35 $\pm$ 0.09	28.34 $\pm$ 0.05	30 $\pm$ 4
39.2. $\pm$ 0.1	33.69 $\pm$ 0.08	35.83 $\pm$ 0.04	29.69 $\pm$ 0.02	29 $\pm$ 1

Each of these models is for dilute solutions without interparticle interactions. Although analysis with these models gave good results, some deviations between data and models were observed in the Guinier-Porod model (Figure 5.24). This deviation increased upon temperature change from 34.5 to 39.2  $^{\circ}\text{C}$ . At low-Q values, scattering data display a slight Q-dependence, suggesting an elongation of the scattering particle.

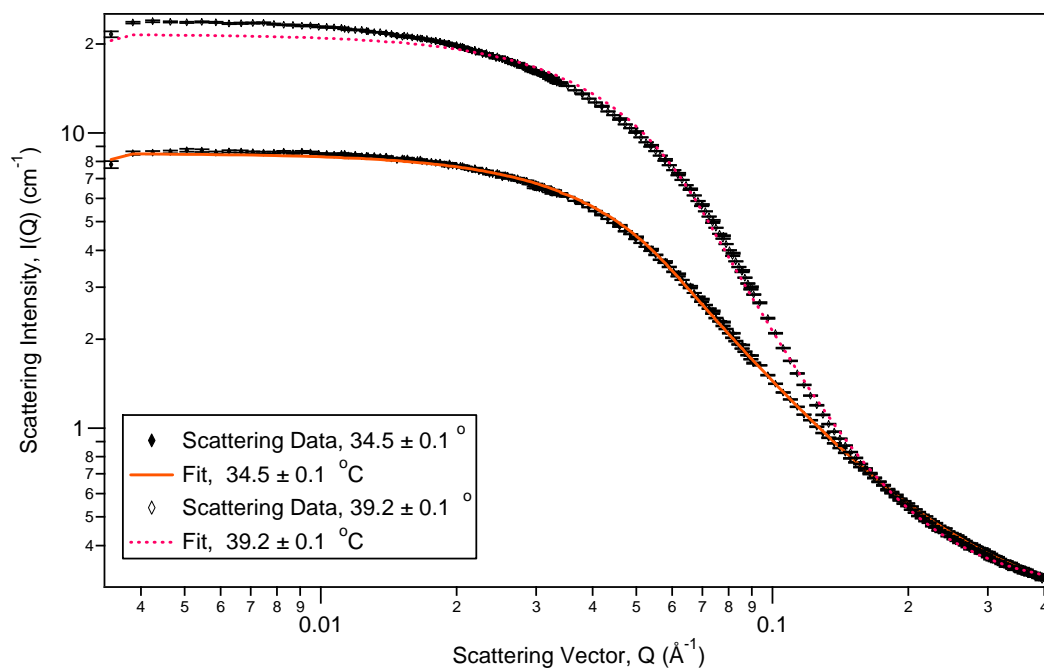


**Figure 5.24:** Scattering in Region II of  $\omega=0.23$  solution, fit with 2-region Guinier-Porod model. Notice deviation between fit and data at low-Q, indicating a second Guinier region within the data.

Analysis with the three-region Guinier-Porod model showed a better fit to the data than nearly all previous fits, based on  $\chi^2$  values. Only the linear Guinier model at 34.5 °C has a lower  $\chi^2$  value than the three-region Guinier-Porod model at this temperature. The three-region Guinier-Porod model has lower  $\chi^2$  values than all previous models at 39.2 °C. This signifies that the particle is not perfectly spherical. At 39.2 °C, for example, the reduced  $\chi^2$  of the two-region fit is approximately 15, while that of the three-region fit 4.8. It is acknowledged that the reduced  $\chi^2$  of the three-region fit is still large, however, it is better than the two-region, and so it is used here. Figure 5.25 displays the three-region Guinier-Porod models fit to the Region II data. Results of the three-region Guinier-Porod model are shown in Table 5.10.

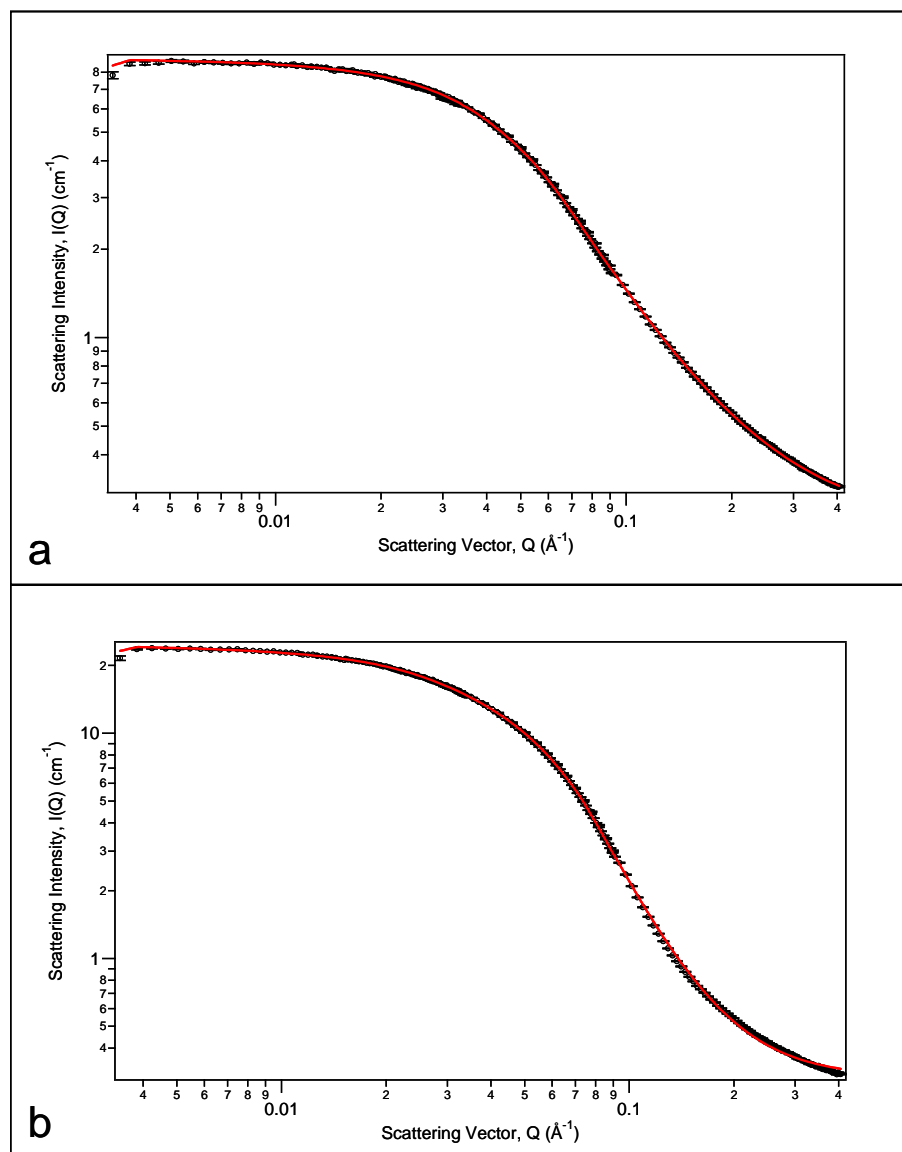


**Figure 5.25:** Region II data of  $\omega=0.23$  17R4/D<sub>2</sub>O solution at (a)  $34.5 \pm 0.1$  °C and (b)  $39.2 \pm 0.1$  °C, fit by the three-region Guinier-Porod model. The three-region Guinier-Porod model was determined to be a better fit than the two-region model through both visual inspection of the fits and reduced  $\chi^2$  values.

**Table 5.10:** Results from  $\omega=0.23$  solution in Region II analyzed with three-region Guinier-Porod model; error is 99%.

Temperature	°C	34.5	±	0.1	39.2	±	0.1
Guinier Scale, G	-	8.1	±	0.3	20.9	±	0.8
Intermediate Q-scaling 2, $n_2$	-	29.5	±	0.4	35.1	±	0.7
2nd Radius of Gyration $R_{g2}$	Å	0.011	±	0.008	0.026	±	0.008
Intermediate Q-scaling 1, $n_1$	-	20.9	±	0.9	24.2	±	0.1
1st Radius of Gyration, $R_{g1}$	Å	0.40	±	0.06	0.286	±	0.008
Porod Exponent, m	-	1.94	±	0.01	3.065	±	0.008
Background, B	cm <sup>-1</sup>	0.233	±	0.002	0.30	±	0.01

The three-region Guinier-Porod fits also indicate that a spherical scattering particle should not be assumed in Region II. The intermediate-regime exponents,  $m_1$ , determined with this fit are slightly greater than zero at both 34.5 and 39.2 °C. This suggests a slight elongation of the particle, from a sphere to an ellipsoid. Although this elongation is observed, the first radius of gyration of the ellipsoid is similar to the  $R_g$  values determined via the dilute solution fits, which assumed a spherical body (Table 5.9). Similarity among these values indicates reliability in estimates of particle dimension. Fits that assume a spherical scattering body are also important to compare to DLS analysis, which also assumes a spherical body. It is difficult to convert these  $R_g$  values to radii and length values because of the ellipsoidal nature of the particle.

It is important to note that all determined particle dimensions appear to be rather small for micelle formation. For example, the Pluronic L64, PEO<sub>13</sub>PPO<sub>30</sub>PEO<sub>13</sub>, has a micelle size of 102 Å.<sup>80, 82</sup> Also, the scattering data could not be fitted by core-shell models (both spherical and oblate bodies were attempted), usually used to model micelle scattering. When the model parameters were kept within physical ranges, the models fitted the scattering data poorly. One would



assume that the expected flower-type micelles of the Reverse Pluronic would scatter in this typical core-shell pattern, but scattering from such flower-type micelles has been shown to require a more involved fit.<sup>99</sup> Therefore, it is suspected that this scattering does not represent a typical core-shell spherical micelle.

Although it is difficult to claim that micelles are formed in Region II, it is apparent that an aggregate of some sort is formed by the copolymer in solution. Porod exponents,  $m$ , (Table 5.11) around two at 34.5 °C and near three at 39.2 °C indicate copolymer chains are probably grouping and collapsing together, forming a very dense mass fractal or very rough surface fractal near 40 °C. If the approximate volume of one copolymer chain is compared with the spherical volume of  $2.7 \times 10^5 \text{ \AA}^3$ , calculated using an rough radius of gyration of 30 Å (based on the  $R_g$  values in Table 5.9), then the approximate number of 17R4 chains in this aggregate can be determined (See Appendix C.2 for calculations). This estimates that about sixty 17R4 chains have come together to form an aggregate in Region II. This calculation assumes no D<sub>2</sub>O molecules are held within the aggregate. The number of chains contained within this aggregate is certain to differ given an elliptical form or the addition of D<sub>2</sub>O molecules within the aggregate, but this is a good estimate and clearly indicates that the scattering in Region II is not from unimers in solution.

**Table 5.11:** Porod exponents,  $m$ , of copolymer aggregates from  $\omega=0.23$  17R4/D<sub>2</sub>O solution in Region II. Errors are given at the 99% level.

Temperature (°C)	$m$ , Linear Porod Fit	$m_2$ , Correlation Length Model	$m$ , 3-Region Guinier-Porod
34.5 ± 0.1	2.093 ± 0.005	2.427 ± 0.006	1.94 ± 0.01
39.2 ± 0.1	2.975 ± 0.005	3.115 ± 0.005	3.065 ± 0.008

### *Reversibility of aggregation*

The  $\omega=0.23$  17R4/D<sub>2</sub>O solution was heated into the two-phase region (Region III) and then cooled back to 25.1 and 6.7 °C. Scattering data indicated that phase separation in Region III and the aggregate formation in Region II are reversible. Clusters reform in solution upon cooling into Region I. This reversibility of aggregation formation is shown in Figure 5.26.

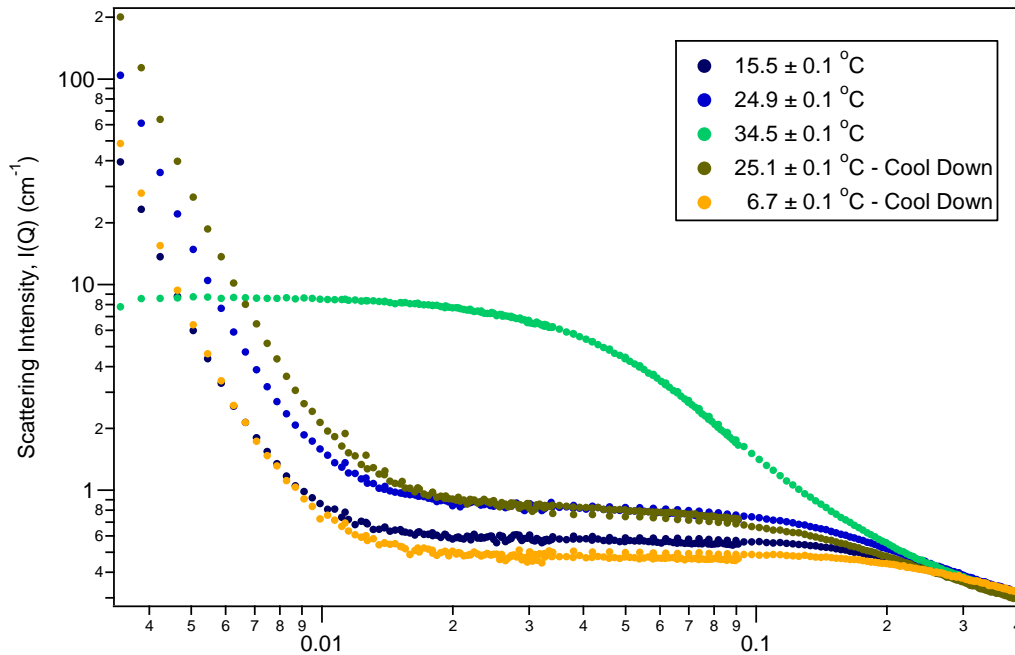


**Figure 5.26:** The  $\omega=0.23$  17R4/D<sub>2</sub>O sample was heated through each of the regions in the phase diagram. The solution was heated to 44.0 °C and then brought back to 25.1 °C. It was then cooled even further to 6.7 °C. Although the solution was phase separated at 44.0 °C, no signs of separate phases persist at 25.1 °C during the cool-down (this would be noted by structure factor peaks in scattering data). Also, it is apparent that aggregates from Region II do not persist, and clusters reform in Region I.

### *Summary of Region II*

As the 17R4/D<sub>2</sub>O solution enters Region II, SANS data for the  $\omega=0.23$  solution indicate that clusters break down and copolymers form ellipsoidal

aggregates. Zero-shear viscosities of the  $\omega=0.23$  solution in Region II are slightly less than those in Region I. This also indicates that there are fewer interactions among copolymers in Region II, i.e. that clusters have broken down.

It is unclear whether aggregates in Region II are micelles. DLS and SANS analyses result in similar dimensions of these copolymer aggregates in Region II ( $R_g \sim 30 \text{ \AA}$ ). The small size of the scattering particles and the failure of traditional “core-shell” models to describe the SANS scattering data suggest that micelles have not formed in solution. Instead, the copolymers seem only to aggregate in an unorganized manner, perhaps on the way to becoming micelles.

## 5.5 Summary

The Reverse Pluronic 17R4 displays three distinct regions of solution characteristics in  $D_2O$ , depending on concentration and temperature. The one-phase region was examined by SANS, DLS, and rheometric techniques. The transitions between regions were examined by visual observations. The resulting phase diagram is very similar to that of Zhou and Chu<sup>80</sup> for 17R4 in  $H_2O$  (Figure 5.27). This is in spite of the possible contamination and impurity of the commercially available Pluronic-R copolymers.<sup>6</sup> The phase separation curve of 17R4/ $D_2O$  has similar curvature to the cloud-point curve of 17R4/ $H_2O$ . The curve in  $D_2O$  does occur at lower temperatures than that in  $H_2O$ . This is not unexpected. Similar results have been seen in other systems when  $H_2O$  was replaced with  $D_2O$  as the solvent.<sup>25</sup>

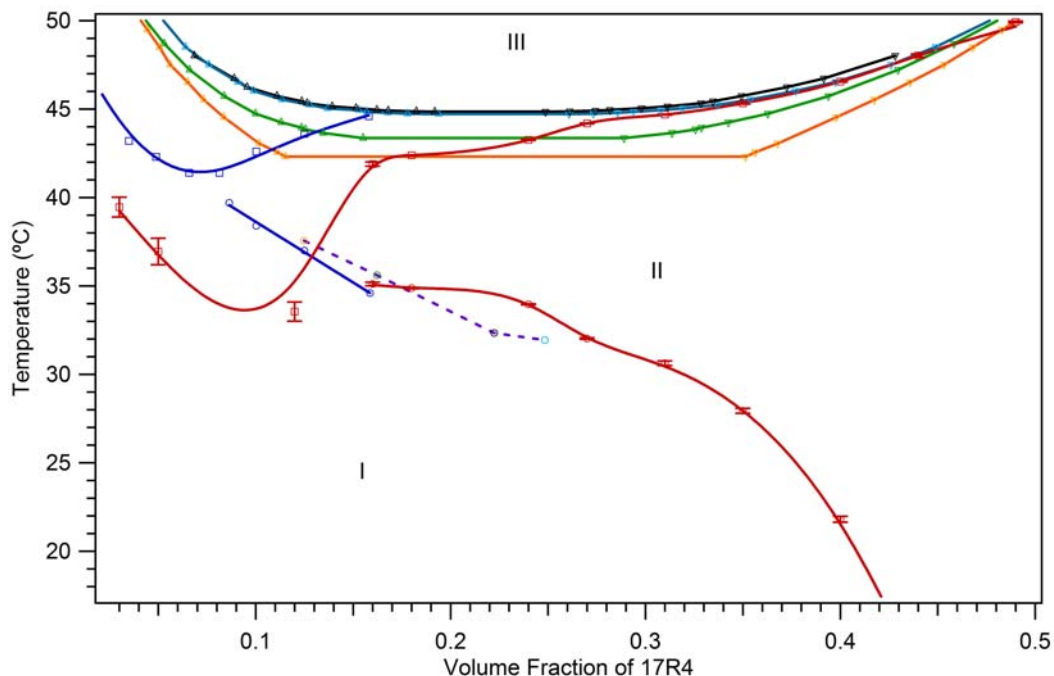


**Figure 5.27:** Phase diagram of 17R4/D<sub>2</sub>O determined here (red), compared with those of 17R4/H<sub>2</sub>O determined by Zhou and Chu (blue)<sup>80</sup> and Jacobs et al. ( $\phi=0.125$  is in orange;  $\phi=0.163$ , green;  $\phi=0.226$ , black, and  $\phi=0.246$ , light blue).<sup>83</sup> Squares and circles represent the cloud-point curves and aggregation curves, respectively. Upper triangles represent the upper phase of the coexisting phases, while upside down triangles are the lower phase. The purple dashed line is the aggregation curve, determined by Jacobs et al. All lines are shown to guide the eye, and do not represent lines of best fit.

There are differences when these curves are compared to the coexistence curve of the 17R4/H<sub>2</sub>O system, determined by Jacobs et al.<sup>83</sup> Jacobs et al. examined coexisting phases at multiple temperatures, determining the concentration of both phases at each temperature. This is in contrast to the techniques used here and by Zhou and Chu, where only the temperature of phase separation was determined per solution concentration. Jacobs et al. observed a different coexistence curve with each solution concentration examined. It is suspected that a non-equilibrium state occurs in these solutions following the aggregate formation in Region II. This continues to be examined by Jacobs et al.

The 17R4/H<sub>2</sub>O cloud-point curve and the coexistence curves intersect at the same concentration and temperature. Currently, the coexistence curves of 17R4/D<sub>2</sub>O solutions are also being determined.<sup>83</sup> It is expected that this solution will also show multiple curves, and that these curves will intersect with the phase separation curve that was determined here. At high concentrations, the D<sub>2</sub>O cloud-point curve appears to align with the 17R4/H<sub>2</sub>O coexistence curves. It will be important to compare the D<sub>2</sub>O curves in this area as well. Finally, comparing the aggregation curves of 17R4 in H<sub>2</sub>O and D<sub>2</sub>O solutions, aggregation appears to occur at extremely similar temperatures in each system. This suggests little solvent isotope effects on aggregate formation.

Each region of the 17R4/D<sub>2</sub>O solution offers different copolymer configurations. Cartoon visuals of each of these are shown in Figure 5.28. Within Region I, at low temperatures and concentrations, solutions appear turbid and  $\omega=0.23$  solutions have a viscosity more than 10 times that of water. SANS scattering from  $\omega=0.23$  and  $\omega=0.11$  solutions exhibited two distinct scattering regions: that of a large “cluster” and that of copolymer unimers in solution. SANS experiments suggest that copolymer unimers exist in this region as clusters. It is assumed that these unimers are “tethered” together at the PPO blocks. In this way, these blocks minimize interactions with the solvent. The size of these clusters could not be determined through SANS, as they are larger than the SANS detection limit. Interestingly, in the lowest concentration examined,  $\omega=9.5 \times 10^{-3}$ , unimers existed alone in solution at temperatures below 39.2 °C; clusters were observed to appear as temperature was increased. Unimer chains were found to have an  $R_g$  of  $\sim 4-15 \text{ \AA}$ , varying slightly with

temperature and concentration. A more precise measurement at low temperatures could not be made because this structure is also at the limit of SANS detection.

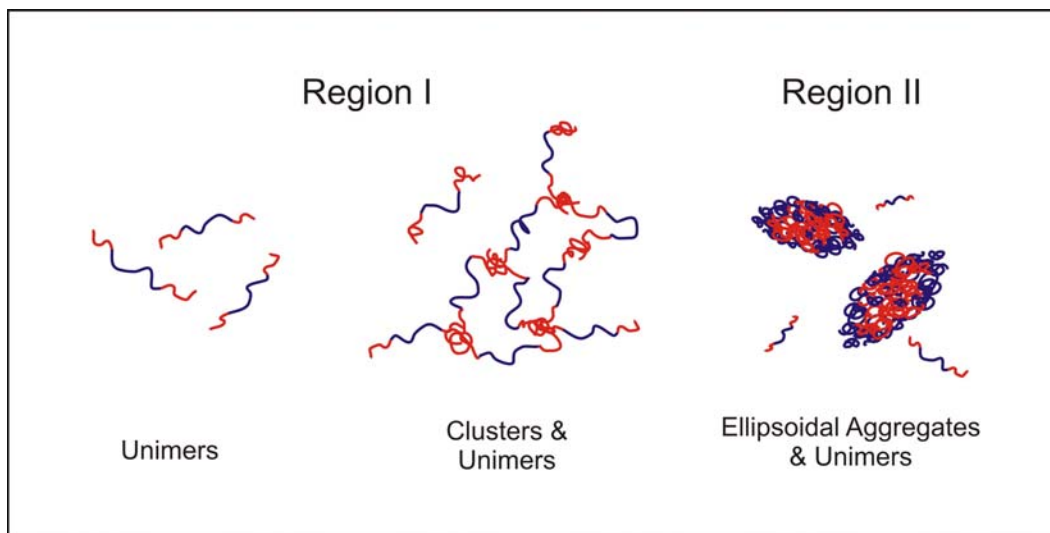


**Figure 5.28:** Cartoon visuals of each copolymer configuration. In each structure, blue represents PEO and red represents PPO blocks. In Region I, free unimers and clusters were observed. It is unknown whether unimers coexist in solution with clusters, as is depicted. Ellipsoidal aggregates with unimers were observed in Region II.

Clusters in this region are similar to those presented by Mortensen et al.<sup>78</sup> It is believed that this network is the cause of turbidity in the sample. The clearing of turbid solutions by Zhou and Chu<sup>80</sup> through filtration was not reproduced by either Jacobs et al.<sup>83</sup> or in this work. This turbidity prevented the use of DLS techniques within Region I. It is suspected that filtration by Zhou and Chu caused the disruption of the unimer networks in solution. If DLS measurements were taken quickly following filtration, it would be possible to follow the formation of aggregates with this technique. It is unclear why this filtration disrupted clusters in Region I in the work by Zhou and Chu, but was not able to be replicated. Zhou and Chu made no

mention of whether the sample eventually re-clouded over time. A study by Ho et al. examined a similar situation of cluster disruption in PEO/water.<sup>96</sup> Clusters in PEO/water solutions could be broken by filtration, but reformed within 24 hours. Because of the inability to replicate the clearing observed by Zhou and Chu, it is not believed that impurities and “anomalous micellization” cause this turbidity.

The solution of 17R4 in D<sub>2</sub>O is a very dynamic system. This clouding is observed to dissipate over time and film formation is seen at the air-solvent interface. This suggests that the system has a long true equilibrium time, and so it is difficult to be certain that any measurements taken are on an equilibrated system.

At intermediate concentrations and temperatures, a rapid change in solution appearance is observed. The turbid solution of Region I quickly clears upon entering Region II. DLS and SANS data suggest similar sizes of aggregates in solution. SANS analyses indicate that the aggregates may have a slightly ellipsoidal shape, and the radius of gyration associated with the length of the aggregate is similar in value to the hydrodynamic radius found through DLS techniques,  $\sim 37$  Å and  $\sim 32$  Å, respectively (averaged from results at 34.5 and 39.2 °C for SANS and 35 and 40 °C for DLS results).

DLS results indicate that unimers are still present in solution in Region II ( $R_h \sim 6$  Å). Unimers were not observed in Region II from the SANS data, but it is possible that scattering from the unimers was overshadowed by scattering from aggregates. That is, the scattering peak of the unimer would have been within the Porod regime of the aggregate scattering intensity. The small presence (only 2-9 % of total scattering peak area by DLS) of unimers in solution may cause such scattering

to be hidden by the more dominant aggregate. It is probable that such unimers do exist in solution with aggregates, as is the case with micelle solutions.<sup>9</sup>

Mortensen et al. observed networking into the micelle region, as well as a very strong interaction peak, suggesting a network of interconnected micelles in solutions of 25R8 and D<sub>2</sub>O.<sup>78</sup> However, cluster scattering is observed to dissipate completely in Region II of 17R4/D<sub>2</sub>O. This indicates that aggregates form and are not interconnected.

It is difficult to state that micelle formation has occurred within Region II of this system. Aggregate size and Porod exponents suggest that the unimers are coming together to form multi-chain aggregates. It is possible that such aggregates are the start of micelle formation. The inability to fit any core-shell model to the data also suggests that these aggregates are not true micelles. At the highest concentration examined here,  $\omega=0.23$ , the close vicinity of the aggregation and phase separation temperatures causes a highly interactive and possibly non-equilibrated system. It is possible that micelles may form at higher concentrations.

It would be intriguing to look more closely at the cluster network within Region I. Both the overall dimensions and the gradual formation of the cluster are interesting. Examination of the overall cluster configuration would require a different scattering technique, such as ultra small angle neutron scattering (USANS) in order to observe cluster dimensions at larger length scales. Hainbuchner et al. examined the gradual decrease of cluster scattering intensity between the unimer and micelle phases of Reverse Pluronic 25R4 through USANS and SANS techniques.<sup>100</sup> It would also be possible to examine the disappearance of the clusters between Regions I and II of the



17R4/D<sub>2</sub>O system by investigating SANS scattering at smaller temperature increments. This would determine if there is an abrupt formation of aggregates and loss of clusters, or if this is a gradual process.

Further examination of a 17R4/D<sub>2</sub>O sample in Region II is required for better interpretation of the aggregate formation. Again, examining at smaller temperature intervals may offer clues into the formation of these structures. Use of deuterium-substitution in one block of the copolymer may also aid in better determining the locations of blocks within aggregates. For example, matching the contrast factor of the PEO block with the solvent (H<sub>2</sub>O/D<sub>2</sub>O mixture) would cause only scattering from the PPO block to be observed. By doing this with both blocks and comparing results, a general indication of where each block resides can be formed. Because the scattering length densities of both blocks are so similar, it was not possible to obtain such a picture without this partial deuteration. Because an H<sub>2</sub>O/D<sub>2</sub>O solvent mixture would be needed for the technique, however, it is important to consider the changes such a solvent isotope exchange might cause.

## Chapter 6: Diblock Poly(ethylene oxide)-Polybutadiene in Organic Solvents

Micelle formation by block copolymers in organic solvents has been studied extensively. However, much of this work has been on styrene- or diene-based systems.<sup>5, 10, 12, 101</sup> As discussed in Chapter 1, micelles in organic solvents are formed through different driving forces than those in aqueous solutions. In these solvents, micelles tend to exist at low temperatures, and disassemble with increasing temperature: a characteristic opposite to that in aqueous systems.

### 6.1 Introduction

Poly(ethylene oxide)-polybutadiene (PEO-PB) copolymers have been thoroughly investigated in aqueous solutions.<sup>102-117</sup> Micelles, as well as vesicles, self-assemble in solutions of this copolymer at concentrations less than 18 weight percent.<sup>107, 109</sup> Jain et al. have observed spherical and worm-like micelles and even networks of worm-like micelles with connecting junctions.<sup>107-109</sup> At higher concentrations, such assemblies form packed morphologies, such as body-centered cubic phases.<sup>109</sup>

Jain et al.,<sup>107</sup> with Won et al.,<sup>114</sup> explored the self-aggregation of dilute (1 wt %) PEO-PB copolymers with 1,2-microstructure PB (that is, the PB blocks were

attached at the first and second carbons, leaving double bonded carbons three and four extending away from the copolymer backbone). The morphologies formed by PEO-PB in water were explored through cryo-transmission electron microscopy (CTEM), as a function of PB repeating units ( $N_{PB}$ ) and weight fraction of PEO ( $\omega_{PEO}$ ) in the diblock.<sup>107, 114</sup> The dependence of micelle and vesicle formations on these copolymer characteristics are reflected in the morphology diagram shown in Figure 6.1. For a copolymer with  $N_{PB} \approx 90$ , at  $\omega_{PEO} < \sim 0.34$ , bilayer vesicles are formed in aqueous solutions (1 wt % overall copolymer concentration). For the same  $N_{PB}$  and overall copolymer concentration, spherical micelles are formed at  $\omega_{PEO} > \sim 0.62$ . Between these PEO weight fractions, solutions with worm-like cylindrical micelles develop.

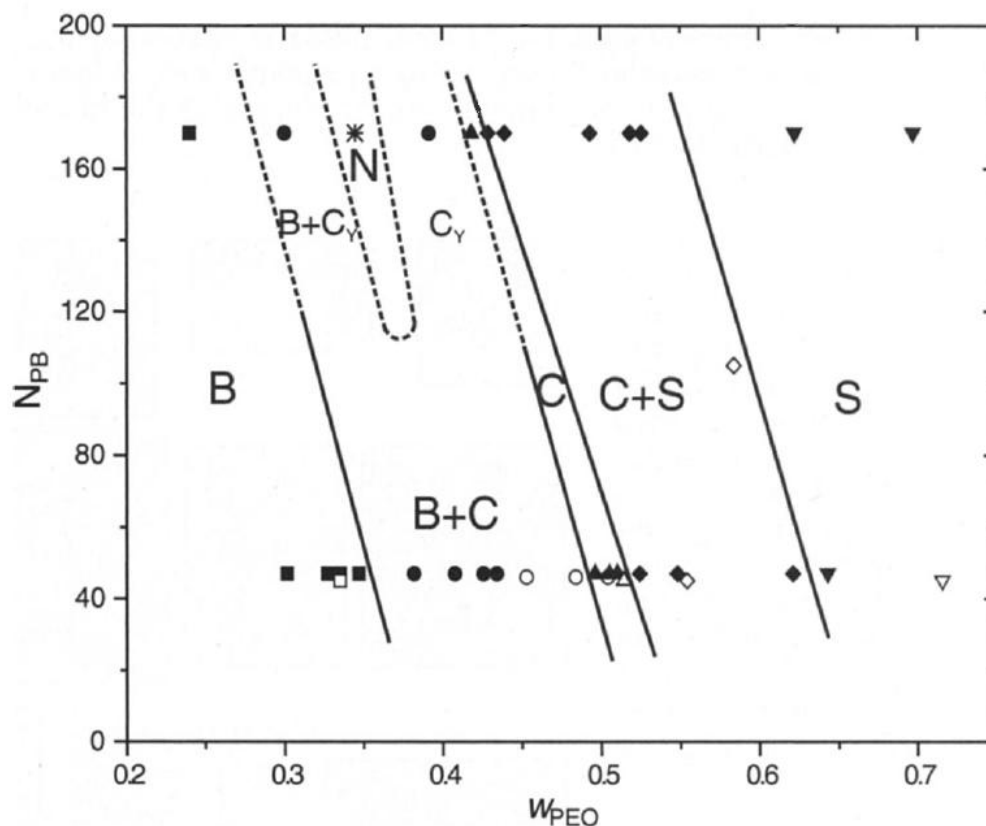


**Figure 6.1:** Self-aggregate morphologies formed in 1 wt % aqueous PEO-PB solutions, as a function of PB repeating units ( $N_{PB}$ ) and weight fraction PEO ( $w_{PEO}$ ), determined by Jain et al.<sup>107</sup> and Won et al.<sup>114</sup> Vesicle bilayers (B), worm-like cylindrical micelles (C), and spherical micelles (S) are formed. Cylindrical micelles with Y-junctions ( $C_Y$ ) also occur in copolymers with higher  $N_{PB}$ . A network (N) phase also appears which is accompanied by phase separation. Data determined by Jain et al. appears as filled symbols. Open symbols depict data from Won et al.

The aggregate formations of a PEO-PB copolymer with 50% weight fraction PEO ( $w_{PEO}=0.50$ ) were examined by Won et al.<sup>115</sup> through small angle neutron scattering, small angle x-ray scattering, and birefringence measurements. At solutions of less than 5% total copolymer, the copolymer forms worm-like micelles in solution (Figure 6.2a). The worm-like micelle phase was observed to continue to slightly higher concentrations at temperatures above 60 °C. Between 5 and 10 % copolymer, a nematic phase of linear cylindrical micelles exists. In this phase,

cylindrical micelles align in one direction. At concentrations above 10%, the cylinders pack into hexagonal packing structure. These solutions were not observed at temperatures lower than 25 °C, and no spherical micelles were observed. A CTEM image of the worm-like micelles in a 1 % copolymer solution is reproduced in Figure 6.2b.

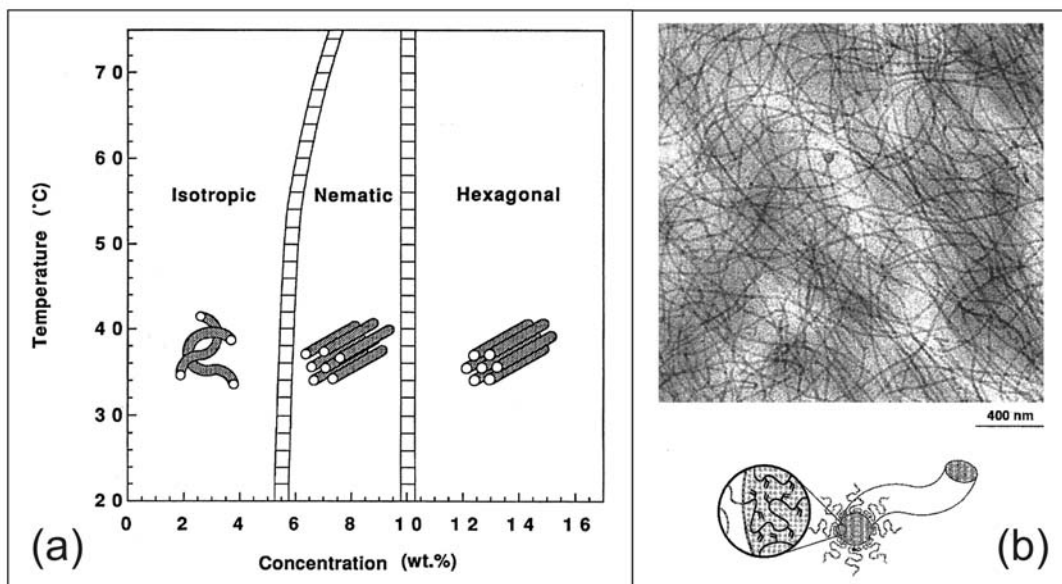


**Figure 6.2:** (a) Morphologies of PEO-PB/water solutions with  $\omega_{\text{PEO}}=0.50$ , determined by Won et al.<sup>115</sup> (b) CTEM image of worm-like cylindrical micelles in PEO-PB/water solutions (1% solution).<sup>115</sup>

Recently, Ploetz and Greer examined the PEO<sub>132</sub>-PB<sub>89</sub> block copolymer in organic solvents.<sup>118</sup> This is the only known investigation on this copolymer in non-aqueous solvents. Ploetz and Greer studied the micelle formation of this copolymer in methanol, cyclohexane, and the partially miscible solvent system of methanol-cyclohexane. The copolymer used by Ploetz and Greer contained PB with 1,4-

microstructures, and so the double bond of the PB is included within the copolymer chain as the PB units are connected at carbons one and four.

In methanol, the PEO<sub>132</sub>-PB<sub>89</sub> forms micelles with PEO residing in the shell and PB in the core of the micelle.<sup>118</sup> This configuration was verified using the nonpolar chiral probe, (-)- $\alpha$ -pinene. When this probe is placed in methanol, phase separation occurs, and a methanol-rich phase and pinene-rich phase result. The amount of pinene present in the methanol-rich phase was monitored via measurement of the optical rotation of the solution. When PEO-PB copolymer was added to the solution, the amount of (-)- $\alpha$ -pinene in the methanol-rich phase increased, shown as an increase in the optical rotation of the phase. The optical rotation of the methanol-rich phase was shown to be dependent on the concentration of copolymer added to the solution. Ploetz and Greer suggest that this is an indication that the probe is encapsulated within the hydrophobic core of the micelle, allowing solvation in the methanol-rich phase.

Dynamic light scattering measurements of PEO<sub>132</sub>-PB<sub>89</sub> in methanol (0.05, 0.1, and 0.2 wt %) showed three distinct hydrodynamic radii in solution (Figure 6.3).<sup>118</sup> The smallest  $R_h$  was less than 1 nm in size and was believed to be associated with unimers in solution. Two larger  $R_h$  values of ~20 nm and ~260 nm were also observed. Ploetz and Greer based their interpretation of these scattering bodies on the work by Jain et al.<sup>107</sup> Assuming the findings in the aqueous solutions could be extrapolated to organic solvents, the PEO<sub>132</sub>-PB<sub>89</sub> copolymer should create solutions of cylindrical or cylindrical and spherical micelles.<sup>118</sup> (In Figure 6.1, see  $N_{PB} \sim 90$  and  $\omega_{PEO} = 0.5$ .) Interestingly, there is little change in  $R_h$  values with temperature.<sup>118</sup> It is

noted by Ploetz and Greer that the extrapolation of morphologies from aqueous to organic solutions may not be accurate.<sup>118</sup> Also, the polybutadiene structure used by Ploetz and Greer is different than that used by Jain et al. (Figure 6.4), also adding complexity in extrapolation from the Jain et al. findings.

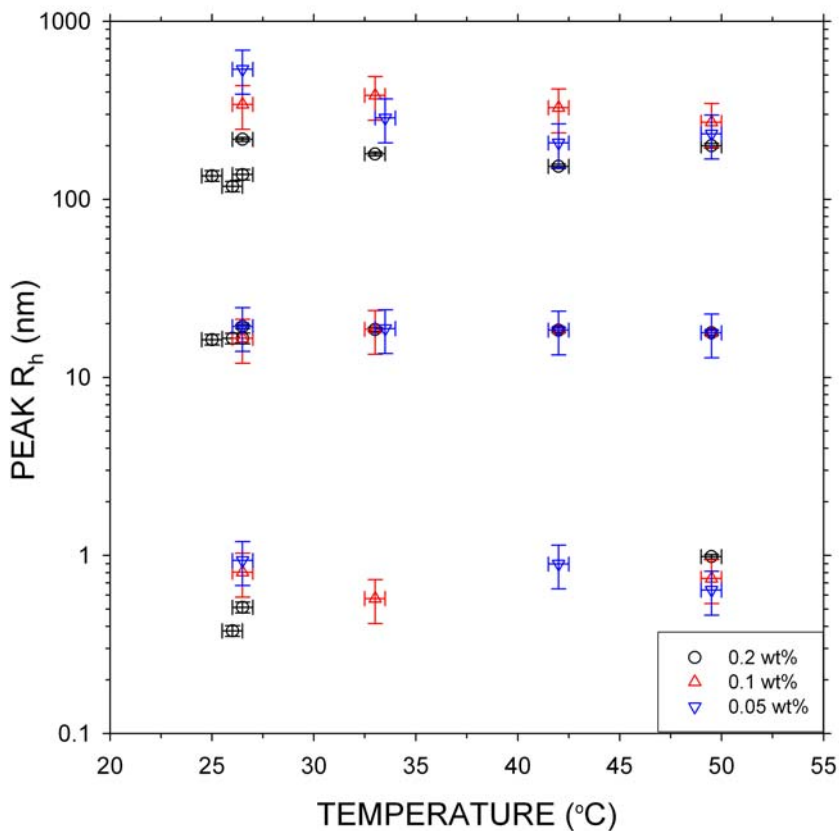


**Figure 6.3:** Dynamic light scattering results depicting three distinct hydrodynamic radii in solutions of PEO<sub>132</sub>-PB<sub>89</sub> in methanol, from Ploetz and Greer.<sup>118</sup>

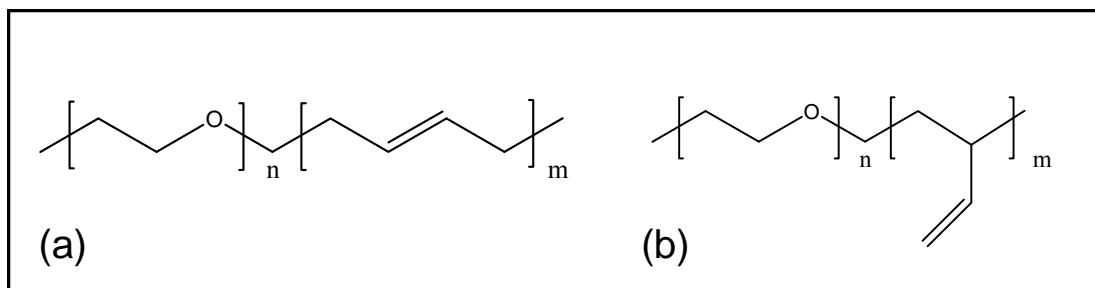


**Figure 6.4:** Molecular structures of poly(propylene oxide)-polybutadiene with (a) 1,4-microstructure polybutadiene and (b) 1,2-microstructure polybutadiene, used by Ploetz and Greer<sup>118</sup> and Jain et al.,<sup>107</sup> respectively. Here  $n$  and  $m$  represent the number of repeating units of PEO and PB.

Molecular probe experiments also allowed Ploetz and Greer to determine the copolymer micelle configuration in cyclohexane.<sup>118</sup> In this case, the hydrophilic dye Rose Bengal was used to show that PEO<sub>132</sub>-PB<sub>89</sub> forms reverse micelles in this nonpolar solvent. That is, PB resides in the shell of the micelles, while PEO resides at the core. When placed in cyclohexane alone, Rose Bengal adheres to the vial and air-solvent interface, not dissolving in solution. Upon the addition of 0.2 wt % PEO<sub>132</sub>-PB<sub>89</sub>, the dye is observed to dissolve in the solution. It was proposed that this solvation occurs when the dye is contained within copolymer micelles. This then demonstrates that the micelles have hydrophilic cores, made of PEO, and hydrophobic shells, PB.

Dynamic light scattering was performed on PEO<sub>132</sub>-PB<sub>89</sub>/cyclohexane solutions (0.05, 0.1, and 0.2 wt %) (Figure 6.5).<sup>118</sup> As with the methanol solutions, the results from Jain et al. in aqueous solutions were extrapolated to explain the findings in the organic solvent. At low temperatures (less than 42 °C) PEO<sub>132</sub>-PB<sub>89</sub> formed cylindrical reverse micelles, marked by a large  $R_h$  value of ~100 nm. At higher temperatures, the scattering intensity of the solution dropped by a factor of ten and a second  $R_h$  of smaller size appeared. This smaller  $R_h$  was concluded to be



associated with spherical micelles. The larger  $R_h$  was still observed at these higher temperatures, suggesting there is a transition from cylindrical to coexisting spherical and cylindrical reverse micelles. Interestingly, scattering from unimers was only observed in one concentration and at one temperature, while such scattering was apparent from most methanol solutions. The authors conclude that this may indicate that micelles form more readily in cyclohexane than in methanol.

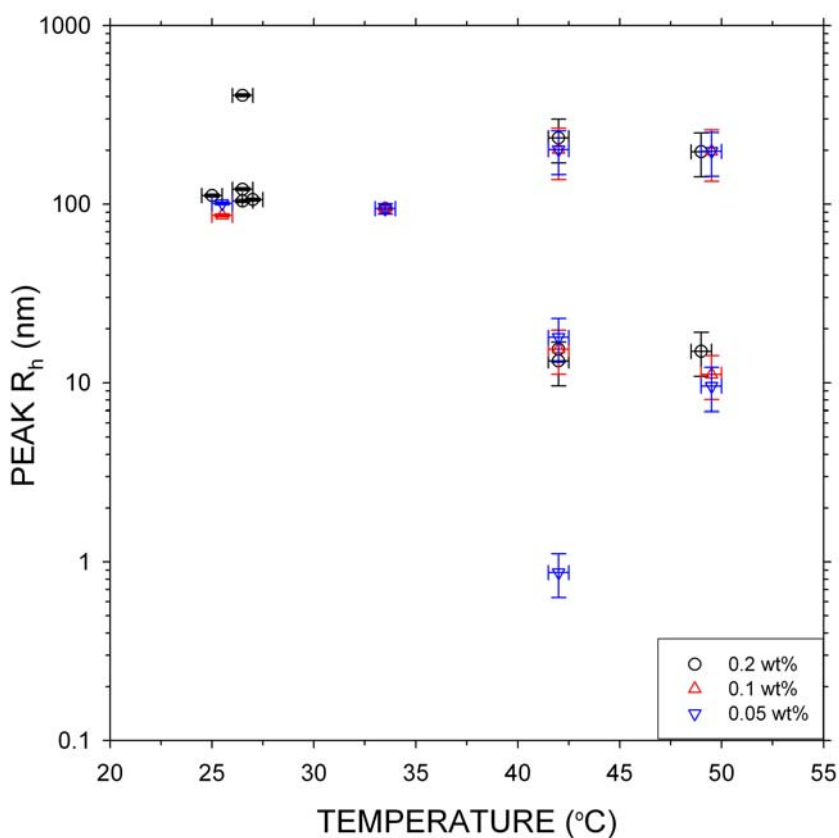


**Figure 6.5:** Dynamic light scattering results from solutions of PEO<sub>132</sub>-PB<sub>89</sub> in cyclohexane, from Ploetz and Greer.<sup>118</sup> The appearance of a smaller hydrodynamic radius above 40 °C is presumed to be due to the transition from cylindrical to coexisting cylindrical and spherical micelles.

Here, exploration of the PEO<sub>132</sub>-PB<sub>89</sub> morphologies in organic solvents is continued. Small angle neutron scattering has been used to confirm the self-aggregation morphologies of this copolymer in deuterated methanol and deuterated cyclohexane. This technique offers greater insight into the conformation of scattering bodies in these solutions than the DLS method previously used, which assumes a spherical body shape. The extrapolation of morphologies from aqueous solutions is also examined.

## 6.2 Experimental

### 6.2.1 Solution preparation

Poly(ethylene oxide)-polybutadiene, PEO<sub>132</sub>-PB<sub>89</sub>, was used as received from Polymer Source, Inc. This copolymer was thoroughly described in Chapter 3. Deuterated methanol (CD<sub>3</sub>OD, 99.8%,  $\rho=0.89$  g/mL) and deuterated cyclohexane (C<sub>6</sub>D<sub>12</sub>, 99.5%,  $\rho=0.89$  g/mL) were obtained from Cambridge Isotopes, Inc. CD<sub>3</sub>OD was dried over 3 Å molecular sieves (Aldrich) and filtered through a 0.2 µm nylon filter before use. C<sub>6</sub>D<sub>12</sub> used in SANS measurements was dried over 4 Å molecular sieves (Sigma). C<sub>6</sub>D<sub>12</sub> used in DLS measurements was not dried.

Samples in deuterated solvents were prepared as to be the same mol % concentration as those used by Ploetz and Greer in protonated solvents. The 0.2 wt % samples in protonated solvents corresponded to a methanol sample of  $5.8 \times 10^{-4}$  mol % and a cyclohexane sample of  $1.5 \times 10^{-3}$  mol %. A 0.17 wt % ( $5.7 \times 10^{-4}$  mol %) sample of PEO<sub>132</sub>-PB<sub>89</sub> in CD<sub>3</sub>OD was prepared, as were a 0.17 wt % ( $1.5 \times 10^{-3}$  mol

%) PEO<sub>132</sub>-PB<sub>89</sub>/C<sub>6</sub>D<sub>12</sub> sample and a 0.18 wt % ( $1.6 \times 10^{-3}$  mol %) PEO<sub>132</sub>-PB<sub>89</sub>/C<sub>6</sub>D<sub>12</sub> sample. These solutions were prepared by massing the desired amount of polymer into a glass vial with a Teflon-lined lid, and solvent was added until the total desired weight was achieved. A Mettler H80 balance ( $\pm 0.1$  mg) was used for all measurements. Sample weights were corrected for buoyancy. A mass density value of 1.0 g/mL for PEO<sub>132</sub>-PB<sub>89</sub>, was estimated as a weight average of PEO and PB densities, 1.147 g/mL<sup>45</sup> and 0.89 g/mL<sup>119</sup>, respectively. All solutions were sonicated to ensure mixing. The 0.17 wt % PEO<sub>132</sub>-PB<sub>89</sub>/C<sub>6</sub>D<sub>12</sub> sample was used in SANS experiments, while the 0.18 wt % PEO<sub>132</sub>-PB<sub>89</sub>/C<sub>6</sub>D<sub>12</sub> sample was used in DLS experiments.

### 6.2.2 Dynamic light scattering

Dynamic light scattering instrumentation and procedures were the same as those described in Chapter 2. Samples were placed in the reservoir of a Neslab RTE-111 constant-temperature bath as the DLS instrument came to the desired temperature. Samples were shaken as removed from the bath and placed in the DLS sample cell. Once in the cell, samples were allowed to equilibrate for 15-20 minutes.

Temperatures of PEO<sub>132</sub>-PB<sub>89</sub>/CD<sub>3</sub>OD sample (0.17 wt %) are reported based upon the instrument temperature. The uncertainty in the sample temperature is large due to air circulation around the DLS instrument. A  $\pm 2$  °C error is reported, as it was observed that sample temperatures varied  $\pm 2$  °C from the instrument temperature when both were greater than 40 °C. Dynamic light scattering of PEO<sub>132</sub>-PB<sub>89</sub>/CD<sub>3</sub>OD

was taken at 26, 42, and 53 ( $\pm 2$ ) °C. Temperatures of the PEO<sub>132</sub>-PB<sub>89</sub>/C<sub>6</sub>D<sub>12</sub> sample (0.18 wt %) were measured with a thermocouple in the solution and are reported to the  $\pm 0.1$  °C. Scattering from this sample was measured at 22.3, 29.1, 37.3, 45.2, 48.4, 54.8, and 61.7 °C.

For both samples, scattering data were taken in multiple iterations at each temperature. Each repetition was analyzed separately, and a 10% error was estimated for hydrodynamic radii results from the PEO<sub>132</sub>-PB<sub>89</sub>/C<sub>6</sub>D<sub>12</sub>. In the CD<sub>3</sub>OD, the uncertainty in viscosity of CD<sub>3</sub>OD was large (~40%), and so a 40% error was estimated for hydrodynamic radii results from this solution. (See Appendix A) Results from each repetition were then averaged as described in Chapter 2.

### 6.2.3 Solvent properties

#### *Refractive indices*

Refractive index measurements were made on the deuterated solvents as a function of temperature using a traditional Abbé refractometer. Refractive indices (at 589.3 nm wavelength) were plotted as a function of temperature and a linear equation was determined for this relationship in each solvent (Figure 6.6). The refractive index of CD<sub>3</sub>OD as a function of temperature had the relationship

$$n_{\text{CD}_3\text{OD}} = 1.332 - 3.9 \times 10^{-4} T, \quad (6.1)$$

and the refractive index of C<sub>6</sub>D<sub>12</sub> had the relationship

$$n_{\text{C}_6\text{D}_{12}} = 1.4316 - 5.4 \times 10^{-4} T, \quad (6.2)$$

with T in °C. Errors for the fitting parameters are found in Appendix D.1.

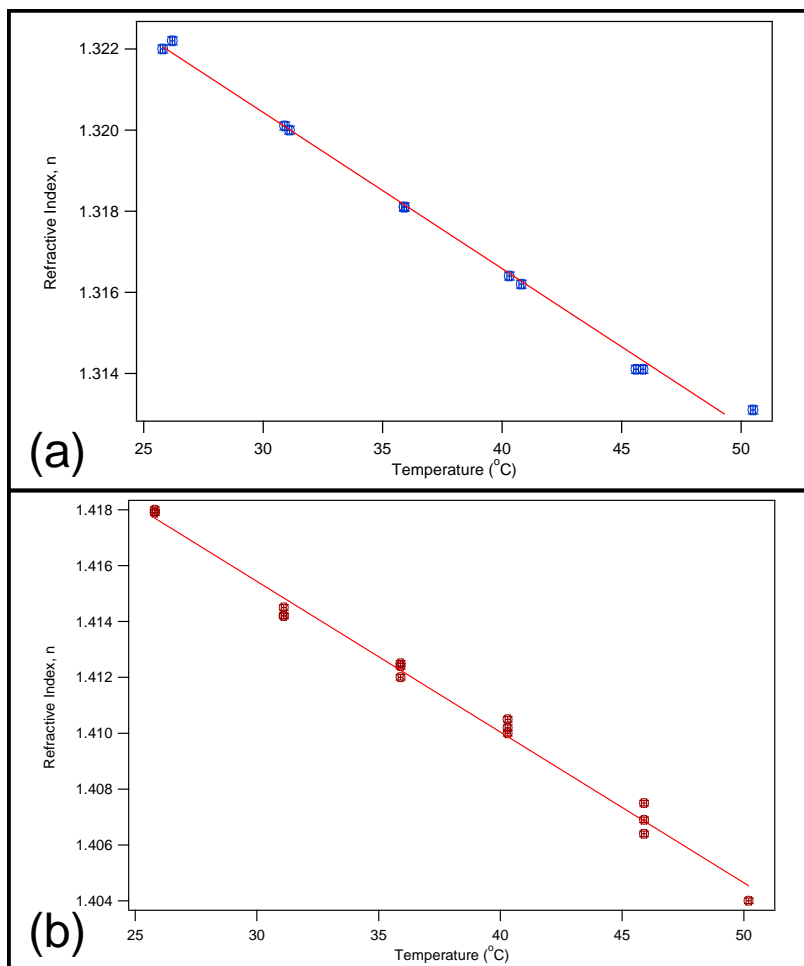


**Figure 6.6:** Refractive indices of (a) CD<sub>3</sub>OD and (b) C<sub>6</sub>D<sub>12</sub> as a function of temperature (°C).

### *Viscosities*

Viscosity values for the deuterated solvents were found in the literature.<sup>120, 121</sup>

The natural logarithms of these values were plotted as a function of 1/T (in Kelvin) to obtain a linear fit, as proposed by Dixon and Schiessler.<sup>120</sup> These linear relationships were used to determine viscosity values at the temperatures used here. These relationships can also be found in Appendix D.2.

## 6.2.4 Small angle neutron scattering

### *Procedure*

The 0.17 wt % PEO<sub>132</sub>-PB<sub>89</sub>/CD<sub>3</sub>OD sample and the 0.17 wt % PEO<sub>132</sub>-PB<sub>89</sub>/C<sub>6</sub>D<sub>12</sub> sample were used in small angle neutron scattering analyses. SANS configurations were the same as those described in Chapter 2. Data from both samples were taken at  $21.3 \pm 1.0$ ,  $30.6 \pm 1.1$ ,  $39.9 \pm 1.2$ ,  $49.3 \pm 1.3$ ,  $58.6 \pm 1.4$ , and  $67.9 \pm 1.6$  °C.

### *Analysis methods*

#### *--CD<sub>3</sub>OD*

Linear Porod and Guinier plots were used to gain insight into scattering particle dimension and size. Prior to these plots, incoherent background scattering was removed from the scattering intensity data. Based upon the method first presented by Müller,<sup>122</sup> the incoherent background, B, at high-Q was estimated by fitting the asymptotic slope of data plotted on  $I(Q)*Q^4$  versus  $Q^4$  axes. The value of this slope was then removed from the  $I(Q)$  data, and the error in the slope was propagated with the  $I(Q)$  error. The linear Porod plot was performed as described in Chapter 2, over the Q-range 0.003-0.01 Å<sup>-2</sup>. Linear Guinier plots were done over the Q-range 0.003-0.02 Å<sup>-2</sup>.

Nonlinear form factor models were also fitted to the scattering data from the copolymer in CD<sub>3</sub>OD. The Schulz sphere model, explained in Chapter 2, was used over the full Q-range. The scattering length density of the sphere was held at  $5.2 \times 10^{-7}$  Å<sup>-2</sup>, the weighted average PEO and PB scattering length densities. (See

Appendix B for all scattering length density calculations and explanations.) The scattering length density of the solvent was held constant at  $5.8 \times 10^{-6} \text{ \AA}^{-2}$ .

The core-shell sphere form factor model was also used, with a polydisperse core radius. This model was also discussed in Chapter 2. This model was fitted over the entire Q-range. The scattering length density of the core was held constant at  $4.1 \times 10^{-7} \text{ \AA}^{-2}$ , the scattering length density of PB. In this manner, it was assumed no mixing of PEO and PB blocks occurred at the core of the micelle. The scattering length density of the solvent was held at  $5.8 \times 10^{-6} \text{ \AA}^{-2}$ . The shell scattering length density was permitted to float between  $6.4 \times 10^{-7} \text{ \AA}^{-2}$  and  $5.8 \times 10^{-6} \text{ \AA}^{-2}$ , the values for PEO and  $C_6D_{12}$ , respectively. In this way, solvent molecules that had permeated the shell of the micelle were accounted for.

-- $C_6D_{12}$

Linear Porod plots in the intermediate regime allowed the determination of the  $I(Q)$  scaling with Q for assemblies in PEO<sub>132</sub>-PB<sub>89</sub>/ $C_6D_{12}$  solutions. Prior to these plots, background scattering was estimated and removed, as described above. Porod plots were performed on a Q-range of 0.003-0.01  $\text{\AA}^{-2}$ .

At low temperatures, an intermediate Q-scaling exponent of about 2 was observed, which can be indicative of multiple scattering bodies. For example, this can indicate a 2-D body, such as a lamella. The non-linear dilute lamella form factor model,<sup>56</sup> available from NIST,<sup>53</sup> was used to analyze the 0.17 wt % PEO<sub>132</sub>-PB<sub>89</sub> in  $C_6D_{12}$  scattering data taken below 39.9 °C.

This lamellar model was described in Chapter 2. The model was fitted to the data over the entire Q-range of scattering data, and the scattering length density of the solvent was held at  $6.7 \times 10^{-6} \text{ \AA}^{-2}$ . The scattering length density of the scattering body was held at the weight average scattering length density of the copolymer,  $5.2 \times 10^{-7} \text{ \AA}^{-2}$ .

Intermediate  $I(Q)$  proportional to  $Q^{-2}$  is also indicative of worm-like cylinders. Scattering from worm-like or “polymer like” micelles has unique characteristics over different Q-ranges (Figure 6.7).<sup>57, 123</sup> At very low-Q, the Guinier regime is observed. As described in Chapter 2, this regime contains information regarding the overall length scale of the assembly. In the intermediate regime, two Q-scaling behaviors are observed. At lower-Q, scattering follows that of polymer power-laws: In good solvents, the cylinder will expand and will be self avoiding. Such behavior is noted by  $I(Q) \sim Q^{-5/3}$ .<sup>57, 123</sup> Bad solvents will cause the micelle to collapse. A fully collapsed micelle will have  $I(Q) \sim Q^{-3}$ .<sup>49</sup> Micelles will act as Gaussian chains in theta-solvents,<sup>57, 123</sup> in which polymer-polymer and polymer-solvent interactions are equal.<sup>9</sup> In theta- solvents,  $I(Q)$  will scale with  $Q^{-2}$ .<sup>57, 123</sup> Still within the intermediate regime, but at higher-Q, a cross-over to scattering which scales with  $Q^{-1}$  will be observed.<sup>57, 123</sup> This scattering is representative of the stiff cylinder form of the micelle at a smaller, local scale.<sup>57, 123</sup> Finally, as the cross-section of the cylinder is probed, an abrupt decrease in  $I(Q)$  is observed, and the Porod regime is approached. Each of these scattering regimes usually spans a large Q-range, and so all these regimes are not usually visible using only one scattering technique.<sup>57</sup>



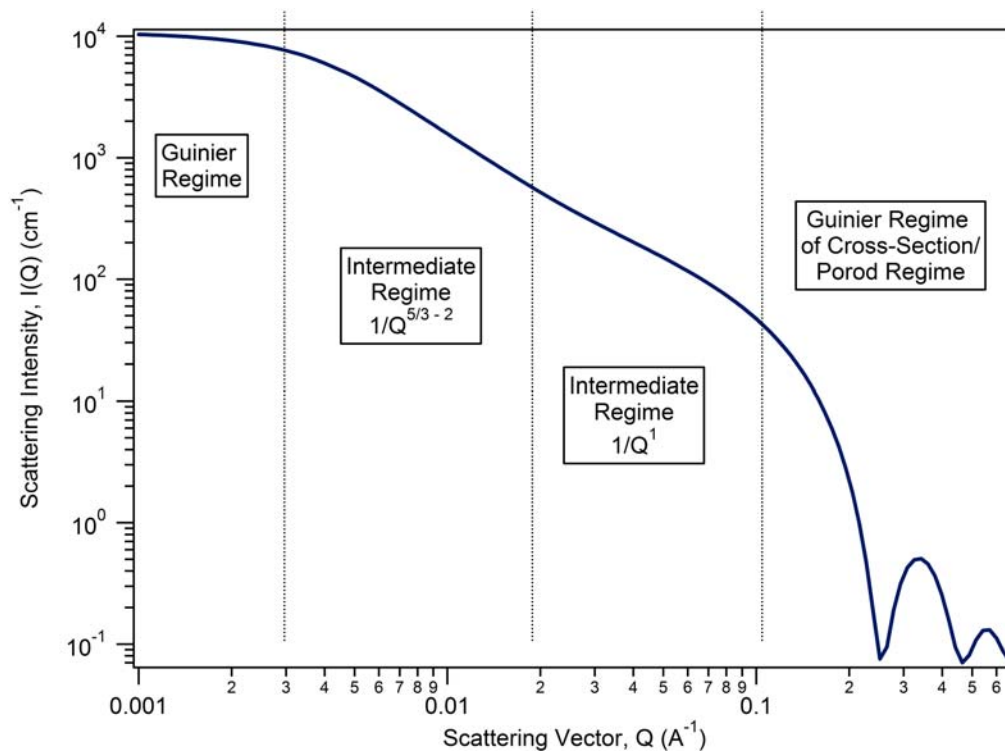


**Figure 6.7:** Example scattering from a flexible cylinder, depicting the different scattering regimes. At high- $Q$ , higher order oscillations would be smeared out if polydispersity in the length or cross-section of the cylinder is included.

The cross-over from polymer-like to cylindrical scattering ( $Q^{-2}$  to  $Q^{-1}$ , for example) is only apparent if the contour length,  $l_p$ , is much less than the overall length,  $L$ .<sup>57, 123</sup> The contour length is the length scale over which the cylinder can be viewed as being rigid. Also,  $l_p$  must be much greater than the cross-sectional radius of the cylinder,  $R_{cs}$ .<sup>57, 123</sup> If  $l_p$  is similar in value to either of these other dimensions, the  $Q^{-1}$  scattering of the stiff cylinder may be masked.<sup>57, 123</sup> That is, it will be “obscured by the exponential decay due to the finite radius of the cylinder on the high- $Q$  side and due to the finite overall size of the flexible coil on the low- $Q$  side.”<sup>123</sup>

A second non-linear model was used on scattering data from the 0.17 wt % PEO<sub>132</sub>-PB<sub>89</sub> in C<sub>6</sub>D<sub>12</sub> solution in order to confirm the existence of worm-like micelles. The flexible cylinder with a polydisperse cross-sectional radius and

excluded volume,<sup>57,58</sup> available from NIST,<sup>53</sup> was used. This model was described in Chapter 2, and was used over the entire Q-range of the scattering data. Again, the scattering length densities of the solvent and copolymer assembly were held at  $6.7 \times 10^{-6} \text{ \AA}^{-2}$  and  $5.2 \times 10^{-7} \text{ \AA}^{-2}$ , respectively.

At temperatures of 49.3 °C and above, scattering above the incoherent background resembled that of spherical assemblies, and was verified through Porod plots over the Q-range 0.003-0.01  $\text{\AA}^{-2}$ . Linear Guinier plots were performed following the removal of background scattering. These were performed over the Q-range 0.003-0.02  $\text{\AA}^{-2}$ .

Non-linear plots performed on data at high temperatures included the spherical form factor model with Schulz polydispersity and the core-shell sphere form factor with polydisperse core. Both of these models were described in Chapter 2. Both of these models were fitted to the data over the Q-range 0.003-0.05  $\text{\AA}^{-2}$ . When performing the Schulz sphere fit, the scattering length densities of the sphere and solvent were held at  $5.2 \times 10^{-7} \text{ \AA}^{-2}$  and  $6.7 \times 10^{-6} \text{ \AA}^{-2}$ , respectively. Scattering length densities were held at  $6.4 \times 10^{-7}$ ,  $4.1 \times 10^{-7}$ , and  $6.7 \times 10^{-6} \text{ \AA}^{-2}$  for the core, shell, and solvent, respectively. By holding these scattering length densities constant, it was presumed that no mixing of copolymer blocks occurred within the shell and core, and that no solvent molecules entered the micelle.

## 6.3 Results and discussion

### 6.3.1 Copolymer in deuterated methanol

#### *Dynamic light scattering*

Through dynamic light scattering techniques, only two hydrodynamic radii values were observed from the 0.17 wt % solution of PEO<sub>132</sub>-PB<sub>89</sub>/CD<sub>3</sub>OD (Table 6.1). Several samples also showed hydrodynamic radii in the millimeter length scale. Such scattering has been considered to be due to dust.

Interestingly, Ploetz and Greer saw three distinct  $R_h$  values in solutions of protonated methanol.<sup>118</sup> Figure 6.8 compares the hydrodynamic radii from the protonated and deuterated solvents. Hydrodynamic radii in CD<sub>3</sub>OD are of the same magnitude of the unimer and first micelle observed in CH<sub>3</sub>OH. Recall that this first micelle was expected to be spherical based upon extrapolation from PEO-PB/water solutions,<sup>107, 118</sup> and such an interpretation will be continued here.

**Table 6.1:** Hydrodynamic radii of PEO<sub>132</sub>-PB<sub>89</sub> formations in CD<sub>3</sub>OD, 0.17 wt %

Temperature		°C <sup>a</sup>	26	42	53
Mean Signal Intensity		Hz	634509	629488	26954
Unimer	Peak Area	-	0.249	0.029	0.076
	Mean	nm	0.26	0.33	0.5
	Position	nm	0.30	0.34	0.6
	Error of Position	nm	0.06	0.09	0.1
Spherical Micelle	Peak Area	-	0.751	0.971	0.812
	Mean	nm	13	13	12
	Position	nm	13	13	11
	Error of Position	nm	2	2	2

<sup>a</sup>: Error in temperature is  $\pm 2$  °C.

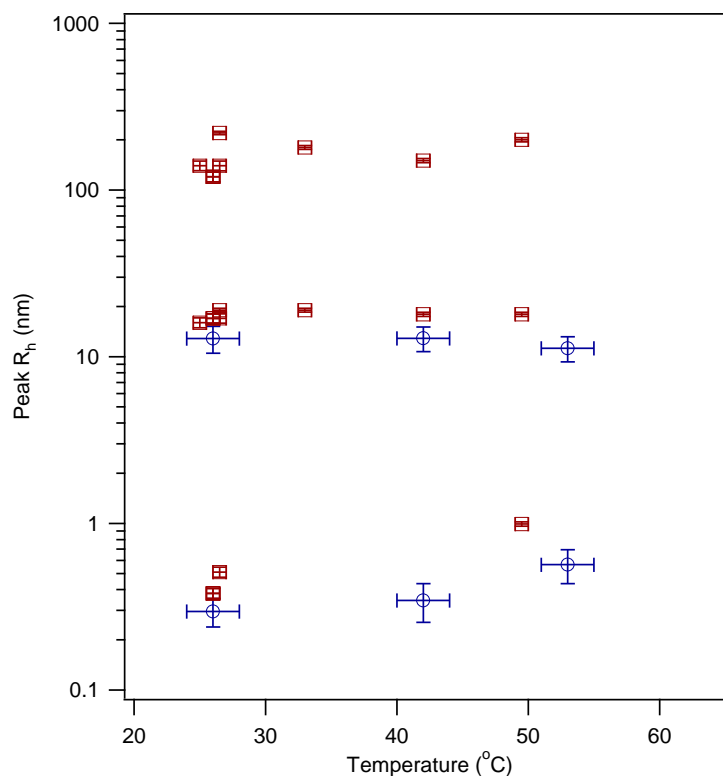


**Figure 6.8:** Hydrodynamic radii of PEO<sub>132</sub>-PB<sub>89</sub> in deuterated methanol (CD<sub>3</sub>OD) (blue) and protonated methanol (CH<sub>3</sub>OH) (red), from Ploetz and Greer.<sup>118</sup> No radii from second micelles ( $R_h \sim 200$  nm) are observed in the deuterated solvent.

### *Small angle neutron scattering*

Small angle neutron scattering of 0.17 wt % solution PEO<sub>132</sub>-PB<sub>89</sub> in CD<sub>3</sub>OD have little variation over the 50 °C temperature range examined (Figure 6.9). Near-zero Q-scaling at the intermediate-to-Guinier regimes suggests spherical assemblies in solution. Linear Porod plots in the intermediate regime confirm this near-zero Q-exponent. An example Porod plot (at 21.3 °C) is shown in Figure 6.10, and the intermediate Q-scaling exponents,  $n$ , for all temperatures are listed in Table 6.2. The slight deviation from  $Q^0$  scaling may be explained by polydispersity in the size of the assembly or slight elongation from a spherical form.<sup>47</sup>

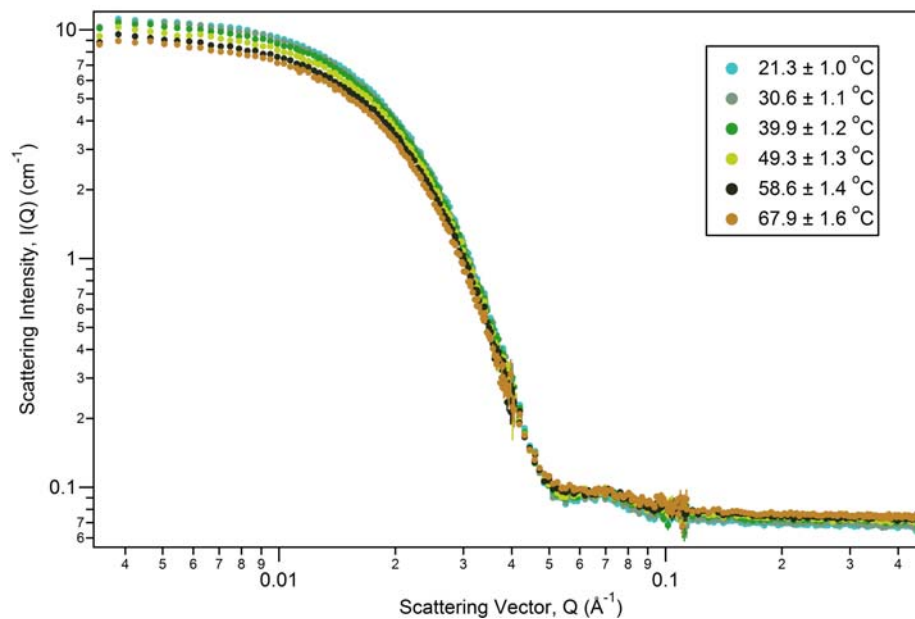


**Figure 6.9:** Small angle neutron scattering data from 0.17 wt % solution PEO<sub>132</sub>-PB<sub>89</sub> in CD<sub>3</sub>OD.

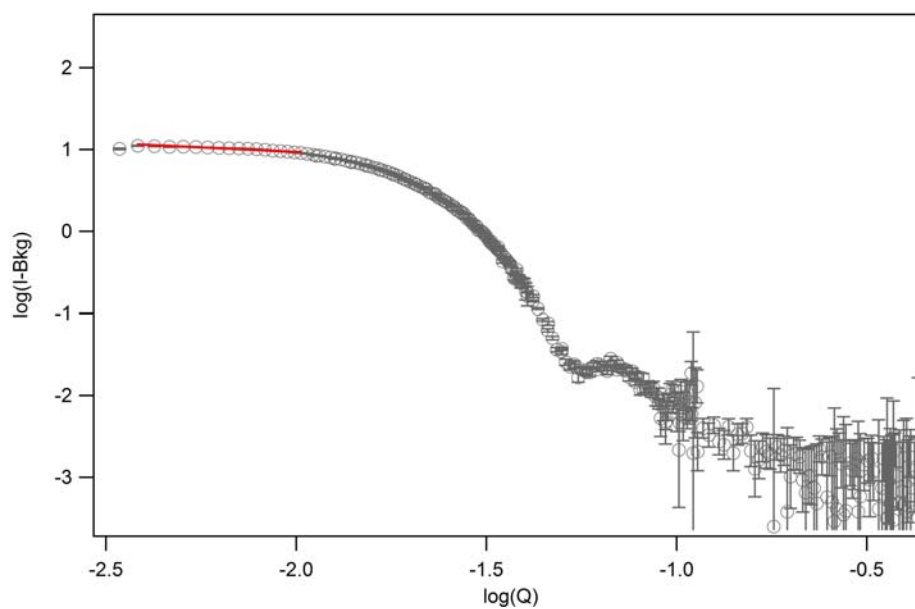


**Figure 6.10:** Linear Porod plot from 0.17 wt % solution PEO<sub>132</sub>-PB<sub>89</sub> in CD<sub>3</sub>OD at 21.3 °C. The Q-scaling exponent of the intermediate regime,  $n$ , is determined by the slope of the fitted line.

**Table 6.2:** Intermediate Q-scaling exponents,  $n$ , for 0.17 wt % solution PEO<sub>132</sub>-PB<sub>89</sub> in CD<sub>3</sub>OD. Exponents are nearly zero, suggesting spherical bodies. Errors are reported at 99% level.

Temperature, (°C)	Intermediate Q-scaling Exponent, $n$		
21.3	0.22	±	0.02
30.6	0.22	±	0.02
39.9	0.24	±	0.02
49.3	0.24	±	0.02
58.6	0.25	±	0.02
67.9	0.25	±	0.02

Linear Guinier plots of scattering data offered estimates of the radii of gyration for each assembly. Figure 6.11 shows an example plot for 21.3 °C. Table 6.3 lists all  $R_g$  values as well as the corresponding spherical radii. It is clear that there is little change in assembly size over the temperature range examined.

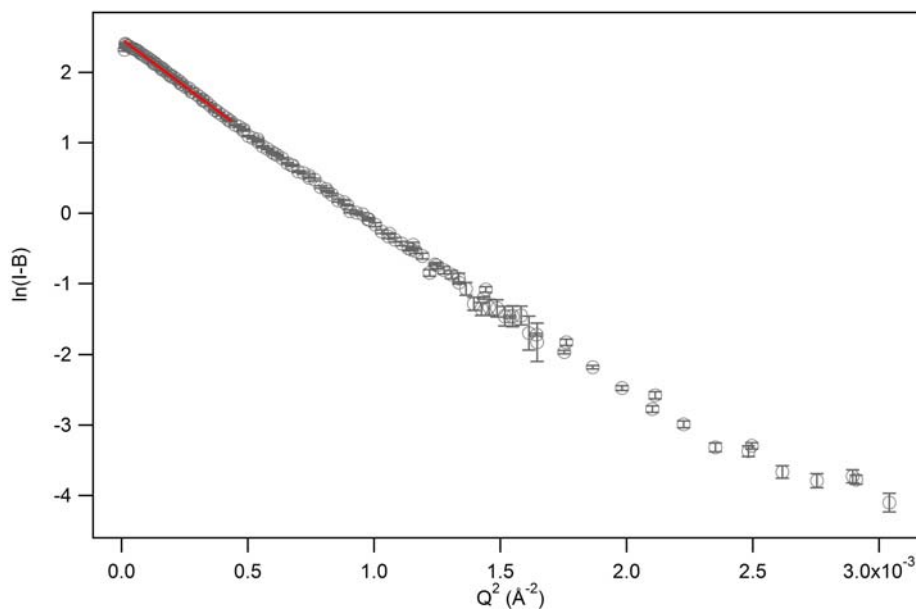


**Figure 6.11:** Linear Guinier plot of 0.17 wt % solution PEO<sub>132</sub>-PB<sub>89</sub> in CD<sub>3</sub>OD at 21.3 °C.

**Table 6.3:** Radii of gyration ( $R_g$ ) and spherical radii ( $R$ ) of 0.17 wt % solution PEO<sub>132</sub>-PB<sub>89</sub> in CD<sub>3</sub>OD determined through linear Guinier plots. Errors are at 99% level.

Temperature, (°C)	Radius of Gyration, $R_g$ (Å)	Spherical Radius, $R$ (Å)
21.3	89.7 ± 0.5	115.8 ± 0.6
30.6	89.7 ± 0.5	115.8 ± 0.6
39.9	88.8 ± 0.5	114.7 ± 0.7
49.3	88.3 ± 0.5	114.0 ± 0.7
58.6	88.3 ± 0.5	114.0 ± 0.7
67.9	89.7 ± 0.6	115.8 ± 0.7

Nonlinear models were also used to fit to the data. Fits with a spherical model, with Schulz polydispersity, offered results similar to the linear Guinier fits. An example fit is shown in Figure 6.12, and radii and polydispersity of these spheres at all temperatures examined are reported in Table 6.4. (Complete fit results are available in Appendix D.3.) It is important to note that the scattering length density of the sphere was held at  $5.2 \times 10^{-7} \text{ \AA}^2$ , which corresponds to the weighted average scattering length density of the copolymer only, and thus these results presume no CD<sub>3</sub>OD was present within the spherical body.

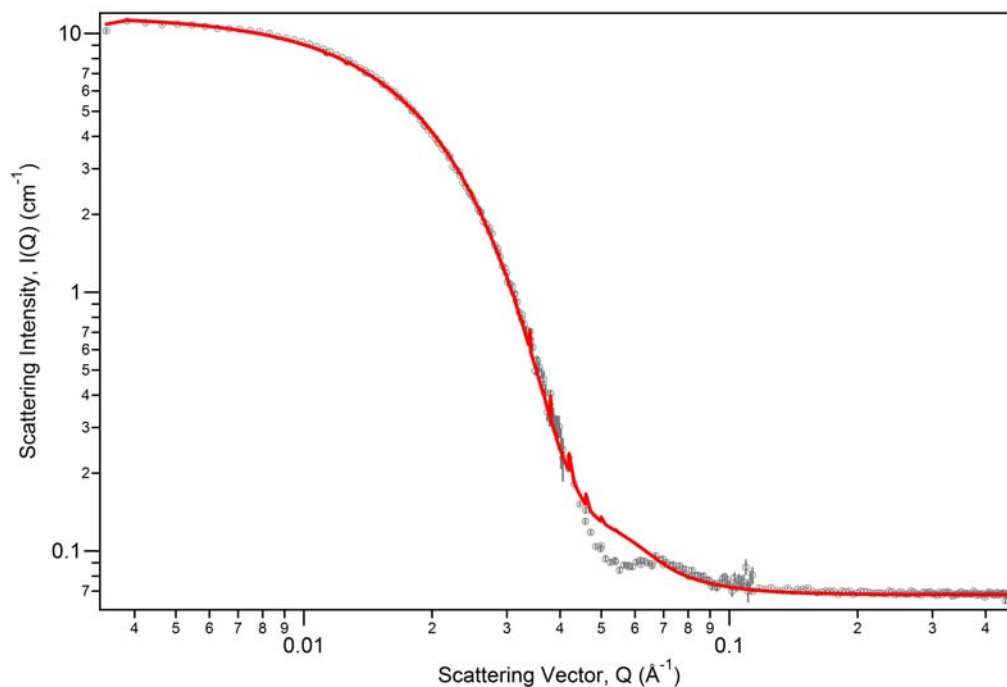


**Figure 6.12:** SANS data of 0.17 wt % PEO<sub>132</sub>-PB<sub>89</sub> in CD<sub>3</sub>OD at 21.3 °C. Red solid line represents fit with Schulz sphere model.

**Table 6.4:** Spherical radii and polydispersities in radii of 0.17 wt % PEO<sub>132</sub>-PB<sub>89</sub> in CD<sub>3</sub>OD, determined through Schulz sphere model. Error is reported at 99% level.

Temperature, (°C)	Mean Radius, R (Å)	Polydispersity, $\rho$ ( $\sigma/R$ )
21.3	92.6 ± 0.2	0.187 ± 0.001
30.6	93.1 ± 0.3	0.183 ± 0.002
39.9	93.4 ± 0.3	0.179 ± 0.003
49.3	93.2 ± 0.2	0.178 ± 0.001
58.6	92.6 ± 0.4	0.181 ± 0.003
67.9	92.0 ± 0.2	0.192 ± 0.001

Finally, the spherical core-shell model, with a polydisperse core, was used to fit the scattering data in for copolymer CD<sub>3</sub>OD. This model is often used to represent micelle assemblies. With this fit, the scattering length density of the core was held constant, assuming only PB was present in the core of the micelle. The scattering length density of the shell was a fitted parameter, as described in the experimental section. In this manner, any presence of CD<sub>3</sub>OD in the shell was accounted for. This



model, fitted to scattering data at 21.3 °C, is illustrated in Figure 6.13. Resulting dimensions for micelles at all temperatures are detailed in Table 6.5 (complete fit results are in Appendix D.3). This model offers similar results to the previous fits.

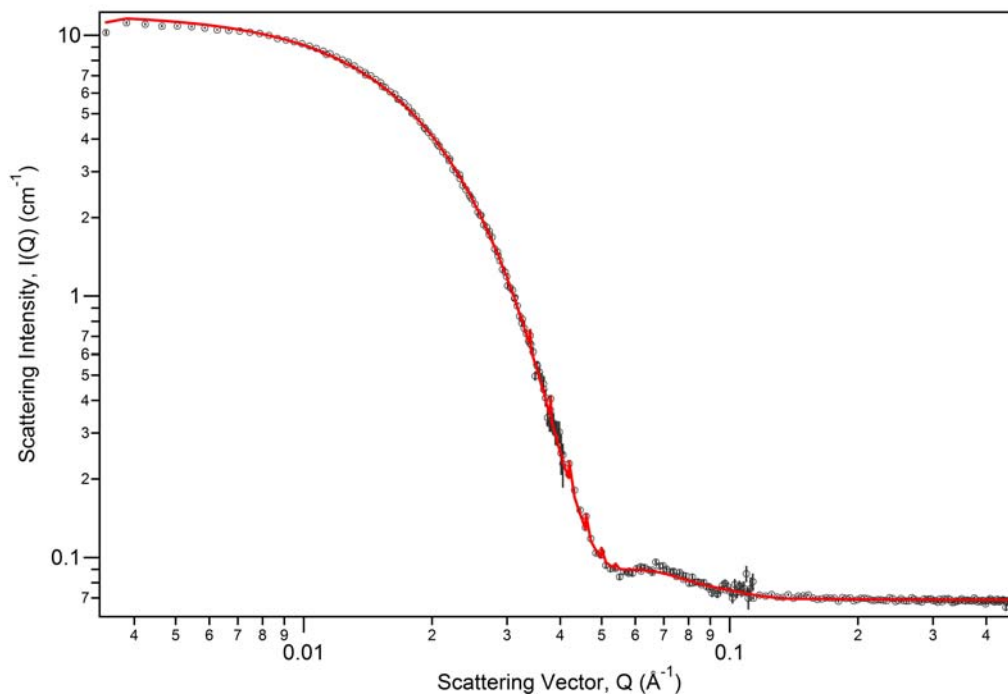


**Figure 6.13:** Scattering data of 0.17 wt % PEO<sub>132</sub>-PB<sub>89</sub> in CD<sub>3</sub>OD at 21.3 °C, fitted by the polydisperse core-shell model (solid red line).

**Table 6.5:** Polydisperse core-shell model results, obtained from fits to 0.17 wt % PEO<sub>132</sub>-PB<sub>89</sub> in CD<sub>3</sub>OD SANS data. 99% error is shown.

Temperature (°C)	Average Core Radius R <sub>c</sub> , (Å)	Polydispersity in Core Radius ρ, σ/R <sub>c</sub>	Shell Thickness, T, (Å)	Scattering Length Density of Shell (Å <sup>-2</sup> )
21.3	23.8 ± 0.3	0.663 ± 0.009	69.0 ± 0.6	2.8x10 <sup>-6</sup> ± 1.x10 <sup>-7</sup>
30.6	24 ± 1	0.66 ± 0.03	70 ± 1	2.84x10 <sup>-6</sup> ± 8.x10 <sup>-8</sup>
39.9	22.6 ± 0.9	0.68 ± 0.02	71 ± 1	2.9x10 <sup>-6</sup> ± 1.x10 <sup>-7</sup>
49.3	22 ± 2	0.68 ± 0.05	71 ± 2	2.9x10 <sup>-6</sup> ± 2.x10 <sup>-7</sup>
58.6	20 ± 2	0.74 ± 0.06	73 ± 2	2.8x10 <sup>-6</sup> ± 2.x10 <sup>-7</sup>
67.9	21 ± 1	0.73 ± 0.03	72 ± 1	2.1x10 <sup>-6</sup> ± 2.x10 <sup>-7</sup>

### *Summary of CD<sub>3</sub>OD results*

Each of the SANS analysis techniques offers similar results regarding the shape and dimension of the PEO<sub>132</sub>-PB<sub>89</sub> assemblies in CD<sub>3</sub>OD (Table 6.6). This

suggests reliability in these sizes. Also important is the comparison between DLS and SANS data. Here again, similar outcomes are seen between techniques (also see Table 6.6). The hydrodynamic radii and spherical radii are only slightly larger than the radii determined through non-linear models. This may suggest there is a small solvent layer surrounding the micelles. Through these techniques, it is clear that PEO<sub>132</sub>-PB<sub>89</sub> forms spherical micelles with total spherical radii around 100 Å in solutions of CD<sub>3</sub>OD.

Again, it is interesting to point out that Ploetz and Greer saw three distinct assemblies in CH<sub>3</sub>OH.<sup>118</sup> These were presumed to be unimers, spherical micelles, and cylindrical micelles. The size of the assemblies in CD<sub>3</sub>OD corresponds with that of the spherical micelles in CH<sub>3</sub>OH. SANS techniques used here have confirmed that these assemblies have a spherical shape in CD<sub>3</sub>OD. It is probable that such a shape extends to these assemblies in CH<sub>3</sub>OH, based upon the similarity in size.

At this time, it is unclear why the copolymer only forms spherical micelles in CD<sub>3</sub>OD while both spherical and cylindrical micelles form in the protonated solvent. Literature has shown that solvent isotope effects can change critical micelle temperatures and aggregation number.<sup>20, 23, 124, 125</sup> However, no prior research has shown such an extreme difference in copolymer assemblies in solvents with different isotopes. The hydrogen bonds in CD<sub>3</sub>OD (both within the solvent and between the solvent and PEO) are presumed to be stronger than those in CH<sub>3</sub>OH, based upon H<sub>2</sub>O/D<sub>2</sub>O literature.<sup>19</sup> It is possible that the hydrogen bonds between solvent and copolymer are more favorable in CD<sub>3</sub>OD than in CH<sub>3</sub>OH, and so the copolymer remains in the spherical formation, with a greater number of these bonds. Often,

copolymers are assumed to behave in the same manner in isotopically different solvents. The difference in copolymer self-assembly observed here shows that this is not always the case.

**Table 6.6:** Comparison of spherical micelle dimensions from all SANS analysis techniques for PEO<sub>132</sub>-PB<sub>89</sub> in CD<sub>3</sub>OD. Spherical radii were determined via radii of gyration from linear Guinier fits. Mean radii from Schulz sphere model, and the polydisperse core-shell model gave the final dimensions. Polydispersities in the core dimensions are not taken into account here. Hydrodynamic radii are determined from DLS analysis. Errors are at the 99% level.

Temperature, (°C)	Spherical Radius, R (Å)	Mean Radius, R (Å)	Core Radius + Shell Thickness, R <sub>c</sub> + T (Å)	Hydrodynamic Radius, R <sub>h</sub> (Å)
21.3 ± 1.0	115.8 ± 0.6	92.6 ± 0.2	92.8 ± 0.7	
26 ± 2				130 ± 20
30.6 ± 1.1	115.8 ± 0.6	93.1 ± 0.3	93 ± 2	
39.9 ± 1.2	114.7 ± 0.7	93.4 ± 0.3	94 ± 1	
42 ± 2				130 ± 20
49.3 ± 1.3	114.0 ± 0.7	93.2 ± 0.2	93 ± 3	
53 ± 2				120 ± 20
58.6 ± 1.4	114.0 ± 0.7	92.6 ± 0.4	93 ± 3	
67.9 ± 1.6	115.8 ± 0.7	92.0 ± 0.2	93 ± 2	

### 6.3.2 Copolymer in deuterated cyclohexane

#### *Dynamic light scattering*

DLS results from the 0.17 wt % PEO<sub>132</sub>-PB<sub>89</sub>/C<sub>6</sub>D<sub>12</sub> were very similar to those obtained from the 0.2 wt % PEO<sub>132</sub>-PB<sub>89</sub>/C<sub>6</sub>H<sub>12</sub> solution by Ploetz and Greer (Figure 6.14, Table 6.7). At temperatures below 45 °C, one hydrodynamic radius is detected. Based upon Ploetz and Greer's interpretation, this hydrodynamic radius corresponds to worm-like cylindrical micelles.<sup>118</sup> As temperature increases, two smaller hydrodynamic radii appear and coexist with the larger radius. It is believed that these smaller radii correspond to spherical micelles and unimers. As in the CD<sub>3</sub>OD solutions, hydrodynamic radii at the micrometer to millimeter length scales were also observed. It is thought that these correspond to dust.

**Table 6.7:** Hydrodynamic radii of PEO<sub>132</sub>-PB<sub>89</sub> formations in C<sub>6</sub>D<sub>12</sub>, 0.17 wt %. Errors are at 99% level.

Temperature	°C <sup>a</sup>	22.3	29.1	37.3	45.2	48.4	54.8	61.7	
Mean Signal Intensity	Hz	634509	629488	671430	79633	8938	5848	6390	
Unimer	Peak Area	-			0.21	0.20	0.19	0.23	
	Mean	nm			0.30	0.82	1.12	1.53	
	Position	nm			0.33	0.85	1.03	1.44	
	Error of Position	nm			0.01	0.04	0.04	0.06	
Spherical Micelle	Peak Area	-			0.142	0.357	0.410	0.311	
	Mean	nm			37	22.8	26.3	20.3	
	Position	nm			35	18.1	14.9	17.3	
	Error of Position	nm			1	0.8	0.7	0.7	
Wormlike Micelle	Peak Area	-	0.933	0.970	0.897	0.614	0.279	0.182	
	Mean	nm	230	240	175	214	186	360	206
	Position	nm	220	240	174	177	151	260	187
	Error of Position	nm	10	10	8	8	7	10	8

a: Error in temperature is ± 0.1 °C

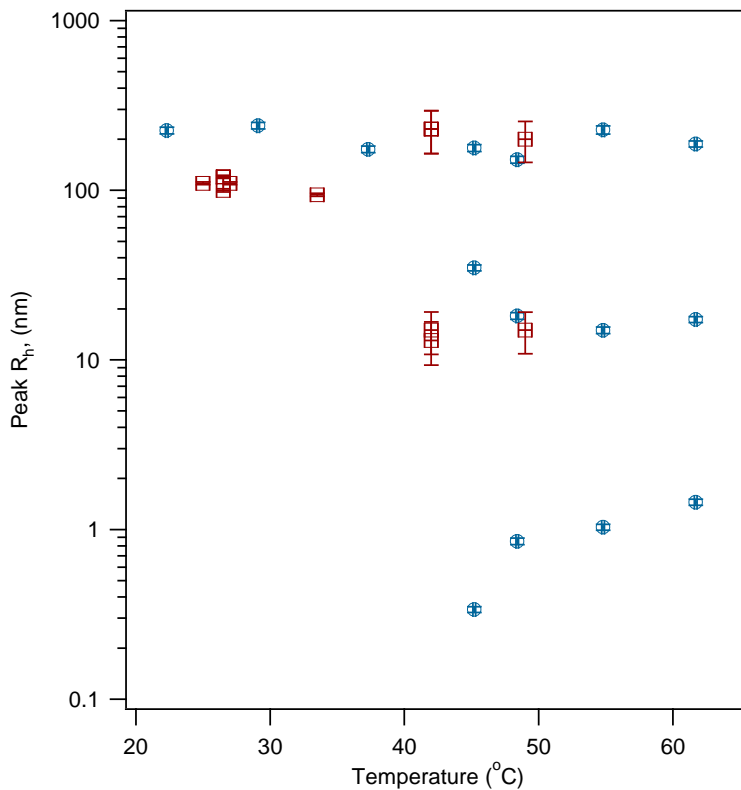


**Figure 6.14:** Hydrodynamic radii of PEO<sub>132</sub>-PB<sub>89</sub> in deuterated cyclohexane (C<sub>6</sub>D<sub>12</sub>, 0.18 wt %, blue) with those observed in protonated cyclohexane (CH<sub>3</sub>OH, 0.20 wt %, red), from Ploetz and Greer.<sup>118</sup> Note that these concentrations correspond to the same mol %.

As observed by Ploetz and Greer in CH<sub>3</sub>OH,<sup>118</sup> the mean scattering intensity also decreased significantly upon transition from cylindrical micelles to coexisting cylindrical and spherical micelles in C<sub>6</sub>D<sub>12</sub> (Figure 6.15). Ploetz and Greer explained this decrease to be caused by the shift to spheres in solution. These results duplicate such a shift, leading to further evidence that such is the case.

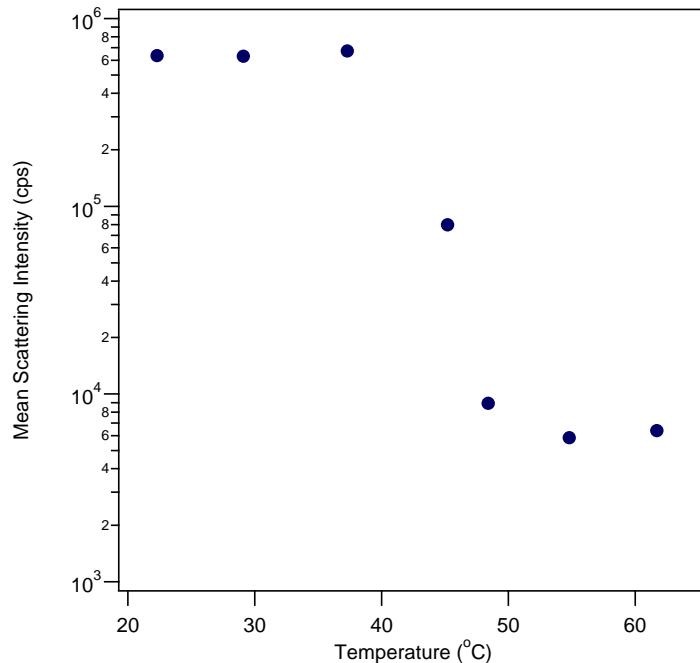


**Figure 6.15:** The mean scattering intensity of the 0.18 wt % PEO<sub>132</sub>-PB<sub>89</sub>/C<sub>6</sub>D<sub>12</sub> solution drops dramatically as the assemblies transition from cylindrical micelles to coexisting cylindrical and spherical micelles. Mean scattering intensity is in counts per second (cps).

The DLS results for PEO<sub>132</sub>-PB<sub>89</sub> in protonated and deuterated cyclohexane are very similar, suggesting that the isotopic difference between the solvents does not greatly affect the copolymer. This is presumably because of the lack of hydrogen bonding in this solvent. There is, however, more unimer in C<sub>6</sub>D<sub>12</sub> than in C<sub>6</sub>H<sub>12</sub>, as indicated by the small  $R_h$  around 1 nm. This would indicate that the deuterated solvent is less selective than its protonated counterpart.

The unimers also appear to get slightly larger as temperature is increased. This suggests that copolymer chains are more solvated and stretched in solution. Both this and the transition to smaller micelles indicate that the solvent becomes less selective with increasing temperature. Recall from Chapter 1 that this is expected

with organic solvents, as micelles transition to unimers with increasing temperature as solvents become more compatible with the carbon backbones of the copolymer.

### *Small angle neutron scattering*

Small angle neutron scattering data of 0.17 wt % PEO<sub>132</sub>-PB<sub>89</sub> in C<sub>6</sub>D<sub>12</sub> mirrors the DLS results of 0.18 wt % PEO<sub>132</sub>-PB<sub>89</sub> in C<sub>6</sub>D<sub>12</sub> and 0.20 wt % PEO<sub>132</sub>-PB<sub>89</sub> in C<sub>6</sub>H<sub>12</sub>. Examining the SANS data over the ~20-70 °C (Figure 6.16), a large assembly exists at 39.9 °C and below. Note that this assembly is so large that the scattering extends beyond the SANS window at low-Q, and no Guinier regime exists. At 49.3 °C, a dramatic change in scattering data is observed. Assemblies become smaller, noted by the appearance of a Guinier regime ( $I(Q)$  scaling with  $\sim Q^0$  and low-Q). Also, the intermediate-regime is obscured by the Guinier and Porod regimes (noted by a drop in  $I(Q)$ ). This suggests a spherical assembly in solution.



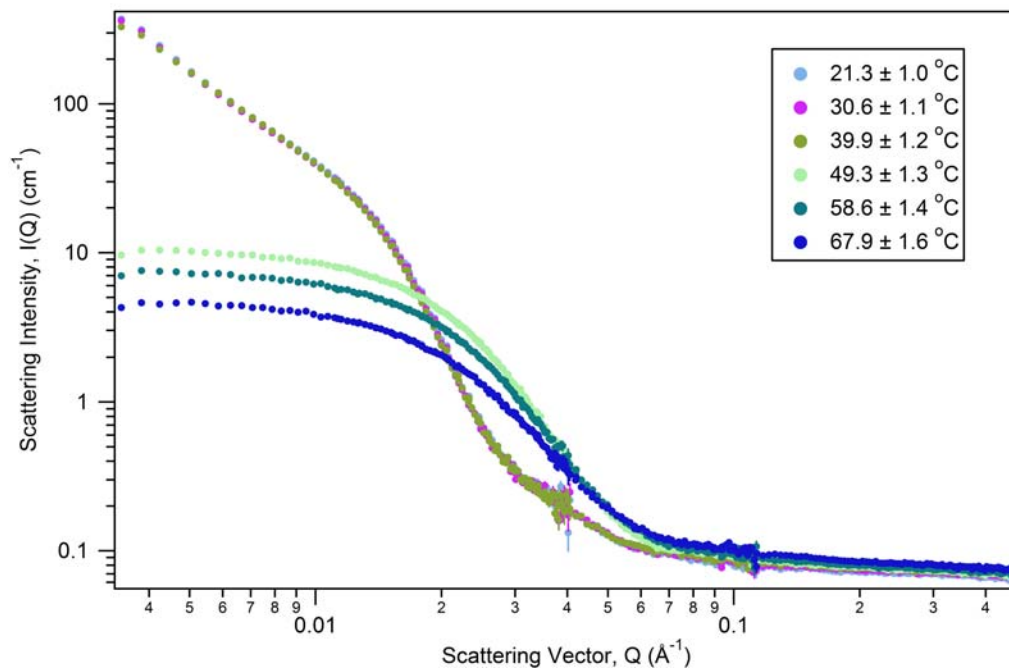


**Figure 6.16:** SANS scattering intensity data of 0.17 wt % PEO<sub>132</sub>-PB<sub>89</sub> in C<sub>6</sub>D<sub>12</sub>

*--Low Temperatures*

Linear Porod plots performed in the intermediate regime of scattering data at 39.9 °C and below reveal a Q-scaling exponent,  $n$ , (where  $I(Q)$  is proportional to  $1/Q^n$ ) of  $\sim 2$ . An example fit is shown in Figure 6.17, and the exponents at all temperatures are found in Table 6.8.

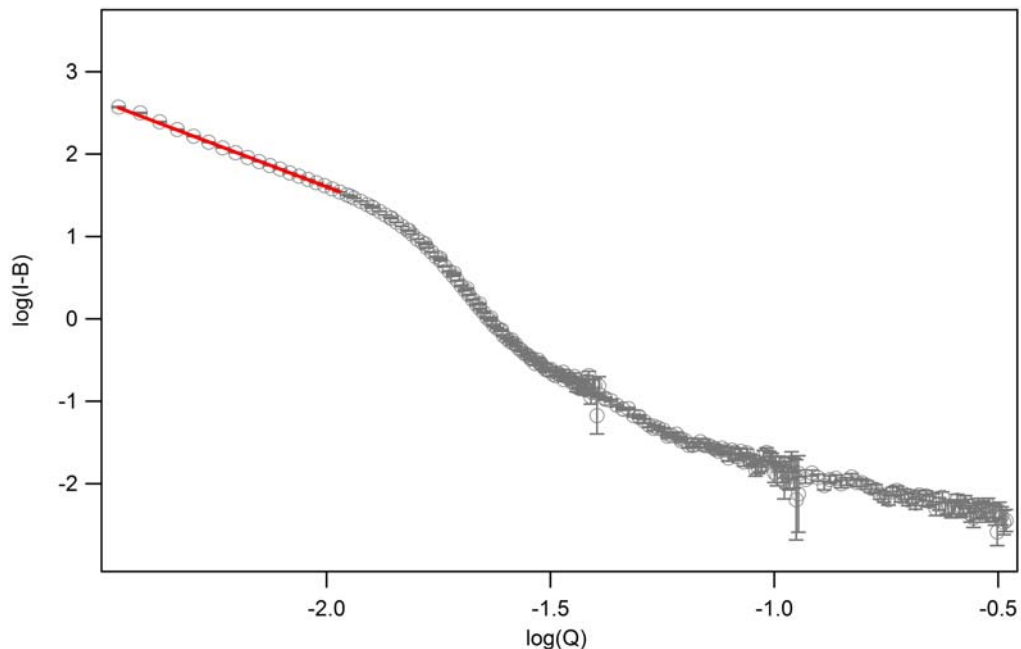


**Figure 6.17:** Linear Porod plot of SANS scattering data of 0.17 wt % solution PEO<sub>132</sub>-PB<sub>89</sub> in C<sub>6</sub>D<sub>12</sub> at 21.3 °C.

**Table 6.8:** Intermediate Q-scaling exponents, n, for 0.17 wt % solution PEO<sub>132</sub>-PB<sub>89</sub> in C<sub>6</sub>D<sub>12</sub>. Errors are shown at 99% level.

Temperature, (°C)	Intermediate Q-scaling Exponent, n		
21.3	2.07	±	0.02
30.6	2.07	±	0.02
39.9	2.06	±	0.01

Because the intermediate Q-scaling exponent of 2 can be associated with multiple scattering bodies, two separate non-linear models were tried here. The lamella form factor scattering model was fitted to the data. As seen in Figure 6.18, and by the goodness of fit (reduced  $\chi^2$  of 11.02), this is a poor fit to the data, and so the scattering assemblies are not considered to have this form.

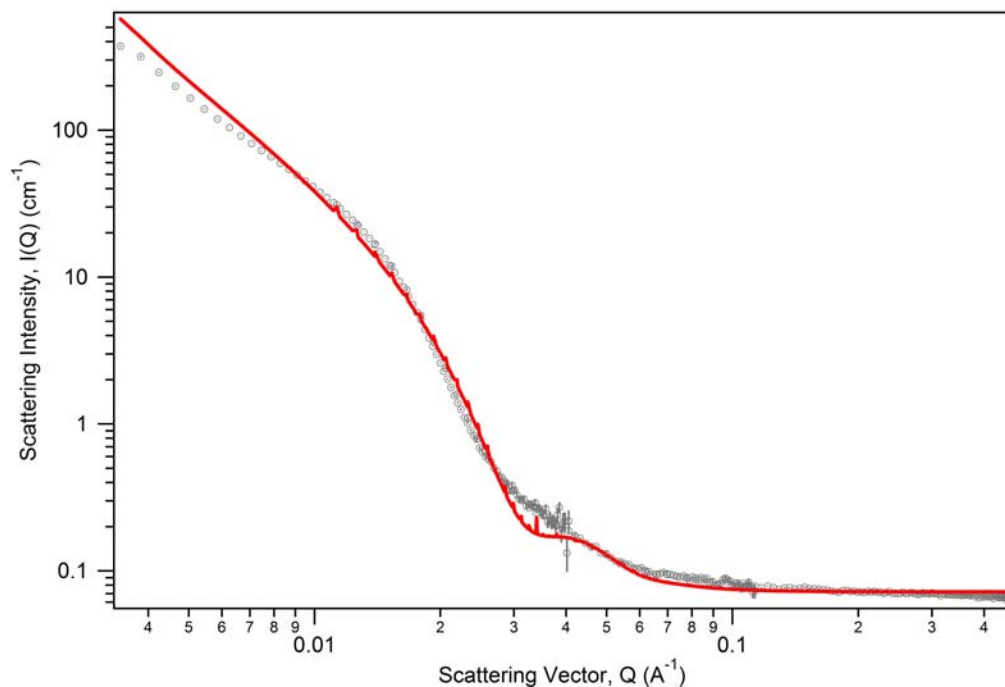


**Figure 6.18:** Example fit of lamellae form factor model to SANS data of 0.17 wt % solution PEO<sub>132</sub>-PB<sub>89</sub> in C<sub>6</sub>D<sub>12</sub> at 21.3 °C.

Flexible cylinders can also have a  $Q$ -scaling near 2, similar to that seen in Gaussian polymer chains. The fact that worm-like cylindrical micelles are observed in water solutions of this copolymer<sup>107</sup> leads one to believe that the same might be true in organic solutions. Also, cylindrical micelles are often observed at temperatures between spherical micellar and lamellar regions. Because this copolymer is observed to transition into a spherical body at high temperatures, it is more likely that the assemblies at low temperatures are cylindrical micelles, rather than lamellae. Because  $I(Q)$  scales with an intermediate exponent slightly greater than 2, this may indicate that the solvent is slightly “bad,” causing the worm-like micelles to slightly collapse upon themselves. While no  $Q^{-1}$  scattering is observed, it

may be obscured within the decrease in  $I(Q)$ , indicating that the cross-section and persistence length of the flexible cylinder are of similar length scales.

Scattering data were fitted to the flexible cylinder model, with polydisperse cross-sectional radius and excluded volume. A sample fit is shown in Figure 6.19, and fit results are shown in Table 6.9. Note that there is some discrepancy in the fitting from the scattering data at high- $Q$ . Additional polydispersity, such as in the persistence length, would cause high- $Q$  scattering to be smeared to a further extent. The model can only take into account polydispersity in the radius, and so high- $Q$  oscillations are observed in the fit. It is also important to note that because the scattering data extend beyond the SANS window, the overall contour length,  $L$ , of the cylinder is difficult to determine accurately. Here, the model will only be used for  $R_{cs}$  and  $l_p$  dimensions. Due to the poor fitting at high- $Q$  and the uncertainty in  $L$ , the reduced  $\chi^2$  value is large,  $\sim 4$ , but is much better than that of the lamella model.

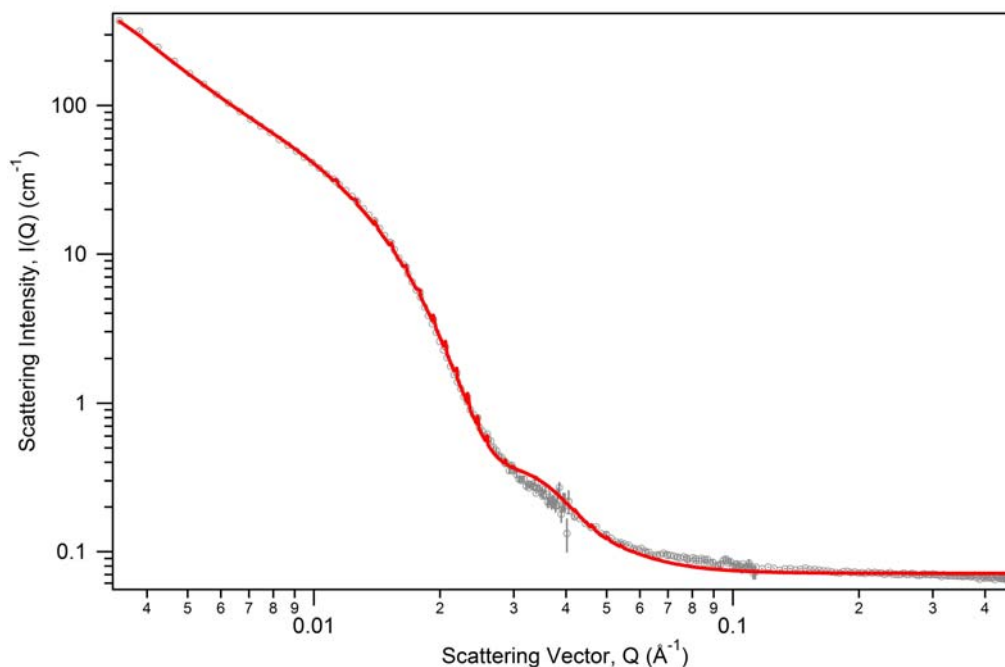


**Figure 6.19:** SANS data from PEO<sub>132</sub>-PB<sub>89</sub> in C<sub>6</sub>D<sub>12</sub> at 21.3 °C, fit with flexible cylinder model with polydisperse cross-sectional radius and excluded volume.

**Table 6.9:** Parameters of flexible cylinder with excluded volume and polydispersity in the cross-sectional radius fit to SANS data from PEO<sub>132</sub>-PB<sub>89</sub> in C<sub>6</sub>D<sub>12</sub>. The contour length cannot be trusted, as the scattering data extended beyond the SANS detection limit. Errors are shown at 99% level.

Temperature (°C)	Contour Length, L (Å)	Kuhn Length, b (Å)	Cross-Sectional Radius, R <sub>cs</sub> (Å)	Polydispersity of Radius, p (σ/R <sub>cs</sub> )
21.3	2.x10 <sup>6</sup> ± 3.x10 <sup>6</sup>	590 ± 20	139.6 ± 0.3	0.179 ± 0.003
30.6	2.x10 <sup>6</sup> ± 4.x10 <sup>6</sup>	600 ± 20	140.1 ± 0.3	0.180 ± 0.003
39.9	4.x10 <sup>4</sup> ± 2.x10 <sup>4</sup>	630 ± 20	139.7 ± 0.3	0.190 ± 0.003

### --High Temperatures

At 49.3 °C and above, the SANS scattering resembles that of spherical bodies.

Note that at high-Q, above  $Q \sim 0.06 \text{ \AA}^{-2}$ , the scattering intensity does not remain constant following the Porod region of the spherical bodies (Figure 6.20), but rather decreases slowly at high-Q. Scattering intensity at this high-Q region also increases with increasing temperature. Such scattering at high-Q may be indicative of

copolymer unimers in solution. This hypothesis is corroborated by the appearance of unimers in the DLS data from these solutions, which was discussed above.

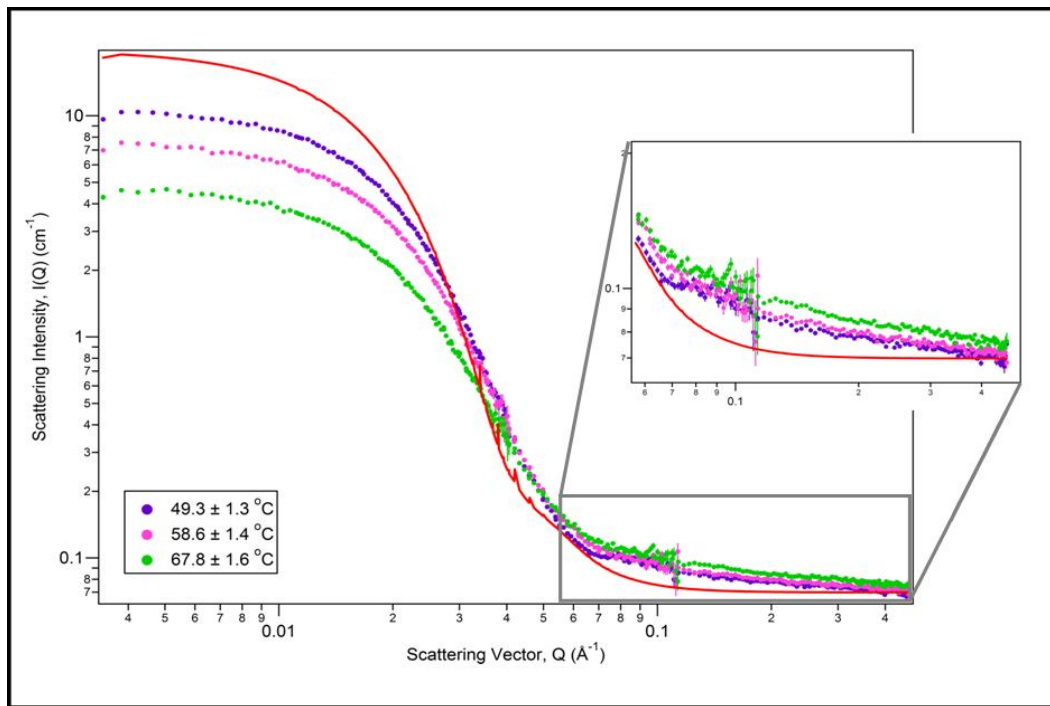


**Figure 6.20:** Scattering from spherical bodies in PEO<sub>132</sub>-PB<sub>89</sub> in C<sub>6</sub>D<sub>12</sub> at high temperatures. The red line displays expected scattering from Schulz spheres alone. Note that at high-Q, scattering intensity from the PEO<sub>132</sub>-PB<sub>89</sub> solution has a Q-dependence.

Linear Porod plots within the Guinier/intermediate regimes confirm that  $I(Q)$  has little dependence on  $Q$  (Table 6.10). Figure 6.21 shows an example fit. Q-scaling exponents in this Q-range slightly larger than 0 may indicate a small elongation of the copolymer assemblies.

**Table 6.10:** Intermediate Q-scaling exponents,  $n$ , for 0.17 wt % solution PEO<sub>132</sub>-PB<sub>89</sub> in C<sub>6</sub>D<sub>12</sub>. Errors are shown at 99% level.

Temperature, (°C)	Intermediate Q-scaling Exponent, $n$
49.3	0.23 ± 0.02
58.6	0.23 ± 0.03
67.9	0.23 ± 0.03

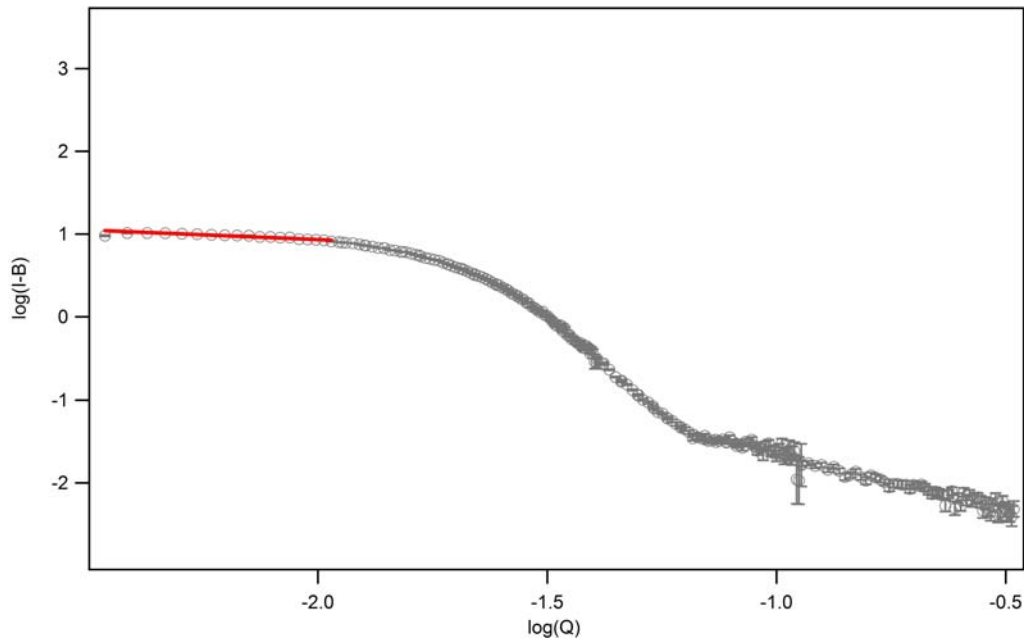


**Figure 6.21:** Example of linear Porod plot of spherical assemblies in the 0.17 wt % PEO<sub>132</sub>-PB<sub>89</sub>/C<sub>6</sub>D<sub>12</sub> solution at 49.3 °C.

Spherical dimensions were determined through linear Guinier plots and the nonlinear spherical form factor model with a Schulz distribution. These were fitted over the spherical portion of the scattering data. That is, the scattering at high-Q that corresponded to unimer scattering was not included in the fits. Figure 6.22 demonstrates examples of such fits, and the results from all temperatures are listed in Table 6.11. These results suggest that the spherical bodies become smaller as temperature is increased. This corresponds well with the increase in unimer scattering intensity at high-Q. It is expected that spherical micelles will become smaller with increasing temperature, and unimer concentration will increase.

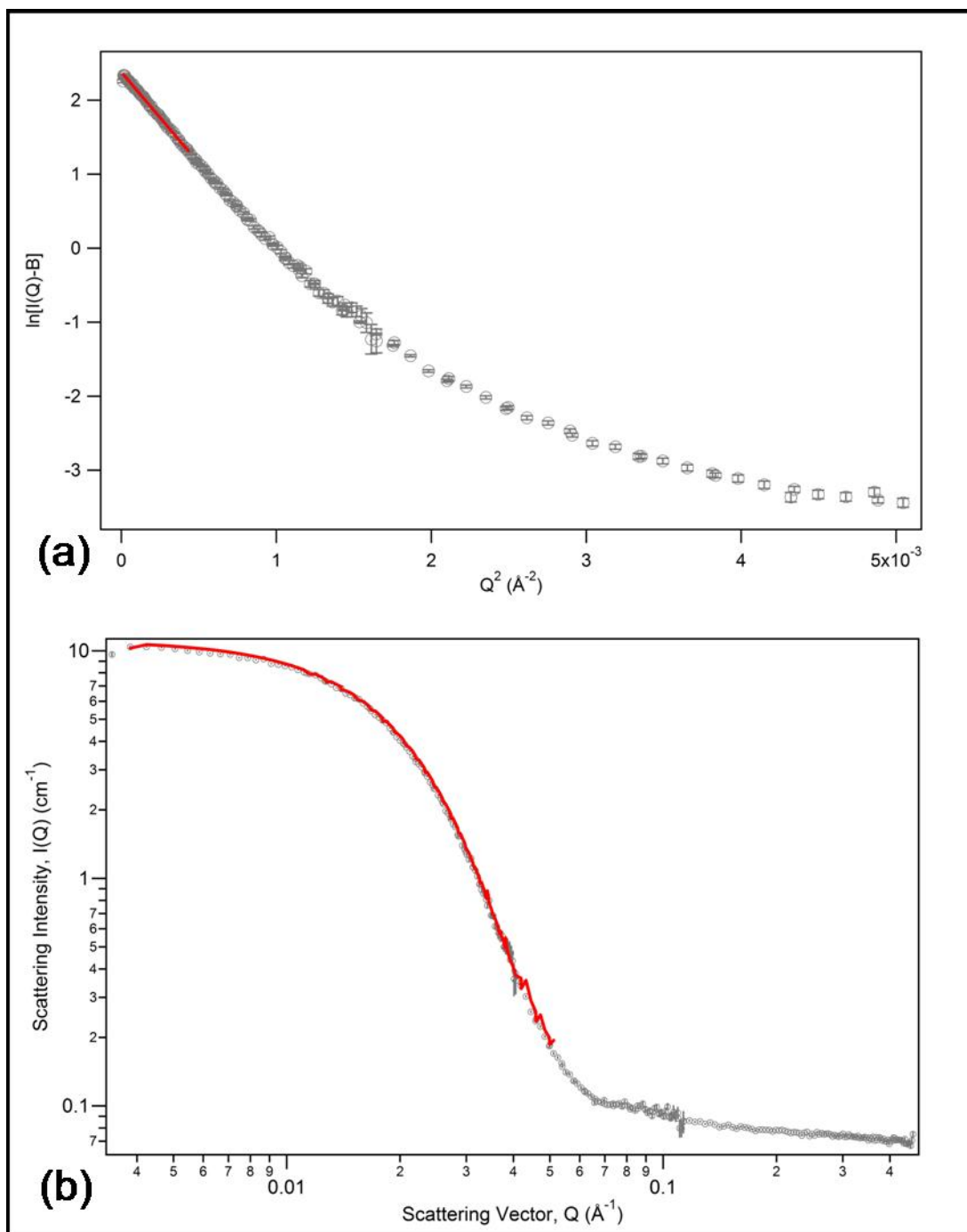


**Figure 6.22:** Example of SANS scattering from 0.17 wt % PEO<sub>132</sub>-PB<sub>89</sub> in C<sub>6</sub>D<sub>12</sub> at 49.3 °C, fit with (a) linear Guinier model and (b) the Schulz sphere model.



**Table 6.11:** Dimensions of spherical micelles for 0.17 wt % PEO<sub>132</sub>-PB<sub>89</sub> in C<sub>6</sub>D<sub>12</sub> as determined through linear Guinier plots and fits with Schulz sphere form factor models. Errors are shown at the 99% level.

Temperature, (°C)	Linear Guinier Plot			Spherical Form Factor with Schulz Polydispersity				
	Radius of Gyration, R <sub>g</sub> (Å)		Spherical Radius, R (Å)		Mean Radius, R (Å)			Polydispersity p
49.3	86.0	± 0.5	111.1	± 0.7	78.4	± 0.9	0.265	± 0.006
58.6	82.4	± 0.5	106.5	± 0.1	72.8	± 0.4	0.281	± 0.002
67.9	80.6	± 0.7	104.2	± 0.7	66	± 3	0.32	± 0.02

Finally, the nonlinear model of a core-shell sphere was used with polydispersity in the core radius. Again, high-Q scattering was excluded from the fitting. Scattering length densities were held constant so that it was assumed that PEO alone was present in the core and PB was solely present in the shell. It is doubtful that this assumption is true, however, as it is likely that some the copolymer blocks may intermingle slightly within the micelle structure, and it is probable that solvent molecules extend into the shell.

When the scattering length densities were not held constant, however, the model resulted in unrealistic results. Negative shell thicknesses and core scattering length densities closer to those of PB than PEO are examples of such unrealistic results. It has previously been shown by Ploetz and Greer that the core of these micelles in C<sub>6</sub>H<sub>12</sub> is hydrophilic,<sup>118</sup> and so the scattering length density should be closer to that of PEO. When the scattering length densities are held constant, the model appears to fit the data well (Figure 6.23). However, errors in the fitting parameters are large (Table 6.12), again suggesting this model may be too simple for the micelles in this system.

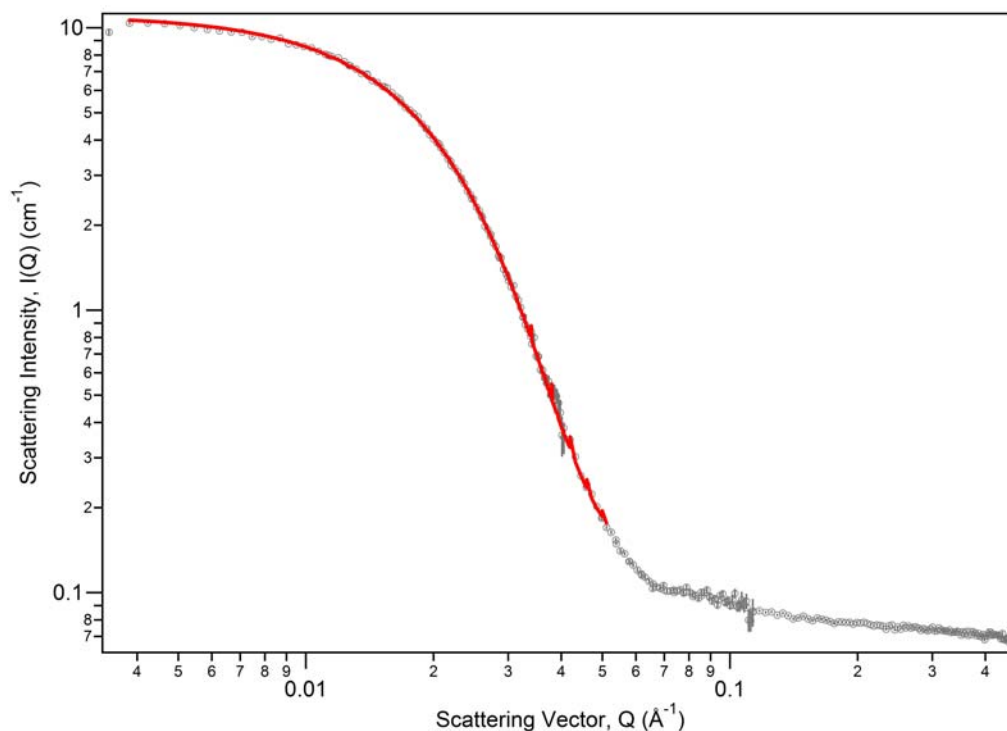


**Figure 6.23:** Example fitting of polydisperse core-shell model to 0.17 wt % PEO<sub>132</sub>-PB<sub>89</sub> in C<sub>6</sub>D<sub>12</sub> at 49.3 °C.

**Table 6.12:** Polydisperse core-shell model fitting parameters for 0.17 wt % PEO<sub>132</sub>-PB<sub>89</sub> in C<sub>6</sub>D<sub>12</sub>. Errors are shown at 99% level.

Temperature (°C)	Average Core Radius R <sub>c</sub> , (Å)		Polydispersity in Core Radius p, σ/R <sub>c</sub>			Shell Thickness, T, (Å)		
49.3	70	± 10	0.29	± 0.03		10	± 10	
58.6	60	± 10	0.31	± 0.03		10	± 10	
67.9	61	± 6	0.33	± 0.03		6	± 6	

Examining the results in a general manner, however, shows similar results to the previous fits to this data. The total radius (radius of the core plus shell thickness) is of the same length scale as that determined with the sphere form factor model, and this radius is observed to decrease with increasing temperature. The largest error is found in the shell thickness. This may be because this was assumed include only PB molecules, not accounting for solvent in the shell. Difficulties in fitting may also

arise because the scattering data at high-Q were obscured with unimer scattering, and the full Q-range could not be used in the fitting.

A more extensive model may be necessary to fit these data. For example, a spherical micelle with polymer chains attached at the surface has been presented for block copolymer micelles by Pedersen and Gerstenberg.<sup>126</sup> At this time, such a model has not been prepared by NIST for fitting in IGOR Pro, and is not used here. Such a model should be used in the future to complete the examination of these PEO<sub>132</sub>-PB<sub>89</sub> micelles.

#### *Summary of C<sub>6</sub>D<sub>12</sub> results*

Table 6.13 compares DLS and SANS results for 0.17 wt % solution of PEO<sub>132</sub>-PB<sub>89</sub> in C<sub>6</sub>D<sub>12</sub> at low temperatures. Below temperatures around 40 °C, DLS results showed the existence of large scattering bodies in solutions of PEO<sub>132</sub>-PB<sub>89</sub> in C<sub>6</sub>D<sub>12</sub>, with hydrodynamic radii of approximately 2000 Å. The shape of these scattering bodies was investigated through SANS techniques. It was confirmed that these bodies have the shape of worm-like cylinders. While the total contour length scale was outside the range of the SANS window, it was found that these worm-like micelles have a cross-sectional radius of approximately 140 Å and a persistence length ( $l_p=b/2$ ) of 300 Å. The similarity between persistence length and the cross-sectional radius dimensions confirms why no I(Q) scaling with 1/Q was observed in the SANS scattering data.

**Table: 6.13:** Dimensions of flexible cylinders in PEO<sub>132</sub>-PB<sub>89</sub> in C<sub>6</sub>D<sub>12</sub>. Hydrodynamic radii were determined through DLS of 0.18 wt % solution. Kuhn lengths ( $=2 \cdot l_p$ ) and cross-sectional radii determined through the flexible cylinder model with excluded volume and polydisperse cross-sectional radius fit to SANS data of 0.17 wt % solution.

Temperature (°C)	Hydrodynamic Radius, R <sub>h</sub> (Å)			Kuhn Length, b (Å)			Cross-Sectional Radius, R <sub>cs</sub> (Å)		
21.3 ± 1.0				590 ± 20			139.6 ± 0.3		
22.3 ± 0.1	2242 ± 101								
29.1 ± 0.1	2392 ± 107								
30.6 ± 1.1				600 ± 20			140.1 ± 0.3		
37.3 ± 0.1	1737 ± 78								
39.9 ± 1.2				630 ± 20			139.7 ± 0.3		
45.2 ± 0.1	1769 ± 83								
48.4 ± 0.1	1512 ± 69								
54.8 ± 0.1	2621 ± 112								
61.7 ± 0.1	1866 ± 77								

It is interesting that the worm-like assembly was seen at all temperatures through DLS techniques, but was only visible below 50 °C through SANS techniques. This indicates that the percent of all the assemblies in the solution that have this form is rather small. The peak area of the DLS results is a sign of this (reported in Table 6.7). Above 50 °C, the percentage of these assemblies in solution is so low that its neutron scattering intensity was obscured by that of the spherical assemblies in solution.

Near 50 °C, a change in scattering body size and shape is observed through both DLS and SANS techniques. A scattering body of smaller R<sub>h</sub> appears in DLS results, and this has a much larger peak area than the cylindrical body. DLS also indicates the appearance of unimer bodies in solution at higher temperatures. SANS data also indicates that these scattering bodies are spherical.

Table 6.14 compares the radii dimensions of these spherical bodies, as determined through multiple analysis techniques. In this table, the dimensions of the

“mean radius” and the “average total radius” appear small in comparison to the others listed. This is because the techniques used to determine these values (the Schulz sphere model and core-shell model, respectively) included polydispersity. Other analysis techniques, the linear Guinier plot and DLS, reported dimensions only of the larger micelles in the population. Taking this into consideration, all dimensions determined are similar.

**Table 6.14:** Comparison of spherical dimensions of PEO<sub>132</sub>-PB<sub>89</sub> micelles in C<sub>6</sub>D<sub>12</sub>. Hydrodynamic radii are determined through DLS, spherical radii are determined through linear Guinier plots, the mean radii were established through fits with the Schulz sphere form factor model, and the average total radius was calculated through fits to the polydisperse core-shell model.

Temperature (°C)	Hydrodynamic Radius, R <sub>h</sub> (Å)			Spherical Radius, R (Å)			Mean Radius, R (Å)			Average Total Radius, R <sub>c</sub> +T (Å)		
45.2 ± 0.1	360	±	10									
48.4 ± 0.1	181	±	8									
49.3 ± 1.3				111.1	±	0.7	78.4	±	0.9	80	±	10
54.8 ± 0.1	149	±	7									
58.6 ± 1.4				106.5	±	0.1	72.8	±	0.4	70	±	10
61.7 ± 0.1	173	±	7									
67.9 ± 1.6				104.2	±	0.7	66	±	3	67	±	8

These results from deuterated cyclohexane compare well with those observed by Ploetz and Greer through DLS studies on PEO<sub>132</sub>-PB<sub>89</sub> in protonated cyclohexane.<sup>118</sup> SANS investigations made here confirm the assumptions made by Ploetz and Greer. This copolymer self-assembles into worm-like micelles below 50 °C. As temperature is increased, these assemblies disassemble into spherical micelles and unimers. It is presumed that if the temperature were increased still further, the spherical micelles would also break down.

## 6.4 Conclusions

Through SANS analyses in deuterated methanol, it has been shown that PEO<sub>132</sub>-PB<sub>89</sub> forms spherical micelles. These micelles change little over the temperature span of approximately 20-70 °C. DLS analyses in this same solvent show the presence of unimers in solution with these spherical micelles. In deuterated cyclohexane, this copolymer forms reverse micelles that change shape with increasing temperature. Below 50 °C, worm-like, or flexible cylinder, micelles also exist in solution. As temperature is increased, these micelles transform into spherical micelles.

This copolymer has only previously been investigated in organic solvents through DLS techniques by Ploetz and Greer.<sup>118</sup> In methanol, the copolymer was observed to form two distinct micelle formations. It was proposed that these were of cylindrical and spherical forms. Reverse micelles, that is, with hydrophilic PEO at the core, form in cyclohexane. At low temperatures, cylindrical micelles exist, disassembling into spherical micelles with increasing temperature. Ploetz and Greer proposed these micelle shapes based upon extrapolation from aqueous systems. Here, the shape of these micellar assemblies has been confirmed.

Solvent isotopic effects were observed to affect micelle shape in solutions of PEO<sub>132</sub>-PB<sub>89</sub>. It is often assumed that copolymers will behave in the same manner in protonated and deuterated solvents. This copolymer forms both cylindrical and spherical micelles in protonated methanol. However, in deuterated methanol, only spherical micelles are observed. It is believed that such differences are due to stronger PEO/methanol hydrogen bonds in the deuterated solvent. Such bonds would

be more favored, and so the spherical formation is kept, as it offers more opportunity for hydrogen bonds. A literature search presented systems in which solvent isotope differences have affected spherical critical micelle temperature and even micelle size and aggregation number.<sup>20, 23, 124, 125</sup> However, no work displaying this disparity in micelle formations was found. No hydrogen bonding occurs between copolymer and solvent in cyclohexane solutions, and so, the isotope difference should not greatly affect the micelle assemblies; such was observed here.

## Chapter 7: Summary and Conclusions

Self-aggregation in three dilute copolymer systems has been examined. Two triblock copolymer systems and one diblock system have been investigated in aqueous and organic solvents, respectively. The self-aggregation characteristics of these systems have proven rich and complex.

The triblock Pluronic P85,  $\text{PEO}_{25}\text{-PPO}_{40}\text{-PEO}_{25}$ , was examined in  $\text{D}_2\text{O}$  under pressure through small angle neutron scattering. In dilute solutions (less than 10% volume fraction) and at low temperatures, this copolymer forms spherical micelles. These micelles transition to cylindrical micelles and further to lamellae with increasing temperature.<sup>45, 67, 69, 70</sup> It was shown that the addition of pressure raises the temperature of transition between each of these aggregate formations.<sup>30</sup>

P85 in  $\text{D}_2\text{O}$  also phase separates at high temperatures. The phase transition was observed to decrease with increasing pressure.<sup>30</sup> The phase separation is noted by the appearance of a demixed lamellae phase; that is, lamellae formations with solvent pockets. This phase had not been seen previously at ambient pressures.

Aqueous solutions of the Reverse Pluronic 17R4,  $\text{PPO}_{14}\text{-PEO}_{24}\text{-PPO}_{14}$ , were also examined. This triblock system has a multifaceted phase diagram. The phase diagram of 17R4 in  $\text{D}_2\text{O}$  contains three distinct regions: Region I is cloudy and one-phase, Region II is clear and one-phase, and Region III has two coexisting phases. The phase diagram was determined via visual inspection of solution clearing between Regions I and II. Visual observance of phase separation identified the transition to



Region III. The phase diagram of 17R4 in H<sub>2</sub>O had been previously examined by Zhou and Chu, using similar techniques.<sup>80</sup>

The phase diagrams of 17R4/D<sub>2</sub>O and 17R4/H<sub>2</sub>O are surprisingly similar given the years between the experiments and the impurities often attributed to similar commercial triblocks. Transition lines of the 17R4/D<sub>2</sub>O system coincide well with in shape with those in the H<sub>2</sub>O system, but transitions do occur at lower temperatures in the D<sub>2</sub>O system. This was not unexpected. Zhou and Chu reported the clearing of Region I with solution filtration, but this clearing could not be repeated for 17R4 in D<sub>2</sub>O.

The phase diagrams of these aqueous 17R4 systems are also being investigated by Jacobs et al.<sup>83</sup> Using refractive index measurements, Jacobs et al. determine the concentrations of the coexisting phases at a number of temperatures above the phase transition temperature. Intriguing differences exist between the transition lines of Jacobs et al. and those determined through traditional cloud-point techniques. The disparities between these phase diagrams suggest non-equilibrium states in one or all of the systems. These variations merit further investigation, which is being pursued by Jacobs et al.

The copolymer structures within each region of 17R4 in D<sub>2</sub>O were investigated. Three samples of concentration and temperatures within Region I were examined through SANS in the 17R4/D<sub>2</sub>O system. Unimers were observed to exist freely at very low concentration and temperature. As temperature or concentration is increased, these unimers aggregate to form clusters, or a network of clusters, in solution. This network most likely consists of PPO blocks “knotted” together in a

manner so as to reduce PPO-D<sub>2</sub>O interactions. PEO blocks still extend into, and are solvated by, D<sub>2</sub>O. These networks are about a micron in size and are presumably the cause of the cloudy and opaque appearance of the solution in this Region. It is proposed that Zhou and Chu<sup>80</sup> were able to break these networks by filtration, temporarily clearing the solution.

One sample was also analyzed within Region II by SANS and DLS techniques. Within this region, copolymer chains self-assemble into an aggregate with a slight elliptical shape. Fits of the SANS data could not reliably determine whether these aggregates were the flower-like micelles that are expected from Reverse Pluronics.<sup>5</sup> While Zhou and Chu originally deemed these aggregates “micelles,”<sup>80</sup> the assemblies are much smaller than traditional micelles, and the SANS scattering cannot be fitted by the usual core-shell model.

Further analysis of the SANS data with a more complex, flower-like micelle model or even molecular probe experiments would help confirm the formation of these assemblies. For example, one could monitor the solvation of a hydrophobic molecule in solutions of 17R4 in D<sub>2</sub>O, as temperature is increased from Region I to Region II. Solvation of such a molecule would suggest that the Region II aggregates have a hydrophobic core. It would also be interesting to take SANS data at higher concentrations within Region II. Further, a contrast-matched SANS study would more clearly define the location of PEO and PPO blocks within the copolymer assemblies.

Finally, the diblock copolymer PEO<sub>132</sub>-PB<sub>89</sub> was examined in organic solvents. This copolymer was previously studied by Ploetz and Greer<sup>40, 118</sup> in

cyclohexane and methanol, and in the partially miscible mixed solvent cyclohexane-methanol.<sup>118</sup> Here, the formations of self-aggregation assemblies in deuterated cyclohexane and deuterated methanol were examined.

In deuterated methanol, PEO<sub>132</sub>-PB<sub>89</sub> forms spherical micelles, which coexist with unimer chains in solution. There is little change in the size or shape of these micelles over a 50 °C temperature span. The size of these micelles is similar to one assembly seen in the PEO<sub>132</sub>-PB<sub>89</sub>/CH<sub>3</sub>OH system that Ploetz and Greer had suggested to be spherical micelles. Through SANS data here, this hypothesis appears to be correct.

This PEO<sub>132</sub>-PB<sub>89</sub>/methanol system also offered an interesting example of solvent isotope effects on copolymer self-assemblies. Ploetz and Greer saw the formation of two distinct micellar assemblies in the PEO<sub>132</sub>-PB<sub>89</sub> system, presumably cylindrical and spherical micelles.<sup>40, 118</sup> However, in the deuterated solvent system, only spherical micelles are present and no cylindrical micelle formation is observed. While previously literature reports changes in micelle size, aggregation number, and critical micelle temperatures due to differences in solvent isotopes,<sup>20, 23, 124, 125</sup> no earlier reports of such a difference in assembly formations has been found. This finding demonstrates the importance of approaching copolymer systems in deuterated solvents differently than protonated solvents. Often such systems are assumed to behave in identical manners. While their behavior is often similar, it is important to recognize the possibility of differences in solution and aggregate behaviors.

Deuterated and protonated PEO<sub>132</sub>-PB<sub>89</sub> and cyclohexane systems were found to behave in similar manners, presumably because of the lack of hydrogen bonding.

Here, SANS experiments were able to confirm the assembly formations proposed by Ploetz and Greer.<sup>40, 118</sup> At low temperatures, cylindrical micelles exist in solution. As the temperature is increased, these cylindrical micelles disassemble into spherical micelles, coexisting with unimers. The spherical micelles continue to decrease in size with increasing temperature, while the unimer concentration increases. Such transitions are typical of copolymers in organic systems, as they are enthalpically driven, as opposed to the entropically driven aqueous systems.

These systems offer many opportunities for further studies. While Ploetz and Greer showed the presence of micelles in the cyclohexane system through molecular probe experiments,<sup>40, 118</sup> the SANS data acquired here could not be fitted by a traditional core-shell model. Further analysis with another model, allowing for both micelles and attached unimer chains may prove useful and informative. Such a model has been discussed in the literature,<sup>126</sup> but is not readily available from NIST. Isotope effects in the methanol system could be further pursued through investigation of a deuterated copolymer/protonated solvent system. Finally, SANS inspection of the micelle assemblies seen by Ploetz and Greer in the cyclohexane-methanol mixed solvent system would also be fascinating.

## Appendices

### Appendix A: Determination of Uncertainties in DLS Analyses

Anisimov advised that the DynaLS software generally overestimates the standard deviation values in hydrodynamic radius ( $R_h$ ) values.<sup>41</sup> Because of this, a more realistic estimate of error was desired.

When Equations (2.5)-(2.7) are rearranged, the following relationship describes  $R_h$ :

$$R_h = \frac{8}{3} \frac{k_B T}{\eta} \frac{\pi n^2}{\lambda^2} \frac{1}{\Gamma} \sin^2\left(\frac{\theta}{2}\right). \quad (\text{A.1})$$

Propagation of error as:

$$u_{R_h} = \sqrt{u_T^2 \left(\frac{\partial R_h}{\partial T}\right)^2 + u_\eta^2 \left(\frac{\partial R_h}{\partial \eta}\right)^2 + u_n^2 \left(\frac{\partial R_h}{\partial n}\right)^2 + u_\lambda^2 \left(\frac{\partial R_h}{\partial \lambda}\right)^2 + u_\Gamma^2 \left(\frac{\partial R_h}{\partial \Gamma}\right)^2 + u_\theta^2 \left(\frac{\partial R_h}{\partial \theta}\right)^2}, \quad (\text{A.2})$$

where  $u$  is the 99% uncertainty, results in:<sup>40</sup>

$$u_{R_h} = R \sqrt{\left(\frac{u_T}{T}\right)^2 + \left(\frac{u_\eta}{\eta}\right)^2 + \left(\frac{2u_n}{n}\right)^2 + \left(\frac{2u_\lambda}{\lambda}\right)^2 + \left(\frac{u_\Gamma}{\Gamma}\right)^2 + \left(\frac{u_\theta}{\tan\left(\frac{\theta}{2}\right)}\right)^2}. \quad (\text{A.3})$$

Uncertainties in temperature, refractive index, and viscosity values were discussed within each chapter for the different copolymer systems. These values, as well as uncertainties in other variables are restated in Table A.1. Uncertainty in laser

wavelength is estimated at  $\pm 5\%$ , as done by Ploetz.<sup>40</sup> That in the scattering angle is  $\pm 0.01^\circ$ .

In systems with only one type of scattering body present, the autocorrelation function (ACF) is described by:<sup>34</sup>

$$g_2(\tau) = 1 + p \exp(-2\Gamma\tau), \quad (\text{A.4})$$

where  $g_2(\tau)$  is the normalized ACF,  $p$  is the mean square scattering light intensity,  $\tau$  is the correlation time, and  $\Gamma$  is the decay rate of the exponential function.<sup>34</sup>  $\Gamma$  can be determined by the slope of a  $\ln(g_2(t)-1)$  as a function of  $\tau$  plot. However, in a polydisperse system, it is more difficult to determine  $\Gamma$ , as described in Chapter 2.

Because of the difficulty in determining  $\Gamma$ , propagation of error was only performed on one DLS data set from each of the poly(ethylene oxide)-polybutadiene systems in order to make a general statement of error. These copolymer systems were used because they showed systems with one type of scattering body at one or more temperatures. Here, the third iteration of data collection at  $37.3^\circ\text{C}$  was used from the  $\text{C}_6\text{D}_{12}$  data, and the first iteration of data collection at  $42^\circ\text{C}$  was used from the  $\text{CD}_3\text{OD}$  system. A 99% uncertainty was estimated as three times the standard deviation of the  $\Gamma$  value. The error was found to be  $\sim 1.5\%$  of the  $\Gamma$  value in the  $\text{C}_6\text{D}_{12}$  system and  $\sim 6\%$  in the  $\text{CD}_3\text{OD}$  system.

**Table A.1:** Uncertainties in DLS and PEO-PB copolymer system characteristics, used to calculate uncertainty in  $R_h$ .

Variable	Value in $C_6D_{12}^a$	99% Uncertainty	Value in $CD_3OD^b$	99% Uncertainty
n	1.43	0.00	1.3	0.0
$\lambda$	632.8 nm	3.164 nm	632.8 nm	3.164 nm
$\theta$	90°	0.01°	90°	0.01°
$\Gamma$	590 Hz	9 Hz	9075.5 Hz	571.5 Hz
T	310.4 K	0.1 K	299 K	2 K
$\eta$	0.79 cP	0.04 cP	0.7 cP	0.3 cP

a: Values of variables and uncertainties at 37.3 °C,  $\Gamma$  determined for third DLS iteration at this temperature. b: Values of variables and uncertainties at 42 °C,  $\Gamma$  determined from the first DLS iteration at this temperature.

From the uncertainties in Table A.1 for the  $C_6D_{12}$  system, the overall uncertainty in  $R_h$  for PEO<sub>132</sub>-PB<sub>89</sub> at 37.3 °C was found to be approximately 5%. Ploetz showed that the uncertainty in  $\Gamma$  depends on the value of scattering intensity.<sup>40</sup> Data sets with low scattering intensity have greater uncertainty in  $\Gamma$ . Because error in  $\Gamma$  should become larger in samples with less scattering intensity (for example, as cylindrical micelles become spherical), and because error in  $\Gamma$  should also increase in samples with several kinds of scattering bodies, a 10% error in  $R_h$  is applied to all PEO<sub>132</sub>-PB<sub>89</sub>/ $C_6D_{12}$  DLS analyses.

In the  $CD_3OD$  system, however, there is a much greater uncertainty in viscosity. This uncertainty becomes the controlling variable in the overall uncertainty. That is, for the DLS data from 42 °C, the uncertainty in viscosity is ~ 40%, as is the overall uncertainty in  $R_h$ . Because of this, a 40% uncertainty is applied to all  $R_h$  values determined for the  $CD_3OD$  system.

Finally, uncertainty must be addressed in the 17R4/ $D_2O$  system. No DLS data set displayed scattering from only one kind of scattering body, and so it is not possible to estimate  $\Gamma$  and the uncertainty in  $\Gamma$ . The uncertainties in all other

variables are listed in Table A.2. If a 5% uncertainty in  $\Gamma$  is estimated, an overall uncertainty in  $R_h$  of  $\sim 8\%$  at  $35\text{ }^\circ\text{C}$  is obtained. Therefore, a conservative 10% uncertainty in all  $R_h$  values is applied in the 17R4/D<sub>2</sub>O system.

**Table A.2:** Uncertainties in DLS and 17R4/D<sub>2</sub>O copolymer system characteristics, used to calculate uncertainty in  $R_h$ .

Variable	Value in 17R4/D <sub>2</sub> O <sup>a</sup>	99% Uncertainty
n	1.325	0.008
$\lambda$	632.8 nm	3.164 nm
$\theta$	90°	0.01°
$\Gamma$		5%
T	308 K	2 K
$\eta$	10.3 cP	0.6 cP

a: Variable values and uncertainties at  $35\text{ }^\circ\text{C}$ , uncertainty in  $\Gamma$  estimated at  $\pm 5\%$ .



## Appendix B: Scattering Length Density Calculations

Scattering length density,  $\rho_n$ , depends upon the nuclei within the molecule.  $\rho_n$  is related to the neutron scattering length,  $b$ , of all the atoms within a molecule that has total volume,  $v_{\text{molecule}}$ .<sup>42, 43, 45</sup>

$$\rho_n = \frac{\sum b}{V_{\text{molecule}}} . \quad (\text{B.1})$$

Atoms have unique scattering length values which vary dramatically with atomic number, and even between isotopes of the same element. This is because neutrons scatter from the nuclei of an atom, as opposed to the surrounding electrons that scatter light and x-rays.<sup>42, 43</sup> For example, hydrogen has a  $b = -3.739 \times 10^{-13}$  cm, where the negative sign represents that scattered neutrons are out of phase with incident neutrons. Deuterium, on the other hand, has a  $b = 6.671 \times 10^{-13}$  cm.<sup>42, 43, 45</sup>

The NIST Center for Neutron Research (NCNR) provides a scattering length density calculator online which determines the scattering length density of a molecule or solvent, given the molecular compound and its density.<sup>127</sup> This calculator was used to determine the scattering length densities for all compounds in this dissertation.

While the densities of solvents could be found in their corresponding material safety data sheets and polymer densities were found in literature, copolymer densities had to be calculated. The PEO<sub>132</sub>-PB<sub>89</sub> copolymer is 54.7 wt% PEO, and 45.3 wt% PB. These percentages were applied to the densities of each polymer, and these were added to obtain the weight average density of the copolymer, 1.03 g/cm<sup>3</sup>. This density was

used in scattering length density calculations. All densities and scattering length densities of polymers and solvents used here are found in Table B.1.

**Table B.1:** Densities and scattering length densities of solvents and polymers

	Compound	Density (g/cm <sup>3</sup> )	Scattering Length Density (Å <sup>-2</sup> )
d-water	D <sub>2</sub> O	1.10 <sup>a</sup>	6.3x10 <sup>-6</sup>
d-cyclohexane	C <sub>6</sub> D <sub>12</sub>	0.89 <sup>b</sup>	6.7x10 <sup>-6</sup>
d-methanol	CD <sub>3</sub> OD	0.89 <sup>c</sup>	5.8x10 <sup>-6</sup>
PEO	C <sub>2</sub> H <sub>4</sub> O	1.127 <sup>d</sup>	6.4x10 <sup>-7</sup>
PPO	C <sub>3</sub> H <sub>6</sub> O	1.004 <sup>d</sup>	3.4x10 <sup>-7</sup>
PB	C <sub>4</sub> H <sub>6</sub>	0.89 <sup>e</sup>	4.1x10 <sup>-7</sup>
PEO <sub>132</sub> -PB <sub>89</sub>	C <sub>2</sub> H <sub>4</sub> OC <sub>4</sub> H <sub>6</sub>	1.03	5.2x10 <sup>-7</sup>

a: Density value from D<sub>2</sub>O material safety data sheet (MSDS) from Cambridge Isotope Laboratories. b: Density value from MSDS from Cambridge Isotope Laboratories. c: Density value from CD<sub>3</sub>OD MSDS from Cambridge Isotope Laboratories. d: Density values from Hammouda.<sup>45</sup> e: Density value from Wignall.<sup>119</sup> Scattering length densities for 17R4 and P85 copolymers were not needed in the SANS analyses used.

## Appendix C: Reverse Pluronic 17R4 in D<sub>2</sub>O

### C.1 Temperatures of interest in the phase diagram

Aggregation temperatures of 17R4 in D<sub>2</sub>O are presented in Table C.1. Recall that this was noted by the appearance of clearing in the solution. Here, the last temperature at which a solution was observed to be cloudy is noted, as is the first temperature the solution was observed to be clear. The aggregation temperature is assumed to lie between these two temperatures. The midpoint of these temperatures is used as the data point in Figure 5.9. The error bars in Figure 5.9 represent the full range between the temperatures discussed above, including error in those temperatures.

Similarly, the phase transition temperatures are also noted in Table C.2-C.3. The phase transition was observed through two techniques: the cloud-point technique, in which the solution became highly milky and opaque, and the observance of phase separation. The cloud-point temperatures are shown in Table C.2 and the phase separation temperatures are given in Table C.3. As above, the last temperature at which a solution was observed to be clear or one phase is indicated, as is the first temperature at which the cloud-point or phase separation was observed. Again, the transition point is believed to be between these temperatures, and the midpoint was used in Figure 4.9. Error bars in this figure represent the entire range of temperatures in which the transition may occur.

**Table C.1:** Aggregation temperatures for 17R4 in D<sub>2</sub>O.

$\omega$	Aggregation Temperature								
	Last Temperature of Cloudy Solution °C			First Temperature with Clear Solution °C			Midpoint Temperature °C	Total Range °C	+/- from Midpoint °C
0.028									
0.048									
0.12									
0.16	35.02	±	0.01	35.21	±	0.01	35.11	0.21	0.10
0.17	34.85	±	0.01	34.90	±	0.01	34.88	0.08	0.04
0.23	33.94	±	0.01	33.98	±	0.01	33.96	0.06	0.03
0.27	32.01	±	0.01	32.06	±	0.01	32.03	0.08	0.04
0.30	30.51	±	0.01	30.75	±	0.01	30.63	0.26	0.13
0.33	27.81	±	0.01	28.08	±	0.01	27.94	0.29	0.14
0.39	21.65	±	0.01	21.97	±	0.01	21.81	0.34	0.17
0.43	12.76	±	1.01	13.21	±	1.01	12.99	2.47	1.24
0.48	less than 0 °C								

**Table C.2:** Cloud-point temperatures for 17R4 in D<sub>2</sub>O.

$\omega$	Cloudpoint Temperature								
	Last Temperature of Clear Solution °C			First Temperature where Cloudpoint Observed °C			Midpoint Temperature °C	Total Range °C	+/- from Midpoint °C
0.028									
0.048									
0.12									
0.16									
0.17									
0.23	43.16	±	0.01	43.22	±	0.01	43.19	0.08	0.04
0.27									
0.30									
0.33	45.29	±	0.01	45.38	±	0.01	45.33	0.10	0.05
0.39	46.55	±	0.01	46.58	±	0.01	46.56	0.05	0.03
0.43	47.96	±	0.01	48.11	±	0.01	48.03	0.17	0.09
0.48	49.89	±	0.01	49.97	±	0.01	49.93	0.10	0.05

**Table C.3:** Phase separation temperatures for 17R4/D<sub>2</sub>O solutions.

$\omega$	Phase Separation Temperature								
	Last Temperature of One-Phase Solution °C			First Temperature with Two-Phase Solution °C			Midpoint Temperature °C	Total Range °C	+/- from Midpoint °C
0.028	38.91	±	0.01	40.01	±	0.01	39.46	1.12	0.56
0.048	36.21	±	0.01	37.69	±	0.01	36.95	1.50	0.75
0.12	33.02	±	0.01	34.08	±	0.01	33.55	1.07	0.54
0.16	41.78	±	0.01	42.01	±	0.01	41.89	0.25	0.12
0.17	42.38	±	0.01	42.40	±	0.01	42.39	0.04	0.02
0.23	43.24	±	0.01	43.29	±	0.01	43.26	0.06	0.03
0.27	44.18	±	0.01	44.20	±	0.01	44.19	0.04	0.02
0.30	44.67	±	0.01	44.71	±	0.01	44.69	0.06	0.03
0.33									
0.39									
0.43									
0.48									

## C.2: Calculations of 17R4 unimer volume and estimation of number of unimers in Region II aggregate

### *Estimation of the volume of one 17R4 molecule:*

The volume of one 17R4 molecule is estimated by the sum of PPO and PEO volumes.

Values of monomer volumes from Hammouda.<sup>9</sup>

PPO volume: 28 PPO molecules  $\times$  57.77 cm<sup>3</sup>/mol = 1618 cm<sup>3</sup>/mol PPO in 17R4

PEO volume: 24 PEO molecules  $\times$  39.04 cm<sup>3</sup>/mol = 937 cm<sup>3</sup>/mol PEO in 17R4

Total volume of 17R4 molecule:

$$2555 \text{ cm}^3/\text{mol 17R4} = 4.2 \times 10^3 \text{ \AA}^3/\text{molecule}$$

If a spherical body is assumed,  $V=4/3\pi R^3$ . If the volume found above is used,  $R \approx 10 \text{ \AA}$ .

### *Estimation of the number of unimer chains in Region II aggregates:*

If an approximate radius of gyration of 30 Å is used, the number of 17R4 unimers in this aggregate can be determined. A spherical body is assumed, and the volume found above is used for a 17R4 molecule.

$$R = \sqrt{\frac{5}{3}} R_g \approx 39 \text{ \AA}, V_{\text{agg}} \approx 2.5 \times 10^5 \text{ \AA}^3$$

$$\frac{V_{\text{agg}}}{V_{17R4}} = \frac{2.5 \times 10^5 \text{ \AA}^3}{4.2 \times 10^3 \text{ \AA}^3} \approx 60 \text{ unimers}$$

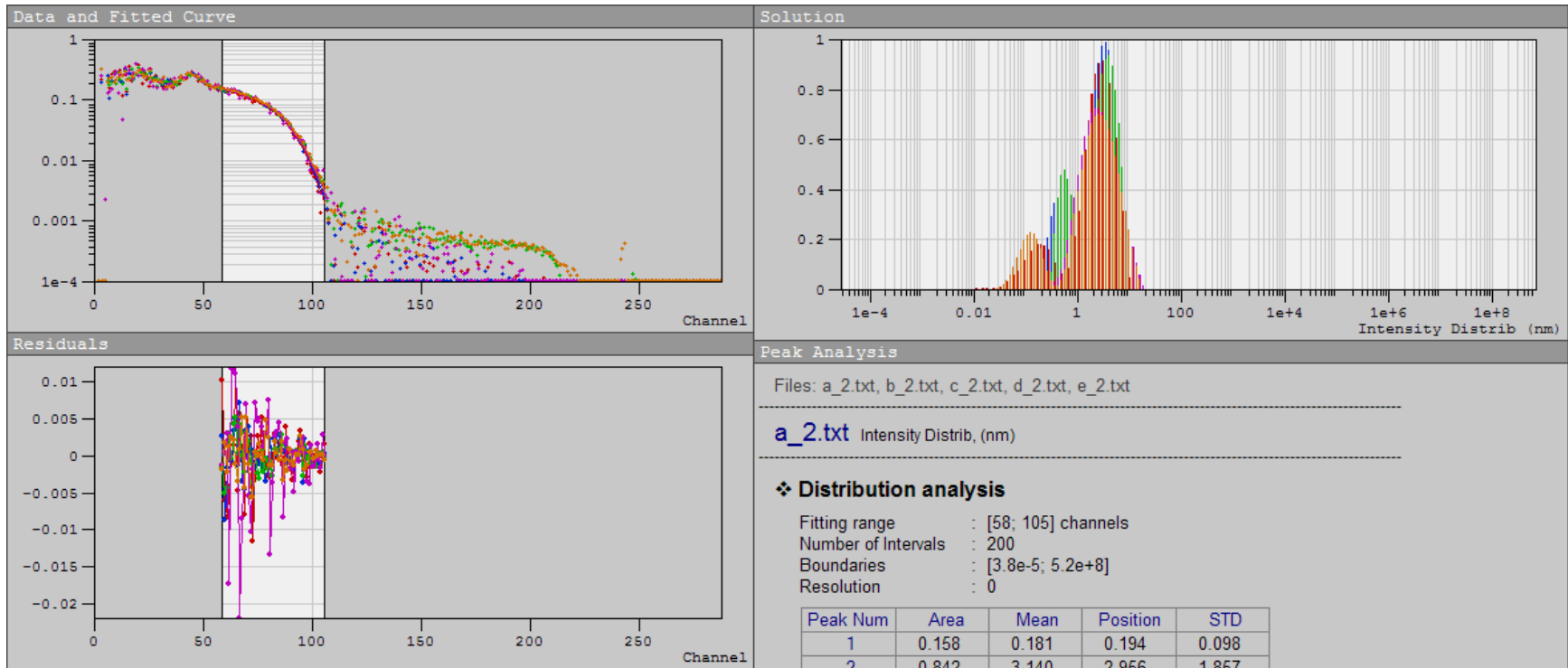
### C.3: DLS and SANS data

Results are presented for below DynaLS analyses of 17R4/D<sub>2</sub>O DLS data at 35 and 39 °C in Table C.4. Figures of DynaLS results follow these tables. Analyses of SANS data from the 17R4 solutions are also presented. All Region I data are presented first. The  $\omega=0.23$  solution data are presented, followed by the dilute solutions:  $\omega=0.11$  and  $\omega=9.5 \times 10^{-3}$ . Region II data from the  $\omega=0.23$  solution are then presented.

**Table C.4:** DynaLS analysis results of DLS data from 17R4 in D<sub>2</sub>O. Standard deviations “STD” are those presented by the DynaLS program and were not reported in Chapter 5. See Chapter 2 and Appendix A for further information regarding DLS error. Uncertainty in temperature is  $\pm 1$  °C.

Temperature T (°C)	Solvent Refractive Index n	Solution Viscosity $\eta$ (cP)	Mean Signal Intensity (Hz)	Channel Numbers in Analysis	Data Acquisition Time (s)	Peak 1 - Unimer				Peak 2 - Micelle			
						Area -	Mean (nm)	Position (nm)	STD (nm)	Area -	Mean (nm)	Position (nm)	STD (nm)
35	1.32	10.3	8585.35	58-105	90	0.158	0.181	0.194	0.10	0.842	3.14	2.956	1.9
			8622.88	58-105	200	0.199	0.443	0.414	0.15	0.801	3.482	3.438	1.8
			8624.17	58-105	300	0.253	0.621	0.56	0.20	0.747	3.977	4	2.0
			8496.34	58-105	60	0.125	0.129	0.123	0.07	0.875	3.444	2.184	2.9
			8495.37	58-105	309	0.172	0.133	0.123	0.07	0.828	3.607	2.541	2.8
39	1.32	10.3	22349.5	58-105	92	0.152	0.568	0.567	0.14	0.848	2.969	2.994	1.1
			22488.0	58-105	202	0.135	0.477	0.488	0.09	0.865	2.877	2.994	0.9
			22403.1	58-105	301	0.115	0.434	0.419	0.10	0.885	2.862	2.994	1.1
			22353.9	58-105	60	0.05	0.418	0.419	0.09	0.95	2.767	2.574	1.2
			22341.9	58-105	301	0.138	0.573	0.567	0.10	0.862	2.899	2.994	0.9

35 °C





39 °C

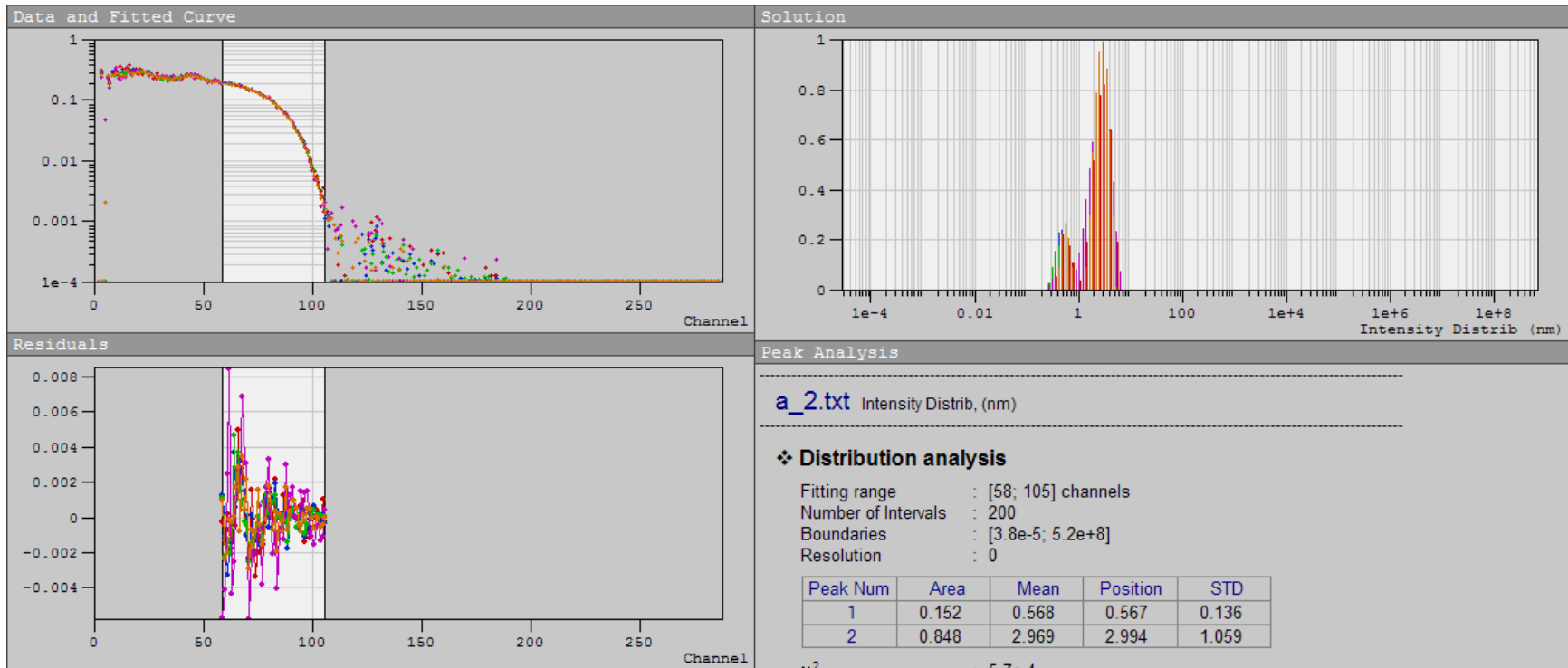


**Table C.5:** Results from fittings by the correlation length model to 17R4/D<sub>2</sub>O data for  $\omega=0.23$ . The entire Q-range was used. Errors are reported to 99% level.

Temperature	°C	15.5	±	0.1	24.9	±	0.1	29.8	±	0.1
Porod Scale, A		2.7E-08	±	5.E-09	4.7E-08	±	6.E-09	5.6E-08	±	7.E-09
Cluster Porod		3.52	±	0.03	3.59	±	0.03	3.60	±	0.02
I(0), C	cm <sup>-1</sup>	0.321	±	0.008	0.579	±	0.007	0.943	±	0.007
Correlation Length, $\xi$	Å	3.95	±	0.07	5.14	±	0.04	6.78	±	0.03
Unimer Porod		3.1	±	0.1	2.60	±	0.05	2.33	±	0.03
Background, B	cm <sup>-1</sup>	0.255	±	0.003	0.243	±	0.002	0.228	±	0.001
$\chi^2 \times 10^{-3}$		1.6			2.0			2.3		
Reduced $\chi^2$		2.6			2.9			3.1		

**Table C.6:** Linear Porod Plot results for 17R4 in D<sub>2</sub>O in Region I of  $\omega=0.23$ , performed over Q-range 0.28-0.41 Å<sup>-1</sup>. These plots were performed after removing  $\frac{A}{Q^{m_1}}$  and background terms, which were determined from the correlation length model. Errors are reported at 99% level.

Temperature (°C)	Porod Exponent, m	$\chi^2$	Reduced $\chi^2$
15.5 ± 0.1	2.2 ± 0.1	17	0.7
24.9 ± 0.1	2.1 ± 0.1	19	0.7
29.8 ± 0.1	1.97 ± 0.07	17	0.7

**Table C.7:** Results from linear Guinier fits of 17R4/D<sub>2</sub>O for  $\omega=0.23$ . These fits were performed over a Q-range of 0.13-0.90 Å<sup>-1</sup>, after the removal of the correlation length model  $\frac{A}{Q^{m_1}}$  and background terms. Errors are reported at 99% level.

Temperature °C	Guinier Slope	$\chi^2 \times 10^{-2}$	Reduced $\chi^2$	Radius of Gyration, R <sub>g</sub> Å
15.5 ± 0.1	-10 ± 2	6.4	0.2	5.6 ± 0.6
24.9 ± 0.1	-22 ± 1	7.7	0.2	8.2 ± 0.2
29.8 ± 0.1	-40.4 ± 0.9	10	0.3	11.0 ± 0.1

**Table C.8:** Two-region Guinier-Porod model results for 17R4 in D<sub>2</sub>O, within Region I of  $\omega=0.23$ . The cluster term,  $\frac{A}{Q^{m_1}}$ , from the correlation length model was removed prior to fitting. The intermediate regime exponent, n, was held at 0, and the model was applied over the Q-range 0.017-0.40 Å<sup>-1</sup>. Errors are reported at 99% level.

Temperature	°C	15.5	±	0.1	24.9	±	0.1	29.8	±	0.1
Guinier Scale, G		0.586	±	0.001	0.74	±	0.03	1.04	±	0.01
Intermediate Q-scaling*, n		0	±	0	0	±	0	0	±	0
Radius of Gyration, R <sub>g</sub>	Å	4.03	±	0.03	6.5	±	0.2	9.0	±	0.6
Porod Exponent, m		0.595	±	0.009	0.91	±	0.09	1.11	±	0.03
Background, B	cm <sup>-1</sup>	0	±	0	0.09	±	0.03	0.12	±	0.01
$\chi^2 \times 10^{-3}$		1.4			1.3			2.7		
Reduced $\chi^2$		2.5			2.5			3.5		

**Table C.9:** Correlation length model results for  $\omega=0.11$  17R4 in D<sub>2</sub>O sample. The model was fitted over the entire Q-range. All errors are reported at 99% level.

Temperature	°C	11.90	±	1.0	30.60	±	1.1
Porod Scale, A		6.E-08	±	2.E-08	6.5E-08	±	9.E-09
Cluster Porod Exponent, $m_1$		3.20	±	0.05	3.59	±	0.03
I(0), C	cm <sup>-1</sup>	0.367	±	0.007	0.881	±	0.008
Correlation Length, $\xi$	Å	4.52	±	0.06	7.54	±	0.04
Unimer Porod Exponent, $m_2$		2.42	±	0.07	2.11	±	0.03
Background, B	cm <sup>-1</sup>	0.165	±	0.006	0.156	±	0.003
$\chi^2 \times 10^{-3}$		1.1			1.4		
Reduced $\chi^2$		2.2			2.4		

**Table C.10:** Two-region Guinier-Porod model results for  $\omega=9.5 \times 10^{-3}$  17R4 in D<sub>2</sub>O sample. The model was fitted over the entire Q-range at 11.9-30.6 °C. At 39.9 °C, the model was fitted over two Q-ranges: 0.034-0.019 Å<sup>-1</sup> to analyze a large scattering body and 0.019-0.40 Å<sup>-1</sup> to analyze unimer scattering. At 39.9 °C at low-Q, the Porod exponent, m, was held at 4. All errors are reported at 99% level.

	°C							Unimer			Cluster					
		11.9	±	1.0	21.3	±	1.0	30.6	±	1.1	39.9	±	1.2	39.9	±	1.2
Temperature	°C	11.9	±	1.0	21.3	±	1.0	30.6	±	1.1	39.9	±	1.2	39.9	±	1.2
Guinier Scale, G		0.047	±	0.002	0.047	±	0.002	0.038	±	0.002	0.027	±	0.001	0.06	±	0.03
Intermediate Q-scaling*, n		0.18	±	0.04	0.19	±	0.04	0.27	±	0.04	0.39	±	0.04	0.9	±	0.3
Radius of Gyration, $R_g$	Å	12.5	±	0.8	12.5	±	0.8	11.3	±	0.7	9.8	±	0.6	220	±	40
Porod Exponent, m		1.2	±	0.1	1.2	±	0.1	1.3	±	0.1	1.5	±	0.2	4	±	0
Background, B	cm <sup>-1</sup>	0.045	±	0.002	0.045	±	0.002	0.047	±	0.002	0.048	±	0.002	0.15	±	0.01
$\chi^2 \times 10^{-2}$		2.4			2.7			2.7			2.0			0.6		
Reduced $\chi^2$		1.0			1.1			1.1			2.1			1.1		

**Table C.11:** Results from the correlation length model fits of  $\omega=0.23$  17R4 in D<sub>2</sub>O within Region II. A was held at  $10^{-12}$  and n was held at 3, effectively removing the clustering portion for this fit. It is expected that the  $\chi^2$  values are large because of the cluster term has been fixed in this manner. All errors are reported at 99% level.

Temperature	°C	34.5	±	0.1	39.2.	±	0.1
Porod Scale, A		$1 \times 10^{-12}$	±	0	$1 \times 10^{-12}$	±	0
Cluster Porod Exponent, $m_1$		3	±	0	3	±	0
I(0), C	cm <sup>-1</sup>	8.50	±	0.02	20.66	±	0.03
Correlation Length, $\xi$	Å	20.99	±	0.05	20.68	±	0.02
Unimer Porod Exponent, $m_2$		2.427	±	0.006	3.115	±	0.005
Background, B	cm <sup>-1</sup>	0.279	±	0.001	0.2864	±	0.0009
$\chi^2 \times 10^{-3}$		6.6			56		
Reduced $\chi^2$		5.3			15.4		

**Table C.12:** Linear Guinier plot results fit to  $\omega=0.23$  17R4/D<sub>2</sub>O within Region II. The background term from the correlation length model was removed before these fits were performed. Fits were done over the Q-range 0.0038-0.045 Å<sup>-1</sup>. All errors are reported at 99% level.

Temperature (°C)	Guinier Slope	$\chi^2 \times 10^{-3}$	Reduced $\chi^2$	Radius of Gyration, $R_g$ Å
34.5 ± 0.1	-301 ± 2	0.3	1.6	30.0 ± 0.1
39.2. ± 0.1	-378 ± 2	3.8	6.0	33.69 ± 0.08

**Table C.13:** Linear Porod fit results to  $\omega=0.23$  17R4/D<sub>2</sub>O within Region II. The correlation length model background was removed prior to fitting. These fits were performed over the Q-range 0.070-0.28 Å<sup>-1</sup>. All errors are reported at 99% level.

Temperature (°C)	Porod Exponent, m	$\chi^2 \times 10^{-3}$	Reduced $\chi^2$
34.5 ± 0.1	2.093 ± 0.005	1.1	4.0
39.2 ± 0.1	2.975 ± 0.005	5.0	8.4

**Table C.14:** Results from the two-region Guinier-Porod model fit to  $\omega=0.23$  17R4/D<sub>2</sub>O within Region II. The intermediate Q-scaling, n, was held at 0 to represent a 3-D body shape, and the entire Q-range was used in the fits. All errors are reported at 99% level.

Temperature	°C	34.5 ± 0.1	39.2 ± 0.1
Guinier Scale, G		8.32 ± 0.02	21.35 ± 0.02
Intermediate Q-scaling, n		0 ± 0	0 ± 0
Radius of Gyration, R <sub>g</sub>	Å	28.34 ± 0.05	29.69 ± 0.02
Porod Exponent, m		1.884 ± 0.006	2.884 ± 0.006
Background, B	cm <sup>-1</sup>	0.223 ± 0.002	0.285 ± 0.001
$\chi^2 \times 10^{-3}$		3.6	47
Reduced $\chi^2$		3.9	14.1

**Table C.15:** Results from the three-region Guinier-Porod model fit to  $\omega=0.23$  17R4/D<sub>2</sub>O within Region II. The entire Q-range was used for fits. All errors are reported at 99% level.

Temperature	°C	34.5	±	0.1	39.2	±	0.1
Guinier Scale, G	-	8.1	±	0.3	20.9	±	0.8
Intermediate Q-scaling 2, $n_2$	-	0.011	±	0.008	0.026	±	0.008
2nd Radius of Gyration $R_{g2}$	Å	29.5	±	0.4	35.1	±	0.7
Intermediate Q-scaling 1, $n_1$	-	0.40	±	0.06	0.286	±	0.008
1st Radius of Gyration, $R_{g1}$	Å	20.9	±	0.9	24.2	±	0.1
Porod Exponent, m	-	1.94	±	0.01	3.065	±	0.008
Background, B	cm <sup>-1</sup>	0.233	±	0.002	0.30		0.01
$\chi^2 \times 10^{-2}$		7.7			54		
Reduced $\chi^2$		1.8			4.8		

## Appendix D: Poly(ethylene oxide)-polybutadiene in organic solvents

### D.1 Solvent Refractive Indices

Refractive indices of the deuterated organic solvents, methanol and cyclohexane ( $\text{CD}_3\text{OD}$  and  $\text{C}_6\text{D}_{12}$ ), were measured at a series of temperatures using an Abbé refractometer. These were plotted as a function of temperature. The refractometry data and linear equations for these relationships are presented below. See Figure 6.6 for the graphic visualization of these linear relationships.

**Table D.1:** Refractive indices of  $\text{CD}_3\text{OD}$  over a series of temperatures.

Refractometer Temperature °C	Temperature Error °C	Refractive Index, n	Refractive Index Error
25.8	0.1	1.3220	0.0001
26.2	0.1	1.3222	0.0001
30.9	0.1	1.3201	0.0001
31.1	0.1	1.3200	0.0001
35.9	0.1	1.3181	0.0001
35.9	0.1	1.3181	0.0001
40.3	0.1	1.3164	0.0001
40.8	0.1	1.3162	0.0001
45.6	0.1	1.3141	0.0001
45.9	0.1	1.3141	0.0001
50.5	0.1	1.3131	0.0001

The refractive index of  $\text{CD}_3\text{OD}$  as a function of temperature follows the equation:

$$n_{\text{CD}_3\text{OD}} = 1.332 - 3.9 \times 10^{-4} T, \quad (6.1)$$

where the 99% uncertainty in the slope is  $1 \times 10^{-5}$  and the uncertainty in the y-intercept is  $4 \times 10^{-4}$ .



**Table D.2:** Refractive indices of C<sub>6</sub>D<sub>12</sub> over a series of temperatures.

Refractometer Temperature °C	Temperature Error °C	Refractive Index, n	Refractive Index Error
50.2	0.1	1.4040	0.0001
45.9	0.1	1.4064	0.0001
45.9	0.1	1.4075	0.0001
45.9	0.1	1.4069	0.0001
40.3	0.1	1.4102	0.0001
40.3	0.1	1.4100	0.0001
40.3	0.1	1.4105	0.0001
35.9	0.1	1.4125	0.0001
35.9	0.1	1.4120	0.0001
35.9	0.1	1.4124	0.0001
31.1	0.1	1.4142	0.0001
31.1	0.1	1.4142	0.0001
31.1	0.1	1.4145	0.0001
25.8	0.1	1.4179	0.0001
25.8	0.1	1.4179	0.0001
25.8	0.1	1.4180	0.0001

The refractive index of C<sub>6</sub>D<sub>12</sub> has the following relationship with temperature:

$$n_{\text{C}_6\text{D}_{12}} = 1.4316 - 5.4 \times 10^{-4} T, \quad (6.2)$$

where the 99% uncertainty in the slope is  $\pm 1 \times 10^{-5}$  and the uncertainty in the y-intercept is  $\pm 4 \times 10^{-4}$ .

## D.2 Solvent Viscosities

Solvent viscosity values as a function of temperature were found in the literature.<sup>120, 121</sup> The natural logarithm of these viscosities was plotted as a function of  $1/T$ , where  $T$  was in Kelvin, as shown in the work by Dixon and Schiessler.<sup>120</sup> Viscosity values for each deuterated organic solvent and these linear relationships are presented below.

**Table D.3:** Viscosity values of CD<sub>3</sub>OD as a function of temperature, from Holz et al.<sup>121</sup>

Viscosity cP	ln(V)	Temperature (K)	1/T (1/K)
0.702	-0.353822	288.15	0.00347
0.602	-0.507498	298.15	0.003354
0.528	-0.638659	308.15	0.003245

When the natural logarithm of the viscosity values is plotted as a function of the reciprocal of temperature, the following linear relationship is found:

$$\ln(\eta_{\text{CD}_3\text{OD}}) = -4.7 + 1300(1/T). \quad (\text{D.1})$$

The 99% error in the slope is  $\pm 100$ , and that in the y-intercept is  $\pm 0.3$ .

**Table D.4:** Viscosity values of C<sub>6</sub>D<sub>12</sub> as a function of temperature, from Dixon and Schiessler.<sup>120</sup>

Viscosity cP	ln(V)	Temperature (K)	1/T (1/K)
1.045	0.044017	293.18	0.003411
0.776	-0.253603	310.96	0.003216
0.5613	-0.5775	333.18	0.003001

The linear relationship between natural logarithm of viscosity and the inverse of temperature for C<sub>6</sub>D<sub>12</sub> follows the equation:

$$\ln(\eta_{\text{C}_6\text{D}_{12}}) = -5.13 + 1518(1/T). \quad (\text{D.2})$$

The error in the slope is  $\pm 15$ , while the error in the y-intercept is  $\pm 0.03$ .

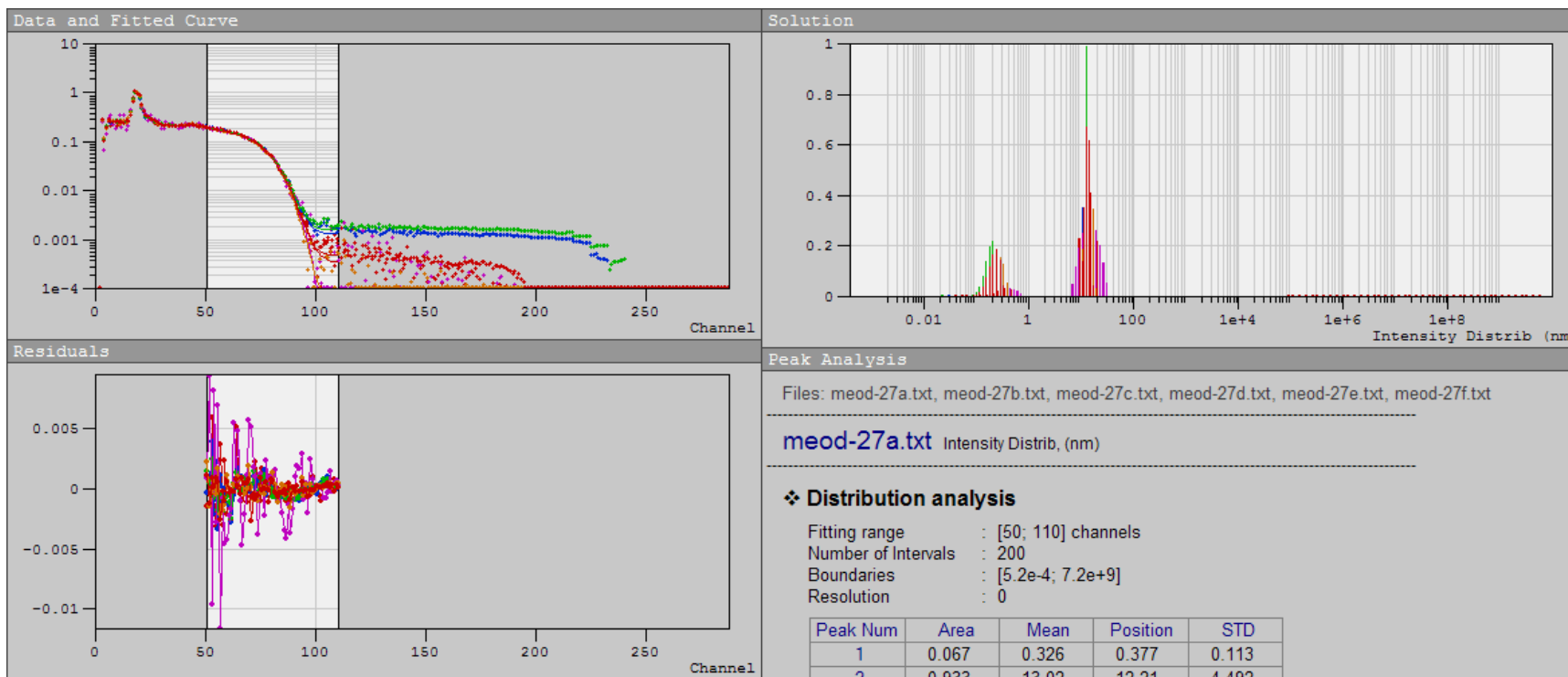
### D.3 Analyses Data

The data from SANS and DLS analyses of the copolymer poly(ethylene oxide)<sub>132</sub>-polybutadiene<sub>89</sub> in organic solvents are presented here. The results in CD<sub>3</sub>OD are presented first, followed by the results from the C<sub>6</sub>D<sub>12</sub> solutions. DynaLS DLS analysis results are summarized in tables. All SANS analyses are also presented.

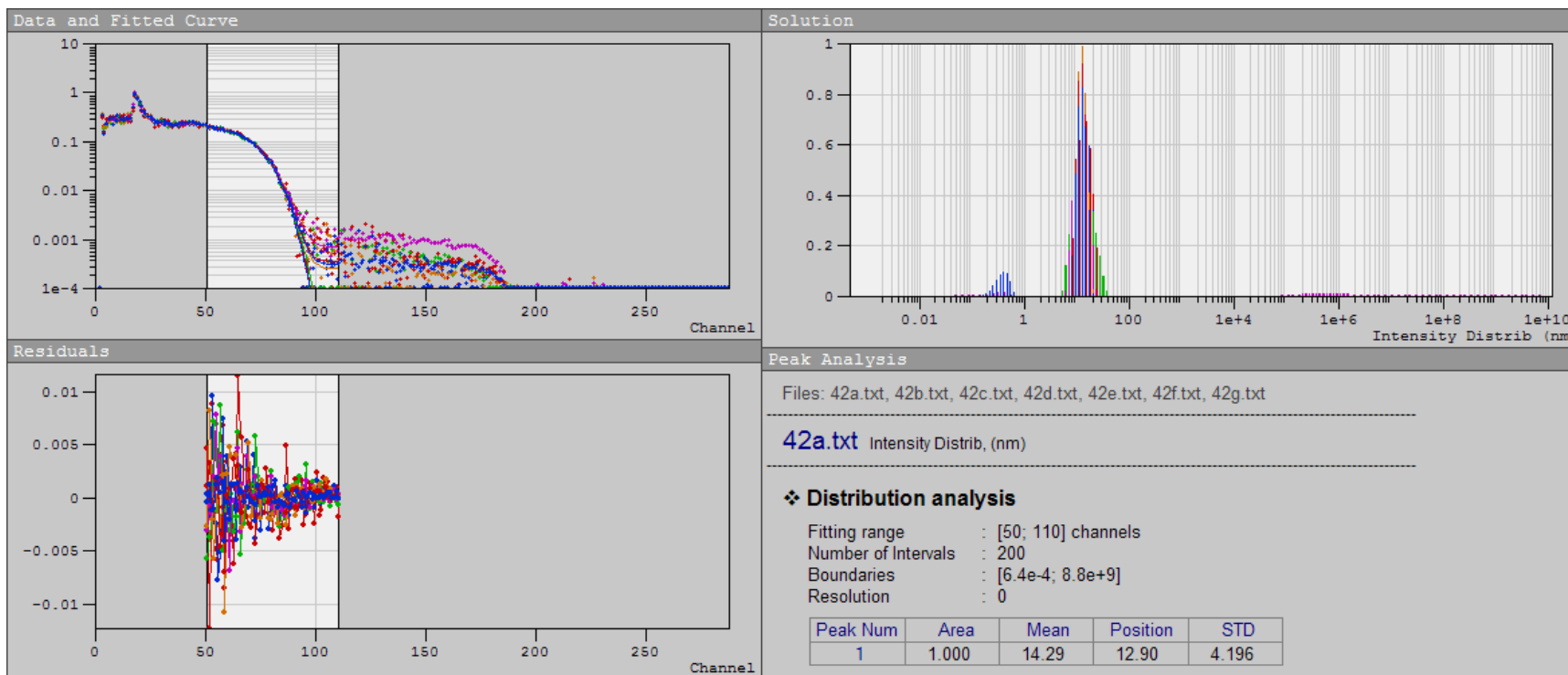
**Table D.5:** DynaLS analysis results of DLS data from PEO<sub>132</sub>-PB<sub>89</sub> in CD<sub>3</sub>OD. Standard deviations “STD” are those presented by the DynaLS program and were not reported in Chapter 6. See Chapter 2 and Appendix A for further information regarding DLS error.

Cell Temperature °C	Solvent Refractive Index n	Solvent Viscosity η cP	Mean Signal Intensity Hz	Channel Numbers in Analysis	Data Acquisition Time sec	unimer				spherical micelle				dust			
						Area -	Mean nm	Position nm	STD nm	Area -	Mean nm	Position nm	STD nm	Area	Mean	Position	STD
26	1.3	0.7	46741.5	50-110	40	0.067	0.326	0.377	0.11	0.933	13.02	12.21	4.5				
			44817.3		148	0.295	0.206	0.239	0.07	0.705	11.66	12.21	3.3				
			43734.6		260	0.380	0.170	0.206	0.06	0.620	11.42	12.21	3.1				
			39940.9		11	0.087	0.401	0.438	0.13	0.913	15.28	14.20	5.7				
			39647.4		117	0.311	0.249	0.278	0.07	0.689	13.58	14.20	2.7				
			39573.8		450	0.352	0.209	0.239	0.07	0.648	12.57	12.21	2.8				
42	1.3	0.6	26238.4	50-110	16	0				1.000	14.29	12.90	4.2				
			26242.7		50	0				1.000	14.00	12.90	3.7				
			26940.4		57	0				1.000	14.41	12.90	6.3				
			27095.8		137	0.018	0.332	0.342	0.11	0.982	11.86	12.90	4.7				
			27390.1		66	0				1.000	12.46	12.90	3.5				
			27413.7		129	0.051	0.279	0.294	0.09	0.949	12.09	12.90	3.5				
			27354.8		316	0.132	0.368	0.398	0.13	0.868	12.24	12.90	3.5				
53	1.3	0.5	25369	50-110	10					0.977	13.86	11.84	8.4	0.023	1.70E+05	8.90E+04	1.50E+05
			26676.4		56					0.579	8.85	8.749	2.3	0.421	3.10E+06	2.70E+04	1.00E+07
			26491.7		91					0.66	9.081	8.749	2.0	0.34	2.00E+07	1.40E+06	4.40E+07
			26815.4		29	0.08	0.698	0.778	0.24	0.92	15.05	13.77	6.5				
			26839.2		109	0.085	0.436	0.494	0.16	0.915	11.85	11.84	4.1				
			26794.9		158	0.155	0.459	0.494	0.17	0.845	12.03	11.84	4.0				
			26879.5		203	0.213	0.454	0.494	0.17	0.787	12.09	11.84	3.8				

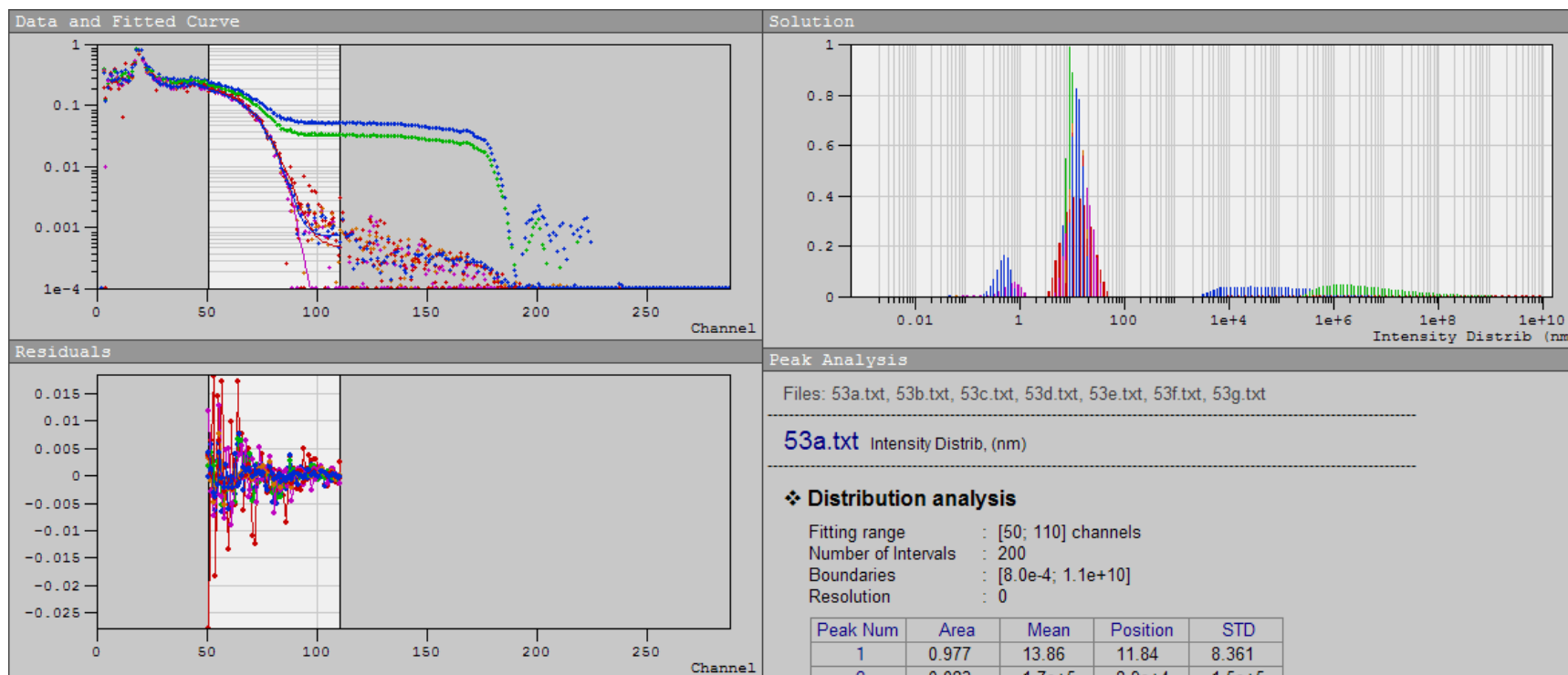
26 °C



42 °C



53 °C



All SANS data errors are presented at 99% level.

**Table D.6:** Linear Guinier Plot results for PEO<sub>132</sub>-PB<sub>89</sub> in CD<sub>3</sub>OD. These plots were done over the Q-range 0.003-0.02 Å<sup>-1</sup>.

Temperature, (°C)	Guinier Slope			$\chi^2 \times 10^{-2}$	Reduced $\chi^2$	Radius of Gyration, R <sub>g</sub> (Å)		Spherical Radius, R (Å)	
21.3	2683	±	27	1.3	1.6	89.7	± 0.5	115.8	± 0.6
30.6	2680	±	30	1.2	1.5	89.7	± 0.5	115.8	± 0.6
39.9	2630	±	30	1.0	1.4	88.8	± 0.5	114.7	± 0.7
49.3	2600	±	30	0.8	1.3	88.3	± 0.5	114.0	± 0.7
58.6	2600	±	30	0.4	0.9	88.3	± 0.5	114.0	± 0.7
67.9	2680	±	33	0.8	1.3	89.7	± 0.6	115.8	± 0.7

**Table D.7:** Linear Porod Plot results for PEO<sub>132</sub>-PB<sub>89</sub> in CD<sub>3</sub>OD, performed over Q-range 0.003-0.01 Å<sup>-1</sup>.

Temperature, (°C)	Intermediate Q-scaling Exponent, n			$\chi^2$	Reduced $\chi^2$
21.3	0.22	±	0.02	78	2.1
30.6	0.22	±	0.02	88	2.3
39.9	0.24	±	0.02	62	1.9
49.3	0.24	±	0.02	57	1.8
58.6	0.25	±	0.02	36	1.5
67.9	0.25	±	0.02	41	1.6



**Table D.8:** Results from non-linear Schulz sphere model analyses of PEO<sub>132</sub>-PB<sub>89</sub> in CD<sub>3</sub>OD SANS data. The entire Q-range was used in the analyses. The scattering length densities of the sphere and solvent were held at  $5.2 \times 10^{-7} \text{ \AA}^{-2}$  and  $5.8 \times 10^{-6} \text{ \AA}^{-2}$ , respectively.

Temperature (°C)	Scale		Mean Radius, R (Å)		Polydispersity $\rho, \sigma/R$		Background B (cm <sup>-1</sup> sr <sup>-1</sup> )		$\chi^2 \times 10^{-3}$	Reduced $\chi^2$
21.3	6.25E-04	± 3.E-06	92.6	± 0.2	0.187	± 0.001	6.80E-02	± 3.E-04	4	3.7
30.6	6.09E-04	± 3.E-06	93.1	± 0.3	0.183	± 0.002	6.92E-02	± 3.E-04	3.9	3.7
39.9	5.93E-04	± 3.E-06	93.4	± 0.3	0.179	± 0.003	7.19E-02	± 3.E-04	3.3	3.4
49.3	5.62E-04	± 3.E-06	93.2	± 0.2	0.178	± 0.001	7.30E-02	± 3.E-04	2.9	3.2
58.6	5.25E-04	± 3.E-06	92.6	± 0.4	0.181	± 0.003	7.42E-02	± 3.E-04	2.2	2.7
67.9	4.90E-04	± 3.E-06	92.0	± 0.2	0.192	± 0.001	7.58E-02	± 3.E-04	1.6	2.4

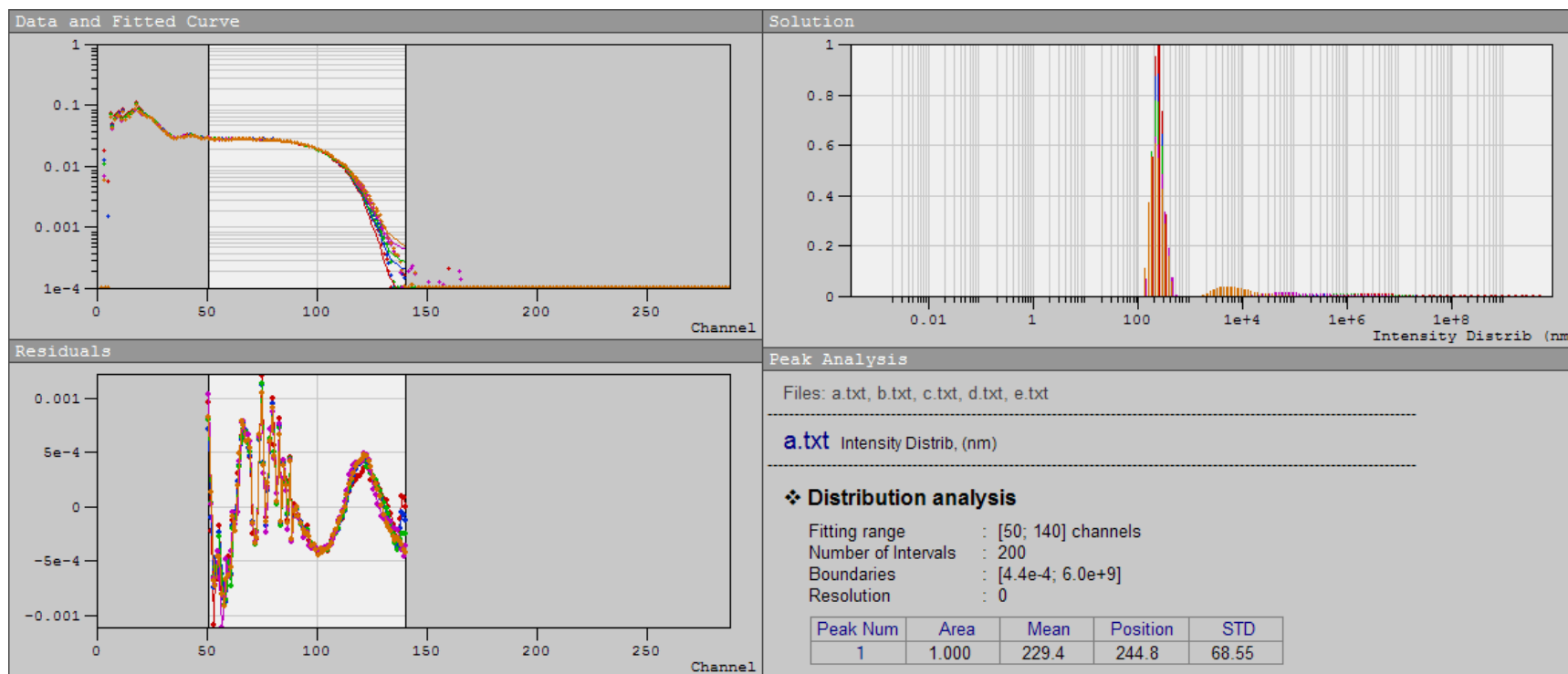
**Table D.9:** Results from non-linear polydisperse core-shell model analyses of PEO<sub>132</sub>-PB<sub>89</sub> in CD<sub>3</sub>OD SANS data. The entire Q-range was used in the analyses. The scattering length densities of the core and solvent were held at  $4.1 \times 10^{-7} \text{ \AA}^{-2}$  and  $5.8 \times 10^{-6} \text{ \AA}^{-1}$ , respectively.

Temperature (°C)	Scale		Average Core Radius R <sub>c</sub> (Å)		Polydispersity in Core Radius $\rho, \sigma/R_c$		Shell Thickness, T, (Å)		Scattering Length Density of Shell (Å <sup>-2</sup> )		Background B (cm <sup>-1</sup> )		$\chi^2 \times 10^{-2}$	Reduced $\chi^2$
21.3	5.9E-03	± 4.E-04	23.8	± 0.3	0.663	± 0.009	69.0	± 0.6	2.8E-06	± 1.E-07	6.89E-02	± 3.E-04	6.1	1.5
30.6	5.9E-03	± 6.E-04	24	± 1	0.66	± 0.03	70	± 1	2.84E-06	± 8.E-08	7.00E-02	± 3.E-04	6.1	1.5
39.9	6.0E-03	± 8.E-04	22.6	± 0.9	0.68	± 0.02	71	± 1	2.9E-06	± 1.E-07	7.26E-02	± 3.E-04	6.4	1.5
49.3	6.E-03	± 1.E-03	22	± 2	0.68	± 0.05	71	± 2	2.9E-06	± 2.E-07	7.37E-02	± 3.E-04	6.4	1.5
58.6	6.E-03	± 1.E-03	20	± 2	0.74	± 0.06	73	± 2	2.8E-06	± 2.E-07	7.47E-02	± 3.E-04	5.6	1.4
67.9	3.8E-03	± 2.E-04	21	± 1	0.73	± 0.03	72	± 1	2.1E-06	± 2.E-07	7.62E-02	± 3.E-04	6.2	1.5

**Table D.10:** DynaLS analysis results of DLS data from PEO<sub>132</sub>-PB<sub>89</sub> in C<sub>6</sub>D<sub>12</sub>. Standard deviations “STD” are those presented by the DynaLS program and were reported in Chapter 6. See Chapter 2 and Appendix A for further information regarding DLS error.

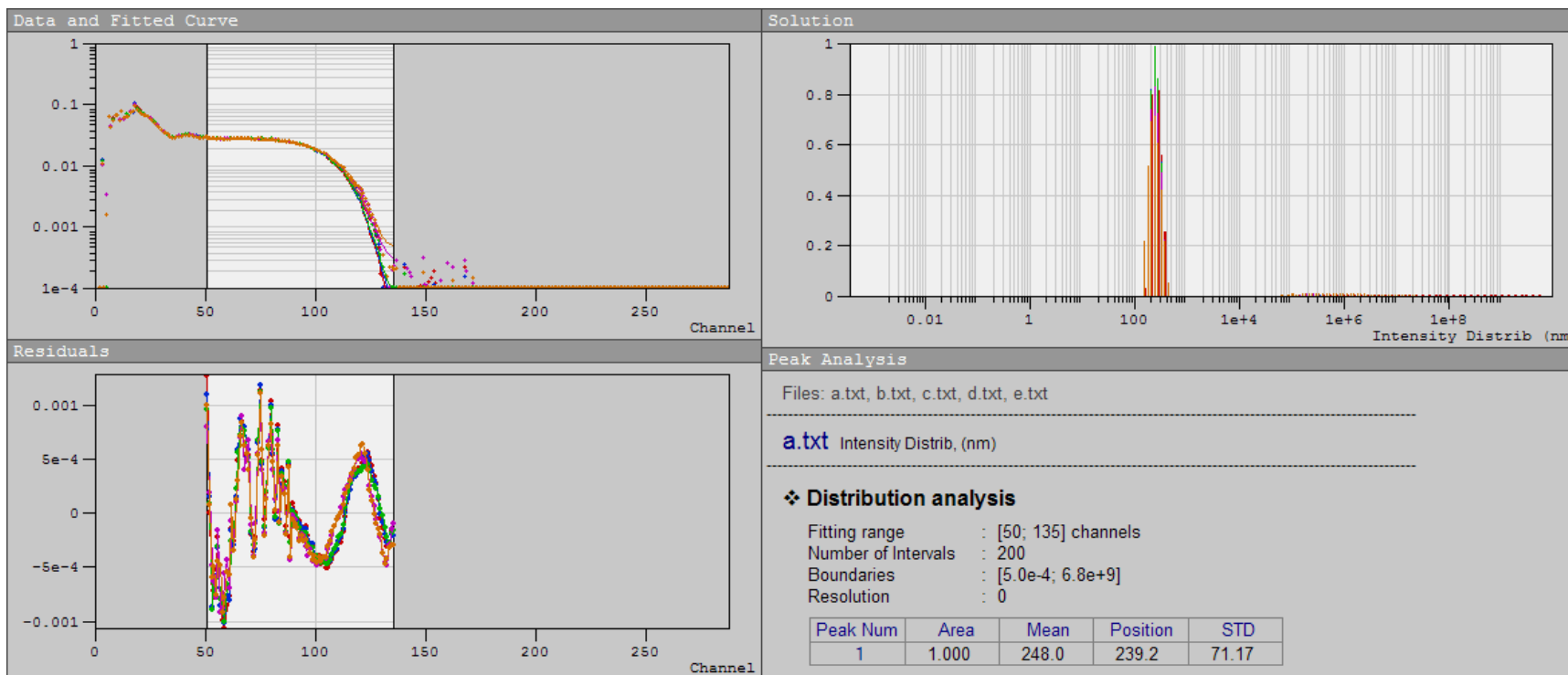
Sample Temperature °C	Solvent Refractive Index n	Solvent Viscosity η cP	Mean Signal Intensity Hz	Channel Numbers in Analysis	Data Acquisition Time sec	unimer				spherical micelle				wormlike micelle				dust				
						Area	Mean	Position	STD	Area	Mean	Position	STD	Area	Mean	Position	STD	Area	Mean	Position	STD	
22.3	1.43	1.0	629916	1-140	102										1.000	229.4	244.8	69				
			631941		203						0.961	226.0	244.8	69	0.039	1.6E+06	1.2E+06	1.1E+06				
			633628		301						0.940	230.4	210.5	72	0.06	1.5E+06	7.4E+05	1.4E+06				
			637185		78						0.903	235.9	210.5	82	0.097	6.3E+05	1.0E+05	8.9E+05				
			639874		304						0.861	230.7	210.5	80	0.139	1.3E+04	5043	1.5E+04				
29.1	1.43	0.90	625469	1-135	62									1.000	248.0	239.2	71					
			626918		90						1.000	243.2	239.2	72								
			628127		131						1.000	240.8	239.2	74								
			633898		30						0.944	242.0	239.2	77	0.056	1.4E+06	7.3E+05	1.2E+06				
			633026		60						0.907	239.2	239.2	78	0.093	1.7E+06	4.0E+05	2.2E+06				
37.3	1.43	0.79	621982	1-135	95									0.748	143.8	152.9	39	0.252	3.6E+07	9.5E+06	4.5E+07	
			633903		123						0.738	141.1	152.9	39	0.262	3.8E+07	1.1E+07	4.6E+07				
			696430		30						1.000	204.3	206.9	36								
			699991		61						1.000	196.4	177.8	39								
			704843		103						1.000	189.8	177.8	44								
45.2	1.43	0.70	75147.6	1-135	94	0.198	0.336	0.358	0.10	0.054	26.18	24.76	5.4	0.748	230.4	130.7	232					
			76660.4		204	0.237	0.318	0.358	0.09	0.043	26.75	24.76	5.0	0.673	173.1	130.7	105	0.047	5.30E+06	6.20E+05	8.70E+06	
			77633.6		308	0.264	0.290	0.308	0.08	0.154	43.77	38.98	10	0.539	190.7	176.9	89	0.042	4.50E+04	7762	6.40E+04	
			80719.8		91	0.162	0.282	0.308	0.07	0.365	57.43	52.75	12	0.474	322.8	278.5	116					
			81587.5		313	0.292	0.257	0.308	0.07	0.280	53.50	52.75	11	0.428	264.8	278.5	73					
			82792.3		67	0.123	0.349	0.358	0.10	0.049	25.79	24.76	4.5	0.748	161.0	130.7	100	0.08	3788	1990	3294	
			82892.1		101	0.164	0.325	0.358	0.09	0.049	23.66	24.76	3.4	0.688	152.5	112.4	84	0.099	1680	1264	984.1	
			8913.76		94	0.277	0.930	0.952	0.40	0.337	27.18	22.80	13	0.280	173.9	162.9	91	0.105	9.90E+06	1.70E+05	3.00E+07	
			8891.51		204	0.278	0.810	0.818	0.33	0.315	23.31	19.60	10	0.281	152.1	162.9	70	0.125	1.50E+07	2.70E+05	4.60E+07	
			8928.05		62	0.115	0.853	0.952	0.36	0.463	24.45	16.85	15	0.266	279.8	189.5	216	0.155	5.70E+06	5.10E+04	2.00E+07	
8872.15	308	0.159	0.660	0.703	0.25	0.318	18.42	14.48	8.8	0.176	137.6	120.4	76	0.347	8.60E+06	8316	4.50E+07					
9007.12	91	0.179	0.855	0.818	0.37	0.354	20.41	16.85	10	0.394	185.5	120.4	149	0.074	3.70E+06	6.90E+04	1.00E+07					
9004.7																						
54.8	1.43	0.61	5506.04	1-150	102	0.269	1.464	1.222	0.86	0.460	30.18	21.63	25	0.097	681.2	329.2	572	0.174	5.70E+06	2.30E+04	2.30E+07	
			5807.47		201	0.182	0.962	0.903	0.43	0.272	15.65	13.74	7.4	0.048	178.7	154.5	70	0.498	2.30E+07	3.10E+04	1.50E+08	
			5783.03		303	0.221	0.903	0.903	0.38	0.295	15.71	13.74	6.7	0.057	209.2	179.8	79	0.427	1.70E+07	3.10E+04	9.70E+07	
			5882.98		59					0.772	57.16	11.81	122	0.228	1.10E+07	2.60E+04	5.90E+07					
			5949.03		226	0.199	1.270	1.050	0.69	0.419	25.08	15.98	24	0.064	510.9	383.0	314	0.317	1.60E+07	3.10E+04	9.40E+07	
			6010.45		302	0.227	1.106	1.050	0.58	0.332	20.60	13.74	16	0.071	315.7	283.0	182	0.37	2.50E+07	4.20E+04	1.60E+08	
			5997.04		368	0.262	1.020	1.050	0.49	0.321	19.66	13.74	14	0.080	287.2	243.3	175	0.337	2.00E+07	4.20E+04	1.10E+08	
			6326.45		91	0.204	1.913	1.872	1.02	0.320	19.24	18.10	12	0.298	166.8	150.4	107	0.178	3.10E+07	1.60E+05	1.50E+08	
6317.46	201	0.252	1.764	1.609	1.04	0.306	22.20	18.10	13	0.246	189.6	175.0	109	0.195	2.50E+07	1.20E+05	1.10E+08					
6360.12	304	0.203	1.305	1.189	0.66	0.241	17.90	15.56	9.0	0.132	149.2	150.4	59	0.424	2.90E+07	1.90E+04	1.90E+08					
6538.14	66	0.185	1.653	1.609	0.85	0.364	19.47	15.56	14	0.172	244.7	203.6	158	0.279	2.10E+07	4.70E+04	1.10E+08					
6410.75	240	0.274	1.289	1.189	0.63	0.303	21.86	18.10	11	0.116	232.7	203.6	114	0.307	1.60E+07	3.00E+04	8.70E+07					
6389.99	327	0.253	1.236	1.189	0.58	0.329	20.87	18.10	10	0.126	255.9	236.8	120	0.293	1.40E+07	3.50E+04	7.00E+07					

22.3 °C

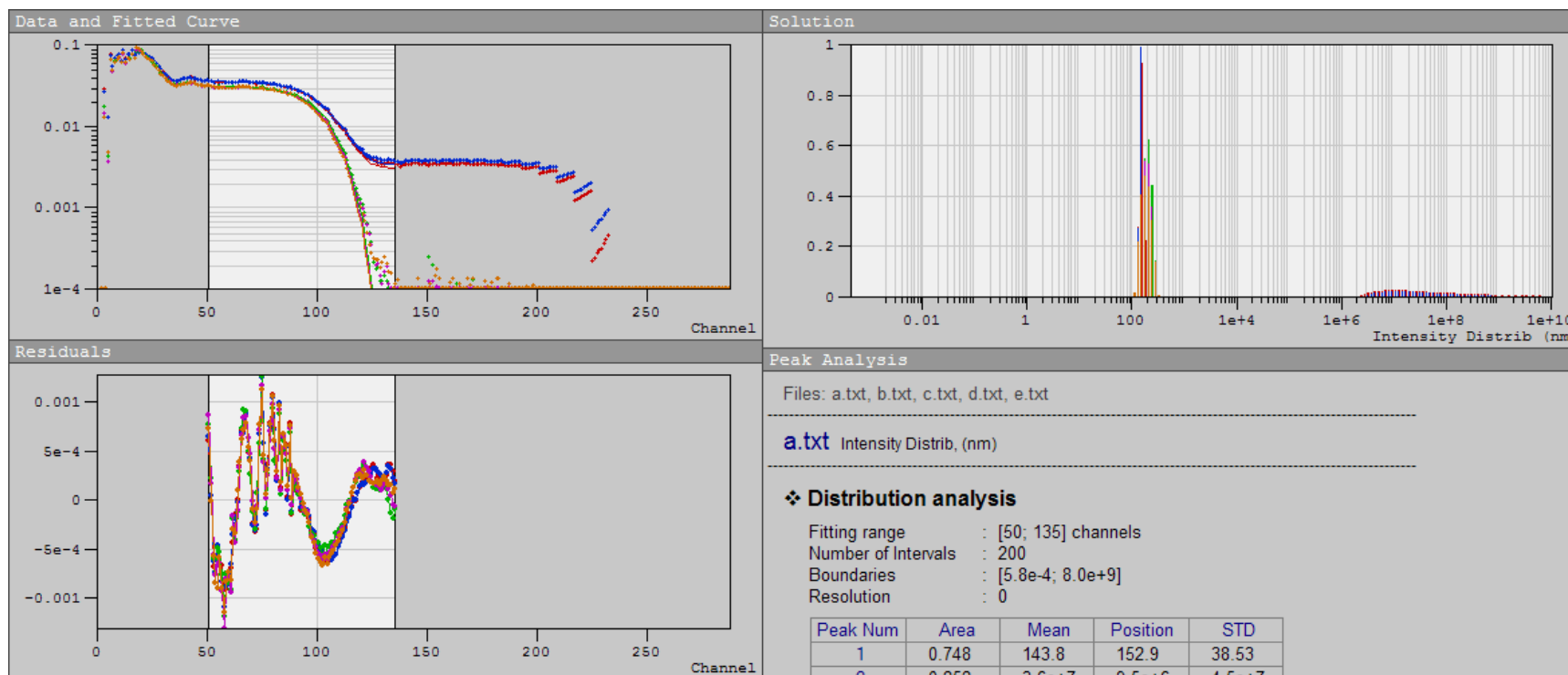


Peak Num	Area	Mean	Position	STD
1	1.000	229.4	244.8	68.55

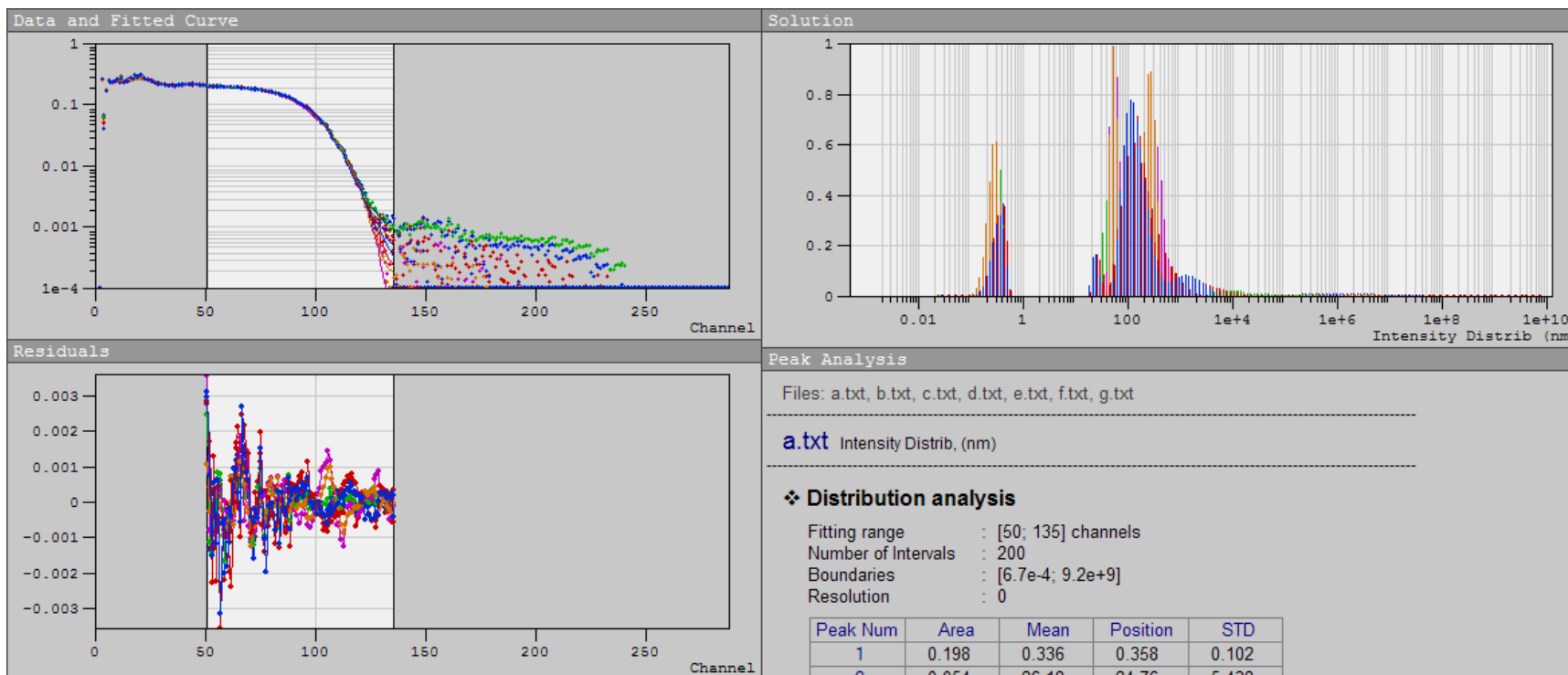
29.1°C



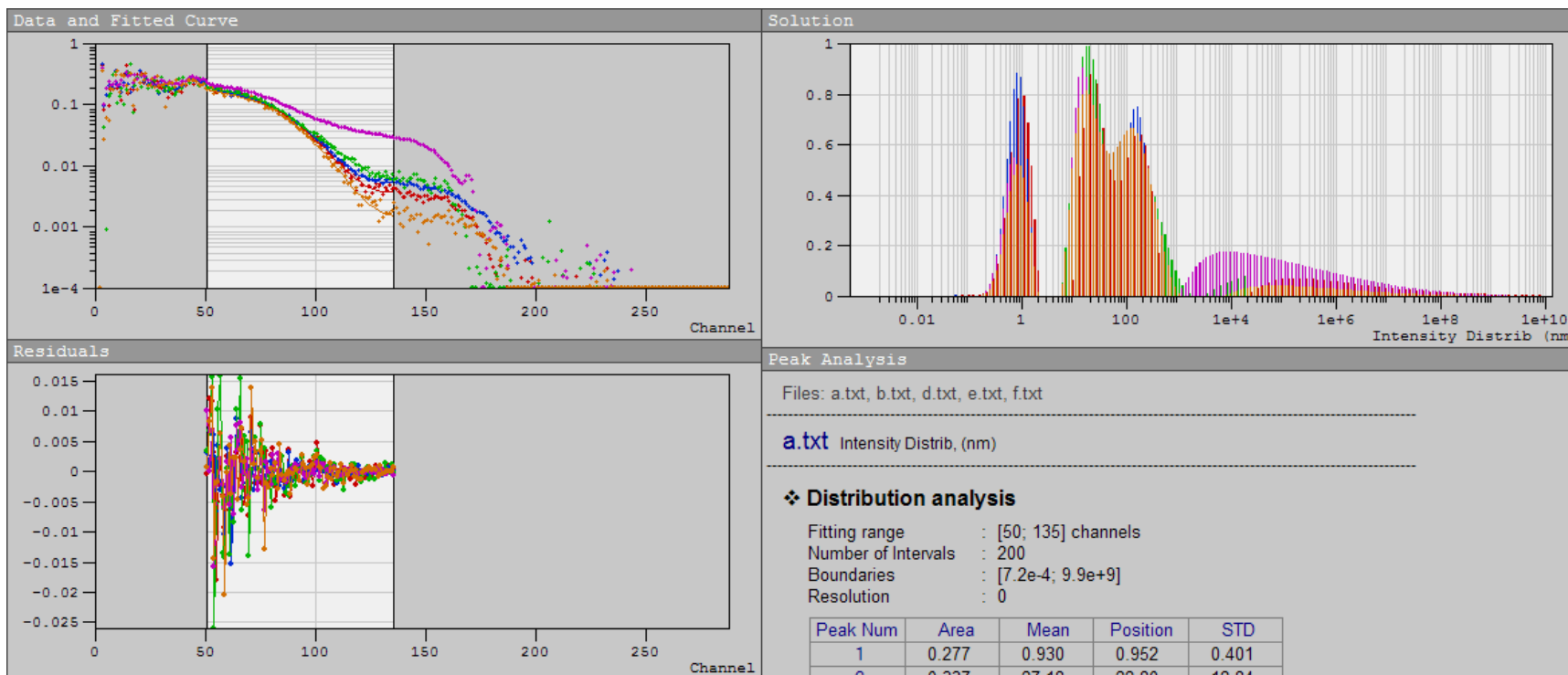
37.3 °C



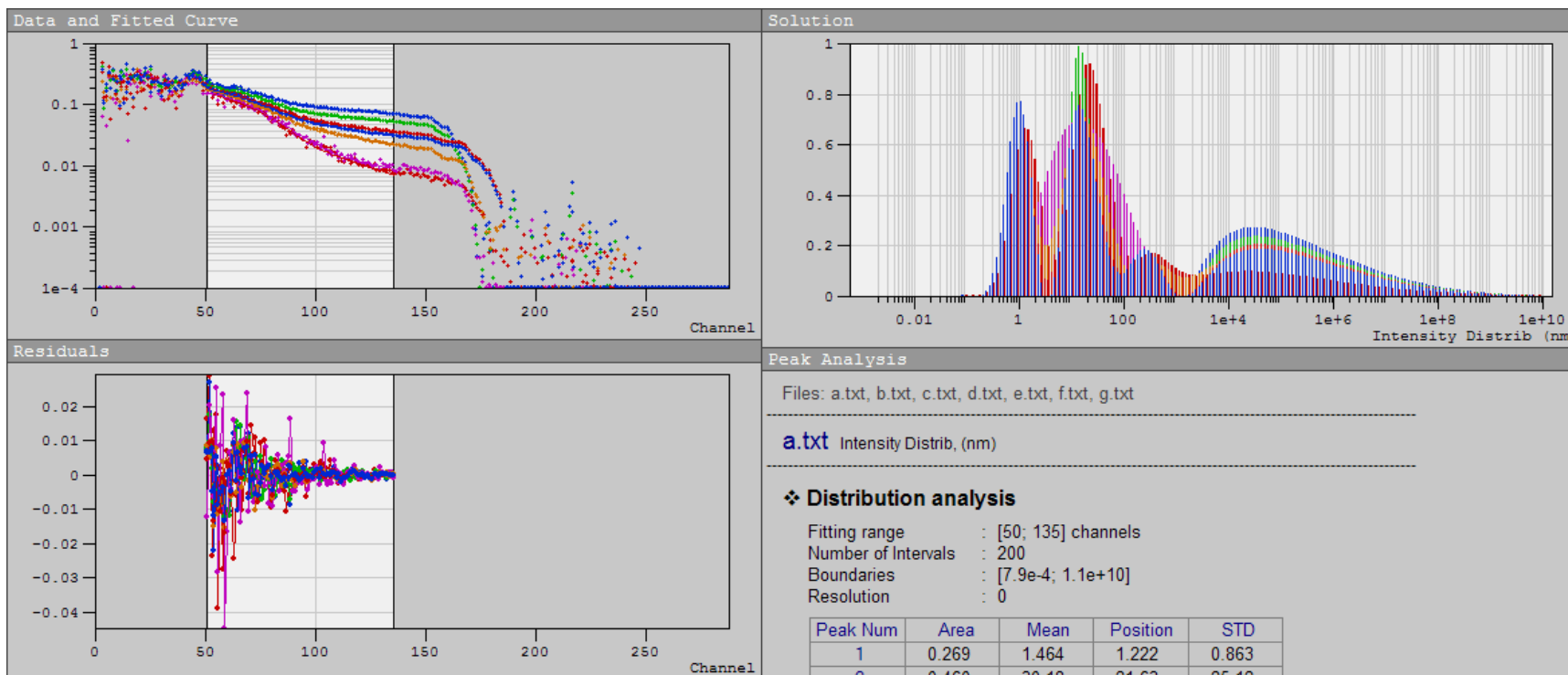
45.2 °C



48.4 °C



54.8 °C





61.7 °C

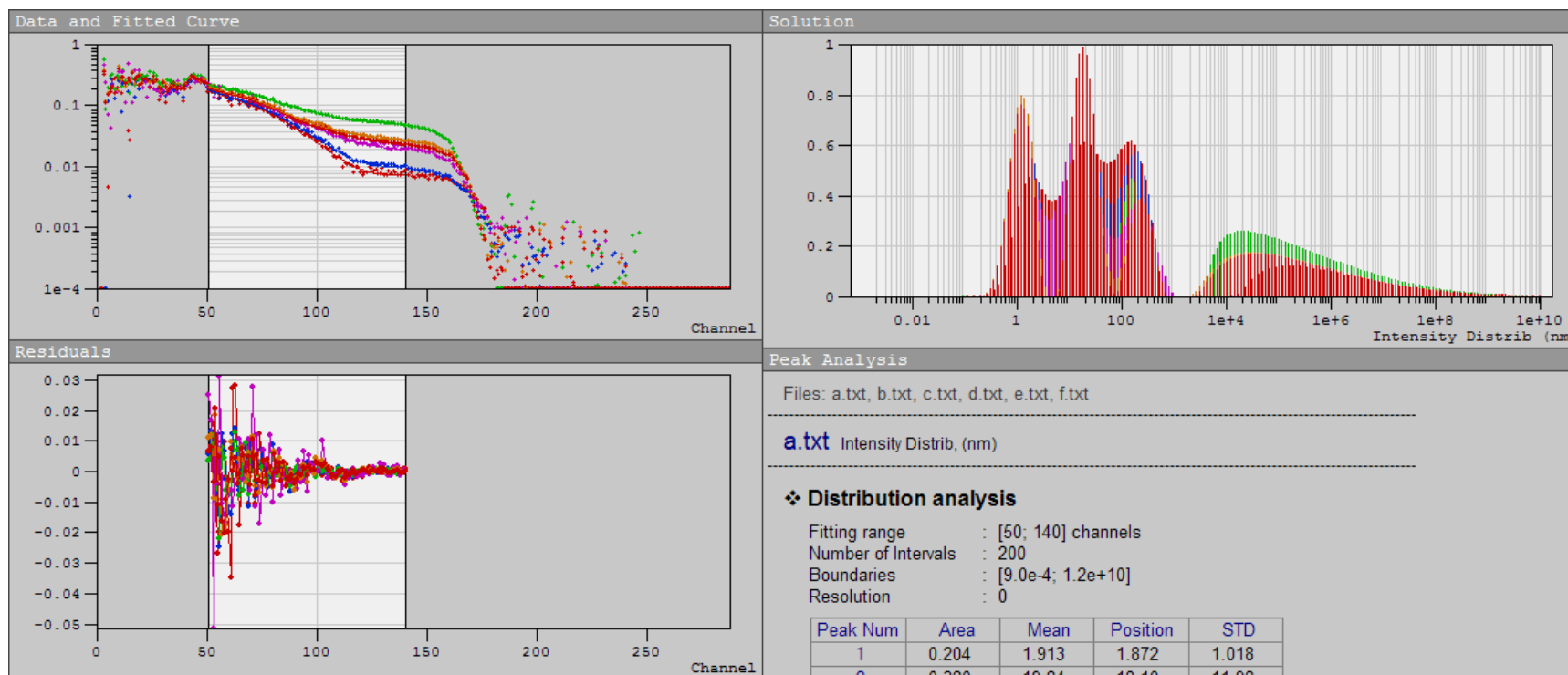


**Table D.11:** Linear Porod Plot results for PEO<sub>132</sub>-PB<sub>89</sub> in C<sub>6</sub>D<sub>12</sub>. These plots were done over the Q-range 0.003-0.01 Å<sup>-1</sup>.

Temperature, (°C)	Intermediate Q-scaling Exponent, n		$\chi^2 \times 10^{-2}$	Reduced $\chi^2$
21.3	2.07	± 0.02	1.0	2.3
30.6	2.07	± 0.02	1.0	2.3
39.9	2.06	± 0.01	1.0	2.4
49.3	0.23	± 0.02	1.2	2.5
58.6	0.23	± 0.03	0.9	2.1
67.9	0.23	± 0.03	0.9	2.2

**Table D.12:** Results from the nonlinear lamellae model with polydisperse bilayer thickness, for PEO<sub>132</sub>-PB<sub>89</sub> in C<sub>6</sub>D<sub>12</sub> at low temperatures. Due to the very large overall error, noted by large reduced  $\chi^2$  values, these results were not used. The scattering length densities of the bilayer and solvent were held at  $5.2 \times 10^{-7}$  Å<sup>-2</sup> and  $6.7 \times 10^{-6}$  Å<sup>-2</sup>, respectively.

Temperature (°C)	scale		Bilayer Thickness $\delta$ (Å)		Polydispersity of Thickness $\rho$ ( $\sigma/\delta$ )			Background (cm <sup>-1</sup> )		$\chi^2 \times 10^{-4}$	Reduced $\chi^2$
21.3	1.101E-03	± 3.E-06	192.4	± 0.4	0.169	± 0.004	7.23E-02	± 3.E-04	3.5	11	
30.6	1.068E-03	± 3.E-06	193.2	± 0.4	0.163	± 0.004	7.44E-02	± 3.E-04	3.5	11	
39.9	1.060E-03	± 3.E-06	194.0	± 0.4	0.174	± 0.004	7.63E-02	± 3.E-04	3.2	11	

**Table D.13:** Results from the nonlinear flexible cylinder model with polydisperse cross-sectional radius and excluded volume, for PEO<sub>132</sub>-PB<sub>89</sub> in C<sub>6</sub>D<sub>12</sub> at low temperatures. The scattering length densities of the cylinder and solvent were held at  $5.2 \times 10^{-7} \text{ \AA}^{-2}$  and  $6.7 \times 10^{-6} \text{ \AA}^{-2}$ , respectively.

Temperature (°C)	scale		Contour Length, L (Å)		Kuhn Length, b (Å)		Cross-Sectional Radius, R <sub>cs</sub> (Å)		Polydispersity of Radius, p (σ/R <sub>cs</sub> )		Background (cm <sup>-1</sup> )		χ <sup>2</sup> × 10 <sup>-3</sup>	Reduced χ <sup>2</sup>
21.3	9.18 × 10 <sup>-4</sup>	± 8 × 10 <sup>-6</sup>	2 × 10 <sup>6</sup>	± 3 × 10 <sup>6</sup>	590	± 20	139.6	± 0.3	0.179	± 0.003	0.0716	± 2.E-04	5.5	4.4
30.6	0.0	± 0.1	2 × 10 <sup>6</sup>	± 4 × 10 <sup>6</sup>	600	± 20	140.1	± 0.3	0.180	± 0.003	0.0737	± 3.E-04	5.3	4.3
39.9	8.56 × 10 <sup>-4</sup>	± 6 × 10 <sup>-6</sup>	4.4 × 10 <sup>4</sup>	± 2 × 10 <sup>4</sup>	630	± 20	139.7	± 0.3	0.190	± 0.003	0.0758	± 3.E-04	5.3	4.3

**Table D.14:** Linear Guinier Plot results for PEO<sub>132</sub>-PB<sub>89</sub> in C<sub>6</sub>D<sub>12</sub>. These plots were done over the Q-range 0.003-0.02 Å<sup>-1</sup>, on the high-temperature data.

Temperature, (°C)	Guinier Slope			χ <sup>2</sup>	Reduced χ <sup>2</sup>	Radius of Gyration, R <sub>g</sub> (Å)		Spherical Radius, R (Å)	
49.3	2467	± 30		89	1.3	86.0	± 0.5	111.1	± 0.7
58.6	2270	± 3		99	1.4	82.5	± 0.05	106.5	± 0.1
67.9	2170	± 30		61	1.1	80.7	± 0.6	104.2	± 0.7

**Table D.15:** Results from the Schulz sphere model, for PEO<sub>132</sub>-PB<sub>89</sub> in C<sub>6</sub>D<sub>12</sub> at high temperatures. Due to scattering from unimers as well, this model was only fit over the Q-range 0.003-0.05 Å<sup>-2</sup>. The scattering length densities of the sphere and solvent were held at 5.2 × 10<sup>-7</sup> Å<sup>-2</sup> and 6.7 × 10<sup>-6</sup> Å<sup>-2</sup>, respectively.

Temperature (°C)	Scale	Mean Radius, R (Å)	Polydispersity p, σ/R	Background B (cm <sup>-1</sup> sr <sup>-1</sup> )	χ <sup>2</sup> × 10 <sup>-2</sup>	Reduced χ <sup>2</sup>
49.3	6.84 × 10 <sup>-4</sup> ± 5. × 10 <sup>-6</sup>	78.4 ± 0.9	0.265 ± 0.006	0.094 ± 0.005	3.0	1.5
58.6	5.53 × 10 <sup>-4</sup> ± 4. × 10 <sup>-6</sup>	72.8 ± 0.4	0.281 ± 0.002	0.114 ± 0.004	2.0	1.2
67.9	3.8 × 10 <sup>-4</sup> ± 1. × 10 <sup>-5</sup>	66 ± 3	0.32 ± 0.02	0.123 ± 0.008	1.3	1.0

**Table D.16:** Polydisperse core-shell model results for PEO<sub>132</sub>-PB<sub>89</sub> in C<sub>6</sub>D<sub>12</sub> at high temperatures. Due to scattering from unimers as well, this model was only fit over the Q-range 0.003-0.05 Å<sup>-2</sup>. The scattering length densities of the core and shell were held at 6.4 × 10<sup>-7</sup> and 4.1 × 10<sup>-7</sup> Å<sup>-2</sup>, respectively. That of the solvent was held at 6.7 × 10<sup>-6</sup> Å<sup>-2</sup>.

Temperature (°C)	Scale	Average Core Radius R <sub>c</sub> (Å)	Polydispersity in Core Radius p, σ/R <sub>c</sub>	Shell Thickness, T, (Å)	Background B (cm <sup>-1</sup> )	χ <sup>2</sup> × 10 <sup>-2</sup>	Reduced χ <sup>2</sup>
49.3	7.39 × 10 <sup>-4</sup> ± 3.0 × 10 <sup>-5</sup>	70 ± 10	0.29 ± 0.03	10 ± 10	0.096 ± 0.006	3.0	1.5
58.6	6.03 × 10 <sup>-4</sup> ± 3.0 × 10 <sup>-5</sup>	60 ± 10	0.31 ± 0.03	10 ± 10	0.116 ± 0.009	2.0	1.3
67.9	4.08 × 10 <sup>-4</sup> ± 2.1 × 10 <sup>-5</sup>	61 ± 6	0.33 ± 0.03	6 ± 6	0.125 ± 0.009	1.3	1.0

## **Appendix E: Small Angle Neutron Scattering Data**

The reduced small angle neutron scattering data for all copolymer solutions is attached. 17R4 data is presented first, and includes all temperatures and concentrations which were presented in Chapter 5. PEO<sub>132</sub>-PB<sub>89</sub> data follows; the deuterated methanol solutions are presented prior to the deuterated cyclohexane.

ω=0.228 17R4/D <sub>2</sub> O 15.5 °C					ω=0.228 17R4/D <sub>2</sub> O 24.9 °C						
Q	I(Q)	Std DevI(Q)	sigmaQ	meanQ	Shadow Factor	Q	I(Q)	Std DevI(Q)	sigmaQ	meanQ	Shadow Factor
0.003433	39.54	1.058	0.001073	0.003607	0.9568	0.003433	104.4	2.822	0.001073	0.003607	0.9568
0.003837	23.28	0.7953	0.001077	0.003977	0.9999	0.003837	61.08	2.082	0.001077	0.003977	0.9999
0.004241	13.67	0.3524	0.001079	0.004367	1	0.004241	35.06	0.9084	0.001079	0.004367	1
0.004645	8.772	0.1864	0.001082	0.00476	1	0.004645	22.09	0.4684	0.001082	0.00476	1
0.005049	5.986	0.1195	0.001087	0.005155	1	0.005049	14.83	0.2578	0.001087	0.005155	1
0.005453	4.364	0.07834	0.001092	0.005551	1	0.005453	10.49	0.1796	0.001092	0.005551	1
0.005857	3.317	0.06353	0.001098	0.005948	1	0.005857	7.666	0.1159	0.001098	0.005948	1
0.006261	2.562	0.05556	0.001104	0.006346	1	0.006261	5.891	0.08896	0.001104	0.006346	1
0.006665	2.136	0.04175	0.001111	0.006745	1	0.006665	4.705	0.06243	0.001111	0.006745	1
0.007069	1.801	0.03851	0.001119	0.007144	1	0.007069	3.86	0.05406	0.001119	0.007144	1
0.007473	1.546	0.0341	0.001127	0.007544	1	0.007473	3.189	0.05032	0.001127	0.007544	1
0.007876	1.349	0.02757	0.001136	0.007944	1	0.007876	2.701	0.04101	0.001136	0.007944	1
0.00828	1.174	0.02854	0.001145	0.008345	1	0.00828	2.353	0.03758	0.001145	0.008345	1
0.008684	1.053	0.02375	0.001155	0.008746	1	0.008684	2.075	0.034	0.001155	0.008746	1
0.009088	0.9852	0.02	0.001165	0.009147	1	0.009088	1.863	0.03057	0.001165	0.009147	1
0.009492	0.9195	0.01918	0.001176	0.009548	1	0.009492	1.738	0.02553	0.001176	0.009548	1
0.009896	0.8627	0.01885	0.001187	0.00995	1	0.009896	1.587	0.02441	0.001187	0.00995	1
0.0103	0.808	0.01767	0.001198	0.01035	1	0.0103	1.483	0.02453	0.001198	0.01035	1
0.0107	0.8112	0.01848	0.00121	0.01075	1	0.0107	1.363	0.02249	0.00121	0.01075	1
0.01111	0.7398	0.01768	0.001222	0.01116	1	0.01111	1.296	0.02084	0.001222	0.01116	1
0.0113	0.7835	0.01253	0.002193	0.01149	1	0.0113	1.36	0.02472	0.002193	0.01149	1
0.01151	0.7224	0.01621	0.001234	0.01156	1	0.01151	1.215	0.02062	0.001234	0.01156	1
0.01192	0.6809	0.01629	0.001247	0.01196	1	0.01192	1.209	0.01962	0.001247	0.01196	1
0.01232	0.707	0.01591	0.00126	0.01236	1	0.01232	1.136	0.01944	0.00126	0.01236	1
0.01263	0.6992	0.01003	0.002214	0.0128	1	0.01263	1.147	0.01399	0.002214	0.0128	1
0.01272	0.6864	0.01607	0.001273	0.01277	1	0.01272	1.084	0.01801	0.001273	0.01277	1
0.01313	0.6453	0.01482	0.001287	0.01317	1	0.01313	1.078	0.02004	0.001287	0.01317	1
0.01353	0.6463	0.01418	0.0013	0.01357	1	0.01353	1.023	0.0173	0.0013	0.01357	1
0.01393	0.6565	0.01346	0.001315	0.01397	1	0.01393	1.011	0.01631	0.001315	0.01397	1
0.01396	0.6634	0.008515	0.002239	0.01412	1	0.01396	1.043	0.01109	0.002239	0.01412	1
0.01434	0.6325	0.0141	0.001329	0.01438	1	0.01434	0.9943	0.01725	0.001329	0.01438	1
0.01474	0.6401	0.01352	0.001344	0.01478	1	0.01474	0.9789	0.01556	0.001344	0.01478	1
0.01515	0.644	0.01291	0.001359	0.01518	1	0.01515	0.9715	0.01561	0.001359	0.01518	1
0.01529	0.6299	0.00862	0.002266	0.01543	1	0.01529	0.9692	0.009802	0.002266	0.01543	1
0.01555	0.626	0.0127	0.001374	0.01558	1	0.01555	0.9587	0.01645	0.001374	0.01558	1
0.01595	0.6203	0.01363	0.001389	0.01599	1	0.01595	0.9535	0.01607	0.001389	0.01599	1
0.01636	0.606	0.01451	0.001405	0.01639	1	0.01636	0.9512	0.01648	0.001405	0.01639	1
0.01662	0.6242	0.006958	0.002296	0.01675	1	0.01662	0.939	0.00867	0.002296	0.01675	1
0.01676	0.6276	0.01308	0.001421	0.01679	1	0.01676	0.9362	0.01487	0.001421	0.01679	1
0.01717	0.6103	0.01408	0.001437	0.0172	1	0.01717	0.9327	0.01612	0.001437	0.0172	1
0.01757	0.6111	0.01349	0.001453	0.0176	1	0.01757	0.9157	0.01534	0.001453	0.0176	1
0.01795	0.621	0.00709	0.002328	0.01807	1	0.01795	0.9095	0.008825	0.002328	0.01807	1
0.01797	0.6024	0.01387	0.00147	0.018	1	0.01797	0.9282	0.01655	0.00147	0.018	1
0.01838	0.6043	0.01167	0.001486	0.01841	1	0.01838	0.8813	0.01634	0.001486	0.01841	1
0.01878	0.5903	0.01358	0.001503	0.01881	1	0.01878	0.8907	0.01544	0.001503	0.01881	1
0.01918	0.611	0.01294	0.00152	0.01921	1	0.01918	0.9015	0.0139	0.00152	0.01921	1
0.01928	0.6077	0.007537	0.002363	0.01939	1	0.01928	0.8916	0.007637	0.002363	0.01939	1
0.01959	0.5887	0.01222	0.001537	0.01962	1	0.01959	0.8772	0.01356	0.001537	0.01962	1
0.01999	0.58	0.01183	0.001555	0.02002	1	0.01999	0.8414	0.01386	0.001555	0.02002	1
0.0204	0.5883	0.01215	0.001572	0.02042	1	0.0204	0.8636	0.0149	0.001572	0.02042	1
0.02061	0.5931	0.007719	0.0024	0.02072	1	0.02061	0.8793	0.007451	0.0024	0.02072	1
0.0208	0.5844	0.01418	0.00159	0.02083	1	0.0208	0.8321	0.01525	0.00159	0.02083	1
0.0212	0.5796	0.01208	0.001608	0.02123	1	0.0212	0.8554	0.01421	0.001608	0.02123	1
0.02161	0.5995	0.01263	0.001626	0.02163	1	0.02161	0.8624	0.01413	0.001626	0.02163	1
0.02194	0.5952	0.006414	0.002438	0.02204	1	0.02194	0.8711	0.007935	0.002438	0.02204	1
0.02201	0.5749	0.01216	0.001644	0.02203	1	0.02201	0.8757	0.01448	0.001644	0.02203	1
0.02241	0.6117	0.01312	0.001662	0.02244	1	0.02241	0.8827	0.01306	0.001662	0.02244	1
0.02282	0.5858	0.01261	0.00168	0.02284	1	0.02282	0.8728	0.01401	0.00168	0.02284	1
0.02322	0.5847	0.01171	0.001699	0.02324	1	0.02322	0.847	0.01382	0.001699	0.02324	1
0.02327	0.5933	0.006314	0.002479	0.02336	1	0.02327	0.864	0.007442	0.002479	0.02336	1
0.02363	0.5876	0.01117	0.001717	0.02365	1	0.02363	0.8517	0.01368	0.001717	0.02365	1
0.02403	0.5925	0.0127	0.001736	0.02405	1	0.02403	0.8624	0.01375	0.001736	0.02405	1
0.02443	0.5995	0.0112	0.001755	0.02445	1	0.02443	0.843	0.01467	0.001755	0.02445	1
0.0246	0.5996	0.005941	0.002521	0.02469	1	0.0246	0.8577	0.007157	0.002521	0.02469	1
0.02484	0.5776	0.0135	0.001774	0.02486	1	0.02484	0.8381	0.01462	0.001774	0.02486	1
0.02524	0.5566	0.01247	0.001793	0.02526	1	0.02524	0.8492	0.0154	0.001793	0.02526	1
0.02564	0.6038	0.01503	0.001812	0.02566	1	0.02564	0.843	0.01612	0.001812	0.02566	1
0.02593	0.5918	0.005338	0.002565	0.02601	1	0.02593	0.8494	0.007275	0.002565	0.02601	1
0.02605	0.5978	0.01475	0.001831	0.02607	1	0.02605	0.839	0.0165	0.001831	0.02607	1
0.02645	0.5636	0.01354	0.001851	0.02647	1	0.02645	0.8239	0.01565	0.001851	0.02647	1
0.02685	0.5747	0.0147	0.00187	0.02687	1	0.02685	0.8368	0.01744	0.00187	0.02687	1
0.02726	0.5831	0.005903	0.002611	0.02734	1	0.02726	0.8579	0.006402	0.002611	0.02734	1
0.02726	0.5895	0.01281	0.00189	0.02728	1	0.02726	0.838	0.0162	0.00189	0.02728	1
0.02766	0.6059	0.01519	0.001909	0.02768	1	0.02766	0.8617	0.01826	0.001909	0.02768	1
0.02807	0.6077	0.01766	0.001929	0.02808	1	0.02807	0.8677	0.01753	0.001929	0.02808	1
0.02847	0.6043	0.01541	0.001949	0.02849	1	0.02847	0.8436	0.01634	0.001949	0.02849	1
0.02859	0.5878	0.005553	0.002658	0.02866	1	0.02859	0.8456	0.006654	0.002658	0.02866	1
0.02887	0.5694	0.01719	0.001968	0.02889	1	0.02887	0.8139	0.01913	0.001968	0.02889	1
0.02928	0.583	0.01435	0.001988	0.02929	1	0.02928	0.7962	0.01904	0.001988	0.02929	1
0.02968	0.5841	0.01731	0.002008	0.0297	1	0.02968	0.8431	0.01863	0.002008	0.0297	1
0.02991	0.5887	0.00559	0.002707	0.02999	1	0.02991	0.8403	0.006467	0.002707	0.02999	1

ω=0.228 17R4/D <sub>2</sub> O 15.5 °C					ω=0.228 17R4/D <sub>2</sub> O 24.9 °C						
Q	I(Q)	Std Dev(I(Q))	sigmaQ	meanQ	Shadow Factor	Q	I(Q)	Std Dev(I(Q))	sigmaQ	meanQ	Shadow Factor
0.03008	0.6064	0.01591	0.002028	0.0301	1	0.03008	0.8603	0.01806	0.002028	0.0301	1
0.03049	0.573	0.0164	0.002049	0.0305	1	0.03049	0.8435	0.01875	0.002049	0.0305	1
0.03089	0.5667	0.01586	0.002069	0.03091	1	0.03089	0.83	0.01731	0.002069	0.03091	1
0.03124	0.5833	0.005669	0.002756	0.03131	1	0.03124	0.8313	0.006287	0.002756	0.03131	1
0.03129	0.5795	0.01589	0.002089	0.03131	1	0.03129	0.8411	0.0195	0.002089	0.03131	1
0.0317	0.5709	0.01424	0.002109	0.03171	1	0.0317	0.8459	0.02025	0.002109	0.03171	1
0.0321	0.5554	0.01648	0.00213	0.03212	1	0.0321	0.7968	0.01862	0.00213	0.03212	1
0.0325	0.565	0.01548	0.00215	0.03252	1	0.0325	0.8122	0.01718	0.00215	0.03252	1
0.03257	0.5746	0.004726	0.002807	0.03264	1	0.03257	0.8376	0.005901	0.002807	0.03264	1
0.03291	0.5774	0.01609	0.002171	0.03292	1	0.03291	0.8316	0.02036	0.002171	0.03292	1
0.03331	0.569	0.01555	0.002191	0.03333	1	0.03331	0.8367	0.01941	0.002191	0.03333	1
0.03372	0.5759	0.0157	0.002212	0.03373	1	0.03372	0.874	0.01825	0.002212	0.03373	1
0.0339	0.5799	0.004857	0.00286	0.03396	1	0.0339	0.831	0.005745	0.00286	0.03396	1
0.03399	0.5939	0.003006	0.004794	0.03426	1	0.03399	0.8434	0.003596	0.004794	0.03426	1
0.03523	0.5803	0.004824	0.002913	0.03529	1	0.03523	0.8279	0.00551	0.002913	0.03529	1
0.03656	0.576	0.004924	0.002967	0.03662	1	0.03656	0.8307	0.005173	0.002967	0.03662	1
0.03788	0.58	0.004843	0.003023	0.03794	1	0.03788	0.819	0.005783	0.003023	0.03794	1
0.03798	0.5984	0.002783	0.00489	0.03823	1	0.03798	0.8427	0.003798	0.00489	0.03823	1
0.03921	0.5802	0.004419	0.003079	0.03927	1	0.03921	0.8194	0.004955	0.003079	0.03927	1
0.04054	0.5809	0.004578	0.003136	0.04059	1	0.04054	0.8105	0.005284	0.003136	0.04059	1
0.04187	0.5724	0.004299	0.003194	0.04192	1	0.04187	0.818	0.004721	0.003194	0.04192	1
0.04197	0.5961	0.003373	0.004996	0.0422	1	0.04197	0.8365	0.003765	0.004996	0.0422	1
0.0432	0.5798	0.004887	0.003253	0.04325	1	0.0432	0.8242	0.005207	0.003253	0.04325	1
0.04452	0.57	0.004248	0.003312	0.04457	1	0.04452	0.806	0.005205	0.003312	0.04457	1
0.04585	0.5673	0.003853	0.003372	0.0459	1	0.04585	0.8044	0.00505	0.003372	0.0459	1
0.04596	0.588	0.003043	0.00511	0.04617	1	0.04597	0.8312	0.003208	0.00511	0.04617	1
0.04718	0.5717	0.004141	0.003433	0.04722	1	0.04718	0.8026	0.005269	0.003433	0.04722	1
0.0485	0.5634	0.00407	0.003495	0.04855	1	0.0485	0.7983	0.004745	0.003495	0.04855	1
0.04983	0.5631	0.004159	0.003557	0.04987	1	0.04983	0.8047	0.00503	0.003557	0.04987	1
0.04996	0.5866	0.002725	0.005233	0.05014	1	0.04996	0.8258	0.003535	0.005233	0.05014	1
0.05116	0.5702	0.004004	0.00362	0.0512	1	0.05116	0.7931	0.004597	0.00362	0.0512	1
0.05248	0.5673	0.003962	0.003683	0.05252	1	0.05248	0.7919	0.004962	0.003683	0.05252	1
0.05381	0.5672	0.004003	0.003746	0.05385	1	0.05381	0.7962	0.004857	0.003746	0.05385	1
0.05394	0.5867	0.002641	0.005363	0.05412	1	0.05394	0.8221	0.003304	0.005363	0.05412	1
0.05514	0.5679	0.003736	0.003811	0.05517	1	0.05514	0.7917	0.004692	0.003811	0.05517	1
0.05646	0.5627	0.003677	0.003875	0.0565	1	0.05646	0.7865	0.004259	0.003875	0.0565	1
0.05779	0.5616	0.003374	0.00394	0.05782	1	0.05779	0.7836	0.004081	0.00394	0.05782	1
0.05793	0.5862	0.002745	0.0055	0.05809	1	0.05793	0.8173	0.003134	0.0055	0.05809	1
0.05911	0.5588	0.003433	0.004006	0.05915	1	0.05911	0.7788	0.004199	0.004006	0.05915	1
0.06044	0.5544	0.003905	0.004071	0.06047	1	0.06044	0.7834	0.004594	0.004071	0.06047	1
0.06176	0.5643	0.003893	0.004138	0.0618	1	0.06176	0.7782	0.004023	0.004138	0.0618	1
0.06192	0.5819	0.002804	0.005643	0.06207	1	0.06192	0.8102	0.002803	0.005643	0.06207	1
0.06309	0.563	0.003745	0.004204	0.06312	1	0.06309	0.7708	0.004054	0.004204	0.06312	1
0.06441	0.558	0.003451	0.004271	0.06444	1	0.06441	0.7751	0.004022	0.004271	0.06444	1
0.06573	0.553	0.003558	0.004338	0.06577	1	0.06573	0.7728	0.003893	0.004338	0.06577	1
0.0659	0.5839	0.002728	0.005791	0.06604	1	0.0659	0.8052	0.003007	0.005791	0.06604	1
0.06706	0.5559	0.003299	0.004406	0.06709	1	0.06706	0.7689	0.004264	0.004406	0.06709	1
0.06838	0.5518	0.003371	0.004474	0.06841	1	0.06838	0.7716	0.003713	0.004474	0.06841	1
0.06971	0.5533	0.003243	0.004542	0.06974	1	0.06971	0.766	0.004143	0.004542	0.06974	1
0.06988	0.5786	0.002406	0.005945	0.07001	1	0.06988	0.7976	0.002903	0.005945	0.07001	1
0.07103	0.5491	0.003235	0.00461	0.07106	1	0.07103	0.762	0.003625	0.00461	0.07106	1
0.07235	0.5522	0.003497	0.004679	0.07238	1	0.07235	0.7548	0.004013	0.004679	0.07238	1
0.07367	0.5505	0.003157	0.004747	0.0737	1	0.07367	0.754	0.003671	0.004747	0.0737	1
0.07386	0.5817	0.002547	0.006104	0.07399	1	0.07386	0.7914	0.002835	0.006104	0.07399	1
0.075	0.5495	0.003206	0.004816	0.07503	1	0.075	0.7529	0.003734	0.004816	0.07503	1
0.07632	0.5575	0.003233	0.004886	0.07635	1	0.07632	0.7511	0.003748	0.004886	0.07635	1
0.07764	0.548	0.00314	0.004955	0.07767	1	0.07764	0.7532	0.003828	0.004955	0.07767	1
0.07783	0.5771	0.002245	0.006266	0.07796	1	0.07784	0.7829	0.003249	0.006266	0.07796	1
0.07896	0.5467	0.003211	0.005025	0.07899	1	0.07896	0.749	0.003489	0.005025	0.07899	1
0.08028	0.5474	0.003287	0.005094	0.08031	1	0.08028	0.749	0.003641	0.005094	0.08031	1
0.08161	0.5503	0.003093	0.005164	0.08163	1	0.08161	0.7409	0.004054	0.005164	0.08163	1
0.08181	0.5738	0.002219	0.006433	0.08192	1	0.08181	0.7769	0.003109	0.006434	0.08192	1
0.08293	0.5554	0.003643	0.005235	0.08295	1	0.08293	0.7372	0.004022	0.005235	0.08295	1
0.08425	0.55	0.003407	0.005305	0.08427	1	0.08425	0.7382	0.003885	0.005305	0.08427	1
0.08557	0.5462	0.003684	0.005375	0.08559	1	0.08557	0.739	0.004651	0.005375	0.08559	1
0.08578	0.5715	0.002496	0.006604	0.08589	1	0.08578	0.7662	0.003425	0.006604	0.08589	1
0.08689	0.545	0.004053	0.005446	0.08691	1	0.08689	0.7264	0.004644	0.005446	0.08691	1
0.08821	0.5413	0.004449	0.005517	0.08823	1	0.08821	0.731	0.004891	0.005517	0.08823	1
0.08953	0.5476	0.004432	0.005588	0.08955	1	0.08953	0.7215	0.004739	0.005588	0.08955	1
0.08975	0.5701	0.002309	0.006778	0.08985	1	0.08975	0.759	0.002612	0.006778	0.08985	1
0.09084	0.5474	0.004816	0.005659	0.09087	1	0.09084	0.7202	0.005217	0.005659	0.09087	1
0.09371	0.5622	0.002197	0.006955	0.09381	1	0.09371	0.7498	0.002857	0.006955	0.09381	1
0.09768	0.5623	0.002195	0.007136	0.09777	1	0.09768	0.7432	0.002802	0.007136	0.09777	1
0.1016	0.5626	0.002305	0.007318	0.1017	1	0.1016	0.7359	0.002723	0.007318	0.1017	1
0.1056	0.5575	0.002351	0.007503	0.1057	1	0.1056	0.7252	0.00242	0.007503	0.1057	1
0.1095	0.5548	0.002269	0.007691	0.1096	1	0.1095	0.7156	0.002517	0.007691	0.1096	1
0.1135	0.5571	0.00226	0.00788	0.1136	1	0.1135	0.7119	0.002503	0.00788	0.1136	1
0.1174	0.552	0.002182	0.008071	0.1175	1	0.1174	0.7036	0.002196	0.008071	0.1175	1
0.1214	0.5493	0.001904	0.008264	0.1215	1	0.1214	0.6957	0.002282	0.008264	0.1215	1
0.1253	0.5453	0.002027	0.008458	0.1254	1	0.1253	0.6831	0.002083	0.008458	0.1254	1
0.1293	0.5443	0.001992	0.008654	0.1293	1	0.1293	0.6784	0.002241	0.008654	0.1293	1

ω=0.228 17R4/D <sub>2</sub> O 15.5 °C					ω=0.228 17R4/D <sub>2</sub> O 24.9 °C						
Q	I(Q)	Std Dev(I(Q))	sigmaQ	meanQ	Shadow Factor	Q	I(Q)	Std Dev(I(Q))	sigmaQ	meanQ	Shadow Factor
0.1332	0.539	0.002052	0.008851	0.1332	1	0.1332	0.6668	0.002282	0.008851	0.1333	1
0.1371	0.5372	0.00201	0.00905	0.1372	1	0.1371	0.6577	0.002474	0.00905	0.1372	1
0.141	0.5305	0.002077	0.009249	0.1411	1	0.141	0.6501	0.002265	0.009249	0.1411	1
0.1449	0.5284	0.001898	0.00945	0.145	1	0.1449	0.6433	0.002165	0.00945	0.145	1
0.1489	0.5251	0.002181	0.009651	0.1489	1	0.1489	0.6315	0.002213	0.009651	0.1489	1
0.1528	0.5195	0.001958	0.009853	0.1528	1	0.1528	0.6216	0.001952	0.009853	0.1528	1
0.1567	0.5151	0.001713	0.01006	0.1567	1	0.1567	0.6117	0.001992	0.01006	0.1567	1
0.1606	0.5126	0.001899	0.01026	0.1606	1	0.1606	0.6049	0.001899	0.01026	0.1606	1
0.1645	0.5054	0.001694	0.01046	0.1645	1	0.1645	0.5936	0.001929	0.01046	0.1645	1
0.1683	0.5003	0.001688	0.01067	0.1684	1	0.1683	0.5866	0.001953	0.01067	0.1684	1
0.1722	0.4996	0.001644	0.01087	0.1723	1	0.1722	0.5768	0.00186	0.01087	0.1723	1
0.1761	0.4941	0.001613	0.01108	0.1762	1	0.1761	0.5706	0.001956	0.01108	0.1762	1
0.18	0.4876	0.001675	0.01129	0.18	1	0.18	0.5584	0.001999	0.01129	0.18	1
0.1838	0.4878	0.001661	0.01149	0.1839	1	0.1838	0.5547	0.002013	0.01149	0.1839	1
0.1877	0.4829	0.001805	0.0117	0.1877	1	0.1877	0.545	0.00173	0.0117	0.1877	1
0.1915	0.4792	0.001663	0.01191	0.1916	1	0.1915	0.5362	0.001779	0.01191	0.1916	1
0.1954	0.4718	0.001694	0.01212	0.1954	1	0.1954	0.527	0.001718	0.01212	0.1954	1
0.1992	0.4688	0.001458	0.01232	0.1993	1	0.1992	0.5215	0.001726	0.01232	0.1993	1
0.2031	0.4631	0.001581	0.01253	0.2031	1	0.2031	0.515	0.001689	0.01253	0.2031	1
0.2069	0.459	0.001696	0.01274	0.2069	1	0.2069	0.5071	0.001742	0.01274	0.2069	1
0.2107	0.4573	0.00168	0.01295	0.2108	1	0.2107	0.5025	0.001863	0.01295	0.2108	1
0.2145	0.4535	0.001543	0.01316	0.2146	1	0.2145	0.4949	0.001515	0.01316	0.2146	1
0.2184	0.4481	0.001613	0.01336	0.2184	1	0.2184	0.4884	0.001656	0.01336	0.2184	1
0.2222	0.4404	0.001587	0.01357	0.2222	1	0.2222	0.4803	0.001646	0.01357	0.2222	1
0.226	0.4388	0.001563	0.01378	0.226	1	0.226	0.4733	0.001658	0.01378	0.226	1
0.2297	0.4381	0.001516	0.01399	0.2298	1	0.2297	0.4713	0.001642	0.01399	0.2298	1
0.2335	0.436	0.001384	0.0142	0.2336	1	0.2335	0.4639	0.001429	0.0142	0.2336	1
0.2373	0.4291	0.001404	0.0144	0.2373	1	0.2373	0.4579	0.001545	0.0144	0.2373	1
0.2411	0.4262	0.001493	0.01461	0.2411	1	0.2411	0.4518	0.001543	0.01461	0.2411	1
0.2448	0.4203	0.001547	0.01482	0.2449	1	0.2448	0.4518	0.001611	0.01482	0.2449	1
0.2486	0.4187	0.001663	0.01503	0.2486	1	0.2486	0.4407	0.001779	0.01503	0.2486	1
0.2523	0.4146	0.001511	0.01524	0.2524	1	0.2523	0.4399	0.001587	0.01524	0.2524	1
0.2561	0.4119	0.00173	0.01544	0.2561	1	0.2561	0.4321	0.001948	0.01544	0.2561	1
0.2598	0.4117	0.001626	0.01565	0.2598	1	0.2598	0.4272	0.001834	0.01565	0.2598	1
0.2635	0.4075	0.001918	0.01586	0.2636	1	0.2635	0.4267	0.001739	0.01586	0.2636	1
0.2673	0.4007	0.001826	0.01606	0.2673	1	0.2673	0.4218	0.001657	0.01606	0.2673	1
0.271	0.3994	0.001655	0.01627	0.271	1	0.271	0.4159	0.001741	0.01627	0.271	1
0.2747	0.3924	0.001722	0.01648	0.2747	1	0.2747	0.4135	0.001648	0.01648	0.2747	1
0.2784	0.3942	0.001527	0.01668	0.2784	1	0.2784	0.4085	0.001701	0.01668	0.2784	1
0.282	0.3921	0.001741	0.01689	0.2821	1	0.282	0.4028	0.001708	0.01689	0.2821	1
0.2857	0.3882	0.001814	0.0171	0.2857	1	0.2857	0.4018	0.001738	0.0171	0.2857	1
0.2894	0.3888	0.001732	0.0173	0.2894	1	0.2894	0.3963	0.001761	0.0173	0.2894	1
0.293	0.3859	0.001832	0.01751	0.2931	1	0.293	0.397	0.001751	0.01751	0.2931	1
0.2967	0.38	0.001573	0.01771	0.2967	1	0.2967	0.389	0.001627	0.01771	0.2967	1
0.3003	0.3753	0.00183	0.01791	0.3004	1	0.3003	0.3858	0.001503	0.01792	0.3004	1
0.304	0.3716	0.001566	0.01812	0.304	1	0.304	0.3818	0.001646	0.01812	0.304	1
0.3076	0.3696	0.001607	0.01832	0.3076	1	0.3076	0.3765	0.00158	0.01832	0.3076	1
0.3112	0.3681	0.001774	0.01853	0.3112	1	0.3112	0.3765	0.001649	0.01853	0.3113	1
0.3148	0.3654	0.001718	0.01873	0.3149	1	0.3148	0.3748	0.001591	0.01873	0.3149	1
0.3184	0.3595	0.001792	0.01893	0.3185	1	0.3184	0.3685	0.001717	0.01893	0.3185	1
0.322	0.3572	0.00152	0.01913	0.322	1	0.322	0.3684	0.001642	0.01913	0.3221	1
0.3256	0.3568	0.001416	0.01934	0.3256	1	0.3256	0.3624	0.00164	0.01934	0.3256	1
0.3292	0.3538	0.001725	0.01954	0.3292	1	0.3292	0.3603	0.001666	0.01954	0.3292	1
0.3327	0.3488	0.001632	0.01974	0.3328	1	0.3327	0.3581	0.001837	0.01974	0.3328	1
0.3363	0.3498	0.001814	0.01994	0.3363	1	0.3363	0.3591	0.001625	0.01994	0.3363	1
0.3398	0.3469	0.001621	0.02014	0.3399	1	0.3399	0.3548	0.00185	0.02014	0.3399	1
0.3434	0.3485	0.001757	0.02034	0.3434	1	0.3434	0.3498	0.001611	0.02034	0.3434	1
0.3469	0.3417	0.001611	0.02054	0.3469	1	0.3469	0.3496	0.001752	0.02054	0.3469	1
0.3504	0.3402	0.001787	0.02074	0.3505	1	0.3504	0.3472	0.001593	0.02074	0.3505	1
0.3539	0.3415	0.00169	0.02094	0.354	1	0.3539	0.3432	0.001487	0.02094	0.354	1
0.3574	0.3373	0.001479	0.02114	0.3575	1	0.3574	0.34	0.001798	0.02114	0.3575	1
0.3609	0.3369	0.001524	0.02133	0.361	1	0.3609	0.3419	0.001818	0.02133	0.361	1
0.3644	0.3352	0.001583	0.02153	0.3644	1	0.3644	0.3411	0.001631	0.02153	0.3644	1
0.3679	0.3309	0.001827	0.02173	0.3679	1	0.3679	0.3387	0.001713	0.02173	0.3679	1
0.3713	0.33	0.001667	0.02192	0.3714	1	0.3713	0.3315	0.001476	0.02192	0.3714	1
0.3748	0.3282	0.001607	0.02212	0.3748	1	0.3748	0.3309	0.001414	0.02212	0.3748	1
0.3782	0.326	0.001783	0.02231	0.3783	1	0.3782	0.3325	0.001645	0.02231	0.3783	1
0.3817	0.327	0.001701	0.02251	0.3817	1	0.3817	0.3321	0.001667	0.02251	0.3817	1
0.3851	0.3231	0.001692	0.0227	0.3851	1	0.3851	0.3242	0.00147	0.0227	0.3851	1
0.3885	0.3215	0.001538	0.0229	0.3885	1	0.3885	0.3256	0.001625	0.0229	0.3885	1
0.3919	0.322	0.001572	0.02309	0.3919	1	0.3919	0.324	0.001469	0.02309	0.3919	1
0.3953	0.3193	0.001805	0.02328	0.3953	1	0.3953	0.3244	0.001673	0.02328	0.3953	1
0.3987	0.3167	0.001558	0.02348	0.3987	1	0.3987	0.3211	0.001541	0.02348	0.3987	1
0.4021	0.3148	0.001484	0.02367	0.4021	1	0.4021	0.3221	0.001695	0.02367	0.4021	1
0.4054	0.3177	0.001807	0.02386	0.4054	1	0.4054	0.3187	0.001704	0.02386	0.4054	1



ω=0.228 17R4/D <sub>2</sub> O 29.8 °C					ω=0.228 17R4/D <sub>2</sub> O 34.5 °C						
Q	I(Q)	Std DevI(Q)	sigmaQ	meanQ	Shadow Factor	Q	I(Q)	Std DevI(Q)	sigmaQ	meanQ	Shadow Factor
0.003433	134.4	3.629	0.001073	0.003607	0.9568	0.003433	7.815	0.2139	0.001073	0.003607	0.9568
0.003837	77.66	2.651	0.001077	0.003977	0.9999	0.003837	8.547	0.1119	0.001077	0.003977	0.9999
0.004241	44.37	1.164	0.001079	0.004367	1	0.004241	8.577	0.09951	0.001079	0.004367	1
0.004645	27.87	0.5774	0.001082	0.00476	1	0.004645	8.623	0.09626	0.001082	0.00476	1
0.005049	18.8	0.3418	0.001087	0.005155	1	0.005049	8.732	0.09922	0.001087	0.005155	1
0.005453	13.34	0.2078	0.001092	0.005551	1	0.005453	8.702	0.08792	0.001092	0.005551	1
0.005857	9.957	0.1357	0.001098	0.005948	1	0.005857	8.574	0.07409	0.001098	0.005948	1
0.006261	7.622	0.1055	0.001104	0.006346	1	0.006261	8.666	0.07243	0.001104	0.006346	1
0.006665	6.14	0.07534	0.001111	0.006745	1	0.006665	8.641	0.06934	0.001111	0.006745	1
0.007069	5.029	0.06594	0.001119	0.007144	1	0.007069	8.603	0.06759	0.001119	0.007144	1
0.007473	4.214	0.05006	0.001127	0.007544	1	0.007473	8.571	0.06465	0.001127	0.007544	1
0.007876	3.615	0.04493	0.001136	0.007944	1	0.007876	8.575	0.06244	0.001136	0.007944	1
0.00828	3.084	0.03732	0.001145	0.008345	1	0.00828	8.633	0.06007	0.001145	0.008345	1
0.008684	2.706	0.03573	0.001155	0.008746	1	0.008684	8.537	0.06204	0.001155	0.008746	1
0.009088	2.513	0.03551	0.001165	0.009147	1	0.009088	8.628	0.0557	0.001165	0.009147	1
0.009492	2.245	0.03105	0.001176	0.009548	1	0.009492	8.588	0.06246	0.001176	0.009548	1
0.009896	2.092	0.02878	0.001187	0.00995	1	0.009896	8.494	0.05115	0.001187	0.00995	1
0.0103	1.949	0.02571	0.001198	0.01035	1	0.0103	8.478	0.05588	0.001198	0.01035	1
0.0107	1.881	0.02795	0.00121	0.01075	1	0.0107	8.442	0.05135	0.00121	0.01075	1
0.01111	1.779	0.02325	0.001222	0.01116	1	0.01111	8.479	0.05351	0.001222	0.01116	1
0.0113	1.885	0.027	0.001293	0.01149	1	0.0113	8.499	0.03426	0.001293	0.01149	1
0.01151	1.65	0.02434	0.001234	0.01156	1	0.01151	8.382	0.04803	0.001234	0.01156	1
0.01192	1.617	0.0221	0.001247	0.01196	1	0.01192	8.44	0.04987	0.001247	0.01196	1
0.01232	1.566	0.02312	0.00126	0.01236	1	0.01232	8.332	0.04652	0.00126	0.01236	1
0.01263	1.597	0.0172	0.002214	0.0128	1	0.01263	8.362	0.03415	0.002214	0.0128	1
0.01272	1.49	0.02082	0.001273	0.01277	1	0.01272	8.346	0.04618	0.001273	0.01277	1
0.01313	1.484	0.02112	0.001287	0.01317	1	0.01313	8.345	0.0472	0.001287	0.01317	1
0.01353	1.463	0.01814	0.0013	0.01357	1	0.01353	8.29	0.04295	0.0013	0.01357	1
0.01393	1.42	0.02122	0.001315	0.01397	1	0.01393	8.273	0.04812	0.001315	0.01397	1
0.01396	1.46	0.01398	0.002239	0.01412	1	0.01396	8.299	0.03064	0.002239	0.01412	1
0.01434	1.358	0.01846	0.001329	0.01438	1	0.01434	8.189	0.04694	0.001329	0.01438	1
0.01474	1.373	0.01907	0.001344	0.01478	1	0.01474	8.085	0.04349	0.001344	0.01478	1
0.01515	1.354	0.01769	0.001359	0.01518	1	0.01515	8.186	0.04688	0.001359	0.01518	1
0.01529	1.376	0.01174	0.002266	0.01543	1	0.01529	8.159	0.031	0.002266	0.01543	1
0.01555	1.332	0.01832	0.001374	0.01558	1	0.01555	8.183	0.04662	0.001374	0.01558	1
0.01595	1.353	0.01639	0.001389	0.01599	1	0.01595	8.078	0.04507	0.001389	0.01599	1
0.01636	1.293	0.01816	0.001405	0.01639	1	0.01636	8.084	0.04393	0.001405	0.01639	1
0.01662	1.31	0.01084	0.002296	0.01675	1	0.01662	8.119	0.03116	0.002296	0.01675	1
0.01676	1.293	0.01801	0.001421	0.01679	1	0.01676	8.018	0.04533	0.001421	0.01679	1
0.01717	1.315	0.01928	0.001437	0.0172	1	0.01717	7.979	0.04098	0.001437	0.0172	1
0.01757	1.267	0.01703	0.001453	0.0176	1	0.01757	7.98	0.04458	0.001453	0.0176	1
0.01795	1.292	0.009683	0.002328	0.01807	1	0.01795	7.932	0.0282	0.002328	0.01807	1
0.01797	1.272	0.01881	0.00147	0.018	1	0.01797	7.916	0.04507	0.00147	0.018	1
0.01838	1.29	0.019	0.001486	0.01841	1	0.01838	7.941	0.04542	0.001486	0.01841	1
0.01878	1.248	0.01903	0.001503	0.01881	1	0.01878	7.821	0.03956	0.001503	0.01881	1
0.01918	1.262	0.01759	0.00152	0.01921	1	0.01918	7.736	0.04229	0.00152	0.01921	1
0.01928	1.266	0.009851	0.002363	0.01939	1	0.01928	7.881	0.02474	0.002363	0.01939	1
0.01959	1.231	0.01643	0.001537	0.01962	1	0.01959	7.762	0.03914	0.001537	0.01962	1
0.01999	1.223	0.01791	0.001555	0.02002	1	0.01999	7.714	0.04076	0.001555	0.02002	1
0.0204	1.251	0.01575	0.001572	0.02042	1	0.0204	7.727	0.04185	0.001572	0.02042	1
0.02061	1.248	0.00928	0.0024	0.02072	1	0.02061	7.716	0.02252	0.0024	0.02072	1
0.0208	1.205	0.01758	0.00159	0.02083	1	0.0208	7.651	0.04243	0.00159	0.02083	1
0.0212	1.219	0.01623	0.001608	0.02123	1	0.0212	7.572	0.03719	0.001608	0.02123	1
0.02161	1.223	0.01657	0.001626	0.02163	1	0.02161	7.524	0.04077	0.001626	0.02163	1
0.02194	1.236	0.009865	0.002438	0.02204	1	0.02194	7.59	0.02314	0.002438	0.02204	1
0.02201	1.174	0.01539	0.001644	0.02203	1	0.02201	7.509	0.03948	0.001644	0.02203	1
0.02241	1.204	0.01592	0.001662	0.02244	1	0.02241	7.412	0.03817	0.001662	0.02244	1
0.02282	1.205	0.017	0.00168	0.02284	1	0.02282	7.449	0.03712	0.00168	0.02284	1
0.02322	1.209	0.01709	0.001699	0.02324	1	0.02322	7.347	0.03984	0.001699	0.02324	1
0.02327	1.217	0.008501	0.002479	0.02336	1	0.02327	7.444	0.02154	0.002479	0.02336	1
0.02363	1.204	0.01661	0.001717	0.02365	1	0.02363	7.262	0.03862	0.001717	0.02365	1
0.02403	1.239	0.017	0.001736	0.02405	1	0.02403	7.244	0.03722	0.001736	0.02405	1
0.02443	1.205	0.01485	0.001755	0.02445	1	0.02443	7.248	0.03525	0.001755	0.02445	1
0.0246	1.209	0.008142	0.002521	0.02469	1	0.0246	7.313	0.02344	0.002521	0.02469	1
0.02484	1.204	0.01714	0.001774	0.02486	1	0.02484	7.261	0.04152	0.001774	0.02486	1
0.02524	1.207	0.0176	0.001793	0.02526	1	0.02524	7.077	0.04077	0.001793	0.02526	1
0.02564	1.172	0.01763	0.001812	0.02566	1	0.02564	7.183	0.04386	0.001812	0.02566	1
0.02593	1.196	0.008379	0.002565	0.02601	1	0.02593	7.16	0.02242	0.002565	0.02601	1
0.02605	1.201	0.01804	0.001831	0.02607	1	0.02605	7.033	0.04565	0.001831	0.02607	1
0.02645	1.18	0.01816	0.001851	0.02647	1	0.02645	7.047	0.04875	0.001851	0.02647	1
0.02685	1.156	0.01898	0.00187	0.02687	1	0.02685	7.014	0.04036	0.00187	0.02687	1
0.02726	1.189	0.007678	0.002611	0.02734	1	0.02726	7.016	0.02286	0.002611	0.02734	1
0.02726	1.185	0.01705	0.00189	0.02728	1	0.02726	6.924	0.04436	0.00189	0.02728	1
0.02766	1.184	0.02131	0.001909	0.02768	1	0.02766	6.911	0.05107	0.001909	0.02768	1
0.02807	1.151	0.0217	0.001929	0.02808	1	0.02807	6.839	0.04801	0.001929	0.02808	1
0.02847	1.147	0.0197	0.001949	0.02849	1	0.02847	6.842	0.04645	0.001949	0.02849	1
0.02859	1.187	0.006748	0.002658	0.02866	1	0.02859	6.879	0.01903	0.002658	0.02866	1
0.02887	1.162	0.02142	0.001968	0.02889	1	0.02887	6.749	0.05009	0.001968	0.02889	1
0.02928	1.193	0.02221	0.001988	0.02929	1	0.02928	6.741	0.05462	0.001988	0.02929	1
0.02968	1.167	0.02188	0.002008	0.0297	1	0.02968	6.54	0.04991	0.002008	0.0297	1
0.02991	1.184	0.007921	0.002707	0.02999	1	0.02991	6.711	0.02014	0.002707	0.02999	1

$\omega=0.228$ 17R4/D <sub>2</sub> O 29.8 °C						$\omega=0.228$ 17R4/D <sub>2</sub> O 34.5 °C					
Q	I(Q)	Std DevI(Q)	sigmaQ	meanQ	Shadow Factor	Q	I(Q)	Std DevI(Q)	sigmaQ	meanQ	Shadow Factor
0.03008	1.161	0.02214	0.002028	0.0301	1	0.03008	6.523	0.04619	0.002028	0.0301	1
0.03049	1.153	0.01882	0.002049	0.0305	1	0.03049	6.479	0.04492	0.002049	0.0305	1
0.03089	1.15	0.02207	0.002069	0.03091	1	0.03089	6.453	0.05487	0.002069	0.03091	1
0.03124	1.168	0.007765	0.002756	0.03131	1	0.03124	6.575	0.02053	0.002756	0.03131	1
0.03129	1.193	0.02241	0.002089	0.03131	1	0.03129	6.481	0.04938	0.002089	0.03131	1
0.0317	1.217	0.02058	0.002109	0.03171	1	0.0317	6.442	0.04615	0.002109	0.03171	1
0.0321	1.17	0.02097	0.00213	0.03212	1	0.0321	6.35	0.05413	0.00213	0.03212	1
0.0325	1.151	0.02178	0.00215	0.03252	1	0.0325	6.271	0.04948	0.00215	0.03252	1
0.03257	1.166	0.007108	0.002807	0.03264	1	0.03257	6.398	0.01692	0.002807	0.03264	1
0.03291	1.14	0.02246	0.002171	0.03292	1	0.03291	6.351	0.04941	0.002171	0.03292	1
0.03331	1.146	0.02133	0.002191	0.03333	1	0.03331	6.205	0.05116	0.002191	0.03333	1
0.03372	1.159	0.02175	0.002212	0.03373	1	0.03372	6.204	0.05168	0.002212	0.03373	1
0.0339	1.174	0.006707	0.00286	0.03396	1	0.0339	6.228	0.01609	0.00286	0.03396	1
0.03399	1.181	0.004545	0.004794	0.03426	1	0.03399	6.224	0.02741	0.004794	0.03426	1
0.03523	1.166	0.005858	0.002913	0.03529	1	0.03523	6.078	0.01454	0.002913	0.03529	1
0.03656	1.164	0.006807	0.002967	0.03662	1	0.03656	5.888	0.01521	0.002967	0.03662	1
0.03788	1.161	0.006088	0.003023	0.03794	1	0.03788	5.781	0.01549	0.003023	0.03794	1
0.03798	1.167	0.003801	0.00489	0.03823	1	0.03798	5.761	0.02816	0.00489	0.03823	1
0.03921	1.14	0.006667	0.003079	0.03927	1	0.03921	5.592	0.01453	0.003079	0.03927	1
0.04054	1.13	0.006646	0.003136	0.04059	1	0.04054	5.434	0.01552	0.003136	0.04059	1
0.04187	1.127	0.006278	0.003194	0.04192	1	0.04187	5.27	0.01392	0.003194	0.04192	1
0.04197	1.153	0.004145	0.004996	0.0422	1	0.04197	5.285	0.02814	0.004996	0.0422	1
0.0432	1.115	0.005936	0.003253	0.04325	1	0.0432	5.109	0.0132	0.003253	0.04325	1
0.04452	1.114	0.006038	0.003312	0.04457	1	0.04452	4.95	0.01241	0.003312	0.04457	1
0.04585	1.1	0.005584	0.003372	0.0459	1	0.04585	4.817	0.01264	0.003372	0.0459	1
0.04597	1.14	0.004211	0.00511	0.04617	1	0.04597	4.855	0.02355	0.00511	0.04617	1
0.04718	1.09	0.005987	0.003433	0.04722	1	0.04718	4.642	0.01296	0.003433	0.04722	1
0.0485	1.093	0.005152	0.003495	0.04855	1	0.0485	4.536	0.01108	0.003495	0.04855	1
0.04983	1.086	0.005184	0.003557	0.04987	1	0.04983	4.365	0.01103	0.003557	0.04987	1
0.04996	1.123	0.003889	0.005233	0.05014	1	0.04996	4.438	0.02352	0.005233	0.05014	1
0.05116	1.087	0.005247	0.00362	0.0512	1	0.05116	4.239	0.01059	0.00362	0.0512	1
0.05248	1.079	0.005482	0.003683	0.05252	1	0.05248	4.112	0.01073	0.003683	0.05252	1
0.05381	1.074	0.005213	0.003746	0.05385	1	0.05381	3.98	0.01025	0.003746	0.05385	1
0.05394	1.108	0.003775	0.005363	0.05412	1	0.05394	4.033	0.02129	0.005363	0.05412	1
0.05514	1.063	0.004739	0.003811	0.05517	1	0.05514	3.865	0.01031	0.003811	0.05517	1
0.05646	1.075	0.004668	0.003875	0.0565	1	0.05646	3.717	0.01017	0.003875	0.0565	1
0.05779	1.05	0.004783	0.00394	0.05782	1	0.05779	3.624	0.008705	0.00394	0.05782	1
0.05793	1.096	0.003941	0.0055	0.05809	1	0.05793	3.664	0.01928	0.0055	0.05809	1
0.05911	1.048	0.004725	0.004006	0.05915	1	0.05911	3.511	0.009289	0.004006	0.05915	1
0.06044	1.04	0.004947	0.004071	0.06047	1	0.06044	3.381	0.009201	0.004071	0.06047	1
0.06176	1.036	0.004939	0.004138	0.0618	1	0.06176	3.267	0.008417	0.004138	0.0618	1
0.06192	1.077	0.004241	0.005643	0.06207	1	0.06192	3.329	0.01712	0.005643	0.06207	1
0.06309	1.03	0.004363	0.004204	0.06312	1	0.06309	3.173	0.007943	0.004204	0.06312	1
0.06441	1.026	0.004402	0.004271	0.06444	1	0.06441	3.058	0.007845	0.004271	0.06444	1
0.06573	1.018	0.004543	0.004338	0.06577	1	0.06573	2.983	0.007919	0.004338	0.06577	1
0.0659	1.057	0.003701	0.005791	0.06604	1	0.0659	3.016	0.01645	0.005791	0.06604	1
0.06706	1.022	0.004657	0.004406	0.06709	1	0.06706	2.871	0.007375	0.004406	0.06709	1
0.06838	1.007	0.004413	0.004474	0.06841	1	0.06838	2.783	0.007358	0.004474	0.06841	1
0.06971	1.003	0.004559	0.004542	0.06974	1	0.06971	2.681	0.007517	0.004542	0.06974	1
0.06988	1.042	0.003475	0.005945	0.07001	1	0.06988	2.731	0.01314	0.005945	0.07001	1
0.07103	0.9975	0.004298	0.00461	0.07106	1	0.07103	2.611	0.006936	0.00461	0.07106	1
0.07235	0.9978	0.004483	0.004679	0.07238	1	0.07235	2.537	0.00753	0.004679	0.07238	1
0.07367	0.9897	0.004029	0.004747	0.0737	1	0.07367	2.442	0.006799	0.004747	0.0737	1
0.07386	1.027	0.003874	0.006104	0.07399	1	0.07386	2.492	0.01201	0.006104	0.07399	1
0.075	0.9916	0.004415	0.004816	0.07503	1	0.075	2.358	0.006629	0.004816	0.07503	1
0.07632	0.9756	0.004331	0.004886	0.07635	1	0.07632	2.298	0.006966	0.004886	0.07635	1
0.07764	0.9614	0.004181	0.004955	0.07767	1	0.07764	2.22	0.006473	0.004955	0.07767	1
0.07784	1.009	0.003906	0.006267	0.07796	1	0.07784	2.285	0.01036	0.006267	0.07796	1
0.07896	0.962	0.004204	0.005025	0.07899	1	0.07896	2.165	0.006387	0.005025	0.07899	1
0.08028	0.966	0.004304	0.005094	0.08031	1	0.08028	2.093	0.006469	0.005094	0.08031	1
0.08161	0.9487	0.0042	0.005164	0.08163	1	0.08161	2.024	0.00633	0.005164	0.08163	1
0.08181	0.992	0.003472	0.006434	0.08192	1	0.08181	2.093	0.008585	0.006434	0.08192	1
0.08293	0.9479	0.004383	0.005235	0.08295	1	0.08293	1.971	0.006986	0.005235	0.08295	1
0.08425	0.9373	0.004604	0.005305	0.08427	1	0.08425	1.92	0.006538	0.005305	0.08427	1
0.08557	0.9397	0.004609	0.005375	0.08559	1	0.08557	1.859	0.00711	0.005375	0.08559	1
0.08578	0.9618	0.002685	0.006604	0.08589	1	0.08578	1.911	0.007013	0.006604	0.08589	1
0.08689	0.9245	0.004936	0.005446	0.08691	1	0.08689	1.815	0.007334	0.005446	0.08691	1
0.08821	0.9168	0.005333	0.005517	0.08823	1	0.08821	1.764	0.007619	0.005517	0.08823	1
0.08953	0.9147	0.005419	0.005588	0.08955	1	0.08953	1.709	0.006452	0.005588	0.08955	1
0.08975	0.9552	0.003477	0.006778	0.08985	1	0.08975	1.76	0.005589	0.006778	0.08985	1
0.09084	0.8983	0.005659	0.005659	0.09087	1	0.09084	1.659	0.00786	0.005659	0.09087	1
0.09371	0.93	0.002843	0.006956	0.09381	1	0.09371	1.632	0.005576	0.006956	0.09381	1
0.09768	0.9223	0.003055	0.007136	0.09777	1	0.09768	1.511	0.004882	0.007136	0.09777	1
0.1016	0.8983	0.00289	0.007318	0.1017	1	0.1016	1.412	0.004877	0.007318	0.1017	1
0.1056	0.8836	0.002883	0.007503	0.1057	1	0.1056	1.321	0.004167	0.007503	0.1057	1
0.1095	0.8638	0.002929	0.007691	0.1096	1	0.1095	1.25	0.004227	0.007691	0.1096	1
0.1135	0.8448	0.003141	0.00788	0.1136	1	0.1135	1.18	0.003704	0.00788	0.1136	1
0.1174	0.8304	0.002425	0.008071	0.1175	1	0.1174	1.11	0.003336	0.008071	0.1175	1
0.1214	0.8128	0.0026	0.008264	0.1215	1	0.1214	1.062	0.003263	0.008264	0.1215	1
0.1253	0.7952	0.002531	0.008458	0.1254	1	0.1253	1.011	0.003424	0.008458	0.1254	1
0.1293	0.7814	0.002363	0.008654	0.1293	1	0.1293	0.9618	0.002929	0.008654	0.1293	1

$\theta=0.228$ 17R4/D <sub>2</sub> O 29.8 °C						$\theta=0.228$ 17R4/D <sub>2</sub> O 34.5 °C					
Q	I(Q)	Std Dev(I(Q))	sigmaQ	meanQ	Shadow Factor	Q	I(Q)	Std Dev(I(Q))	sigmaQ	meanQ	Shadow Factor
0.1332	0.7594	0.002532	0.008851	0.1333	1	0.1332	0.9271	0.002795	0.008851	0.1333	1
0.1371	0.7416	0.002391	0.00905	0.1372	1	0.1371	0.888	0.002806	0.00905	0.1372	1
0.141	0.7304	0.002632	0.009249	0.1411	1	0.141	0.8554	0.002713	0.009249	0.1411	1
0.1449	0.7149	0.002511	0.00945	0.145	1	0.1449	0.825	0.002972	0.00945	0.145	1
0.1489	0.701	0.00227	0.009651	0.1489	1	0.1489	0.7901	0.002573	0.009651	0.1489	1
0.1528	0.6827	0.002204	0.009853	0.1528	1	0.1528	0.7657	0.002563	0.009853	0.1528	1
0.1567	0.6718	0.002049	0.01006	0.1567	1	0.1567	0.7377	0.00226	0.01006	0.1567	1
0.1606	0.6581	0.002013	0.01026	0.1606	1	0.1606	0.718	0.002395	0.01026	0.1606	1
0.1645	0.6437	0.002052	0.01046	0.1645	1	0.1645	0.6981	0.002408	0.01046	0.1645	1
0.1683	0.6287	0.002154	0.01067	0.1684	1	0.1683	0.6772	0.002334	0.01067	0.1684	1
0.1722	0.6212	0.00192	0.01087	0.1723	1	0.1722	0.6578	0.002125	0.01087	0.1723	1
0.1761	0.6047	0.001822	0.01108	0.1762	1	0.1761	0.6409	0.002097	0.01108	0.1762	1
0.18	0.5899	0.001863	0.01129	0.18	1	0.18	0.6211	0.002223	0.01129	0.18	1
0.1838	0.5831	0.002139	0.01149	0.1839	1	0.1838	0.6073	0.002029	0.01149	0.1839	1
0.1877	0.5679	0.001784	0.0117	0.1877	1	0.1877	0.5939	0.001993	0.0117	0.1877	1
0.1916	0.558	0.001871	0.01191	0.1916	1	0.1916	0.5766	0.001836	0.01191	0.1916	1
0.1954	0.5494	0.00186	0.01212	0.1954	1	0.1954	0.5657	0.00174	0.01212	0.1954	1
0.1992	0.5412	0.001687	0.01232	0.1993	1	0.1992	0.5557	0.001766	0.01232	0.1993	1
0.2031	0.5316	0.001825	0.01253	0.2031	1	0.2031	0.5425	0.001749	0.01253	0.2031	1
0.2069	0.5195	0.00159	0.01274	0.2069	1	0.2069	0.5299	0.001737	0.01274	0.2069	1
0.2107	0.5142	0.001727	0.01295	0.2108	1	0.2107	0.5194	0.001765	0.01295	0.2108	1
0.2145	0.5049	0.001723	0.01316	0.2146	1	0.2145	0.5086	0.001667	0.01316	0.2146	1
0.2184	0.4948	0.001749	0.01336	0.2184	1	0.2184	0.5021	0.001692	0.01336	0.2184	1
0.2222	0.4886	0.001617	0.01357	0.2222	1	0.2222	0.4918	0.001685	0.01357	0.2222	1
0.226	0.4803	0.001446	0.01378	0.226	1	0.226	0.4832	0.001628	0.01378	0.226	1
0.2297	0.4717	0.001524	0.01399	0.2298	1	0.2297	0.4767	0.001613	0.01399	0.2298	1
0.2335	0.4663	0.001423	0.0142	0.2336	1	0.2335	0.4661	0.001475	0.0142	0.2336	1
0.2373	0.4574	0.001518	0.0144	0.2373	1	0.2373	0.4597	0.001563	0.0144	0.2373	1
0.2411	0.4564	0.001465	0.01461	0.2411	1	0.2411	0.4569	0.001559	0.01461	0.2411	1
0.2448	0.4463	0.001538	0.01482	0.2449	1	0.2448	0.4463	0.001611	0.01482	0.2449	1
0.2486	0.4436	0.001812	0.01503	0.2486	1	0.2486	0.4408	0.001594	0.01503	0.2486	1
0.2523	0.4389	0.001702	0.01524	0.2524	1	0.2523	0.4373	0.001748	0.01524	0.2524	1
0.2561	0.4324	0.001696	0.01544	0.2561	1	0.2561	0.4326	0.001883	0.01544	0.2561	1
0.2598	0.4276	0.00183	0.01565	0.2598	1	0.2598	0.427	0.001784	0.01565	0.2598	1
0.2635	0.422	0.001794	0.01586	0.2636	1	0.2635	0.419	0.001651	0.01586	0.2636	1
0.2673	0.4163	0.001599	0.01606	0.2673	1	0.2673	0.4145	0.001708	0.01606	0.2673	1
0.271	0.4109	0.001824	0.01627	0.271	1	0.271	0.408	0.001655	0.01627	0.271	1
0.2747	0.4091	0.001833	0.01648	0.2747	1	0.2747	0.4062	0.00171	0.01648	0.2747	1
0.2784	0.4035	0.001882	0.01668	0.2784	1	0.2784	0.4005	0.001901	0.01668	0.2784	1
0.282	0.3994	0.001643	0.01689	0.2821	1	0.282	0.3966	0.001683	0.01689	0.2821	1
0.2857	0.3986	0.001943	0.0171	0.2857	1	0.2857	0.3924	0.001706	0.0171	0.2857	1
0.2894	0.3905	0.001748	0.0173	0.2894	1	0.2894	0.39	0.001897	0.0173	0.2894	1
0.293	0.3859	0.001715	0.01751	0.2931	1	0.293	0.3867	0.001863	0.01751	0.2931	1
0.2967	0.3853	0.001723	0.01771	0.2967	1	0.2967	0.3809	0.001774	0.01771	0.2967	1
0.3003	0.3795	0.001797	0.01792	0.3004	1	0.3003	0.3795	0.001712	0.01792	0.3004	1
0.304	0.375	0.001822	0.01812	0.304	1	0.304	0.3741	0.001741	0.01812	0.304	1
0.3076	0.3735	0.001494	0.01832	0.3076	1	0.3076	0.3699	0.001607	0.01832	0.3076	1
0.3112	0.3685	0.001694	0.01853	0.3113	1	0.3112	0.3676	0.001585	0.01853	0.3113	1
0.3148	0.3643	0.001667	0.01873	0.3149	1	0.3148	0.3648	0.001674	0.01873	0.3149	1
0.3184	0.3628	0.001799	0.01893	0.3185	1	0.3184	0.3597	0.001861	0.01893	0.3185	1
0.322	0.3602	0.001616	0.01913	0.3221	1	0.322	0.3548	0.001571	0.01913	0.3221	1
0.3256	0.3574	0.002007	0.01934	0.3256	1	0.3256	0.3549	0.001467	0.01934	0.3256	1
0.3292	0.3542	0.001448	0.01954	0.3292	1	0.3292	0.3527	0.001682	0.01954	0.3292	1
0.3327	0.3506	0.001598	0.01974	0.3328	1	0.3327	0.3496	0.001512	0.01974	0.3328	1
0.3363	0.3487	0.001722	0.01994	0.3363	1	0.3363	0.3481	0.001651	0.01994	0.3363	1
0.3399	0.3485	0.001525	0.02014	0.3399	1	0.3399	0.3444	0.001717	0.02014	0.3399	1
0.3434	0.343	0.001734	0.02034	0.3434	1	0.3434	0.3414	0.001609	0.02034	0.3434	1
0.3469	0.3434	0.001591	0.02054	0.3469	1	0.3469	0.3393	0.001776	0.02054	0.3469	1
0.3504	0.3406	0.001696	0.02074	0.3505	1	0.3504	0.3382	0.001688	0.02074	0.3505	1
0.3539	0.338	0.001753	0.02094	0.354	1	0.3539	0.3346	0.001518	0.02094	0.354	1
0.3574	0.3362	0.001732	0.02114	0.3575	1	0.3574	0.3345	0.001777	0.02114	0.3575	1
0.3609	0.3334	0.001586	0.02133	0.361	1	0.3609	0.3321	0.001559	0.02133	0.361	1
0.3644	0.3321	0.001746	0.02153	0.3644	1	0.3644	0.3306	0.001638	0.02153	0.3644	1
0.3679	0.3288	0.001577	0.02173	0.3679	1	0.3679	0.3257	0.001411	0.02173	0.3679	1
0.3713	0.3282	0.001483	0.02192	0.3714	1	0.3713	0.3253	0.001629	0.02192	0.3714	1
0.3748	0.3252	0.001534	0.02212	0.3748	1	0.3748	0.3228	0.001646	0.02212	0.3748	1
0.3782	0.3237	0.001639	0.02231	0.3783	1	0.3782	0.3218	0.001784	0.02231	0.3783	1
0.3817	0.3216	0.001779	0.02251	0.3817	1	0.3817	0.3201	0.001765	0.02251	0.3817	1
0.3851	0.3203	0.001701	0.0227	0.3851	1	0.3851	0.3173	0.001621	0.0227	0.3851	1
0.3885	0.3218	0.001479	0.0229	0.3885	1	0.3885	0.3157	0.001643	0.0229	0.3885	1
0.3919	0.3186	0.001729	0.02309	0.3919	1	0.3919	0.3169	0.001537	0.02309	0.3919	1
0.3953	0.3181	0.001753	0.02328	0.3953	1	0.3953	0.3121	0.001654	0.02328	0.3953	1
0.3987	0.3125	0.001505	0.02348	0.3987	1	0.3987	0.3136	0.00171	0.02348	0.3987	1
0.4021	0.311	0.001733	0.02367	0.4021	1	0.4021	0.3106	0.001707	0.02367	0.4021	1
0.4054	0.3149	0.001696	0.02386	0.4054	1	0.4054	0.3119	0.001684	0.02386	0.4054	1

$\phi=0.228$ 17R4/D <sub>2</sub> O 39.2 °C						$\phi=0.228$ 17R4/D <sub>2</sub> O 25.1 °C (cooling)					
Q	I(Q)	Std Dev(I(Q))	sigmaQ	meanQ	Shadow Factor	Q	I(Q)	Std Dev(I(Q))	sigmaQ	meanQ	Shadow Factor
0.003433	21.56	0.4818	0.001073	0.003607	0.9568	0.003433	200.3	5.505	0.001073	0.003607	0.9568
0.003837	23.64	0.1637	0.001077	0.003977	0.9999	0.003837	113.4	4.008	0.001077	0.003977	0.9999
0.004241	23.87	0.1726	0.001079	0.004367	1	0.004241	63.74	1.695	0.001079	0.004367	1
0.004645	23.75	0.1438	0.001082	0.00476	1	0.004645	39.84	0.8291	0.001082	0.00476	1
0.005049	23.67	0.1301	0.001087	0.005155	1	0.005049	26.64	0.4702	0.001087	0.005155	1
0.005453	23.76	0.1411	0.001092	0.005551	1	0.005453	18.66	0.2907	0.001092	0.005551	1
0.005857	23.66	0.1436	0.001098	0.005948	1	0.005857	13.66	0.19	0.001098	0.005948	1
0.006261	23.45	0.1205	0.001104	0.006346	1	0.006261	10.18	0.1489	0.001104	0.006346	1
0.006665	23.5	0.1134	0.001111	0.006745	1	0.006665	8.027	0.09863	0.001111	0.006745	1
0.007069	23.55	0.1172	0.001119	0.007144	1	0.007069	6.444	0.08142	0.001119	0.007144	1
0.007473	23.59	0.1085	0.001127	0.007544	1	0.007473	5.19	0.06453	0.001127	0.007544	1
0.007876	23.35	0.1072	0.001136	0.007944	1	0.007876	4.353	0.05223	0.001136	0.007944	1
0.00828	23.22	0.09703	0.001145	0.008345	1	0.00828	3.586	0.04548	0.001145	0.008345	1
0.008684	23.16	0.1051	0.001155	0.008746	1	0.008684	3.065	0.03517	0.001155	0.008746	1
0.009088	23.02	0.09799	0.001165	0.009147	1	0.009088	2.64	0.03487	0.001165	0.009147	1
0.009492	23.11	0.1032	0.001176	0.009548	1	0.009492	2.421	0.03137	0.001176	0.009548	1
0.009896	22.86	0.08581	0.001187	0.00995	1	0.009896	2.138	0.03028	0.001187	0.00995	1
0.0103	22.82	0.1032	0.001198	0.01035	1	0.0103	1.939	0.02698	0.001198	0.01035	1
0.0107	22.75	0.08202	0.00121	0.01075	1	0.0107	1.824	0.02825	0.00121	0.01075	1
0.01111	22.71	0.09274	0.001222	0.01116	1	0.01111	1.638	0.02332	0.001222	0.01116	1
0.0113	22.48	0.06842	0.002193	0.01149	1	0.0113	1.887	0.03819	0.002193	0.01149	1
0.01151	22.36	0.08925	0.001234	0.01156	1	0.01151	1.523	0.02457	0.001234	0.01156	1
0.01192	22.31	0.08645	0.001247	0.01196	1	0.01192	1.47	0.02304	0.001247	0.01196	1
0.01232	22.31	0.08937	0.00126	0.01236	1	0.01232	1.334	0.02116	0.00126	0.01236	1
0.01263	22.12	0.06	0.002214	0.0128	1	0.01263	1.48	0.02174	0.002214	0.0128	1
0.01272	22.06	0.07445	0.001273	0.01277	1	0.01272	1.274	0.01966	0.001273	0.01277	1
0.01313	21.93	0.08424	0.001287	0.01317	1	0.01313	1.29	0.0182	0.001287	0.01317	1
0.01353	21.9	0.07689	0.0013	0.01357	1	0.01353	1.2	0.01717	0.0013	0.01357	1
0.01393	21.69	0.07538	0.001315	0.01397	1	0.01393	1.192	0.01767	0.001315	0.01397	1
0.01396	21.74	0.0506	0.002239	0.01412	1	0.01396	1.243	0.01452	0.002239	0.01412	1
0.01434	21.62	0.07727	0.001329	0.01438	1	0.01434	1.107	0.01705	0.001329	0.01438	1
0.01474	21.32	0.07233	0.001344	0.01478	1	0.01474	1.081	0.01683	0.001344	0.01478	1
0.01515	21.16	0.07582	0.001359	0.01518	1	0.01515	1.072	0.01595	0.001359	0.01518	1
0.01529	21.36	0.05519	0.002266	0.01543	1	0.01529	1.106	0.01092	0.002266	0.01543	1
0.01555	21.23	0.07405	0.001374	0.01558	1	0.01555	1.025	0.01615	0.001374	0.01558	1
0.01595	21.06	0.07482	0.001389	0.01599	1	0.01595	1.024	0.01716	0.001389	0.01599	1
0.01636	20.96	0.07575	0.001405	0.01639	1	0.01636	0.9833	0.01758	0.001405	0.01639	1
0.01662	20.87	0.04843	0.002296	0.01675	1	0.01662	1.03	0.01015	0.002296	0.01675	1
0.01676	20.84	0.0683	0.001421	0.01679	1	0.01676	1.016	0.01779	0.001421	0.01679	1
0.01717	20.75	0.0746	0.001437	0.0172	1	0.01717	0.9597	0.01717	0.001437	0.0172	1
0.01757	20.56	0.07119	0.001453	0.0176	1	0.01757	0.9426	0.01696	0.001453	0.0176	1
0.01795	20.45	0.04534	0.002328	0.01807	1	0.01795	0.9753	0.009244	0.002328	0.01807	1
0.01797	20.48	0.06788	0.00147	0.018	1	0.01797	0.9778	0.01513	0.00147	0.018	1
0.01838	20.37	0.06559	0.001486	0.01841	1	0.01838	0.9251	0.01494	0.001486	0.01841	1
0.01878	20.18	0.07301	0.001503	0.01881	1	0.01878	0.9353	0.01535	0.001503	0.01881	1
0.01918	20.04	0.07137	0.00152	0.01921	1	0.01918	0.9135	0.01589	0.00152	0.01921	1
0.01928	19.99	0.04926	0.002363	0.01939	1	0.01928	0.9381	0.00811	0.002363	0.01939	1
0.01959	19.78	0.06502	0.001537	0.01962	1	0.01959	0.9118	0.01626	0.001537	0.01962	1
0.01999	19.8	0.06732	0.001555	0.02002	1	0.01999	0.9062	0.01581	0.001555	0.02002	1
0.0204	19.59	0.06461	0.001572	0.02042	1	0.0204	0.8945	0.01465	0.001572	0.02042	1
0.02061	19.52	0.04039	0.0024	0.02072	1	0.02061	0.924	0.007994	0.0024	0.02072	1
0.0208	19.35	0.06297	0.00159	0.02083	1	0.0208	0.8861	0.01479	0.00159	0.02083	1
0.0212	19.2	0.06525	0.001608	0.02123	1	0.0212	0.8971	0.01533	0.001608	0.02123	1
0.02161	18.98	0.06679	0.001626	0.02163	1	0.02161	0.8581	0.01437	0.001626	0.02163	1
0.02194	19.1	0.0455	0.002438	0.02204	1	0.02194	0.9034	0.007823	0.002438	0.02204	1
0.02201	18.82	0.06168	0.001644	0.02203	1	0.02201	0.8863	0.01392	0.001644	0.02203	1
0.02241	18.86	0.06042	0.001662	0.02244	1	0.02241	0.8973	0.01484	0.001662	0.02244	1
0.02282	18.5	0.06275	0.00168	0.02284	1	0.02282	0.8675	0.0146	0.00168	0.02284	1
0.02322	18.5	0.06405	0.001699	0.02324	1	0.02322	0.8812	0.01359	0.001699	0.02324	1
0.02327	18.58	0.03715	0.002479	0.02336	1	0.02327	0.8816	0.007022	0.002479	0.02336	1
0.02363	18.29	0.06014	0.001717	0.02365	1	0.02363	0.9034	0.01399	0.001717	0.02365	1
0.02403	18.21	0.06247	0.001736	0.02405	1	0.02403	0.8802	0.01359	0.001736	0.02405	1
0.02443	17.93	0.05631	0.001755	0.02445	1	0.02443	0.8668	0.0141	0.001755	0.02445	1
0.0246	18.14	0.04026	0.002521	0.02469	1	0.0246	0.8826	0.006957	0.002521	0.02469	1
0.02484	17.88	0.06154	0.001774	0.02486	1	0.02484	0.8919	0.01472	0.001774	0.02486	1
0.02524	17.77	0.06574	0.001793	0.02526	1	0.02524	0.8501	0.0146	0.001793	0.02526	1
0.02564	17.74	0.06356	0.001812	0.02566	1	0.02564	0.8305	0.01546	0.001812	0.02566	1
0.02593	17.64	0.04065	0.002565	0.02601	1	0.02593	0.8722	0.007024	0.002565	0.02601	1
0.02605	17.52	0.0727	0.001831	0.02607	1	0.02605	0.8449	0.01539	0.001831	0.02607	1
0.02645	17.29	0.07485	0.001851	0.02647	1	0.02645	0.8568	0.01523	0.001851	0.02647	1
0.02685	17.14	0.07075	0.00187	0.02687	1	0.02685	0.8321	0.01777	0.00187	0.02687	1
0.02726	17.26	0.03385	0.002611	0.02734	1	0.02726	0.868	0.006391	0.002611	0.02734	1
0.02726	17.04	0.0665	0.00189	0.02728	1	0.02726	0.8368	0.01625	0.00189	0.02728	1
0.02766	16.94	0.07771	0.001909	0.02768	1	0.02766	0.8651	0.01668	0.001909	0.02768	1
0.02807	16.69	0.07396	0.001929	0.02808	1	0.02807	0.8551	0.0164	0.001929	0.02808	1
0.02847	16.65	0.07426	0.001949	0.02849	1	0.02847	0.8191	0.01832	0.001949	0.02849	1
0.02859	16.7	0.02887	0.002658	0.02866	1	0.02859	0.8508	0.00577	0.002658	0.02866	1
0.02887	16.51	0.07999	0.001968	0.02889	1	0.02887	0.8357	0.0189	0.001968	0.02889	1
0.02928	16.22	0.07617	0.001988	0.02929	1	0.02928	0.8419	0.01669	0.001988	0.02929	1
0.02968	16.11	0.07516	0.002008	0.0297	1	0.02968	0.8632	0.01764	0.002008	0.0297	1
0.02991	16.32	0.03345	0.002707	0.02999	1	0.02991	0.8612	0.006463	0.002707	0.02999	1

$\phi=0.228$ 17R4/D <sub>2</sub> O 39.2 °C						$\phi=0.228$ 17R4/D <sub>2</sub> O 25.1 °C (cooling)					
Q	I(Q)	Std DevI(Q)	sigmaQ	meanQ	Shadow Factor	Q	I(Q)	Std DevI(Q)	sigmaQ	meanQ	Shadow Factor
0.03008	16	0.07371	0.002028	0.0301	1	0.03008	0.815	0.01872	0.002028	0.0301	1
0.03049	15.85	0.08309	0.002049	0.0305	1	0.03049	0.7909	0.01778	0.002049	0.0305	1
0.03089	15.85	0.08926	0.002069	0.03091	1	0.03089	0.8075	0.01988	0.002069	0.03091	1
0.03124	15.81	0.03099	0.002756	0.03131	1	0.03124	0.8492	0.006784	0.002756	0.03131	1
0.03129	15.67	0.06996	0.002089	0.03131	1	0.03129	0.8327	0.01753	0.002089	0.03131	1
0.0317	15.53	0.075	0.002109	0.03171	1	0.0317	0.8553	0.01863	0.002109	0.03171	1
0.0321	15.28	0.07294	0.00213	0.03212	1	0.0321	0.8376	0.01994	0.00213	0.03212	1
0.0325	15.13	0.07548	0.00215	0.03252	1	0.0325	0.8211	0.02108	0.00215	0.03252	1
0.03257	15.39	0.03097	0.002807	0.03264	1	0.03257	0.8434	0.006309	0.002807	0.03264	1
0.03291	14.99	0.08338	0.002171	0.03292	1	0.03291	0.8389	0.01916	0.002171	0.03292	1
0.03331	14.78	0.06423	0.002191	0.03333	1	0.03331	0.8359	0.01832	0.002191	0.03333	1
0.03372	14.7	0.07983	0.002212	0.03373	1	0.03372	0.838	0.01822	0.002212	0.03373	1
0.0339	14.82	0.03289	0.00286	0.03396	1	0.0339	0.845	0.006071	0.00286	0.03396	1
0.03399	14.75	0.07306	0.004794	0.03426	1	0.03399	0.7714	0.003707	0.004794	0.03426	1
0.03523	14.4	0.02596	0.002913	0.03529	1	0.03523	0.843	0.005619	0.002913	0.03529	1
0.03656	13.93	0.02963	0.002967	0.03662	1	0.03656	0.8382	0.005991	0.002967	0.03662	1
0.03788	13.55	0.02759	0.003023	0.03794	1	0.03788	0.8295	0.006076	0.003023	0.03794	1
0.03798	13.54	0.07164	0.00489	0.03823	1	0.03798	0.7614	0.003782	0.00489	0.03823	1
0.03921	13.07	0.02465	0.003079	0.03927	1	0.03921	0.8268	0.005496	0.003079	0.03927	1
0.04054	12.68	0.02472	0.003136	0.04059	1	0.04054	0.8245	0.004959	0.003136	0.04059	1
0.04187	12.28	0.02288	0.003194	0.04192	1	0.04187	0.821	0.005301	0.003194	0.04192	1
0.04197	12.31	0.06902	0.004996	0.0422	1	0.04197	0.7615	0.003783	0.004996	0.0422	1
0.0432	11.82	0.02284	0.003253	0.04325	1	0.0432	0.8249	0.005444	0.003253	0.04325	1
0.04452	11.47	0.02087	0.003312	0.04457	1	0.04452	0.8072	0.005007	0.003312	0.04457	1
0.04585	11.08	0.01937	0.003372	0.0459	1	0.04585	0.8088	0.004853	0.003372	0.0459	1
0.04596	11.16	0.06091	0.00511	0.04617	1	0.04597	0.7508	0.003576	0.00511	0.04617	1
0.04718	10.68	0.02003	0.003433	0.04722	1	0.04718	0.8038	0.005053	0.003433	0.04722	1
0.0485	10.37	0.0181	0.003495	0.04855	1	0.0485	0.8069	0.004539	0.003495	0.04855	1
0.04983	10.01	0.017	0.003557	0.04987	1	0.04983	0.8038	0.004706	0.003557	0.04987	1
0.04996	10.08	0.05557	0.005233	0.05014	1	0.04996	0.746	0.002889	0.005233	0.05014	1
0.05116	9.648	0.01706	0.00362	0.0512	1	0.05116	0.7954	0.004549	0.00362	0.0512	1
0.05248	9.292	0.01518	0.003683	0.05252	1	0.05248	0.794	0.004686	0.003683	0.05252	1
0.05381	8.982	0.01716	0.003746	0.05385	1	0.05381	0.7939	0.004514	0.003746	0.05385	1
0.05394	9.07	0.05206	0.005363	0.05412	1	0.05394	0.7425	0.003196	0.005363	0.05412	1
0.05514	8.683	0.01544	0.003811	0.05517	1	0.05514	0.7879	0.004338	0.003811	0.05517	1
0.05646	8.385	0.01657	0.003875	0.0565	1	0.05646	0.7872	0.004357	0.003875	0.0565	1
0.05779	8.053	0.01527	0.00394	0.05782	1	0.05779	0.7845	0.004103	0.00394	0.05782	1
0.05793	8.122	0.04785	0.0055	0.05809	1	0.05793	0.7353	0.003173	0.0055	0.05809	1
0.05911	7.77	0.01452	0.004006	0.05915	1	0.05911	0.7848	0.003977	0.004006	0.05915	1
0.06044	7.476	0.01449	0.004071	0.06047	1	0.06044	0.7784	0.004442	0.004071	0.06047	1
0.06176	7.188	0.01328	0.004138	0.0618	1	0.06176	0.7797	0.004121	0.004138	0.0618	1
0.06192	7.279	0.04203	0.005643	0.06207	1	0.06192	0.7299	0.002869	0.005643	0.06207	1
0.06309	6.927	0.01309	0.004204	0.06312	1	0.06309	0.7807	0.004042	0.004204	0.06312	1
0.06441	6.653	0.01268	0.004271	0.06444	1	0.06441	0.7808	0.003966	0.004271	0.06444	1
0.06573	6.409	0.01219	0.004338	0.06577	1	0.06573	0.7754	0.003952	0.004338	0.06577	1
0.0659	6.46	0.03883	0.005791	0.06604	1	0.0659	0.7213	0.002618	0.005791	0.06604	1
0.06706	6.142	0.01242	0.004406	0.06709	1	0.06706	0.7739	0.003745	0.004406	0.06709	1
0.06838	5.877	0.01128	0.004474	0.06841	1	0.06838	0.7691	0.003784	0.004474	0.06841	1
0.06971	5.653	0.01058	0.004542	0.06974	1	0.06971	0.7639	0.003741	0.004542	0.06974	1
0.06988	5.712	0.03434	0.005945	0.07001	1	0.06988	0.7157	0.003067	0.005945	0.07001	1
0.07103	5.419	0.01046	0.00461	0.07106	1	0.07103	0.7656	0.003513	0.00461	0.07106	1
0.07235	5.206	0.01023	0.004679	0.07238	1	0.07235	0.7673	0.003928	0.004679	0.07238	1
0.07367	4.958	0.009597	0.004747	0.0737	1	0.07367	0.7553	0.003912	0.004747	0.0737	1
0.07386	5.043	0.03058	0.006104	0.07399	1	0.07386	0.7102	0.003213	0.006104	0.07399	1
0.075	4.774	0.01005	0.004816	0.07503	1	0.075	0.7549	0.003652	0.004816	0.07503	1
0.07632	4.553	0.009532	0.004886	0.07635	1	0.07632	0.7496	0.003689	0.004886	0.07635	1
0.07764	4.376	0.00944	0.004955	0.07767	1	0.07764	0.7473	0.003669	0.004955	0.07767	1
0.07783	4.478	0.02465	0.006266	0.07796	1	0.07784	0.7048	0.00296	0.006267	0.07796	1
0.07896	4.197	0.008851	0.005025	0.07899	1	0.07896	0.7506	0.003856	0.005025	0.07899	1
0.08028	4.002	0.00916	0.005094	0.08031	1	0.08028	0.7447	0.00376	0.005094	0.08031	1
0.08161	3.828	0.009457	0.005164	0.08163	1	0.08161	0.738	0.003958	0.005164	0.08163	1
0.08181	3.908	0.02024	0.006433	0.08192	1	0.08181	0.698	0.002436	0.006434	0.08192	1
0.08293	3.668	0.009453	0.005235	0.08295	1	0.08293	0.7367	0.004241	0.005235	0.08295	1
0.08425	3.516	0.00922	0.005305	0.08427	1	0.08425	0.7404	0.004134	0.005305	0.08427	1
0.08557	3.383	0.009755	0.005375	0.08559	1	0.08557	0.7396	0.004162	0.005375	0.08559	1
0.08578	3.415	0.01631	0.006604	0.08589	1	0.08578	0.6928	0.00278	0.006604	0.08589	1
0.08689	3.231	0.00993	0.005446	0.08691	1	0.08689	0.7307	0.004408	0.005446	0.08691	1
0.08821	3.088	0.01042	0.005517	0.08823	1	0.08821	0.731	0.004673	0.005517	0.08823	1
0.08953	2.952	0.009834	0.005588	0.08955	1	0.08953	0.7299	0.004946	0.005588	0.08955	1
0.08975	3.007	0.01365	0.006778	0.08985	1	0.08975	0.6866	0.002597	0.006778	0.08985	1
0.09084	2.833	0.01027	0.005659	0.09087	1	0.09084	0.726	0.005367	0.005659	0.09087	1
0.09371	2.658	0.01234	0.006955	0.09381	1	0.09371	0.6775	0.002328	0.006956	0.09381	1
0.09768	2.356	0.01056	0.007136	0.09777	1	0.09768	0.6659	0.002358	0.007136	0.09777	1
0.1016	2.093	0.008783	0.007318	0.1017	1	0.1016	0.6595	0.002374	0.007318	0.1017	1
0.1056	1.867	0.007905	0.007503	0.1057	1	0.1056	0.6513	0.002663	0.007503	0.1057	1
0.1095	1.689	0.007056	0.007691	0.1096	1	0.1095	0.6412	0.002582	0.007691	0.1096	1
0.1135	1.531	0.005639	0.00788	0.1136	1	0.1135	0.641	0.002356	0.00788	0.1136	1
0.1174	1.402	0.005057	0.008071	0.1175	1	0.1174	0.6293	0.002141	0.008071	0.1175	1
0.1214	1.289	0.00437	0.008264	0.1215	1	0.1214	0.6228	0.002198	0.008264	0.1215	1
0.1253	1.194	0.004349	0.008458	0.1254	1	0.1253	0.6219	0.0024	0.008458	0.1254	1
0.1293	1.108	0.003572	0.008654	0.1293	1	0.1293	0.6105	0.002034	0.008654	0.1293	1

ω=0.228 17R4/D <sub>2</sub> O 39.2 °C						ω=0.228 17R4/D <sub>2</sub> O 25.1 °C (cooling)					
Q	I(Q)	Std Dev(I(Q))	sigmaQ	meanQ	Shadow Factor	Q	I(Q)	Std Dev(I(Q))	sigmaQ	meanQ	Shadow Factor
0.1332	1.032	0.003206	0.008851	0.1332	1	0.1332	0.6003	0.002309	0.008851	0.1333	1
0.1371	0.9727	0.003592	0.00905	0.1372	1	0.1371	0.5927	0.00215	0.00905	0.1372	1
0.141	0.9211	0.002968	0.009249	0.1411	1	0.141	0.5838	0.002184	0.009249	0.1411	1
0.1449	0.8719	0.002861	0.00945	0.145	1	0.1449	0.5754	0.001969	0.00945	0.145	1
0.1489	0.8287	0.002988	0.009651	0.1489	1	0.1489	0.5719	0.002062	0.009651	0.1489	1
0.1528	0.7919	0.002662	0.009853	0.1528	1	0.1528	0.5621	0.001887	0.009853	0.1528	1
0.1567	0.7558	0.002499	0.01006	0.1567	1	0.1567	0.5528	0.001925	0.01006	0.1567	1
0.1606	0.7297	0.002473	0.01026	0.1606	1	0.1606	0.5474	0.001929	0.01026	0.1606	1
0.1645	0.7039	0.002387	0.01046	0.1645	1	0.1645	0.5377	0.002049	0.01046	0.1645	1
0.1683	0.6787	0.002144	0.01067	0.1684	1	0.1683	0.5324	0.001909	0.01067	0.1684	1
0.1722	0.657	0.00217	0.01087	0.1723	1	0.1722	0.5249	0.001774	0.01087	0.1723	1
0.1761	0.6388	0.00219	0.01108	0.1762	1	0.1761	0.5153	0.001891	0.01108	0.1762	1
0.18	0.6162	0.001924	0.01129	0.18	1	0.18	0.5088	0.001545	0.01129	0.18	1
0.1838	0.6009	0.00205	0.01149	0.1839	1	0.1838	0.5054	0.001738	0.01149	0.1839	1
0.1877	0.5838	0.001929	0.0117	0.1877	1	0.1877	0.4977	0.001781	0.0117	0.1877	1
0.1915	0.5688	0.002005	0.01191	0.1916	1	0.1916	0.4901	0.001644	0.01191	0.1916	1
0.1954	0.5547	0.001903	0.01212	0.1954	1	0.1954	0.4817	0.001652	0.01212	0.1954	1
0.1992	0.5443	0.001537	0.01232	0.1993	1	0.1992	0.4793	0.001681	0.01232	0.1993	1
0.2031	0.5289	0.001876	0.01253	0.2031	1	0.2031	0.4697	0.001552	0.01253	0.2031	1
0.2069	0.5167	0.001676	0.01274	0.2069	1	0.2069	0.4674	0.001663	0.01274	0.2069	1
0.2107	0.5034	0.0019	0.01295	0.2108	1	0.2107	0.4591	0.00162	0.01295	0.2108	1
0.2145	0.4954	0.001744	0.01316	0.2146	1	0.2145	0.4531	0.00156	0.01316	0.2146	1
0.2184	0.484	0.001688	0.01336	0.2184	1	0.2184	0.4473	0.001402	0.01336	0.2184	1
0.2222	0.4777	0.001554	0.01357	0.2222	1	0.2222	0.4422	0.001598	0.01357	0.2222	1
0.226	0.4651	0.001623	0.01378	0.226	1	0.226	0.4393	0.001593	0.01378	0.226	1
0.2297	0.4601	0.001614	0.01399	0.2298	1	0.2297	0.4287	0.001541	0.01399	0.2298	1
0.2335	0.4499	0.001519	0.0142	0.2336	1	0.2335	0.4248	0.001409	0.0142	0.2336	1
0.2373	0.445	0.001612	0.0144	0.2373	1	0.2373	0.4189	0.001389	0.0144	0.2373	1
0.2411	0.4418	0.001431	0.01461	0.2411	1	0.2411	0.4182	0.00145	0.01461	0.2411	1
0.2448	0.4302	0.001641	0.01482	0.2449	1	0.2448	0.4109	0.001677	0.01482	0.2449	1
0.2486	0.4277	0.001515	0.01503	0.2486	1	0.2486	0.4075	0.001566	0.01503	0.2486	1
0.2523	0.4203	0.001643	0.01524	0.2524	1	0.2523	0.4052	0.001658	0.01524	0.2524	1
0.2561	0.4156	0.001847	0.01544	0.2561	1	0.2561	0.3996	0.001663	0.01544	0.2561	1
0.2598	0.4082	0.001697	0.01565	0.2598	1	0.2598	0.3953	0.001559	0.01565	0.2598	1
0.2635	0.4066	0.001834	0.01586	0.2636	1	0.2635	0.3928	0.001772	0.01586	0.2636	1
0.2673	0.4011	0.001778	0.01606	0.2673	1	0.2673	0.3905	0.001557	0.01606	0.2673	1
0.271	0.3956	0.001961	0.01627	0.271	1	0.271	0.3852	0.001746	0.01627	0.271	1
0.2747	0.3889	0.001779	0.01648	0.2747	1	0.2747	0.3789	0.001643	0.01648	0.2747	1
0.2784	0.3896	0.001648	0.01668	0.2784	1	0.2784	0.379	0.001743	0.01668	0.2784	1
0.282	0.3844	0.001686	0.01689	0.2821	1	0.282	0.3745	0.001503	0.01689	0.2821	1
0.2857	0.3834	0.001588	0.0171	0.2857	1	0.2857	0.3705	0.001663	0.0171	0.2857	1
0.2894	0.3768	0.001756	0.0173	0.2894	1	0.2894	0.3663	0.001582	0.0173	0.2894	1
0.293	0.3746	0.001482	0.01751	0.2931	1	0.293	0.3655	0.001531	0.01751	0.2931	1
0.2967	0.3716	0.001687	0.01771	0.2967	1	0.2967	0.3603	0.001627	0.01771	0.2967	1
0.3003	0.366	0.001742	0.01791	0.3004	1	0.3003	0.3583	0.001624	0.01792	0.3004	1
0.304	0.3602	0.001653	0.01812	0.304	1	0.304	0.3538	0.001608	0.01812	0.304	1
0.3076	0.3579	0.001841	0.01832	0.3076	1	0.3076	0.3507	0.001496	0.01832	0.3076	1
0.3112	0.3552	0.001829	0.01853	0.3112	1	0.3112	0.3451	0.001504	0.01853	0.3113	1
0.3148	0.3526	0.001713	0.01873	0.3149	1	0.3148	0.3434	0.001572	0.01873	0.3149	1
0.3184	0.3525	0.001638	0.01893	0.3185	1	0.3184	0.3436	0.001777	0.01893	0.3185	1
0.322	0.3472	0.001714	0.01913	0.322	1	0.322	0.3426	0.001683	0.01913	0.3221	1
0.3256	0.3445	0.001767	0.01934	0.3256	1	0.3256	0.3352	0.001543	0.01934	0.3256	1
0.3292	0.3402	0.001688	0.01954	0.3292	1	0.3292	0.3323	0.001671	0.01954	0.3292	1
0.3327	0.3404	0.001669	0.01974	0.3328	1	0.3327	0.3323	0.0015	0.01974	0.3328	1
0.3363	0.3386	0.001785	0.01994	0.3363	1	0.3363	0.3284	0.001544	0.01994	0.3363	1
0.3398	0.3372	0.001742	0.02014	0.3399	1	0.3399	0.3261	0.001556	0.02014	0.3399	1
0.3434	0.3318	0.001627	0.02034	0.3434	1	0.3434	0.3238	0.001565	0.02034	0.3434	1
0.3469	0.3322	0.001812	0.02054	0.3469	1	0.3469	0.321	0.001762	0.02054	0.3469	1
0.3504	0.3336	0.00168	0.02074	0.3505	1	0.3504	0.3222	0.001696	0.02074	0.3505	1
0.3539	0.328	0.001844	0.02094	0.354	1	0.3539	0.319	0.001719	0.02094	0.354	1
0.3574	0.3261	0.001707	0.02114	0.3575	1	0.3574	0.3162	0.001468	0.02114	0.3575	1
0.3609	0.3226	0.00174	0.02133	0.361	1	0.3609	0.3175	0.001384	0.02133	0.361	1
0.3644	0.3226	0.001702	0.02153	0.3644	1	0.3644	0.3147	0.001657	0.02153	0.3644	1
0.3679	0.3198	0.001543	0.02173	0.3679	1	0.3679	0.3128	0.001575	0.02173	0.3679	1
0.3713	0.3206	0.00163	0.02192	0.3714	1	0.3713	0.3102	0.001603	0.02192	0.3714	1
0.3748	0.3188	0.001601	0.02212	0.3748	1	0.3748	0.308	0.001694	0.02212	0.3748	1
0.3782	0.3173	0.001643	0.02231	0.3783	1	0.3782	0.3089	0.001564	0.02231	0.3783	1
0.3817	0.314	0.001579	0.02251	0.3817	1	0.3817	0.3039	0.001716	0.02251	0.3817	1
0.3851	0.3145	0.001796	0.0227	0.3851	1	0.3851	0.3011	0.001607	0.0227	0.3851	1
0.3885	0.3115	0.001643	0.0229	0.3885	1	0.3885	0.3009	0.001636	0.0229	0.3885	1
0.3919	0.3108	0.001763	0.02309	0.3919	1	0.3919	0.2981	0.001588	0.02309	0.3919	1
0.3953	0.3062	0.001725	0.02328	0.3953	1	0.3953	0.3008	0.001526	0.02328	0.3953	1
0.3987	0.3109	0.001867	0.02348	0.3987	1	0.3987	0.2991	0.001669	0.02348	0.3987	1
0.4021	0.308	0.001552	0.02367	0.4021	1	0.4021	0.2964	0.001661	0.02367	0.4021	1
0.4054	0.3067	0.001613	0.02386	0.4054	1	0.4054	0.2946	0.001387	0.02386	0.4054	1

$\theta=0.228$ 17R4/D <sub>2</sub> O 6.7 °C (cooling)						$\theta=0.111$ 17R4/D <sub>2</sub> O 11.9 °C					
Q	I(Q)	Std Dev(I(Q))	sigmaQ	meanQ	Shadow Factor	Q	I(Q)	Std Dev(I(Q))	sigmaQ	meanQ	Shadow Factor
0.003433	48.59	1.299	0.001073	0.003607	0.9568	0.003433	12.44	0.2768	0.001068	0.003607	0.9568
0.003837	27.86	1.019	0.001077	0.003977	0.9999	0.003837	8.281	0.2491	0.001071	0.003977	0.9999
0.004241	15.48	0.4506	0.001079	0.004367	1	0.004241	5.077	0.1709	0.001072	0.004367	1
0.004645	9.413	0.2194	0.001082	0.00476	1	0.004645	3.384	0.09732	0.001074	0.00476	1
0.005049	6.381	0.1233	0.001087	0.005155	1	0.005049	2.585	0.0765	0.001077	0.005155	1
0.005453	4.619	0.08552	0.001092	0.005551	1	0.005453	1.94	0.07251	0.001081	0.005551	1
0.005857	3.41	0.06924	0.001098	0.005948	1	0.005857	1.624	0.05679	0.001085	0.005948	1
0.006261	2.59	0.04908	0.001104	0.006346	1	0.006261	1.371	0.05386	0.00109	0.006346	1
0.006665	2.138	0.04031	0.001111	0.006745	1	0.006665	1.136	0.04794	0.001096	0.006745	1
0.007069	1.734	0.03654	0.001119	0.007144	1	0.007069	1.072	0.04228	0.001101	0.007144	1
0.007473	1.475	0.0327	0.001127	0.007544	1	0.007473	0.9976	0.03758	0.001108	0.007544	1
0.007876	1.316	0.02506	0.001136	0.007944	1	0.007876	0.8801	0.03255	0.001115	0.007944	1
0.00828	1.114	0.02507	0.001145	0.008345	1	0.00828	0.8067	0.03609	0.001122	0.008345	1
0.008684	1.037	0.02501	0.001155	0.008746	1	0.008684	0.7696	0.03004	0.001129	0.008746	1
0.009088	0.9092	0.02062	0.001165	0.009147	1	0.009088	0.7544	0.02686	0.001137	0.009147	1
0.009492	0.8359	0.02025	0.001176	0.009548	1	0.009492	0.6794	0.02842	0.001146	0.009548	1
0.009896	0.7277	0.0177	0.001187	0.00995	1	0.009896	0.6811	0.0246	0.001154	0.00995	1
0.0103	0.7567	0.01673	0.001198	0.01035	1	0.0103	0.6824	0.02495	0.001163	0.01035	1
0.0107	0.7158	0.01663	0.00121	0.01075	1	0.0107	0.685	0.023	0.001173	0.01075	1
0.01111	0.6689	0.01754	0.001222	0.01116	1	0.01111	0.6204	0.0234	0.001182	0.01116	1
0.0113	0.6935	0.01259	0.002193	0.01149	1	0.0113	0.613	0.01073	0.00217	0.01149	1
0.01151	0.6339	0.01668	0.001234	0.01156	1	0.01151	0.6292	0.02342	0.001192	0.01156	1
0.01192	0.6078	0.0171	0.001247	0.01196	1	0.01192	0.5778	0.02336	0.001202	0.01196	1
0.01232	0.5923	0.01512	0.00126	0.01236	1	0.01232	0.5751	0.02142	0.001213	0.01236	1
0.01263	0.6018	0.01081	0.002214	0.0128	1	0.01263	0.59	0.00976	0.002186	0.0128	1
0.01272	0.5702	0.01472	0.001273	0.01277	1	0.01272	0.586	0.02198	0.001223	0.01277	1
0.01313	0.5809	0.01508	0.001287	0.01317	1	0.01313	0.6164	0.01972	0.001234	0.01317	1
0.01353	0.5436	0.01422	0.0013	0.01357	1	0.01353	0.5774	0.02013	0.001246	0.01357	1
0.01393	0.5548	0.01295	0.001315	0.01397	1	0.01393	0.5879	0.0198	0.001257	0.01397	1
0.01396	0.5527	0.008239	0.002239	0.01412	1	0.01396	0.5753	0.009188	0.002205	0.01412	1
0.01434	0.5469	0.01323	0.001329	0.01438	1	0.01434	0.5825	0.01907	0.001269	0.01438	1
0.01474	0.5506	0.01222	0.001344	0.01478	1	0.01474	0.5592	0.01806	0.001281	0.01478	1
0.01515	0.5337	0.0128	0.001359	0.01518	1	0.01515	0.5835	0.01965	0.001293	0.01518	1
0.01529	0.5311	0.007406	0.002266	0.01543	1	0.01529	0.572	0.007763	0.002226	0.01543	1
0.01555	0.5202	0.01249	0.001374	0.01558	1	0.01555	0.5425	0.01852	0.001305	0.01558	1
0.01595	0.488	0.01214	0.001389	0.01599	1	0.01595	0.5796	0.01645	0.001318	0.01599	1
0.01636	0.5097	0.01183	0.001405	0.01639	1	0.01636	0.5443	0.01831	0.001331	0.01639	1
0.01662	0.5238	0.006861	0.002296	0.01675	1	0.01662	0.5589	0.007084	0.002249	0.01675	1
0.01676	0.5011	0.01263	0.001421	0.01679	1	0.01676	0.549	0.01743	0.001344	0.01679	1
0.01717	0.5236	0.01361	0.001437	0.0172	1	0.01717	0.5527	0.01844	0.001357	0.0172	1
0.01757	0.5169	0.01248	0.001453	0.0176	1	0.01757	0.557	0.01961	0.00137	0.0176	1
0.01795	0.5107	0.006541	0.002328	0.01807	1	0.01795	0.5447	0.007236	0.002275	0.01807	1
0.01797	0.4951	0.01328	0.00147	0.018	1	0.01797	0.5369	0.01694	0.001384	0.018	1
0.01838	0.4824	0.01202	0.001486	0.01841	1	0.01838	0.5987	0.01731	0.001397	0.01841	1
0.01878	0.4968	0.01166	0.001503	0.01881	1	0.01878	0.5581	0.01919	0.001411	0.01881	1
0.01918	0.5047	0.01292	0.00152	0.01921	1	0.01918	0.5467	0.01872	0.001425	0.01921	1
0.01928	0.5034	0.007252	0.002363	0.01939	1	0.01928	0.5421	0.007245	0.002302	0.01939	1
0.01959	0.4809	0.01138	0.001537	0.01962	1	0.01959	0.5859	0.01902	0.00144	0.01962	1
0.01999	0.5066	0.01178	0.001555	0.02002	1	0.01999	0.5426	0.01715	0.001454	0.02002	1
0.0204	0.4902	0.01204	0.001572	0.02042	1	0.0204	0.5411	0.01766	0.001468	0.02042	1
0.02061	0.4975	0.005935	0.0024	0.02072	1	0.02061	0.5423	0.006439	0.002331	0.02072	1
0.0208	0.4954	0.01287	0.00159	0.02083	1	0.0208	0.5768	0.01669	0.001483	0.02083	1
0.0212	0.4804	0.01186	0.001608	0.02123	1	0.0212	0.5286	0.0162	0.001498	0.02123	1
0.02161	0.483	0.01132	0.001626	0.02163	1	0.02161	0.5492	0.0174	0.001513	0.02163	1
0.02194	0.4879	0.005799	0.002438	0.02204	1	0.02194	0.5327	0.006256	0.002362	0.02204	1
0.02201	0.4866	0.01196	0.001644	0.02203	1	0.02201	0.5387	0.01561	0.001528	0.02203	1
0.02241	0.5006	0.01151	0.001662	0.02244	1	0.02241	0.5476	0.01762	0.001543	0.02244	1
0.02282	0.4897	0.01229	0.00168	0.02284	1	0.02282	0.56	0.01715	0.001558	0.02284	1
0.02322	0.4826	0.009988	0.001699	0.02324	1	0.02322	0.5395	0.01584	0.001574	0.02324	1
0.02327	0.4795	0.006017	0.002479	0.02336	1	0.02327	0.5293	0.006656	0.002394	0.02336	1
0.02363	0.4852	0.01028	0.001717	0.02365	1	0.02363	0.5374	0.01634	0.001589	0.02365	1
0.02403	0.4936	0.01152	0.001736	0.02405	1	0.02403	0.5297	0.01812	0.001605	0.02405	1
0.02443	0.4849	0.01147	0.001755	0.02445	1	0.02443	0.5465	0.01665	0.001621	0.02445	1
0.0246	0.4849	0.005419	0.002521	0.02469	1	0.0246	0.5292	0.006875	0.002428	0.02469	1
0.02484	0.4882	0.01147	0.001774	0.02486	1	0.02484	0.4988	0.01714	0.001637	0.02486	1
0.02524	0.4898	0.01198	0.001793	0.02526	1	0.02524	0.5448	0.0195	0.001653	0.02526	1
0.02564	0.4606	0.01132	0.001812	0.02566	1	0.02564	0.5614	0.01855	0.001669	0.02566	1
0.02593	0.4873	0.005548	0.002565	0.02601	1	0.02593	0.5291	0.005625	0.002464	0.02601	1
0.02605	0.4712	0.0122	0.001831	0.02607	1	0.02605	0.559	0.02036	0.001685	0.02607	1
0.02645	0.4552	0.01302	0.001851	0.02647	1	0.02645	0.5309	0.01878	0.001701	0.02647	1
0.02685	0.469	0.01271	0.00187	0.02687	1	0.02685	0.5023	0.02108	0.001718	0.02687	1
0.02726	0.4782	0.005463	0.002611	0.02734	1	0.02726	0.528	0.005524	0.0025	0.02734	1
0.02726	0.4813	0.01236	0.00189	0.02728	1	0.02726	0.5221	0.02071	0.001734	0.02728	1
0.02766	0.4854	0.01544	0.001909	0.02768	1	0.02766	0.5164	0.02134	0.001751	0.02768	1
0.02807	0.4741	0.01394	0.001929	0.02808	1	0.02807	0.5395	0.0242	0.001767	0.02808	1
0.02847	0.5125	0.01504	0.001949	0.02849	1	0.02847	0.5389	0.02114	0.001784	0.02849	1
0.02859	0.4805	0.004785	0.002658	0.02866	1	0.02859	0.5266	0.006415	0.002538	0.02866	1
0.02887	0.4596	0.01517	0.001968	0.02889	1	0.02887	0.5335	0.02259	0.001801	0.02889	1
0.02928	0.4693	0.01352	0.001988	0.02929	1	0.02928	0.5509	0.02345	0.001818	0.02929	1
0.02968	0.4484	0.01524	0.002008	0.0297	1	0.02968	0.5382	0.02072	0.001835	0.0297	1
0.02991	0.4793	0.005468	0.002707	0.02999	1	0.02991	0.5341	0.005454	0.002578	0.02999	1

φ=0.228 17R4/D <sub>2</sub> O 6.7 °C (cooling)					φ=0.111 17R4/D <sub>2</sub> O 11.9 °C						
Q	I(Q)	Std Dev(I(Q))	sigmaQ	meanQ	Shadow Factor	Q	I(Q)	Std Dev(I(Q))	sigmaQ	meanQ	Shadow Factor
0.03008	0.5024	0.01433	0.002028	0.0301	1	0.03008	0.5361	0.02066	0.001852	0.0301	1
0.03049	0.4527	0.01474	0.002049	0.0305	1	0.03049	0.5198	0.01942	0.001869	0.0305	1
0.03089	0.4876	0.01524	0.002069	0.03091	1	0.03089	0.5319	0.02186	0.001886	0.03091	1
0.03124	0.4692	0.00495	0.002756	0.03131	1	0.03124	0.5321	0.005441	0.002618	0.03131	1
0.03129	0.4572	0.01362	0.002089	0.03131	1	0.03129	0.5227	0.0211	0.001903	0.03131	1
0.0317	0.4918	0.01529	0.002109	0.03171	1	0.0317	0.5193	0.02299	0.00192	0.03171	1
0.0321	0.4438	0.01593	0.00213	0.03212	1	0.0321	0.5485	0.02358	0.001938	0.03212	1
0.0325	0.4921	0.01555	0.00215	0.03252	1	0.0325	0.5468	0.02296	0.001955	0.03252	1
0.03257	0.4738	0.004876	0.002807	0.03264	1	0.03257	0.5273	0.005025	0.00266	0.03264	1
0.03291	0.4938	0.01392	0.002171	0.03292	1	0.03291	0.5661	0.023	0.001973	0.03292	1
0.03331	0.5076	0.01474	0.002191	0.03333	1	0.03331	0.5085	0.02183	0.00199	0.03333	1
0.03372	0.4765	0.01407	0.002212	0.03373	1	0.03372	0.5296	0.02267	0.002008	0.03373	1
0.0339	0.4769	0.004228	0.00286	0.03396	1	0.0339	0.5209	0.005052	0.002703	0.03396	1
0.03399	0.4998	0.00285	0.004794	0.03426	1	0.034	0.5433	0.002017	0.004701	0.03428	1
0.03523	0.4759	0.004024	0.002913	0.03529	1	0.03523	0.5203	0.004841	0.002746	0.03529	1
0.03656	0.4758	0.004493	0.002967	0.03662	1	0.03656	0.5199	0.00502	0.002791	0.03662	1
0.03788	0.4722	0.003948	0.003023	0.03794	1	0.03788	0.5256	0.004632	0.002837	0.03794	1
0.03798	0.5059	0.002845	0.00489	0.03823	1	0.03799	0.5429	0.002173	0.004777	0.03824	1
0.03921	0.4817	0.003917	0.003079	0.03927	1	0.03921	0.5212	0.004654	0.002883	0.03927	1
0.04054	0.4695	0.004514	0.003136	0.04059	1	0.04054	0.5123	0.004709	0.00293	0.04059	1
0.04187	0.4718	0.004265	0.003194	0.04192	1	0.04187	0.5137	0.004521	0.002979	0.04192	1
0.04197	0.5008	0.002633	0.004996	0.0422	1	0.04199	0.5375	0.002338	0.00486	0.04221	1
0.0432	0.4768	0.003811	0.003253	0.04325	1	0.0432	0.508	0.003914	0.003027	0.04325	1
0.04452	0.474	0.003881	0.003312	0.04457	1	0.04452	0.5142	0.004479	0.003077	0.04457	1
0.04585	0.467	0.003688	0.003372	0.0459	1	0.04585	0.5171	0.004247	0.003127	0.0459	1
0.04597	0.5028	0.003132	0.00511	0.04617	1	0.04598	0.5348	0.00252	0.004951	0.04619	1
0.04718	0.4713	0.004093	0.003433	0.04722	1	0.04718	0.5096	0.004335	0.003178	0.04722	1
0.0485	0.4663	0.004037	0.003495	0.04855	1	0.0485	0.5121	0.003864	0.00323	0.04855	1
0.04983	0.4739	0.004032	0.003557	0.04987	1	0.04983	0.5077	0.004088	0.003282	0.04987	1
0.04996	0.4991	0.0026	0.005233	0.05014	1	0.04998	0.5335	0.002349	0.005049	0.05016	1
0.05116	0.4721	0.003675	0.00362	0.0512	1	0.05116	0.5114	0.003919	0.003334	0.0512	1
0.05248	0.4701	0.003495	0.003683	0.05252	1	0.05248	0.5136	0.003776	0.003388	0.05252	1
0.05381	0.4642	0.004011	0.003746	0.05385	1	0.05381	0.5094	0.00383	0.003441	0.05385	1
0.05394	0.4995	0.00256	0.005363	0.05412	1	0.05397	0.531	0.002411	0.005154	0.05414	1
0.05514	0.4688	0.003534	0.003811	0.05517	1	0.05514	0.5059	0.003756	0.003495	0.05517	1
0.05646	0.4743	0.003553	0.003875	0.0565	1	0.05646	0.5071	0.003849	0.00355	0.0565	1
0.05779	0.4644	0.003327	0.00394	0.05782	1	0.05779	0.5089	0.003829	0.003605	0.05782	1
0.05793	0.4962	0.00255	0.0055	0.05809	1	0.05795	0.5307	0.002442	0.005264	0.05812	1
0.05911	0.4682	0.003385	0.004006	0.05915	1	0.05911	0.5041	0.003813	0.00366	0.05915	1
0.06044	0.4675	0.003319	0.004071	0.06047	1	0.06044	0.5041	0.003823	0.003716	0.06047	1
0.06176	0.4664	0.00326	0.004138	0.0618	1	0.06176	0.5012	0.003866	0.003772	0.0618	1
0.06192	0.4943	0.002468	0.005643	0.06207	1	0.06194	0.523	0.002126	0.00538	0.06209	1
0.06309	0.4692	0.003222	0.004204	0.06312	1	0.06309	0.504	0.003659	0.003829	0.06312	1
0.06441	0.4704	0.003035	0.004271	0.06444	1	0.06441	0.5001	0.003351	0.003886	0.06444	1
0.06573	0.4628	0.003056	0.004338	0.06577	1	0.06573	0.5026	0.003458	0.003943	0.06577	1
0.0659	0.4934	0.002346	0.005791	0.06604	1	0.06593	0.52	0.002058	0.0055	0.06607	1
0.06706	0.4676	0.003109	0.004406	0.06709	1	0.06706	0.5051	0.003346	0.004001	0.06709	1
0.06838	0.4596	0.003131	0.004474	0.06841	1	0.06838	0.4921	0.00343	0.004059	0.06841	1
0.06971	0.4674	0.003346	0.004542	0.06974	1	0.06971	0.4974	0.003665	0.004117	0.06974	1
0.06988	0.493	0.00238	0.005945	0.07001	1	0.06991	0.5163	0.001816	0.005626	0.07004	1
0.07103	0.4634	0.003189	0.00461	0.07106	1	0.07103	0.4969	0.003247	0.004175	0.07106	1
0.07235	0.4662	0.002971	0.004679	0.07238	1	0.07235	0.4976	0.003298	0.004234	0.07238	1
0.07367	0.461	0.003002	0.004747	0.0737	1	0.07367	0.4931	0.00349	0.004293	0.0737	1
0.07386	0.4973	0.002395	0.006104	0.07399	1	0.07389	0.5148	0.001785	0.005756	0.07402	1
0.075	0.4636	0.00284	0.004816	0.07503	1	0.075	0.4919	0.003616	0.004352	0.07503	1
0.07632	0.4622	0.003149	0.004886	0.07635	1	0.07632	0.4906	0.003082	0.004411	0.07635	1
0.07764	0.4611	0.003034	0.004955	0.07767	1	0.07764	0.4871	0.003039	0.004471	0.07767	1
0.07784	0.494	0.002598	0.006267	0.07796	1	0.07787	0.5108	0.001969	0.00589	0.07799	1
0.07896	0.463	0.003045	0.005025	0.07899	1	0.07896	0.4869	0.003445	0.004531	0.07899	1
0.08028	0.4659	0.002889	0.005094	0.08031	1	0.08028	0.4917	0.003492	0.004591	0.08031	1
0.08161	0.464	0.003017	0.005164	0.08163	1	0.08161	0.4874	0.003835	0.004651	0.08163	1
0.08181	0.4893	0.002187	0.006434	0.08192	1	0.08184	0.5036	0.001673	0.006028	0.08196	1
0.08293	0.462	0.003284	0.005235	0.08295	1	0.08293	0.4849	0.00373	0.004711	0.08295	1
0.08425	0.4617	0.003429	0.005305	0.08427	1	0.08425	0.4802	0.003473	0.004772	0.08427	1
0.08557	0.4576	0.003606	0.005375	0.08559	1	0.08557	0.4753	0.004011	0.004833	0.08559	1
0.08578	0.491	0.0023	0.006604	0.08589	1	0.08581	0.5011	0.001741	0.006169	0.08592	1
0.08689	0.466	0.003551	0.005446	0.08691	1	0.08689	0.4845	0.004206	0.004893	0.08691	1
0.08821	0.4571	0.003731	0.005517	0.08823	1	0.08821	0.4831	0.004687	0.004954	0.08823	1
0.08953	0.4562	0.004117	0.005588	0.08955	1	0.08953	0.4697	0.004328	0.005016	0.08955	1
0.08975	0.4871	0.002039	0.006778	0.08985	1	0.08978	0.4983	0.002054	0.006314	0.08989	1
0.09084	0.465	0.004179	0.005659	0.09087	1	0.09084	0.4754	0.004252	0.005077	0.09087	1
0.09371	0.4881	0.002052	0.006956	0.09381	1	0.09375	0.49	0.001713	0.006461	0.09385	1
0.09768	0.4876	0.002241	0.007136	0.09777	1	0.09771	0.4913	0.00197	0.006612	0.09781	1
0.1016	0.4844	0.002065	0.007318	0.1017	1	0.1017	0.4863	0.001755	0.006764	0.1018	1
0.1056	0.4845	0.001774	0.007503	0.1057	1	0.1056	0.4817	0.001665	0.00692	0.1057	1
0.1095	0.4877	0.00196	0.007691	0.1096	1	0.1096	0.473	0.00175	0.007077	0.1097	1
0.1135	0.4868	0.001944	0.00788	0.1136	1	0.1135	0.4727	0.001738	0.007237	0.1136	1
0.1174	0.481	0.001855	0.008071	0.1175	1	0.1175	0.469	0.001703	0.007398	0.1176	1
0.1214	0.4803	0.001861	0.008264	0.1215	1	0.1214	0.4638	0.001534	0.007561	0.1215	1
0.1253	0.4781	0.001763	0.008458	0.1254	1	0.1254	0.4569	0.001701	0.007726	0.1254	1
0.1293	0.4828	0.001969	0.008654	0.1293	1	0.1293	0.4512	0.001466	0.007892	0.1294	1



$\phi=0.228$ 17R4/D <sub>2</sub> O 6.7 °C (cooling)						$\phi=0.111$ 17R4/D <sub>2</sub> O 11.9 °C					
Q	I(Q)	Std Dev(I(Q))	sigmaQ	meanQ	Shadow Factor	Q	I(Q)	Std Dev(I(Q))	sigmaQ	meanQ	Shadow Factor
0.1332	0.4773	0.001834	0.008851	0.1333	1	0.1332	0.4477	0.001478	0.00806	0.1333	1
0.1371	0.4736	0.001869	0.00905	0.1372	1	0.1372	0.4412	0.001495	0.008229	0.1372	1
0.141	0.4718	0.001591	0.009249	0.1411	1	0.1411	0.4359	0.001334	0.008399	0.1411	1
0.1449	0.4746	0.001919	0.00945	0.145	1	0.145	0.4332	0.001422	0.00857	0.1451	1
0.1489	0.4705	0.001703	0.009651	0.1489	1	0.1489	0.4302	0.001494	0.008742	0.149	1
0.1528	0.4669	0.001711	0.009853	0.1528	1	0.1528	0.4248	0.001315	0.008915	0.1529	1
0.1567	0.4657	0.001708	0.01006	0.1567	1	0.1567	0.4202	0.001383	0.009089	0.1568	1
0.1606	0.4644	0.001776	0.01026	0.1606	1	0.1606	0.4153	0.001319	0.009264	0.1607	1
0.1645	0.4605	0.001667	0.01046	0.1645	1	0.1645	0.4086	0.001339	0.009439	0.1646	1
0.1683	0.4604	0.00172	0.01067	0.1684	1	0.1684	0.4074	0.001348	0.009615	0.1685	1
0.1722	0.4593	0.001602	0.01087	0.1723	1	0.1723	0.3998	0.001264	0.009792	0.1723	1
0.1761	0.455	0.0017	0.01108	0.1762	1	0.1762	0.3961	0.001295	0.009969	0.1762	1
0.18	0.452	0.001751	0.01129	0.18	1	0.18	0.3897	0.001161	0.01015	0.1801	1
0.1838	0.448	0.001777	0.01149	0.1839	1	0.1839	0.3882	0.001198	0.01032	0.184	1
0.1877	0.4473	0.00144	0.0117	0.1877	1	0.1878	0.3838	0.001239	0.0105	0.1878	1
0.1916	0.4433	0.001668	0.01191	0.1916	1	0.1916	0.3791	0.001184	0.01068	0.1917	1
0.1954	0.442	0.00155	0.01212	0.1954	1	0.1955	0.3735	0.001137	0.01086	0.1955	1
0.1992	0.4402	0.001618	0.01232	0.1993	1	0.1993	0.3687	0.001122	0.01104	0.1994	1
0.2031	0.4374	0.001738	0.01253	0.2031	1	0.2032	0.3646	0.001205	0.01122	0.2032	1
0.2069	0.4363	0.001457	0.01274	0.2069	1	0.207	0.3615	0.00105	0.0114	0.207	1
0.2107	0.4333	0.001703	0.01295	0.2108	1	0.2108	0.3581	0.001201	0.01158	0.2109	1
0.2145	0.4277	0.001373	0.01316	0.2146	1	0.2146	0.3537	0.001122	0.01176	0.2147	1
0.2184	0.4298	0.001541	0.01336	0.2184	1	0.2184	0.3499	0.001094	0.01194	0.2185	1
0.2222	0.4223	0.001465	0.01357	0.2222	1	0.2222	0.3456	0.001102	0.01212	0.2223	1
0.226	0.4219	0.001663	0.01378	0.226	1	0.226	0.3416	0.001121	0.0123	0.2261	1
0.2297	0.4182	0.001478	0.01399	0.2298	1	0.2298	0.3387	0.001106	0.01248	0.2299	1
0.2335	0.4173	0.001319	0.0142	0.2336	1	0.2336	0.334	0.001091	0.01266	0.2337	1
0.2373	0.4124	0.001345	0.0144	0.2373	1	0.2374	0.3321	0.001147	0.01284	0.2374	1
0.2411	0.4114	0.001595	0.01461	0.2411	1	0.2412	0.3282	0.000949	0.01303	0.2412	1
0.2448	0.4103	0.001708	0.01482	0.2449	1	0.2449	0.3274	0.001314	0.01321	0.245	1
0.2486	0.4068	0.001526	0.01503	0.2486	1	0.2487	0.321	0.001256	0.01339	0.2487	1
0.2523	0.4054	0.001632	0.01524	0.2524	1	0.2524	0.3187	0.001212	0.01357	0.2525	1
0.2561	0.3974	0.001575	0.01544	0.2561	1	0.2562	0.3166	0.001207	0.01375	0.2562	1
0.2598	0.4008	0.001571	0.01565	0.2598	1	0.2599	0.3119	0.001305	0.01393	0.2599	1
0.2635	0.3969	0.001735	0.01586	0.2636	1	0.2636	0.3083	0.001308	0.01411	0.2637	1
0.2673	0.3964	0.001705	0.01606	0.2673	1	0.2674	0.3079	0.001101	0.01429	0.2674	1
0.271	0.3926	0.001575	0.01627	0.271	1	0.2711	0.3036	0.001289	0.01447	0.2711	1
0.2747	0.3873	0.001602	0.01648	0.2747	1	0.2748	0.3016	0.001372	0.01465	0.2748	1
0.2784	0.3868	0.001523	0.01668	0.2784	1	0.2785	0.2976	0.001247	0.01483	0.2785	1
0.282	0.3811	0.00164	0.01689	0.2821	1	0.2821	0.2969	0.001196	0.01501	0.2822	1
0.2857	0.3837	0.001676	0.0171	0.2857	1	0.2858	0.2947	0.001195	0.01519	0.2859	1
0.2894	0.3788	0.001466	0.0173	0.2894	1	0.2895	0.2918	0.001203	0.01537	0.2895	1
0.293	0.3839	0.001675	0.01751	0.2931	1	0.2932	0.2881	0.001219	0.01555	0.2932	1
0.2967	0.3749	0.001781	0.01771	0.2967	1	0.2968	0.2861	0.001198	0.01572	0.2968	1
0.3003	0.3744	0.001763	0.01792	0.3004	1	0.3005	0.2843	0.001149	0.0159	0.3005	1
0.304	0.3692	0.001678	0.01812	0.304	1	0.3041	0.2815	0.0012	0.01608	0.3041	1
0.3076	0.3677	0.001759	0.01832	0.3076	1	0.3077	0.2798	0.001253	0.01626	0.3077	1
0.3112	0.3651	0.001642	0.01853	0.3113	1	0.3113	0.2761	0.001299	0.01644	0.3114	1
0.3148	0.3626	0.001529	0.01873	0.3149	1	0.3149	0.2731	0.001253	0.01661	0.315	1
0.3184	0.3613	0.001676	0.01893	0.3185	1	0.3186	0.2701	0.001232	0.01679	0.3186	1
0.322	0.3631	0.001676	0.01913	0.3221	1	0.3221	0.2695	0.001384	0.01697	0.3222	1
0.3256	0.3601	0.001524	0.01934	0.3256	1	0.3257	0.2679	0.001154	0.01714	0.3258	1
0.3292	0.3557	0.001772	0.01954	0.3292	1	0.3293	0.2678	0.001188	0.01732	0.3293	1
0.3327	0.3543	0.001852	0.01974	0.3328	1	0.3329	0.2634	0.001274	0.01749	0.3329	1
0.3363	0.3545	0.001689	0.01994	0.3363	1	0.3364	0.2618	0.001216	0.01767	0.3364	1
0.3399	0.3519	0.001689	0.02014	0.3399	1	0.34	0.2599	0.001315	0.01785	0.34	1
0.3434	0.3444	0.001501	0.02034	0.3434	1	0.3435	0.2567	0.001133	0.01802	0.3435	1
0.3469	0.3448	0.001727	0.02054	0.3469	1	0.347	0.2565	0.001208	0.01819	0.3471	1
0.3504	0.345	0.001639	0.02074	0.3505	1	0.3506	0.2545	0.001208	0.01837	0.3506	1
0.3539	0.3435	0.001671	0.02094	0.354	1	0.3541	0.2532	0.001168	0.01854	0.3541	1
0.3574	0.3403	0.001566	0.02114	0.3575	1	0.3576	0.2525	0.001136	0.01872	0.3576	1
0.3609	0.3386	0.001646	0.02133	0.361	1	0.3611	0.2505	0.001161	0.01889	0.3611	1
0.3644	0.3374	0.001597	0.02153	0.3644	1	0.3645	0.2503	0.001159	0.01906	0.3646	1
0.3679	0.3353	0.001551	0.02173	0.3679	1	0.368	0.2462	0.001149	0.01923	0.368	1
0.3713	0.333	0.001492	0.02192	0.3714	1	0.3715	0.2456	0.001164	0.0194	0.3715	1
0.3748	0.3355	0.001479	0.02212	0.3748	1	0.3749	0.2442	0.001151	0.01958	0.375	1
0.3782	0.3304	0.001808	0.02231	0.3783	1	0.3784	0.2429	0.001138	0.01975	0.3784	1
0.3817	0.3293	0.001642	0.02251	0.3817	1	0.3818	0.2431	0.001207	0.01992	0.3818	1
0.3851	0.3258	0.001636	0.0227	0.3851	1	0.3852	0.2406	0.001206	0.02009	0.3853	1
0.3885	0.3262	0.001798	0.0229	0.3885	1	0.3886	0.2391	0.00128	0.02026	0.3887	1
0.3919	0.3236	0.001538	0.02309	0.3919	1	0.3921	0.2386	0.001166	0.02043	0.3921	1
0.3953	0.3228	0.001776	0.02328	0.3953	1	0.3954	0.2366	0.001351	0.0206	0.3955	1
0.3987	0.3222	0.001707	0.02348	0.3987	1	0.3988	0.2366	0.001253	0.02076	0.3989	1
0.4021	0.3182	0.001543	0.02367	0.4021	1	0.4022	0.2335	0.001303	0.02093	0.4022	1
0.4054	0.3191	0.001671	0.02386	0.4054	1	0.4056	0.2328	0.001329	0.0211	0.4056	1

ω=0.111 17R4/D <sub>2</sub> O 30.6 °C						ω=0.111 17R4/D <sub>2</sub> O 49.3 °C					
Q	I(Q)	Std Dev(I(Q))	sigmaQ	meanQ	Shadow Factor	Q	I(Q)	Std Dev(I(Q))	sigmaQ	meanQ	Shadow Factor
0.003433	143.7	3.581	0.001068	0.003607	0.9568	0.003433	19.89	0.7788	0.001068	0.003607	0.9568
0.003837	85.72	2.828	0.001071	0.003977	0.9999	0.003837	11.88	0.4752	0.001071	0.003977	0.9999
0.004241	48.75	1.295	0.001072	0.004367	1	0.004241	7.153	0.2589	0.001072	0.004367	1
0.004645	31	0.6833	0.001074	0.00476	1	0.004645	5.208	0.1573	0.001074	0.00476	1
0.005049	20.81	0.3973	0.001077	0.005155	1	0.005049	4.093	0.1175	0.001077	0.005155	1
0.005453	14.56	0.2633	0.001081	0.005551	1	0.005453	3.321	0.08905	0.001081	0.005551	1
0.005857	10.73	0.1726	0.001085	0.005948	1	0.005857	2.987	0.08431	0.001085	0.005948	1
0.006261	8.147	0.1354	0.00109	0.006346	1	0.006261	2.61	0.06603	0.00109	0.006346	1
0.006665	6.467	0.09618	0.001096	0.006745	1	0.006665	2.469	0.06442	0.001096	0.006745	1
0.007069	5.229	0.08897	0.001101	0.007144	1	0.007069	2.386	0.0635	0.001101	0.007144	1
0.007473	4.346	0.06788	0.001108	0.007544	1	0.007473	2.21	0.05518	0.001108	0.007544	1
0.007876	3.775	0.06477	0.001115	0.007944	1	0.007876	2.232	0.0523	0.001115	0.007944	1
0.00828	3.066	0.05424	0.001122	0.008345	1	0.00828	2.134	0.05113	0.001122	0.008345	1
0.008684	2.776	0.054	0.001129	0.008746	1	0.008684	2.098	0.05314	0.001129	0.008746	1
0.009088	2.483	0.04585	0.001137	0.009147	1	0.009088	2.116	0.05065	0.001137	0.009147	1
0.009492	2.266	0.04006	0.001146	0.009548	1	0.009492	1.962	0.04926	0.001146	0.009548	1
0.009896	2.022	0.03907	0.001154	0.00995	1	0.009896	2.04	0.04149	0.001154	0.00995	1
0.0103	1.896	0.03658	0.001163	0.01035	1	0.0103	1.898	0.04127	0.001163	0.01035	1
0.0107	1.821	0.04102	0.001173	0.01075	1	0.0107	1.956	0.04353	0.001173	0.01075	1
0.01111	1.648	0.03439	0.001182	0.01116	1	0.01111	1.912	0.03876	0.001182	0.01116	1
0.0113	1.783	0.03103	0.00217	0.01149	1	0.0113	1.953	0.01589	0.00217	0.01149	1
0.01151	1.625	0.03471	0.001192	0.01156	1	0.01151	1.944	0.03669	0.001192	0.01156	1
0.01192	1.532	0.03307	0.001202	0.01196	1	0.01192	1.921	0.03918	0.001202	0.01196	1
0.01232	1.499	0.03521	0.001213	0.01236	1	0.01232	1.97	0.03911	0.001213	0.01236	1
0.01263	1.489	0.01924	0.002186	0.0128	1	0.01263	1.927	0.01419	0.002186	0.0128	1
0.01272	1.403	0.02978	0.001223	0.01277	1	0.01272	1.851	0.03479	0.001223	0.01277	1
0.01313	1.405	0.03122	0.001234	0.01317	1	0.01313	1.865	0.03613	0.001234	0.01317	1
0.01353	1.369	0.02893	0.001246	0.01357	1	0.01353	1.931	0.03511	0.001246	0.01357	1
0.01393	1.344	0.02852	0.001257	0.01397	1	0.01393	1.925	0.03359	0.001257	0.01397	1
0.01396	1.322	0.01341	0.002205	0.01412	1	0.01396	1.9	0.01353	0.002205	0.01412	1
0.01434	1.26	0.02941	0.001269	0.01438	1	0.01434	1.878	0.03611	0.001269	0.01438	1
0.01474	1.279	0.02756	0.001281	0.01478	1	0.01474	1.896	0.03495	0.001281	0.01478	1
0.01515	1.286	0.02516	0.001293	0.01518	1	0.01515	1.908	0.03267	0.001293	0.01518	1
0.01529	1.231	0.01249	0.002226	0.01543	1	0.01529	1.861	0.01338	0.002226	0.01543	1
0.01555	1.192	0.02626	0.001305	0.01558	1	0.01555	1.903	0.03365	0.001305	0.01558	1
0.01595	1.175	0.02662	0.001318	0.01599	1	0.01595	1.923	0.03466	0.001318	0.01599	1
0.01636	1.165	0.02596	0.001331	0.01639	1	0.01636	1.943	0.03581	0.001331	0.01639	1
0.01662	1.185	0.01229	0.002249	0.01675	1	0.01662	1.872	0.01326	0.002249	0.01675	1
0.01676	1.215	0.02484	0.001344	0.01679	1	0.01676	1.927	0.03362	0.001344	0.01679	1
0.01717	1.214	0.02648	0.001357	0.0172	1	0.01717	1.847	0.03239	0.001357	0.0172	1
0.01757	1.156	0.02325	0.00137	0.0176	1	0.01757	1.856	0.03414	0.00137	0.0176	1
0.01795	1.125	0.01171	0.002275	0.01807	1	0.01795	1.865	0.0129	0.002275	0.01807	1
0.01797	1.111	0.02527	0.001384	0.018	1	0.01797	1.868	0.03565	0.001384	0.018	1
0.01838	1.169	0.02598	0.001397	0.01841	1	0.01838	1.887	0.03591	0.001397	0.01841	1
0.01878	1.163	0.02487	0.001411	0.01881	1	0.01878	1.89	0.03259	0.001411	0.01881	1
0.01918	1.165	0.02344	0.001425	0.01921	1	0.01918	1.862	0.03381	0.001425	0.01921	1
0.01928	1.098	0.01022	0.002302	0.01939	1	0.01928	1.863	0.01175	0.002302	0.01939	1
0.01959	1.166	0.02415	0.00144	0.01962	1	0.01959	1.931	0.03319	0.00144	0.01962	1
0.01999	1.089	0.02316	0.001454	0.02002	1	0.01999	1.926	0.03482	0.001454	0.02002	1
0.0204	1.137	0.02386	0.001468	0.02042	1	0.0204	1.88	0.0311	0.001468	0.02042	1
0.02061	1.091	0.009638	0.002331	0.02072	1	0.02061	1.836	0.01353	0.002331	0.02072	1
0.0208	1.105	0.02338	0.001483	0.02083	1	0.0208	1.875	0.03247	0.001483	0.02083	1
0.0212	1.125	0.02476	0.001498	0.02123	1	0.0212	1.859	0.03524	0.001498	0.02123	1
0.02161	1.102	0.02273	0.001513	0.02163	1	0.02161	1.844	0.032	0.001513	0.02163	1
0.02194	1.07	0.008713	0.002362	0.02204	1	0.02194	1.854	0.01254	0.002362	0.02204	1
0.02201	1.108	0.0229	0.001528	0.02203	1	0.02201	1.776	0.03111	0.001528	0.02203	1
0.02241	1.062	0.02211	0.001543	0.02244	1	0.02241	1.832	0.03427	0.001543	0.02244	1
0.02282	1.092	0.0235	0.001558	0.02284	1	0.02282	1.871	0.03148	0.001558	0.02284	1
0.02322	1.098	0.02397	0.001574	0.02324	1	0.02322	1.808	0.03484	0.001574	0.02324	1
0.02327	1.065	0.009289	0.002394	0.02336	1	0.02327	1.847	0.01102	0.002394	0.02336	1
0.02363	1.066	0.02286	0.001589	0.02365	1	0.02363	1.845	0.03131	0.001589	0.02365	1
0.02403	1.081	0.02286	0.001605	0.02405	1	0.02403	1.869	0.03294	0.001605	0.02405	1
0.02443	1.112	0.02295	0.001621	0.02445	1	0.02443	1.863	0.02844	0.001621	0.02445	1
0.0246	1.039	0.008334	0.002428	0.02469	1	0.0246	1.844	0.01149	0.002428	0.02469	1
0.02484	1.106	0.02374	0.001637	0.02486	1	0.02484	1.863	0.03447	0.001637	0.02486	1
0.02524	1.119	0.02557	0.001653	0.02526	1	0.02524	1.862	0.03494	0.001653	0.02526	1
0.02564	1.077	0.0276	0.001669	0.02566	1	0.02564	1.842	0.03685	0.001669	0.02566	1
0.02593	1.043	0.00716	0.002464	0.02601	1	0.02593	1.836	0.01229	0.002464	0.02601	1
0.02605	1.048	0.0269	0.001685	0.02607	1	0.02605	1.857	0.0361	0.001685	0.02607	1
0.02645	1.105	0.02692	0.001701	0.02647	1	0.02645	1.782	0.03695	0.001701	0.02647	1
0.02685	0.9967	0.02621	0.001718	0.02687	1	0.02685	1.867	0.03855	0.001718	0.02687	1
0.02726	1.051	0.007976	0.0025	0.02734	1	0.02726	1.828	0.01012	0.0025	0.02734	1
0.02726	1.056	0.02826	0.001734	0.02728	1	0.02726	1.844	0.04037	0.001734	0.02728	1
0.02766	1.05	0.02846	0.001751	0.02768	1	0.02766	1.836	0.03882	0.001751	0.02768	1
0.02807	1.083	0.03011	0.001767	0.02808	1	0.02807	1.852	0.04132	0.001767	0.02808	1
0.02847	1.056	0.02939	0.001784	0.02849	1	0.02847	1.876	0.03969	0.001784	0.02849	1
0.02859	1.018	0.007572	0.002538	0.02866	1	0.02859	1.821	0.009354	0.002538	0.02866	1
0.02887	1.056	0.03041	0.001801	0.02889	1	0.02887	1.805	0.04256	0.001801	0.02889	1
0.02928	1.088	0.03314	0.001818	0.02929	1	0.02928	1.898	0.04322	0.001818	0.02929	1
0.02968	0.9952	0.03215	0.001835	0.0297	1	0.02968	1.788	0.03886	0.001835	0.0297	1
0.02991	1.017	0.007209	0.002578	0.02999	1	0.02991	1.837	0.008825	0.002578	0.02999	1

$\omega=0.111$ 17R4/D <sub>2</sub> O 30.6 °C						$\omega=0.111$ 17R4/D <sub>2</sub> O 49.3 °C					
Q	I(Q)	Std Dev(I(Q))	sigmaQ	meanQ	Shadow Factor	Q	I(Q)	Std Dev(I(Q))	sigmaQ	meanQ	Shadow Factor
0.03008	1.06	0.02836	0.001852	0.0301	1	0.03008	1.835	0.04345	0.001852	0.0301	1
0.03049	1.054	0.02934	0.001869	0.0305	1	0.03049	1.888	0.04099	0.001869	0.0305	1
0.03089	1.063	0.02796	0.001886	0.03091	1	0.03089	1.783	0.04507	0.001886	0.03091	1
0.03124	1.023	0.007606	0.002618	0.03131	1	0.03124	1.81	0.01012	0.002618	0.03131	1
0.03129	1.053	0.0279	0.001903	0.03131	1	0.03129	1.84	0.0429	0.001903	0.03131	1
0.0317	1.033	0.02973	0.00192	0.03171	1	0.0317	1.752	0.04265	0.00192	0.03171	1
0.0321	0.9853	0.02909	0.001938	0.03212	1	0.0321	1.713	0.03931	0.001938	0.03212	1
0.0325	0.9784	0.03244	0.001955	0.03252	1	0.0325	1.718	0.03973	0.001955	0.03252	1
0.03257	1.015	0.008003	0.00266	0.03264	1	0.03257	1.82	0.009524	0.00266	0.03264	1
0.03291	1.099	0.02717	0.001973	0.03292	1	0.03291	1.737	0.04602	0.001973	0.03292	1
0.03331	0.9798	0.02905	0.00199	0.03333	1	0.03331	1.787	0.04053	0.00199	0.03333	1
0.03372	1.008	0.0279	0.002008	0.03373	1	0.03372	1.775	0.04388	0.002008	0.03373	1
0.0339	1	0.007198	0.002703	0.03396	1	0.0339	1.816	0.009176	0.002703	0.03396	1
0.03399	1.009	0.003594	0.0047	0.03426	1	0.03399	1.799	0.005401	0.0047	0.03426	1
0.03523	1.006	0.006042	0.002746	0.03529	1	0.03523	1.816	0.00808	0.002746	0.03529	1
0.03656	0.9897	0.006619	0.002791	0.03662	1	0.03656	1.817	0.008805	0.002791	0.03662	1
0.03788	0.9893	0.006748	0.002837	0.03794	1	0.03788	1.822	0.007896	0.002837	0.03794	1
0.03798	0.9972	0.002783	0.004775	0.03823	1	0.03798	1.816	0.004772	0.004775	0.03823	1
0.03921	0.9719	0.006081	0.002883	0.03927	1	0.03921	1.813	0.008485	0.002883	0.03927	1
0.04054	0.9845	0.006571	0.00293	0.04059	1	0.04054	1.834	0.00788	0.00293	0.04059	1
0.04187	0.9567	0.005985	0.002979	0.04192	1	0.04187	1.824	0.008528	0.002979	0.04192	1
0.04197	0.9845	0.003217	0.004859	0.0422	1	0.04197	1.841	0.004792	0.004859	0.0422	1
0.0432	0.9728	0.006162	0.003027	0.04325	1	0.0432	1.83	0.008583	0.003027	0.04325	1
0.04452	0.9423	0.00569	0.003077	0.04457	1	0.04452	1.843	0.007327	0.003077	0.04457	1
0.04585	0.9513	0.005818	0.003127	0.0459	1	0.04585	1.872	0.008041	0.003127	0.0459	1
0.04597	0.9673	0.003386	0.00495	0.04617	1	0.04597	1.885	0.005277	0.00495	0.04617	1
0.04718	0.9527	0.005535	0.003178	0.04722	1	0.04718	1.878	0.00726	0.003178	0.04722	1
0.0485	0.9257	0.005062	0.00323	0.04855	1	0.0485	1.89	0.00776	0.00323	0.04855	1
0.04983	0.9282	0.005656	0.003282	0.04987	1	0.04983	1.904	0.007476	0.003282	0.04987	1
0.04996	0.9467	0.002893	0.005048	0.05014	1	0.04996	1.949	0.006567	0.005048	0.05014	1
0.05116	0.9305	0.005254	0.003334	0.0512	1	0.05116	1.939	0.007595	0.003334	0.0512	1
0.05248	0.9145	0.005495	0.003388	0.05252	1	0.05248	1.948	0.007173	0.003388	0.05252	1
0.05381	0.9158	0.004941	0.003441	0.05385	1	0.05381	1.969	0.007238	0.003441	0.05385	1
0.05394	0.9318	0.003214	0.005152	0.05412	1	0.05394	2.029	0.005921	0.005152	0.05412	1
0.05514	0.9072	0.005049	0.003495	0.05517	1	0.05514	2	0.007507	0.003495	0.05517	1
0.05646	0.9027	0.00523	0.00355	0.0565	1	0.05646	2.027	0.007708	0.00355	0.0565	1
0.05779	0.8949	0.00515	0.003605	0.05782	1	0.05779	2.046	0.0076	0.003605	0.05782	1
0.05793	0.9138	0.003544	0.005262	0.05809	1	0.05793	2.116	0.007735	0.005262	0.05809	1
0.05911	0.8923	0.004693	0.00366	0.05915	1	0.05911	2.079	0.007047	0.00366	0.05915	1
0.06044	0.8804	0.005112	0.003716	0.06047	1	0.06044	2.126	0.007549	0.003716	0.06047	1
0.06176	0.8805	0.004819	0.003772	0.0618	1	0.06176	2.148	0.007107	0.003772	0.0618	1
0.06192	0.9004	0.003255	0.005378	0.06207	1	0.06192	2.219	0.006793	0.005378	0.06207	1
0.06309	0.8691	0.004915	0.003829	0.06312	1	0.06309	2.173	0.007025	0.003829	0.06312	1
0.06441	0.8714	0.004503	0.003886	0.06444	1	0.06441	2.218	0.006989	0.003886	0.06444	1
0.06573	0.8576	0.00438	0.003943	0.06577	1	0.06573	2.252	0.007648	0.003943	0.06577	1
0.0659	0.8828	0.003273	0.005499	0.06604	1	0.0659	2.311	0.006925	0.005499	0.06604	1
0.06706	0.8508	0.004374	0.004001	0.06709	1	0.06706	2.297	0.007839	0.004001	0.06709	1
0.06838	0.8488	0.004334	0.004059	0.06841	1	0.06838	2.316	0.007399	0.004059	0.06841	1
0.06971	0.8392	0.004247	0.004117	0.06974	1	0.06971	2.351	0.006857	0.004117	0.06974	1
0.06988	0.861	0.002817	0.005624	0.07001	1	0.06988	2.381	0.005354	0.005624	0.07001	1
0.07103	0.8355	0.003981	0.004175	0.07106	1	0.07103	2.376	0.007292	0.004175	0.07106	1
0.07235	0.8283	0.004449	0.004234	0.07238	1	0.07235	2.394	0.007273	0.004234	0.07238	1
0.07367	0.8172	0.004248	0.004293	0.0737	1	0.07367	2.416	0.006471	0.004293	0.0737	1
0.07386	0.8456	0.002707	0.005754	0.07399	1	0.07386	2.393	0.005818	0.005754	0.07399	1
0.075	0.8192	0.004133	0.004352	0.07503	1	0.075	2.428	0.006914	0.004352	0.07503	1
0.07632	0.8139	0.004265	0.004411	0.07635	1	0.07632	2.412	0.007049	0.004411	0.07635	1
0.07764	0.8007	0.004123	0.004471	0.07767	1	0.07764	2.403	0.007309	0.004471	0.07767	1
0.07784	0.8253	0.00295	0.005888	0.07796	1	0.07784	2.347	0.007352	0.005888	0.07796	1
0.07896	0.806	0.004054	0.004531	0.07899	1	0.07896	2.39	0.006933	0.004531	0.07899	1
0.08028	0.8003	0.004171	0.004591	0.08031	1	0.08028	2.339	0.007219	0.004591	0.08031	1
0.08161	0.7889	0.004454	0.004651	0.08163	1	0.08161	2.291	0.007115	0.004651	0.08163	1
0.08181	0.8078	0.002474	0.006026	0.08192	1	0.08181	2.217	0.007999	0.006026	0.08192	1
0.08293	0.7819	0.00419	0.004711	0.08295	1	0.08293	2.239	0.007901	0.004711	0.08295	1
0.08425	0.7663	0.004551	0.004772	0.08427	1	0.08425	2.184	0.007651	0.004772	0.08427	1
0.08557	0.7637	0.004554	0.004833	0.08559	1	0.08557	2.106	0.0081	0.004833	0.08559	1
0.08578	0.7879	0.002676	0.006167	0.08589	1	0.08578	2.015	0.008947	0.006167	0.08589	1
0.08689	0.75	0.005244	0.004893	0.08691	1	0.08689	2.036	0.008405	0.004893	0.08691	1
0.08821	0.7598	0.005452	0.004954	0.08823	1	0.08821	1.974	0.009386	0.004954	0.08823	1
0.08953	0.7449	0.005465	0.005016	0.08955	1	0.08953	1.883	0.00922	0.005016	0.08955	1
0.08975	0.777	0.002571	0.006312	0.08985	1	0.08975	1.789	0.008853	0.006312	0.08985	1
0.09084	0.7407	0.005348	0.005077	0.09087	1	0.09084	1.81	0.008539	0.005077	0.09087	1
0.09371	0.7533	0.002345	0.006459	0.09381	1	0.09371	1.535	0.009317	0.006459	0.09381	1
0.09768	0.7317	0.002298	0.006609	0.09777	1	0.09768	1.293	0.007955	0.006609	0.09777	1
0.1016	0.7196	0.002203	0.006762	0.1017	1	0.1016	1.101	0.006555	0.006762	0.1017	1
0.1056	0.7006	0.002111	0.006917	0.1057	1	0.1056	0.9185	0.00504	0.006917	0.1057	1
0.1095	0.6855	0.002007	0.007075	0.1096	1	0.1095	0.7848	0.003881	0.007075	0.1096	1
0.1135	0.6683	0.001938	0.007234	0.1136	1	0.1135	0.6737	0.003356	0.007234	0.1136	1
0.1174	0.6518	0.00202	0.007396	0.1175	1	0.1174	0.5863	0.003038	0.007396	0.1175	1
0.1214	0.6389	0.001879	0.007559	0.1215	1	0.1214	0.519	0.002378	0.007559	0.1215	1
0.1253	0.6253	0.001939	0.007723	0.1254	1	0.1253	0.4666	0.002422	0.007723	0.1254	1
0.1293	0.6079	0.001845	0.007889	0.1293	1	0.1293	0.4216	0.001898	0.007889	0.1293	1

$\omega=0.111$ 17R4/D <sub>2</sub> O 30.6 °C						$\omega=0.111$ 17R4/D <sub>2</sub> O 49.3 °C					
Q	I(Q)	Std DevI(Q)	sigmaQ	meanQ	Shadow Factor	Q	I(Q)	Std DevI(Q)	sigmaQ	meanQ	Shadow Factor
0.1332	0.5996	0.001843	0.008057	0.1333	1	0.1332	0.3873	0.00178	0.008057	0.1333	1
0.1371	0.5836	0.001971	0.008226	0.1372	1	0.1371	0.3593	0.001792	0.008226	0.1372	1
0.141	0.5711	0.001582	0.008396	0.1411	1	0.141	0.3356	0.001599	0.008396	0.1411	1
0.1449	0.5545	0.001736	0.008567	0.145	1	0.1449	0.3161	0.001729	0.008567	0.145	1
0.1489	0.5446	0.001573	0.008739	0.1489	1	0.1489	0.2989	0.001393	0.008739	0.1489	1
0.1528	0.5371	0.001709	0.008912	0.1528	1	0.1528	0.2827	0.001356	0.008912	0.1528	1
0.1567	0.5217	0.001731	0.009086	0.1567	1	0.1567	0.2716	0.001369	0.009086	0.1567	1
0.1606	0.5105	0.001582	0.00926	0.1606	1	0.1606	0.2592	0.001271	0.00926	0.1606	1
0.1645	0.5006	0.001593	0.009436	0.1645	1	0.1645	0.2493	0.001213	0.009436	0.1645	1
0.1683	0.4886	0.001418	0.009612	0.1684	1	0.1683	0.24	0.001191	0.009612	0.1684	1
0.1722	0.4793	0.001564	0.009788	0.1723	1	0.1722	0.2337	0.001192	0.009788	0.1723	1
0.1761	0.4699	0.001513	0.009965	0.1762	1	0.1761	0.224	0.00104	0.009965	0.1762	1
0.18	0.4604	0.001403	0.01014	0.18	1	0.18	0.2208	0.001115	0.01014	0.18	1
0.1838	0.4514	0.001492	0.01032	0.1839	1	0.1838	0.213	0.000971	0.01032	0.1839	1
0.1877	0.4432	0.001227	0.0105	0.1877	1	0.1877	0.2093	0.000984	0.0105	0.1877	1
0.1916	0.4355	0.001263	0.01068	0.1916	1	0.1916	0.2033	0.001078	0.01068	0.1916	1
0.1954	0.4262	0.001255	0.01086	0.1954	1	0.1954	0.1981	0.000941	0.01086	0.1954	1
0.1992	0.4179	0.001362	0.01104	0.1993	1	0.1992	0.1949	0.000977	0.01104	0.1993	1
0.2031	0.4097	0.001276	0.01122	0.2031	1	0.2031	0.19	0.000937	0.01122	0.2031	1
0.2069	0.4055	0.001281	0.0114	0.2069	1	0.2069	0.1872	0.000958	0.0114	0.2069	1
0.2107	0.3971	0.001259	0.01158	0.2108	1	0.2107	0.1818	0.000964	0.01158	0.2108	1
0.2145	0.389	0.001163	0.01176	0.2146	1	0.2145	0.18	0.000893	0.01176	0.2146	1
0.2184	0.3827	0.001192	0.01194	0.2184	1	0.2184	0.1772	0.000922	0.01194	0.2184	1
0.2222	0.3761	0.001193	0.01212	0.2222	1	0.2222	0.174	0.00089	0.01212	0.2222	1
0.226	0.3741	0.001127	0.0123	0.226	1	0.226	0.1721	0.000838	0.0123	0.226	1
0.2297	0.3639	0.001087	0.01248	0.2298	1	0.2297	0.1692	0.000976	0.01248	0.2298	1
0.2335	0.3583	0.001083	0.01266	0.2336	1	0.2335	0.1665	0.000846	0.01266	0.2336	1
0.2373	0.3535	0.001211	0.01284	0.2373	1	0.2373	0.1641	0.000841	0.01284	0.2373	1
0.2411	0.3476	0.001292	0.01302	0.2411	1	0.2411	0.1624	0.000898	0.01302	0.2411	1
0.2448	0.3446	0.001172	0.0132	0.2449	1	0.2448	0.1592	0.000844	0.0132	0.2449	1
0.2486	0.3404	0.001178	0.01338	0.2486	1	0.2486	0.1584	0.000877	0.01338	0.2486	1
0.2523	0.3383	0.001276	0.01356	0.2524	1	0.2523	0.1563	0.000925	0.01356	0.2524	1
0.2561	0.3333	0.001264	0.01374	0.2561	1	0.2561	0.1567	0.000982	0.01374	0.2561	1
0.2598	0.3296	0.001161	0.01392	0.2598	1	0.2598	0.1538	0.000863	0.01392	0.2598	1
0.2635	0.3251	0.001283	0.0141	0.2636	1	0.2635	0.1517	0.000897	0.0141	0.2636	1
0.2673	0.3186	0.00128	0.01428	0.2673	1	0.2673	0.1498	0.000978	0.01428	0.2673	1
0.271	0.3154	0.001163	0.01446	0.271	1	0.271	0.1496	0.000968	0.01446	0.271	1
0.2747	0.314	0.001286	0.01464	0.2747	1	0.2747	0.1467	0.000985	0.01464	0.2747	1
0.2784	0.3063	0.001257	0.01482	0.2784	1	0.2784	0.145	0.000901	0.01482	0.2784	1
0.282	0.3067	0.001174	0.015	0.2821	1	0.282	0.1457	0.001082	0.015	0.2821	1
0.2857	0.3014	0.001171	0.01518	0.2857	1	0.2857	0.1447	0.000907	0.01518	0.2857	1
0.2894	0.2998	0.001238	0.01536	0.2894	1	0.2894	0.1437	0.000945	0.01536	0.2894	1
0.293	0.2964	0.001325	0.01554	0.2931	1	0.293	0.1422	0.000949	0.01554	0.2931	1
0.2967	0.2903	0.001249	0.01572	0.2967	1	0.2967	0.1406	0.000996	0.01572	0.2967	1
0.3003	0.2899	0.001291	0.0159	0.3004	1	0.3003	0.139	0.000995	0.0159	0.3004	1
0.304	0.2862	0.001257	0.01607	0.304	1	0.304	0.1394	0.001023	0.01607	0.304	1
0.3076	0.2831	0.001255	0.01625	0.3076	1	0.3076	0.1384	0.001013	0.01625	0.3076	1
0.3112	0.2824	0.001253	0.01643	0.3113	1	0.3112	0.1376	0.001043	0.01643	0.3113	1
0.3148	0.2817	0.001097	0.01661	0.3149	1	0.3148	0.1357	0.000844	0.01661	0.3149	1
0.3184	0.2787	0.00138	0.01678	0.3185	1	0.3184	0.1329	0.000895	0.01678	0.3185	1
0.322	0.2756	0.001201	0.01696	0.3221	1	0.322	0.1339	0.000879	0.01696	0.3221	1
0.3256	0.271	0.001158	0.01714	0.3256	1	0.3256	0.1338	0.001016	0.01714	0.3256	1
0.3292	0.2713	0.001184	0.01731	0.3292	1	0.3292	0.1342	0.000984	0.01731	0.3292	1
0.3327	0.2685	0.001255	0.01749	0.3328	1	0.3327	0.1327	0.00111	0.01749	0.3328	1
0.3363	0.2649	0.001122	0.01766	0.3363	1	0.3363	0.1335	0.001017	0.01766	0.3363	1
0.3399	0.2609	0.001231	0.01784	0.3399	1	0.3399	0.1307	0.000987	0.01784	0.3399	1
0.3434	0.2604	0.001247	0.01801	0.3434	1	0.3434	0.13	0.000981	0.01801	0.3434	1
0.3469	0.2579	0.001251	0.01819	0.3469	1	0.3469	0.1298	0.000955	0.01819	0.3469	1
0.3504	0.2582	0.001329	0.01836	0.3505	1	0.3504	0.1278	0.00094	0.01836	0.3505	1
0.3539	0.255	0.001233	0.01854	0.354	1	0.3539	0.1266	0.001039	0.01854	0.354	1
0.3574	0.2546	0.001126	0.01871	0.3575	1	0.3574	0.1281	0.000941	0.01871	0.3575	1
0.3609	0.2512	0.001263	0.01888	0.361	1	0.3609	0.1269	0.000991	0.01888	0.361	1
0.3644	0.2505	0.001116	0.01905	0.3644	1	0.3644	0.128	0.001012	0.01905	0.3644	1
0.3679	0.2483	0.001341	0.01923	0.3679	1	0.3679	0.1263	0.001012	0.01923	0.3679	1
0.3713	0.2474	0.001169	0.0194	0.3714	1	0.3713	0.1262	0.000934	0.0194	0.3714	1
0.3748	0.2446	0.001321	0.01957	0.3748	1	0.3748	0.1254	0.001003	0.01957	0.3748	1
0.3782	0.2446	0.001293	0.01974	0.3783	1	0.3782	0.1239	0.000892	0.01974	0.3783	1
0.3817	0.2429	0.00128	0.01991	0.3817	1	0.3817	0.1239	0.000871	0.01991	0.3817	1
0.3851	0.2406	0.001212	0.02008	0.3851	1	0.3851	0.1242	0.000905	0.02008	0.3851	1
0.3885	0.2386	0.001268	0.02025	0.3885	1	0.3885	0.1238	0.000996	0.02025	0.3885	1
0.3919	0.2378	0.001253	0.02042	0.3919	1	0.3919	0.1218	0.000863	0.02042	0.3919	1
0.3953	0.2369	0.001143	0.02059	0.3953	1	0.3953	0.1226	0.001014	0.02059	0.3953	1
0.3987	0.234	0.001156	0.02076	0.3987	1	0.3987	0.1221	0.000983	0.02076	0.3987	1
0.4021	0.2349	0.001245	0.02092	0.4021	1	0.4021	0.1223	0.000956	0.02092	0.4021	1
0.4054	0.2334	0.001213	0.02109	0.4054	1	0.4054	0.1215	0.000974	0.02109	0.4054	1

$\omega=9.54 \times 10^{-3}$ 17R4/D <sub>2</sub> O 11.9 °C					$\omega=9.54 \times 10^{-3}$ 17R4/D <sub>2</sub> O 21.3 °C						
Q	I(Q)	Std Dev(I(Q))	sigmaQ	meanQ	Shadow Factor	Q	I(Q)	Std Dev(I(Q))	sigmaQ	meanQ	Shadow Factor
0.003433	0.2354	0.1032	0.001068	0.003607	0.9568	0.003433	0.2356	0.09494	0.001068	0.003607	0.9568
0.003837	0.1736	0.08189	0.001071	0.003977	0.9999	0.003837	0.1921	0.0825	0.001071	0.003977	0.9999
0.004241	0.2405	0.06769	0.001072	0.004367	1	0.004241	0.2846	0.06498	0.001072	0.004367	1
0.004645	0.2466	0.0529	0.001074	0.00476	1	0.004645	0.2402	0.05798	0.001074	0.00476	1
0.005049	0.1713	0.04648	0.001077	0.005155	1	0.005049	0.2575	0.05117	0.001077	0.005155	1
0.005453	0.1721	0.04126	0.001081	0.005551	1	0.005453	0.1882	0.03614	0.001081	0.005551	1
0.005857	0.1391	0.03522	0.001085	0.005948	1	0.005857	0.1644	0.03145	0.001085	0.005948	1
0.006261	0.1182	0.03084	0.00109	0.006346	1	0.006261	0.1545	0.03005	0.00109	0.006346	1
0.006665	0.1526	0.0256	0.001096	0.006745	1	0.006665	0.1642	0.02472	0.001096	0.006745	1
0.007069	0.177	0.02504	0.001101	0.007144	1	0.007069	0.1737	0.02149	0.001101	0.007144	1
0.007473	0.1575	0.02118	0.001108	0.007544	1	0.007473	0.149	0.02223	0.001108	0.007544	1
0.007876	0.1431	0.01796	0.001115	0.007944	1	0.007876	0.1671	0.02098	0.001115	0.007944	1
0.00828	0.1773	0.01883	0.001122	0.008345	1	0.00828	0.1808	0.01814	0.001122	0.008345	1
0.008684	0.1629	0.01687	0.001129	0.008746	1	0.008684	0.171	0.01704	0.001129	0.008746	1
0.009088	0.1229	0.01676	0.001137	0.009147	1	0.009088	0.1245	0.01608	0.001137	0.009147	1
0.009492	0.1539	0.01601	0.001146	0.009548	1	0.009492	0.2015	0.01835	0.001146	0.009548	1
0.009896	0.1134	0.01697	0.001154	0.00995	1	0.009896	0.1351	0.01497	0.001154	0.00995	1
0.0103	0.1663	0.01375	0.001163	0.01035	1	0.0103	0.1728	0.01539	0.001163	0.01035	1
0.0107	0.1589	0.01437	0.001173	0.01075	1	0.0107	0.1555	0.01405	0.001173	0.01075	1
0.01111	0.1313	0.01348	0.001182	0.01116	1	0.01111	0.1564	0.01345	0.001182	0.01116	1
0.0113	0.1416	0.005718	0.00217	0.01149	1	0.0113	0.1508	0.006447	0.00217	0.01149	1
0.01151	0.1495	0.01391	0.001192	0.01156	1	0.01151	0.1748	0.01348	0.001192	0.01156	1
0.01192	0.1566	0.01283	0.001202	0.01196	1	0.01192	0.173	0.01193	0.001202	0.01196	1
0.01232	0.137	0.01192	0.001213	0.01236	1	0.01232	0.1382	0.01179	0.001213	0.01236	1
0.01263	0.1476	0.005194	0.002186	0.0128	1	0.01263	0.1529	0.005486	0.002186	0.0128	1
0.01272	0.1576	0.01194	0.001223	0.01277	1	0.01272	0.1584	0.01194	0.001223	0.01277	1
0.01313	0.1407	0.01201	0.001234	0.01317	1	0.01313	0.1568	0.01165	0.001234	0.01317	1
0.01353	0.1634	0.0115	0.001246	0.01357	1	0.01353	0.1612	0.01165	0.001246	0.01357	1
0.01393	0.1613	0.01103	0.001257	0.01397	1	0.01393	0.1503	0.01078	0.001257	0.01397	1
0.01396	0.1466	0.004453	0.002205	0.01412	1	0.01396	0.1517	0.00461	0.002205	0.01412	1
0.01434	0.1389	0.01131	0.001269	0.01438	1	0.01434	0.1577	0.01253	0.001269	0.01438	1
0.01474	0.1366	0.01086	0.001281	0.01478	1	0.01474	0.1728	0.01034	0.001281	0.01478	1
0.01515	0.1455	0.0108	0.001293	0.01518	1	0.01515	0.155	0.01055	0.001293	0.01518	1
0.01529	0.1415	0.0043	0.002226	0.01543	1	0.01529	0.1457	0.004337	0.002226	0.01543	1
0.01555	0.1619	0.01031	0.001305	0.01558	1	0.01555	0.17	0.01149	0.001305	0.01558	1
0.01595	0.1509	0.0102	0.001318	0.01599	1	0.01595	0.1439	0.01091	0.001318	0.01599	1
0.01636	0.1287	0.01069	0.001331	0.01639	1	0.01636	0.1646	0.01165	0.001331	0.01639	1
0.01662	0.1353	0.003842	0.002249	0.01675	1	0.01662	0.1513	0.004251	0.002249	0.01675	1
0.01676	0.1284	0.01019	0.001344	0.01679	1	0.01676	0.1422	0.01014	0.001344	0.01679	1
0.01717	0.133	0.01007	0.001357	0.0172	1	0.01717	0.151	0.01055	0.001357	0.0172	1
0.01757	0.1368	0.009746	0.00137	0.0176	1	0.01757	0.1539	0.0107	0.00137	0.0176	1
0.01795	0.1387	0.003818	0.002275	0.01807	1	0.01795	0.1449	0.004503	0.002275	0.01807	1
0.01797	0.134	0.01	0.001384	0.018	1	0.01797	0.1408	0.0104	0.001384	0.018	1
0.01838	0.1392	0.008743	0.001397	0.01841	1	0.01838	0.1414	0.00979	0.001397	0.01841	1
0.01878	0.148	0.0109	0.001411	0.01881	1	0.01878	0.147	0.0106	0.001411	0.01881	1
0.01918	0.147	0.01091	0.001425	0.01921	1	0.01918	0.1412	0.01071	0.001425	0.01921	1
0.01928	0.1362	0.003754	0.002302	0.01939	1	0.01928	0.144	0.00357	0.002302	0.01939	1
0.01959	0.1433	0.009319	0.00144	0.01962	1	0.01959	0.1521	0.009906	0.00144	0.01962	1
0.01999	0.1305	0.0104	0.001454	0.02002	1	0.01999	0.144	0.009963	0.001454	0.02002	1
0.0204	0.1416	0.009073	0.001468	0.02042	1	0.0204	0.1545	0.01074	0.001468	0.02042	1
0.02061	0.1346	0.003586	0.002331	0.02072	1	0.02061	0.1445	0.003479	0.002331	0.02072	1
0.0208	0.1379	0.009707	0.001483	0.02083	1	0.0208	0.1544	0.01031	0.001483	0.02083	1
0.0212	0.1332	0.01032	0.001498	0.02123	1	0.0212	0.1462	0.009662	0.001498	0.02123	1
0.02161	0.1361	0.01002	0.001513	0.02163	1	0.02161	0.143	0.009788	0.001513	0.02163	1
0.02194	0.1336	0.003195	0.002362	0.02204	1	0.02194	0.1398	0.003605	0.002362	0.02204	1
0.02201	0.1363	0.009615	0.001528	0.02203	1	0.02201	0.1396	0.01043	0.001528	0.02203	1
0.02241	0.1514	0.009763	0.001543	0.02244	1	0.02241	0.143	0.009861	0.001543	0.02244	1
0.02282	0.1333	0.009945	0.001558	0.02284	1	0.02282	0.1289	0.01034	0.001558	0.02284	1
0.02322	0.132	0.009095	0.001574	0.02324	1	0.02322	0.1391	0.01022	0.001574	0.02324	1
0.02327	0.1282	0.00288	0.002394	0.02336	1	0.02327	0.1359	0.003112	0.002394	0.02336	1
0.02363	0.1404	0.009151	0.001589	0.02365	1	0.02363	0.1361	0.009472	0.001589	0.02365	1
0.02403	0.1399	0.009255	0.001605	0.02405	1	0.02403	0.1334	0.009803	0.001605	0.02405	1
0.02443	0.1373	0.008282	0.001621	0.02445	1	0.02443	0.1383	0.009324	0.001621	0.02445	1
0.0246	0.1298	0.00307	0.002428	0.02469	1	0.0246	0.1305	0.00316	0.002428	0.02469	1
0.02484	0.1453	0.01028	0.001637	0.02486	1	0.02484	0.1535	0.009948	0.001637	0.02486	1
0.02524	0.1283	0.01008	0.001653	0.02526	1	0.02524	0.1349	0.01097	0.001653	0.02526	1
0.02564	0.1452	0.0109	0.001669	0.02566	1	0.02564	0.1584	0.01059	0.001669	0.02566	1
0.02593	0.1247	0.002982	0.002464	0.02601	1	0.02593	0.1369	0.003186	0.002464	0.02601	1
0.02605	0.1318	0.011	0.001685	0.02607	1	0.02605	0.1368	0.01093	0.001685	0.02607	1
0.02645	0.1376	0.01128	0.001701	0.02647	1	0.02645	0.1612	0.01083	0.001701	0.02647	1
0.02685	0.1446	0.01217	0.001718	0.02687	1	0.02685	0.1266	0.01134	0.001718	0.02687	1
0.02726	0.1268	0.002939	0.0025	0.02734	1	0.02726	0.1343	0.002848	0.0025	0.02734	1
0.02726	0.1265	0.01249	0.001734	0.02728	1	0.02726	0.1258	0.01105	0.001734	0.02728	1
0.02766	0.1572	0.01123	0.001751	0.02768	1	0.02766	0.1442	0.01086	0.001751	0.02768	1
0.02807	0.1357	0.01153	0.001767	0.02808	1	0.02807	0.1434	0.01209	0.001767	0.02808	1
0.02847	0.1283	0.01248	0.001784	0.02849	1	0.02847	0.1368	0.0132	0.001784	0.02849	1
0.02859	0.1269	0.002689	0.002538	0.02866	1	0.02859	0.1273	0.002731	0.002538	0.02866	1
0.02887	0.1678	0.01498	0.001801	0.02889	1	0.02887	0.1451	0.01246	0.001801	0.02889	1
0.02928	0.1303	0.01233	0.001818	0.02929	1	0.02928	0.1517	0.01162	0.001818	0.02929	1
0.02968	0.1344	0.01305	0.001835	0.0297	1	0.02968	0.1318	0.01272	0.001835	0.0297	1
0.02991	0.1271	0.002569	0.002578	0.02999	1	0.02991	0.1308	0.00291	0.002578	0.02999	1

$\omega=9.54 \times 10^{-3}$ 17R4/D <sub>2</sub> O 11.9 °C					$\omega=9.54 \times 10^{-3}$ 17R4/D <sub>2</sub> O 21.3 °C						
Q	I(Q)	Std Dev(I(Q))	sigmaQ	meanQ	Shadow Factor	Q	I(Q)	Std Dev(I(Q))	sigmaQ	meanQ	Shadow Factor
0.03008	0.1319	0.01084	0.001852	0.0301	1	0.03008	0.1409	0.01185	0.001852	0.0301	1
0.03049	0.126	0.01196	0.001869	0.0305	1	0.03049	0.1308	0.01249	0.001869	0.0305	1
0.03089	0.1178	0.01283	0.001886	0.03091	1	0.03089	0.1523	0.01453	0.001886	0.03091	1
0.03124	0.1266	0.002717	0.002618	0.03131	1	0.03124	0.1309	0.002929	0.002618	0.03131	1
0.03129	0.1342	0.01225	0.001903	0.03131	1	0.03129	0.1229	0.0109	0.001903	0.03131	1
0.0317	0.1229	0.01121	0.00192	0.03171	1	0.0317	0.1376	0.01253	0.00192	0.03171	1
0.0321	0.1286	0.01219	0.001938	0.03212	1	0.0321	0.1321	0.01414	0.001938	0.03212	1
0.0325	0.1238	0.01331	0.001955	0.03252	1	0.0325	0.1536	0.01274	0.001955	0.03252	1
0.03257	0.1269	0.002566	0.00266	0.03264	1	0.03257	0.1327	0.002667	0.00266	0.03264	1
0.03291	0.1271	0.0112	0.001973	0.03292	1	0.03291	0.1399	0.01216	0.001973	0.03292	1
0.03331	0.1237	0.01197	0.00199	0.03333	1	0.03331	0.1415	0.01213	0.00199	0.03333	1
0.03372	0.138	0.01306	0.002008	0.03373	1	0.03372	0.1265	0.01348	0.002008	0.03373	1
0.0339	0.1208	0.002662	0.002703	0.03396	1	0.0339	0.1271	0.002632	0.002703	0.03396	1
0.03399	0.1265	0.001372	0.0047	0.03426	1	0.03399	0.1302	0.001378	0.0047	0.03426	1
0.03523	0.1222	0.002688	0.002746	0.03529	1	0.03523	0.127	0.002252	0.002746	0.03529	1
0.03656	0.1209	0.002406	0.002791	0.03662	1	0.03656	0.1301	0.002639	0.002791	0.03662	1
0.03788	0.1232	0.002296	0.002837	0.03794	1	0.03788	0.1244	0.002386	0.002837	0.03794	1
0.03798	0.1234	0.00125	0.004775	0.03823	1	0.03798	0.1285	0.001339	0.004775	0.03823	1
0.03921	0.1243	0.002017	0.002883	0.03927	1	0.03921	0.1251	0.002461	0.002883	0.03927	1
0.04054	0.1194	0.002131	0.00293	0.04059	1	0.04054	0.1222	0.002451	0.00293	0.04059	1
0.04187	0.1184	0.002232	0.002979	0.04192	1	0.04187	0.1245	0.002399	0.002979	0.04192	1
0.04197	0.1199	0.001325	0.004859	0.0422	1	0.04197	0.1271	0.001283	0.004859	0.0422	1
0.0432	0.119	0.001975	0.003027	0.04325	1	0.0432	0.1222	0.002152	0.003027	0.04325	1
0.04452	0.1184	0.002251	0.003077	0.04457	1	0.04452	0.1217	0.002221	0.003077	0.04457	1
0.04585	0.1164	0.002095	0.003127	0.0459	1	0.04585	0.1144	0.002194	0.003127	0.0459	1
0.04597	0.1181	0.001102	0.00495	0.04617	1	0.04597	0.1217	0.00132	0.00495	0.04617	1
0.04718	0.1148	0.001943	0.003178	0.04722	1	0.04718	0.1215	0.002262	0.003178	0.04722	1
0.0485	0.1141	0.001978	0.00323	0.04855	1	0.0485	0.1161	0.001957	0.00323	0.04855	1
0.04983	0.1118	0.001857	0.003282	0.04987	1	0.04983	0.1198	0.002137	0.003282	0.04987	1
0.04996	0.1154	0.001218	0.005048	0.05014	1	0.04996	0.1204	0.001113	0.005048	0.05014	1
0.05116	0.1122	0.001978	0.003334	0.0512	1	0.05116	0.1163	0.001815	0.003334	0.0512	1
0.05248	0.112	0.001946	0.003388	0.05252	1	0.05248	0.113	0.001905	0.003388	0.05252	1
0.05381	0.1112	0.00207	0.003441	0.05385	1	0.05381	0.1166	0.00182	0.003441	0.05385	1
0.05394	0.1127	0.001198	0.005152	0.05412	1	0.05394	0.1172	0.001249	0.005152	0.05412	1
0.05514	0.1062	0.001788	0.003495	0.05517	1	0.05514	0.1158	0.001992	0.003495	0.05517	1
0.05646	0.11	0.00191	0.00355	0.0565	1	0.05646	0.1152	0.001884	0.00355	0.0565	1
0.05779	0.1121	0.001656	0.003605	0.05782	1	0.05779	0.1114	0.001777	0.003605	0.05782	1
0.05793	0.1098	0.001118	0.005262	0.05809	1	0.05793	0.1142	0.001214	0.005262	0.05809	1
0.05911	0.1082	0.00189	0.00366	0.05915	1	0.05911	0.1144	0.001891	0.00366	0.05915	1
0.06044	0.1023	0.001698	0.003716	0.06047	1	0.06044	0.1103	0.001739	0.003716	0.06047	1
0.06176	0.1052	0.00175	0.003772	0.0618	1	0.06176	0.1076	0.001764	0.003772	0.0618	1
0.06192	0.1082	0.001077	0.005378	0.06207	1	0.06192	0.1131	0.001059	0.005378	0.06207	1
0.06309	0.1037	0.00178	0.003829	0.06312	1	0.06309	0.1099	0.001838	0.003829	0.06312	1
0.06441	0.1074	0.001662	0.003886	0.06444	1	0.06441	0.1086	0.001725	0.003886	0.06444	1
0.06573	0.1041	0.001636	0.003943	0.06577	1	0.06573	0.1063	0.001736	0.003943	0.06577	1
0.0659	0.1058	0.001135	0.005499	0.06604	1	0.0659	0.1087	0.001094	0.005499	0.06604	1
0.06706	0.1015	0.001738	0.004001	0.06709	1	0.06706	0.1079	0.00162	0.004001	0.06709	1
0.06838	0.09862	0.001521	0.004059	0.06841	1	0.06838	0.1045	0.001766	0.004059	0.06841	1
0.06971	0.1005	0.001652	0.004117	0.06974	1	0.06971	0.1048	0.00164	0.004117	0.06974	1
0.06988	0.1024	0.001004	0.005624	0.07001	1	0.06988	0.105	0.001042	0.005624	0.07001	1
0.07103	0.1025	0.00154	0.004175	0.07106	1	0.07103	0.1056	0.001691	0.004175	0.07106	1
0.07235	0.102	0.001585	0.004234	0.07238	1	0.07235	0.1047	0.001571	0.004234	0.07238	1
0.07367	0.1012	0.001453	0.004293	0.0737	1	0.07367	0.102	0.001599	0.004293	0.0737	1
0.07386	0.1006	0.000987	0.005754	0.07399	1	0.07386	0.1007	0.000995	0.005754	0.07399	1
0.075	0.09919	0.001551	0.004352	0.07503	1	0.075	0.1001	0.001676	0.004352	0.07503	1
0.07632	0.09893	0.001452	0.004411	0.07635	1	0.07632	0.101	0.001523	0.004411	0.07635	1
0.07764	0.09523	0.001503	0.004471	0.07767	1	0.07764	0.1011	0.001495	0.004471	0.07767	1
0.07784	0.09599	0.000987	0.005888	0.07796	1	0.07784	0.1007	0.000919	0.005888	0.07796	1
0.07896	0.09536	0.001532	0.004531	0.07899	1	0.07896	0.1004	0.001635	0.004531	0.07899	1
0.08028	0.09518	0.001598	0.004591	0.08031	1	0.08028	0.0986	0.001594	0.004591	0.08031	1
0.08161	0.09412	0.001718	0.004651	0.08163	1	0.08161	0.09479	0.001562	0.004651	0.08163	1
0.08181	0.09602	0.000862	0.006026	0.08192	1	0.08181	0.09711	0.000958	0.006026	0.08192	1
0.08293	0.09476	0.001701	0.004711	0.08295	1	0.08293	0.09469	0.001725	0.004711	0.08295	1
0.08425	0.09114	0.001566	0.004772	0.08427	1	0.08425	0.09371	0.00169	0.004772	0.08427	1
0.08557	0.09278	0.001704	0.004833	0.08559	1	0.08557	0.09145	0.001748	0.004833	0.08559	1
0.08578	0.09119	0.00103	0.006167	0.08589	1	0.08578	0.09609	0.000879	0.006167	0.08589	1
0.08689	0.08883	0.001777	0.004893	0.08691	1	0.08689	0.09463	0.001976	0.004893	0.08691	1
0.08821	0.09071	0.002062	0.004954	0.08823	1	0.08821	0.0954	0.00209	0.004954	0.08823	1
0.08953	0.08976	0.002129	0.005016	0.08955	1	0.08953	0.09065	0.002059	0.005016	0.08955	1
0.08975	0.09155	0.000824	0.006312	0.08985	1	0.08975	0.09346	0.000807	0.006312	0.08985	1
0.09084	0.08781	0.002101	0.005077	0.09087	1	0.09084	0.09363	0.002163	0.005077	0.09087	1
0.09371	0.08872	0.000859	0.006459	0.09381	1	0.09371	0.09187	0.000754	0.006459	0.09381	1
0.09768	0.08669	0.000808	0.006609	0.09777	1	0.09768	0.08728	0.000941	0.006609	0.09777	1
0.1016	0.08531	0.000871	0.006762	0.1017	1	0.1016	0.08631	0.000815	0.006762	0.1017	1
0.1056	0.0827	0.000761	0.006917	0.1057	1	0.1056	0.08467	0.00091	0.006917	0.1057	1
0.1095	0.08154	0.000801	0.007075	0.1096	1	0.1095	0.08437	0.000823	0.007075	0.1096	1
0.1135	0.08091	0.000744	0.007234	0.1136	1	0.1135	0.08365	0.00077	0.007234	0.1136	1
0.1174	0.07999	0.000765	0.007396	0.1175	1	0.1174	0.08062	0.000784	0.007396	0.1175	1
0.1214	0.07794	0.000751	0.007559	0.1215	1	0.1214	0.07844	0.000766	0.007559	0.1215	1
0.1253	0.07631	0.000824	0.007723	0.1254	1	0.1253	0.07749	0.000767	0.007723	0.1254	1
0.1293	0.07527	0.000672	0.007889	0.1293	1	0.1293	0.07693	0.000685	0.007889	0.1293	1

$\omega=9.54 \times 10^{-3}$ 17R4/D <sub>2</sub> O 11.9 °C					$\omega=9.54 \times 10^{-3}$ 17R4/D <sub>2</sub> O 21.3 °C						
Q	I(Q)	Std Dev(I(Q))	sigmaQ	meanQ	Shadow Factor	Q	I(Q)	Std Dev(I(Q))	sigmaQ	meanQ	Shadow Factor
0.1332	0.07444	0.000682	0.008057	0.1333	1	0.1332	0.075	0.000701	0.008057	0.1333	1
0.1371	0.07286	0.000715	0.008226	0.1372	1	0.1371	0.07371	0.000701	0.008226	0.1372	1
0.141	0.07275	0.000687	0.008396	0.1411	1	0.141	0.07304	0.000753	0.008396	0.1411	1
0.1449	0.07188	0.000735	0.008567	0.145	1	0.1449	0.07189	0.000687	0.008567	0.145	1
0.1489	0.07054	0.000669	0.008739	0.1489	1	0.1489	0.07099	0.000675	0.008739	0.1489	1
0.1528	0.06948	0.000693	0.008912	0.1528	1	0.1528	0.07118	0.0007	0.008912	0.1528	1
0.1567	0.06934	0.0007	0.009086	0.1567	1	0.1567	0.06919	0.000663	0.009086	0.1567	1
0.1606	0.06761	0.000715	0.00926	0.1606	1	0.1606	0.06893	0.00068	0.00926	0.1606	1
0.1645	0.06647	0.000662	0.009436	0.1645	1	0.1645	0.06819	0.000657	0.009436	0.1645	1
0.1683	0.0664	0.0006	0.009612	0.1684	1	0.1683	0.06808	0.000643	0.009612	0.1684	1
0.1722	0.06715	0.000688	0.009788	0.1723	1	0.1722	0.0679	0.000629	0.009788	0.1723	1
0.1761	0.06555	0.000581	0.009965	0.1762	1	0.1761	0.06612	0.000648	0.009965	0.1762	1
0.18	0.0648	0.000616	0.01014	0.18	1	0.18	0.06438	0.000603	0.01014	0.18	1
0.1838	0.06465	0.000596	0.01032	0.1839	1	0.1838	0.06463	0.000598	0.01032	0.1839	1
0.1877	0.06494	0.000553	0.0105	0.1877	1	0.1877	0.06653	0.000598	0.0105	0.1877	1
0.1916	0.06366	0.00063	0.01068	0.1916	1	0.1916	0.06335	0.000595	0.01068	0.1916	1
0.1954	0.06325	0.00055	0.01086	0.1954	1	0.1954	0.06447	0.000554	0.01086	0.1954	1
0.1992	0.06305	0.000574	0.01104	0.1993	1	0.1992	0.06394	0.000606	0.01104	0.1993	1
0.2031	0.06324	0.000577	0.01122	0.2031	1	0.2031	0.06297	0.000577	0.01122	0.2031	1
0.2069	0.06257	0.000564	0.0114	0.2069	1	0.2069	0.06251	0.000569	0.0114	0.2069	1
0.2107	0.0615	0.000601	0.01158	0.2108	1	0.2107	0.06185	0.000574	0.01158	0.2108	1
0.2145	0.06169	0.000603	0.01176	0.2146	1	0.2145	0.06121	0.000538	0.01176	0.2146	1
0.2184	0.06153	0.000584	0.01194	0.2184	1	0.2184	0.06171	0.000523	0.01194	0.2184	1
0.2222	0.05992	0.000562	0.01212	0.2222	1	0.2222	0.06168	0.000505	0.01212	0.2222	1
0.226	0.06009	0.000539	0.0123	0.226	1	0.226	0.06105	0.000532	0.0123	0.226	1
0.2297	0.05959	0.000512	0.01248	0.2298	1	0.2297	0.06125	0.000536	0.01248	0.2298	1
0.2335	0.05994	0.000553	0.01266	0.2336	1	0.2335	0.06118	0.000541	0.01266	0.2336	1
0.2373	0.0599	0.000534	0.01284	0.2373	1	0.2373	0.06107	0.000516	0.01284	0.2373	1
0.2411	0.05874	0.000568	0.01302	0.2411	1	0.2411	0.06019	0.000578	0.01302	0.2411	1
0.2448	0.05905	0.000563	0.0132	0.2449	1	0.2448	0.05953	0.000588	0.0132	0.2449	1
0.2486	0.05924	0.000591	0.01338	0.2486	1	0.2486	0.06	0.000635	0.01338	0.2486	1
0.2523	0.05774	0.000592	0.01356	0.2524	1	0.2523	0.0592	0.000617	0.01356	0.2524	1
0.2561	0.058	0.000608	0.01374	0.2561	1	0.2561	0.05857	0.000631	0.01374	0.2561	1
0.2598	0.05906	0.000591	0.01392	0.2598	1	0.2598	0.05884	0.000619	0.01392	0.2598	1
0.2635	0.05854	0.000653	0.0141	0.2636	1	0.2635	0.0586	0.000707	0.0141	0.2636	1
0.2673	0.05863	0.000535	0.01428	0.2673	1	0.2673	0.05755	0.000554	0.01428	0.2673	1
0.271	0.05731	0.000625	0.01446	0.271	1	0.271	0.05859	0.000629	0.01446	0.271	1
0.2747	0.05794	0.000673	0.01464	0.2747	1	0.2747	0.05717	0.00068	0.01464	0.2747	1
0.2784	0.05675	0.000655	0.01482	0.2784	1	0.2784	0.05777	0.000664	0.01482	0.2784	1
0.282	0.05708	0.000681	0.015	0.2821	1	0.282	0.05764	0.000752	0.015	0.2821	1
0.2857	0.05636	0.000623	0.01518	0.2857	1	0.2857	0.05624	0.000639	0.01518	0.2857	1
0.2894	0.05571	0.00063	0.01536	0.2894	1	0.2894	0.05677	0.000627	0.01536	0.2894	1
0.293	0.05588	0.000597	0.01554	0.2931	1	0.293	0.05607	0.000623	0.01554	0.2931	1
0.2967	0.05569	0.000678	0.01572	0.2967	1	0.2967	0.05798	0.000601	0.01572	0.2967	1
0.3003	0.05669	0.000674	0.0159	0.3004	1	0.3003	0.05654	0.000709	0.0159	0.3004	1
0.304	0.05469	0.000633	0.01607	0.304	1	0.304	0.0551	0.000648	0.01607	0.304	1
0.3076	0.05497	0.000698	0.01625	0.3076	1	0.3076	0.05636	0.000674	0.01625	0.3076	1
0.3112	0.05537	0.000603	0.01643	0.3113	1	0.3112	0.05455	0.000635	0.01643	0.3113	1
0.3148	0.05575	0.000716	0.01661	0.3149	1	0.3148	0.05567	0.000702	0.01661	0.3149	1
0.3184	0.05584	0.000682	0.01678	0.3185	1	0.3184	0.05738	0.000629	0.01678	0.3185	1
0.322	0.05504	0.000613	0.01696	0.3221	1	0.322	0.05611	0.000602	0.01696	0.3221	1
0.3256	0.05547	0.000609	0.01714	0.3256	1	0.3256	0.05515	0.000626	0.01714	0.3256	1
0.3292	0.05476	0.000688	0.01731	0.3292	1	0.3292	0.05481	0.000654	0.01731	0.3292	1
0.3327	0.05498	0.000693	0.01749	0.3328	1	0.3327	0.05431	0.000744	0.01749	0.3328	1
0.3363	0.05443	0.000618	0.01766	0.3363	1	0.3363	0.05501	0.000621	0.01766	0.3363	1
0.3399	0.05394	0.000578	0.01784	0.3399	1	0.3399	0.05515	0.000623	0.01784	0.3399	1
0.3434	0.05469	0.000682	0.01801	0.3434	1	0.3434	0.05466	0.000651	0.01801	0.3434	1
0.3469	0.05406	0.000659	0.01819	0.3469	1	0.3469	0.05386	0.000657	0.01819	0.3469	1
0.3504	0.05291	0.000657	0.01836	0.3505	1	0.3504	0.05412	0.000706	0.01836	0.3505	1
0.3539	0.05395	0.000681	0.01854	0.354	1	0.3539	0.0549	0.000617	0.01854	0.354	1
0.3574	0.05367	0.000658	0.01871	0.3575	1	0.3574	0.05403	0.000675	0.01871	0.3575	1
0.3609	0.05449	0.00068	0.01888	0.361	1	0.3609	0.05398	0.000669	0.01888	0.361	1
0.3644	0.05434	0.000628	0.01905	0.3644	1	0.3644	0.05415	0.000627	0.01905	0.3644	1
0.3679	0.05552	0.000608	0.01923	0.3679	1	0.3679	0.05499	0.000658	0.01923	0.3679	1
0.3713	0.05377	0.000638	0.0194	0.3714	1	0.3713	0.05366	0.000719	0.0194	0.3714	1
0.3748	0.05448	0.000599	0.01957	0.3748	1	0.3748	0.0535	0.000651	0.01957	0.3748	1
0.3782	0.0545	0.000602	0.01974	0.3783	1	0.3782	0.05274	0.000667	0.01974	0.3783	1
0.3817	0.05214	0.000663	0.01991	0.3817	1	0.3817	0.05304	0.000652	0.01991	0.3817	1
0.3851	0.05394	0.000628	0.02008	0.3851	1	0.3851	0.0532	0.000637	0.02008	0.3851	1
0.3885	0.05311	0.000682	0.02025	0.3885	1	0.3885	0.05416	0.000663	0.02025	0.3885	1
0.3919	0.05318	0.000688	0.02042	0.3919	1	0.3919	0.05367	0.000691	0.02042	0.3919	1
0.3953	0.05276	0.000728	0.02059	0.3953	1	0.3953	0.05268	0.000634	0.02059	0.3953	1
0.3987	0.05192	0.000577	0.02076	0.3987	1	0.3987	0.05238	0.000693	0.02076	0.3987	1
0.4021	0.05244	0.000676	0.02092	0.4021	1	0.4021	0.05293	0.000671	0.02092	0.4021	1
0.4054	0.05273	0.000723	0.02109	0.4054	1	0.4054	0.05416	0.000606	0.02109	0.4054	1

$\omega=9.54 \times 10^{-3}$ 17R4/D <sub>2</sub> O 30.6 °C					$\omega=9.54 \times 10^{-3}$ 17R4/D <sub>2</sub> O 39.9 °C						
Q	I(Q)	Std Dev(I(Q))	sigmaQ	meanQ	Shadow Factor	Q	I(Q)	Std Dev(I(Q))	sigmaQ	meanQ	Shadow Factor
0.003433	0.4267	0.1587	0.001068	0.003607	0.9568	0.003433	10.07	0.3273	0.001068	0.003607	0.9568
0.003837	0.4079	0.1145	0.001071	0.003977	0.9999	0.003837	8.801	0.2646	0.001071	0.003977	0.9999
0.004241	0.5092	0.09392	0.001072	0.004367	1	0.004241	7.244	0.1934	0.001072	0.004367	1
0.004645	0.4291	0.08223	0.001074	0.00476	1	0.004645	6.059	0.1618	0.001074	0.00476	1
0.005049	0.3275	0.06661	0.001077	0.005155	1	0.005049	4.979	0.1468	0.001077	0.005155	1
0.005453	0.244	0.05561	0.001081	0.005551	1	0.005453	4.336	0.1358	0.001081	0.005551	1
0.005857	0.1987	0.04947	0.001085	0.005948	1	0.005857	3.849	0.1083	0.001085	0.005948	1
0.006261	0.2017	0.04717	0.00109	0.006346	1	0.006261	3.224	0.1052	0.00109	0.006346	1
0.006665	0.2287	0.04418	0.001096	0.006745	1	0.006665	2.776	0.09355	0.001096	0.006745	1
0.007069	0.2557	0.04097	0.001101	0.007144	1	0.007069	2.369	0.08158	0.001101	0.007144	1
0.007473	0.2583	0.03579	0.001108	0.007544	1	0.007473	1.969	0.07701	0.001108	0.007544	1
0.007876	0.2	0.03402	0.001115	0.007944	1	0.007876	1.837	0.0733	0.001115	0.007944	1
0.00828	0.2476	0.03053	0.001122	0.008345	1	0.00828	1.545	0.06183	0.001122	0.008345	1
0.008684	0.2505	0.0318	0.001129	0.008746	1	0.008684	1.253	0.05651	0.001129	0.008746	1
0.009088	0.2068	0.02941	0.001137	0.009147	1	0.009088	1.021	0.04521	0.001137	0.009147	1
0.009492	0.2118	0.02885	0.001146	0.009548	1	0.009492	0.8529	0.04494	0.001146	0.009548	1
0.009896	0.2056	0.02456	0.001154	0.00995	1	0.009896	0.7644	0.03899	0.001154	0.00995	1
0.0103	0.1758	0.02586	0.001163	0.01035	1	0.0103	0.6432	0.03895	0.001163	0.01035	1
0.0107	0.2328	0.02447	0.001173	0.01075	1	0.0107	0.5814	0.03502	0.001173	0.01075	1
0.01111	0.2008	0.02324	0.001182	0.01116	1	0.01111	0.5598	0.03368	0.001182	0.01116	1
0.0113	0.176	0.007724	0.00217	0.01149	1	0.0113	0.5712	0.01632	0.00217	0.01149	1
0.01151	0.2131	0.02321	0.001192	0.01156	1	0.01151	0.4567	0.02954	0.001192	0.01156	1
0.01192	0.1941	0.02254	0.001202	0.01196	1	0.01192	0.4433	0.02825	0.001202	0.01196	1
0.01232	0.165	0.01939	0.001213	0.01236	1	0.01232	0.3823	0.02529	0.001213	0.01236	1
0.01263	0.1772	0.006474	0.002186	0.0128	1	0.01263	0.4029	0.009394	0.002186	0.0128	1
0.01272	0.1755	0.02121	0.001223	0.01277	1	0.01272	0.3427	0.02621	0.001223	0.01277	1
0.01313	0.1717	0.0175	0.001234	0.01317	1	0.01313	0.367	0.02397	0.001234	0.01317	1
0.01353	0.1807	0.01856	0.001246	0.01357	1	0.01353	0.3795	0.02471	0.001246	0.01357	1
0.01393	0.197	0.01844	0.001257	0.01397	1	0.01393	0.2892	0.02201	0.001257	0.01397	1
0.01396	0.1676	0.005821	0.002205	0.01412	1	0.01396	0.3039	0.007439	0.002205	0.01412	1
0.01434	0.1468	0.01776	0.001269	0.01438	1	0.01434	0.26	0.02034	0.001269	0.01438	1
0.01474	0.1826	0.01895	0.001281	0.01478	1	0.01474	0.3251	0.02444	0.001281	0.01478	1
0.01515	0.1793	0.0179	0.001293	0.01518	1	0.01515	0.2641	0.02037	0.001293	0.01518	1
0.01529	0.1578	0.004846	0.002226	0.01543	1	0.01529	0.2645	0.005757	0.002226	0.01543	1
0.01555	0.1612	0.01685	0.001305	0.01558	1	0.01555	0.2497	0.01944	0.001305	0.01558	1
0.01595	0.1615	0.01739	0.001318	0.01599	1	0.01595	0.2307	0.0199	0.001318	0.01599	1
0.01636	0.1774	0.01871	0.001331	0.01639	1	0.01636	0.2401	0.02046	0.001331	0.01639	1
0.01662	0.1567	0.00498	0.002249	0.01675	1	0.01662	0.2319	0.005004	0.002249	0.01675	1
0.01676	0.1703	0.01745	0.001344	0.01679	1	0.01676	0.2374	0.01947	0.001344	0.01679	1
0.01717	0.1497	0.01586	0.001357	0.0172	1	0.01717	0.2009	0.01794	0.001357	0.0172	1
0.01757	0.1804	0.01759	0.00137	0.0176	1	0.01757	0.2478	0.0189	0.00137	0.0176	1
0.01795	0.1578	0.004524	0.002275	0.01807	1	0.01795	0.2062	0.004846	0.002275	0.01807	1
0.01797	0.139	0.01684	0.001384	0.018	1	0.01797	0.1766	0.01679	0.001384	0.018	1
0.01838	0.1255	0.01384	0.001397	0.01841	1	0.01838	0.1966	0.01764	0.001397	0.01841	1
0.01878	0.1631	0.01721	0.001411	0.01881	1	0.01878	0.1925	0.01794	0.001411	0.01881	1
0.01918	0.1723	0.01724	0.001425	0.01921	1	0.01918	0.182	0.01873	0.001425	0.01921	1
0.01928	0.1524	0.004334	0.002302	0.01939	1	0.01928	0.1849	0.004887	0.002302	0.01939	1
0.01959	0.1741	0.01641	0.00144	0.01962	1	0.01959	0.1923	0.0162	0.00144	0.01962	1
0.01999	0.1363	0.015	0.001454	0.02002	1	0.01999	0.2193	0.01922	0.001454	0.02002	1
0.0204	0.1701	0.01692	0.001468	0.02042	1	0.0204	0.1878	0.01774	0.001468	0.02042	1
0.02061	0.1488	0.003904	0.002331	0.02072	1	0.02061	0.1782	0.003852	0.002331	0.02072	1
0.0208	0.1621	0.01588	0.001483	0.02083	1	0.0208	0.1865	0.01719	0.001483	0.02083	1
0.0212	0.1648	0.01734	0.001498	0.02123	1	0.0212	0.1939	0.01813	0.001498	0.02123	1
0.02161	0.1664	0.01653	0.001513	0.02163	1	0.02161	0.1685	0.01686	0.001513	0.02163	1
0.02194	0.144	0.004008	0.002362	0.02204	1	0.02194	0.17	0.003873	0.002362	0.02204	1
0.02201	0.1537	0.01643	0.001528	0.02203	1	0.02201	0.1743	0.0169	0.001528	0.02203	1
0.02241	0.1825	0.01667	0.001543	0.02244	1	0.02241	0.1517	0.01518	0.001543	0.02244	1
0.02282	0.1232	0.01506	0.001558	0.02284	1	0.02282	0.1821	0.01742	0.001558	0.02284	1
0.02322	0.1483	0.0174	0.001574	0.02324	1	0.02322	0.1382	0.01536	0.001574	0.02324	1
0.02327	0.1394	0.00369	0.002394	0.02336	1	0.02327	0.1668	0.003887	0.002394	0.02336	1
0.02363	0.1477	0.01529	0.001589	0.02365	1	0.02363	0.2136	0.01883	0.001589	0.02365	1
0.02403	0.1575	0.01597	0.001605	0.02405	1	0.02403	0.171	0.0165	0.001605	0.02405	1
0.02443	0.1487	0.01513	0.001621	0.02445	1	0.02443	0.1812	0.01607	0.001621	0.02445	1
0.0246	0.1458	0.003589	0.002428	0.02469	1	0.0246	0.1608	0.004082	0.002428	0.02469	1
0.02484	0.1269	0.01541	0.001637	0.02486	1	0.02484	0.149	0.01635	0.001637	0.02486	1
0.02524	0.1326	0.01565	0.001653	0.02526	1	0.02524	0.1562	0.01788	0.001653	0.02526	1
0.02564	0.1747	0.01809	0.001669	0.02566	1	0.02564	0.1845	0.01901	0.001669	0.02566	1
0.02593	0.1429	0.003797	0.002464	0.02601	1	0.02593	0.1574	0.00392	0.002464	0.02601	1
0.02605	0.1357	0.01986	0.001685	0.02607	1	0.02605	0.1584	0.01899	0.001685	0.02607	1
0.02645	0.1367	0.01707	0.001701	0.02647	1	0.02645	0.1377	0.01568	0.001701	0.02647	1
0.02685	0.1385	0.02041	0.001718	0.02687	1	0.02685	0.1616	0.01736	0.001718	0.02687	1
0.02726	0.1384	0.003234	0.0025	0.02734	1	0.02726	0.1531	0.0036	0.0025	0.02734	1
0.02726	0.138	0.01797	0.001734	0.02728	1	0.02726	0.1682	0.01805	0.001734	0.02728	1
0.02766	0.1542	0.01807	0.001751	0.02768	1	0.02766	0.1777	0.02083	0.001751	0.02768	1
0.02807	0.1554	0.02223	0.001767	0.02808	1	0.02807	0.1553	0.01935	0.001767	0.02808	1
0.02847	0.1207	0.0188	0.001784	0.02849	1	0.02847	0.1525	0.02039	0.001784	0.02849	1
0.02859	0.1334	0.0032	0.002538	0.02866	1	0.02859	0.1481	0.003295	0.002538	0.02866	1
0.02887	0.1414	0.01899	0.001801	0.02889	1	0.02887	0.1672	0.02063	0.001801	0.02889	1
0.02928	0.1819	0.02048	0.001818	0.02929	1	0.02928	0.1765	0.02054	0.001818	0.02929	1
0.02968	0.1503	0.02183	0.001835	0.0297	1	0.02968	0.1608	0.02036	0.001835	0.0297	1
0.02991	0.1362	0.003088	0.002578	0.02999	1	0.02991	0.1492	0.003428	0.002578	0.02999	1



$\omega=9.54 \times 10^{-3}$ 17R4/D <sub>2</sub> O 30.6 °C					$\omega=9.54 \times 10^{-3}$ 17R4/D <sub>2</sub> O 39.9 °C						
Q	I(Q)	Std Dev(I(Q))	sigmaQ	meanQ	Shadow Factor	Q	I(Q)	Std Dev(I(Q))	sigmaQ	meanQ	Shadow Factor
0.03008	0.1438	0.01972	0.001852	0.0301	1	0.03008	0.1525	0.0194	0.001852	0.0301	1
0.03049	0.1558	0.02056	0.001869	0.0305	1	0.03049	0.1336	0.01913	0.001869	0.0305	1
0.03089	0.1101	0.01838	0.001886	0.03091	1	0.03089	0.1815	0.02197	0.001886	0.03091	1
0.03124	0.14	0.003115	0.002618	0.03131	1	0.03124	0.1486	0.003266	0.002618	0.03131	1
0.03129	0.1988	0.02271	0.001903	0.03131	1	0.03129	0.1133	0.01983	0.001903	0.03131	1
0.0317	0.1337	0.02091	0.00192	0.03171	1	0.0317	0.1341	0.02023	0.00192	0.03171	1
0.0321	0.1614	0.02066	0.001938	0.03212	1	0.0321	0.1534	0.02128	0.001938	0.03212	1
0.0325	0.1737	0.02196	0.001955	0.03252	1	0.0325	0.2011	0.02452	0.001955	0.03252	1
0.03257	0.1406	0.002906	0.00266	0.03264	1	0.03257	0.1473	0.003413	0.00266	0.03264	1
0.03291	0.1211	0.01763	0.001973	0.03292	1	0.03291	0.1603	0.02056	0.001973	0.03292	1
0.03331	0.1475	0.0206	0.00199	0.03333	1	0.03331	0.1665	0.02253	0.00199	0.03333	1
0.03372	0.171	0.02353	0.002008	0.03373	1	0.03372	0.1681	0.02317	0.002008	0.03373	1
0.0339	0.1334	0.002988	0.002703	0.03396	1	0.0339	0.1413	0.003313	0.002703	0.03396	1
0.03399	0.1359	0.001282	0.0047	0.03426	1	0.03399	0.1449	0.001296	0.0047	0.03426	1
0.03523	0.1382	0.003097	0.002746	0.03529	1	0.03523	0.1449	0.002945	0.002746	0.03529	1
0.03656	0.1296	0.002737	0.002791	0.03662	1	0.03656	0.1366	0.00308	0.002791	0.03662	1
0.03788	0.1349	0.002707	0.002837	0.03794	1	0.03788	0.136	0.002572	0.002837	0.03794	1
0.03798	0.133	0.001483	0.004775	0.03823	1	0.03798	0.141	0.00138	0.004775	0.03823	1
0.03921	0.1295	0.002702	0.002883	0.03927	1	0.03921	0.1351	0.002867	0.002883	0.03927	1
0.04054	0.1275	0.002605	0.00293	0.04059	1	0.04054	0.1386	0.002546	0.00293	0.04059	1
0.04187	0.1258	0.002753	0.002979	0.04192	1	0.04187	0.1337	0.002688	0.002979	0.04192	1
0.04197	0.1291	0.001296	0.004859	0.0422	1	0.04197	0.1368	0.001206	0.004859	0.0422	1
0.0432	0.1278	0.002658	0.003027	0.04325	1	0.0432	0.1357	0.002516	0.003027	0.04325	1
0.04452	0.1293	0.002447	0.003077	0.04457	1	0.04452	0.1304	0.002418	0.003077	0.04457	1
0.04585	0.1263	0.002446	0.003127	0.0459	1	0.04585	0.1308	0.002294	0.003127	0.0459	1
0.04597	0.1263	0.000977	0.00495	0.04617	1	0.04597	0.1342	0.001281	0.00495	0.04617	1
0.04718	0.1256	0.002491	0.003178	0.04722	1	0.04718	0.1294	0.00235	0.003178	0.04722	1
0.0485	0.1215	0.002387	0.00323	0.04855	1	0.0485	0.1297	0.002264	0.00323	0.04855	1
0.04983	0.1235	0.002365	0.003282	0.04987	1	0.04983	0.1302	0.00237	0.003282	0.04987	1
0.04996	0.1243	0.001122	0.005048	0.05014	1	0.04996	0.1298	0.001232	0.005048	0.05014	1
0.05116	0.1224	0.002305	0.003334	0.0512	1	0.05116	0.1263	0.002203	0.003334	0.0512	1
0.05248	0.1236	0.002316	0.003388	0.05252	1	0.05248	0.127	0.002436	0.003388	0.05252	1
0.05381	0.1205	0.002229	0.003441	0.05385	1	0.05381	0.125	0.002348	0.003441	0.05385	1
0.05394	0.1221	0.001283	0.005152	0.05412	1	0.05394	0.1266	0.001148	0.005152	0.05412	1
0.05514	0.1219	0.00207	0.003495	0.05517	1	0.05514	0.1223	0.00196	0.003495	0.05517	1
0.05646	0.1181	0.002109	0.00355	0.0565	1	0.05646	0.1191	0.002048	0.00355	0.0565	1
0.05779	0.1176	0.002074	0.003605	0.05782	1	0.05779	0.1222	0.002037	0.003605	0.05782	1
0.05793	0.118	0.001135	0.005262	0.05809	1	0.05793	0.1227	0.001079	0.005262	0.05809	1
0.05911	0.1176	0.00201	0.00366	0.05915	1	0.05911	0.1187	0.002032	0.00366	0.05915	1
0.06044	0.1129	0.001987	0.003716	0.06047	1	0.06044	0.1199	0.002141	0.003716	0.06047	1
0.06176	0.1128	0.00198	0.003772	0.0618	1	0.06176	0.1179	0.002014	0.003772	0.0618	1
0.06192	0.1173	0.00109	0.005378	0.06207	1	0.06192	0.1199	0.001034	0.005378	0.06207	1
0.06309	0.1126	0.001912	0.003829	0.06312	1	0.06309	0.1174	0.00195	0.003829	0.06312	1
0.06441	0.1123	0.00201	0.003886	0.06444	1	0.06441	0.1185	0.002006	0.003886	0.06444	1
0.06573	0.1092	0.001903	0.003943	0.06577	1	0.06573	0.1137	0.001908	0.003943	0.06577	1
0.0659	0.1124	0.001165	0.005499	0.06604	1	0.0659	0.1163	0.001159	0.005499	0.06604	1
0.06706	0.1102	0.00195	0.004001	0.06709	1	0.06706	0.1139	0.001843	0.004001	0.06709	1
0.06838	0.1087	0.001765	0.004059	0.06841	1	0.06838	0.1116	0.001863	0.004059	0.06841	1
0.06971	0.106	0.001888	0.004117	0.06974	1	0.06971	0.1091	0.001856	0.004117	0.06974	1
0.06988	0.1082	0.001121	0.005624	0.07001	1	0.06988	0.1137	0.001054	0.005624	0.07001	1
0.07103	0.1102	0.001903	0.004175	0.07106	1	0.07103	0.1118	0.001828	0.004175	0.07106	1
0.07235	0.1077	0.00176	0.004234	0.07238	1	0.07235	0.1154	0.001897	0.004234	0.07238	1
0.07367	0.1063	0.00188	0.004293	0.0737	1	0.07367	0.1112	0.001828	0.004293	0.0737	1
0.07386	0.1056	0.000913	0.005754	0.07399	1	0.07386	0.1109	0.001053	0.005754	0.07399	1
0.075	0.1049	0.001743	0.004352	0.07503	1	0.075	0.108	0.00181	0.004352	0.07503	1
0.07632	0.1037	0.001796	0.004411	0.07635	1	0.07632	0.1085	0.00183	0.004411	0.07635	1
0.07764	0.1053	0.001803	0.004471	0.07767	1	0.07764	0.106	0.001747	0.004471	0.07767	1
0.07784	0.1033	0.001001	0.005888	0.07796	1	0.07784	0.1082	0.000947	0.005888	0.07796	1
0.07896	0.09965	0.001715	0.004531	0.07899	1	0.07896	0.1062	0.001943	0.004531	0.07899	1
0.08028	0.1018	0.001817	0.004591	0.08031	1	0.08028	0.1054	0.001762	0.004591	0.08031	1
0.08161	0.1003	0.0019	0.004651	0.08163	1	0.08161	0.103	0.001881	0.004651	0.08163	1
0.08181	0.1027	0.000975	0.006026	0.08192	1	0.08181	0.1054	0.00086	0.006026	0.08192	1
0.08293	0.1008	0.001845	0.004711	0.08295	1	0.08293	0.1009	0.001755	0.004711	0.08295	1
0.08425	0.101	0.00187	0.004772	0.08427	1	0.08425	0.1007	0.001887	0.004772	0.08427	1
0.08557	0.09799	0.001947	0.004833	0.08559	1	0.08557	0.09989	0.002166	0.004833	0.08559	1
0.08578	0.09956	0.000983	0.006167	0.08589	1	0.08578	0.1015	0.000902	0.006167	0.08589	1
0.08689	0.09518	0.002092	0.004893	0.08691	1	0.08689	0.1009	0.002108	0.004893	0.08691	1
0.08821	0.09743	0.002278	0.004954	0.08823	1	0.08821	0.1022	0.002462	0.004954	0.08823	1
0.08953	0.09414	0.002434	0.005016	0.08955	1	0.08953	0.1006	0.002546	0.005016	0.08955	1
0.08975	0.09624	0.00091	0.006312	0.08985	1	0.08975	0.0992	0.000867	0.006312	0.08985	1
0.09084	0.09409	0.002502	0.005077	0.09087	1	0.09084	0.101	0.002815	0.005077	0.09087	1
0.09371	0.09478	0.000969	0.006459	0.09381	1	0.09371	0.09841	0.00098	0.006459	0.09381	1
0.09768	0.09238	0.000945	0.006609	0.09777	1	0.09768	0.09653	0.000945	0.006609	0.09777	1
0.1016	0.08844	0.000916	0.006762	0.1017	1	0.1016	0.09321	0.00098	0.006762	0.1017	1
0.1056	0.08754	0.000843	0.006917	0.1057	1	0.1056	0.091	0.000805	0.006917	0.1057	1
0.1095	0.08575	0.000721	0.007075	0.1096	1	0.1095	0.08968	0.000799	0.007075	0.1096	1
0.1135	0.08551	0.000729	0.007234	0.1136	1	0.1135	0.08691	0.000861	0.007234	0.1136	1
0.1174	0.08275	0.000828	0.007396	0.1175	1	0.1174	0.08556	0.000705	0.007396	0.1175	1
0.1214	0.0832	0.0008	0.007559	0.1215	1	0.1214	0.08437	0.000749	0.007559	0.1215	1
0.1253	0.08061	0.000761	0.007723	0.1254	1	0.1253	0.08302	0.00084	0.007723	0.1254	1
0.1293	0.07841	0.000732	0.007889	0.1293	1	0.1293	0.08216	0.000709	0.007889	0.1293	1

$\alpha=9.54 \times 10^{-3}$ 17R4/D <sub>2</sub> O 30.6 °C						$\alpha=9.54 \times 10^{-3}$ 17R4/D <sub>2</sub> O 39.9 °C					
Q	I(Q)	Std Dev(I(Q))	sigmaQ	meanQ	Shadow Factor	Q	I(Q)	Std Dev(I(Q))	sigmaQ	meanQ	Shadow Factor
0.1332	0.07735	0.000689	0.008057	0.1333	1	0.1332	0.08015	0.000677	0.008057	0.1333	1
0.1371	0.07647	0.000717	0.008226	0.1372	1	0.1371	0.07796	0.000804	0.008226	0.1372	1
0.141	0.07544	0.000761	0.008396	0.1411	1	0.141	0.07668	0.000732	0.008396	0.1411	1
0.1449	0.07441	0.000716	0.008567	0.145	1	0.1449	0.07573	0.000769	0.008567	0.145	1
0.1489	0.07304	0.000692	0.008739	0.1489	1	0.1489	0.07474	0.000664	0.008739	0.1489	1
0.1528	0.07279	0.000706	0.008912	0.1528	1	0.1528	0.07273	0.000662	0.008912	0.1528	1
0.1567	0.07073	0.000705	0.009086	0.1567	1	0.1567	0.07292	0.000668	0.009086	0.1567	1
0.1606	0.07034	0.000664	0.00926	0.1606	1	0.1606	0.07138	0.000713	0.00926	0.1606	1
0.1645	0.06961	0.000632	0.009436	0.1645	1	0.1645	0.07107	0.000667	0.009436	0.1645	1
0.1683	0.06841	0.000653	0.009612	0.1684	1	0.1683	0.07018	0.000623	0.009612	0.1684	1
0.1722	0.06787	0.000603	0.009788	0.1723	1	0.1722	0.07015	0.000697	0.009788	0.1723	1
0.1761	0.06734	0.000626	0.009965	0.1762	1	0.1761	0.06874	0.000627	0.009965	0.1762	1
0.18	0.06597	0.000644	0.01014	0.18	1	0.18	0.06754	0.000576	0.01014	0.18	1
0.1838	0.06585	0.000611	0.01032	0.1839	1	0.1838	0.06763	0.000616	0.01032	0.1839	1
0.1877	0.06629	0.000566	0.0105	0.1877	1	0.1877	0.06819	0.000654	0.0105	0.1877	1
0.1916	0.06568	0.000574	0.01068	0.1916	1	0.1916	0.06659	0.000554	0.01068	0.1916	1
0.1954	0.06428	0.000576	0.01086	0.1954	1	0.1954	0.06473	0.000563	0.01086	0.1954	1
0.1992	0.06461	0.000621	0.01104	0.1993	1	0.1992	0.06533	0.000603	0.01104	0.1993	1
0.2031	0.0641	0.000555	0.01122	0.2031	1	0.2031	0.06522	0.000604	0.01122	0.2031	1
0.2069	0.06416	0.000538	0.0114	0.2069	1	0.2069	0.06416	0.000588	0.0114	0.2069	1
0.2107	0.06327	0.00055	0.01158	0.2108	1	0.2107	0.06449	0.000597	0.01158	0.2108	1
0.2145	0.06294	0.000618	0.01176	0.2146	1	0.2145	0.06359	0.000565	0.01176	0.2146	1
0.2184	0.06237	0.000607	0.01194	0.2184	1	0.2184	0.0632	0.000597	0.01194	0.2184	1
0.2222	0.06225	0.000537	0.01212	0.2222	1	0.2222	0.06293	0.000534	0.01212	0.2222	1
0.226	0.06124	0.00058	0.0123	0.226	1	0.226	0.06112	0.000555	0.0123	0.226	1
0.2297	0.06108	0.000527	0.01248	0.2298	1	0.2297	0.06116	0.000578	0.01248	0.2298	1
0.2335	0.06239	0.000526	0.01266	0.2336	1	0.2335	0.06232	0.000551	0.01266	0.2336	1
0.2373	0.06074	0.000506	0.01284	0.2373	1	0.2373	0.06247	0.000532	0.01284	0.2373	1
0.2411	0.06087	0.000587	0.01302	0.2411	1	0.2411	0.06168	0.000575	0.01302	0.2411	1
0.2448	0.06046	0.000571	0.0132	0.2449	1	0.2448	0.06059	0.000567	0.0132	0.2449	1
0.2486	0.0592	0.000594	0.01338	0.2486	1	0.2486	0.05927	0.00058	0.01338	0.2486	1
0.2523	0.06088	0.000599	0.01356	0.2524	1	0.2523	0.061	0.000557	0.01356	0.2524	1
0.2561	0.05845	0.000636	0.01374	0.2561	1	0.2561	0.05972	0.000575	0.01374	0.2561	1
0.2598	0.05902	0.00065	0.01392	0.2598	1	0.2598	0.05891	0.000592	0.01392	0.2598	1
0.2635	0.05944	0.000578	0.0141	0.2636	1	0.2635	0.05914	0.000557	0.0141	0.2636	1
0.2673	0.05838	0.000629	0.01428	0.2673	1	0.2673	0.05913	0.000603	0.01428	0.2673	1
0.271	0.06022	0.000629	0.01446	0.271	1	0.271	0.05827	0.000608	0.01446	0.271	1
0.2747	0.05736	0.000632	0.01464	0.2747	1	0.2747	0.05861	0.00057	0.01464	0.2747	1
0.2784	0.0574	0.000618	0.01482	0.2784	1	0.2784	0.05965	0.000679	0.01482	0.2784	1
0.282	0.05901	0.000706	0.015	0.2821	1	0.282	0.05795	0.000631	0.015	0.2821	1
0.2857	0.05825	0.000701	0.01518	0.2857	1	0.2857	0.05828	0.000622	0.01518	0.2857	1
0.2894	0.05761	0.000598	0.01536	0.2894	1	0.2894	0.0577	0.000673	0.01536	0.2894	1
0.293	0.05653	0.000579	0.01554	0.2931	1	0.293	0.0567	0.000646	0.01554	0.2931	1
0.2967	0.05706	0.000659	0.01572	0.2967	1	0.2967	0.05725	0.000643	0.01572	0.2967	1
0.3003	0.05624	0.000724	0.0159	0.3004	1	0.3003	0.05842	0.000678	0.0159	0.3004	1
0.304	0.05543	0.000668	0.01607	0.304	1	0.304	0.05763	0.000653	0.01607	0.304	1
0.3076	0.05716	0.000646	0.01625	0.3076	1	0.3076	0.0566	0.000684	0.01625	0.3076	1
0.3112	0.05642	0.000604	0.01643	0.3113	1	0.3112	0.05723	0.00066	0.01643	0.3113	1
0.3148	0.05659	0.000699	0.01661	0.3149	1	0.3148	0.05645	0.000648	0.01661	0.3149	1
0.3184	0.05757	0.000692	0.01678	0.3185	1	0.3184	0.05743	0.000629	0.01678	0.3185	1
0.322	0.05592	0.000598	0.01696	0.3221	1	0.322	0.05754	0.000626	0.01696	0.3221	1
0.3256	0.05593	0.000705	0.01714	0.3256	1	0.3256	0.05652	0.000699	0.01714	0.3256	1
0.3292	0.05597	0.000649	0.01731	0.3292	1	0.3292	0.05618	0.000659	0.01731	0.3292	1
0.3327	0.05561	0.000619	0.01749	0.3328	1	0.3327	0.05611	0.000662	0.01749	0.3328	1
0.3363	0.05565	0.000624	0.01766	0.3363	1	0.3363	0.05554	0.000653	0.01766	0.3363	1
0.3399	0.05594	0.000634	0.01784	0.3399	1	0.3399	0.05645	0.000679	0.01784	0.3399	1
0.3434	0.05494	0.00063	0.01801	0.3434	1	0.3434	0.0558	0.000616	0.01801	0.3434	1
0.3469	0.0547	0.00061	0.01819	0.3469	1	0.3469	0.05503	0.00067	0.01819	0.3469	1
0.3504	0.05459	0.000702	0.01836	0.3505	1	0.3504	0.0549	0.000708	0.01836	0.3505	1
0.3539	0.05521	0.000632	0.01854	0.354	1	0.3539	0.05605	0.00071	0.01854	0.354	1
0.3574	0.05399	0.000661	0.01871	0.3575	1	0.3574	0.05493	0.000655	0.01871	0.3575	1
0.3609	0.05481	0.000644	0.01888	0.361	1	0.3609	0.05476	0.000751	0.01888	0.361	1
0.3644	0.05448	0.000666	0.01905	0.3644	1	0.3644	0.055	0.000707	0.01905	0.3644	1
0.3679	0.05473	0.000573	0.01923	0.3679	1	0.3679	0.05581	0.000648	0.01923	0.3679	1
0.3713	0.05455	0.000652	0.0194	0.3714	1	0.3713	0.05528	0.000651	0.0194	0.3714	1
0.3748	0.05421	0.000636	0.01957	0.3748	1	0.3748	0.054	0.000625	0.01957	0.3748	1
0.3782	0.05471	0.000691	0.01974	0.3783	1	0.3782	0.05373	0.000622	0.01974	0.3783	1
0.3817	0.05387	0.00073	0.01991	0.3817	1	0.3817	0.05364	0.00061	0.01991	0.3817	1
0.3851	0.05328	0.000635	0.02008	0.3851	1	0.3851	0.05403	0.000719	0.02008	0.3851	1
0.3885	0.05365	0.000697	0.02025	0.3885	1	0.3885	0.05543	0.000763	0.02025	0.3885	1
0.3919	0.05352	0.000601	0.02042	0.3919	1	0.3919	0.05381	0.000673	0.02042	0.3919	1
0.3953	0.05358	0.000717	0.02059	0.3953	1	0.3953	0.05399	0.000652	0.02059	0.3953	1
0.3987	0.05336	0.000732	0.02076	0.3987	1	0.3987	0.05406	0.000687	0.02076	0.3987	1
0.4021	0.0548	0.000695	0.02092	0.4021	1	0.4021	0.05553	0.000769	0.02092	0.4021	1
0.4054	0.05333	0.000733	0.02109	0.4054	1	0.4054	0.05542	0.000724	0.02109	0.4054	1

$\theta=9.54 \times 10^{-3}$ 17R4/D <sub>2</sub> O 49.3 °C					$\theta=9.54 \times 10^{-3}$ 17R4/D <sub>2</sub> O 49.3 °C						
Q	I(Q)	Std Dev(I(Q))	sigmaQ	meanQ	Shadow Factor	Q	I(Q)	Std Dev(I(Q))	sigmaQ	meanQ	Shadow Factor
0.003433	137.9	3.522	0.001068	0.003607	0.9568	0.03008	0.1744	0.02344	0.001852	0.0301	1
0.003837	83.42	3.067	0.001071	0.003977	0.9999	0.03049	0.136	0.02002	0.001869	0.0305	1
0.004241	47.48	1.417	0.001072	0.004367	1	0.03089	0.1436	0.01929	0.001886	0.03091	1
0.004645	29.15	0.7452	0.001074	0.00476	1	0.03124	0.1568	0.003377	0.002618	0.03131	1
0.005049	18.54	0.4272	0.001077	0.005155	1	0.03129	0.1212	0.02024	0.001903	0.03131	1
0.005453	12.91	0.2657	0.001081	0.005551	1	0.0317	0.1395	0.01929	0.00192	0.03171	1
0.005857	9.308	0.2031	0.001085	0.005948	1	0.0321	0.1167	0.02111	0.001938	0.03212	1
0.006261	6.877	0.1717	0.00109	0.006346	1	0.0325	0.1321	0.02005	0.001955	0.03252	1
0.006665	5.192	0.1336	0.001096	0.006745	1	0.03257	0.1488	0.003204	0.00266	0.03264	1
0.007069	4.135	0.0999	0.001101	0.007144	1	0.03291	0.1775	0.02367	0.001973	0.03292	1
0.007473	3.341	0.09809	0.001108	0.007544	1	0.03331	0.1726	0.02056	0.00199	0.03333	1
0.007876	2.612	0.07411	0.001115	0.007944	1	0.03372	0.1579	0.01939	0.002008	0.03373	1
0.00828	2.196	0.06836	0.001122	0.008345	1	0.0339	0.149	0.003096	0.002703	0.03396	1
0.008684	1.687	0.0691	0.001129	0.008746	1	0.03399	0.1512	0.001301	0.0047	0.03426	1
0.009088	1.427	0.05401	0.001137	0.009147	1	0.03523	0.1455	0.00286	0.002746	0.03529	1
0.009492	1.188	0.05317	0.001146	0.009548	1	0.03656	0.1438	0.002722	0.002791	0.03662	1
0.009896	1.024	0.04294	0.001154	0.00995	1	0.03788	0.1399	0.002871	0.002837	0.03794	1
0.0103	0.8903	0.03772	0.001163	0.01035	1	0.03798	0.1458	0.001322	0.004775	0.03823	1
0.0107	0.809	0.04027	0.001173	0.01075	1	0.03921	0.1447	0.002766	0.002883	0.03927	1
0.01111	0.7425	0.03888	0.001182	0.01116	1	0.04054	0.1373	0.00279	0.00293	0.04059	1
0.0113	0.8152	0.02309	0.00217	0.01149	1	0.04187	0.1401	0.002467	0.002979	0.04192	1
0.01151	0.6397	0.03437	0.001192	0.01156	1	0.04197	0.1417	0.001235	0.004859	0.0422	1
0.01192	0.5596	0.03151	0.001202	0.01196	1	0.0432	0.1398	0.00262	0.003027	0.04325	1
0.01232	0.5266	0.03262	0.001213	0.01236	1	0.04452	0.1363	0.002741	0.003077	0.04457	1
0.01263	0.5444	0.01338	0.002186	0.0128	1	0.04585	0.13	0.002539	0.003127	0.0459	1
0.01272	0.5095	0.03034	0.001223	0.01277	1	0.04597	0.1402	0.001258	0.00495	0.04617	1
0.01313	0.4153	0.02825	0.001234	0.01317	1	0.04718	0.1378	0.00246	0.003178	0.04722	1
0.01353	0.431	0.02498	0.001246	0.01357	1	0.0485	0.1314	0.00236	0.00323	0.04855	1
0.01393	0.3833	0.02631	0.001257	0.01397	1	0.04983	0.1334	0.00243	0.003282	0.04987	1
0.01396	0.4023	0.009034	0.002205	0.01412	1	0.04996	0.1368	0.001294	0.005048	0.05014	1
0.01434	0.3884	0.02282	0.001269	0.01438	1	0.05116	0.1361	0.002271	0.003334	0.0512	1
0.01474	0.3585	0.02212	0.001281	0.01478	1	0.05248	0.1365	0.002295	0.003388	0.05252	1
0.01515	0.3222	0.02133	0.001293	0.01518	1	0.05381	0.133	0.002351	0.003441	0.05385	1
0.01529	0.3249	0.007328	0.002226	0.01543	1	0.05394	0.1348	0.001362	0.005152	0.05412	1
0.01555	0.2995	0.02003	0.001305	0.01558	1	0.05514	0.1313	0.0021	0.003495	0.05517	1
0.01595	0.3008	0.02152	0.001318	0.01599	1	0.05646	0.13	0.002148	0.00355	0.0565	1
0.01636	0.2802	0.02097	0.001331	0.01639	1	0.05779	0.1332	0.002089	0.003605	0.05782	1
0.01662	0.2779	0.005827	0.002249	0.01675	1	0.05793	0.1358	0.00132	0.005262	0.05809	1
0.01676	0.2398	0.01947	0.001344	0.01679	1	0.05911	0.1319	0.002153	0.00366	0.05915	1
0.01717	0.2553	0.01969	0.001357	0.0172	1	0.06044	0.1251	0.002143	0.003716	0.06047	1
0.01757	0.2695	0.02022	0.00137	0.0176	1	0.06176	0.1302	0.002106	0.003772	0.0618	1
0.01795	0.2469	0.005532	0.002275	0.01807	1	0.06192	0.1344	0.001265	0.005378	0.06207	1
0.01797	0.2209	0.01867	0.001384	0.018	1	0.06309	0.1292	0.002132	0.003829	0.06312	1
0.01838	0.238	0.01764	0.001397	0.01841	1	0.06441	0.1371	0.002053	0.003886	0.06444	1
0.01878	0.2173	0.01869	0.001411	0.01881	1	0.06573	0.1313	0.002198	0.003943	0.06577	1
0.01918	0.2108	0.01664	0.001425	0.01921	1	0.0659	0.1334	0.001134	0.005499	0.06604	1
0.01928	0.221	0.004916	0.002302	0.01939	1	0.06706	0.1342	0.001987	0.004001	0.06709	1
0.01959	0.231	0.01978	0.00144	0.01962	1	0.06838	0.1302	0.00191	0.004059	0.06841	1
0.01999	0.1978	0.01848	0.001454	0.02002	1	0.06971	0.1305	0.002029	0.004117	0.06974	1
0.0204	0.2021	0.01702	0.001468	0.02042	1	0.06988	0.1349	0.001082	0.005624	0.07001	1
0.02061	0.2044	0.004252	0.002331	0.02072	1	0.07103	0.1357	0.001905	0.004175	0.07106	1
0.0208	0.1876	0.01669	0.001483	0.02083	1	0.07235	0.1372	0.001996	0.004234	0.07238	1
0.0212	0.195	0.01686	0.001498	0.02123	1	0.07367	0.1332	0.001848	0.004293	0.0737	1
0.02161	0.208	0.01692	0.001513	0.02163	1	0.07386	0.1344	0.0012	0.005754	0.07399	1
0.02194	0.1826	0.003848	0.002362	0.02204	1	0.075	0.136	0.001871	0.004352	0.07503	1
0.02201	0.2078	0.0174	0.001528	0.02203	1	0.07632	0.1339	0.001962	0.004411	0.07635	1
0.02241	0.1792	0.01636	0.001543	0.02244	1	0.07764	0.133	0.002016	0.004471	0.07767	1
0.02282	0.1913	0.01721	0.001558	0.02284	1	0.07784	0.1326	0.000954	0.005888	0.07796	1
0.02322	0.1676	0.01672	0.001574	0.02324	1	0.07896	0.1327	0.001992	0.004531	0.07899	1
0.02327	0.1732	0.003876	0.002394	0.02336	1	0.08028	0.1293	0.001849	0.004591	0.08031	1
0.02363	0.1898	0.01695	0.001589	0.02365	1	0.08161	0.1272	0.001971	0.004651	0.08163	1
0.02403	0.1982	0.01636	0.001605	0.02405	1	0.08181	0.1297	0.000971	0.006026	0.08192	1
0.02443	0.1909	0.01518	0.001621	0.02445	1	0.08293	0.1275	0.001948	0.004711	0.08295	1
0.0246	0.1708	0.004014	0.002428	0.02469	1	0.08425	0.1233	0.002108	0.004772	0.08427	1
0.02484	0.165	0.01647	0.001637	0.02486	1	0.08557	0.124	0.002224	0.004833	0.08559	1
0.02524	0.166	0.01777	0.001653	0.02526	1	0.08578	0.1229	0.001003	0.006167	0.08589	1
0.02564	0.176	0.01931	0.001669	0.02566	1	0.08689	0.1201	0.002128	0.004893	0.08691	1
0.02593	0.1595	0.00347	0.002464	0.02601	1	0.08821	0.1203	0.00238	0.004954	0.08823	1
0.02605	0.1719	0.01811	0.001685	0.02607	1	0.08953	0.1179	0.002493	0.005016	0.08955	1
0.02645	0.1588	0.01862	0.001701	0.02647	1	0.08975	0.1144	0.0011	0.006312	0.08985	1
0.02685	0.1434	0.01813	0.001718	0.02687	1	0.09084	0.1126	0.00248	0.005077	0.09087	1
0.02726	0.1628	0.003731	0.0025	0.02734	1	0.09371	0.1104	0.000889	0.006459	0.09381	1
0.02726	0.1768	0.02094	0.001734	0.02728	1	0.09768	0.1032	0.000876	0.006609	0.09777	1
0.02766	0.1678	0.01895	0.001751	0.02768	1	0.1016	0.0984	0.000788	0.006762	0.1017	1
0.02807	0.1371	0.02051	0.001767	0.02808	1	0.1056	0.09532	0.000827	0.006917	0.1057	1
0.02847	0.1649	0.02101	0.001784	0.02849	1	0.1095	0.09183	0.000734	0.007075	0.1096	1
0.02859	0.1571	0.003555	0.002538	0.02866	1	0.1135	0.08921	0.00084	0.007234	0.1136	1
0.02887	0.1506	0.02094	0.001801	0.02889	1	0.1174	0.08685	0.000848	0.007396	0.1175	1
0.02928	0.2009	0.02049	0.001818	0.02929	1	0.1214	0.08506	0.000733	0.007559	0.1215	1
0.02968	0.1625	0.02254	0.001835	0.0297	1	0.1253	0.08392	0.000787	0.007723	0.1254	1
0.02991	0.1568	0.003025	0.002578	0.02999	1	0.1293	0.08112	0.000731	0.007889	0.1293	1

$\alpha=9.54 \times 10^{-3}$  17R4/D<sub>2</sub>O 49.3 °C

Q	I(Q)	Std Dev(I(Q))	sigmaQ	meanQ	Shadow Factor
0.1332	0.08103	0.000736	0.008057	0.1333	1
0.1371	0.07754	0.000721	0.008226	0.1372	1
0.141	0.07639	0.000681	0.008396	0.1411	1
0.1449	0.07535	0.00067	0.008567	0.145	1
0.1489	0.07443	0.000662	0.008739	0.1489	1
0.1528	0.07355	0.000699	0.008912	0.1528	1
0.1567	0.07324	0.000647	0.009086	0.1567	1
0.1606	0.07062	0.000605	0.00926	0.1606	1
0.1645	0.07031	0.000677	0.009436	0.1645	1
0.1683	0.07018	0.000626	0.009612	0.1684	1
0.1722	0.07002	0.000623	0.009788	0.1723	1
0.1761	0.069	0.00057	0.009965	0.1762	1
0.18	0.0682	0.00063	0.01014	0.18	1
0.1838	0.0672	0.000682	0.01032	0.1839	1
0.1877	0.06747	0.000643	0.0105	0.1877	1
0.1916	0.0663	0.000587	0.01068	0.1916	1
0.1954	0.06459	0.000633	0.01086	0.1954	1
0.1992	0.06579	0.000591	0.01104	0.1993	1
0.2031	0.06448	0.000563	0.01122	0.2031	1
0.2069	0.06416	0.000597	0.0114	0.2069	1
0.2107	0.06343	0.000601	0.01158	0.2108	1
0.2145	0.0637	0.00058	0.01176	0.2146	1
0.2184	0.06363	0.000535	0.01194	0.2184	1
0.2222	0.06339	0.000585	0.01212	0.2222	1
0.226	0.06136	0.000583	0.0123	0.226	1
0.2297	0.06239	0.000549	0.01248	0.2298	1
0.2335	0.06264	0.000549	0.01266	0.2336	1
0.2373	0.06229	0.000499	0.01284	0.2373	1
0.2411	0.06081	0.000572	0.01302	0.2411	1
0.2448	0.05975	0.000606	0.0132	0.2449	1
0.2486	0.06121	0.000612	0.01338	0.2486	1
0.2523	0.06031	0.00058	0.01356	0.2524	1
0.2561	0.0599	0.000583	0.01374	0.2561	1
0.2598	0.05998	0.00065	0.01392	0.2598	1
0.2635	0.06007	0.000637	0.0141	0.2636	1
0.2673	0.05775	0.000704	0.01428	0.2673	1
0.271	0.06099	0.000655	0.01446	0.271	1
0.2747	0.05892	0.000603	0.01464	0.2747	1
0.2784	0.05905	0.000611	0.01482	0.2784	1
0.282	0.05863	0.000643	0.015	0.2821	1
0.2857	0.05795	0.000601	0.01518	0.2857	1
0.2894	0.05772	0.000704	0.01536	0.2894	1
0.293	0.05777	0.000628	0.01554	0.2931	1
0.2967	0.05779	0.000641	0.01572	0.2967	1
0.3003	0.05817	0.000681	0.0159	0.3004	1
0.304	0.05758	0.000581	0.01607	0.304	1
0.3076	0.05814	0.000603	0.01625	0.3076	1
0.3112	0.05817	0.000684	0.01643	0.3113	1
0.3148	0.05638	0.000664	0.01661	0.3149	1
0.3184	0.05806	0.000623	0.01678	0.3185	1
0.322	0.05676	0.00064	0.01696	0.3221	1
0.3256	0.05649	0.000702	0.01714	0.3256	1
0.3292	0.05675	0.000653	0.01731	0.3292	1
0.3327	0.05524	0.000638	0.01749	0.3328	1
0.3363	0.05731	0.000696	0.01766	0.3363	1
0.3399	0.05642	0.000684	0.01784	0.3399	1
0.3434	0.05671	0.000728	0.01801	0.3434	1
0.3469	0.0567	0.000655	0.01819	0.3469	1
0.3504	0.05552	0.00064	0.01836	0.3505	1
0.3539	0.05563	0.000608	0.01854	0.354	1
0.3574	0.05513	0.000712	0.01871	0.3575	1
0.3609	0.0564	0.00076	0.01888	0.361	1
0.3644	0.05491	0.000633	0.01905	0.3644	1
0.3679	0.05564	0.000631	0.01923	0.3679	1
0.3713	0.05613	0.000668	0.0194	0.3714	1
0.3748	0.05504	0.000635	0.01957	0.3748	1
0.3782	0.05468	0.000753	0.01974	0.3783	1
0.3817	0.05418	0.000733	0.01991	0.3817	1
0.3851	0.05493	0.000625	0.02008	0.3851	1
0.3885	0.05661	0.000658	0.02025	0.3885	1
0.3919	0.05484	0.000706	0.02042	0.3919	1
0.3953	0.05523	0.000712	0.02059	0.3953	1
0.3987	0.05516	0.00056	0.02076	0.3987	1
0.4021	0.05533	0.000698	0.02092	0.4021	1
0.4054	0.05631	0.000653	0.02109	0.4054	1

PEO <sub>132</sub> -PB <sub>89</sub> /CD <sub>3</sub> OD 21.3 °C					PEO <sub>132</sub> -PB <sub>89</sub> /CD <sub>3</sub> OD 30.6 °C						
Q	I(Q)	Std Dev(I(Q))	sigmaQ	meanQ	Shadow Factor	Q	I(Q)	Std Dev(I(Q))	sigmaQ	meanQ	Shadow Factor
0.003433	10.24	0.1994	0.001072	0.003606	0.9585	0.003433	10.3	0.2257	0.001072	0.003606	0.9585
0.003837	11.17	0.1529	0.001076	0.003977	0.9999	0.003837	10.89	0.1308	0.001076	0.003977	0.9999
0.004241	11.01	0.1333	0.001078	0.004367	1	0.004241	10.77	0.1176	0.001078	0.004367	1
0.004645	10.83	0.1257	0.001081	0.00476	1	0.004645	10.62	0.118	0.001081	0.00476	1
0.005049	10.85	0.1051	0.001086	0.005155	1	0.005049	10.77	0.1061	0.001086	0.005155	1
0.005453	10.79	0.1062	0.001091	0.005551	1	0.005453	10.55	0.1053	0.001091	0.005551	1
0.005857	10.65	0.09769	0.001097	0.005948	1	0.005857	10.53	0.1042	0.001097	0.005948	1
0.006261	10.48	0.09519	0.001103	0.006346	1	0.006261	10.44	0.09356	0.001103	0.006346	1
0.006665	10.43	0.0865	0.001111	0.006745	1	0.006665	10.24	0.09544	0.001111	0.006745	1
0.007069	10.38	0.07918	0.001118	0.007144	1	0.007069	10.1	0.08477	0.001118	0.007144	1
0.007473	10.26	0.08373	0.001127	0.007544	1	0.007473	10.02	0.0771	0.001127	0.007544	1
0.007876	10.16	0.07994	0.001135	0.007944	1	0.007876	9.808	0.06704	0.001135	0.007944	1
0.00828	9.977	0.0751	0.001145	0.008345	1	0.00828	9.753	0.08286	0.001145	0.008345	1
0.008684	9.719	0.07537	0.001154	0.008746	1	0.008684	9.626	0.07361	0.001154	0.008746	1
0.009088	9.588	0.06709	0.001164	0.009147	1	0.009088	9.485	0.07124	0.001164	0.009147	1
0.009492	9.448	0.06796	0.001175	0.009548	1	0.009492	9.259	0.07084	0.001175	0.009548	1
0.009896	9.273	0.06375	0.001186	0.00995	1	0.009896	8.983	0.06493	0.001186	0.00995	1
0.0103	9.091	0.06505	0.001197	0.01035	1	0.0103	8.913	0.06436	0.001197	0.01035	1
0.0107	8.9	0.06639	0.001209	0.01075	1	0.0107	8.671	0.07064	0.001209	0.01075	1
0.01111	8.692	0.0599	0.001221	0.01116	1	0.01111	8.451	0.05848	0.001221	0.01116	1
0.0113	8.431	0.05326	0.002191	0.01149	1	0.0113	8.266	0.051	0.002191	0.01149	1
0.01151	8.5	0.0532	0.001233	0.01156	1	0.01151	8.306	0.0561	0.001233	0.01156	1
0.01192	8.242	0.05124	0.001246	0.01196	1	0.01192	8.126	0.05611	0.001246	0.01196	1
0.01232	8.045	0.05231	0.001259	0.01236	1	0.01232	7.858	0.05297	0.001259	0.01236	1
0.01263	7.736	0.05141	0.002212	0.0128	1	0.01263	7.623	0.04337	0.002212	0.0128	1
0.01272	7.873	0.05169	0.001272	0.01277	1	0.01272	7.629	0.05637	0.001272	0.01277	1
0.01313	7.623	0.05587	0.001286	0.01317	1	0.01313	7.512	0.05667	0.001286	0.01317	1
0.01353	7.354	0.04959	0.0013	0.01357	1	0.01353	7.3	0.05875	0.0013	0.01357	1
0.01393	7.184	0.04666	0.001314	0.01397	1	0.01393	7.053	0.0474	0.001314	0.01397	1
0.01396	7.04	0.04132	0.002236	0.01412	1	0.01396	6.928	0.04638	0.002236	0.01412	1
0.01434	6.988	0.04911	0.001328	0.01438	1	0.01434	6.716	0.05079	0.001328	0.01438	1
0.01474	6.759	0.04105	0.001343	0.01478	1	0.01474	6.629	0.04558	0.001343	0.01478	1
0.01515	6.574	0.04541	0.001358	0.01518	1	0.01515	6.364	0.04065	0.001358	0.01518	1
0.01529	6.361	0.04332	0.002264	0.01543	1	0.01529	6.23	0.03879	0.002264	0.01543	1
0.01555	6.307	0.04381	0.001373	0.01558	1	0.01555	6.146	0.04198	0.001373	0.01558	1
0.01595	6.062	0.04436	0.001389	0.01599	1	0.01595	5.902	0.04258	0.001389	0.01599	1
0.01636	5.936	0.04424	0.001404	0.01639	1	0.01636	5.772	0.04382	0.001404	0.01639	1
0.01662	5.686	0.03701	0.002294	0.01675	1	0.01662	5.596	0.03898	0.002294	0.01675	1
0.01676	5.662	0.04436	0.00142	0.01679	1	0.01676	5.517	0.04553	0.00142	0.01679	1
0.01717	5.505	0.04447	0.001436	0.0172	1	0.01717	5.335	0.03836	0.001436	0.0172	1
0.01757	5.303	0.04633	0.001453	0.0176	1	0.01757	5.137	0.03914	0.001453	0.0176	1
0.01795	5.016	0.03769	0.002326	0.01807	1	0.01795	4.928	0.03692	0.002326	0.01807	1
0.01797	5.082	0.03911	0.001469	0.018	1	0.01797	4.917	0.04037	0.001469	0.018	1
0.01838	4.882	0.04055	0.001486	0.01841	1	0.01838	4.698	0.03926	0.001486	0.01841	1
0.01878	4.65	0.03883	0.001503	0.01881	1	0.01878	4.59	0.03718	0.001503	0.01881	1
0.01918	4.429	0.04005	0.00152	0.01921	1	0.01918	4.406	0.03912	0.00152	0.01921	1
0.01928	4.381	0.03298	0.002361	0.01939	1	0.01928	4.278	0.03216	0.002361	0.01939	1
0.01959	4.244	0.03801	0.001537	0.01962	1	0.01959	4.197	0.03256	0.001537	0.01962	1
0.01999	4.081	0.03679	0.001554	0.02002	1	0.01999	4.036	0.03541	0.001554	0.02002	1
0.0204	3.929	0.03462	0.001572	0.02042	1	0.0204	3.826	0.03351	0.001572	0.02042	1
0.02061	3.806	0.02668	0.002398	0.02072	1	0.02061	3.729	0.02594	0.002398	0.02072	1
0.0208	3.75	0.03246	0.001589	0.02083	1	0.0208	3.684	0.0338	0.001589	0.02083	1
0.0212	3.573	0.03261	0.001607	0.02123	1	0.0212	3.489	0.03367	0.001607	0.02123	1
0.02161	3.475	0.02935	0.001625	0.02163	1	0.02161	3.367	0.03136	0.001625	0.02163	1
0.02194	3.303	0.02669	0.002436	0.02204	1	0.02194	3.238	0.02428	0.002436	0.02204	1
0.02201	3.35	0.03132	0.001643	0.02203	1	0.02201	3.214	0.03053	0.001643	0.02203	1
0.02241	3.06	0.03003	0.001661	0.02244	1	0.02241	3.043	0.02754	0.001661	0.02244	1
0.02282	2.969	0.027	0.00168	0.02284	1	0.02282	2.926	0.03047	0.00168	0.02284	1
0.02322	2.916	0.02759	0.001698	0.02324	1	0.02322	2.813	0.02848	0.001698	0.02324	1
0.02327	2.821	0.0209	0.002477	0.02336	1	0.02327	2.774	0.01982	0.002477	0.02336	1
0.02363	2.653	0.02986	0.001717	0.02365	1	0.02363	2.648	0.02995	0.001717	0.02365	1
0.02403	2.556	0.02798	0.001736	0.02405	1	0.02403	2.531	0.02758	0.001736	0.02405	1
0.02443	2.447	0.02581	0.001754	0.02445	1	0.02443	2.415	0.02471	0.001754	0.02445	1
0.0246	2.399	0.01969	0.002519	0.02469	1	0.0246	2.357	0.02033	0.002519	0.02469	1
0.02484	2.347	0.02685	0.001773	0.02486	1	0.02484	2.323	0.02808	0.001773	0.02486	1
0.02524	2.244	0.02846	0.001792	0.02526	1	0.02524	2.207	0.02543	0.001792	0.02526	1
0.02564	2.099	0.0288	0.001812	0.02566	1	0.02564	2.046	0.02875	0.001812	0.02566	1
0.02593	2.041	0.01707	0.002563	0.02601	1	0.02593	1.995	0.0144	0.002563	0.02601	1
0.02605	2.039	0.02721	0.001831	0.02607	1	0.02605	2.024	0.02971	0.001831	0.02607	1
0.02645	1.877	0.02494	0.00185	0.02647	1	0.02645	1.858	0.02861	0.00185	0.02647	1
0.02685	1.835	0.02611	0.00187	0.02687	1	0.02685	1.759	0.02909	0.00187	0.02687	1
0.02726	1.77	0.02863	0.001889	0.02728	1	0.02726	1.672	0.02619	0.001889	0.02728	1
0.02726	1.718	0.01114	0.002609	0.02734	1	0.02726	1.69	0.01203	0.002609	0.02734	1
0.02766	1.68	0.02869	0.001909	0.02768	1	0.02766	1.564	0.02896	0.001909	0.02768	1
0.02807	1.517	0.02656	0.001928	0.02808	1	0.02807	1.484	0.02923	0.001928	0.02808	1
0.02847	1.477	0.02449	0.001948	0.02849	1	0.02847	1.424	0.02709	0.001948	0.02849	1
0.02859	1.426	0.01084	0.002656	0.02866	1	0.02859	1.383	0.01018	0.002656	0.02866	1
0.02887	1.367	0.02701	0.001968	0.02889	1	0.02887	1.361	0.02663	0.001968	0.02889	1
0.02928	1.266	0.02643	0.001988	0.02929	1	0.02928	1.244	0.02579	0.001988	0.02929	1
0.02968	1.237	0.02762	0.002008	0.0297	1	0.02968	1.192	0.02298	0.002008	0.0297	1
0.02991	1.187	0.009084	0.002705	0.02999	1	0.02991	1.147	0.009584	0.002705	0.02999	1

PEO <sub>132</sub> -PB <sub>89</sub> /CD <sub>3</sub> OD 21.3 °C					PEO <sub>132</sub> -PB <sub>89</sub> /CD <sub>3</sub> OD 30.6 °C						
Q	I(Q)	Std Dev(I(Q))	sigmaQ	meanQ	Shadow Factor	Q	I(Q)	Std Dev(I(Q))	sigmaQ	meanQ	Shadow Factor
0.03008	1.096	0.02521	0.002028	0.0301	1	0.007069	1.136	0.02426	0.002028	0.0301	1
0.03049	1.077	0.02472	0.002048	0.0305	1	0.007069	1.062	0.02273	0.002048	0.0305	1
0.03089	1.054	0.01999	0.002068	0.03091	1	0.007069	1.002	0.02268	0.002068	0.03091	1
0.03124	0.9801	0.008521	0.002754	0.03131	1	0.007069	0.9472	0.007701	0.002754	0.03131	1
0.03129	0.9862	0.02297	0.002089	0.03131	1	0.007069	0.9501	0.02323	0.002089	0.03131	1
0.0317	0.9172	0.024	0.002109	0.03171	1	0.007069	0.8922	0.02296	0.002109	0.03171	1
0.0321	0.837	0.02034	0.002129	0.03212	1	0.007069	0.8222	0.02022	0.002129	0.03212	1
0.0325	0.7884	0.02311	0.00215	0.03252	1	0.007069	0.7875	0.02345	0.00215	0.03252	1
0.03257	0.8158	0.006809	0.002806	0.03264	1	0.007069	0.7802	0.007239	0.002806	0.03264	1
0.03291	0.7523	0.02321	0.00217	0.03292	1	0.007069	0.7404	0.02039	0.00217	0.03292	1
0.03331	0.7171	0.01964	0.002191	0.03333	1	0.007069	0.7379	0.02163	0.002191	0.03333	1
0.03372	0.6727	0.02043	0.002212	0.03373	1	0.007069	0.6922	0.02059	0.002212	0.03373	1
0.0339	0.6616	0.006367	0.002858	0.03396	1	0.007069	0.6473	0.005974	0.002858	0.03396	1
0.03399	0.7054	0.02229	0.004785	0.03426	1	0.007069	0.6853	0.02194	0.004785	0.03426	1
0.03412	0.6523	0.02101	0.002232	0.03413	1	0.007069	0.6438	0.02079	0.002232	0.03413	1
0.03452	0.6115	0.02236	0.002253	0.03454	1	0.007069	0.6006	0.02389	0.002253	0.03454	1
0.03493	0.4963	0.02026	0.002274	0.03494	1	0.007069	0.5181	0.02539	0.002274	0.03494	1
0.03523	0.5502	0.00623	0.002911	0.03529	1	0.007069	0.5235	0.005338	0.002911	0.03529	1
0.03533	0.5428	0.02138	0.002295	0.03534	1	0.007069	0.5249	0.02116	0.002295	0.03534	1
0.03573	0.5128	0.0237	0.002316	0.03575	1	0.007069	0.5255	0.02375	0.002316	0.03575	1
0.03614	0.4864	0.02391	0.002336	0.03615	1	0.007069	0.4697	0.02208	0.002336	0.03615	1
0.03654	0.463	0.02999	0.002357	0.03655	1	0.007069	0.3953	0.0265	0.002357	0.03655	1
0.03656	0.4407	0.004778	0.002966	0.03662	1	0.007069	0.4352	0.004949	0.002966	0.03662	1
0.03694	0.4092	0.0309	0.002378	0.03696	1	0.007069	0.4019	0.02537	0.002378	0.03696	1
0.03735	0.3438	0.02576	0.0024	0.03736	1	0.007069	0.3551	0.02201	0.0024	0.03736	1
0.03775	0.3255	0.02282	0.002421	0.03776	1	0.007069	0.3757	0.02467	0.002421	0.03776	1
0.03788	0.3677	0.004658	0.003021	0.03794	1	0.007069	0.3545	0.004501	0.003021	0.03794	1
0.03798	0.406	0.0135	0.004881	0.03823	1	0.007069	0.3862	0.01319	0.004881	0.03823	1
0.03815	0.3314	0.02936	0.002442	0.03817	1	0.007069	0.2811	0.02283	0.002442	0.03817	1
0.03856	0.3276	0.03045	0.002463	0.03857	1	0.007069	0.3717	0.02586	0.002463	0.03857	1
0.03896	0.3007	0.03139	0.002484	0.03897	1	0.007069	0.3273	0.029	0.002484	0.03897	1
0.03921	0.2991	0.004069	0.003077	0.03927	1	0.007069	0.294	0.003761	0.003077	0.03927	1
0.03936	0.3001	0.03342	0.002506	0.03938	1	0.007069	0.2839	0.02439	0.002506	0.03938	1
0.03977	0.3028	0.02996	0.002527	0.03978	1	0.007069	0.2664	0.03534	0.002527	0.03978	1
0.04017	0.2514	0.04405	0.002548	0.04018	1	0.007069	0.3015	0.048	0.002548	0.04018	1
0.04054	0.2474	0.003339	0.003134	0.04059	1	0.007069	0.244	0.003366	0.003134	0.04059	1
0.04057	0.2291	0.04392	0.00257	0.04059	1	0.007069	0.2212	0.03866	0.00257	0.04059	1
0.04187	0.2082	0.003243	0.003192	0.04192	1	0.007069	0.2027	0.003199	0.003192	0.04192	1
0.04197	0.2291	0.007166	0.004987	0.0422	1	0.007069	0.2212	0.006652	0.004987	0.0422	1
0.0432	0.1811	0.002773	0.003251	0.04325	1	0.007069	0.1704	0.003202	0.003251	0.04325	1
0.04452	0.152	0.002803	0.003311	0.04457	1	0.007069	0.1452	0.002685	0.003311	0.04457	1
0.04585	0.1303	0.002806	0.003371	0.0459	1	0.007069	0.129	0.002867	0.003371	0.0459	1
0.04597	0.1438	0.003809	0.005102	0.04617	1	0.007069	0.1407	0.003533	0.005102	0.04617	1
0.04718	0.1181	0.002391	0.003432	0.04722	1	0.007069	0.1156	0.002358	0.003432	0.04722	1
0.0485	0.1041	0.002226	0.003493	0.04855	1	0.007069	0.1074	0.002449	0.003493	0.04855	1
0.04983	0.1021	0.002529	0.003555	0.04987	1	0.007069	0.1034	0.002363	0.003555	0.04987	1
0.04996	0.1049	0.001622	0.005225	0.05014	1	0.007069	0.1046	0.001934	0.005225	0.05014	1
0.05116	0.09335	0.002238	0.003618	0.0512	1	0.007069	0.09014	0.002186	0.003618	0.0512	1
0.05248	0.0904	0.002188	0.003681	0.05252	1	0.007069	0.09274	0.002284	0.003681	0.05252	1
0.05381	0.09184	0.002208	0.003745	0.05385	1	0.007069	0.08979	0.002215	0.003745	0.05385	1
0.05394	0.09069	0.001413	0.005355	0.05412	1	0.007069	0.09082	0.001272	0.005355	0.05412	1
0.05514	0.08435	0.002147	0.003809	0.05517	1	0.007069	0.08591	0.002294	0.003809	0.05517	1
0.05646	0.0883	0.002134	0.003874	0.0565	1	0.007069	0.09098	0.002045	0.003874	0.0565	1
0.05779	0.08807	0.002026	0.003939	0.05782	1	0.007069	0.09122	0.002132	0.003939	0.05782	1
0.05793	0.08702	0.001412	0.005492	0.05809	1	0.007069	0.08947	0.001213	0.005492	0.05809	1
0.05911	0.08695	0.002245	0.004004	0.05915	1	0.007069	0.09066	0.002023	0.004004	0.05915	1
0.06044	0.09068	0.001994	0.00407	0.06047	1	0.007069	0.09323	0.002085	0.00407	0.06047	1
0.06176	0.09215	0.001951	0.004137	0.0618	1	0.007069	0.09363	0.00213	0.004137	0.0618	1
0.06192	0.08875	0.00128	0.005635	0.06207	1	0.007069	0.08878	0.001357	0.005635	0.06207	1
0.06309	0.09155	0.002013	0.004203	0.06312	1	0.007069	0.09177	0.002043	0.004203	0.06312	1
0.06441	0.08981	0.00201	0.00427	0.06444	1	0.007069	0.09001	0.002033	0.00427	0.06444	1
0.06573	0.08764	0.001944	0.004337	0.06577	1	0.007069	0.09045	0.001929	0.004337	0.06577	1
0.0659	0.08938	0.001245	0.005784	0.06604	1	0.007069	0.09041	0.00137	0.005784	0.06604	1
0.06706	0.09593	0.001974	0.004405	0.06709	1	0.007069	0.09255	0.00195	0.004405	0.06709	1
0.06838	0.0927	0.001984	0.004473	0.06841	1	0.007069	0.09464	0.001967	0.004473	0.06841	1
0.06971	0.0931	0.001861	0.004541	0.06974	1	0.007069	0.09413	0.001789	0.004541	0.06974	1
0.06988	0.08854	0.001217	0.005938	0.07001	1	0.007069	0.08852	0.001407	0.005938	0.07001	1
0.07103	0.09029	0.001851	0.004609	0.07106	1	0.007069	0.09412	0.001994	0.004609	0.07106	1
0.07235	0.08835	0.00173	0.004678	0.07238	1	0.007069	0.09387	0.001853	0.004678	0.07238	1
0.07367	0.08862	0.001899	0.004746	0.0737	1	0.007069	0.08982	0.001935	0.004746	0.0737	1
0.07386	0.08776	0.001386	0.006097	0.07399	1	0.007069	0.08666	0.001411	0.006097	0.07399	1
0.075	0.08458	0.001758	0.004815	0.07503	1	0.007069	0.08802	0.001849	0.004815	0.07503	1
0.07632	0.08765	0.001795	0.004885	0.07635	1	0.007069	0.09022	0.001765	0.004885	0.07635	1
0.07764	0.08545	0.001972	0.004954	0.07767	1	0.007069	0.08595	0.001769	0.004954	0.07767	1
0.07784	0.08246	0.001339	0.00626	0.07796	1	0.007069	0.08358	0.001224	0.00626	0.07796	1
0.07896	0.0849	0.001842	0.005024	0.07899	1	0.007069	0.08627	0.001809	0.005024	0.07899	1
0.08028	0.07958	0.001745	0.005094	0.08031	1	0.007069	0.0833	0.001854	0.005094	0.08031	1
0.08161	0.08424	0.001957	0.005164	0.08163	1	0.007069	0.08389	0.001933	0.005164	0.08163	1
0.08181	0.0798	0.001385	0.006427	0.08192	1	0.007069	0.07993	0.000928	0.006427	0.08192	1
0.08293	0.0804	0.002051	0.005234	0.08295	1	0.007069	0.08169	0.002103	0.005234	0.08295	1
0.08425	0.08066	0.002027	0.005304	0.08427	1	0.007069	0.07919	0.002316	0.005304	0.08427	1

PEO <sub>132</sub> -PB <sub>89</sub> /CD <sub>3</sub> OD 21.3 °C					PEO <sub>132</sub> -PB <sub>89</sub> /CD <sub>3</sub> OD 30.6 °C						
Q	I(Q)	Std Dev(I(Q))	sigmaQ	meanQ	Shadow Factor	Q	I(Q)	Std Dev(I(Q))	sigmaQ	meanQ	Shadow Factor
0.08557	0.07984	0.00197	0.005375	0.08559	1	0.007069	0.07669	0.002116	0.005375	0.08559	1
0.08578	0.07863	0.001261	0.006598	0.08589	1	0.007069	0.0796	0.001342	0.006598	0.08589	1
0.08689	0.08017	0.002235	0.005445	0.08691	1	0.007069	0.08362	0.00222	0.005445	0.08691	1
0.08821	0.07744	0.002392	0.005516	0.08823	1	0.007069	0.08442	0.002457	0.005516	0.08823	1
0.08953	0.07733	0.002396	0.005587	0.08955	1	0.007069	0.07894	0.002255	0.005587	0.08955	1
0.08975	0.0757	0.001099	0.006772	0.08985	1	0.007069	0.07775	0.000934	0.006772	0.08985	1
0.09084	0.07305	0.002644	0.005658	0.09087	1	0.007069	0.07471	0.002502	0.005658	0.09087	1
0.09216	0.07486	0.002536	0.005729	0.09219	1	0.007069	0.0771	0.002463	0.005729	0.09219	1
0.09348	0.07239	0.00266	0.0058	0.0935	1	0.007069	0.07624	0.002779	0.0058	0.0935	1
0.09371	0.07262	0.001029	0.006949	0.09381	1	0.007069	0.07443	0.001108	0.006949	0.09381	1
0.0948	0.07508	0.002718	0.005872	0.09482	1	0.007069	0.07891	0.003037	0.005872	0.09482	1
0.09612	0.07797	0.003211	0.005943	0.09614	1	0.007069	0.08231	0.003063	0.005943	0.09614	1
0.09743	0.07967	0.002696	0.006015	0.09746	1	0.007069	0.07624	0.003406	0.006015	0.09746	1
0.09768	0.07514	0.001152	0.00713	0.09777	1	0.007069	0.07557	0.001217	0.00713	0.09777	1
0.09875	0.07738	0.003221	0.006086	0.09877	1	0.007069	0.07714	0.003079	0.006086	0.09877	1
0.1001	0.07402	0.003324	0.006158	0.1001	1	0.007069	0.0781	0.003672	0.006158	0.1001	1
0.1014	0.06996	0.003477	0.00623	0.1014	1	0.007069	0.07911	0.003471	0.00623	0.1014	1
0.1016	0.07248	0.00111	0.007313	0.1017	1	0.007069	0.07414	0.001118	0.007313	0.1017	1
0.1027	0.07884	0.003889	0.006302	0.1027	1	0.007069	0.07843	0.00404	0.006302	0.1027	1
0.104	0.07335	0.003765	0.006374	0.104	1	0.007069	0.07579	0.004047	0.006374	0.104	1
0.1053	0.07755	0.003902	0.006446	0.1053	1	0.007069	0.07706	0.004539	0.006446	0.1053	1
0.1056	0.07382	0.00104	0.007498	0.1057	1	0.007069	0.07546	0.001043	0.007498	0.1057	1
0.1066	0.07538	0.004964	0.006518	0.1067	1	0.007069	0.07647	0.004858	0.006518	0.1067	1
0.108	0.07601	0.004953	0.006591	0.108	1	0.007069	0.07583	0.005986	0.006591	0.108	1
0.1093	0.08655	0.006165	0.006663	0.1093	1	0.007069	0.08426	0.005039	0.006663	0.1093	1
0.1095	0.07371	0.001068	0.007685	0.1096	1	0.007069	0.0767	0.00105	0.007685	0.1096	1
0.1106	0.06977	0.006707	0.006735	0.1106	1	0.007069	0.07529	0.007736	0.006735	0.1106	1
0.1119	0.07595	0.008037	0.006808	0.1119	1	0.007069	0.07975	0.005582	0.006808	0.1119	1
0.1132	0.08073	0.006021	0.00688	0.1132	1	0.007069	0.06744	0.007703	0.00688	0.1132	1
0.1135	0.06986	0.001034	0.007875	0.1136	1	0.007069	0.07402	0.001044	0.007875	0.1136	1
0.1174	0.07177	0.00102	0.008066	0.1175	1	0.007069	0.07266	0.000973	0.008066	0.1175	1
0.1214	0.07108	0.001028	0.008259	0.1215	1	0.007069	0.07177	0.001012	0.008259	0.1215	1
0.1253	0.07213	0.000911	0.008453	0.1254	1	0.007069	0.073	0.00089	0.008453	0.1254	1
0.1293	0.07054	0.000943	0.008649	0.1293	1	0.007069	0.07146	0.000946	0.008649	0.1293	1
0.1332	0.0703	0.000932	0.008847	0.1333	1	0.007069	0.07209	0.000834	0.008847	0.1333	1
0.1371	0.07196	0.000856	0.009045	0.1372	1	0.007069	0.0723	0.000965	0.009045	0.1372	1
0.141	0.06977	0.000896	0.009245	0.1411	1	0.007069	0.07123	0.000959	0.009245	0.1411	1
0.1449	0.07114	0.000922	0.009445	0.145	1	0.007069	0.07264	0.000928	0.009445	0.145	1
0.1489	0.07125	0.000869	0.009647	0.1489	1	0.007069	0.07418	0.000774	0.009647	0.1489	1
0.1528	0.07191	0.000898	0.009849	0.1528	1	0.007069	0.07178	0.000881	0.009849	0.1528	1
0.1567	0.06991	0.000845	0.01005	0.1567	1	0.007069	0.07203	0.000908	0.01005	0.1567	1
0.1606	0.06907	0.000915	0.01026	0.1606	1	0.007069	0.07058	0.000785	0.01026	0.1606	1
0.1645	0.06944	0.000776	0.01046	0.1645	1	0.007069	0.07075	0.000867	0.01046	0.1645	1
0.1683	0.07012	0.000844	0.01067	0.1684	1	0.007069	0.07071	0.000735	0.01067	0.1684	1
0.1722	0.06987	0.00089	0.01087	0.1723	1	0.007069	0.07113	0.000782	0.01087	0.1723	1
0.1761	0.06975	0.000758	0.01108	0.1762	1	0.007069	0.07064	0.000852	0.01108	0.1762	1
0.18	0.06805	0.000886	0.01128	0.18	1	0.007069	0.06967	0.000821	0.01128	0.18	1
0.1838	0.07013	0.000728	0.01149	0.1839	1	0.007069	0.07137	0.000846	0.01149	0.1839	1
0.1877	0.06966	0.000788	0.0117	0.1877	1	0.007069	0.0707	0.000794	0.0117	0.1877	1
0.1916	0.06992	0.000784	0.0119	0.1916	1	0.007069	0.06996	0.00085	0.0119	0.1916	1
0.1954	0.06818	0.000805	0.01211	0.1954	1	0.007069	0.07068	0.000752	0.01211	0.1954	1
0.1992	0.06882	0.000816	0.01232	0.1993	1	0.007069	0.06999	0.00081	0.01232	0.1993	1
0.2031	0.06974	0.000761	0.01253	0.2031	1	0.007069	0.06989	0.000779	0.01253	0.2031	1
0.2069	0.06975	0.000806	0.01274	0.2069	1	0.007069	0.07066	0.000834	0.01274	0.2069	1
0.2107	0.06959	0.000733	0.01294	0.2108	1	0.007069	0.07006	0.000754	0.01294	0.2108	1
0.2145	0.06872	0.000722	0.01315	0.2146	1	0.007069	0.06891	0.000711	0.01315	0.2146	1
0.2184	0.06845	0.000718	0.01336	0.2184	1	0.007069	0.06985	0.000703	0.01336	0.2184	1
0.2222	0.06883	0.000674	0.01357	0.2222	1	0.007069	0.06998	0.000675	0.01357	0.2222	1
0.226	0.06885	0.000763	0.01378	0.226	1	0.007069	0.06961	0.000768	0.01378	0.226	1
0.2297	0.06854	0.000788	0.01399	0.2298	1	0.007069	0.07137	0.000732	0.01399	0.2298	1
0.2335	0.06828	0.000698	0.01419	0.2336	1	0.007069	0.07007	0.000675	0.01419	0.2336	1
0.2373	0.07002	0.000702	0.0144	0.2373	1	0.007069	0.07148	0.000755	0.0144	0.2373	1
0.2411	0.06957	0.0008	0.01461	0.2411	1	0.007069	0.07032	0.000723	0.01461	0.2411	1
0.2448	0.06785	0.000834	0.01482	0.2449	1	0.007069	0.06954	0.000821	0.01482	0.2449	1
0.2486	0.06837	0.000792	0.01503	0.2486	1	0.007069	0.0694	0.000886	0.01503	0.2486	1
0.2523	0.06959	0.000881	0.01523	0.2524	1	0.007069	0.06892	0.000827	0.01523	0.2524	1
0.2561	0.0683	0.000834	0.01544	0.2561	1	0.007069	0.06949	0.000878	0.01544	0.2561	1
0.2598	0.06809	0.000834	0.01565	0.2598	1	0.007069	0.06994	0.000795	0.01565	0.2598	1
0.2635	0.06821	0.000832	0.01586	0.2636	1	0.007069	0.06989	0.000852	0.01586	0.2636	1
0.2673	0.07011	0.000856	0.01606	0.2673	1	0.007069	0.0709	0.000839	0.01606	0.2673	1
0.271	0.06926	0.000899	0.01627	0.271	1	0.007069	0.07049	0.000855	0.01627	0.271	1
0.2747	0.06815	0.000879	0.01648	0.2747	1	0.007069	0.06958	0.000817	0.01648	0.2747	1
0.2784	0.06819	0.000859	0.01668	0.2784	1	0.007069	0.06868	0.000862	0.01668	0.2784	1
0.282	0.06752	0.000889	0.01689	0.2821	1	0.007069	0.06902	0.000796	0.01689	0.2821	1
0.2857	0.06929	0.000851	0.01709	0.2857	1	0.007069	0.06969	0.000859	0.01709	0.2857	1
0.2894	0.069	0.000838	0.0173	0.2894	1	0.007069	0.06968	0.000878	0.0173	0.2894	1
0.293	0.06923	0.000916	0.0175	0.2931	1	0.007069	0.07022	0.000912	0.0175	0.2931	1
0.2967	0.06949	0.000765	0.01771	0.2967	1	0.007069	0.07048	0.000894	0.01771	0.2967	1
0.3003	0.06818	0.000881	0.01791	0.3004	1	0.007069	0.06975	0.000903	0.01791	0.3004	1
0.304	0.06838	0.000946	0.01812	0.304	1	0.007069	0.0693	0.000834	0.01812	0.304	1
0.3076	0.06738	0.00092	0.01832	0.3076	1	0.007069	0.07006	0.000964	0.01832	0.3076	1

PEO <sub>132</sub> -PB <sub>89</sub> /CD <sub>3</sub> OD 21.3 °C					PEO <sub>132</sub> -PB <sub>89</sub> /CD <sub>3</sub> OD 30.6 °C						
Q	I(Q)	Std Dev(I(Q))	sigmaQ	meanQ	Shadow Factor	Q	I(Q)	Std Dev(I(Q))	sigmaQ	meanQ	Shadow Factor
0.3112	0.06923	0.000968	0.01852	0.3113	1	0.007069	0.07008	0.000928	0.01852	0.3113	1
0.3148	0.06769	0.000916	0.01873	0.3149	1	0.007069	0.06868	0.000993	0.01873	0.3149	1
0.3184	0.0694	0.000924	0.01893	0.3185	1	0.007069	0.06868	0.00091	0.01893	0.3185	1
0.322	0.06874	0.000895	0.01913	0.3221	1	0.007069	0.06931	0.000811	0.01913	0.3221	1
0.3256	0.06952	0.001023	0.01933	0.3256	1	0.007069	0.06958	0.000965	0.01933	0.3256	1
0.3292	0.06897	0.00086	0.01954	0.3292	1	0.007069	0.06808	0.000884	0.01954	0.3292	1
0.3327	0.06716	0.000819	0.01974	0.3328	1	0.007069	0.06937	0.000904	0.01974	0.3328	1
0.3363	0.06735	0.000873	0.01994	0.3363	1	0.007069	0.06998	0.000925	0.01994	0.3363	1
0.3399	0.06821	0.000948	0.02014	0.3399	1	0.007069	0.0694	0.000835	0.02014	0.3399	1
0.3434	0.06798	0.000879	0.02034	0.3434	1	0.007069	0.06812	0.000892	0.02034	0.3434	1
0.3469	0.06854	0.000847	0.02054	0.3469	1	0.007069	0.06972	0.000891	0.02054	0.3469	1
0.3504	0.06949	0.000983	0.02074	0.3505	1	0.007069	0.06998	0.000889	0.02074	0.3505	1
0.3539	0.06839	0.000851	0.02094	0.354	1	0.007069	0.069	0.000843	0.02094	0.354	1
0.3574	0.06811	0.000975	0.02113	0.3575	1	0.007069	0.06785	0.000874	0.02113	0.3575	1
0.3609	0.06869	0.000961	0.02133	0.361	1	0.007069	0.06818	0.000954	0.02133	0.361	1
0.3644	0.06829	0.00094	0.02153	0.3644	1	0.007069	0.06659	0.000894	0.02153	0.3644	1
0.3679	0.06826	0.000816	0.02173	0.3679	1	0.007069	0.07013	0.000902	0.02173	0.3679	1
0.3713	0.0681	0.000924	0.02192	0.3714	1	0.007069	0.06696	0.000936	0.02192	0.3714	1
0.3748	0.06995	0.00096	0.02212	0.3748	1	0.007069	0.06932	0.000865	0.02212	0.3748	1
0.3782	0.06884	0.000914	0.02231	0.3783	1	0.007069	0.06975	0.000887	0.02231	0.3783	1
0.3817	0.06756	0.000855	0.02251	0.3817	1	0.007069	0.06832	0.000918	0.02251	0.3817	1
0.3851	0.06829	0.000919	0.0227	0.3851	1	0.007069	0.06921	0.00088	0.0227	0.3851	1
0.3885	0.06772	0.000999	0.0229	0.3885	1	0.007069	0.06833	0.000962	0.0229	0.3885	1
0.3919	0.06847	0.000843	0.02309	0.3919	1	0.007069	0.06961	0.000875	0.02309	0.3919	1
0.3953	0.06826	0.001019	0.02328	0.3953	1	0.007069	0.06889	0.001015	0.02328	0.3953	1
0.3987	0.06642	0.000894	0.02347	0.3987	1	0.007069	0.06886	0.000993	0.02347	0.3987	1
0.4021	0.06818	0.000915	0.02367	0.4021	1	0.007069	0.06926	0.00095	0.02367	0.4021	1
0.4054	0.0687	0.000969	0.02386	0.4054	1	0.007069	0.06782	0.00095	0.02386	0.4054	1
0.4088	0.06959	0.000967	0.02405	0.4088	1	0.007069	0.07042	0.001066	0.02405	0.4088	1
0.4121	0.06833	0.000967	0.02424	0.4121	1	0.007069	0.07009	0.000814	0.02424	0.4121	1
0.4155	0.06785	0.000873	0.02443	0.4155	1	0.007069	0.06903	0.000876	0.02443	0.4155	1
0.4188	0.06754	0.001017	0.02462	0.4188	1	0.007069	0.06904	0.000934	0.02462	0.4188	1
0.4221	0.0688	0.000894	0.02481	0.4221	1	0.007069	0.06832	0.000983	0.02481	0.4221	1
0.4254	0.06904	0.00104	0.02499	0.4254	1	0.007069	0.06872	0.001027	0.02499	0.4254	1
0.4287	0.0675	0.001217	0.02518	0.4287	1	0.007069	0.06944	0.001033	0.02518	0.4287	1
0.432	0.06812	0.001196	0.02537	0.432	1	0.007069	0.06813	0.00125	0.02537	0.432	1
0.4352	0.06831	0.001301	0.02556	0.4353	1	0.007069	0.06731	0.00112	0.02556	0.4353	1
0.4385	0.06892	0.001541	0.02574	0.4385	1	0.007069	0.07021	0.001412	0.02574	0.4385	1
0.4417	0.06823	0.001408	0.02593	0.4418	1	0.007069	0.06604	0.00156	0.02593	0.4418	1
0.445	0.06434	0.001688	0.02611	0.445	1	0.007069	0.06729	0.001132	0.02611	0.445	1
0.4482	0.06842	0.001759	0.0263	0.4482	1	0.007069	0.07326	0.001773	0.0263	0.4482	1
0.4514	0.06709	0.001909	0.02648	0.4515	1	0.007069	0.06701	0.001799	0.02648	0.4515	1
0.4546	0.06698	0.001999	0.02666	0.4547	1	0.007069	0.06733	0.001597	0.02666	0.4547	1
0.4578	0.06664	0.001489	0.02685	0.4579	1	0.007069	0.06703	0.001528	0.02685	0.4579	1
0.461	0.06818	0.002496	0.02703	0.461	1	0.007069	0.06853	0.002562	0.02703	0.461	1

PEO <sub>132</sub> -PB <sub>89</sub> /CD <sub>3</sub> OD 39.9 °C					PEO <sub>132</sub> -PB <sub>89</sub> /CD <sub>3</sub> OD 49.3 °C						
Q	I(Q)	Std Dev(I(Q))	sigmaQ	meanQ	Shadow Factor	Q	I(Q)	Std Dev(I(Q))	sigmaQ	meanQ	Shadow Factor
0.003433	10.16	0.2014	0.001072	0.003606	0.9585	0.003433	9.377	0.2129	0.001072	0.003606	0.9585
0.003837	10.76	0.1317	0.001076	0.003977	0.9999	0.003837	10.27	0.1378	0.001076	0.003977	0.9999
0.004241	10.55	0.1031	0.001078	0.004367	1	0.004241	10.02	0.1087	0.001078	0.004367	1
0.004645	10.57	0.09781	0.001081	0.00476	1	0.004645	9.833	0.1015	0.001081	0.00476	1
0.005049	10.33	0.102	0.001086	0.005155	1	0.005049	9.685	0.1047	0.001086	0.005155	1
0.005453	10.18	0.09363	0.001091	0.005551	1	0.005453	9.426	0.09947	0.001091	0.005551	1
0.005857	10.08	0.09104	0.001097	0.005948	1	0.005857	9.443	0.08925	0.001097	0.005948	1
0.006261	10.03	0.08972	0.001103	0.006346	1	0.006261	9.538	0.08032	0.001103	0.006346	1
0.006665	9.829	0.08732	0.001111	0.006745	1	0.006665	9.36	0.08527	0.001111	0.006745	1
0.007069	9.799	0.08545	0.001118	0.007144	1	0.007069	9.141	0.08723	0.001118	0.007144	1
0.007473	9.632	0.08132	0.001127	0.007544	1	0.007473	8.975	0.07741	0.001127	0.007544	1
0.007876	9.348	0.07713	0.001135	0.007944	1	0.007876	8.923	0.07397	0.001135	0.007944	1
0.00828	9.414	0.06382	0.001145	0.008345	1	0.00828	8.8	0.07415	0.001145	0.008345	1
0.008684	9.091	0.06648	0.001154	0.008746	1	0.008684	8.59	0.06971	0.001154	0.008746	1
0.009088	9.124	0.07284	0.001164	0.009147	1	0.009088	8.468	0.05854	0.001164	0.009147	1
0.009492	8.915	0.0662	0.001175	0.009548	1	0.009492	8.47	0.06638	0.001175	0.009548	1
0.009896	8.693	0.07051	0.001186	0.00995	1	0.009896	8.172	0.06135	0.001186	0.00995	1
0.0103	8.509	0.06094	0.001197	0.01035	1	0.0103	7.979	0.06594	0.001197	0.01035	1
0.0107	8.43	0.05771	0.001209	0.01075	1	0.0107	7.905	0.05755	0.001209	0.01075	1
0.01111	8.246	0.05849	0.001221	0.01116	1	0.01111	7.695	0.05606	0.001221	0.01116	1
0.0113	8.082	0.04748	0.001291	0.01149	1	0.0113	7.645	0.04724	0.001291	0.01149	1
0.01151	7.984	0.05828	0.001233	0.01156	1	0.01151	7.469	0.05906	0.001233	0.01156	1
0.01192	7.891	0.05503	0.001246	0.01196	1	0.01192	7.304	0.05537	0.001246	0.01196	1
0.01232	7.73	0.05377	0.001259	0.01236	1	0.01232	7.195	0.04689	0.001259	0.01236	1
0.01263	7.433	0.04382	0.002212	0.0128	1	0.01263	7.056	0.04036	0.002212	0.0128	1
0.01272	7.525	0.05994	0.001272	0.01277	1	0.01272	7.076	0.05083	0.001272	0.01277	1
0.01313	7.292	0.05568	0.001286	0.01317	1	0.01313	6.86	0.04976	0.001286	0.01317	1
0.01353	7.046	0.04779	0.0013	0.01357	1	0.01353	6.551	0.04722	0.0013	0.01357	1
0.01393	6.796	0.04631	0.001314	0.01397	1	0.01393	6.392	0.0495	0.001314	0.01397	1
0.01396	6.805	0.04294	0.002236	0.01412	1	0.01396	6.477	0.04288	0.002236	0.01412	1
0.01434	6.609	0.04834	0.001328	0.01438	1	0.01434	6.197	0.04151	0.001328	0.01438	1



PEO <sub>132</sub> -PB <sub>89</sub> /CD <sub>3</sub> OD 39.9 °C					PEO <sub>132</sub> -PB <sub>89</sub> /CD <sub>3</sub> OD 49.3 °C						
Q	I(Q)	Std Dev(I(Q))	sigmaQ	meanQ	Shadow Factor	Q	I(Q)	Std Dev(I(Q))	sigmaQ	meanQ	Shadow Factor
0.01474	6.418	0.04593	0.001343	0.01478	1	0.01474	5.947	0.04575	0.001343	0.01478	1
0.01515	6.2	0.04495	0.001358	0.01518	1	0.01515	5.839	0.04402	0.001358	0.01518	1
0.01529	6.118	0.03993	0.002264	0.01543	1	0.01529	5.779	0.04025	0.002264	0.01543	1
0.01555	5.972	0.04211	0.001373	0.01558	1	0.01555	5.595	0.04533	0.001373	0.01558	1
0.01595	5.729	0.04514	0.001389	0.01599	1	0.01595	5.46	0.04195	0.001389	0.01599	1
0.01636	5.554	0.04245	0.001404	0.01639	1	0.01636	5.284	0.04398	0.001404	0.01639	1
0.01662	5.493	0.03545	0.002294	0.01675	1	0.01662	5.165	0.0342	0.002294	0.01675	1
0.01676	5.364	0.03682	0.00142	0.01679	1	0.01676	5.15	0.04464	0.00142	0.01679	1
0.01717	5.164	0.04294	0.001436	0.0172	1	0.01717	4.973	0.03907	0.001436	0.0172	1
0.01757	4.963	0.04103	0.001453	0.0176	1	0.01757	4.701	0.03944	0.001453	0.0176	1
0.01795	4.853	0.0326	0.002326	0.01807	1	0.01795	4.604	0.03164	0.002326	0.01807	1
0.01797	4.754	0.03973	0.001469	0.018	1	0.01797	4.603	0.03688	0.001469	0.018	1
0.01838	4.641	0.04116	0.001486	0.01841	1	0.01838	4.379	0.03438	0.001486	0.01841	1
0.01878	4.416	0.03529	0.001503	0.01881	1	0.01878	4.27	0.03351	0.001503	0.01881	1
0.01918	4.316	0.03625	0.00152	0.01921	1	0.01918	4.031	0.03942	0.00152	0.01921	1
0.01928	4.264	0.03054	0.002361	0.01939	1	0.01928	4.034	0.0296	0.002361	0.01939	1
0.01959	4.105	0.03728	0.001537	0.01962	1	0.01959	3.881	0.03462	0.001537	0.01962	1
0.01999	3.952	0.03351	0.001554	0.02002	1	0.01999	3.714	0.03529	0.001554	0.02002	1
0.0204	3.778	0.03466	0.001572	0.02042	1	0.0204	3.554	0.03234	0.001572	0.02042	1
0.02061	3.703	0.02673	0.002398	0.02072	1	0.02061	3.519	0.02619	0.002398	0.02072	1
0.0208	3.587	0.03504	0.001589	0.02083	1	0.0208	3.428	0.03106	0.001589	0.02083	1
0.0212	3.426	0.03181	0.001607	0.02123	1	0.0212	3.194	0.03188	0.001607	0.02123	1
0.02161	3.276	0.0341	0.001625	0.02163	1	0.02161	3.106	0.02977	0.001625	0.02163	1
0.02194	3.2	0.02393	0.002436	0.02204	1	0.02194	3.032	0.02198	0.002436	0.02204	1
0.02201	3.129	0.02986	0.001643	0.02203	1	0.02201	2.936	0.03	0.001643	0.02203	1
0.02241	2.978	0.03053	0.001661	0.02244	1	0.02241	2.825	0.02746	0.001661	0.02244	1
0.02282	2.858	0.02866	0.00168	0.02284	1	0.02282	2.676	0.02867	0.00168	0.02284	1
0.02322	2.721	0.02611	0.001698	0.02324	1	0.02322	2.574	0.02889	0.001698	0.02324	1
0.02327	2.713	0.02258	0.002477	0.02336	1	0.02327	2.581	0.01951	0.002477	0.02336	1
0.02363	2.598	0.02916	0.001717	0.02365	1	0.02363	2.486	0.02641	0.001717	0.02365	1
0.02403	2.421	0.02442	0.001736	0.02405	1	0.02403	2.367	0.02552	0.001736	0.02405	1
0.02443	2.361	0.02433	0.001754	0.02445	1	0.02443	2.235	0.02574	0.001754	0.02445	1
0.0246	2.325	0.01754	0.002519	0.02469	1	0.0246	2.192	0.01771	0.002519	0.02469	1
0.02484	2.214	0.02578	0.001773	0.02486	1	0.02484	2.104	0.02592	0.001773	0.02486	1
0.02524	2.141	0.02863	0.001792	0.02526	1	0.02524	1.981	0.02716	0.001792	0.02526	1
0.02564	2.055	0.02844	0.001812	0.02566	1	0.02564	1.967	0.02973	0.001812	0.02566	1
0.02593	1.976	0.01506	0.002563	0.02601	1	0.02593	1.882	0.01327	0.002563	0.02601	1
0.02605	1.903	0.02596	0.001831	0.02607	1	0.02605	1.813	0.02613	0.001831	0.02607	1
0.02645	1.782	0.02542	0.00185	0.02647	1	0.02645	1.695	0.02762	0.00185	0.02647	1
0.02685	1.752	0.02945	0.00187	0.02687	1	0.02685	1.626	0.02807	0.00187	0.02687	1
0.02726	1.663	0.02685	0.001889	0.02728	1	0.02726	1.56	0.02518	0.001889	0.02728	1
0.02726	1.639	0.01328	0.002609	0.02734	1	0.02726	1.569	0.01141	0.002609	0.02734	1
0.02766	1.519	0.0273	0.001909	0.02768	1	0.02766	1.52	0.02834	0.001909	0.02768	1
0.02807	1.45	0.02882	0.001928	0.02808	1	0.02807	1.415	0.02766	0.001928	0.02808	1
0.02847	1.385	0.02824	0.001948	0.02849	1	0.02847	1.28	0.02754	0.001948	0.02849	1
0.02859	1.376	0.009916	0.002656	0.02866	1	0.02859	1.311	0.01029	0.002656	0.02866	1
0.02887	1.288	0.02652	0.001968	0.02889	1	0.02887	1.199	0.02536	0.001968	0.02889	1
0.02928	1.271	0.02627	0.001988	0.02929	1	0.02928	1.189	0.02485	0.001988	0.02929	1
0.02968	1.189	0.02548	0.002008	0.0297	1	0.02968	1.183	0.02744	0.002008	0.0297	1
0.02991	1.131	0.008416	0.002705	0.02999	1	0.02991	1.084	0.008946	0.002705	0.02999	1
0.03008	1.089	0.0246	0.002028	0.0301	1	0.03008	1.012	0.02178	0.002028	0.0301	1
0.03049	1.027	0.02536	0.002048	0.0305	1	0.03049	0.9762	0.02137	0.002048	0.0305	1
0.03089	0.9668	0.02378	0.002068	0.03091	1	0.03089	0.9679	0.02334	0.002068	0.03091	1
0.03124	0.935	0.008275	0.002754	0.03131	1	0.03124	0.8962	0.007821	0.002754	0.03131	1
0.03129	0.9054	0.024	0.002089	0.03131	1	0.03129	0.9003	0.02056	0.002089	0.03131	1
0.0317	0.8747	0.02302	0.002109	0.03171	1	0.0317	0.8762	0.02315	0.002109	0.03171	1
0.0321	0.7393	0.02006	0.002129	0.03212	1	0.0321	0.7951	0.02121	0.002129	0.03212	1
0.0325	0.7401	0.01969	0.00215	0.03252	1	0.0325	0.7468	0.02078	0.00215	0.03252	1
0.03257	0.7681	0.006884	0.002806	0.03264	1	0.03257	0.7396	0.006958	0.002806	0.03264	1
0.03291	0.7472	0.02206	0.00217	0.03292	1	0.03291	0.6869	0.01969	0.00217	0.03292	1
0.03331	0.7168	0.02125	0.002191	0.03333	1	0.03331	0.6483	0.01951	0.002191	0.03333	1
0.03372	0.6252	0.02039	0.002212	0.03373	1	0.03372	0.6329	0.01967	0.002212	0.03373	1
0.0339	0.6349	0.006097	0.002858	0.03396	1	0.0339	0.606	0.005981	0.002858	0.03396	1
0.03399	0.6682	0.02154	0.004785	0.03426	1	0.03399	0.6477	0.02099	0.004785	0.03426	1
0.03412	0.6395	0.0216	0.002232	0.03413	1	0.03412	0.5869	0.01794	0.002232	0.03413	1
0.03452	0.5901	0.02199	0.002253	0.03454	1	0.03452	0.5271	0.02329	0.002253	0.03454	1
0.03493	0.527	0.02085	0.002274	0.03494	1	0.03493	0.4989	0.02023	0.002274	0.03494	1
0.03523	0.5259	0.005409	0.002911	0.03529	1	0.03523	0.5012	0.005211	0.002911	0.03529	1
0.03533	0.4839	0.0228	0.002295	0.03534	1	0.03533	0.4848	0.02198	0.002295	0.03534	1
0.03573	0.4925	0.02343	0.002316	0.03575	1	0.03573	0.472	0.02267	0.002316	0.03575	1
0.03614	0.4605	0.02243	0.002336	0.03615	1	0.03614	0.3971	0.02259	0.002336	0.03615	1
0.03654	0.4003	0.02797	0.002357	0.03655	1	0.03654	0.4199	0.02308	0.002357	0.03655	1
0.03656	0.4213	0.004774	0.002966	0.03662	1	0.03656	0.4033	0.00444	0.002966	0.03662	1
0.03694	0.4436	0.02835	0.002378	0.03696	1	0.03694	0.3418	0.02553	0.002378	0.03696	1
0.03735	0.3583	0.02074	0.0024	0.03736	1	0.03735	0.3559	0.02245	0.0024	0.03736	1
0.03775	0.3867	0.02565	0.002421	0.03776	1	0.03775	0.2866	0.02388	0.002421	0.03776	1
0.03788	0.3464	0.004271	0.003021	0.03794	1	0.03788	0.3351	0.004336	0.003021	0.03794	1
0.03798	0.3827	0.01244	0.004881	0.03823	1	0.03798	0.3691	0.01229	0.004881	0.03823	1
0.03815	0.3091	0.03553	0.002442	0.03817	1	0.03815	0.3328	0.028	0.002442	0.03817	1
0.03856	0.344	0.02574	0.002463	0.03857	1	0.03856	0.3427	0.02785	0.002463	0.03857	1
0.03896	0.3178	0.03495	0.002484	0.03897	1	0.03896	0.301	0.03103	0.002484	0.03897	1

PEO <sub>132</sub> -PB <sub>89</sub> /CD <sub>3</sub> OD 39.9 °C					PEO <sub>132</sub> -PB <sub>89</sub> /CD <sub>3</sub> OD 49.3 °C						
Q	I(Q)	Std Dev(I(Q))	sigmaQ	meanQ	Shadow Factor	Q	I(Q)	Std Dev(I(Q))	sigmaQ	meanQ	Shadow Factor
0.03921	0.2828	0.003909	0.003077	0.03927	1	0.03921	0.2757	0.003751	0.003077	0.03927	1
0.03936	0.2714	0.03046	0.002506	0.03938	1	0.03936	0.3083	0.04537	0.002506	0.03938	1
0.03977	0.2697	0.03899	0.002527	0.03978	1	0.03977	0.311	0.0363	0.002527	0.03978	1
0.04017	0.2388	0.03489	0.002548	0.04018	1	0.04017	0.1954	0.03512	0.002548	0.04018	1
0.04054	0.2341	0.003518	0.003134	0.04059	1	0.04054	0.2271	0.003189	0.003134	0.04059	1
0.04057	0.2744	0.0341	0.00257	0.04059	1	0.04057	0.2524	0.03561	0.00257	0.04059	1
0.04187	0.1982	0.002986	0.003192	0.04192	1	0.04187	0.1957	0.003151	0.003192	0.04192	1
0.04197	0.2221	0.006584	0.004987	0.0422	1	0.04197	0.2149	0.006399	0.004987	0.0422	1
0.0432	0.1741	0.002935	0.003251	0.04325	1	0.0432	0.1704	0.00302	0.003251	0.04325	1
0.04452	0.1461	0.002637	0.003311	0.04457	1	0.04452	0.1444	0.003062	0.003311	0.04457	1
0.04585	0.1275	0.002621	0.003371	0.0459	1	0.04585	0.1299	0.002713	0.003371	0.0459	1
0.04597	0.1414	0.003631	0.005102	0.04617	1	0.04597	0.1384	0.003319	0.005102	0.04617	1
0.04718	0.1187	0.00256	0.003432	0.04722	1	0.04718	0.1201	0.002615	0.003432	0.04722	1
0.0485	0.1085	0.002315	0.003493	0.04855	1	0.0485	0.1088	0.002272	0.003493	0.04855	1
0.04983	0.1015	0.002341	0.003555	0.04987	1	0.04983	0.1031	0.002307	0.003555	0.04987	1
0.04996	0.1052	0.001807	0.005225	0.05014	1	0.04996	0.1065	0.001814	0.005225	0.05014	1
0.05116	0.09616	0.002386	0.003618	0.0512	1	0.05116	0.09881	0.002232	0.003618	0.0512	1
0.05248	0.09237	0.002283	0.003681	0.05252	1	0.05248	0.0942	0.002345	0.003681	0.05252	1
0.05381	0.09605	0.002288	0.003745	0.05385	1	0.05381	0.09085	0.002122	0.003745	0.05385	1
0.05394	0.09236	0.00163	0.005355	0.05412	1	0.05394	0.09536	0.001457	0.005355	0.05412	1
0.05514	0.08901	0.002115	0.003809	0.05517	1	0.05514	0.09047	0.002179	0.003809	0.05517	1
0.05646	0.09376	0.0022	0.003874	0.0565	1	0.05646	0.09618	0.002106	0.003874	0.0565	1
0.05779	0.09452	0.002152	0.003939	0.05782	1	0.05779	0.09147	0.002157	0.003939	0.05782	1
0.05793	0.09021	0.001275	0.005492	0.05809	1	0.05793	0.09201	0.001459	0.005492	0.05809	1
0.05911	0.09014	0.002116	0.004004	0.05915	1	0.05911	0.09361	0.002144	0.004004	0.05915	1
0.06044	0.09711	0.002334	0.00407	0.06047	1	0.06044	0.09376	0.002063	0.00407	0.06047	1
0.06176	0.09179	0.002111	0.004137	0.0618	1	0.06176	0.09875	0.001995	0.004137	0.0618	1
0.06192	0.09131	0.001541	0.005635	0.06207	1	0.06192	0.09145	0.001268	0.005635	0.06207	1
0.06309	0.09702	0.002237	0.004203	0.06312	1	0.06309	0.09596	0.002108	0.004203	0.06312	1
0.06441	0.0945	0.002218	0.00427	0.06444	1	0.06441	0.09317	0.00202	0.00427	0.06444	1
0.06573	0.09686	0.001886	0.004337	0.06577	1	0.06573	0.09191	0.001836	0.004337	0.06577	1
0.0659	0.09103	0.001381	0.005784	0.06604	1	0.0659	0.09134	0.001265	0.005784	0.06604	1
0.06706	0.0985	0.002064	0.004405	0.06709	1	0.06706	0.09466	0.001883	0.004405	0.06709	1
0.06838	0.09631	0.001981	0.004473	0.06841	1	0.06838	0.09495	0.001838	0.004473	0.06841	1
0.06971	0.09738	0.001918	0.004541	0.06974	1	0.06971	0.09953	0.001872	0.004541	0.06974	1
0.06988	0.09143	0.001302	0.005938	0.07001	1	0.06988	0.09264	0.001221	0.005938	0.07001	1
0.07103	0.09493	0.002038	0.004609	0.07106	1	0.07103	0.09728	0.00187	0.004609	0.07106	1
0.07235	0.09526	0.001958	0.004678	0.07238	1	0.07235	0.09394	0.001932	0.004678	0.07238	1
0.07367	0.09505	0.001942	0.004746	0.0737	1	0.07367	0.09008	0.00198	0.004746	0.0737	1
0.07386	0.08932	0.001286	0.006097	0.07399	1	0.07386	0.09152	0.001086	0.006097	0.07399	1
0.075	0.09076	0.001757	0.004815	0.07503	1	0.075	0.09226	0.001901	0.004815	0.07503	1
0.07632	0.09342	0.001877	0.004885	0.07635	1	0.07632	0.09084	0.001869	0.004885	0.07635	1
0.07764	0.08924	0.001884	0.004954	0.07767	1	0.07764	0.08872	0.002003	0.004954	0.07767	1
0.07784	0.08675	0.001202	0.00626	0.07796	1	0.07784	0.08767	0.001146	0.00626	0.07796	1
0.07896	0.08689	0.001885	0.005024	0.07899	1	0.07896	0.08922	0.001936	0.005024	0.07899	1
0.08028	0.08793	0.001934	0.005094	0.08031	1	0.08028	0.08864	0.001902	0.005094	0.08031	1
0.08161	0.08813	0.001845	0.005164	0.08163	1	0.08161	0.08655	0.001805	0.005164	0.08163	1
0.08181	0.08358	0.001358	0.006427	0.08192	1	0.08181	0.08586	0.001089	0.006427	0.08192	1
0.08293	0.08646	0.00215	0.005234	0.08295	1	0.08293	0.08714	0.002128	0.005234	0.08295	1
0.08425	0.08491	0.002074	0.005304	0.08427	1	0.08425	0.08458	0.002308	0.005304	0.08427	1
0.08557	0.08344	0.002063	0.005375	0.08559	1	0.08557	0.08298	0.002206	0.005375	0.08559	1
0.08578	0.08152	0.001134	0.006598	0.08589	1	0.08578	0.08178	0.001106	0.006598	0.08589	1
0.08689	0.0852	0.002332	0.005445	0.08691	1	0.08689	0.08515	0.002105	0.005445	0.08691	1
0.08821	0.08454	0.002355	0.005516	0.08823	1	0.08821	0.08382	0.002444	0.005516	0.08823	1
0.08953	0.08136	0.002556	0.005587	0.08955	1	0.08953	0.08128	0.002295	0.005587	0.08955	1
0.08975	0.08029	0.001111	0.006772	0.08985	1	0.08975	0.07935	0.001054	0.006772	0.08985	1
0.09084	0.08152	0.002646	0.005658	0.09087	1	0.09084	0.08042	0.002551	0.005658	0.09087	1
0.09216	0.07964	0.002734	0.005729	0.09219	1	0.09216	0.08243	0.002637	0.005729	0.09219	1
0.09348	0.08055	0.003068	0.0058	0.0935	1	0.09348	0.07785	0.002805	0.0058	0.0935	1
0.09371	0.07694	0.001103	0.006949	0.09381	1	0.09371	0.07883	0.001047	0.006949	0.09381	1
0.0948	0.08097	0.002854	0.005872	0.09482	1	0.0948	0.08353	0.00271	0.005872	0.09482	1
0.09612	0.08193	0.002775	0.005943	0.09614	1	0.09612	0.08499	0.003179	0.005943	0.09614	1
0.09743	0.08752	0.002872	0.006015	0.09746	1	0.09743	0.0887	0.003194	0.006015	0.09746	1
0.09768	0.07756	0.001191	0.00713	0.09777	1	0.09768	0.07955	0.00112	0.00713	0.09777	1
0.09875	0.07283	0.003047	0.006086	0.09877	1	0.09875	0.08296	0.003162	0.006086	0.09877	1
0.1001	0.08318	0.003285	0.006158	0.1001	1	0.1001	0.08326	0.003489	0.006158	0.1001	1
0.1014	0.06824	0.00346	0.00623	0.1014	1	0.1014	0.07612	0.003371	0.00623	0.1014	1
0.1016	0.07628	0.001005	0.007313	0.1017	1	0.1016	0.07634	0.001032	0.007313	0.1017	1
0.1027	0.08325	0.003964	0.006302	0.1027	1	0.1027	0.08679	0.003991	0.006302	0.1027	1
0.104	0.08656	0.0038	0.006374	0.104	1	0.104	0.0877	0.00448	0.006374	0.104	1
0.1053	0.07582	0.003905	0.006446	0.1053	1	0.1053	0.08117	0.004055	0.006446	0.1053	1
0.1056	0.0769	0.000979	0.007498	0.1057	1	0.1056	0.07991	0.00088	0.007498	0.1057	1
0.1066	0.08128	0.005399	0.006518	0.1067	1	0.1066	0.07771	0.005391	0.006518	0.1067	1
0.108	0.07545	0.005332	0.006591	0.108	1	0.108	0.08255	0.0064	0.006591	0.108	1
0.1093	0.07787	0.005738	0.006663	0.1093	1	0.1093	0.08868	0.005861	0.006663	0.1093	1
0.1095	0.07769	0.000928	0.007685	0.1096	1	0.1095	0.07881	0.00106	0.007685	0.1096	1
0.1106	0.06728	0.006247	0.006735	0.1106	1	0.1106	0.07035	0.006195	0.006735	0.1106	1
0.1119	0.06341	0.005473	0.006808	0.1119	1	0.1119	0.08195	0.006249	0.006808	0.1119	1
0.1132	0.08306	0.008321	0.00688	0.1132	1	0.1132	0.07536	0.00624	0.00688	0.1132	1
0.1135	0.07599	0.000887	0.007875	0.1136	1	0.1135	0.07593	0.001082	0.007875	0.1136	1
0.1174	0.07443	0.000925	0.008066	0.1175	1	0.1174	0.07777	0.001003	0.008066	0.1175	1

PEO <sub>132</sub> -PB <sub>89</sub> /CD <sub>3</sub> OD 39.9 °C					PEO <sub>132</sub> -PB <sub>89</sub> /CD <sub>3</sub> OD 49.3 °C						
Q	I(Q)	Std Dev(I(Q))	sigmaQ	meanQ	Shadow Factor	Q	I(Q)	Std Dev(I(Q))	sigmaQ	meanQ	Shadow Factor
0.1214	0.07586	0.001026	0.008259	0.1215	1	0.1214	0.07721	0.001058	0.008259	0.1215	1
0.1253	0.0763	0.000976	0.008453	0.1254	1	0.1253	0.07727	0.001029	0.008453	0.1254	1
0.1293	0.07368	0.001014	0.008649	0.1293	1	0.1293	0.07561	0.000919	0.008649	0.1293	1
0.1332	0.07501	0.001028	0.008847	0.1333	1	0.1332	0.07586	0.000968	0.008847	0.1333	1
0.1371	0.07514	0.000906	0.009045	0.1372	1	0.1371	0.07633	0.000866	0.009045	0.1372	1
0.141	0.07446	0.00087	0.009245	0.1411	1	0.141	0.07424	0.000847	0.009245	0.1411	1
0.1449	0.07427	0.000989	0.009445	0.145	1	0.1449	0.07704	0.000948	0.009445	0.145	1
0.1489	0.07586	0.000907	0.009647	0.1489	1	0.1489	0.07688	0.000877	0.009647	0.1489	1
0.1528	0.07401	0.001017	0.009849	0.1528	1	0.1528	0.07483	0.00091	0.009849	0.1528	1
0.1567	0.07306	0.000878	0.01005	0.1567	1	0.1567	0.0756	0.000906	0.01005	0.1567	1
0.1606	0.07201	0.000871	0.01026	0.1606	1	0.1606	0.0753	0.000874	0.01026	0.1606	1
0.1645	0.07309	0.000896	0.01046	0.1645	1	0.1645	0.07438	0.000861	0.01046	0.1645	1
0.1683	0.0712	0.000691	0.01067	0.1684	1	0.1683	0.07458	0.000819	0.01067	0.1684	1
0.1722	0.07322	0.000861	0.01087	0.1723	1	0.1722	0.07385	0.000773	0.01087	0.1723	1
0.1761	0.07183	0.000789	0.01108	0.1762	1	0.1761	0.0744	0.000777	0.01108	0.1762	1
0.18	0.07301	0.000831	0.01128	0.18	1	0.18	0.07367	0.000805	0.01128	0.18	1
0.1838	0.07177	0.0008	0.01149	0.1839	1	0.1838	0.07352	0.000766	0.01149	0.1839	1
0.1877	0.07259	0.00086	0.0117	0.1877	1	0.1877	0.07413	0.000808	0.0117	0.1877	1
0.1916	0.07392	0.000832	0.0119	0.1916	1	0.1916	0.0746	0.000792	0.0119	0.1916	1
0.1954	0.0732	0.000865	0.01211	0.1954	1	0.1954	0.07466	0.00087	0.01211	0.1954	1
0.1992	0.07279	0.000767	0.01232	0.1993	1	0.1992	0.07482	0.000825	0.01232	0.1993	1
0.2031	0.07285	0.000852	0.01253	0.2031	1	0.2031	0.07468	0.000824	0.01253	0.2031	1
0.2069	0.07327	0.000773	0.01274	0.2069	1	0.2069	0.07336	0.00081	0.01274	0.2069	1
0.2107	0.07428	0.000814	0.01294	0.2108	1	0.2107	0.0751	0.000765	0.01294	0.2108	1
0.2145	0.07137	0.000731	0.01315	0.2146	1	0.2145	0.07381	0.000699	0.01315	0.2146	1
0.2184	0.07269	0.000696	0.01336	0.2184	1	0.2184	0.07311	0.000746	0.01336	0.2184	1
0.2222	0.07215	0.000727	0.01357	0.2222	1	0.2222	0.07259	0.000839	0.01357	0.2222	1
0.226	0.07192	0.000752	0.01378	0.226	1	0.226	0.07373	0.000703	0.01378	0.226	1
0.2297	0.07245	0.000788	0.01399	0.2298	1	0.2297	0.0745	0.000737	0.01399	0.2298	1
0.2335	0.07176	0.000748	0.01419	0.2336	1	0.2335	0.07348	0.000722	0.01419	0.2336	1
0.2373	0.07301	0.000756	0.0144	0.2373	1	0.2373	0.07366	0.000689	0.0144	0.2373	1
0.2411	0.07329	0.000748	0.01461	0.2411	1	0.2411	0.07267	0.000739	0.01461	0.2411	1
0.2448	0.07145	0.000835	0.01482	0.2449	1	0.2448	0.07384	0.000848	0.01482	0.2449	1
0.2486	0.07192	0.000795	0.01503	0.2486	1	0.2486	0.07293	0.000859	0.01503	0.2486	1
0.2523	0.07122	0.000834	0.01523	0.2524	1	0.2523	0.07257	0.000829	0.01523	0.2524	1
0.2561	0.07275	0.000845	0.01544	0.2561	1	0.2561	0.07385	0.000872	0.01544	0.2561	1
0.2598	0.07261	0.000866	0.01565	0.2598	1	0.2598	0.0736	0.000858	0.01565	0.2598	1
0.2635	0.07383	0.000951	0.01586	0.2636	1	0.2635	0.07364	0.000903	0.01586	0.2636	1
0.2673	0.0729	0.000836	0.01606	0.2673	1	0.2673	0.0744	0.00081	0.01606	0.2673	1
0.271	0.07242	0.000896	0.01627	0.271	1	0.271	0.07062	0.000912	0.01627	0.271	1
0.2747	0.07194	0.000791	0.01648	0.2747	1	0.2747	0.0727	0.00079	0.01648	0.2747	1
0.2784	0.07246	0.001022	0.01668	0.2784	1	0.2784	0.07362	0.000857	0.01668	0.2784	1
0.282	0.07079	0.000841	0.01689	0.2821	1	0.282	0.07263	0.000928	0.01689	0.2821	1
0.2857	0.07507	0.000942	0.01709	0.2857	1	0.2857	0.07475	0.000854	0.01709	0.2857	1
0.2894	0.07352	0.000832	0.0173	0.2894	1	0.2894	0.0725	0.000956	0.0173	0.2894	1
0.293	0.07189	0.000904	0.0175	0.2931	1	0.293	0.07249	0.000925	0.0175	0.2931	1
0.2967	0.07209	0.000897	0.01771	0.2967	1	0.2967	0.07362	0.000907	0.01771	0.2967	1
0.3003	0.07329	0.00095	0.01791	0.3004	1	0.3003	0.07347	0.000857	0.01791	0.3004	1
0.304	0.07301	0.000821	0.01812	0.304	1	0.304	0.07196	0.000939	0.01812	0.304	1
0.3076	0.07206	0.000866	0.01832	0.3076	1	0.3076	0.07365	0.000885	0.01832	0.3076	1
0.3112	0.07268	0.000923	0.01852	0.3113	1	0.3112	0.07316	0.000896	0.01852	0.3113	1
0.3148	0.07344	0.000886	0.01873	0.3149	1	0.3148	0.07382	0.000945	0.01873	0.3149	1
0.3184	0.07228	0.000885	0.01893	0.3185	1	0.3184	0.07447	0.000864	0.01893	0.3185	1
0.322	0.07275	0.000917	0.01913	0.3221	1	0.322	0.07252	0.000938	0.01913	0.3221	1
0.3256	0.07157	0.001	0.01933	0.3256	1	0.3256	0.07324	0.00086	0.01933	0.3256	1
0.3292	0.0722	0.000918	0.01954	0.3292	1	0.3292	0.07288	0.001055	0.01954	0.3292	1
0.3327	0.07104	0.000934	0.01974	0.3328	1	0.3327	0.07401	0.000955	0.01974	0.3328	1
0.3363	0.07201	0.000912	0.01994	0.3363	1	0.3363	0.07294	0.001018	0.01994	0.3363	1
0.3399	0.07323	0.000904	0.02014	0.3399	1	0.3399	0.07198	0.000909	0.02014	0.3399	1
0.3434	0.07168	0.000841	0.02034	0.3434	1	0.3434	0.07173	0.000884	0.02034	0.3434	1
0.3469	0.073	0.000887	0.02054	0.3469	1	0.3469	0.07359	0.000877	0.02054	0.3469	1
0.3504	0.07276	0.000952	0.02074	0.3505	1	0.3504	0.07261	0.000966	0.02074	0.3505	1
0.3539	0.07253	0.00084	0.02094	0.354	1	0.3539	0.072	0.000974	0.02094	0.354	1
0.3574	0.07283	0.000924	0.02113	0.3575	1	0.3574	0.07276	0.000884	0.02113	0.3575	1
0.3609	0.07122	0.000929	0.02133	0.361	1	0.3609	0.07074	0.000956	0.02133	0.361	1
0.3644	0.07221	0.001012	0.02153	0.3644	1	0.3644	0.07244	0.001056	0.02153	0.3644	1
0.3679	0.07211	0.000878	0.02173	0.3679	1	0.3679	0.07354	0.001011	0.02173	0.3679	1
0.3713	0.0697	0.000863	0.02192	0.3714	1	0.3713	0.07159	0.00083	0.02192	0.3714	1
0.3748	0.0712	0.000848	0.02212	0.3748	1	0.3748	0.07309	0.000959	0.02212	0.3748	1
0.3782	0.07201	0.00094	0.02231	0.3783	1	0.3782	0.07415	0.001	0.02231	0.3783	1
0.3817	0.07153	0.000914	0.02251	0.3817	1	0.3817	0.07038	0.000889	0.02251	0.3817	1
0.3851	0.07263	0.000964	0.0227	0.3851	1	0.3851	0.0727	0.00086	0.0227	0.3851	1
0.3885	0.07064	0.000854	0.0229	0.3885	1	0.3885	0.07197	0.000975	0.0229	0.3885	1
0.3919	0.07174	0.000839	0.02309	0.3919	1	0.3919	0.07305	0.001057	0.02309	0.3919	1
0.3953	0.07002	0.000912	0.02328	0.3953	1	0.3953	0.07183	0.000973	0.02328	0.3953	1
0.3987	0.07247	0.001006	0.02347	0.3987	1	0.3987	0.07165	0.001128	0.02347	0.3987	1
0.4021	0.07215	0.000983	0.02367	0.4021	1	0.4021	0.07302	0.000937	0.02367	0.4021	1
0.4054	0.07176	0.000929	0.02386	0.4054	1	0.4054	0.07137	0.000852	0.02386	0.4054	1
0.4088	0.07274	0.000994	0.02405	0.4088	1	0.4088	0.0737	0.000862	0.02405	0.4088	1
0.4121	0.07178	0.000905	0.02424	0.4121	1	0.4121	0.07403	0.000906	0.02424	0.4121	1
0.4155	0.07059	0.000927	0.02443	0.4155	1	0.4155	0.07312	0.000968	0.02443	0.4155	1

PEO <sub>132</sub> -PB <sub>89</sub> /CD <sub>3</sub> OD 39.9 °C						PEO <sub>132</sub> -PB <sub>89</sub> /CD <sub>3</sub> OD 49.3 °C					
Q	I(Q)	Std Dev(I(Q))	sigmaQ	meanQ	Shadow Factor	Q	I(Q)	Std Dev(I(Q))	sigmaQ	meanQ	Shadow Factor
0.4188	0.07137	0.000977	0.02462	0.4188	1	0.4188	0.07309	0.000997	0.02462	0.4188	1
0.4221	0.07174	0.00101	0.02481	0.4221	1	0.4221	0.07237	0.001056	0.02481	0.4221	1
0.4254	0.07213	0.001039	0.02499	0.4254	1	0.4254	0.0739	0.000948	0.02499	0.4254	1
0.4287	0.07219	0.001227	0.02518	0.4287	1	0.4287	0.07133	0.001158	0.02518	0.4287	1
0.432	0.07163	0.001295	0.02537	0.432	1	0.432	0.07318	0.00119	0.02537	0.432	1
0.4352	0.07178	0.001347	0.02556	0.4353	1	0.4352	0.07234	0.00127	0.02556	0.4353	1
0.4385	0.07153	0.00147	0.02574	0.4385	1	0.4385	0.0705	0.001329	0.02574	0.4385	1
0.4417	0.07072	0.001597	0.02593	0.4418	1	0.4417	0.07072	0.001605	0.02593	0.4418	1
0.445	0.07063	0.001429	0.02611	0.445	1	0.445	0.07261	0.00159	0.02611	0.445	1
0.4482	0.07128	0.001637	0.0263	0.4482	1	0.4482	0.07114	0.001926	0.0263	0.4482	1
0.4514	0.06792	0.001896	0.02648	0.4515	1	0.4514	0.07183	0.001636	0.02648	0.4515	1
0.4546	0.06821	0.002069	0.02666	0.4547	1	0.4546	0.07271	0.001962	0.02666	0.4547	1
0.4578	0.06977	0.001782	0.02685	0.4579	1	0.4578	0.07379	0.001902	0.02685	0.4579	1
0.461	0.0709	0.002376	0.02703	0.461	1	0.461	0.0761	0.003018	0.02703	0.461	1

PEO <sub>132</sub> -PB <sub>89</sub> /CD <sub>3</sub> OD 58.6 °C						PEO <sub>132</sub> -PB <sub>89</sub> /CD <sub>3</sub> OD 67.9 °C					
Q	I(Q)	Std Dev(I(Q))	sigmaQ	meanQ	Shadow Factor	Q	I(Q)	Std Dev(I(Q))	sigmaQ	meanQ	Shadow Factor
0.003433	8.816	0.1984	0.001072	0.003606	0.9585	0.003433	8.62	0.1757	0.001072	0.003606	0.9585
0.003837	9.556	0.1295	0.001076	0.003977	0.9999	0.003837	8.946	0.1255	0.001076	0.003977	0.9999
0.004241	9.365	0.1088	0.001078	0.004367	1	0.004241	8.804	0.1018	0.001078	0.004367	1
0.004645	9.204	0.1085	0.001081	0.00476	1	0.004645	8.908	0.101	0.001081	0.00476	1
0.005049	9.037	0.1042	0.001086	0.005155	1	0.005049	8.663	0.1044	0.001086	0.005155	1
0.005453	8.952	0.09414	0.001091	0.005551	1	0.005453	8.63	0.09629	0.001091	0.005551	1
0.005857	8.903	0.09136	0.001097	0.005948	1	0.005857	8.38	0.08712	0.001097	0.005948	1
0.006261	8.818	0.0761	0.001103	0.006346	1	0.006261	8.364	0.08283	0.001103	0.006346	1
0.006665	8.553	0.08305	0.001111	0.006745	1	0.006665	8.135	0.07545	0.001111	0.006745	1
0.007069	8.469	0.07753	0.001118	0.007144	1	0.007069	8.035	0.07865	0.001118	0.007144	1
0.007473	8.475	0.0787	0.001127	0.007544	1	0.007473	7.985	0.0784	0.001127	0.007544	1
0.007876	8.275	0.0717	0.001135	0.007944	1	0.007876	7.836	0.06672	0.001135	0.007944	1
0.00828	8.095	0.0738	0.001145	0.008345	1	0.00828	7.723	0.07168	0.001145	0.008345	1
0.008684	8.104	0.07022	0.001154	0.008746	1	0.008684	7.682	0.05918	0.001154	0.008746	1
0.009088	7.851	0.05784	0.001164	0.009147	1	0.009088	7.537	0.0678	0.001164	0.009147	1
0.009492	7.838	0.05934	0.001175	0.009548	1	0.009492	7.447	0.05876	0.001175	0.009548	1
0.009896	7.613	0.0584	0.001186	0.00995	1	0.009896	7.165	0.05905	0.001186	0.00995	1
0.0103	7.489	0.0607	0.001197	0.01035	1	0.0103	7.127	0.05519	0.001197	0.01035	1
0.0107	7.361	0.05703	0.001209	0.01075	1	0.0107	6.909	0.04957	0.001209	0.01075	1
0.01111	7.117	0.05185	0.001221	0.01116	1	0.01111	6.803	0.05051	0.001221	0.01116	1
0.0113	6.996	0.04055	0.002191	0.01149	1	0.0113	6.535	0.0394	0.002191	0.01149	1
0.01151	7.023	0.05689	0.001233	0.01156	1	0.01151	6.681	0.05192	0.001233	0.01156	1
0.01192	6.874	0.05093	0.001246	0.01196	1	0.01192	6.51	0.049	0.001246	0.01196	1
0.01232	6.645	0.04919	0.001259	0.01236	1	0.01232	6.202	0.04551	0.001259	0.01236	1
0.01263	6.454	0.03785	0.002212	0.0128	1	0.01263	6.026	0.03998	0.002212	0.0128	1
0.01272	6.482	0.0507	0.001272	0.01277	1	0.01272	6.176	0.04742	0.001272	0.01277	1
0.01313	6.306	0.04325	0.001286	0.01317	1	0.01313	5.979	0.04263	0.001286	0.01317	1
0.01353	6.166	0.0492	0.0013	0.01357	1	0.01353	5.773	0.04432	0.0013	0.01357	1
0.01393	5.918	0.04397	0.001314	0.01397	1	0.01393	5.667	0.04196	0.001314	0.01397	1
0.01396	5.907	0.0406	0.002236	0.01412	1	0.01396	5.467	0.03665	0.002236	0.01412	1
0.01434	5.748	0.04299	0.001328	0.01438	1	0.01434	5.471	0.04217	0.001328	0.01438	1
0.01474	5.607	0.04415	0.001343	0.01478	1	0.01474	5.256	0.03722	0.001343	0.01478	1
0.01515	5.435	0.04591	0.001358	0.01518	1	0.01515	5.031	0.03942	0.001358	0.01518	1
0.01529	5.319	0.03595	0.002264	0.01543	1	0.01529	4.954	0.02938	0.002264	0.01543	1
0.01555	5.246	0.04095	0.001373	0.01558	1	0.01555	4.902	0.042	0.001373	0.01558	1
0.01595	5.097	0.04078	0.001389	0.01599	1	0.01595	4.756	0.04033	0.001389	0.01599	1
0.01636	4.942	0.04115	0.001404	0.01639	1	0.01636	4.627	0.0384	0.001404	0.01639	1
0.01662	4.799	0.03085	0.002294	0.01675	1	0.01662	4.452	0.03147	0.002294	0.01675	1
0.01676	4.773	0.04099	0.00142	0.01679	1	0.01676	4.476	0.04055	0.00142	0.01679	1
0.01717	4.563	0.04086	0.001436	0.0172	1	0.01717	4.28	0.037	0.001436	0.0172	1
0.01757	4.488	0.03804	0.001453	0.0176	1	0.01757	4.157	0.03577	0.001453	0.0176	1
0.01795	4.275	0.02975	0.002326	0.01807	1	0.01795	3.962	0.02927	0.002326	0.01807	1
0.01797	4.283	0.03839	0.001469	0.018	1	0.01797	3.992	0.03693	0.001469	0.018	1
0.01838	4.096	0.038	0.001486	0.01841	1	0.01838	3.786	0.03431	0.001486	0.01841	1
0.01878	3.94	0.03504	0.001503	0.01881	1	0.01878	3.654	0.03483	0.001503	0.01881	1
0.01918	3.806	0.03323	0.00152	0.01921	1	0.01918	3.527	0.03323	0.00152	0.01921	1
0.01928	3.739	0.02751	0.002361	0.01939	1	0.01928	3.46	0.02405	0.002361	0.01939	1
0.01959	3.651	0.03425	0.001537	0.01962	1	0.01959	3.377	0.03311	0.001537	0.01962	1
0.01999	3.473	0.03483	0.001554	0.02002	1	0.01999	3.27	0.03154	0.001554	0.02002	1
0.0204	3.375	0.0324	0.001572	0.02042	1	0.0204	3.117	0.02988	0.001572	0.02042	1
0.02061	3.268	0.02542	0.002398	0.02072	1	0.02061	3.033	0.02307	0.002398	0.02072	1
0.0208	3.149	0.03075	0.001589	0.02083	1	0.0208	2.912	0.02852	0.001589	0.02083	1
0.0212	3.027	0.02998	0.001607	0.02123	1	0.0212	2.815	0.02652	0.001607	0.02123	1
0.02161	2.9	0.031	0.001625	0.02163	1	0.02161	2.737	0.03165	0.001625	0.02163	1
0.02194	2.829	0.02197	0.002436	0.02204	1	0.02194	2.615	0.02088	0.002436	0.02204	1
0.02201	2.776	0.02964	0.001643	0.02203	1	0.02201	2.549	0.02739	0.001643	0.02203	1
0.02241	2.682	0.02879	0.001661	0.02244	1	0.02241	2.447	0.02686	0.001661	0.02244	1
0.02282	2.493	0.02729	0.00168	0.02284	1	0.02282	2.355	0.02664	0.00168	0.02284	1
0.02322	2.383	0.02673	0.001698	0.02324	1	0.02322	2.27	0.02581	0.001698	0.02324	1
0.02327	2.411	0.01988	0.002477	0.02336	1	0.02327	2.241	0.01885	0.002477	0.02336	1
0.02363	2.289	0.02488	0.001717	0.02365	1	0.02363	2.105	0.02363	0.001717	0.02365	1
0.02403	2.202	0.02517	0.001736	0.02405	1	0.02403	2.031	0.02382	0.001736	0.02405	1

PEO <sub>132</sub> -PB <sub>89</sub> /CD <sub>3</sub> OD 58.6 °C					PEO <sub>132</sub> -PB <sub>89</sub> /CD <sub>3</sub> OD 67.9 °C						
Q	I(Q)	Std Dev(I(Q))	sigmaQ	meanQ	Shadow Factor	Q	I(Q)	Std Dev(I(Q))	sigmaQ	meanQ	Shadow Factor
0.02443	2.098	0.02498	0.001754	0.02445	1	0.02443	1.927	0.02267	0.001754	0.02445	1
0.0246	2.047	0.01708	0.002519	0.02469	1	0.0246	1.898	0.01714	0.002519	0.02469	1
0.02484	1.957	0.02373	0.001773	0.02486	1	0.02484	1.863	0.02468	0.001773	0.02486	1
0.02524	1.896	0.02733	0.001792	0.02526	1	0.02524	1.727	0.02455	0.001792	0.02526	1
0.02564	1.811	0.02766	0.001812	0.02566	1	0.02564	1.657	0.02597	0.001812	0.02566	1
0.02593	1.724	0.01359	0.002563	0.02601	1	0.02593	1.612	0.01236	0.002563	0.02601	1
0.02605	1.729	0.02608	0.001831	0.02607	1	0.02605	1.586	0.02366	0.001831	0.02607	1
0.02645	1.61	0.02402	0.00185	0.02647	1	0.02645	1.501	0.02516	0.00185	0.02647	1
0.02685	1.535	0.02515	0.00187	0.02687	1	0.02685	1.412	0.0256	0.00187	0.02687	1
0.02726	1.481	0.02613	0.001889	0.02728	1	0.02726	1.345	0.02361	0.001889	0.02728	1
0.02726	1.455	0.01171	0.002609	0.02734	1	0.02726	1.362	0.01064	0.002609	0.02734	1
0.02766	1.389	0.02651	0.001909	0.02768	1	0.02766	1.311	0.02644	0.001909	0.02768	1
0.02807	1.339	0.02457	0.001928	0.02808	1	0.02807	1.183	0.02286	0.001928	0.02808	1
0.02847	1.261	0.02434	0.001948	0.02849	1	0.02847	1.159	0.02615	0.001948	0.02849	1
0.02859	1.226	0.009242	0.002656	0.02866	1	0.02859	1.145	0.009601	0.002656	0.02866	1
0.02887	1.167	0.02201	0.001968	0.02889	1	0.02887	1.061	0.02451	0.001968	0.02889	1
0.02928	1.083	0.02346	0.001988	0.02929	1	0.02928	1.039	0.02425	0.001988	0.02929	1
0.02968	1.02	0.02229	0.002008	0.0297	1	0.02968	0.9655	0.02382	0.002008	0.0297	1
0.02991	1.032	0.009226	0.002705	0.02999	1	0.02991	0.9483	0.008583	0.002705	0.02999	1
0.03008	0.9904	0.02373	0.002028	0.0301	1	0.03008	0.8788	0.02202	0.002028	0.0301	1
0.03049	0.9448	0.02148	0.002048	0.0305	1	0.03049	0.8719	0.02262	0.002048	0.0305	1
0.03089	0.9091	0.02318	0.002068	0.03091	1	0.03089	0.7932	0.0218	0.002068	0.03091	1
0.03124	0.8406	0.007258	0.002754	0.03131	1	0.03124	0.7943	0.006852	0.002754	0.03131	1
0.03129	0.8271	0.01939	0.002089	0.03131	1	0.03129	0.7574	0.02263	0.002089	0.03131	1
0.0317	0.7851	0.02424	0.002109	0.03171	1	0.0317	0.7113	0.01911	0.002109	0.03171	1
0.0321	0.7309	0.02127	0.002129	0.03212	1	0.0321	0.6622	0.02046	0.002129	0.03212	1
0.0325	0.7271	0.02238	0.00215	0.03252	1	0.0325	0.6212	0.02023	0.00215	0.03252	1
0.03257	0.7065	0.006717	0.002806	0.03264	1	0.03257	0.6627	0.006131	0.002806	0.03264	1
0.03291	0.6538	0.02014	0.00217	0.03292	1	0.03291	0.6135	0.01911	0.00217	0.03292	1
0.03331	0.6108	0.01964	0.002191	0.03333	1	0.03331	0.5798	0.01958	0.002191	0.03333	1
0.03372	0.5982	0.01751	0.002212	0.03373	1	0.03372	0.547	0.01928	0.002212	0.03373	1
0.0339	0.5732	0.006001	0.002858	0.03396	1	0.0339	0.5346	0.005123	0.002858	0.03396	1
0.03399	0.6163	0.01905	0.004785	0.03426	1	0.03399	0.578	0.01808	0.004785	0.03426	1
0.03412	0.5518	0.01835	0.002232	0.03413	1	0.03412	0.5475	0.01685	0.002232	0.03413	1
0.03452	0.5268	0.02107	0.002253	0.03454	1	0.03452	0.4756	0.01932	0.002253	0.03454	1
0.03493	0.4977	0.02081	0.002274	0.03494	1	0.03493	0.4578	0.01959	0.002274	0.03494	1
0.03523	0.47	0.005132	0.002911	0.03529	1	0.03523	0.4433	0.005249	0.002911	0.03529	1
0.03533	0.4777	0.0225	0.002295	0.03534	1	0.03533	0.452	0.02208	0.002295	0.03534	1
0.03573	0.4247	0.01864	0.002316	0.03575	1	0.03573	0.4047	0.0194	0.002316	0.03575	1
0.03614	0.3644	0.02265	0.002336	0.03615	1	0.03614	0.3764	0.0236	0.002336	0.03615	1
0.03654	0.399	0.02378	0.002357	0.03655	1	0.03654	0.3441	0.02111	0.002357	0.03655	1
0.03656	0.3863	0.004541	0.002966	0.03662	1	0.03656	0.3692	0.00481	0.002966	0.03662	1
0.03694	0.3911	0.02497	0.002378	0.03696	1	0.03694	0.3637	0.0231	0.002378	0.03696	1
0.03735	0.3629	0.02474	0.0024	0.03736	1	0.03735	0.286	0.01874	0.0024	0.03736	1
0.03775	0.3017	0.02335	0.002421	0.03776	1	0.03775	0.3356	0.02219	0.002421	0.03776	1
0.03788	0.3253	0.003761	0.003021	0.03794	1	0.03788	0.304	0.004025	0.003021	0.03794	1
0.03798	0.3568	0.01116	0.004881	0.03823	1	0.03798	0.3414	0.01021	0.004881	0.03823	1
0.03815	0.2831	0.02502	0.002442	0.03817	1	0.03815	0.2699	0.02651	0.002442	0.03817	1
0.03856	0.3121	0.02291	0.002463	0.03857	1	0.03856	0.2746	0.02654	0.002463	0.03857	1
0.03896	0.2354	0.02092	0.002484	0.03897	1	0.03896	0.2722	0.03	0.002484	0.03897	1
0.03921	0.2693	0.003754	0.003077	0.03927	1	0.03921	0.2565	0.003612	0.003077	0.03927	1
0.03936	0.2644	0.03048	0.002506	0.03938	1	0.03936	0.2567	0.03013	0.002506	0.03938	1
0.03977	0.2132	0.02541	0.002527	0.03978	1	0.03977	0.3115	0.05195	0.002527	0.03978	1
0.04017	0.24	0.04674	0.002548	0.04018	1	0.04017	0.2242	0.03071	0.002548	0.04018	1
0.04054	0.2247	0.003614	0.003134	0.04059	1	0.04054	0.2169	0.003282	0.003134	0.04059	1
0.04057	0.2355	0.04035	0.00257	0.04059	1	0.04057	0.2191	0.03227	0.00257	0.04059	1
0.04187	0.1914	0.003076	0.003192	0.04192	1	0.04187	0.1882	0.002804	0.003192	0.04192	1
0.04197	0.2147	0.006097	0.004987	0.0422	1	0.04197	0.2087	0.005803	0.004987	0.0422	1
0.0432	0.1657	0.003021	0.003251	0.04325	1	0.0432	0.1688	0.002896	0.003251	0.04325	1
0.04452	0.1487	0.002621	0.003311	0.04457	1	0.04452	0.1458	0.00264	0.003311	0.04457	1
0.04585	0.1289	0.002695	0.003371	0.0459	1	0.04585	0.1319	0.002542	0.003371	0.0459	1
0.04597	0.1391	0.003556	0.005102	0.04617	1	0.04597	0.1415	0.003005	0.005102	0.04617	1
0.04718	0.1192	0.00262	0.003432	0.04722	1	0.04718	0.1216	0.00253	0.003432	0.04722	1
0.0485	0.1061	0.002407	0.003493	0.04855	1	0.0485	0.1144	0.002388	0.003493	0.04855	1
0.04983	0.1069	0.002361	0.003555	0.04987	1	0.04983	0.1111	0.002375	0.003555	0.04987	1
0.04996	0.1087	0.001726	0.005225	0.05014	1	0.04996	0.112	0.001792	0.005225	0.05014	1
0.05116	0.09831	0.00245	0.003618	0.0512	1	0.05116	0.1037	0.002164	0.003618	0.0512	1
0.05248	0.0988	0.002301	0.003681	0.05252	1	0.05248	0.1052	0.002439	0.003681	0.05252	1
0.05381	0.09962	0.002299	0.003745	0.05385	1	0.05381	0.09874	0.00217	0.003745	0.05385	1
0.05394	0.09581	0.001373	0.005355	0.05412	1	0.05394	0.09996	0.001342	0.005355	0.05412	1
0.05514	0.09499	0.002135	0.003809	0.05517	1	0.05514	0.09891	0.002129	0.003809	0.05517	1
0.05646	0.09682	0.002164	0.003874	0.0565	1	0.05646	0.1024	0.002089	0.003874	0.0565	1
0.05779	0.09679	0.002169	0.003939	0.05782	1	0.05779	0.09953	0.002187	0.003939	0.05782	1
0.05793	0.09372	0.001305	0.005492	0.05809	1	0.05793	0.09696	0.001259	0.005492	0.05809	1
0.05911	0.09637	0.002002	0.004004	0.05915	1	0.05911	0.09801	0.001973	0.004004	0.05915	1
0.06044	0.09779	0.001939	0.00407	0.06047	1	0.06044	0.09852	0.002228	0.00407	0.06047	1
0.06176	0.09352	0.002127	0.004137	0.0618	1	0.06176	0.09709	0.001946	0.004137	0.0618	1
0.06192	0.0919	0.001451	0.005635	0.06207	1	0.06192	0.09734	0.001227	0.005635	0.06207	1
0.06309	0.09685	0.002022	0.004203	0.06312	1	0.06309	0.09466	0.002039	0.004203	0.06312	1
0.06441	0.09314	0.001881	0.00427	0.06444	1	0.06441	0.09533	0.002069	0.00427	0.06444	1
0.06573	0.09707	0.002089	0.004337	0.06577	1	0.06573	0.0978	0.002135	0.004337	0.06577	1

PEO <sub>132</sub> -PB <sub>89</sub> /CD <sub>3</sub> OD 58.6 °C					PEO <sub>132</sub> -PB <sub>89</sub> /CD <sub>3</sub> OD 67.9 °C						
Q	I(Q)	Std Dev(I(Q))	sigmaQ	meanQ	Shadow Factor	Q	I(Q)	Std Dev(I(Q))	sigmaQ	meanQ	Shadow Factor
0.0659	0.09253	0.001433	0.005784	0.06604	1	0.0659	0.09416	0.00127	0.005784	0.06604	1
0.06706	0.09888	0.001859	0.004405	0.06709	1	0.06706	0.09891	0.001923	0.004405	0.06709	1
0.06838	0.09672	0.001978	0.004473	0.06841	1	0.06838	0.0959	0.001959	0.004473	0.06841	1
0.06971	0.09774	0.001885	0.004541	0.06974	1	0.06971	0.09839	0.00192	0.004541	0.06974	1
0.06988	0.09394	0.001409	0.005938	0.07001	1	0.06988	0.09278	0.001199	0.005938	0.07001	1
0.07103	0.09847	0.001999	0.004609	0.07106	1	0.07103	0.09669	0.001973	0.004609	0.07106	1
0.07235	0.09414	0.001846	0.004678	0.07238	1	0.07235	0.09749	0.001904	0.004678	0.07238	1
0.07367	0.09186	0.001896	0.004746	0.0737	1	0.07367	0.09275	0.001851	0.004746	0.0737	1
0.07386	0.09113	0.001121	0.006097	0.07399	1	0.07386	0.0915	0.001211	0.006097	0.07399	1
0.075	0.09095	0.001781	0.004815	0.07503	1	0.075	0.09094	0.001859	0.004815	0.07503	1
0.07632	0.09507	0.001787	0.004885	0.07635	1	0.07632	0.09259	0.001888	0.004885	0.07635	1
0.07764	0.08853	0.001956	0.004954	0.07767	1	0.07764	0.09118	0.001997	0.004954	0.07767	1
0.07784	0.08837	0.001278	0.00626	0.07796	1	0.07784	0.09016	0.001355	0.00626	0.07796	1
0.07896	0.09072	0.00191	0.005024	0.07899	1	0.07896	0.09242	0.001852	0.005024	0.07899	1
0.08028	0.08886	0.001881	0.005094	0.08031	1	0.08028	0.09456	0.001797	0.005094	0.08031	1
0.08161	0.0867	0.001841	0.005164	0.08163	1	0.08161	0.09186	0.001816	0.005164	0.08163	1
0.08181	0.08703	0.001109	0.006427	0.08192	1	0.08181	0.08765	0.001046	0.006427	0.08192	1
0.08293	0.08801	0.002057	0.005234	0.08295	1	0.08293	0.08992	0.001996	0.005234	0.08295	1
0.08425	0.0879	0.002139	0.005304	0.08427	1	0.08425	0.0876	0.002137	0.005304	0.08427	1
0.08557	0.08221	0.002073	0.005375	0.08559	1	0.08557	0.08558	0.002117	0.005375	0.08559	1
0.08578	0.08653	0.001115	0.006598	0.08589	1	0.08578	0.08376	0.001089	0.006598	0.08589	1
0.08689	0.08764	0.00221	0.005445	0.08691	1	0.08689	0.09061	0.002319	0.005445	0.08691	1
0.08821	0.08268	0.002288	0.005516	0.08823	1	0.08821	0.08708	0.002411	0.005516	0.08823	1
0.08953	0.08393	0.002425	0.005587	0.08955	1	0.08953	0.08507	0.00245	0.005587	0.08955	1
0.08975	0.08131	0.001067	0.006772	0.08985	1	0.08975	0.08469	0.001169	0.006772	0.08985	1
0.09084	0.08368	0.002369	0.005658	0.09087	1	0.09084	0.08742	0.002787	0.005658	0.09087	1
0.09216	0.07998	0.002563	0.005729	0.09219	1	0.09216	0.08463	0.002505	0.005729	0.09219	1
0.09348	0.07847	0.002921	0.0058	0.0935	1	0.09348	0.08334	0.00282	0.0058	0.0935	1
0.09371	0.08009	0.001118	0.006949	0.09381	1	0.09371	0.08182	0.001207	0.006949	0.09381	1
0.0948	0.08513	0.002816	0.005872	0.09482	1	0.0948	0.09106	0.002983	0.005872	0.09482	1
0.09612	0.08021	0.002855	0.005943	0.09614	1	0.09612	0.08719	0.003165	0.005943	0.09614	1
0.09743	0.08436	0.003177	0.006015	0.09746	1	0.09743	0.09189	0.003456	0.006015	0.09746	1
0.09768	0.08181	0.001026	0.00713	0.09777	1	0.09768	0.08422	0.00127	0.00713	0.09777	1
0.09875	0.085	0.003328	0.006086	0.09877	1	0.09875	0.08912	0.003753	0.006086	0.09877	1
0.1001	0.08331	0.003459	0.006158	0.1001	1	0.1001	0.08472	0.003236	0.006158	0.1001	1
0.1014	0.08319	0.00357	0.00623	0.1014	1	0.1014	0.07958	0.003586	0.00623	0.1014	1
0.1016	0.07909	0.001007	0.007313	0.1017	1	0.1016	0.08204	0.001085	0.007313	0.1017	1
0.1027	0.0837	0.004025	0.006302	0.1027	1	0.1027	0.08503	0.004054	0.006302	0.1027	1
0.104	0.07533	0.00417	0.006374	0.104	1	0.104	0.07746	0.004268	0.006374	0.104	1
0.1053	0.08536	0.004294	0.006446	0.1053	1	0.1053	0.08362	0.004575	0.006446	0.1053	1
0.1056	0.07867	0.001036	0.007498	0.1057	1	0.1056	0.08194	0.001009	0.007498	0.1057	1
0.1066	0.08245	0.004629	0.006518	0.1067	1	0.1066	0.08644	0.004806	0.006518	0.1067	1
0.108	0.08552	0.004957	0.006591	0.108	1	0.108	0.07638	0.006224	0.006591	0.108	1
0.1093	0.08996	0.005468	0.006663	0.1093	1	0.1093	0.09039	0.007075	0.006663	0.1093	1
0.1095	0.07891	0.001028	0.007685	0.1096	1	0.1095	0.08168	0.001037	0.007685	0.1096	1
0.1106	0.06716	0.00698	0.006735	0.1106	1	0.1106	0.06758	0.006775	0.006735	0.1106	1
0.1119	0.07632	0.005849	0.006808	0.1119	1	0.1119	0.08608	0.007108	0.006808	0.1119	1
0.1132	0.07629	0.005689	0.00688	0.1132	1	0.1132	0.08883	0.009037	0.00688	0.1132	1
0.1135	0.07845	0.001155	0.007875	0.1136	1	0.1135	0.0802	0.00099	0.007875	0.1136	1
0.1174	0.07944	0.000924	0.008066	0.1175	1	0.1174	0.07848	0.000862	0.008066	0.1175	1
0.1214	0.07627	0.001117	0.008259	0.1215	1	0.1214	0.07882	0.000974	0.008259	0.1215	1
0.1253	0.07883	0.001071	0.008453	0.1254	1	0.1253	0.07986	0.001044	0.008453	0.1254	1
0.1293	0.07719	0.001024	0.008649	0.1293	1	0.1293	0.07746	0.000958	0.008649	0.1293	1
0.1332	0.07984	0.001104	0.008847	0.1333	1	0.1332	0.07971	0.00093	0.008847	0.1333	1
0.1371	0.0775	0.000862	0.009045	0.1372	1	0.1371	0.08018	0.000857	0.009045	0.1372	1
0.141	0.07546	0.000968	0.009245	0.1411	1	0.141	0.0774	0.000987	0.009245	0.1411	1
0.1449	0.07628	0.000894	0.009445	0.145	1	0.1449	0.07766	0.000939	0.009445	0.145	1
0.1489	0.07713	0.001004	0.009647	0.1489	1	0.1489	0.07862	0.000957	0.009647	0.1489	1
0.1528	0.07706	0.000983	0.009849	0.1528	1	0.1528	0.07882	0.000893	0.009849	0.1528	1
0.1567	0.0765	0.000965	0.01005	0.1567	1	0.1567	0.07803	0.00083	0.01005	0.1567	1
0.1606	0.07653	0.000995	0.01026	0.1606	1	0.1606	0.07735	0.000839	0.01026	0.1606	1
0.1645	0.07668	0.000827	0.01046	0.1645	1	0.1645	0.07691	0.000803	0.01046	0.1645	1
0.1683	0.075	0.000832	0.01067	0.1684	1	0.1683	0.07659	0.000835	0.01067	0.1684	1
0.1722	0.07493	0.000867	0.01087	0.1723	1	0.1722	0.07562	0.000828	0.01087	0.1723	1
0.1761	0.07511	0.000816	0.01108	0.1762	1	0.1761	0.07592	0.000875	0.01108	0.1762	1
0.18	0.07495	0.00083	0.01128	0.18	1	0.18	0.07657	0.000897	0.01128	0.18	1
0.1838	0.07586	0.000768	0.01149	0.1839	1	0.1838	0.07651	0.000842	0.01149	0.1839	1
0.1877	0.07436	0.000805	0.0117	0.1877	1	0.1877	0.07789	0.000879	0.0117	0.1877	1
0.1916	0.07446	0.000822	0.0119	0.1916	1	0.1916	0.07623	0.000867	0.0119	0.1916	1
0.1954	0.07561	0.000794	0.01211	0.1954	1	0.1954	0.07627	0.000797	0.01211	0.1954	1
0.1992	0.07425	0.000791	0.01232	0.1993	1	0.1992	0.0757	0.000787	0.01232	0.1993	1
0.2031	0.07592	0.000827	0.01253	0.2031	1	0.2031	0.07693	0.000736	0.01253	0.2031	1
0.2069	0.0743	0.000751	0.01274	0.2069	1	0.2069	0.07604	0.000875	0.01274	0.2069	1
0.2107	0.07548	0.000773	0.01294	0.2108	1	0.2107	0.07761	0.000739	0.01294	0.2108	1
0.2145	0.0727	0.000765	0.01315	0.2146	1	0.2145	0.07631	0.00081	0.01315	0.2146	1
0.2184	0.07553	0.000784	0.01336	0.2184	1	0.2184	0.07699	0.000727	0.01336	0.2184	1
0.2222	0.07347	0.000744	0.01357	0.2222	1	0.2222	0.07483	0.000755	0.01357	0.2222	1
0.226	0.07548	0.000764	0.01378	0.226	1	0.226	0.07665	0.000753	0.01378	0.226	1
0.2297	0.07448	0.000761	0.01399	0.2298	1	0.2297	0.07608	0.000713	0.01399	0.2298	1
0.2335	0.0735	0.000724	0.01419	0.2336	1	0.2335	0.07615	0.00072	0.01419	0.2336	1
0.2373	0.0754	0.000766	0.0144	0.2373	1	0.2373	0.07591	0.000754	0.0144	0.2373	1

PEO <sub>132</sub> -PB <sub>89</sub> /CD <sub>3</sub> OD 58.6 °C					PEO <sub>132</sub> -PB <sub>89</sub> /CD <sub>3</sub> OD 67.9 °C						
Q	I(Q)	Std Dev(I(Q))	sigmaQ	meanQ	Shadow Factor	Q	I(Q)	Std Dev(I(Q))	sigmaQ	meanQ	Shadow Factor
0.2411	0.07453	0.000798	0.01461	0.2411	1	0.2411	0.07662	0.00079	0.01461	0.2411	1
0.2448	0.07415	0.000859	0.01482	0.2449	1	0.2448	0.07563	0.000903	0.01482	0.2449	1
0.2486	0.07395	0.000833	0.01503	0.2486	1	0.2486	0.07512	0.000853	0.01503	0.2486	1
0.2523	0.0745	0.000818	0.01523	0.2524	1	0.2523	0.07506	0.000801	0.01523	0.2524	1
0.2561	0.07504	0.000881	0.01544	0.2561	1	0.2561	0.07529	0.000842	0.01544	0.2561	1
0.2598	0.07322	0.000801	0.01565	0.2598	1	0.2598	0.07643	0.00086	0.01565	0.2598	1
0.2635	0.07433	0.000854	0.01586	0.2636	1	0.2635	0.07598	0.00096	0.01586	0.2636	1
0.2673	0.07369	0.000853	0.01606	0.2673	1	0.2673	0.07631	0.000865	0.01606	0.2673	1
0.271	0.0738	0.000973	0.01627	0.271	1	0.271	0.07534	0.000821	0.01627	0.271	1
0.2747	0.07442	0.000902	0.01648	0.2747	1	0.2747	0.07572	0.000757	0.01648	0.2747	1
0.2784	0.07268	0.00085	0.01668	0.2784	1	0.2784	0.07492	0.000752	0.01668	0.2784	1
0.282	0.07325	0.000851	0.01689	0.2821	1	0.282	0.07651	0.00085	0.01689	0.2821	1
0.2857	0.07447	0.000786	0.01709	0.2857	1	0.2857	0.07629	0.000885	0.01709	0.2857	1
0.2894	0.0751	0.000968	0.0173	0.2894	1	0.2894	0.07548	0.000946	0.0173	0.2894	1
0.293	0.0732	0.000888	0.0175	0.2931	1	0.293	0.07637	0.000895	0.0175	0.2931	1
0.2967	0.0743	0.000798	0.01771	0.2967	1	0.2967	0.07485	0.000864	0.01771	0.2967	1
0.3003	0.07369	0.000867	0.01791	0.3004	1	0.3003	0.07462	0.000919	0.01791	0.3004	1
0.304	0.07493	0.000865	0.01812	0.304	1	0.304	0.07508	0.000944	0.01812	0.304	1
0.3076	0.07305	0.000905	0.01832	0.3076	1	0.3076	0.07428	0.000947	0.01832	0.3076	1
0.3112	0.07491	0.000927	0.01852	0.3113	1	0.3112	0.07467	0.000941	0.01852	0.3113	1
0.3148	0.07436	0.000815	0.01873	0.3149	1	0.3148	0.07586	0.000934	0.01873	0.3149	1
0.3184	0.07435	0.000946	0.01893	0.3185	1	0.3184	0.07562	0.000886	0.01893	0.3185	1
0.322	0.07511	0.000848	0.01913	0.3221	1	0.322	0.07562	0.000882	0.01913	0.3221	1
0.3256	0.07388	0.000945	0.01933	0.3256	1	0.3256	0.07418	0.00096	0.01933	0.3256	1
0.3292	0.07341	0.000927	0.01954	0.3292	1	0.3292	0.07456	0.00097	0.01954	0.3292	1
0.3327	0.07387	0.000892	0.01974	0.3328	1	0.3327	0.07612	0.0009	0.01974	0.3328	1
0.3363	0.07244	0.00097	0.01994	0.3363	1	0.3363	0.07425	0.000756	0.01994	0.3363	1
0.3399	0.07347	0.00099	0.02014	0.3399	1	0.3399	0.07599	0.000938	0.02014	0.3399	1
0.3434	0.07313	0.000955	0.02034	0.3434	1	0.3434	0.07487	0.000892	0.02034	0.3434	1
0.3469	0.07497	0.00092	0.02054	0.3469	1	0.3469	0.0744	0.000907	0.02054	0.3469	1
0.3504	0.07452	0.000909	0.02074	0.3505	1	0.3504	0.07534	0.00092	0.02074	0.3505	1
0.3539	0.07453	0.001011	0.02094	0.354	1	0.3539	0.07491	0.000867	0.02094	0.354	1
0.3574	0.07358	0.000921	0.02113	0.3575	1	0.3574	0.07382	0.000949	0.02113	0.3575	1
0.3609	0.0736	0.000865	0.02133	0.361	1	0.3609	0.0749	0.000775	0.02133	0.361	1
0.3644	0.07433	0.001012	0.02153	0.3644	1	0.3644	0.07297	0.000914	0.02153	0.3644	1
0.3679	0.07353	0.000874	0.02173	0.3679	1	0.3679	0.07488	0.00093	0.02173	0.3679	1
0.3713	0.0749	0.000906	0.02192	0.3714	1	0.3713	0.0734	0.000883	0.02192	0.3714	1
0.3748	0.07347	0.000935	0.02212	0.3748	1	0.3748	0.07511	0.00093	0.02212	0.3748	1
0.3782	0.0747	0.00095	0.02231	0.3783	1	0.3782	0.07612	0.000943	0.02231	0.3783	1
0.3817	0.07317	0.000991	0.02251	0.3817	1	0.3817	0.07288	0.000903	0.02251	0.3817	1
0.3851	0.0725	0.000929	0.0227	0.3851	1	0.3851	0.07482	0.000904	0.0227	0.3851	1
0.3885	0.07388	0.000925	0.0229	0.3885	1	0.3885	0.07475	0.000961	0.0229	0.3885	1
0.3919	0.07267	0.000941	0.02309	0.3919	1	0.3919	0.07543	0.000903	0.02309	0.3919	1
0.3953	0.07196	0.001017	0.02328	0.3953	1	0.3953	0.07406	0.001006	0.02328	0.3953	1
0.3987	0.07139	0.000987	0.02347	0.3987	1	0.3987	0.07551	0.001063	0.02347	0.3987	1
0.4021	0.07376	0.000944	0.02367	0.4021	1	0.4021	0.07535	0.000978	0.02367	0.4021	1
0.4054	0.07257	0.000988	0.02386	0.4054	1	0.4054	0.07417	0.000905	0.02386	0.4054	1
0.4088	0.07392	0.001039	0.02405	0.4088	1	0.4088	0.07381	0.000944	0.02405	0.4088	1
0.4121	0.07398	0.000983	0.02424	0.4121	1	0.4121	0.07434	0.001034	0.02424	0.4121	1
0.4155	0.07384	0.000917	0.02443	0.4155	1	0.4155	0.07564	0.00099	0.02443	0.4155	1
0.4188	0.07243	0.000956	0.02462	0.4188	1	0.4188	0.07526	0.000997	0.02462	0.4188	1
0.4221	0.07401	0.00096	0.02481	0.4221	1	0.4221	0.07443	0.000855	0.02481	0.4221	1
0.4254	0.07417	0.000956	0.02499	0.4254	1	0.4254	0.07547	0.001082	0.02499	0.4254	1
0.4287	0.07271	0.001012	0.02518	0.4287	1	0.4287	0.07361	0.001162	0.02518	0.4287	1
0.432	0.07446	0.001189	0.02537	0.432	1	0.432	0.07479	0.001384	0.02537	0.432	1
0.4352	0.07224	0.001399	0.02556	0.4353	1	0.4352	0.07299	0.001357	0.02556	0.4353	1
0.4385	0.07272	0.001398	0.02574	0.4385	1	0.4385	0.07359	0.001336	0.02574	0.4385	1
0.4417	0.07475	0.001231	0.02593	0.4418	1	0.4417	0.07438	0.001746	0.02593	0.4418	1
0.445	0.07307	0.001539	0.02611	0.445	1	0.445	0.07511	0.001505	0.02611	0.445	1
0.4482	0.07627	0.001703	0.0263	0.4482	1	0.4482	0.07381	0.001678	0.0263	0.4482	1
0.4514	0.07079	0.001934	0.02648	0.4515	1	0.4514	0.07388	0.001555	0.02648	0.4515	1
0.4546	0.07082	0.001867	0.02666	0.4547	1	0.4546	0.07688	0.002038	0.02666	0.4547	1
0.4578	0.07478	0.002149	0.02685	0.4579	1	0.4578	0.07361	0.002065	0.02685	0.4579	1
0.461	0.07003	0.001864	0.02703	0.461	1	0.461	0.07725	0.002012	0.02703	0.461	1

PEO <sub>132</sub> -PB <sub>89</sub> /C <sub>6</sub> D <sub>12</sub> 21.3 °C						PEO <sub>132</sub> -PB <sub>89</sub> /C <sub>6</sub> D <sub>12</sub> 30.6 °C					
Q	I(Q)	Std Dev(I(Q))	sigmaQ	meanQ	Shadow Factor	Q	I(Q)	Std Dev(I(Q))	sigmaQ	meanQ	Shadow Factor
0.003433	372.4	5.232	0.001072	0.003606	0.9585	0.003433	362.5	4.746	0.001072	0.003606	0.9585
0.003837	316.1	4.623	0.001076	0.003977	0.9999	0.003837	307.9	4.479	0.001076	0.003977	0.9999
0.004241	247	2.93	0.001078	0.004367	1	0.004241	239.6	2.915	0.001078	0.004367	1
0.004645	198.7	2.091	0.001081	0.00476	1	0.004645	192.4	1.956	0.001081	0.00476	1
0.005049	164.7	1.358	0.001086	0.005155	1	0.005049	159.6	1.371	0.001086	0.005155	1
0.005453	139.1	1.056	0.001091	0.005551	1	0.005453	135	1.019	0.001091	0.005551	1
0.005857	119	0.8226	0.001097	0.005948	1	0.005857	115.5	0.8059	0.001097	0.005948	1
0.006261	104	0.6545	0.001103	0.006346	1	0.006261	100.8	0.598	0.001103	0.006346	1
0.006665	91.18	0.5346	0.001111	0.006745	1	0.006665	89.05	0.5329	0.001111	0.006745	1
0.007069	81	0.429	0.001118	0.007144	1	0.007069	78.95	0.4205	0.001118	0.007144	1
0.007473	72.6	0.3594	0.001127	0.007544	1	0.007473	70.57	0.3673	0.001127	0.007544	1
0.007876	65.92	0.2847	0.001135	0.007944	1	0.007876	63.94	0.2888	0.001135	0.007944	1
0.00828	59.22	0.2439	0.001145	0.008345	1	0.00828	57.72	0.2451	0.001145	0.008345	1
0.008684	54	0.2101	0.001154	0.008746	1	0.008684	52.77	0.2115	0.001154	0.008746	1
0.009088	49.41	0.209	0.001164	0.009147	1	0.009088	47.99	0.1974	0.001164	0.009147	1
0.009492	44.98	0.1795	0.001175	0.009548	1	0.009492	43.83	0.1993	0.001175	0.009548	1
0.009896	41.41	0.1646	0.001186	0.00995	1	0.009896	40.03	0.1482	0.001186	0.00995	1
0.0103	37.83	0.1648	0.001197	0.01035	1	0.0103	36.79	0.1542	0.001197	0.01035	1
0.0107	34.69	0.1377	0.001209	0.01075	1	0.0107	33.85	0.1514	0.001209	0.01075	1
0.01111	32.06	0.1405	0.001221	0.01116	1	0.01111	30.96	0.1334	0.001221	0.01116	1
0.0113	30.83	0.5136	0.002191	0.01149	1	0.0113	30.4	0.5278	0.002191	0.01149	1
0.01151	29.25	0.1254	0.001233	0.01156	1	0.01151	28.29	0.1171	0.001233	0.01156	1
0.01192	26.79	0.1195	0.001246	0.01196	1	0.01192	26.19	0.1163	0.001246	0.01196	1
0.01232	24.42	0.1138	0.001259	0.01236	1	0.01232	23.72	0.1021	0.001259	0.01236	1
0.01263	22.91	0.3775	0.002212	0.0128	1	0.01263	22.4	0.3736	0.002212	0.0128	1
0.01272	22.29	0.1066	0.001272	0.01277	1	0.01272	21.43	0.1024	0.001272	0.01277	1
0.01313	20.21	0.09785	0.001286	0.01317	1	0.01313	19.65	0.08994	0.001286	0.01317	1
0.01353	18.3	0.09071	0.001314	0.01357	1	0.01353	17.78	0.08499	0.001314	0.01357	1
0.01393	16.63	0.07791	0.001314	0.01397	1	0.01393	16.07	0.08686	0.001314	0.01397	1
0.01396	16.78	0.2855	0.002236	0.01412	1	0.01396	16.34	0.2804	0.002236	0.01412	1
0.01434	14.89	0.07387	0.001328	0.01438	1	0.01434	14.36	0.07232	0.001328	0.01438	1
0.01474	13.34	0.07251	0.001343	0.01478	1	0.01474	12.87	0.06779	0.001343	0.01478	1
0.01515	12.01	0.06278	0.001358	0.01518	1	0.01515	11.47	0.05754	0.001358	0.01518	1
0.01529	11.87	0.2072	0.002264	0.01543	1	0.01529	11.57	0.2031	0.002264	0.01543	1
0.01555	10.7	0.05702	0.001373	0.01558	1	0.01555	10.18	0.06068	0.001373	0.01558	1
0.01595	9.371	0.06019	0.001389	0.01599	1	0.01595	9.094	0.06254	0.001389	0.01599	1
0.01636	8.489	0.0595	0.001404	0.01639	1	0.01636	8.032	0.054	0.001404	0.01639	1
0.01662	8.186	0.1512	0.002294	0.01675	1	0.01662	7.957	0.1471	0.002294	0.01675	1
0.01676	7.37	0.05466	0.00142	0.01679	1	0.01676	7.023	0.04865	0.00142	0.01679	1
0.01717	6.501	0.05302	0.001436	0.0172	1	0.01717	6.198	0.04743	0.001436	0.0172	1
0.01757	5.745	0.04472	0.001453	0.0176	1	0.01757	5.565	0.04123	0.001453	0.0176	1
0.01795	5.49	0.1037	0.002326	0.01807	1	0.01795	5.305	0.1011	0.002326	0.01807	1
0.01797	5.129	0.0432	0.001469	0.018	1	0.01797	4.802	0.04154	0.001469	0.018	1
0.01838	4.399	0.03814	0.001486	0.01841	1	0.01838	4.222	0.03929	0.001486	0.01841	1
0.01878	3.853	0.03218	0.001503	0.01881	1	0.01878	3.711	0.03472	0.001503	0.01881	1
0.01918	3.377	0.02983	0.00152	0.01921	1	0.01918	3.273	0.03391	0.00152	0.01921	1
0.01928	3.63	0.06797	0.002361	0.01939	1	0.01928	3.522	0.06661	0.002361	0.01939	1
0.01959	2.976	0.02991	0.001537	0.01962	1	0.01959	2.816	0.03086	0.001537	0.01962	1
0.01999	2.598	0.02823	0.001554	0.02002	1	0.01999	2.461	0.02804	0.001554	0.02002	1
0.0204	2.281	0.02662	0.001572	0.02042	1	0.0204	2.194	0.02708	0.001572	0.02042	1
0.02061	2.394	0.04425	0.002398	0.02072	1	0.02061	2.309	0.04304	0.002398	0.02072	1
0.0208	2.023	0.0258	0.001589	0.02083	1	0.0208	1.968	0.02404	0.001589	0.02083	1
0.0212	1.773	0.02365	0.001607	0.02123	1	0.0212	1.734	0.02372	0.001607	0.02123	1
0.02161	1.562	0.0217	0.001625	0.02163	1	0.02161	1.495	0.02342	0.001625	0.02163	1
0.02194	1.589	0.0285	0.002436	0.02204	1	0.02194	1.549	0.02741	0.002436	0.02204	1
0.02201	1.389	0.02009	0.001643	0.02203	1	0.02201	1.342	0.01951	0.001643	0.02203	1
0.02241	1.256	0.02044	0.001661	0.02244	1	0.02241	1.207	0.01969	0.001661	0.02244	1
0.02282	1.106	0.01987	0.00168	0.02284	1	0.02282	1.1	0.01967	0.00168	0.02284	1
0.02322	1.018	0.01812	0.001698	0.02324	1	0.02322	0.9546	0.01745	0.001698	0.02324	1
0.02327	1.096	0.01708	0.002477	0.02336	1	0.02327	1.051	0.01759	0.002477	0.02336	1
0.02363	0.9033	0.01709	0.001717	0.02365	1	0.02363	0.8982	0.01777	0.001717	0.02365	1
0.02403	0.838	0.01665	0.001736	0.02405	1	0.02403	0.8327	0.01584	0.001736	0.02405	1
0.02443	0.7882	0.01625	0.001754	0.02445	1	0.02443	0.7431	0.01533	0.001754	0.02445	1
0.0246	0.7972	0.01176	0.002519	0.02469	1	0.0246	0.7668	0.01077	0.002519	0.02469	1
0.02484	0.6889	0.01656	0.001773	0.02486	1	0.02484	0.6556	0.01437	0.001773	0.02486	1
0.02524	0.6458	0.0151	0.001792	0.02526	1	0.02524	0.6693	0.01694	0.001792	0.02526	1
0.02564	0.6012	0.01629	0.001812	0.02566	1	0.02564	0.5924	0.01579	0.001812	0.02566	1
0.02593	0.6186	0.007616	0.002563	0.02601	1	0.02593	0.5927	0.007984	0.002563	0.02601	1
0.02605	0.5738	0.01682	0.001831	0.02607	1	0.02605	0.5527	0.01628	0.001831	0.02607	1
0.02645	0.5542	0.01681	0.00185	0.02647	1	0.02645	0.491	0.01498	0.00185	0.02647	1
0.02685	0.5037	0.01659	0.00187	0.02687	1	0.02685	0.4754	0.01546	0.00187	0.02687	1
0.02726	0.4786	0.01463	0.001889	0.02728	1	0.02726	0.47	0.01558	0.001889	0.02728	1
0.02726	0.4783	0.00591	0.002609	0.02734	1	0.02726	0.469	0.006358	0.002609	0.02734	1
0.02766	0.4456	0.01625	0.001909	0.02768	1	0.02766	0.4391	0.01545	0.001909	0.02768	1
0.02807	0.4307	0.01582	0.001928	0.02808	1	0.02807	0.424	0.01526	0.001928	0.02808	1
0.02847	0.4088	0.01474	0.001948	0.02849	1	0.02847	0.4014	0.01574	0.001948	0.02849	1
0.02859	0.3915	0.00528	0.002656	0.02866	1	0.02859	0.3937	0.005659	0.002656	0.02866	1
0.02887	0.3933	0.01454	0.001968	0.02889	1	0.02887	0.3973	0.01626	0.001968	0.02889	1
0.02928	0.3508	0.01551	0.001988	0.02929	1	0.02928	0.3411	0.0156	0.001988	0.02929	1
0.02968	0.3824	0.01512	0.002008	0.0297	1	0.02968	0.3751	0.01765	0.002008	0.0297	1
0.02991	0.3511	0.004069	0.002705	0.02999	1	0.02991	0.3355	0.004717	0.002705	0.02999	1



PEO <sub>132</sub> -PB <sub>89</sub> /C <sub>6</sub> D <sub>12</sub> 21.3 °C					PEO <sub>132</sub> -PB <sub>89</sub> /C <sub>6</sub> D <sub>12</sub> 30.6 °C						
Q	I(Q)	Std Dev(I(Q))	sigmaQ	meanQ	Shadow Factor	Q	I(Q)	Std Dev(I(Q))	sigmaQ	meanQ	Shadow Factor
0.03008	0.3554	0.01563	0.002028	0.0301	1	0.03008	0.3014	0.01364	0.002028	0.0301	1
0.03049	0.3295	0.01524	0.002048	0.0305	1	0.03049	0.3313	0.01447	0.002048	0.0305	1
0.03089	0.3076	0.01505	0.002068	0.03091	1	0.03089	0.3133	0.01442	0.002068	0.03091	1
0.03124	0.3016	0.004264	0.002754	0.03131	1	0.03124	0.2885	0.00464	0.002754	0.03131	1
0.03129	0.3076	0.01484	0.002089	0.03131	1	0.03129	0.2864	0.01446	0.002089	0.03131	1
0.0317	0.3089	0.01585	0.002109	0.03171	1	0.0317	0.2856	0.0147	0.002109	0.03171	1
0.0321	0.2764	0.01424	0.002129	0.03212	1	0.0321	0.2773	0.0137	0.002129	0.03212	1
0.0325	0.2863	0.01445	0.00215	0.03252	1	0.0325	0.2848	0.01577	0.00215	0.03252	1
0.03257	0.2691	0.004463	0.002806	0.03264	1	0.03257	0.2662	0.004576	0.002806	0.03264	1
0.03291	0.2842	0.01432	0.00217	0.03292	1	0.03291	0.2956	0.01423	0.00217	0.03292	1
0.03331	0.2732	0.01437	0.002191	0.03333	1	0.03331	0.2539	0.01306	0.002191	0.03333	1
0.03372	0.2905	0.01573	0.002212	0.03373	1	0.03372	0.2766	0.01531	0.002212	0.03373	1
0.0339	0.2479	0.003808	0.002858	0.03396	1	0.0339	0.2523	0.00354	0.002858	0.03396	1
0.03399	0.2676	0.005363	0.004785	0.03426	1	0.03399	0.2667	0.005097	0.004785	0.03426	1
0.03412	0.2688	0.01499	0.002232	0.03413	1	0.03412	0.2806	0.01342	0.002232	0.03413	1
0.03452	0.2667	0.0171	0.002253	0.03454	1	0.03452	0.2736	0.01769	0.002253	0.03454	1
0.03493	0.2525	0.01754	0.002274	0.03494	1	0.03493	0.2432	0.0178	0.002274	0.03494	1
0.03523	0.2363	0.00354	0.002911	0.03529	1	0.03523	0.2274	0.00392	0.002911	0.03529	1
0.03533	0.2423	0.01853	0.002295	0.03534	1	0.03533	0.2749	0.01811	0.002295	0.03534	1
0.03573	0.2648	0.01911	0.002316	0.03575	1	0.03573	0.2315	0.01608	0.002316	0.03575	1
0.03614	0.2146	0.01974	0.002336	0.03615	1	0.03614	0.2132	0.01491	0.002336	0.03615	1
0.03654	0.2326	0.02251	0.002357	0.03655	1	0.03654	0.2272	0.02058	0.002357	0.03655	1
0.03656	0.2097	0.00332	0.002966	0.03662	1	0.03656	0.213	0.003133	0.002966	0.03662	1
0.03694	0.2139	0.02273	0.002378	0.03696	1	0.03694	0.2496	0.0232	0.002378	0.03696	1
0.03735	0.217	0.02164	0.0024	0.03736	1	0.03735	0.2148	0.02116	0.0024	0.03736	1
0.03775	0.2043	0.02163	0.002421	0.03776	1	0.03775	0.2036	0.02125	0.002421	0.03776	1
0.03788	0.2019	0.003578	0.003021	0.03794	1	0.03788	0.2017	0.003085	0.003021	0.03794	1
0.03798	0.206	0.003212	0.004881	0.03823	1	0.03798	0.2104	0.003209	0.004881	0.03823	1
0.03815	0.2406	0.02672	0.002442	0.03817	1	0.03815	0.1594	0.02213	0.002442	0.03817	1
0.03856	0.2701	0.02452	0.002463	0.03857	1	0.03856	0.2032	0.0262	0.002463	0.03857	1
0.03896	0.1789	0.02321	0.002484	0.03897	1	0.03896	0.1771	0.02312	0.002484	0.03897	1
0.03921	0.1935	0.003037	0.003077	0.03927	1	0.03921	0.1925	0.0032	0.003077	0.03927	1
0.03936	0.2174	0.03144	0.002506	0.03938	1	0.03936	0.2432	0.03121	0.002506	0.03938	1
0.03977	0.2178	0.03109	0.002527	0.03978	1	0.03977	0.2202	0.0338	0.002527	0.03978	1
0.04017	0.1324	0.03431	0.002548	0.04018	1	0.04017	0.1733	0.03976	0.002548	0.04018	1
0.04054	0.188	0.003233	0.003134	0.04059	1	0.04054	0.1849	0.003083	0.003134	0.04059	1
0.04057	0.2181	0.0405	0.00257	0.04059	1	0.04057	0.2472	0.03851	0.00257	0.04059	1
0.04187	0.1747	0.002891	0.003192	0.04192	1	0.04187	0.1787	0.003014	0.003192	0.04192	1
0.04197	0.1708	0.00249	0.004987	0.0422	1	0.04197	0.1733	0.002443	0.004987	0.0422	1
0.0432	0.1671	0.00274	0.003251	0.04325	1	0.0432	0.1677	0.002907	0.003251	0.04325	1
0.04452	0.1546	0.002689	0.003311	0.04457	1	0.04452	0.1609	0.002862	0.003311	0.04457	1
0.04585	0.1463	0.002645	0.003371	0.0459	1	0.04585	0.1483	0.002882	0.003371	0.0459	1
0.04597	0.1452	0.002317	0.005102	0.04617	1	0.04597	0.1495	0.001964	0.005102	0.04617	1
0.04718	0.1468	0.002684	0.003432	0.04722	1	0.04718	0.1412	0.002688	0.003432	0.04722	1
0.0485	0.1322	0.002645	0.003493	0.04855	1	0.0485	0.1372	0.002598	0.003493	0.04855	1
0.04983	0.1307	0.002795	0.003555	0.04987	1	0.04983	0.1323	0.002568	0.003555	0.04987	1
0.04996	0.1288	0.001623	0.005225	0.05014	1	0.04996	0.1294	0.001734	0.005225	0.05014	1
0.05116	0.1229	0.002413	0.003618	0.0512	1	0.05116	0.1239	0.002615	0.003618	0.0512	1
0.05248	0.1166	0.002383	0.003681	0.05252	1	0.05248	0.119	0.002311	0.003681	0.05252	1
0.05381	0.1121	0.002361	0.003745	0.05385	1	0.05381	0.1171	0.002116	0.003745	0.05385	1
0.05394	0.1151	0.001623	0.005355	0.05412	1	0.05394	0.1153	0.001494	0.005355	0.05412	1
0.05514	0.1125	0.002339	0.003809	0.05517	1	0.05514	0.1114	0.002472	0.003809	0.05517	1
0.05646	0.1102	0.002332	0.003874	0.0565	1	0.05646	0.1066	0.002235	0.003874	0.0565	1
0.05779	0.1031	0.002309	0.003939	0.05782	1	0.05779	0.1062	0.002165	0.003939	0.05782	1
0.05793	0.1053	0.001435	0.005492	0.05809	1	0.05793	0.1059	0.001484	0.005492	0.05809	1
0.05911	0.1036	0.002096	0.004004	0.05915	1	0.05911	0.1031	0.002142	0.004004	0.05915	1
0.06044	0.1052	0.002245	0.00407	0.06047	1	0.06044	0.1042	0.002133	0.00407	0.06047	1
0.06176	0.1008	0.001984	0.004137	0.0618	1	0.06176	0.1033	0.002106	0.004137	0.0618	1
0.06192	0.09851	0.001482	0.005635	0.06207	1	0.06192	0.09946	0.00119	0.005635	0.06207	1
0.06309	0.09891	0.002075	0.004203	0.06312	1	0.06309	0.1023	0.002253	0.004203	0.06312	1
0.06441	0.09459	0.002152	0.00427	0.06444	1	0.06441	0.09705	0.002035	0.00427	0.06444	1
0.06573	0.0944	0.002191	0.004337	0.06577	1	0.06573	0.09451	0.002075	0.004337	0.06577	1
0.0659	0.09511	0.001239	0.005784	0.06604	1	0.0659	0.098	0.001334	0.005784	0.06604	1
0.06706	0.09534	0.00209	0.004405	0.06709	1	0.06706	0.09985	0.001861	0.004405	0.06709	1
0.06838	0.09769	0.002039	0.004473	0.06841	1	0.06838	0.09847	0.001842	0.004473	0.06841	1
0.06971	0.09531	0.002002	0.004541	0.06974	1	0.06971	0.0972	0.001802	0.004541	0.06974	1
0.06988	0.09437	0.001273	0.005938	0.07001	1	0.06988	0.09537	0.001402	0.005938	0.07001	1
0.07103	0.09465	0.001835	0.004609	0.07106	1	0.07103	0.09663	0.00197	0.004609	0.07106	1
0.07235	0.09332	0.00186	0.004678	0.07238	1	0.07235	0.0934	0.001902	0.004678	0.07238	1
0.07367	0.09164	0.001868	0.004746	0.0737	1	0.07367	0.09312	0.001845	0.004746	0.0737	1
0.07386	0.09193	0.001296	0.006097	0.07399	1	0.07386	0.09307	0.001471	0.006097	0.07399	1
0.075	0.09017	0.001875	0.004815	0.07503	1	0.075	0.09329	0.00176	0.004815	0.07503	1
0.07632	0.0924	0.001723	0.004885	0.07635	1	0.07632	0.09368	0.001855	0.004885	0.07635	1
0.07764	0.09067	0.00173	0.004954	0.07767	1	0.07764	0.09274	0.002015	0.004954	0.07767	1
0.07784	0.08867	0.001257	0.00626	0.07796	1	0.07784	0.09125	0.001263	0.00626	0.07796	1
0.07896	0.08589	0.001803	0.005024	0.07899	1	0.07896	0.09393	0.001965	0.005024	0.07899	1
0.08028	0.09094	0.001993	0.005094	0.08031	1	0.08028	0.09179	0.001891	0.005094	0.08031	1
0.08161	0.08956	0.001829	0.005164	0.08163	1	0.08161	0.09056	0.001864	0.005164	0.08163	1
0.08181	0.08684	0.001277	0.006427	0.08192	1	0.08181	0.08841	0.00123	0.006427	0.08192	1
0.08293	0.08652	0.001937	0.005234	0.08295	1	0.08293	0.08957	0.002059	0.005234	0.08295	1
0.08425	0.09006	0.00208	0.005304	0.08427	1	0.08425	0.09091	0.002129	0.005304	0.08427	1
0.08557	0.08364	0.001981	0.005375	0.08559	1	0.08557	0.08915	0.002141	0.005375	0.08559	1

PEO <sub>132</sub> -PB <sub>89</sub> /C <sub>6</sub> D <sub>12</sub> 21.3 °C					PEO <sub>132</sub> -PB <sub>89</sub> /C <sub>6</sub> D <sub>12</sub> 30.6 °C						
Q	I(Q)	Std DevI(Q)	sigmaQ	meanQ	Shadow Factor	Q	I(Q)	Std DevI(Q)	sigmaQ	meanQ	Shadow Factor
0.08578	0.08784	0.001127	0.006598	0.08589	1	0.08578	0.08852	0.001115	0.006598	0.08589	1
0.08689	0.08901	0.002369	0.005445	0.08691	1	0.08689	0.09081	0.002254	0.005445	0.08691	1
0.08821	0.08383	0.002347	0.005516	0.08823	1	0.08821	0.09057	0.00227	0.005516	0.08823	1
0.08953	0.08477	0.002438	0.005587	0.08955	1	0.08953	0.0883	0.002681	0.005587	0.08955	1
0.08975	0.08414	0.000955	0.006772	0.08985	1	0.08975	0.08767	0.001235	0.006772	0.08985	1
0.09084	0.08008	0.002523	0.005658	0.09087	1	0.09084	0.08602	0.002601	0.005658	0.09087	1
0.09216	0.08105	0.002572	0.005729	0.09219	1	0.09216	0.08417	0.002674	0.005729	0.09219	1
0.09348	0.08201	0.002751	0.0058	0.0935	1	0.09348	0.0769	0.002809	0.0058	0.0935	1
0.09371	0.08258	0.001057	0.006949	0.09381	1	0.09371	0.08399	0.001078	0.006949	0.09381	1
0.0948	0.08722	0.003183	0.005872	0.09482	1	0.0948	0.08837	0.002852	0.005872	0.09482	1
0.09612	0.08931	0.003093	0.005943	0.09614	1	0.09612	0.08627	0.002982	0.005943	0.09614	1
0.09743	0.08672	0.003147	0.006015	0.09746	1	0.09743	0.08764	0.003427	0.006015	0.09746	1
0.09768	0.08345	0.00108	0.00713	0.09777	1	0.09768	0.08553	0.000976	0.00713	0.09777	1
0.09875	0.0854	0.003124	0.006086	0.09877	1	0.09875	0.08609	0.003652	0.006086	0.09877	1
0.1001	0.07898	0.003646	0.006158	0.1001	1	0.1001	0.08337	0.003758	0.006158	0.1001	1
0.1014	0.07795	0.003572	0.00623	0.1014	1	0.1014	0.08221	0.003232	0.00623	0.1014	1
0.1016	0.08258	0.001195	0.007313	0.1017	1	0.1016	0.08291	0.001076	0.007313	0.1017	1
0.1027	0.0826	0.003829	0.006302	0.1027	1	0.1027	0.08483	0.003777	0.006302	0.1027	1
0.104	0.07925	0.004068	0.006374	0.104	1	0.104	0.08369	0.004293	0.006374	0.104	1
0.1053	0.07594	0.005037	0.006446	0.1053	1	0.1053	0.08486	0.004337	0.006446	0.1053	1
0.1056	0.08238	0.001181	0.007498	0.1057	1	0.1056	0.08396	0.001081	0.007498	0.1057	1
0.1066	0.07821	0.004805	0.006518	0.1067	1	0.1066	0.09016	0.004281	0.006518	0.1067	1
0.108	0.0787	0.00606	0.006591	0.108	1	0.108	0.0798	0.007133	0.006591	0.108	1
0.1093	0.08368	0.005194	0.006663	0.1093	1	0.1093	0.08316	0.006193	0.006663	0.1093	1
0.1095	0.07802	0.001036	0.007685	0.1096	1	0.1095	0.07978	0.001006	0.007685	0.1096	1
0.1106	0.07876	0.005526	0.006735	0.1106	1	0.1106	0.07285	0.005141	0.006735	0.1106	1
0.1119	0.07176	0.007095	0.006808	0.1119	1	0.1119	0.07178	0.007111	0.006808	0.1119	1
0.1132	0.07287	0.007973	0.00688	0.1132	1	0.1132	0.07423	0.005575	0.00688	0.1132	1
0.1135	0.07862	0.001092	0.007875	0.1136	1	0.1135	0.08066	0.001138	0.007875	0.1136	1
0.1174	0.07661	0.000969	0.008066	0.1175	1	0.1174	0.07868	0.000933	0.008066	0.1175	1
0.1214	0.07881	0.000904	0.008259	0.1215	1	0.1214	0.0795	0.001006	0.008259	0.1215	1
0.1253	0.0772	0.000984	0.008453	0.1254	1	0.1253	0.07929	0.001014	0.008453	0.1254	1
0.1293	0.07487	0.000941	0.008649	0.1293	1	0.1293	0.07824	0.001101	0.008649	0.1293	1
0.1332	0.07662	0.000997	0.008847	0.1333	1	0.1332	0.07903	0.00111	0.008847	0.1333	1
0.1371	0.07695	0.000938	0.009045	0.1372	1	0.1371	0.07829	0.000985	0.009045	0.1372	1
0.141	0.07533	0.000897	0.009245	0.1411	1	0.141	0.07792	0.000992	0.009245	0.1411	1
0.1449	0.076	0.00093	0.009445	0.145	1	0.1449	0.07911	0.000929	0.009445	0.145	1
0.1489	0.07745	0.000989	0.009647	0.1489	1	0.1489	0.07805	0.00098	0.009647	0.1489	1
0.1528	0.07571	0.001003	0.009849	0.1528	1	0.1528	0.07691	0.000924	0.009849	0.1528	1
0.1567	0.07567	0.000922	0.01005	0.1567	1	0.1567	0.07718	0.000846	0.01005	0.1567	1
0.1606	0.075	0.000972	0.01026	0.1606	1	0.1606	0.07622	0.000909	0.01026	0.1606	1
0.1645	0.0742	0.000876	0.01046	0.1645	1	0.1645	0.07672	0.000815	0.01046	0.1645	1
0.1683	0.07396	0.000891	0.01067	0.1684	1	0.1683	0.07656	0.00082	0.01067	0.1684	1
0.1722	0.07282	0.000808	0.01087	0.1723	1	0.1722	0.07573	0.000887	0.01087	0.1723	1
0.1761	0.0723	0.000871	0.01108	0.1762	1	0.1761	0.07501	0.00097	0.01108	0.1762	1
0.18	0.07175	0.000736	0.01128	0.18	1	0.18	0.07592	0.000836	0.01128	0.18	1
0.1838	0.07338	0.000751	0.01149	0.1839	1	0.1838	0.07552	0.0008	0.01149	0.1839	1
0.1877	0.07369	0.000822	0.0117	0.1877	1	0.1877	0.07505	0.000792	0.0117	0.1877	1
0.1916	0.07237	0.000847	0.0119	0.1916	1	0.1916	0.0755	0.000876	0.0119	0.1916	1
0.1954	0.07286	0.000861	0.01211	0.1954	1	0.1954	0.07411	0.000759	0.01211	0.1954	1
0.1992	0.07174	0.000816	0.01232	0.1993	1	0.1992	0.07422	0.000816	0.01232	0.1993	1
0.2031	0.07215	0.000802	0.01253	0.2031	1	0.2031	0.07388	0.00086	0.01253	0.2031	1
0.2069	0.07117	0.000755	0.01274	0.2069	1	0.2069	0.0731	0.000813	0.01274	0.2069	1
0.2107	0.07271	0.000727	0.01294	0.2108	1	0.2107	0.07483	0.000732	0.01294	0.2108	1
0.2145	0.07171	0.000721	0.01315	0.2146	1	0.2145	0.07401	0.000768	0.01315	0.2146	1
0.2184	0.0725	0.000782	0.01336	0.2184	1	0.2184	0.0742	0.000749	0.01336	0.2184	1
0.2222	0.07147	0.000683	0.01357	0.2222	1	0.2222	0.07292	0.00073	0.01357	0.2222	1
0.226	0.07189	0.000812	0.01378	0.226	1	0.226	0.0736	0.00079	0.01378	0.226	1
0.2297	0.07035	0.000726	0.01399	0.2298	1	0.2297	0.07326	0.000689	0.01399	0.2298	1
0.2335	0.07108	0.000772	0.01419	0.2336	1	0.2335	0.07191	0.000806	0.01419	0.2336	1
0.2373	0.07227	0.000783	0.0144	0.2373	1	0.2373	0.07367	0.000825	0.0144	0.2373	1
0.2411	0.07033	0.000727	0.01461	0.2411	1	0.2411	0.07446	0.00077	0.01461	0.2411	1
0.2448	0.07062	0.00083	0.01482	0.2449	1	0.2448	0.07314	0.000908	0.01482	0.2449	1
0.2486	0.07012	0.000772	0.01503	0.2486	1	0.2486	0.07154	0.000869	0.01503	0.2486	1
0.2523	0.07059	0.000896	0.01523	0.2524	1	0.2523	0.07268	0.00085	0.01523	0.2524	1
0.2561	0.07169	0.000814	0.01544	0.2561	1	0.2561	0.07333	0.000852	0.01544	0.2561	1
0.2598	0.07019	0.000839	0.01565	0.2598	1	0.2598	0.07438	0.000791	0.01565	0.2598	1
0.2635	0.07034	0.000837	0.01586	0.2636	1	0.2635	0.07331	0.000968	0.01586	0.2636	1
0.2673	0.07136	0.000885	0.01606	0.2673	1	0.2673	0.07333	0.000953	0.01606	0.2673	1
0.271	0.07069	0.000883	0.01627	0.271	1	0.271	0.07252	0.00102	0.01627	0.271	1
0.2747	0.0697	0.000791	0.01648	0.2747	1	0.2747	0.07014	0.00099	0.01648	0.2747	1
0.2784	0.06925	0.00084	0.01668	0.2784	1	0.2784	0.0713	0.00092	0.01668	0.2784	1
0.282	0.07002	0.000847	0.01689	0.2821	1	0.282	0.071	0.000818	0.01689	0.2821	1
0.2857	0.07094	0.000783	0.01709	0.2857	1	0.2857	0.07179	0.00085	0.01709	0.2857	1
0.2894	0.07019	0.000948	0.0173	0.2894	1	0.2894	0.07294	0.000926	0.0173	0.2894	1
0.293	0.07028	0.000966	0.0175	0.2931	1	0.293	0.0715	0.000944	0.0175	0.2931	1
0.2967	0.06978	0.000911	0.01771	0.2967	1	0.2967	0.07202	0.000957	0.01771	0.2967	1
0.3003	0.07086	0.000892	0.01791	0.3004	1	0.3003	0.07062	0.000956	0.01791	0.3004	1
0.304	0.07009	0.000786	0.01812	0.304	1	0.304	0.07147	0.00088	0.01812	0.304	1
0.3076	0.06993	0.000973	0.01832	0.3076	1	0.3076	0.07322	0.000955	0.01832	0.3076	1
0.3112	0.06951	0.000947	0.01852	0.3113	1	0.3112	0.0717	0.000945	0.01852	0.3113	1
0.3148	0.068	0.000795	0.01873	0.3149	1	0.3148	0.07108	0.000947	0.01873	0.3149	1

PEO <sub>132</sub> -PB <sub>89</sub> /C <sub>6</sub> D <sub>12</sub> 21.3 °C						PEO <sub>132</sub> -PB <sub>89</sub> /C <sub>6</sub> D <sub>12</sub> 30.6 °C					
Q	I(Q)	Std Dev(I(Q))	sigmaQ	meanQ	Shadow Factor	Q	I(Q)	Std Dev(I(Q))	sigmaQ	meanQ	Shadow Factor
0.3184	0.07007	0.000944	0.01893	0.3185	1	0.3184	0.07222	0.00093	0.01893	0.3185	1
0.322	0.06945	0.000826	0.01913	0.3221	1	0.322	0.07108	0.001031	0.01913	0.3221	1
0.3256	0.06877	0.000974	0.01933	0.3256	1	0.3256	0.07034	0.000948	0.01933	0.3256	1
0.3292	0.06896	0.00091	0.01954	0.3292	1	0.3292	0.0719	0.000962	0.01954	0.3292	1
0.3327	0.0687	0.000881	0.01974	0.3328	1	0.3327	0.07035	0.000913	0.01974	0.3328	1
0.3363	0.06869	0.000991	0.01994	0.3363	1	0.3363	0.07037	0.000897	0.01994	0.3363	1
0.3399	0.06941	0.000889	0.02014	0.3399	1	0.3399	0.06988	0.000909	0.02014	0.3399	1
0.3434	0.06842	0.000812	0.02034	0.3434	1	0.3434	0.06873	0.000876	0.02034	0.3434	1
0.3469	0.06876	0.000814	0.02054	0.3469	1	0.3469	0.07047	0.000904	0.02054	0.3469	1
0.3504	0.06834	0.000945	0.02074	0.3505	1	0.3504	0.07095	0.000956	0.02074	0.3505	1
0.3539	0.06794	0.000797	0.02094	0.354	1	0.3539	0.07165	0.000961	0.02094	0.354	1
0.3574	0.06829	0.000961	0.02113	0.3575	1	0.3574	0.07069	0.000918	0.02113	0.3575	1
0.3609	0.06844	0.000904	0.02133	0.361	1	0.3609	0.06998	0.001006	0.02133	0.361	1
0.3644	0.06889	0.000919	0.02153	0.3644	1	0.3644	0.06958	0.00101	0.02153	0.3644	1
0.3679	0.06803	0.000883	0.02173	0.3679	1	0.3679	0.07051	0.000887	0.02173	0.3679	1
0.3713	0.06777	0.000945	0.02192	0.3714	1	0.3713	0.06941	0.001005	0.02192	0.3714	1
0.3748	0.0688	0.000935	0.02212	0.3748	1	0.3748	0.07147	0.000798	0.02212	0.3748	1
0.3782	0.06965	0.000895	0.02231	0.3783	1	0.3782	0.06984	0.00096	0.02231	0.3783	1
0.3817	0.06681	0.000942	0.02251	0.3817	1	0.3817	0.0689	0.001055	0.02251	0.3817	1
0.3851	0.06851	0.001017	0.0227	0.3851	1	0.3851	0.06951	0.000896	0.0227	0.3851	1
0.3885	0.06542	0.00091	0.0229	0.3885	1	0.3885	0.06776	0.000869	0.0229	0.3885	1
0.3919	0.06776	0.000904	0.02309	0.3919	1	0.3919	0.06987	0.001033	0.02309	0.3919	1
0.3953	0.0675	0.000971	0.02328	0.3953	1	0.3953	0.0679	0.001037	0.02328	0.3953	1
0.3987	0.06617	0.001	0.02347	0.3987	1	0.3987	0.06886	0.00096	0.02347	0.3987	1
0.4021	0.06883	0.00097	0.02367	0.4021	1	0.4021	0.06987	0.000817	0.02367	0.4021	1
0.4054	0.06663	0.001013	0.02386	0.4054	1	0.4054	0.06861	0.00096	0.02386	0.4054	1
0.4088	0.0674	0.001018	0.02405	0.4088	1	0.4088	0.07014	0.000953	0.02405	0.4088	1
0.4121	0.0665	0.00092	0.02424	0.4121	1	0.4121	0.06861	0.001008	0.02424	0.4121	1
0.4155	0.06657	0.000905	0.02443	0.4155	1	0.4155	0.06826	0.000968	0.02443	0.4155	1
0.4188	0.06706	0.000875	0.02462	0.4188	1	0.4188	0.06808	0.000999	0.02462	0.4188	1
0.4221	0.06487	0.000998	0.02481	0.4221	1	0.4221	0.06924	0.000935	0.02481	0.4221	1
0.4254	0.06737	0.001051	0.02499	0.4254	1	0.4254	0.06799	0.000979	0.02499	0.4254	1
0.4287	0.06749	0.001047	0.02518	0.4287	1	0.4287	0.07106	0.001093	0.02518	0.4287	1
0.432	0.06645	0.001167	0.02537	0.432	1	0.432	0.06894	0.001254	0.02537	0.432	1
0.4352	0.06564	0.001196	0.02556	0.4353	1	0.4352	0.06656	0.001417	0.02556	0.4353	1
0.4385	0.06569	0.001555	0.02574	0.4385	1	0.4385	0.0687	0.001425	0.02574	0.4385	1
0.4417	0.06645	0.001651	0.02593	0.4418	1	0.4417	0.06905	0.001725	0.02593	0.4418	1
0.445	0.06538	0.001565	0.02611	0.445	1	0.445	0.06739	0.001404	0.02611	0.445	1
0.4482	0.06637	0.001588	0.0263	0.4482	1	0.4482	0.06992	0.00175	0.0263	0.4482	1
0.4514	0.06634	0.001834	0.02648	0.4515	1	0.4514	0.06649	0.001997	0.02648	0.4515	1
0.4546	0.06325	0.001923	0.02666	0.4547	1	0.4546	0.06765	0.002024	0.02666	0.4547	1
0.4578	0.06965	0.001734	0.02685	0.4579	1	0.4578	0.06731	0.001915	0.02685	0.4579	1
0.461	0.0683	0.002488	0.02703	0.461	1	0.461	0.06678	0.002301	0.02703	0.461	1

PEO <sub>132</sub> -PB <sub>89</sub> /C <sub>6</sub> D <sub>12</sub> 39.9 °C						PEO <sub>132</sub> -PB <sub>89</sub> /C <sub>6</sub> D <sub>12</sub> 49.3 °C					
Q	I(Q)	Std Dev(I(Q))	sigmaQ	meanQ	Shadow Factor	Q	I(Q)	Std Dev(I(Q))	sigmaQ	meanQ	Shadow Factor
0.003433	330.1	4.362	0.001072	0.003606	0.9585	0.003433	9.632	0.2058	0.001072	0.003606	0.9585
0.003837	289.9	3.663	0.001076	0.003977	0.9999	0.003837	10.39	0.1326	0.001076	0.003977	0.9999
0.004241	232.5	2.52	0.001078	0.004367	1	0.004241	10.4	0.1193	0.001078	0.004367	1
0.004645	191.4	1.778	0.001081	0.00476	1	0.004645	10.34	0.1059	0.001081	0.00476	1
0.005049	161	1.311	0.001086	0.005155	1	0.005049	10.2	0.1128	0.001086	0.005155	1
0.005453	137	1.019	0.001091	0.005551	1	0.005453	10.01	0.1027	0.001091	0.005551	1
0.005857	118.3	0.7821	0.001097	0.005948	1	0.005857	9.876	0.09332	0.001097	0.005948	1
0.006261	103.2	0.6614	0.001103	0.006346	1	0.006261	9.743	0.07836	0.001103	0.006346	1
0.006665	91.13	0.4917	0.001111	0.006745	1	0.006665	9.669	0.08861	0.001111	0.006745	1
0.007069	80.9	0.4635	0.001118	0.007144	1	0.007069	9.642	0.08438	0.001118	0.007144	1
0.007473	72.47	0.3743	0.001127	0.007544	1	0.007473	9.321	0.08535	0.001127	0.007544	1
0.007876	65.38	0.3337	0.001135	0.007944	1	0.007876	9.309	0.08288	0.001135	0.007944	1
0.00828	59	0.245	0.001145	0.008345	1	0.00828	9.109	0.0747	0.001145	0.008345	1
0.008684	53.19	0.2213	0.001154	0.008746	1	0.008684	9.191	0.06777	0.001154	0.008746	1
0.009088	48.36	0.1987	0.001164	0.009147	1	0.009088	8.778	0.06611	0.001164	0.009147	1
0.009492	44.15	0.186	0.001175	0.009548	1	0.009492	8.7	0.06263	0.001175	0.009548	1
0.009896	40.65	0.1634	0.001186	0.00995	1	0.009896	8.588	0.06652	0.001186	0.00995	1
0.0103	36.87	0.1623	0.001197	0.01035	1	0.0103	8.48	0.05493	0.001197	0.01035	1
0.0107	33.59	0.1286	0.001209	0.01075	1	0.0107	8.24	0.0637	0.001209	0.01075	1
0.01111	30.63	0.1366	0.001221	0.01116	1	0.01111	8.055	0.05459	0.001221	0.01116	1
0.0113	30.06	0.5301	0.002191	0.01149	1	0.0113	7.971	0.05048	0.002191	0.01149	1
0.01151	28.21	0.1238	0.001233	0.01156	1	0.01151	7.902	0.04907	0.001233	0.01156	1
0.01192	25.34	0.1078	0.001246	0.01196	1	0.01192	7.824	0.0567	0.001246	0.01196	1
0.01232	23.34	0.1005	0.001259	0.01236	1	0.01232	7.58	0.05314	0.001259	0.01236	1
0.01263	22	0.3812	0.002212	0.0128	1	0.01263	7.365	0.04488	0.002212	0.0128	1
0.01272	21.13	0.1019	0.001272	0.01277	1	0.01272	7.322	0.05082	0.001272	0.01277	1
0.01313	19.17	0.095	0.001286	0.01317	1	0.01313	7.134	0.05051	0.001286	0.01317	1
0.01353	17.22	0.08104	0.0013	0.01357	1	0.01353	6.874	0.04254	0.0013	0.01357	1
0.01393	15.44	0.0793	0.001314	0.01397	1	0.01393	6.853	0.05128	0.001314	0.01397	1
0.01396	15.88	0.2786	0.002236	0.01412	1	0.01396	6.803	0.04062	0.002236	0.01412	1
0.01434	13.86	0.08076	0.001328	0.01438	1	0.01434	6.501	0.04478	0.001328	0.01438	1
0.01474	12.31	0.07098	0.001343	0.01478	1	0.01474	6.391	0.04161	0.001343	0.01478	1
0.01515	11.06	0.067	0.001358	0.01518	1	0.01515	6.192	0.047	0.001358	0.01518	1
0.01529	11.15	0.2041	0.002264	0.01543	1	0.01529	6.186	0.03839	0.002264	0.01543	1

PEO <sub>132</sub> -PB <sub>89</sub> /C <sub>6</sub> D <sub>12</sub> 39.9 °C						PEO <sub>132</sub> -PB <sub>89</sub> /C <sub>6</sub> D <sub>12</sub> 49.3 °C					
Q	I(Q)	Std Dev(I(Q))	sigmaQ	meanQ	Shadow Factor	Q	I(Q)	Std Dev(I(Q))	sigmaQ	meanQ	Shadow Factor
0.01555	9.763	0.05732	0.001373	0.01558	1	0.01555	6.116	0.04479	0.001373	0.01558	1
0.01595	8.695	0.05634	0.001389	0.01599	1	0.01595	5.883	0.04427	0.001389	0.01599	1
0.01636	7.68	0.05203	0.001404	0.01639	1	0.01636	5.687	0.04171	0.001404	0.01639	1
0.01662	7.615	0.1408	0.002294	0.01675	1	0.01662	5.587	0.03581	0.002294	0.01675	1
0.01676	6.729	0.04419	0.00142	0.01679	1	0.01676	5.443	0.04168	0.00142	0.01679	1
0.01717	5.953	0.04642	0.001436	0.0172	1	0.01717	5.227	0.04039	0.001436	0.0172	1
0.01757	5.249	0.04315	0.001453	0.0176	1	0.01757	5.105	0.03636	0.001453	0.0176	1
0.01795	5.068	0.09623	0.002326	0.01807	1	0.01795	4.96	0.03417	0.002326	0.01807	1
0.01797	4.596	0.0395	0.001469	0.018	1	0.01797	4.945	0.04117	0.001469	0.018	1
0.01838	4.029	0.03798	0.001486	0.01841	1	0.01838	4.826	0.03886	0.001486	0.01841	1
0.01878	3.585	0.03694	0.001503	0.01881	1	0.01878	4.568	0.03517	0.001503	0.01881	1
0.01918	3.159	0.03088	0.00152	0.01921	1	0.01918	4.392	0.03515	0.00152	0.01921	1
0.01928	3.366	0.0627	0.002361	0.01939	1	0.01928	4.387	0.02981	0.002361	0.01939	1
0.01959	2.704	0.02914	0.001537	0.01962	1	0.01959	4.185	0.03395	0.001537	0.01962	1
0.01999	2.408	0.03018	0.001554	0.02002	1	0.01999	4.038	0.03574	0.001554	0.02002	1
0.0204	2.14	0.0243	0.001572	0.02042	1	0.0204	3.918	0.03456	0.001572	0.02042	1
0.02061	2.236	0.04055	0.002398	0.02072	1	0.02061	3.872	0.02783	0.002398	0.02072	1
0.0208	1.892	0.02486	0.001589	0.02083	1	0.0208	3.761	0.03485	0.001589	0.02083	1
0.0212	1.692	0.02328	0.001607	0.02123	1	0.0212	3.611	0.03464	0.001607	0.02123	1
0.02161	1.514	0.0223	0.001625	0.02163	1	0.02161	3.436	0.02964	0.001625	0.02163	1
0.02194	1.51	0.02624	0.002436	0.02204	1	0.02194	3.364	0.0263	0.002436	0.02204	1
0.02201	1.38	0.0221	0.001643	0.02203	1	0.02201	3.255	0.03198	0.001643	0.02203	1
0.02241	1.238	0.01834	0.001661	0.02244	1	0.02241	3.185	0.03	0.001661	0.02244	1
0.02282	1.073	0.01906	0.00168	0.02284	1	0.02282	3.084	0.02938	0.00168	0.02284	1
0.02322	0.9949	0.01835	0.001698	0.02324	1	0.02322	2.94	0.02676	0.001698	0.02324	1
0.02327	1.062	0.01577	0.002477	0.02336	1	0.02327	2.902	0.0219	0.002477	0.02336	1
0.02363	0.9174	0.01698	0.001717	0.02365	1	0.02363	2.804	0.02828	0.001717	0.02365	1
0.02403	0.8241	0.01698	0.001736	0.02405	1	0.02403	2.646	0.02863	0.001736	0.02405	1
0.02443	0.7512	0.01557	0.001754	0.02445	1	0.02443	2.562	0.02638	0.001754	0.02445	1
0.0246	0.7649	0.01173	0.002519	0.02469	1	0.0246	2.478	0.01951	0.002519	0.02469	1
0.02484	0.7175	0.01728	0.001773	0.02486	1	0.02484	2.475	0.02533	0.001773	0.02486	1
0.02524	0.6198	0.01474	0.001792	0.02526	1	0.02524	2.318	0.02854	0.001792	0.02526	1
0.02564	0.6152	0.01623	0.001812	0.02566	1	0.02564	2.248	0.02949	0.001812	0.02566	1
0.02593	0.5922	0.007144	0.002563	0.02601	1	0.02593	2.159	0.01498	0.002563	0.02601	1
0.02605	0.5462	0.01688	0.001831	0.02607	1	0.02605	2.125	0.0279	0.001831	0.02607	1
0.02645	0.5253	0.01563	0.00185	0.02647	1	0.02645	1.979	0.02845	0.00185	0.02647	1
0.02685	0.4706	0.01461	0.00187	0.02687	1	0.02685	1.927	0.02914	0.00187	0.02687	1
0.02726	0.5071	0.01418	0.001889	0.02728	1	0.02726	1.854	0.02595	0.001889	0.02728	1
0.02726	0.4713	0.006233	0.002609	0.02734	1	0.02726	1.825	0.0129	0.002609	0.02734	1
0.02766	0.4402	0.01398	0.001909	0.02768	1	0.02766	1.732	0.02915	0.001909	0.02768	1
0.02807	0.396	0.01683	0.001928	0.02808	1	0.02807	1.681	0.02968	0.001928	0.02808	1
0.02847	0.4086	0.01591	0.001948	0.02849	1	0.02847	1.559	0.0263	0.001948	0.02849	1
0.02859	0.3888	0.005221	0.002656	0.02866	1	0.02859	1.531	0.01157	0.002656	0.02866	1
0.02887	0.4254	0.0167	0.001968	0.02889	1	0.02887	1.532	0.02551	0.001968	0.02889	1
0.02928	0.3544	0.01697	0.001988	0.02929	1	0.02928	1.394	0.02927	0.001988	0.02929	1
0.02968	0.3701	0.01523	0.002008	0.0297	1	0.02968	1.343	0.02695	0.002008	0.0297	1
0.02991	0.3439	0.004639	0.002705	0.02999	1	0.02991	1.31	0.009676	0.002705	0.02999	1
0.03008	0.341	0.01487	0.002028	0.0301	1	0.03008	1.271	0.02668	0.002028	0.0301	1
0.03049	0.3439	0.01478	0.002048	0.0305	1	0.03049	1.209	0.02597	0.002048	0.0305	1
0.03089	0.3005	0.01445	0.002068	0.03091	1	0.03089	1.224	0.02337	0.002068	0.03091	1
0.03124	0.2936	0.004153	0.002754	0.03131	1	0.03124	1.121	0.008852	0.002754	0.03131	1
0.03129	0.3074	0.01553	0.002089	0.03131	1	0.03129	1.117	0.02425	0.002089	0.03131	1
0.0317	0.3049	0.01665	0.002109	0.03171	1	0.0317	1.083	0.02648	0.002109	0.03171	1
0.0321	0.2685	0.01472	0.002129	0.03212	1	0.0321	1.021	0.02562	0.002129	0.03212	1
0.0325	0.2986	0.01487	0.00215	0.03252	1	0.0325	0.9438	0.02501	0.00215	0.03252	1
0.03257	0.2639	0.003744	0.002806	0.03264	1	0.03257	0.9473	0.008628	0.002806	0.03264	1
0.03291	0.2845	0.01511	0.00217	0.03292	1	0.03291	0.8902	0.02196	0.00217	0.03292	1
0.03331	0.2644	0.01434	0.002191	0.03333	1	0.03331	0.857	0.02399	0.002191	0.03333	1
0.03372	0.2507	0.01472	0.002212	0.03373	1	0.03372	0.8614	0.02141	0.002212	0.03373	1
0.0339	0.2468	0.003717	0.002858	0.03396	1	0.0339	0.8084	0.006784	0.002858	0.03396	1
0.03399	0.2614	0.005153	0.004785	0.03426	1	0.03399	0.8397	0.02201	0.004785	0.03426	1
0.03412	0.2751	0.01419	0.002232	0.03413	1	0.03412	0.759	0.02001	0.002232	0.03413	1
0.03452	0.2393	0.01607	0.002253	0.03454	1	0.03452	0.7996	0.02575	0.002253	0.03454	1
0.03493	0.2343	0.01795	0.002274	0.03494	1	0.03493	0.6872	0.02646	0.002274	0.03494	1
0.03523	0.2234	0.003955	0.002911	0.03529	1	0.03523	0.687	0.005841	0.002911	0.03529	1
0.03533	0.2477	0.01802	0.002295	0.03534	1	0.03533	0.6854	0.02827	0.002295	0.03534	1
0.03573	0.2343	0.01861	0.002316	0.03575	1	0.03573	0.6154	0.02294	0.002316	0.03575	1
0.03614	0.2115	0.01678	0.002336	0.03615	1	0.03614	0.6128	0.02677	0.002336	0.03615	1
0.03654	0.2367	0.01982	0.002357	0.03655	1	0.03654	0.5749	0.0317	0.002357	0.03655	1
0.03656	0.2148	0.003531	0.002966	0.03662	1	0.03656	0.5802	0.005926	0.002966	0.03662	1
0.03694	0.2409	0.02105	0.002378	0.03696	1	0.03694	0.5514	0.02758	0.002378	0.03696	1
0.03735	0.1787	0.02054	0.0024	0.03736	1	0.03735	0.5594	0.02834	0.0024	0.03736	1
0.03775	0.2306	0.02524	0.002421	0.03776	1	0.03775	0.5	0.02526	0.002421	0.03776	1
0.03788	0.1977	0.002946	0.003021	0.03794	1	0.03788	0.5019	0.004589	0.003021	0.03794	1
0.03798	0.2052	0.003175	0.004881	0.03823	1	0.03798	0.5323	0.01439	0.004881	0.03823	1
0.03815	0.1624	0.02323	0.002442	0.03817	1	0.03815	0.4926	0.03055	0.002442	0.03817	1
0.03856	0.2339	0.02807	0.002463	0.03857	1	0.03856	0.5162	0.02883	0.002463	0.03857	1
0.03896	0.2058	0.02195	0.002484	0.03897	1	0.03896	0.4946	0.03089	0.002484	0.03897	1
0.03921	0.1897	0.003075	0.003077	0.03927	1	0.03921	0.4386	0.004179	0.003077	0.03927	1
0.03936	0.182	0.03293	0.002506	0.03938	1	0.03936	0.4686	0.04041	0.002506	0.03938	1
0.03977	0.2357	0.02927	0.002527	0.03978	1	0.03977	0.4339	0.0481	0.002527	0.03978	1
0.04017	0.2192	0.03691	0.002548	0.04018	1	0.04017	0.3613	0.05868	0.002548	0.04018	1

PEO <sub>132</sub> -PB <sub>99</sub> /C <sub>6</sub> D <sub>12</sub> 39.9 °C						PEO <sub>132</sub> -PB <sub>99</sub> /C <sub>6</sub> D <sub>12</sub> 49.3 °C					
Q	I(Q)	Std Dev(I(Q))	sigmaQ	meanQ	Shadow Factor	Q	I(Q)	Std Dev(I(Q))	sigmaQ	meanQ	Shadow Factor
0.04054	0.1844	0.00317	0.003134	0.04059	1	0.04054	0.3824	0.003861	0.003134	0.04059	1
0.04057	0.1908	0.03115	0.00257	0.04059	1	0.04057	0.3545	0.04586	0.00257	0.04059	1
0.04187	0.1727	0.002851	0.003192	0.04192	1	0.04187	0.3377	0.003768	0.003192	0.04192	1
0.04197	0.1714	0.002519	0.004987	0.0422	1	0.04197	0.3479	0.007846	0.004987	0.0422	1
0.0432	0.1712	0.002573	0.003251	0.04325	1	0.0432	0.3028	0.003606	0.003251	0.04325	1
0.04452	0.1511	0.002824	0.003311	0.04457	1	0.04452	0.2592	0.003273	0.003311	0.04457	1
0.04585	0.1454	0.002614	0.003371	0.0459	1	0.04585	0.2358	0.00344	0.003371	0.0459	1
0.04597	0.1458	0.002071	0.005102	0.04617	1	0.04597	0.2408	0.004886	0.005102	0.04617	1
0.04718	0.1454	0.00286	0.003432	0.04722	1	0.04718	0.2233	0.003001	0.003432	0.04722	1
0.0485	0.1352	0.002493	0.003493	0.04855	1	0.0485	0.202	0.002935	0.003493	0.04855	1
0.04983	0.1277	0.002538	0.003555	0.04987	1	0.04983	0.1834	0.002745	0.003555	0.04987	1
0.04996	0.1288	0.001636	0.005225	0.05014	1	0.04996	0.1852	0.002758	0.005225	0.05014	1
0.05116	0.1218	0.002754	0.003618	0.0512	1	0.05116	0.1701	0.002768	0.003618	0.0512	1
0.05248	0.1178	0.002219	0.003681	0.05252	1	0.05248	0.1633	0.002583	0.003681	0.05252	1
0.05381	0.1148	0.002372	0.003745	0.05385	1	0.05381	0.1535	0.002424	0.003745	0.05385	1
0.05394	0.1155	0.001385	0.005355	0.05412	1	0.05394	0.1489	0.002028	0.005355	0.05412	1
0.05514	0.1127	0.002442	0.003809	0.05517	1	0.05514	0.1405	0.002558	0.003809	0.05517	1
0.05646	0.1119	0.002072	0.003874	0.0565	1	0.05646	0.1373	0.002174	0.003874	0.0565	1
0.05779	0.1097	0.002251	0.003939	0.05782	1	0.05779	0.1289	0.00236	0.003939	0.05782	1
0.05793	0.1084	0.001314	0.005492	0.05809	1	0.05793	0.129	0.001566	0.005492	0.05809	1
0.05911	0.1084	0.002335	0.004004	0.05915	1	0.05911	0.1253	0.002125	0.004004	0.05915	1
0.06044	0.1048	0.002214	0.00407	0.06047	1	0.06044	0.1203	0.002154	0.00407	0.06047	1
0.06176	0.1058	0.002025	0.004137	0.0618	1	0.06176	0.1165	0.002197	0.004137	0.0618	1
0.06192	0.1022	0.001381	0.005635	0.06207	1	0.06192	0.1154	0.001526	0.005635	0.06207	1
0.06309	0.1033	0.002081	0.004203	0.06312	1	0.06309	0.1134	0.002163	0.004203	0.06312	1
0.06441	0.09705	0.002156	0.00427	0.06444	1	0.06441	0.1098	0.001992	0.00427	0.06444	1
0.06573	0.1002	0.001965	0.004337	0.06577	1	0.06573	0.1035	0.002156	0.004337	0.06577	1
0.0659	0.09856	0.001499	0.005784	0.06604	1	0.0659	0.1073	0.001474	0.005784	0.06604	1
0.06706	0.09935	0.002006	0.004405	0.06709	1	0.06706	0.1048	0.002059	0.004405	0.06709	1
0.06838	0.1002	0.00209	0.004473	0.06841	1	0.06838	0.1036	0.001999	0.004473	0.06841	1
0.06971	0.1018	0.001908	0.004541	0.06974	1	0.06971	0.1059	0.00209	0.004541	0.06974	1
0.06988	0.09703	0.001228	0.005938	0.07001	1	0.06988	0.1022	0.001301	0.005938	0.07001	1
0.07103	0.0998	0.002019	0.004609	0.07106	1	0.07103	0.101	0.001891	0.004609	0.07106	1
0.07235	0.1005	0.001862	0.004678	0.07238	1	0.07235	0.1014	0.001977	0.004678	0.07238	1
0.07367	0.09816	0.001912	0.004746	0.0737	1	0.07367	0.1022	0.002091	0.004746	0.0737	1
0.07386	0.09648	0.001317	0.006097	0.07399	1	0.07386	0.1	0.00137	0.006097	0.07399	1
0.075	0.09273	0.001885	0.004815	0.07503	1	0.075	0.1011	0.001953	0.004815	0.07503	1
0.07632	0.09609	0.001828	0.004885	0.07635	1	0.07632	0.1025	0.001915	0.004885	0.07635	1
0.07764	0.09728	0.001967	0.004954	0.07767	1	0.07764	0.1004	0.001789	0.004954	0.07767	1
0.07784	0.09418	0.001076	0.00626	0.07796	1	0.07784	0.09957	0.001342	0.00626	0.07796	1
0.07896	0.09351	0.001901	0.005024	0.07899	1	0.07896	0.1045	0.001995	0.005024	0.07899	1
0.08028	0.09405	0.001938	0.005094	0.08031	1	0.08028	0.1005	0.002058	0.005094	0.08031	1
0.08161	0.09073	0.001847	0.005164	0.08163	1	0.08161	0.09888	0.001847	0.005164	0.08163	1
0.08181	0.09162	0.001088	0.006427	0.08192	1	0.08181	0.0968	0.00118	0.006427	0.08192	1
0.08293	0.09219	0.001899	0.005234	0.08295	1	0.08293	0.09774	0.002065	0.005234	0.08295	1
0.08425	0.09275	0.002107	0.005304	0.08427	1	0.08425	0.09546	0.002095	0.005304	0.08427	1
0.08557	0.08731	0.002081	0.005375	0.08559	1	0.08557	0.1003	0.002134	0.005375	0.08559	1
0.08578	0.08977	0.001249	0.006598	0.08589	1	0.08578	0.09766	0.001189	0.006598	0.08589	1
0.08689	0.08858	0.002192	0.005445	0.08691	1	0.08689	0.1	0.002278	0.005445	0.08691	1
0.08821	0.08969	0.002326	0.005516	0.08823	1	0.08821	0.1022	0.002482	0.005516	0.08823	1
0.08953	0.08456	0.002573	0.005587	0.08955	1	0.08953	0.09706	0.002699	0.005587	0.08955	1
0.08975	0.08963	0.001119	0.006772	0.08985	1	0.08975	0.09604	0.001138	0.006772	0.08985	1
0.09084	0.08634	0.002523	0.005658	0.09087	1	0.09084	0.09327	0.002623	0.005658	0.09087	1
0.09216	0.0868	0.002861	0.005729	0.09219	1	0.09216	0.0952	0.002877	0.005729	0.09219	1
0.09348	0.08645	0.00277	0.0058	0.0935	1	0.09348	0.09049	0.002958	0.0058	0.0935	1
0.09371	0.08852	0.001178	0.006949	0.09381	1	0.09371	0.0942	0.001155	0.006949	0.09381	1
0.0948	0.09296	0.002658	0.005872	0.09482	1	0.0948	0.09753	0.002856	0.005872	0.09482	1
0.09612	0.08967	0.002727	0.005943	0.09614	1	0.09612	0.09901	0.002884	0.005943	0.09614	1
0.09743	0.09169	0.003565	0.006015	0.09746	1	0.09743	0.09284	0.0033	0.006015	0.09746	1
0.09768	0.08912	0.001113	0.00713	0.09777	1	0.09768	0.09206	0.00103	0.00713	0.09777	1
0.09875	0.08778	0.003492	0.006086	0.09877	1	0.09875	0.09348	0.003783	0.006086	0.09877	1
0.1001	0.08931	0.003508	0.006158	0.1001	1	0.1001	0.0901	0.003279	0.006158	0.1001	1
0.1014	0.08361	0.003919	0.00623	0.1014	1	0.1014	0.09471	0.003759	0.00623	0.1014	1
0.1016	0.08529	0.00122	0.007313	0.1017	1	0.1016	0.08995	0.001033	0.007313	0.1017	1
0.1027	0.08038	0.003816	0.006302	0.1027	1	0.1027	0.0991	0.003795	0.006302	0.1027	1
0.104	0.08623	0.003623	0.006374	0.104	1	0.104	0.08938	0.00408	0.006374	0.104	1
0.1053	0.08761	0.004473	0.006446	0.1053	1	0.1053	0.08996	0.004614	0.006446	0.1053	1
0.1056	0.08431	0.001169	0.007498	0.1057	1	0.1056	0.08901	0.001173	0.007498	0.1057	1
0.1066	0.09067	0.005611	0.006518	0.1067	1	0.1066	0.09419	0.006496	0.006518	0.1067	1
0.108	0.07587	0.005878	0.006591	0.108	1	0.108	0.09024	0.005477	0.006591	0.108	1
0.1093	0.08797	0.005107	0.006663	0.1093	1	0.1093	0.09326	0.005776	0.006663	0.1093	1
0.1095	0.08382	0.001125	0.007685	0.1096	1	0.1095	0.0884	0.001109	0.007685	0.1096	1
0.1106	0.08259	0.009196	0.006735	0.1106	1	0.1106	0.07987	0.007439	0.006735	0.1106	1
0.1119	0.0787	0.005655	0.006808	0.1119	1	0.1119	0.07959	0.007013	0.006808	0.1119	1
0.1132	0.08846	0.007612	0.00688	0.1132	1	0.1132	0.08524	0.009656	0.00688	0.1132	1
0.1135	0.08338	0.000995	0.007875	0.1136	1	0.1135	0.08583	0.001121	0.007875	0.1136	1
0.1174	0.08196	0.001013	0.008066	0.1175	1	0.1174	0.08619	0.001012	0.008066	0.1175	1
0.1214	0.08303	0.000922	0.008259	0.1215	1	0.1214	0.08499	0.000965	0.008259	0.1215	1
0.1253	0.08254	0.00099	0.008453	0.1254	1	0.1253	0.08536	0.000959	0.008453	0.1254	1
0.1293	0.07921	0.001021	0.008649	0.1293	1	0.1293	0.08329	0.000865	0.008649	0.1293	1
0.1332	0.08257	0.000941	0.008847	0.1333	1	0.1332	0.08452	0.000939	0.008847	0.1333	1
0.1371	0.08152	0.000942	0.009045	0.1372	1	0.1371	0.08279	0.000953	0.009045	0.1372	1

PEO <sub>132</sub> -PB <sub>89</sub> /C <sub>6</sub> D <sub>12</sub> 39.9 °C						PEO <sub>132</sub> -PB <sub>89</sub> /C <sub>6</sub> D <sub>12</sub> 49.3 °C					
Q	I(Q)	Std DevI(Q)	sigmaQ	meanQ	Shadow Factor	Q	I(Q)	Std DevI(Q)	sigmaQ	meanQ	Shadow Factor
0.141	0.07997	0.000911	0.009245	0.1411	1	0.141	0.08071	0.001003	0.009245	0.1411	1
0.1449	0.08196	0.000993	0.009445	0.145	1	0.1449	0.08134	0.000917	0.009445	0.145	1
0.1489	0.08075	0.000909	0.009647	0.1489	1	0.1489	0.08258	0.000928	0.009647	0.1489	1
0.1528	0.07889	0.000919	0.009849	0.1528	1	0.1528	0.08068	0.000878	0.009849	0.1528	1
0.1567	0.07903	0.000982	0.01005	0.1567	1	0.1567	0.07952	0.000964	0.01005	0.1567	1
0.1606	0.0785	0.000902	0.01026	0.1606	1	0.1606	0.08125	0.000878	0.01026	0.1606	1
0.1645	0.07878	0.000846	0.01046	0.1645	1	0.1645	0.0805	0.000874	0.01046	0.1645	1
0.1683	0.07766	0.000886	0.01067	0.1684	1	0.1683	0.07996	0.000875	0.01067	0.1684	1
0.1722	0.07713	0.000826	0.01087	0.1723	1	0.1722	0.07903	0.000774	0.01087	0.1723	1
0.1761	0.07895	0.000883	0.01108	0.1762	1	0.1761	0.07771	0.000872	0.01108	0.1762	1
0.18	0.07597	0.000845	0.01128	0.18	1	0.18	0.07863	0.000826	0.01128	0.18	1
0.1838	0.07775	0.000825	0.01149	0.1839	1	0.1838	0.07865	0.00084	0.01149	0.1839	1
0.1877	0.07633	0.000817	0.0117	0.1877	1	0.1877	0.07837	0.000885	0.0117	0.1877	1
0.1916	0.07684	0.000868	0.0119	0.1916	1	0.1916	0.07842	0.000848	0.0119	0.1916	1
0.1954	0.07655	0.000911	0.01211	0.1954	1	0.1954	0.07734	0.000855	0.01211	0.1954	1
0.1992	0.07614	0.000847	0.01232	0.1993	1	0.1992	0.07834	0.000842	0.01232	0.1993	1
0.2031	0.07672	0.000835	0.01253	0.2031	1	0.2031	0.07807	0.00077	0.01253	0.2031	1
0.2069	0.07682	0.000797	0.01274	0.2069	1	0.2069	0.07846	0.000728	0.01274	0.2069	1
0.2107	0.0781	0.000862	0.01294	0.2108	1	0.2107	0.07767	0.000803	0.01294	0.2108	1
0.2145	0.07589	0.000786	0.01315	0.2146	1	0.2145	0.07694	0.000776	0.01315	0.2146	1
0.2184	0.07715	0.000711	0.01336	0.2184	1	0.2184	0.07615	0.000744	0.01336	0.2184	1
0.2222	0.07551	0.000738	0.01357	0.2222	1	0.2222	0.07677	0.000795	0.01357	0.2222	1
0.226	0.07589	0.000754	0.01378	0.226	1	0.226	0.07648	0.000776	0.01378	0.226	1
0.2297	0.07482	0.000724	0.01399	0.2298	1	0.2297	0.07602	0.000721	0.01399	0.2298	1
0.2335	0.07539	0.000768	0.01419	0.2336	1	0.2335	0.07419	0.00074	0.01419	0.2336	1
0.2373	0.07428	0.000693	0.0144	0.2373	1	0.2373	0.07624	0.000752	0.0144	0.2373	1
0.2411	0.07567	0.000812	0.01461	0.2411	1	0.2411	0.07683	0.000769	0.01461	0.2411	1
0.2448	0.075	0.000804	0.01482	0.2449	1	0.2448	0.07382	0.000836	0.01482	0.2449	1
0.2486	0.07442	0.000826	0.01503	0.2486	1	0.2486	0.07546	0.000815	0.01503	0.2486	1
0.2523	0.07579	0.00085	0.01523	0.2524	1	0.2523	0.07424	0.000732	0.01523	0.2524	1
0.2561	0.07417	0.000796	0.01544	0.2561	1	0.2561	0.07657	0.000871	0.01544	0.2561	1
0.2598	0.07459	0.000839	0.01565	0.2598	1	0.2598	0.07511	0.000835	0.01565	0.2598	1
0.2635	0.07399	0.000885	0.01586	0.2636	1	0.2635	0.07601	0.000946	0.01586	0.2636	1
0.2673	0.07478	0.000897	0.01606	0.2673	1	0.2673	0.07491	0.000876	0.01606	0.2673	1
0.271	0.07193	0.000905	0.01627	0.271	1	0.271	0.07542	0.000944	0.01627	0.271	1
0.2747	0.07361	0.000858	0.01648	0.2747	1	0.2747	0.07551	0.000771	0.01648	0.2747	1
0.2784	0.07418	0.00088	0.01668	0.2784	1	0.2784	0.07483	0.000919	0.01668	0.2784	1
0.282	0.07229	0.000967	0.01689	0.2821	1	0.282	0.0735	0.000814	0.01689	0.2821	1
0.2857	0.07369	0.000862	0.01709	0.2857	1	0.2857	0.07453	0.000912	0.01709	0.2857	1
0.2894	0.07359	0.000842	0.0173	0.2894	1	0.2894	0.07382	0.000989	0.0173	0.2894	1
0.293	0.07398	0.000965	0.0175	0.2931	1	0.293	0.07327	0.000887	0.0175	0.2931	1
0.2967	0.07407	0.00088	0.01771	0.2967	1	0.2967	0.07429	0.000929	0.01771	0.2967	1
0.3003	0.07144	0.000918	0.01791	0.3004	1	0.3003	0.0754	0.000848	0.01791	0.3004	1
0.304	0.07296	0.000976	0.01812	0.304	1	0.304	0.07308	0.000879	0.01812	0.304	1
0.3076	0.07274	0.000984	0.01832	0.3076	1	0.3076	0.07319	0.000931	0.01832	0.3076	1
0.3112	0.0718	0.000859	0.01852	0.3113	1	0.3112	0.07484	0.00085	0.01852	0.3113	1
0.3148	0.07264	0.000971	0.01873	0.3149	1	0.3148	0.07369	0.00092	0.01873	0.3149	1
0.3184	0.07445	0.001014	0.01893	0.3185	1	0.3184	0.07333	0.000923	0.01893	0.3185	1
0.322	0.07207	0.00104	0.01913	0.3221	1	0.322	0.07309	0.000852	0.01913	0.3221	1
0.3256	0.07271	0.00096	0.01933	0.3256	1	0.3256	0.07286	0.001023	0.01933	0.3256	1
0.3292	0.07508	0.001009	0.01954	0.3292	1	0.3292	0.07374	0.000979	0.01954	0.3292	1
0.3327	0.07151	0.000997	0.01974	0.3328	1	0.3327	0.07221	0.000939	0.01974	0.3328	1
0.3363	0.0711	0.000891	0.01994	0.3363	1	0.3363	0.07252	0.000995	0.01994	0.3363	1
0.3399	0.07294	0.000988	0.02014	0.3399	1	0.3399	0.07238	0.000981	0.02014	0.3399	1
0.3434	0.07193	0.000923	0.02034	0.3434	1	0.3434	0.07304	0.000945	0.02034	0.3434	1
0.3469	0.07298	0.000939	0.02054	0.3469	1	0.3469	0.07246	0.000819	0.02054	0.3469	1
0.3504	0.07283	0.000877	0.02074	0.3505	1	0.3504	0.07066	0.000933	0.02074	0.3505	1
0.3539	0.0726	0.000942	0.02094	0.354	1	0.3539	0.07265	0.000997	0.02094	0.354	1
0.3574	0.06997	0.001088	0.02113	0.3575	1	0.3574	0.07147	0.000952	0.02113	0.3575	1
0.3609	0.06994	0.000966	0.02133	0.361	1	0.3609	0.07295	0.00098	0.02133	0.361	1
0.3644	0.07278	0.000965	0.02153	0.3644	1	0.3644	0.07055	0.000945	0.02153	0.3644	1
0.3679	0.07189	0.000914	0.02173	0.3679	1	0.3679	0.07281	0.000893	0.02173	0.3679	1
0.3713	0.07054	0.001012	0.02192	0.3714	1	0.3713	0.0709	0.000886	0.02192	0.3714	1
0.3748	0.07029	0.00099	0.02212	0.3748	1	0.3748	0.07274	0.000911	0.02212	0.3748	1
0.3782	0.07212	0.001031	0.02231	0.3783	1	0.3782	0.07193	0.001042	0.02231	0.3783	1
0.3817	0.07036	0.000878	0.02251	0.3817	1	0.3817	0.07041	0.000924	0.02251	0.3817	1
0.3851	0.07158	0.000958	0.0227	0.3851	1	0.3851	0.07165	0.000878	0.0227	0.3851	1
0.3885	0.06867	0.000993	0.0229	0.3885	1	0.3885	0.06995	0.00088	0.0229	0.3885	1
0.3919	0.07106	0.000991	0.02309	0.3919	1	0.3919	0.06983	0.00096	0.02309	0.3919	1
0.3953	0.07062	0.000994	0.02328	0.3953	1	0.3953	0.07104	0.001022	0.02328	0.3953	1
0.3987	0.07011	0.000964	0.02347	0.3987	1	0.3987	0.06815	0.00104	0.02347	0.3987	1
0.4021	0.07007	0.00101	0.02367	0.4021	1	0.4021	0.07056	0.000948	0.02367	0.4021	1
0.4054	0.07088	0.00098	0.02386	0.4054	1	0.4054	0.0702	0.000891	0.02386	0.4054	1
0.4088	0.07111	0.001008	0.02405	0.4088	1	0.4088	0.07249	0.000902	0.02405	0.4088	1
0.4121	0.07117	0.000815	0.02424	0.4121	1	0.4121	0.07235	0.000905	0.02424	0.4121	1
0.4155	0.06965	0.000984	0.02443	0.4155	1	0.4155	0.07063	0.000967	0.02443	0.4155	1
0.4188	0.07001	0.001011	0.02462	0.4188	1	0.4188	0.07083	0.001026	0.02462	0.4188	1
0.4221	0.07003	0.001069	0.02481	0.4221	1	0.4221	0.07096	0.000937	0.02481	0.4221	1
0.4254	0.07145	0.000973	0.02499	0.4254	1	0.4254	0.07093	0.001034	0.02499	0.4254	1
0.4287	0.07118	0.001212	0.02518	0.4287	1	0.4287	0.07069	0.000992	0.02518	0.4287	1
0.432	0.07209	0.001433	0.02537	0.432	1	0.432	0.07007	0.000953	0.02537	0.432	1
0.4352	0.06803	0.001191	0.02556	0.4353	1	0.4352	0.06857	0.001265	0.02556	0.4353	1

PEO <sub>132</sub> -PB <sub>89</sub> /C <sub>6</sub> D <sub>12</sub> 39.9 °C						PEO <sub>132</sub> -PB <sub>89</sub> /C <sub>6</sub> D <sub>12</sub> 49.3 °C					
Q	I(Q)	Std DevI(Q)	sigmaQ	meanQ	Shadow Factor	Q	I(Q)	Std DevI(Q)	sigmaQ	meanQ	Shadow Factor
0.4385	0.07168	0.001387	0.02574	0.4385	1	0.4385	0.07154	0.001351	0.02574	0.4385	1
0.4417	0.07067	0.00153	0.02593	0.4418	1	0.4417	0.06834	0.001415	0.02593	0.4418	1
0.445	0.07009	0.001889	0.02611	0.445	1	0.445	0.06796	0.001442	0.02611	0.445	1
0.4482	0.06877	0.001747	0.0263	0.4482	1	0.4482	0.06861	0.001693	0.0263	0.4482	1
0.4514	0.06833	0.001871	0.02648	0.4515	1	0.4514	0.06894	0.001558	0.02648	0.4515	1
0.4546	0.07251	0.001851	0.02666	0.4547	1	0.4546	0.06688	0.002209	0.02666	0.4547	1
0.4578	0.07126	0.00199	0.02685	0.4579	1	0.4578	0.07069	0.002028	0.02685	0.4579	1
0.461	0.06951	0.002329	0.02703	0.461	1	0.461	0.07517	0.002115	0.02703	0.461	1
PEO <sub>132</sub> -PB <sub>89</sub> /C <sub>6</sub> D <sub>12</sub> 58.6 °C						PEO <sub>132</sub> -PB <sub>89</sub> /C <sub>6</sub> D <sub>12</sub> 67.9 °C					
Q	I(Q)	Std DevI(Q)	sigmaQ	meanQ	Shadow Factor	Q	I(Q)	Std DevI(Q)	sigmaQ	meanQ	Shadow Factor
0.003433	6.985	0.1575	0.001072	0.003606	0.9585	0.003433	4.277	0.1221	0.001072	0.003606	0.9585
0.003837	7.561	0.1143	0.001076	0.003977	0.9999	0.003837	4.604	0.09096	0.001076	0.003977	0.9999
0.004241	7.483	0.09966	0.001078	0.004367	1	0.004241	4.503	0.08392	0.001078	0.004367	1
0.004645	7.431	0.09952	0.001081	0.00476	1	0.004645	4.594	0.07765	0.001081	0.00476	1
0.005049	7.212	0.09251	0.001086	0.005155	1	0.005049	4.647	0.07252	0.001086	0.005155	1
0.005453	7.185	0.0806	0.001091	0.005551	1	0.005453	4.546	0.07371	0.001091	0.005551	1
0.005857	7.224	0.08398	0.001097	0.005948	1	0.005857	4.379	0.06883	0.001097	0.005948	1
0.006261	7.119	0.07571	0.001103	0.006346	1	0.006261	4.428	0.06212	0.001103	0.006346	1
0.006665	6.767	0.07274	0.001111	0.006745	1	0.006665	4.406	0.06001	0.001111	0.006745	1
0.007069	6.819	0.06671	0.001118	0.007144	1	0.007069	4.268	0.05699	0.001118	0.007144	1
0.007473	6.809	0.07101	0.001127	0.007544	1	0.007473	4.276	0.05918	0.001127	0.007544	1
0.007876	6.724	0.05873	0.001135	0.007944	1	0.007876	4.159	0.05434	0.001135	0.007944	1
0.00828	6.494	0.0667	0.001145	0.008345	1	0.00828	4.046	0.05018	0.001145	0.008345	1
0.008684	6.55	0.05259	0.001154	0.008746	1	0.008684	4.078	0.05227	0.001154	0.008746	1
0.009088	6.336	0.05554	0.001164	0.009147	1	0.009088	3.979	0.04603	0.001164	0.009147	1
0.009492	6.337	0.05229	0.001175	0.009548	1	0.009492	4.038	0.05297	0.001175	0.009548	1
0.009896	6.148	0.05168	0.001186	0.00995	1	0.009896	3.853	0.04428	0.001186	0.00995	1
0.0103	6.19	0.05549	0.001197	0.01035	1	0.0103	3.684	0.03839	0.001197	0.01035	1
0.0107	5.927	0.05161	0.001209	0.01075	1	0.0107	3.731	0.03704	0.001209	0.01075	1
0.01111	5.773	0.05002	0.001221	0.01116	1	0.01111	3.65	0.03885	0.001221	0.01116	1
0.0113	5.634	0.03504	0.002191	0.01149	1	0.0113	3.6	0.02795	0.002191	0.01149	1
0.01151	5.664	0.05299	0.001233	0.01156	1	0.01151	3.563	0.03604	0.001233	0.01156	1
0.01192	5.623	0.04876	0.001246	0.01196	1	0.01192	3.473	0.03897	0.001246	0.01196	1
0.01232	5.431	0.04158	0.001259	0.01236	1	0.01232	3.422	0.03329	0.001259	0.01236	1
0.01263	5.277	0.03388	0.002212	0.0128	1	0.01263	3.359	0.02204	0.002212	0.0128	1
0.01272	5.332	0.04402	0.001272	0.01277	1	0.01272	3.39	0.03631	0.001272	0.01277	1
0.01313	5.285	0.04173	0.001286	0.01317	1	0.01313	3.287	0.03505	0.001286	0.01317	1
0.01353	5.129	0.03956	0.0013	0.01357	1	0.01353	3.217	0.03288	0.0013	0.01357	1
0.01393	4.952	0.04103	0.001314	0.01397	1	0.01393	3.122	0.03317	0.001314	0.01397	1
0.01396	4.878	0.0306	0.002236	0.01412	1	0.01396	3.116	0.02405	0.002236	0.01412	1
0.01434	4.883	0.04215	0.001328	0.01438	1	0.01434	3.071	0.02949	0.001328	0.01438	1
0.01474	4.663	0.03871	0.001343	0.01478	1	0.01474	2.97	0.02884	0.001343	0.01478	1
0.01515	4.658	0.03947	0.001358	0.01518	1	0.01515	2.907	0.03232	0.001358	0.01518	1
0.01529	4.507	0.02635	0.002264	0.01543	1	0.01529	2.863	0.01926	0.002264	0.01543	1
0.01555	4.494	0.03746	0.001373	0.01558	1	0.01555	2.779	0.03135	0.001373	0.01558	1
0.01595	4.367	0.03673	0.001389	0.01599	1	0.01595	2.776	0.02903	0.001389	0.01599	1
0.01636	4.216	0.03756	0.001404	0.01639	1	0.01636	2.7	0.03148	0.001404	0.01639	1
0.01662	4.093	0.02656	0.002294	0.01675	1	0.01662	2.62	0.01808	0.002294	0.01675	1
0.01676	4.149	0.0375	0.00142	0.01679	1	0.01676	2.587	0.02923	0.00142	0.01679	1
0.01717	3.987	0.03617	0.001436	0.0172	1	0.01717	2.557	0.02998	0.001436	0.0172	1
0.01757	3.891	0.03495	0.001453	0.0176	1	0.01757	2.45	0.02737	0.001453	0.0176	1
0.01795	3.711	0.02566	0.002326	0.01807	1	0.01795	2.406	0.01794	0.002326	0.01807	1
0.01797	3.758	0.03482	0.001469	0.018	1	0.01797	2.365	0.02933	0.001469	0.018	1
0.01838	3.631	0.03132	0.001486	0.01841	1	0.01838	2.262	0.02621	0.001486	0.01841	1
0.01878	3.502	0.03214	0.001503	0.01881	1	0.01878	2.218	0.02622	0.001503	0.01881	1
0.01918	3.328	0.03346	0.00152	0.01921	1	0.01918	2.167	0.02482	0.00152	0.01921	1
0.01928	3.319	0.02317	0.002361	0.01939	1	0.01928	2.187	0.01682	0.002361	0.01939	1
0.01959	3.295	0.03378	0.001537	0.01962	1	0.01959	2.111	0.02692	0.001537	0.01962	1
0.01999	3.156	0.03319	0.001554	0.02002	1	0.01999	2.071	0.02641	0.001554	0.02002	1
0.0204	3.06	0.0278	0.001572	0.02042	1	0.0204	1.998	0.02665	0.001572	0.02042	1
0.02061	2.932	0.02117	0.002398	0.02072	1	0.02061	1.952	0.01501	0.002398	0.02072	1
0.0208	2.96	0.03144	0.001589	0.02083	1	0.0208	1.921	0.02566	0.001589	0.02083	1
0.0212	2.788	0.02764	0.001607	0.02123	1	0.0212	1.837	0.02463	0.001607	0.02123	1
0.02161	2.738	0.02825	0.001625	0.02163	1	0.02161	1.727	0.02347	0.001625	0.02163	1
0.02194	2.602	0.01877	0.002436	0.02204	1	0.02194	1.754	0.01445	0.002436	0.02204	1
0.02201	2.575	0.0266	0.001643	0.02203	1	0.02201	1.722	0.02388	0.001643	0.02203	1
0.02241	2.509	0.02803	0.001661	0.02244	1	0.02241	1.67	0.02454	0.001661	0.02244	1
0.02282	2.442	0.02538	0.00168	0.02284	1	0.02282	1.596	0.02204	0.00168	0.02284	1
0.02322	2.299	0.02561	0.001698	0.02324	1	0.02322	1.547	0.02029	0.001698	0.02324	1
0.02327	2.291	0.01605	0.002477	0.02336	1	0.02327	1.54	0.01282	0.002477	0.02336	1
0.02363	2.196	0.02485	0.001717	0.02365	1	0.02363	1.506	0.02024	0.001717	0.02365	1
0.02403	2.166	0.0241	0.001736	0.02405	1	0.02403	1.472	0.02079	0.001736	0.02405	1
0.02443	2.059	0.02399	0.001754	0.02445	1	0.02443	1.358	0.01925	0.001754	0.02445	1
0.0246	1.995	0.01518	0.002519	0.02469	1	0.0246	1.357	0.01186	0.002519	0.02469	1
0.02484	1.951	0.02366	0.001773	0.02486	1	0.02484	1.32	0.02064	0.001773	0.02486	1
0.02524	1.899	0.02474	0.001792	0.02526	1	0.02524	1.301	0.02197	0.001792	0.02526	1
0.02564	1.805	0.02504	0.001812	0.02566	1	0.02564	1.214	0.02144	0.001812	0.02566	1
0.02593	1.74	0.01226	0.002563	0.02601	1	0.02593	1.209	0.008995	0.002563	0.02601	1
0.02605	1.756	0.02603	0.001831	0.02607	1	0.02605	1.141	0.02401	0.001831	0.02607	1

PEO <sub>132</sub> -PB <sub>89</sub> /C <sub>6</sub> D <sub>12</sub> 58.6 °C						PEO <sub>132</sub> -PB <sub>89</sub> /C <sub>6</sub> D <sub>12</sub> 67.9 °C					
Q	I(Q)	Std Dev(I(Q))	sigmaQ	meanQ	Shadow Factor	Q	I(Q)	Std Dev(I(Q))	sigmaQ	meanQ	Shadow Factor
0.02645	1.675	0.02797	0.00185	0.02647	1	0.02645	1.158	0.02166	0.00185	0.02647	1
0.02685	1.597	0.02622	0.00187	0.02687	1	0.02685	1.079	0.02293	0.00187	0.02687	1
0.02726	1.528	0.02541	0.001889	0.02728	1	0.02726	1.103	0.02183	0.001889	0.02728	1
0.02726	1.524	0.01021	0.002609	0.02734	1	0.02726	1.08	0.008737	0.002609	0.02734	1
0.02766	1.434	0.02332	0.001909	0.02768	1	0.02766	1.011	0.02283	0.001909	0.02768	1
0.02807	1.407	0.02794	0.001928	0.02808	1	0.02807	0.9375	0.02084	0.001928	0.02808	1
0.02847	1.375	0.02601	0.001948	0.02849	1	0.02847	0.9551	0.02408	0.001948	0.02849	1
0.02859	1.307	0.009603	0.002656	0.02866	1	0.02859	0.9321	0.008367	0.002656	0.02866	1
0.02887	1.271	0.02576	0.001968	0.02889	1	0.02887	0.8733	0.02086	0.001968	0.02889	1
0.02928	1.216	0.02577	0.001988	0.02929	1	0.02928	0.847	0.0213	0.001988	0.02929	1
0.02968	1.159	0.02531	0.002008	0.0297	1	0.02968	0.8541	0.02215	0.002008	0.0297	1
0.02991	1.139	0.00811	0.002705	0.02999	1	0.02991	0.8159	0.007351	0.002705	0.02999	1
0.03008	1.083	0.02237	0.002028	0.0301	1	0.03008	0.842	0.02137	0.002028	0.0301	1
0.03049	1.028	0.02463	0.002048	0.0305	1	0.03049	0.7818	0.02049	0.002048	0.0305	1
0.03089	1.034	0.02323	0.002068	0.03091	1	0.03089	0.7603	0.01936	0.002068	0.03091	1
0.03124	0.9757	0.007768	0.002754	0.03131	1	0.03124	0.7206	0.006281	0.002754	0.03131	1
0.03129	0.9216	0.02321	0.002089	0.03131	1	0.03129	0.7018	0.02119	0.002089	0.03131	1
0.0317	0.9321	0.02468	0.002109	0.03171	1	0.0317	0.6918	0.02247	0.002109	0.03171	1
0.0321	0.903	0.02344	0.002129	0.03212	1	0.0321	0.6743	0.02015	0.002129	0.03212	1
0.0325	0.8542	0.02145	0.00215	0.03252	1	0.0325	0.6375	0.0195	0.00215	0.03252	1
0.03257	0.8519	0.007274	0.002806	0.03264	1	0.03257	0.6461	0.006069	0.002806	0.03264	1
0.03291	0.7952	0.02078	0.00217	0.03292	1	0.03291	0.6514	0.01854	0.00217	0.03292	1
0.03331	0.7645	0.02125	0.002191	0.03333	1	0.03331	0.6202	0.01807	0.002191	0.03333	1
0.03372	0.7323	0.01981	0.002212	0.03373	1	0.03372	0.5816	0.01944	0.002212	0.03373	1
0.0339	0.7424	0.005862	0.002858	0.03396	1	0.0339	0.5704	0.00535	0.002858	0.03396	1
0.03399	0.7618	0.01811	0.004785	0.03426	1	0.03399	0.6006	0.01299	0.004785	0.03426	1
0.03412	0.7235	0.02318	0.002232	0.03413	1	0.03412	0.5823	0.01966	0.002232	0.03413	1
0.03452	0.7158	0.02242	0.002253	0.03454	1	0.03452	0.5418	0.02066	0.002253	0.03454	1
0.03493	0.6704	0.02258	0.002274	0.03494	1	0.03493	0.5119	0.02046	0.002274	0.03494	1
0.03523	0.6415	0.00555	0.002911	0.03529	1	0.03523	0.5015	0.005036	0.002911	0.03529	1
0.03533	0.624	0.02952	0.002295	0.03534	1	0.03533	0.5013	0.02171	0.002295	0.03534	1
0.03573	0.6264	0.0263	0.002316	0.03575	1	0.03573	0.49	0.02379	0.002316	0.03575	1
0.03614	0.5691	0.02721	0.002336	0.03615	1	0.03614	0.4594	0.0255	0.002336	0.03615	1
0.03654	0.5598	0.02769	0.002357	0.03655	1	0.03654	0.4197	0.02625	0.002357	0.03655	1
0.03656	0.554	0.005188	0.002966	0.03662	1	0.03656	0.4405	0.005177	0.002966	0.03662	1
0.03694	0.5615	0.03018	0.002378	0.03696	1	0.03694	0.4165	0.02911	0.002378	0.03696	1
0.03735	0.4918	0.02991	0.0024	0.03736	1	0.03735	0.4504	0.02821	0.0024	0.03736	1
0.03775	0.4932	0.028	0.002421	0.03776	1	0.03775	0.3705	0.02762	0.002421	0.03776	1
0.03788	0.4894	0.004554	0.003021	0.03794	1	0.03788	0.3982	0.004261	0.003021	0.03794	1
0.03798	0.5083	0.01185	0.004881	0.03823	1	0.03798	0.4243	0.007993	0.004881	0.03823	1
0.03815	0.4249	0.03464	0.002442	0.03817	1	0.03815	0.375	0.03479	0.002442	0.03817	1
0.03856	0.5112	0.03894	0.002463	0.03857	1	0.03856	0.4025	0.03397	0.002463	0.03857	1
0.03896	0.5079	0.0419	0.002484	0.03897	1	0.03896	0.4011	0.03702	0.002484	0.03897	1
0.03921	0.4295	0.004442	0.003077	0.03927	1	0.03921	0.3587	0.003882	0.003077	0.03927	1
0.03936	0.3653	0.03313	0.002506	0.03938	1	0.03936	0.4021	0.0345	0.002506	0.03938	1
0.03977	0.4088	0.03794	0.002527	0.03978	1	0.03977	0.3512	0.0302	0.002527	0.03978	1
0.04017	0.4376	0.05052	0.002548	0.04018	1	0.04017	0.3334	0.05958	0.002548	0.04018	1
0.04054	0.3797	0.004063	0.003134	0.04059	1	0.04054	0.3239	0.004018	0.003134	0.04059	1
0.04057	0.3625	0.05185	0.00257	0.04059	1	0.04057	0.328	0.03593	0.00257	0.04059	1
0.04187	0.3349	0.003625	0.003192	0.04192	1	0.04187	0.2986	0.003587	0.003192	0.04192	1
0.04197	0.3513	0.007192	0.004987	0.0422	1	0.04197	0.3122	0.005477	0.004987	0.0422	1
0.0432	0.2985	0.003685	0.003251	0.04325	1	0.0432	0.2682	0.00349	0.003251	0.04325	1
0.04452	0.2772	0.003356	0.003311	0.04457	1	0.04452	0.2509	0.003475	0.003311	0.04457	1
0.04585	0.2541	0.003392	0.003371	0.0459	1	0.04585	0.2294	0.003419	0.003371	0.0459	1
0.04597	0.2568	0.004715	0.005102	0.04617	1	0.04597	0.2409	0.003844	0.005102	0.04617	1
0.04718	0.2345	0.003278	0.003432	0.04722	1	0.04718	0.2181	0.002997	0.003432	0.04722	1
0.0485	0.2132	0.002971	0.003493	0.04855	1	0.0485	0.201	0.00287	0.003493	0.04855	1
0.04983	0.2039	0.003089	0.003555	0.04987	1	0.04983	0.1935	0.002864	0.003555	0.04987	1
0.04996	0.198	0.002935	0.005225	0.05014	1	0.04996	0.1971	0.002641	0.005225	0.05014	1
0.05116	0.1806	0.002917	0.003618	0.0512	1	0.05116	0.1847	0.002835	0.003618	0.0512	1
0.05248	0.1707	0.002528	0.003681	0.05252	1	0.05248	0.1732	0.002673	0.003681	0.05252	1
0.05381	0.1681	0.002382	0.003745	0.05385	1	0.05381	0.1693	0.002794	0.003745	0.05385	1
0.05394	0.1637	0.00208	0.005355	0.05412	1	0.05394	0.1656	0.002137	0.005355	0.05412	1
0.05514	0.1543	0.002719	0.003809	0.05517	1	0.05514	0.1596	0.002686	0.003809	0.05517	1
0.05646	0.1487	0.002383	0.003874	0.0565	1	0.05646	0.1546	0.002454	0.003874	0.0565	1
0.05779	0.1452	0.002224	0.003939	0.05782	1	0.05779	0.1424	0.002514	0.003939	0.05782	1
0.05793	0.1398	0.001747	0.005492	0.05809	1	0.05793	0.1462	0.001532	0.005492	0.05809	1
0.05911	0.1395	0.002255	0.004004	0.05915	1	0.05911	0.1388	0.002307	0.004004	0.05915	1
0.06044	0.1361	0.002191	0.00407	0.06047	1	0.06044	0.1421	0.002383	0.00407	0.06047	1
0.06176	0.1286	0.002228	0.004137	0.0618	1	0.06176	0.1343	0.002228	0.004137	0.0618	1
0.06192	0.1259	0.001445	0.005635	0.06207	1	0.06192	0.1346	0.001754	0.005635	0.06207	1
0.06309	0.1236	0.002372	0.004203	0.06312	1	0.06309	0.1281	0.002093	0.004203	0.06312	1
0.06441	0.1187	0.002127	0.00427	0.06444	1	0.06441	0.1273	0.002049	0.00427	0.06444	1
0.06573	0.1166	0.002241	0.004337	0.06577	1	0.06573	0.1217	0.002046	0.004337	0.06577	1
0.0659	0.1147	0.001487	0.005784	0.06604	1	0.0659	0.1236	0.001605	0.005784	0.06604	1
0.06706	0.1155	0.002057	0.004405	0.06709	1	0.06706	0.1224	0.00223	0.004405	0.06709	1
0.06838	0.1114	0.001989	0.004473	0.06841	1	0.06838	0.1184	0.002281	0.004473	0.06841	1
0.06971	0.1118	0.002024	0.004541	0.06974	1	0.06971	0.1206	0.002101	0.004541	0.06974	1
0.06988	0.1067	0.001345	0.005938	0.07001	1	0.06988	0.1181	0.001456	0.005938	0.07001	1
0.07103	0.1097	0.00201	0.004609	0.07106	1	0.07103	0.1179	0.002144	0.004609	0.07106	1
0.07235	0.1098	0.001915	0.004678	0.07238	1	0.07235	0.1115	0.00206	0.004678	0.07238	1
0.07367	0.1073	0.001857	0.004746	0.0737	1	0.07367	0.1128	0.001999	0.004746	0.0737	1



PEO <sub>132</sub> -PB <sub>89</sub> /C <sub>6</sub> D <sub>12</sub> 58.6 °C						PEO <sub>132</sub> -PB <sub>89</sub> /C <sub>6</sub> D <sub>12</sub> 67.9 °C					
Q	I(Q)	Std DevI(Q)	sigmaQ	meanQ	Shadow Factor	Q	I(Q)	Std DevI(Q)	sigmaQ	meanQ	Shadow Factor
0.07386	0.1051	0.001251	0.006097	0.07399	1	0.07386	0.1147	0.001456	0.006097	0.07399	1
0.075	0.1037	0.00193	0.004815	0.07503	1	0.075	0.1097	0.001948	0.004815	0.07503	1
0.07632	0.1079	0.002048	0.004885	0.07635	1	0.07632	0.1163	0.001994	0.004885	0.07635	1
0.07764	0.09968	0.001993	0.004954	0.07767	1	0.07764	0.1087	0.002029	0.004954	0.07767	1
0.07784	0.1014	0.001225	0.00626	0.07796	1	0.07784	0.1097	0.001171	0.00626	0.07796	1
0.07896	0.102	0.002039	0.005024	0.07899	1	0.07896	0.1101	0.00195	0.005024	0.07899	1
0.08028	0.1036	0.001782	0.005094	0.08031	1	0.08028	0.1113	0.001858	0.005094	0.08031	1
0.08161	0.1032	0.00204	0.005164	0.08163	1	0.08161	0.1103	0.00206	0.005164	0.08163	1
0.08181	0.09923	0.001188	0.006427	0.08192	1	0.08181	0.1063	0.001353	0.006427	0.08192	1
0.08293	0.1011	0.002092	0.005234	0.08295	1	0.08293	0.1087	0.002167	0.005234	0.08295	1
0.08425	0.1013	0.002114	0.005304	0.08427	1	0.08425	0.1064	0.002292	0.005304	0.08427	1
0.08557	0.09885	0.002156	0.005375	0.08559	1	0.08557	0.1086	0.002422	0.005375	0.08559	1
0.08578	0.09828	0.001229	0.006598	0.08589	1	0.08578	0.1067	0.001317	0.006598	0.08589	1
0.08689	0.09698	0.002101	0.005445	0.08691	1	0.08689	0.1104	0.002415	0.005445	0.08691	1
0.08821	0.1031	0.002255	0.005516	0.08823	1	0.08821	0.1066	0.002538	0.005516	0.08823	1
0.08953	0.09701	0.00252	0.005587	0.08955	1	0.08953	0.1019	0.002797	0.005587	0.08955	1
0.08975	0.09913	0.001076	0.006772	0.08985	1	0.08975	0.1049	0.001128	0.006772	0.08985	1
0.09084	0.1004	0.002695	0.005658	0.09087	1	0.09084	0.1024	0.002838	0.005658	0.09087	1
0.09216	0.09853	0.002885	0.005729	0.09219	1	0.09216	0.103	0.002905	0.005729	0.09219	1
0.09348	0.09049	0.002553	0.0058	0.0935	1	0.09348	0.1057	0.003047	0.0058	0.0935	1
0.09371	0.09533	0.00117	0.006949	0.09381	1	0.09371	0.1016	0.001348	0.006949	0.09381	1
0.0948	0.09422	0.002962	0.005872	0.09482	1	0.0948	0.1072	0.002859	0.005872	0.09482	1
0.09612	0.09676	0.003018	0.005943	0.09614	1	0.09612	0.1101	0.00316	0.005943	0.09614	1
0.09743	0.1028	0.003331	0.006015	0.09746	1	0.09743	0.1134	0.003657	0.006015	0.09746	1
0.09768	0.0959	0.001179	0.00713	0.09777	1	0.09768	0.101	0.001195	0.00713	0.09777	1
0.09875	0.09502	0.003141	0.006086	0.09877	1	0.09875	0.1005	0.003679	0.006086	0.09877	1
0.1001	0.09703	0.003787	0.006158	0.1001	1	0.1001	0.1062	0.003829	0.006158	0.1001	1
0.1014	0.09016	0.003696	0.00623	0.1014	1	0.1014	0.0999	0.004352	0.00623	0.1014	1
0.1016	0.09175	0.000961	0.007313	0.1017	1	0.1016	0.0988	0.001158	0.007313	0.1017	1
0.1027	0.1039	0.003572	0.006302	0.1027	1	0.1027	0.09492	0.003433	0.006302	0.1027	1
0.104	0.08874	0.004494	0.006374	0.104	1	0.104	0.09853	0.004096	0.006374	0.104	1
0.1053	0.08815	0.004345	0.006446	0.1053	1	0.1053	0.1038	0.004461	0.006446	0.1053	1
0.1056	0.09101	0.001131	0.007498	0.1057	1	0.1056	0.09841	0.001226	0.007498	0.1057	1
0.1066	0.08928	0.005455	0.006518	0.1067	1	0.1066	0.1049	0.004562	0.006518	0.1067	1
0.108	0.09326	0.005943	0.006591	0.108	1	0.108	0.09349	0.005809	0.006591	0.108	1
0.1093	0.09872	0.00506	0.006663	0.1093	1	0.1093	0.1054	0.004686	0.006663	0.1093	1
0.1095	0.09423	0.001164	0.007685	0.1096	1	0.1095	0.099	0.001183	0.007685	0.1096	1
0.1106	0.08658	0.007958	0.006735	0.1106	1	0.1106	0.1042	0.007005	0.006735	0.1106	1
0.1119	0.07611	0.008972	0.006808	0.1119	1	0.1119	0.08725	0.006663	0.006808	0.1119	1
0.1132	0.1068	0.009978	0.00688	0.1132	1	0.1132	0.07819	0.00714	0.00688	0.1132	1
0.1135	0.09019	0.001161	0.007875	0.1136	1	0.1135	0.09593	0.001259	0.007875	0.1136	1
0.1174	0.08828	0.001044	0.008066	0.1175	1	0.1174	0.09271	0.000969	0.008066	0.1175	1
0.1214	0.08778	0.001071	0.008259	0.1215	1	0.1214	0.09385	0.001041	0.008259	0.1215	1
0.1253	0.08591	0.001054	0.008453	0.1254	1	0.1253	0.09485	0.0011	0.008453	0.1254	1
0.1293	0.08621	0.000917	0.008649	0.1293	1	0.1293	0.09345	0.001016	0.008649	0.1293	1
0.1332	0.08699	0.000989	0.008847	0.1333	1	0.1332	0.09306	0.001121	0.008847	0.1333	1
0.1371	0.08605	0.000903	0.009045	0.1372	1	0.1371	0.0928	0.001034	0.009045	0.1372	1
0.141	0.08379	0.000851	0.009245	0.1411	1	0.141	0.09099	0.001055	0.009245	0.1411	1
0.1449	0.08418	0.001007	0.009445	0.145	1	0.1449	0.09164	0.000975	0.009445	0.145	1
0.1489	0.08448	0.000942	0.009647	0.1489	1	0.1489	0.09158	0.000928	0.009647	0.1489	1
0.1528	0.0848	0.000901	0.009849	0.1528	1	0.1528	0.08995	0.000944	0.009849	0.1528	1
0.1567	0.08348	0.000906	0.01005	0.1567	1	0.1567	0.08891	0.001057	0.01005	0.1567	1
0.1606	0.08388	0.000901	0.01026	0.1606	1	0.1606	0.08863	0.001034	0.01026	0.1606	1
0.1645	0.08263	0.000941	0.01046	0.1645	1	0.1645	0.08823	0.000884	0.01046	0.1645	1
0.1683	0.08121	0.000855	0.01067	0.1684	1	0.1683	0.08684	0.000929	0.01067	0.1684	1
0.1722	0.08164	0.000899	0.01087	0.1723	1	0.1722	0.08719	0.000909	0.01087	0.1723	1
0.1761	0.08097	0.000822	0.01108	0.1762	1	0.1761	0.08652	0.000827	0.01108	0.1762	1
0.18	0.08058	0.000836	0.01128	0.18	1	0.18	0.08555	0.000965	0.01128	0.18	1
0.1838	0.08118	0.000819	0.01149	0.1839	1	0.1838	0.08547	0.000805	0.01149	0.1839	1
0.1877	0.07941	0.000909	0.0117	0.1877	1	0.1877	0.08507	0.0008	0.0117	0.1877	1
0.1916	0.08006	0.000812	0.0119	0.1916	1	0.1916	0.0853	0.000842	0.0119	0.1916	1
0.1954	0.08059	0.000828	0.01211	0.1954	1	0.1954	0.0843	0.000841	0.01211	0.1954	1
0.1992	0.07924	0.000763	0.01232	0.1993	1	0.1992	0.08372	0.000798	0.01232	0.1993	1
0.2031	0.08	0.000802	0.01253	0.2031	1	0.2031	0.08501	0.000873	0.01253	0.2031	1
0.2069	0.07927	0.000843	0.01274	0.2069	1	0.2069	0.08427	0.000831	0.01274	0.2069	1
0.2107	0.08045	0.0008	0.01294	0.2108	1	0.2107	0.08392	0.000806	0.01294	0.2108	1
0.2145	0.07897	0.0008	0.01315	0.2146	1	0.2145	0.08348	0.000768	0.01315	0.2146	1
0.2184	0.07819	0.000828	0.01336	0.2184	1	0.2184	0.0847	0.000789	0.01336	0.2184	1
0.2222	0.07605	0.000809	0.01357	0.2222	1	0.2222	0.08247	0.000828	0.01357	0.2222	1
0.226	0.07829	0.000783	0.01378	0.226	1	0.226	0.08229	0.000772	0.01378	0.226	1
0.2297	0.07765	0.000709	0.01399	0.2298	1	0.2297	0.0823	0.000824	0.01399	0.2298	1
0.2335	0.07658	0.000698	0.01419	0.2336	1	0.2335	0.08251	0.000785	0.01419	0.2336	1
0.2373	0.07693	0.000767	0.0144	0.2373	1	0.2373	0.0831	0.000726	0.0144	0.2373	1
0.2411	0.07785	0.000789	0.01461	0.2411	1	0.2411	0.08223	0.000755	0.01461	0.2411	1
0.2448	0.07774	0.00088	0.01482	0.2449	1	0.2448	0.08178	0.000951	0.01482	0.2449	1
0.2486	0.07786	0.000811	0.01503	0.2486	1	0.2486	0.08176	0.000912	0.01503	0.2486	1
0.2523	0.07829	0.000854	0.01523	0.2524	1	0.2523	0.08096	0.000847	0.01523	0.2524	1
0.2561	0.07683	0.000813	0.01544	0.2561	1	0.2561	0.08317	0.001011	0.01544	0.2561	1
0.2598	0.0766	0.000788	0.01565	0.2598	1	0.2598	0.08217	0.000805	0.01565	0.2598	1
0.2635	0.07665	0.000877	0.01586	0.2636	1	0.2635	0.08202	0.00093	0.01586	0.2636	1
0.2673	0.07785	0.000817	0.01606	0.2673	1	0.2673	0.08233	0.000872	0.01606	0.2673	1
0.271	0.07577	0.000863	0.01627	0.271	1	0.271	0.08059	0.000959	0.01627	0.271	1

PEO <sub>132</sub> -PB <sub>89</sub> /C <sub>6</sub> D <sub>12</sub> 58.6 °C						PEO <sub>132</sub> -PB <sub>89</sub> /C <sub>6</sub> D <sub>12</sub> 67.9 °C					
Q	I(Q)	Std DevI(Q)	sigmaQ	meanQ	Shadow Factor	Q	I(Q)	Std DevI(Q)	sigmaQ	meanQ	Shadow Factor
0.2747	0.07533	0.000812	0.01648	0.2747	1	0.2747	0.08072	0.000876	0.01648	0.2747	1
0.2784	0.07616	0.000914	0.01668	0.2784	1	0.2784	0.08117	0.001063	0.01668	0.2784	1
0.282	0.07452	0.0009	0.01689	0.2821	1	0.282	0.07965	0.000888	0.01689	0.2821	1
0.2857	0.07571	0.000787	0.01709	0.2857	1	0.2857	0.0806	0.000986	0.01709	0.2857	1
0.2894	0.07708	0.000909	0.0173	0.2894	1	0.2894	0.08208	0.000924	0.0173	0.2894	1
0.293	0.07547	0.000867	0.0175	0.2931	1	0.293	0.0815	0.000992	0.0175	0.2931	1
0.2967	0.07606	0.000933	0.01771	0.2967	1	0.2967	0.08156	0.000927	0.01771	0.2967	1
0.3003	0.07453	0.000909	0.01791	0.3004	1	0.3003	0.08026	0.00093	0.01791	0.3004	1
0.304	0.07433	0.000848	0.01812	0.304	1	0.304	0.08012	0.00087	0.01812	0.304	1
0.3076	0.07477	0.000997	0.01832	0.3076	1	0.3076	0.07917	0.001022	0.01832	0.3076	1
0.3112	0.07562	0.000886	0.01852	0.3113	1	0.3112	0.07994	0.000993	0.01852	0.3113	1
0.3148	0.07532	0.000936	0.01873	0.3149	1	0.3148	0.08085	0.001071	0.01873	0.3149	1
0.3184	0.07548	0.000971	0.01893	0.3185	1	0.3184	0.07859	0.000927	0.01893	0.3185	1
0.322	0.07596	0.000859	0.01913	0.3221	1	0.322	0.0784	0.000894	0.01913	0.3221	1
0.3256	0.07484	0.000987	0.01933	0.3256	1	0.3256	0.07927	0.000924	0.01933	0.3256	1
0.3292	0.074	0.000999	0.01954	0.3292	1	0.3292	0.08006	0.000906	0.01954	0.3292	1
0.3327	0.07356	0.000849	0.01974	0.3328	1	0.3327	0.07889	0.001023	0.01974	0.3328	1
0.3363	0.07335	0.00097	0.01994	0.3363	1	0.3363	0.07734	0.001022	0.01994	0.3363	1
0.3399	0.07404	0.000939	0.02014	0.3399	1	0.3399	0.07816	0.000914	0.02014	0.3399	1
0.3434	0.07464	0.000888	0.02034	0.3434	1	0.3434	0.07559	0.000873	0.02034	0.3434	1
0.3469	0.07562	0.000808	0.02054	0.3469	1	0.3469	0.07908	0.001011	0.02054	0.3469	1
0.3504	0.07407	0.000903	0.02074	0.3505	1	0.3504	0.07774	0.000884	0.02074	0.3505	1
0.3539	0.07397	0.000983	0.02094	0.354	1	0.3539	0.07832	0.001029	0.02094	0.354	1
0.3574	0.07399	0.000886	0.02113	0.3575	1	0.3574	0.0776	0.00098	0.02113	0.3575	1
0.3609	0.07431	0.001029	0.02133	0.361	1	0.3609	0.07802	0.001054	0.02133	0.361	1
0.3644	0.07291	0.00089	0.02153	0.3644	1	0.3644	0.07782	0.000969	0.02153	0.3644	1
0.3679	0.07124	0.000908	0.02173	0.3679	1	0.3679	0.07791	0.000997	0.02173	0.3679	1
0.3713	0.07162	0.00101	0.02192	0.3714	1	0.3713	0.07499	0.000999	0.02192	0.3714	1
0.3748	0.07459	0.000931	0.02212	0.3748	1	0.3748	0.07814	0.000931	0.02212	0.3748	1
0.3782	0.07309	0.00103	0.02231	0.3783	1	0.3782	0.07735	0.001034	0.02231	0.3783	1
0.3817	0.07309	0.000968	0.02251	0.3817	1	0.3817	0.07698	0.000976	0.02251	0.3817	1
0.3851	0.07093	0.000932	0.0227	0.3851	1	0.3851	0.07879	0.000891	0.0227	0.3851	1
0.3885	0.07147	0.000892	0.0229	0.3885	1	0.3885	0.07518	0.001016	0.0229	0.3885	1
0.3919	0.07269	0.001007	0.02309	0.3919	1	0.3919	0.07618	0.000982	0.02309	0.3919	1
0.3953	0.0722	0.000978	0.02328	0.3953	1	0.3953	0.07595	0.001046	0.02328	0.3953	1
0.3987	0.07205	0.00102	0.02347	0.3987	1	0.3987	0.07384	0.001032	0.02347	0.3987	1
0.4021	0.0725	0.000976	0.02367	0.4021	1	0.4021	0.07817	0.000986	0.02367	0.4021	1
0.4054	0.07153	0.000955	0.02386	0.4054	1	0.4054	0.07604	0.000905	0.02386	0.4054	1
0.4088	0.07334	0.000939	0.02405	0.4088	1	0.4088	0.07724	0.001019	0.02405	0.4088	1
0.4121	0.07213	0.000984	0.02424	0.4121	1	0.4121	0.07711	0.000934	0.02424	0.4121	1
0.4155	0.07325	0.000988	0.02443	0.4155	1	0.4155	0.07479	0.000938	0.02443	0.4155	1
0.4188	0.07378	0.001007	0.02462	0.4188	1	0.4188	0.07669	0.000908	0.02462	0.4188	1
0.4221	0.07278	0.00101	0.02481	0.4221	1	0.4221	0.07635	0.00096	0.02481	0.4221	1
0.4254	0.07147	0.000949	0.02499	0.4254	1	0.4254	0.07667	0.001009	0.02499	0.4254	1
0.4287	0.07275	0.001178	0.02518	0.4287	1	0.4287	0.07761	0.001057	0.02518	0.4287	1
0.432	0.07256	0.001349	0.02537	0.432	1	0.432	0.07545	0.001376	0.02537	0.432	1
0.4352	0.0696	0.0013	0.02556	0.4353	1	0.4352	0.07668	0.001375	0.02556	0.4353	1
0.4385	0.07204	0.001333	0.02574	0.4385	1	0.4385	0.07602	0.001348	0.02574	0.4385	1
0.4417	0.07245	0.001321	0.02593	0.4418	1	0.4417	0.07371	0.001534	0.02593	0.4418	1
0.445	0.07109	0.001612	0.02611	0.445	1	0.445	0.07394	0.001873	0.02611	0.445	1
0.4482	0.07269	0.001786	0.0263	0.4482	1	0.4482	0.07475	0.001843	0.0263	0.4482	1
0.4514	0.07212	0.001679	0.02648	0.4515	1	0.4514	0.0746	0.001912	0.02648	0.4515	1
0.4546	0.07158	0.001624	0.02666	0.4547	1	0.4546	0.07429	0.001768	0.02666	0.4547	1
0.4578	0.072	0.001829	0.02685	0.4579	1	0.4578	0.07609	0.002201	0.02685	0.4579	1
0.461	0.06839	0.00214	0.02703	0.461	1	0.461	0.07626	0.003362	0.02703	0.461	1

## References

- (1) Lodge, T. P.; Muthukumar, M. *J. Phys. Chem.* **1996**, 100, 13275-13292.
- (2) Bates, F. S.; Fredrickson, G. H. *Phys. Today* **1999**, 52, 32-38.
- (3) Carraher, C. E., Jr. *Seymour/Carraher's Polymer Chemistry* Marcel Dekker, Inc: New York, NY, 2003.
- (4) Hadjichristidis, N.; Pitsikalis, M.; Iatrou, H. *Adv. Polym. Sci.* **2005**, 189, 1-124.
- (5) Riess, G. *Prog. Polym. Sci.* **2003**, 28, 1107-1170.
- (6) Mortensen, K. *Colloids Surf., A* **2001**, 183-185, 277-292.
- (7) Schmolka, I. R. *J. Am. Oil Chem. Soc.* **1977**, 54, 110-116.
- (8) Lindman, B.; Alexandridis, P. Amphiphilic molecules: small and large. In *Amphiphilic Block Copolymers: Self-Assembly and Application*, ed.; Alexandridis, P. Lindman, B., Eds.; Elsevier: New York, NY, 2000; Ch. pp 1-12.
- (9) Hamley, I. W. *Introduction to Soft Matter: Polymers, Colloids, Amphiphiles, and Liquid Crystals*; Wiley: Chichester, UK, 2000.
- (10) Gohy, J. F. *Adv. Polym. Sci.* **2005**, 190, 65-136.
- (11) Blandamer, M. J.; Cullis, P. M.; Soldia, L. J.; Engberts, J. B. F. N.; Kacperskac, A.; Van Osd, N. M.; Subha, M. C. *Adv. Colloid Interface Sci.* **2000**, 58, 171-209.
- (12) Liu, T. B.; Liu, L.-Z.; Chu, B. Formation of amphiphilic block copolymer micelles in nonaqueous solution. In *Amphiphilic Block Copolymers*, ed.; Alexandridis, P. Lindman, B., Eds.; Elsevier Science B.V.: Amsterdam, The Netherlands, 2000; Ch. pp 115-149.
- (13) Alexandridis, P.; Yang, L. *Macromolecules* **2000**, 33, 3382-3391.
- (14) Greer, S. Personal communication.
- (15) Fiscaro, E.; Compari, C.; Braibanti, A. *Phys. Chem. Chem. Phys.* **2004**, 6, 4156-4166.

- (16) Raghavan, S. University of Maryland, College Park, College Park, MD. Personal communication, 2007.
- (17) Luan, C. H.; Urry, D. W. *J. Phys. Chem.* **1991**, 95, 7896-7900.
- (18) Mukerjee, P.; Kapauan, P.; Meyer, H. G. *J. Phys. Chem.* **1966**, 70, 783-786.
- (19) Engdahl, A.; Nelander, B. *J. Chem. Phys.* **1987**, 86, 1819-1823.
- (20) Chang, N. J.; Kaler, E. W. *J. Phys. Chem.* **1985**, 89, 2996-3000.
- (21) Emerson, M. F.; Holtzer, A. *J. Phys. Chem.* **1967**, 71, 3320-3330.
- (22) Niranjana, P.; Forbes, J.; Greer, S.; Dudowicz, J.; Freed, K.; Douglas, J. J. *J. Chem. Phys.* **2003**, 119, 4070-4083.
- (23) Shvartzman-Cohen, R.; Ren, C.; Szleifer, I.; Yerushalmi-Rozen, R. *Soft Matter* **2009**, 5, 5003-5011.
- (24) Shirota, H.; Kuwabara, N.; Ohkawa, K.; Horie, K. *J. Phys. Chem. B.* **1999**, 103, 10400-10408.
- (25) Bergbreiter, D.; Fu, H. *J. Polym. Sci. Part A: Polym. Chem.* **2008**, 46, 186-193.
- (26) *Material Safety Data Sheet, Methanol, Sigma-Aldrich.*
- (27) *Material Safety Data Sheet, Methanol-d4, Cambridge Isotope Laboratories.*
- (28) *Material Safety Data Sheet, Cyclohexane-d12, Cambridge Isotope Laboratories.*
- (29) *Material Safety Data Sheet, Cyclohexane, Sigma-Aldrich.*
- (30) Clover, B.; Hammouda, B. *Langmuir*. Preprint available at: <http://pubs.acs.org/doi/pdfplus/10.1021/la903961a>.
- (31) Elias, H.-G. *An Introduction to Plastics*; Wiley-VCH: Weinheim, 2003.
- (32) Evans, D. F.; Wennerström, H. *The Colloidal Domain : where physics, chemistry, biology, and technology meet*; Advances in Interfacial Engineering Wiley-VCH: New York, 1999.
- (33) Santos, N. C.; Castanho, M., A. R. B. *Biophys. J.* **1996**, 71, 1641-1650.

- (34) Thomas, J. C. Photon Correlation Spectroscopy: Technique and Instrumentation. In *Photon Correlation Spectroscopy: Multi-component Systems*, ed.; Schmitz, K. S., Ed. SPIE Publications: Bellingham, WA, 1991; Ch. pp 2-18.
- (35) Rubinstein, M.; Colby, R. H. *Polymer Physics*; Oxford University Press: New York, NY, 2003.
- (36) Hiemenz, P. C.; Rajagopalan, R. *Principles of Colloid and Surface Chemistry*; Marcel Dekker, Inc: New York, NY, 1997.
- (37) Lomakin, A.; Teplow, D. B.; Benedek, G. B. Quasielastic Light Scattering for Protein Assembly Studies. In *Amyloid Proteins: Methods and Protocols*, ed.; Sigurdsson, E. M., Ed. Methods in Molecular Biology, Humana Press, Inc.: Totowa, NJ, 2004; Ch. pp 153-174.
- (38) Goldin, A. A. Software for Particle Size Distribution Analysis in Photon Correlation Spectroscopy.  
[http://www.photocor.com/download/manuals/dynals\\_manual.htm](http://www.photocor.com/download/manuals/dynals_manual.htm) (April 16, 2008).
- (39) Einstein, A. *Ann. Phys.* **1906**, 19, 289-306.
- (40) Ploetz, C. D. Micelles of polybutadiene-*b*-poly(ethylene oxide) in a binary solvent system. M.S. Thesis, University of Maryland, College Park, College Park, 2008.
- (41) Anisimov, M. University of Maryland, College Park. Personal communication.
- (42) King, S. M. Small Angle Neutron Scattering.  
<http://www.isis.rl.ac.uk/largescale/loq/documents/sans.htm> (April 7 2008).
- (43) King, S. M. Small-angle Neutron Scattering. In *Modern Techniques for Polymer Characterisation*, ed.; Pethrick, R. A. Dawkins, J. V., Eds.; John Wiley and Sons, Ltd.: New York, NY, 1999; Ch. pp 171-232.
- (44) Glinka, C. J.; Barker, J. G.; Hammouda, B.; Krueger, S.; Moyer, J. J.; Orts, W. J. *J. Appl. Crystallogr.* **1998**, 31, 430-445.
- (45) Hammouda, B. *Probing Nanoscale Structures: The SANS Toolbox*. **2009**, book available online at:  
[www.ncnr.nist.gov/staff/hammouda/the\\_SANS\\_toolbox.pdf](http://www.ncnr.nist.gov/staff/hammouda/the_SANS_toolbox.pdf).
- (46) Hammouda, B.; Ho, D.; Kline, S. *Macromolecules* **2004**, 37, 6932-6937.

- (47) Norman, A. I.; Ho, D.; Karim, A.; Amis, E. J. *J. Colloid Interface Sci.* **2005**, 288, 155-165.
- (48) Roe, R.-J. *Methods of X-ray and Neutron Scattering in Polymer Science*; Topics in Polymer Science, Oxford University Press: New York, NY, 2000.
- (49) Hammouda, B. National Institute of Standards and Technology, Center for Neutron Research, Gaithersburg, MD. Personal communication.
- (50) Porod, G. General Theory. In *Small Angle X-ray Scattering*, ed.; Glatter, O. Kratky, O., Eds.; Academic Press Inc.: New York, NY, 1982; Ch. pp 17-51.
- (51) Hammouda, B. A New Guinier-Porod Model, Unpublished work, 2009.
- (52) Zemb, T. Scattering by Microemulsions. In *Neutrons, X-rays, and Light*, ed.; Lindner, P. Zemb, T., Eds.; Elsevier Science B.V.: New York, NY, 2002; Ch. pp 317-350.
- (53) Kline, S. R. *J. Appl. Crystallogr.* **2006**, 39, 895-900.
- (54) NIST Center for Neutron Research, SANS & USANS Analysis with IGOR Pro. [http://www.ncnr.nist.gov/programs/sans/data/red\\_anal.html](http://www.ncnr.nist.gov/programs/sans/data/red_anal.html).
- (55) Hayter, J. B. In *Physics of Amphiphiles: Micelles, Vesicles, and Microemulsions*, ed.; DeGiorgio, V. Corti, M., Eds.; Academic: New York, 1983; Ch. pp 59-93.
- (56) Nallet, F.; Laversanne, R.; Roux, D. *J. Phys. II France* **1993**, 3, 487-502.
- (57) Pedersen, J. S.; Schurtenberger, P. *Macromolecules* **1996**, 29, 7602-7612.
- (58) Chen, W.-R.; Butler, P. D.; Magid, L. J. *Langmuir* **2006**, 22, 6539-6548.
- (59) *Igor Pro*, WaveMetrics: Lake Oswego, OR, 2009. [www.wavemetrics.com](http://www.wavemetrics.com)
- (60) Zhang, J. Polymer Source, Inc., Personal communication.
- (61) Altinok, H.; Yu, G.-E.; Nixon, K.; Gorry, P. A.; Attwood, D.; Booth, C. *Langmuir* **1997**, 13, 5837-5848.
- (62) Mortensen, K. *Colloids Surf., A* **2001**, 183-185, 277-292.
- (63) Winter, R. *Curr. Opin. Colloid Interface Sci.* **2001**, 6, 303-312.
- (64) Lesemann, M.; Nathan, H.; DiNoia, T. P.; Kirby, C. F.; McHugh, M. A.; van Zanten, J. H.; Paulaitis, M. E. *Ind. Eng. Chem. Res.* **2003**, 42, 6425-6430.

- (65) Lesemann, M.; Thirumoorthy, K.; Kim, Y. J.; Jonas, J.; Paulaitis, M. E. *Langmuir* **1998**, 14, 5339-5341.
- (66) Kostko, A.; Harden, J.; McHugh, M. *Macromolecules* **2009**, 42, 5328-5338.
- (67) Mortensen, K.; Pedersen, J. S. *Macromolecules* **1993**, 26, 805-812.
- (68) Mortensen, K.; Schwahn, D.; Janssen, S. *Phys. Rev. Lett.* **1993**, 71, 1728-1731.
- (69) Mortensen, K. *J. Phys.: Condens. Matter* **1996**, 8, A103-A124.
- (70) Mortensen, K. *Europhys. Lett.* **1992**, 19, 599-604.
- (71) Hammouda, B.; Ho, D.; Kline, S. *Macromolecules* **2002**, 35, 8578-8585.
- (72) Kotaka, T.; Tanaka, T.; Inagaki, H. *Polym. J.* **1972**, 3, 327-337.
- (73) Tanaka, T.; Kotaka, T.; Inagaki, H. *Polym. J.* **1972**, 3, 338-349.
- (74) ten Brinke, G.; Hadziioannou, G. *Macromolecules* **1987**, 20, 486-489.
- (75) Balsara, N. P.; Tirrell, M.; Lodge, T. P. *Macromolecules* **1991**, 24, 1975-1986.
- (76) Tang, W. T.; Hadziioannou, G.; Cotts, P. M.; Smith, B. A.; Frank, C. W. *Polym. Prepr. (Am. Chem. Soc., Div. Polym. Chem.)* **1986**, 27, 107.
- (77) D'Errico, G.; Paduano, L.; Khan, A. *J. Colloid Interface Sci.* **2004**, 279, 379-390.
- (78) Mortensen, K.; Brown, W.; Jorgensen, E. *Macromolecules* **1994**, 27, 5654-5666.
- (79) Altinok, H.; Yu, G.-E.; Nixon, K.; Gorry, P. A.; Attwood, D.; Booth, C. *Langmuir* **1997**, 13, 5837-5848.
- (80) Zhou, Z.; Chu, B. *Macromolecules* **1994**, 27, 2025-2033.
- (81) Zhou, Z.; Chu, B. *Macromolecules* **1987**, 20, 3089-3091.
- (82) Zhou, Z.; Chu, B. *Macromolecules* **1988**, 21, 2548-2554.
- (83) Jacobs, D. T.; Patton, K.; Huff, A. 17R4 in H<sub>2</sub>O, Unpublished work, 2009.

- (84) In *Handbook of Chemistry and Physics*, 73rd ed.; Lide, D. R., Ed. CRC Press: Boca Raton, 1992; Ch. 6, p 13.
- (85) Greer, S. C. Measurement and Control of Temperature. In *Building Scientific Apparatus: A Practical Guide to Design and Construction*, 4th ed.; Moore, J. H., Davis, C. C. Coplan, M. A., Eds.; Cambridge University Press: New York, NY, 2009; Ch. pp 617-619.
- (86) Alexandridis, P.; Hatton, T. A. *Colloids Surf., A* **1995**, 96, 1-46.
- (87) Munoz, M. G.; Monroy, F.; Ortega, F.; Rubio, R. G.; Langevin, D. *Langmuir* **2000**, 16, 1083-1093.
- (88) Nystrom, B.; Walderhaug, H. *J. Phys. Chem.* **1996**, 100, 5433-5439.
- (89) Sedev, R. *Colloids Surf., A* **1999**, 156, 65-70.
- (90) Sedev, R.; Exerowa, D. *Adv. Colloid Interface Sci.* **1999**, 83, 111-136.
- (91) Sedev, R.; Steitz, R.; Findenegg, G. H. *Physica B* **2002**, 315, 267-272.
- (92) Hambardzumyan, A.; Aguié-Béghin, V.; Daoud, M.; Douillard, R. *Langmuir* **2004**, 20, 756-763.
- (93) Prokic, D. *J. Phys. E: Sci. Instrum.* **1982**, 15, 282-284.
- (94) Luten, D. *Phys. Rev.* **1934**, 45, 161-165.
- (95) Hammouda, B. *Polymer* **2009**, 50, 5293-5297.
- (96) Ho, D.; Hammouda, B.; Kline, S. *J. Polym. Sci. Polym. Phys. Ed.* **2003**, 41, 135-138.
- (97) Horkay, F.; Hammouda, B. *Colloid Polym. Sci.* **2008**, 286, 611-620.
- (98) Hammouda, B. Gaithersburg, MD. Personal communication, November 2009.
- (99) Koga, T.; Tanka, F.; Motokawa, R.; Koizumi, S.; Winnik, F. M. *Macromolecules* **2008**, 41, 9413-9422.
- (100) Hainbuchner, M.; Baron, M.; Lo Celso, F.; Triolo, A.; Triolo, R.; Rauch, H. *Physica A* **2002**, 304, 220-229.
- (101) Hamley, I. W., Ed. *The Physics of Block Copolymers.*; Oxford Science Publications: Oxford, U.K., 1998.



- (102) Deng, Y.; Young, R. N.; Ryan, A. J.; Fairclough, J. P. A.; Norman, A. I.; Tack, R. D. *Polymer* **2002**, 43, 7155-7160.
- (103) Discher, B. M.; Bermudez, H.; Hammer, D. A.; Won, Y. Y.; Bates, F. S. *J. Phys. Chem. B* **2002**, 106, 2848-2854.
- (104) Forster, S.; Berton, B.; Hentze, H. P.; Kramer, E.; Antonietti, M.; Lindner, P. *Macromolecules* **2001**, 32, 4610-4623.
- (105) Hentze, H. P.; Kramer, E.; Berton, B.; Forster, S.; Antonietti, M.; Dreja, M. *Macromolecules* **1999**, 32, 5803-5809.
- (106) Hong, S.; Yang, L. Z.; MacKnight, W. J.; Gido, S. P. *Macromolecules* **2001**, 34, 7009-7016.
- (107) Jain, S.; Bates, F. S. *Science* **2003**, 300, 460-464.
- (108) Jain, S.; Bates, F. S. *Macromolecules* **2004**, 37, 1511-1523.
- (109) Jain, S. M.; Gong, X. B.; Scriven, L. E.; Bates, F. S. *Phys. Rev. Lett.* **2006**, 96, 138304.
- (110) Jofre, A.; Hutchison, J. B.; Kishore, R.; Locascio, L. E.; Helmerson, K. *J. Phys. Chem. B* **2007**, 111, 5162-5166.
- (111) Lang, P.; Willner, L.; Pyckhout-Hintzen, W.; Krastev, R. *Langmuir* **2003**, 19, 7597-7603.
- (112) Nordskog, A.; Futterer, T.; von Berlepsh, H.; Bottcher, C.; Heinemann, A.; Schlaad, H.; Hellweg, T. *Phys. Chem. Chem. Phys.* **2004**, 6, 3123-3129.
- (113) Pispas, S.; Hadjichristidis, N. *Langmuir* **2003**, 19, 48-54.
- (114) Won, Y. Y.; Brannan, A. K.; Davis, H. T.; Bates, F. S. *J. Phys. Chem. B* **2002**, 106, 3354-3364.
- (115) Won, Y. Y.; Davis, H. T.; Bates, F. S. *Science* **1999**, 283, 960-963.
- (116) Won, Y. Y.; Davis, H. T.; Bates, F. S. *Macromolecules* **2003**, 36, 953-955.
- (117) Won, Y. Y.; Davis, H. T.; Bates, F. S.; Agamalian, M.; Wignall, G. D. *J. Phys. Chem. B* **2000**, 104, 7134-7143.
- (118) Ploetz, C. D.; Greer, S. *Langmuir* **2009**, 25, 13402-13411.

- (119) Wignall, G. D. Small angle neutron and x-ray scattering. In *Physical Properties of Polymers Handbook*, 2nd ed.; Mark, J. E., Ed. Springer Science: New York, 2007; Ch. 23.
- (120) Dixon, J. A.; Schiessler, R. W. *J. Phys. Chem.* **1954**, 58, 430-432.
- (121) Holz, M.; Mao, X.; Seiferling, D.; Sacco, A. *J. Chem. Phys.* **1996**, 104, 669-679.
- (122) Müller, K. Experimental Practice. In *Small Angle X-ray Scattering*, ed.; Glatter, O. Kratky, O., Eds.; Academic Press: New York, NY, 1982; Ch.
- (123) Schurtenberger, P.; Magid, L. J.; King, S. M.; Lindner, P. *J. Phys. Chem.* **1991**, 95, 4173-4176.
- (124) Edwards, P. J. B.; Jolley, K. W.; Smith, M. H.; Thomsen, S. J.; Boden, N. *Langmuir* **1997**, 13, 2665-2669.
- (125) Wilcoxon, J. P.; Schaefer, D. W.; Kaler, E. W. *J. Chem. Phys.* **1989**, 90, 1909-1917.
- (126) Pedersen, J. S.; Gerstenber, M. S. *Macromolecules* **1996**, 29, 1363-1365.
- (127) Munter, A. Scattering length density calculator.  
<http://www.ncnr.nist.gov/resources/sldcalc.html> (2010).